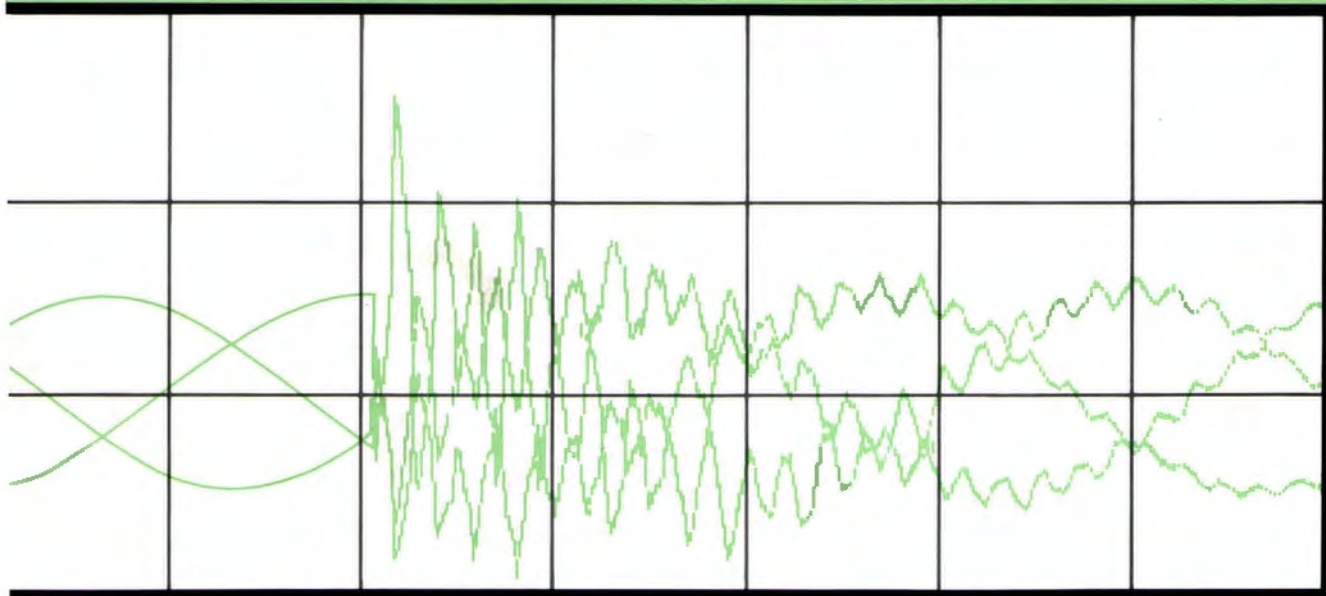


Electromagnetic Transients Program (EMTP)

APPLICATION GUIDE



**EMTP DEVELOPMENT COORDINATION GROUP
ELECTRIC POWER RESEARCH INSTITUTE**

R E P O R T S U M M A R Y

SUBJECTS	Power system planning / Transmission: Protection and control	
TOPICS	Electric transients Electromagnetic transients Power systems	Substations Transmission EMTP code
AUDIENCE	Transmission and distribution planners and designers / Electrical engineers	

Electromagnetic Transients Program (EMTP) Application Guide

The electromagnetic transients program is a versatile computer program that utilities worldwide use to analyze high-speed power system transients. This application guide provides procedures and data to assist engineers experienced in electromagnetic transient analysis based on EMTP.

BACKGROUND	The electromagnetic transients program (EMTP), developed in the early 1970s by the Bonneville Power Administration (BPA), has been widely used for transient analysis. To respond to user needs for program documentation, EPRI and the EMTP Development Coordination Group—composed of BPA, the Canadian Electrical Association, Hydro Quebec, Ontario Hydro, the U.S. Bureau of Reclamation, and the Western Area Power Administration—have developed several EMTP manuals. These include a primer (EL-4202) to introduce the program's input/output format to new users, a workbook (EL-4651) to explain electromagnetic transient principles to engineers with no prior experience in analyzing power system transients, and a rule book (EL-4541) to describe program syntax and conventions.
OBJECTIVE	To develop an EMTP application guide for engineers with experience in electromagnetic transient analysis.
APPROACH	The project team first briefly described problems encountered in preparing EMTP studies and applying the results. They then developed a components guide that describes the structure and limitations of mathematical models available in EMTP; provides guides to data preparation, including typical parameters for a wide range of equipment; and contains suggestions about which model to use in various circumstances. As a first step in developing a study guide, they showed how EMTP can be used to explain the situations under which surges can occur, describing appropriate analysis techniques and developing sample input files.
RESULTS	At present, the applications guide provides documentation for modeling transients related to overhead lines, transformers, circuit breakers, initial conditions in a given scenario, current and voltage sources, and lightning arresters. The study on surges focuses on those generated by the closing

or opening of circuit breakers but includes information on temporary overvoltages and lightning surges.

EPRI PERSPECTIVE The EMTP application guide provides an important bridge between the introductory EMTP documentation in EPRI reports EL-4202 and EL-4651 and the EMTP operation instructions in EPRI report EL-4541. The guide contains equipment data never before available. But because it describes the application of EMTP in areas where unanimity among experts is seldom achievable, these data should be carefully evaluated before they are used in utility EMTP studies. Moreover, the guide addresses only one of many EMTP applications and, because the art of applying EMTP is constantly developing, its study and component sections will need periodic revision.

PROJECT RP2149-1
EPRI Project Manager: J. V. Mitsche
Electrical Systems Division
Contractor: Westinghouse Electric Corporation

For further information on EPRI research programs, call
EPRI Technical Information Specialists (415) 855-2411.

Electromagnetic Transients Program (EMTP) Application Guide

EL-4650
Research Project 2149-1

Final Report, November 1986

Prepared by

WESTINGHOUSE ELECTRIC CORPORATION
Advanced Systems Technology
Power System Engineering Department
777 Penn Center Boulevard
Pittsburgh, Pennsylvania 15235

Principal Investigators
S. F. Mauser
T. E. McDermott

Prepared for

Electric Power Research Institute
3412 Hillview Avenue
Palo Alto, California 94304

EPRI Project Manager
J. V. Mitsche

Power System Planning and Operations Program
Electrical Systems Division

ORDERING INFORMATION

Requests for copies of this report should be directed to Research Reports Center (RRC), Box 50490, Palo Alto, CA 94303, (415) 965-4081. There is no charge for reports requested by EPRI member utilities and affiliates, U.S. utility associations, U.S. government agencies (federal, state, and local), media, and foreign organizations with which EPRI has an information exchange agreement. On request, RRC will send a catalog of EPRI reports.

Electric Power Research Institute and EPRI are registered service marks of Electric Power Research Institute, Inc.

Copyright © 1986 Electric Power Research Institute, Inc. All rights reserved.

NOTICE

This report was prepared by the organization(s) named below as an account of work sponsored by the Electric Power Research Institute, Inc. (EPRI). Neither EPRI, members of EPRI, the organization(s) named below, nor any person acting on behalf of any of them (a) makes any warranty, express or implied, with respect to the use of any information, apparatus, method, or process disclosed in this report or that such use may not infringe privately owned rights; or (b) assumes any liabilities with respect to the use of, or for damages resulting from the use of, any information, apparatus, method, or process disclosed in this report.

Prepared by
Westinghouse Electric Corporation
Pittsburgh, Pennsylvania

ABSTRACT

This document is an outgrowth of a survey and analysis of Electromagnetic Transients Program (EMTP) user needs, in which improved user's documentation was determined to be the single most important enhancement to the EMTP. The Application Guide covers EMTP models and studies, with many examples and typical data. The Application Guide is part of a series of new EMTP user manuals which covers program operation, theory, and application guide lines.

ACKNOWLEDGMENTS

The contractor acknowledges valuable assistance from the Industry Advisors:

Mr. O. J. Garcia	Florida Power & Light Company
Mr. John Kappenman	Minnesota Power & Light Company
Mr. William Torgerson	Puget Sound Power & Light Company

Members of the project team at Westinghouse were Mr. Stephen Mauser, Mr. Thomas McDermott, Mr. Nicholas Abi-Samra, and Mr. Helfried Anderl.

The EPRI project manager has been Mr. James Mitsche.

CONTENTS

<u>Section</u>		<u>Page</u>
INTRODUCTORY MATERIAL		
Summary		S-1
1 Introduction		1-1
COMPONENT GUIDE		
2 Overhead Lines		2-1
3 Transformers		3-1
4 Circuit Breakers		4-1
5 Surge Arresters.		5-1
6 Initial Conditions		6-1
7 Sources.		7-1
STUDY GUIDE		
8 Line Switching		8-1

FIGURES

<u>Figure</u>		<u>Page</u>
1-1	Numerical Oscillations Caused by Inductance Switching	1-3
1-2	Network Connections to Avoid Numerical Oscillations	1-4
1-3	Thyristor With Current-Limiting Reactor and Snubber	1-4
2-1	Infinitesimal Section of a Two-Conductor Transmission Line in the a) Time Domain and b) Frequency Domain.	2-6
2-2	EMTP Single-Conductor Line Model.	2-7
2-3	Physical Interpretation of Meyer-Dommel Weighting Function ^(B)	2-11
2-4	Weighting Functions in Meyer and Dommel's Formulation ^(B)	2-12
2-5	Weighting Functions $a_1(t)$ and $a_2(t)$ in the Marti Formulation	2-12
2-6	System Used for Example 1 for Comparing Results of Different Line Models. A single-line-to-ground fault is applied at Phase C of a 138 mile open-ended line. The fault is not allowed to clear for the duration of the run.	2-14
2-7	Phase B Voltage at the Open Receiving End (REC B) of the 138 Mile Line of the Example 1 as Obtained by a Field Test. Reference (A)	2-19
2-8	REC B Voltage to Ground for Example 1 Using a Distributed and Transposed Constant-Parameter Line Model. Line Parameters Calculated at 60 Hz.	2-19
2-9	REC B Voltage to Ground for Example 1 Using Constant- Parameter Transposed Line Model. Line Parameters Calculated at 500 Hz	2-20
2-10	REC B Voltage to Ground for Example 1 Using Lee's Nontransposed Line Model. Line Parameters Calculated at 60 Hz	2-21
2-11	REC B Voltage to Ground for Example 1 Using Meyer-Dommel Frequency-Dependent Line Model.	2-22
2-12	REC B Voltage to Ground for Example 1 Using Marti's Frequency- Dependent nontransposed Line Model.	2-23
2-13	REC B Voltage to Ground for Example 1 Using Marti's Frequency-Dependent Transposed Line Model	2-24
2-14	Circuit of Example 2. A single-line-to-ground fault is applied to Phase B of an open-ended transmission line, 120 miles long. Fault is not allowed to clear for the duration of the run	2-27
2-15	Faulting Conditions for Example 2. Node Voltage at Faulted Node REC B.	2-27

FIGURES (Cont'd)

<u>Figure</u>		<u>Page</u>
2-16	REC A Voltage to Ground for Example 2, Using the Constant-Parameter Transposed Line Model	2-28
2-17	REC A Voltage to Ground for Example 2, Using the Constant-Parameter Nontransposed Line Model.	2-29
2-18	REC A Voltage to Ground for Example 2, Using the Meyer-Oommel Transposed Line Model.	2-30
2-19	REC A Voltage to Ground for Example 2, Using the Marti Frequency-Dependent Model	2-31
2-20	Variation of the Sequence Resistances Per Unit Length of a Typical 500-kV Flat Configuration Transmission Line Shown in Figure 2-23	2-35
2-21	Variation of the Sequence Inductances Per Unit Length of a Typical 500-kV Flat Configuration Transmission Line Shown in Figure 2-23	2-36
2-22	Variation of the Sequence Surge Impedances for a Typical 500-kV Flat Configuration Transmission Line Shown in Figure 2-23	2-37
2-23	Tower Dimensions for the 500-kV Flat Configuration Transmission Line	2-38
2-24	Equivalent Number of Standard Suspension Insulators (5-3/4" x 10") Which are Used on Different Voltage Levels. Values Reflect the Range In Use	2-39
2-25	Equivalent Number of 5-3/4" x 10" Standard Insulators Used at Voltage Levels Equal to and Greater Than 69 kV.	2-40
2-26	Minimum Phase-to-Ground Clearances at Tower for Lines at Nominal Voltage Levels Equal to and Greater Than 69 kV.	2-41
2-27	Minimum Phase-to-Phase Clearances for Lines at Nominal Voltage Levels Equal to and Greater Than 69 kV.	2-42
2-28	Phase Conductor Heights for Transmission Lines at Nominal Voltage Levels Equal to and Greater Than 69 kV.	2-43
2-29	Positive and Zero Sequence Surge Impedance for Transmission Lines	2-44
2-30	Positive and Zero-Sequence Travelling Wave Velocities for Typical Transmission Lines. To be Used in Conjunction with Figure II.A.28 When Using Distributed Parameter Lines (ITYPE = -1, -2, -3).	2-45
2-31	Positive and Zero-Sequence Line Inductances for Typical Transmission Lines.	2-46
2-32	Positive and Zero-Sequence Capacitances for Typical Transmission Lines.	2-47
2-33	DC Resistance of the Phase Conductor (single or Bundled, as Applicable) for Typical Transmission Lines.	2-48

FIGURES (Cont'd)

<u>Figure</u>		<u>Page</u>
2-34	Positive and Zero Sequence Resistances for Typical Transmission Lines.	2-49
3-1	Equivalent Circuits for Short-Circuit Tests	3-4
3-2	Nonlinear Magnetizing Impedances.	3-7
3-3	Piecewise Nonlinear Inductance.	3-7
3-4	Hysteresis Model With RL Components	3-9
3-5	Type 96 Hysteretic Iron Core Model.	3-9
3-6	Autotransformer Windings.	3-20
3-7	Phase Shifting Transformer Winding Connections.	3-21
3-8	Transformer Test Case System.	3-24
3-9	Single-Line-to-Ground Low Side Fault Saturable TRANSFORMER, Closed Delta Tertiary	3-28
3-10	Single-Line-to-Ground Low Side Fault Saturable TRANSFORMER, Open Delta Tertiary	3-29
3-11	Single-Line-to-Ground Low Side Fault BCTTRAN, Closed Delta Tertiary.	3-30
3-12	Single-Line-to-Ground Low Side Fault BCTTRAN, Open Delta Tertiary.	3-31
3-13	Single-Line-to-Ground Low Side Fault BCTTRAN, Open Delta Tertiary, Type 98 Saturation.	3-32
3-14	Single-Line-to-Ground Low Side Fault BCTTRAN, Open Delta Tertiary, Type 98 Hysteresis.	3-33
3-15	Single-Phase Surge Applied to Transformer	3-34
3-16	Surge Transfer Without Transformer Capacitances	3-37
3-17	Surge Transfer With Transformer Capacitances.	3-38
3-18	Transformer Lowest Insulation Strength (vs. kV)	3-41
3-19	Positive Sequence Impedance of Non-Autotransformers (vs. BIL)	3-42
3-20	Positive Sequence Impedance of Autotransformers (vs. BIL)	3-43
3-21	Core Loss (vs. MVA)	3-44
3-22	Load Loss (vs. MVA)	3-45
3-23	Exciting Current at 100% Voltage (vs. MVA).	3-46
3-24	Exciting Current at 110% Voltage (vs. MVA).	3-47
3-25	Leakage Reactance (vs. MVA)	3-48
3-26	Shell-Form C_{hg} (vs. MVA).	3-50
3-27	Shell-Form C_{h1} (vs. MVA).	3-51
3-28	Shell-Form C_{1g} (vs. MVA).	3-51
3-29	Core-Form C_{hg} (vs. MVA)	3-52

FIGURES (Cont'd)

<u>Figure</u>		<u>Page</u>
3-30	Core-Form C_{hl} (vs. MVA)	3-52
3-31	Core-Form C_{lg} (vs. MVA)	3-53
3-32	Autotransformer C_{hg} (vs. MVA)	3-53
3-33	Autotransformer C_{ht} (vs. MVA)	3-54
3-34	Autotransformer C_{tg} (vs. MVA)	3-54
3-35	Capacitance of Current Transformers (vs. kV).	3-55
3-36	Capacitance of Potential Transformers (vs. kV).	3-56
4-1	Determination of Switch Opening Time.	4-2
4-2	Prestriking Circuit Breaker	4-3
4-3	Distribution of Contact Closing Times	4-3
4-4	TACS Prestrike Logic.	4-4
4-5	Prestrike Circuit Example	4-4
4-6	TACS Control Signals.	4-5
4-7	Load Voltage During Prestrike	4-6
4-8	Simulation of a Restrike.	4-7
4-9	Circuit Connection for the Simulation of Multiple Restrikes .	4-8
4-10	One Pole of an EHV Circuit Breaker With Preinsertion Resistor	4-9
4-11	Single-Phase Line Energization.	4-10
4-12a	Receiving End Voltage with No Resistor.	4-10
4-12b	Receiving End Voltage with Resistor	4-11
4-13	Closing Time of the Circuit Breaker Main Contact.	4-12
4-14	Uniform Distribution for Selecting the Aiming Point Reference Angle Boundaries at 0 and 360 Degrees	4-12
4-15	Closing Times of the Auxiliary and Main Contacts.	4-16
5-1	Types of Metal Oxide Arresters.	5-2
5-2	Nonlinear V-I Characteristic with Flashover	5-2
5-3	Nonlinear Arrester Solution by Compensation	5-3
5-4	Exponential Segments Defining Arrester Characteristic	5-5
5-5	System for Lightning Impulse Test Cases	5-7
5-6	System for Switching Surge Test Cases	5-7
5-7	396-kV SiC Arrester Active Gap in TACS.	5-9
5-8	Case SAMOD1, Lightning Impulse, No Arrester	5-18
5-9	Case SAMOD2, Lightning Impulse, SiC Arrester.	5-19
5-10	Case SAMOD3, Lightning Impulse, MOx Arrester.	5-20
5-11	Case SAMOD4, Switching Surge, No Arrester	5-22

FIGURES (Cont'd)

<u>Figure</u>		<u>Page</u>
5-12	Case SAMOD5, Switching Surge, MOx Gapless, 900-kV Surge . . .	5-23
5-13	Case SAMOD6, Switching Surge, MOx Shunt Gap, 900-kV Surge . .	5-24
5-14	Case SAMOD7, Switching Surge, SiC Active Gap, 900-kV Surge. .	5-25
5-15	Case SAMOD8, Switching Surge, SiC Passive Gap, 900-kV Surge .	5-26
5-16	Variation of a vs. I for a Metal Oxide Arrester	5-33
6-1	Ungrounded Capacitor Bank with Trapped Charge	6-4
6-2	Initialization of Nonlinear Inductance.	6-6
6-3	Phasor Diagram of Three-Phase Inductance Initialization . . .	6-7
6-4a	Excitation System Block Diagram	6-9
6-4b	Hydrogovernor Block Diagram	6-9
6-5a	TACS Excitation System Block Diagram.	6-10
6-5b	TACS Hydrogovernor Block Diagram.	6-10
7-1	Single-Phase Surge Impedance Termination.	7-3
7-2	Paralleled Surge Impedance Terminations	7-3
7-3	Multi-Phase Surge Impedance Termination	7-4
7-4	Load Equivalent Circuits.	7-6
7-5	Frequency Characteristics of Load Models.	7-7
7-6	Impulse Waveshape	7-9
7-7	Double Exponential Representation of 2 x 100 Wave	7-11
7-8	Typical Source Impedances	7-13
8-1	Variation of the Statistical Overvoltage, E_2 , With Source Impedance for a Given System. ($X_1 = X_0$ is assumed.)	8-15
8-2	Effect of Line End Arresters On Reducing the Maximum SOV's Along a 500-kV Line	8-17
8-3	Variation of E_2 with Pole Span.	8-17
8-4	TACS Logic for Calculating Energy Dissipated In the Branch Element Between 8A and 9A	8-19
8-5A	Series Capacitor Bank and Its Protection Scheme	8-20
8-5B	Logic for Firing the Protective Gap Across the Series Capacitor Bank and Its Metal Oxide Protection	8-20
8-6	Deenergization of an Uncompensated 500-kV Line.	8-26
8-7a	RinginG On Transposed Line - Phase A Sending End Voltage. . .	8-26
8-7b	RinginG On an Untransposed Line - Phase A and C Sending End Voltages.	8-27
8-8	Circuit Used for Ring Down Cases.	8-28
8-9	Sending End and Receiving End Voltages for a Transformer- Terminated Transposed Line.	8-35

FIGURES (Cont'd)

<u>Figure</u>		<u>Page</u>
8-10	Schematic of System Used for the Case of Deenergization of a Transformer-Terminated Line	8-36
8-11	Schematic of System Used for Deenergizing a 230-kV Transformer-Terminated Line	8-36
8-12	Receiving End Voltage When Deenergizing the 100-Mile 230-kV Line.	8-37
8-13	Effects of Preinsertion Resistor Size On Maximum Switching Overvoltage	8-43
8-14	Circuit Used in the Approximate Approach for Calculating Energizing and Reclosing SOV's.	8-44
8-15	Equivalent Circuit for Energizing the Line of Figure 8-14 With No Trapped Charge, As Seen From the Sending End.	8-45
8-16	Energizing a Line With No Trapped Charge. Circuit Breaker Closing at Maximum Line-to-Ground Voltage	8-45
8-17	Reclosing the Breakers Into Trapped Charge. The reclosing time delay is not shown	8-36
8-18	Equivalent Circuit for Calculating the Resulting Overvoltage When Reclosing Into 1 Per-Unit Trapped Charge, as Seen from the Sending End	8-47
8-19	Equivalent Circuit for the Making of the Auxiliary Contacts, as Seen From the Sending End.	8-48
8-20	Equivalent Circuit for the Making of the Main Contacts, as Seen From the Sending End	8-48
8-21	Insertion (Solid) and Shorting (Dashed) Transients When Reclosing Into a Line With Trapped Charge Using Preinsertion Resistors	8-49
8-22	System Used for High-Speed Reclosing Into Trapped Charge.	8-52
8-23	System Used for Single-Pole Reclosing Cases	8-57
8-24a	Receiving End Phase A Voltage for Single-Pole Switching Case.	8-58
8-24b	Receiving End Phase B Voltage for Single-Pole Switching Case.	8-58
8-24c	Sending End Phase C Voltage for Single-Pole Switching Case.	8-59
8-25	Simplified Equivalent Circuits for Calculating the Overvoltages Due to Load Rejection.	8-66
8-26	Circuit used for Load Rejection Case.	8-68
8-27	TACS Logic for Overspeeding Generator Due to Load Rejection	8-68
8-28	Frequency of Overspeeding Generator Due to Load Rejection	8-69
8-29a	Overspeeding Generator Terminal Voltage to Ground	8-70
8-29b	Overspeeding Generator Terminal Voltage - Plotted Only to 40 Milliseconds to Show Details of the Waveform	8-71
8-30	Receiving End Terminal Voltage After Load Rejection	8-72

FIGURES (Cont'd)

<u>Figure</u>		<u>Page</u>
8-31	One-Line Diagram of the System Used to Size Shunt Reactors On the Basis of 60-Hz Voltage Rise (Ferranti Effect).	8-77
8-32	Method to Size Shunt Reactors for Line Compensation Levels On a 500-kV Line	8-77
8-33	60 Hz Rise in Receiving-End Voltage For An Unloaded 500-kV Line for Various Shunt Reactor Sizes and Different Line Lengths	8-78
8-34	Typical Voltage Profile On An Uncompensated Line With No Surge Arresters	8-83
8-35	Distribution of SOV's Versus Tower Strength for One Tower and for n Towers.	8-85
8-36	Brown's Assumption.	8-85
8-37	Constants for Use in Brown's Method	8-86
8-38	50% Flashover Voltage, V_{50} , in Per-Unit of the Insulation Length As a Function of ESDD ⁽³⁾	8-99
8-39	Withstand Voltage for Different Insulators Under Different Contamination Conditions ⁽³⁾	8-100
8-40	Outline of Shapes of Tested Insulators in Table 8-37.	8-103
8-41	Lightning Outage Rates for Single-Circuit Horizontal Lines Versus Tower Footing Impedance ⁽²⁾	8-107
8-42	Lightning Outage Rates for Double-Circuit Vertical Lines Versus Tower Footing Impedance ⁽²⁾	8-107
8-43	Estimates of Line Insulation Requirements ⁽⁴⁾	8-111
8-44	Integrating the NESC Requirements Into Figure 8-43.	8-112

TABLES

<u>Table</u>		<u>Page</u>
1-1	Frequency Ranges for EMTP Simulations.	1-7
2-1	Summary of Models for Transmission Lines	2-10
2-2	Cross Reference Between Models Used and File Names	2-16
2-3	Setup for a Uniformly Distributed Transposed Constant-Parameter Line to be Used in Example 1.	2-50
2-4	Setup for a Uniformly Distributed Nontransposed Constant-Parameter Line to be Used in Example 1.	2-51
2-5	Meyer-Dommel Setup for a Frequency-Dependent Line Model to be Used in Example 1.	2-52
2-6	Marti Setup for a Frequency-Dependent Nontransposed Line Model to be Used in Example 1.	2-53
2-7	Results of Example 1	2-17
2-8	Results of Example 2	2-26
2-9	Transient Run for Example 1 With a Uniformly Distributed Transposed Constant-Parameter Line Model	2-54
2-10	Transient Run for Example 1 with a Uniformly Distributed Nontransposed Constant-Parameter Line Model (Lee's Model).	2-56
2-11	Transient Run for Example 1 Using Meyer-Dommel Frequency- Dependent Line Model	2-58
2-12	Transient Run for Example 1 Using Marti Frequency- Dependent Transposed Line Model.	2-61
2-13	Transient Run for Example 1 Using Marti Frequency- Dependent Nontransposed Line Model	2-64
2-14	Transient Run for Example 2 Using Marti's Frequency- Dependent Nontransposed Line Model	2-67
3-1	Sample Transformer Test Data	3-12
3-2	EMTP Saturable Transformer Branch Input.	3-13
3-3	XFORMER Input.	3-14
3-4	XFORMER Output	3-14
3-5	TRELEG Input	3-15
3-6	TRELEG Output.	3-16
3-7	BCTTRAN Input	3-17
3-8	BCTTRAN Output.	3-18
3-9	Convert Input and Output	3-22

TABLES (Cont'd)

<u>Table</u>		<u>Page</u>
3-10	HYSDAT Input and Output.	3-23
3-11	EMTP Input for Single-Line-to-Ground Faults.	3-26
3-12	Single-Line-to-Ground Fault Case Results Peak Transient Magnitudes.	3-27
3-13	Transformer Capacitance Branch Input.	3-35
3-14	Surge Transfer Case Results	3-36
3-15	Transformer Model Characteristics	3-39
4-1	Input Data for a Time-Controlled Switch	4-1
4-2	Input Data for Flashover Switch	4-8
4-3	Input Data for Statistical Switching.	4-14
4-4	Circuit Breaker Characteristics	4-19
5-1	Input Data for Case SAMOD3, Lightning Test System With Gapless Metal Oxide Arrester.	5-12
5-2	Input Data for Case SAMOD8, Switching Surge Test System With Passive-Gap Silicon Carbide Arrester.	5-13
5-3	Input Data for Case SAMOD6, Switching Surge Test System With Shunt-Gap Metal Oxide Arrester.	5-14
5-4	Input Data for Case SAMOD7, Switching Surge Test System With Active-Gap Silicon Carbide Arrester	5-15
5-5	Lightning Impulse Test System Results	5-17
5-6	Switching Surge Test System Results	5-17
5-7	Switching Surge Results - Comparison of Metal Oxide to Silicon Carbide Arresters	5-17
5-8	Arrester Energy Dissipation Approximations.	5-28
5-9	Approximations to Lightning Impulse Discharge Voltage and Current	5-28
5-10	Surge Arrester Model Characteristics.	5-29
5-11	Sparkover Levels.	5-31
5-12	SiC Arrester Energy Discharge Capability [kJ/kV].	5-32
5-13	Metal Oxide Lightning Discharge Parameters.	5-33
5-14	Metal Oxide Arrester Switching Discharge Parameters Metal Oxide Arrester With Shunt Gap - 45/90 Impulse Test.	5-34
5-15	Metal Oxide Arrester Energy Discharge Capability.	5-35
7-1	Lightning Stroke Parameters	7-12
7-2	Typical Phase Angles of Sequence Impedances	7-12
7-3	Important Generator Characteristics	7-14
7-4	Generator Terminal Capacitance to Ground.	7-15
7-5	Typical Generator Impedances.	7-16
7-6	Machine Parameter Conversion Results	7-21

TABLES (Cont'd)

<u>Table</u>		<u>Page</u>
7-7	Derived Model Time Constants	7-21
8-1	Common Origins of SOV's	8-3
8-2	Some Causes of Temporary Overvoltages	8-4
8-3	Typical Magnitudes of Overvoltages.	8-5
8-4	Data for Switched Transmission Lines.	8-6
8-5	Data for Transmission Lines Not to Be Switched.	8-8
8-6	Equivalent Sources.	8-8
8-7	Surge Arresters	8-8
8-8	Transformers.	8-9
8-9	Circuit Breakers.	8-9
8-10	Series and Shunt Compensation	8-10
8-11	Effect of Different Parameters On the Results of Switching Surge Studies	8-14
8-12	Required Outputs for Conducting a Switching Surge Study	8-18
8-13	Tacs Input Data for Calculating Energy.	8-20
8-14	Input for the Deenergization of a Transposed Line	8-29
8-15	Input for the Deenergization of an Untransposed Line.	8-31
8-16	Input for the Deenergization of a Transformer-Terminated Line	8-38
8-17	Input Data Deenergizing the 230-kV Transformer-Terminated Line.	8-40
8-18	Estimated Minimum Deionization or Dead Time (in Cycles of 60 Hz) Required for Automatic Three-Pole Reclosing.	8-51
8-19	Variation of Maximum Receiving End Voltage With Different Preinsertion Resistor Values.	8-52
8-20	Input Data for Reclosing With a 300-Ohm Preinsertion Resistor	8-53
8-21	Input Data for Single-Pole Switching Case	8-60
8-22	Input Data for Single-Pole Switching Probability Runs	8-62
8-23	Input for the Load Rejection Case	8-73
8-24	Charging Characteristics for Different Line Lengths (for a 500-kV Line).	8-80
8-25	Comparison Between EMTP Results and Those Obtained Using Equation 8-15	8-80
8-26	Typical Distributions of Switching Overvoltages	8-81
8-27	Statistical Overvoltages for Distributions of Table 8-26.	8-82
8-28	The Constant K_G As a Function of the SSFOR.	8-87
8-29	The Constant K_E As a Function of the SSFOR.	8-88
8-30	Reference Heights	8-91
8-31	Span Lengths.	8-91

TABLES (Cont'd)

<u>Table</u>		<u>Page</u>
8-32	Clearances.	8-94
8-33	Minimum Tower Strike Distances As Calculated By Equation (8-47).	8-96
8-34	Ranges of the Equivalent Salt Deposit Density, ESDD	8-98
8-35	Required Specific Creep - Inches/kV _{LG} (cm/kV _{LG})	8-101
8-36	Recommended Number of Standard Insulators for 230-kV and 500-kV Lines Based On Power Frequency Contamination Considerations.	8-102
8-37	Leakage Distances for Different Insulators ^(B) Tested Insulators.	8-104
8-38	Suggested Distributions of Lightning Flashes for Engineering Use	8-105
8-39	Calculated Vs. Actual Lightning Tripout Rates Per 100 km Per Year.	8-106
8-40	Assumed E ₂ for the Different Voltage Levels	8-111

Part 1

INTRODUCTORY MATERIAL

SUMMARY

The Electromagnetic Transients Program (EMTP) is a computer program used to simulate electromagnetic, electromechanical, and control system transients on multiphase electric power systems. It was first developed, among many other programs, as a digital computer counterpart to the analog Transient Network Analyzer (TNA). Many other capabilities have been added to the EMTP over a 15-year period, and the program has become widely used in the utility industry.

This document is an outgrowth of a survey and analysis of EMTP user needs, in which improved user's documentation was determined to be the single most important enhancement to the EMTP. The Application Guide covers EMTP models and studies. The Application Guide is part of a series of new EMTP user manuals which covers program operation, theory, and application guide lines.

The Introduction in Section 1 contains general information on time step selection, how much of the power system to model, and other questions which pertain to all EMTP studies. The main body of the Application Guide is divided into two portions, covering EMTP models and EMTP studies. These sections assume some familiarity with the EMTP. Novice users should consider working through the EMTP Primer, which is a training manual, before using the Application Guide, which is intended to be a reference document.

The sections on models include a brief background discussion, examples of data preparation, comparisons between the results of different models, typical data, and suggestions on which models to use in various circumstances. There are, at present, six sections on EMTP models in the Application Guide. These include:

- Section 2: Overhead Lines
- Section 3: Transformers
- Section 4: Circuit Breakers
- Section 5: Surge Arresters
- Section 6: Initial Conditions
- Section 7: Sources

The sections on studies include discussions of objectives, developing system models, selecting and interpreting EMTP output, and using the EMTP study results. Typical study results are also provided to serve as benchmarks. There is, at present, one section on EMTP studies in the Application Guide.

Section 8: Line Switching

Once the new user has completed EMTP training using the EMTP Primer, the Application Guide and Operation Manual are intended to be reference documents for actual engineering studies. It is anticipated that more sections will be added to this Application Guide as EMTP development progresses.

Section 1 INTRODUCTION

This Application Guide is intended to help EMTP users develop appropriate models for power system studies. It contains information on the features of various models, how to use commonly available data to develop the proper input data for the EMTP models, typical data for various components, and examples of the various models. There are also sample studies which are intended to help the user define what input data is required for a study, what cases should be considered and how to use the EMTP's results.

This introductory section contains general information which is applicable to all or most EMTP studies. After reading it, the user can proceed to specific model sections of immediate interest.

1-1. SETTING UP A SYSTEM MODEL

One of the initial questions in conducting an EMTP study concerns how much of the power system to model. A good starting rule of thumb for switching studies is to model the system in detail one or two buses away from each switched bus, depending on the electrical line lengths. This can also be applied to other types of studies. Transformations to different voltage levels can be modeled with the transformer and a source impedance, particularly for transformations to lower voltage levels. Once a basic system model has been developed and tested, the user can add more of the system details to observe their effect on the results. The importance of starting out with a simple model is strongly emphasized. When equivalencing the outlying power system, the traditional short circuit impedances may not be accurate. The Source modeling section contains more details.

1-2. UNITS OF THE PARAMETERS

It is important to use a consistent set of engineering units for the EMTP input data. Many times, the calculated or nameplate data for lines, cables, transformers, machines, etc., is given in per-unit or percent. Per-unit impedances

can be used in the EMTP if care is taken that all values are on the same MVA base and that transformer turns ratios are properly represented. If per-unit impedances are used, all transformer line-to-line voltage transformation ratios will normally be 1:1. When using the TRANSFORMER branch type, wye-wye and delta-delta transformers can have winding turns ratios of 1:1. Wye-delta transformers should have winding turns ratios of 1:1.73. Off-nominal taps would require adjustments to these ratios.

Type 59 machine data presents another problem when the EMTP input data is specified in per-unit. The user normally inputs the per-unit machine reactances on the machine's own MVA base, and the EMTP uses the machine MVA and kV ratings to convert these to physical inductances and resistances. To use per-unit impedances in the rest of the system, the user must perform a change of base on his machine data. For example, assume the per-unit machine data is on a 600-MVA, 22-kV base, and the rest of the input data is on a 100-MVA base. The Type 59 machine MVA rating should be input as 6.0 and the kV rating should be input as 1.0.

It is usually desired to have the transient overvoltage results in per-unit. To do this with per-unit impedances, the user should set the per-unit line-to-ground source voltages equal to 1.0 or some other preswitching voltage. The current base is equal to $100 \text{ MVA} / (\sqrt{3} * \text{kV base})$, in Amperes crest.

A second means of entering the input data in consistent units is often used on Transient Network Analyzers. The user converts the data to physical impedances on a common voltage base, and all transformer line-to-line voltage ratios are 1:1 as described above. If source voltages are specified as 1.0 per-unit line-to-ground, then the transient overvoltage results will be in per-unit. The current base is $1/(\text{system voltage level})$, which will be different in various parts of the system. This system of units offers no advantage over per-unit impedances for EMTP studies because the same amount of data conversion is required.

A third means of entering the input data is to use physical units. This causes the least confusion of any system, and avoids conversion of machine data. The transformer turns ratios correspond to the physical voltage transformation ratios. The disadvantage of this system is that the output voltages and currents are in physical values rather than the more convenient per-unit values.

If an output postprocessing program is available, it is relatively easy to rescale the output to obtain per-unit peak values and plot scales. In that case, the use of physical units for the input data is strongly recommended.

1-3. NETWORK TOPOLOGY REQUIREMENTS

The network must be configured so that switching operations will not create a condition where current in an inductance is left with no path to ground. Switches in the EMTP usually interrupt current at the first time step after a current zero crossing after the specified contact parting time. Alternatively, the current can be interrupted at the first time step after its magnitude drops below a specified threshold. In either case, the switch will effectively chop a small amount of current. In Figure 1-1, the interrupted inductive current has no path to ground. The behavior of the EMTP's trapezoidal rule as a differentiator will then lead to numerical oscillations, with the voltage across the inductance reaching alternate extremes each time step.

Network configurations which avoid this problem are shown in Figure 1-2. The added capacitance in Figure 1-2a might represent a circuit breaker's terminal capacitance. The parallel resistance in Figure 1-2b might represent part of the inductor's losses. It will provide a path for dissipating the current chopped by switch opening.

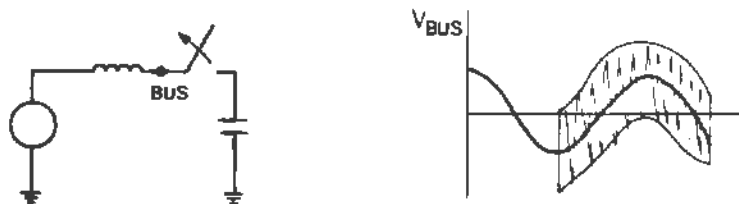


Figure 1-1. Numerical Oscillations Caused by Inductance Switching

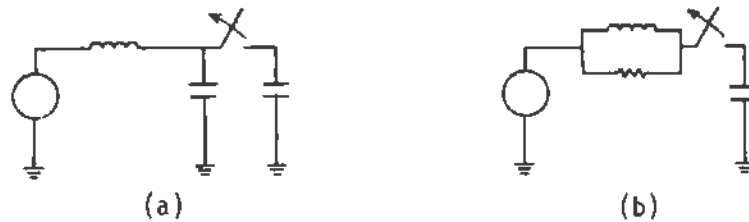


Figure 1-2. Network Connections to Avoid Numerical Oscillations

Similarly, an attempt to instantaneously change the voltage across a capacitance will lead to numerical oscillations. Two rules apply:

1. Do not connect switches in series with an inductance unless current can flow through the inductance for any possible status of the switches in the EMTP model.
2. Do not place voltage sources across a capacitance.

When modeling losses in an inductance, it is wise to put at least part of the losses in a series resistance. This will insure that any dc currents trapped in the inductance by switching operations will eventually decay. Similarly, resistors should be connected in parallel with capacitors if it is desired that dc voltages trapped on the capacitor by switching operations eventually decay.

When modeling thyristor or diode switches it is usually wise to represent current limiting reactors and RC snubber circuits as shown in Figure 1.3 of the Primer, reproduced as Figure 1-3 below. These components limit excessive di/dt and dv/dt on the thyristor both in the real world and in the EMTP, thereby enhancing numerical stability of the simulation. Component sizes can be the actual physical values if available, or can be selected to conform with the time step requirements as discussed below.

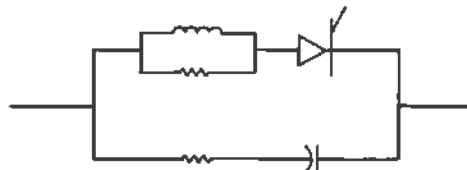


Figure 1-3. Thyristor with Current-Limiting Reactor and Snubber

Floating subnetworks in the EMTP occur when switches open and disconnect part of the system model from any path to ground. Common examples are unloaded delta tertiary windings, which are always floating, and Static VAR or HVDC systems which do not have the additional elements shown in Figure 1-3. The voltages of these networks are mathematically undefined, and the EMTP sets the voltage at one node in the floating subnetwork equal to zero. This may be acceptable for delta tertiary windings, but in general, it is best to include stray capacitances to ground at each terminal of an unloaded delta winding, or at one node in each subnetwork which could become floating. The parallel elements in Figure 1-3 will usually ensure a path to ground for thyristor-switched systems. Very small capacitances can be used so long as they conform to the time step requirements discussed below.

Similarly, stray capacitances are often needed at the terminals of Type 59 machines to enhance stability of the simulation. Usually, values in the range of .001 to .1 microfarads yield good results.

1-4. TIME STEP AND TMAX SELECTION

Selection of the simulation time step is one of the most important decisions an EMTP user must make. There is a balance between computational effort and accuracy which must be achieved. As rules of thumb, the following procedures for determining the maximum acceptable time step are presented.

1. Determine the shortest travel time among the lines and cables which are modeled. This can be calculated as (line length)/(fastest wave velocity). To obtain the maximum time step, this travel time should be divided by 10 for lines which are important to the study, or by 4 for lines which form part of the outlying system.
2. Calculate the period of oscillation for each LC loop according to $T = 1/f = 2\pi\sqrt{LC}$. For loops which will play an important part in the transients of interest, the time step should be no more than 1/20th of the oscillation period. For loops and frequencies of lesser interest, the time step could be as high as 1/4th of the oscillation period.
3. Calculate the RC and L/R time constants for the lumped elements. The time step should not exceed the shortest of these time constants.
4. When simulating thyristor switch control systems with TACS, the time step should not exceed 50 microseconds for a 60-Hertz power system.

5. When simulating Type 59 synchronous machines, the time step should not exceed 100 microseconds. If computation time becomes a problem when simulating long-term machine dynamics with the EMTP, it may be possible to increase the time step provided that some comparisons are made with cases using the 100-microsecond time step.
6. When simulating harmonics or other steady-state or quasi steady-state phenomena, the time step should be approximately equal to one degree of a power frequency cycle, or 50 microseconds for 60-Hertz systems.

These guidelines are intended to provide the maximum time steps usable for acceptable accuracy in the EMTP results. Smaller time steps than the ones suggested above are often preferable. In each study, the user should compare cases with different time steps to ensure that using a smaller time step has no significant effect on the results of interest.

It is generally preferable to choose the time step so that each transmission line's travel time consists of an integer number of time steps. This will limit interpolation errors during the simulation. This requirement is more important for positive sequence travel times, but it is also desirable for the zero sequence travel times. The user could select a time step which is not a "round" number in order to satisfy this condition. It may also be useful to modify transmission line lengths to better match the time step.

The length of time to be simulated, T_{max} , also affects the computational effort. T_{max} should be selected to provide for the following:

1. At least one cycle of pretransient power frequency voltage should be simulated for low to medium frequency switching transients. For high frequency transients this does not apply because various "tricks" are often used to set up the proper initial conditions to simulate the transient immediately, thereby saving computational effort.
2. At least 10 to 20 cycles (at the transient frequency, not 60 Hertz) of the dominant switching transient should be simulated to observe damping rates and ensure that resonances do not occur.
3. Machine dynamics will typically require 1 to 5 seconds of simulation time.
4. When the steady-state condition contains harmonics, especially due to nonlinear elements or thyristor switching, several cycles of pretransient conditions must be simulated to ensure that the correct initial conditions are reached. Five power frequency

cycles are suggested as a starting point, subject to later adjustment by the user.

5. When multiple switching operations, such as reclosing or sequential switching, are simulated, sufficient time between switching operations must be allowed for the transients to decay. It is not necessary to duplicate the physical time delays, which may be several seconds or minutes in real time. Experimentation by the user will be necessary, but the initial cases could begin with three power frequency cycles between switching operations. Alternatively, the user could simulate one switching event, then repeat the case with a second switching event added at a later time, etc.

Proper values of T_{max} for control system simulations can often be determined from knowledge of the control system's natural frequencies and time constants. Field test results and experimentation with the EMTP are also valuable means for determining both T_{max} and the time step.

As further guidance in selecting the time step, T_{max} and the valid frequency range for the models, several frequency bands are defined in Table 1-1 [1].

Table 1-1
FREQUENCY RANGES FOR EMTP SIMULATIONS

<u>Frequency Class</u>	<u>Example Applications</u>	<u>Frequency Range</u>
Dynamic Overvoltages	Control System Dynamics	.01 Hz- 5 kHz
	Transformer Energization	.1 Hz - 3 kHz
	Load Rejection	.1 Hz - 3 kHz
Switching Transients	Line Energization	3 Hz - 15 kHz
	Line Reclosing	d.c. - 15 kHz
	Fault Initiation	10 Hz - 30 kHz
	Fault Clearing	10 Hz - 3 kHz
	Breaker Restrike	10 Hz - 30 kHz
Steep-Fronted Surges	Transient Recovery Voltage	10 Hz - 30 kHz
	Lightning	5 kHz - 3 MHz
GIS Transients	Multiple Restrikes/Voltage Escalation	10 Hz - 3 MHz
	Restrikes	50 kHz- 30 MHz

1. Ardito and Santagostino, "A Review of Digital and Analog Methods of Calculation of Overvoltages in Electric Systems," Cigre Study Committee 33 Overvoltages and Insulation Coordination Colloquium in Budapest, 23-25 September 1985.

1-5. OUTPUT SELECTION

The phasor steady-state solution and the network connectivity table should always be selected as outputs for each case, as potential debugging aids if nothing else.

Time step variable printouts are of limited use in debugging an EMTP case or in evaluating the case results. Plotted variables are much more convenient. However, the variable minima and maxima and the times of switch operation are useful printed outputs. Even though only a few variables may be of significance in applying the study results, the user should plot a large number of voltages and other parameters to assist in verifying the system model for each case. If batch mode plotting is employed, the incentive for plotting many variables is even greater. It is recommended that plot data files be saved a short while so that expanded time scale plots can be made as needed.

When plotting node voltages, all three phases at each bus should be plotted on separate graphs. The same holds true in general for branch currents and voltages. It is sometimes convenient to plot the voltages on each side of a switch or the currents through parallel components on the same graph.

Due to plot data array restrictions in the inhouse plotting program, it may not be possible to plot every point for each variable. The plotting increment should always be an odd number. The user should also consider the effective time step for plotting, bearing in mind that peak magnitudes which occur on the skipped data points will not appear in the plot.

It is usually wise to plot all switch currents and switch differential voltages. For rotating machines, only the terminal voltages and currents and the air gap torque are necessary to plot. Sometimes the rotor speed deviation, field current or the shaft torques will be required. For TACS systems, only the variables which interface as inputs or outputs with the EMTP must be plotted. Sometimes TACS can be used to calculate derived output quantities to simplify evaluation of the study results. However, internal TACS variables might be plotted for debugging purposes as a new model is developed. For thyristor firing control systems, the firing pulses and controlling variables should be plotted on the same graph for several thyristors until the user gains confidence in the model.

When grouping node voltages for statistical output, the three phases at each bus should be grouped on one separate output request card which has a slightly different voltage base from the other buses. This will permit the evaluation of both phase peaks and case peaks. Case peaks are normally used in TNA studies. Case 7 of the Primer illustrates this technique.

1-6. DEBUGGING SUGGESTIONS

The Operation Manual contains brief descriptions of all error messages. If the cause of the error is not obvious, or if the case runs but appears to yield erroneous results, the following steps can be taken:

1. Check each entry of the network connectivity table printout against each element in the user's diagram of the system model, and then check each element of the diagram against the network connectivity table.
2. Check the EMTP input echo and the parameter interpretations on the left-hand side of the printout.
3. Repeat the case after removing rotating machines, frequency-dependent line models, surge arresters, nonlinear inductances and TACS systems.
4. Remove any negative inductances from TRANSFORMER branch types.
5. Check the steady-state solution for consistency as described below under verification of results.
6. If any subnetwork is floating, or is weakly tied to ground, strengthen its path to ground.
7. Repeat the case with a smaller time step.

1-7. VERIFYING THE RESULTS

The single most important tool the user has for verifying the EMTP case results is a basic knowledge of the phenomena to be simulated. Field test results, technical papers, basic textbooks and more experienced engineers can all help. The textbook by Allan Greenwood, *Electrical Transients in Power Systems*, is a useful basic reference. It is preferable that the user review the basics of the phenomena before attempting to simulate it with the EMTP. Learning-by-doing can be very frustrating and very risky when attempting to apply the study results.

When verifying the case results of a new EMT model, the user should always check the input parameter interpretation and the network connectivity table. The steady-state phasor solution should be checked for bus voltage magnitudes at locations where load flow or hand calculation results are available, injected source currents and power, and the MW/MVAR loads of three-phase shunt elements. Line and switch currents should be nearly balanced as well. If there is a message warning about a nonlinear inductance operating outside the linear flux region, make adjustments as described in the Initial Conditions section. Machine model steady-state printouts should be checked for speed, terminal power, field current and air gap torque levels in the steady state.

Preswitching steady-state waveforms should be examined for characteristic harmonic content, which should reach a stable condition before transients are initiated.

Transient frequencies can be verified according to $f = 1/(2\pi\sqrt{LC})$ for lumped circuits, $f = 1/4\tau$ for open-circuited lines and cables, and $f = 1/2\tau$ for short-circuited lines and cables. The lumped circuit surge impedance, $Z = \sqrt{L/C}$, is useful for relating transient voltage and current peak magnitudes in lumped circuits. The traveling wave reflection and transmission coefficients;

$$E_r = (Z_b - Z_a) / (Z_b + Z_a)$$

$$E_t = 2Z_b / (Z_b + Z_a)$$

can be used to check the behavior of traveling waves as they enter stations. Note that inductive terminations will initially appear as open circuits, but then become short circuits in a dc steady state or reactive impedances in an ac steady state. Capacitive terminations will initially appear as short circuits, but then become open circuits in a dc steady state or capacitive impedances in an ac steady state. Shunt capacitors generally increase transient overvoltage magnitudes.

Damping rates of lines and cables, transformers, and series RL loads are generally low, especially at high frequencies. The exceptions would be frequency-dependent overhead lines and resistive shunts to ground.

1-8. IEEE REFERENCES

A bibliography of IEEE papers related to the EMTP follows. Some of the papers focus on the physical characteristics of power system components which bear on EMTP modeling of the device. The papers are grouped in the following categories:

1. General Interest
2. Surge Arresters
3. Circuit Breakers
4. Cables
5. Initial Conditions
6. Overhead Transmission Lines
7. Rotating Machines
8. Sources and Source Equivalents
9. Studies
10. TACS, HVDC and Static VAR Compensators
11. Transformers

There are many additional papers which describe studies which have been performed using the EMTP, and some of them have field or laboratory test results as well. The user should examine the Transactions subject index for the topics of interest. There are also many papers and books on general transient phenomena and power system components which are readily available. Other methods of digitally simulating electromagnetic transients are in use, and references may be found in the IEEE Transactions on Power Apparatus & Systems. The bibliography of the Tutorial Course Text for Digital Simulation of Electrical Transient Phenomena serves as a good starting point for locating this material.

IEEE Papers Index - General Interest Category

IEEE PSE & Education Committee, "Digital Simulation of Electrical Transient Phenomena," (Tutorial Course Text 81 EH0173-5-PWR), Pages 1-59.

Dommel and Meyer, "Computation of Electromagnetic Transients," IEEE Proceedings, Vol. 62, Number 7, July, 1974, Pages 983-993.

Dommel, "Digital Computer Solution of Electromagnetic Transients in Single and Multiphase Networks," PAS 88, Number 4, April, 1969, Pages 388-399.

Dommel, "Nonlinear and Time-Varying Elements in Digital Simulation of Electromagnetic Transients," PAS 90, Number 6, Nov/Dec, 1971, Pages 2561-2567.

Talukdar, "METAP - A Modular and Expandable Program for Simulating Power System Transients," PAS 96, Number 6, Nov/Dec. 1976, Pages 1882-1891.

Meyer, "Machine Translation of an Electromagnetic Transients Program (EMTP) Among Different Computer Systems," PICA Conference Record, Volume 10, 1977, Pages 272-277; PAS 97, Number 2, Mar/Apr, 1978, Page 319 (abstract).

Alvarado, "Parallel Solution of Transient Problems by Trapezoidal Integration," PAS 98, Number 3, May/June, 1979, Pages 1080-1090.

Alvarado, Lasseter, and Sanchez, "Testing of Trapezoidal Integration with Damping for the Solution of Power Transient Problems," PAS 102, Number 12, December, 1983, Pages 3783-3790.

Semlyen and Abdel-Rahman, "A Closed Form Approach for the Calculation of Switching Transients in Power System Networks Using the Compensation Theorem," PAS 102, Number 7, July, 1983, Pages 2021-2028.

Viegas de Vasconcelos, Hoseman, "Transient Studies on a Multiprocessor," PAS 103, Number 11, November, 1984, Pages 3260-3266

Alvarado, Lasseter, Kwon, Mong, "A Module Oriented EMTP Interface," PAS 103, Number 12, December, 1984, Pages 3488-3495.

IEEE Papers Index - Arresters Category

Clayton, Grant, Hedman, Wilson, "Surge Arrester Protection and Very Fast Surges," PAS 102, Number 8, August, 1983, Pages 2400-2412; PAS 102, Number 10, October, 1983, Page 3488 (correction).

Lat, "Analytical Method for the Performance Prediction of Metal Oxide Surge Arresters," PAS 104, Number 10, October, 1985, Pages 2665-2674.

IEEE Papers Index - Breakers Category

Prasad and Herling, "Three Phase Dynamic Simulation of Air Blast Generator Circuit Breakers - Theory and Modeling," PAS 101, Number 6, June, 1982, Pages 1561-1569.

Shindo and Suzuki, "A New Calculation Method of Breakdown Voltage-Time Characteristics of Long Air Gaps," PAS 104, Number 6, June, 1985, Pages 1556-1563.

Tanabe, Ibuki, Sakuma and Yonezawa, "Simulation of the SF6 Arc Behavior by a Cylindrical Arc Model," PAS 104, Number 7, July, 1985, Pages 1903-1909.

IEEE Papers Index - Cables Category

Nagaoka and Ametani, "Transient Calculations on Crossbonded Cables," PAS 102, Number 4, April, 1983, Pages 779-787.

Greenfield, "Transient Behavior of Short and Long Cables," PAS 103, Number 11, November, 1984, Pages 3193-3203.

IEEE Papers Index - Initial Conditions Category

Brandwajn, Meyer and Dommel, "Synchronous Machine Initialization for Unbalanced Network Conditions within an Electromagnetic Transients Program," PICA Conference Record, Volume 11, 1979, Pages 38-41.

Van Dommelen, "Optimization of Initial Values of Mechanical Variables of Turbine-Generator Units in an Electromagnetic Transients Program," PAS 100, Number 12, December, 1981, Pages 4990-4994 .

Makram, Koerber and Kruempel, "An Accurate Computer Method for Obtaining Boundary Conditions in Faulted Power Systems," PAS 101, Number 9, September, 1982, Pages 3252-3260.

IEEE Papers Index - Lines Category

Meyer and Dommel, "Numerical Modelling of Frequency-Dependent Transmission Line Parameters in an Electromagnetic Transients Program," PAS 93, Number 5, Sept/Oct, 1974, Pages 1401-1409.

Semlyen and Dabuleanu, "Fast and Accurate Switching Transient Calculations on Transmission Lines with Ground Return Using Recursive Convolutions," PAS 94, Number 2, Mar/Apr, 1975, Pages 561-571.

Ametani, "A Highly Efficient Method for Calculating Transmission Line Transients," PAS 95, Number 4, Sept/Oct, 1976, Pages 1545-1551.

Semlyen and Roth, "Calculation of Exponential Step Responses Accurately for Three Base Frequencies," PAS 96, Number 2, Mar/Apr, 1977, Pages 667-672.

Semlyen, "Ground Return Parameters of Transmission Lines - An Asymptotic Analysis for Very High Frequencies," PAS 100, Number 3, March, 1981, Pages 1031-1038.

Hauer, "State-Space Modeling of Transmission Line Dynamics Via Nonlinear Optimization," PAS 100, Number 12, December, 1981, Pages 4918-4925.

Semlyen, "Contributions to the Theory of Calculation of Electromagnetic Transients on Transmission Lines with Frequency Dependent Parameters," PAS 100, Number 2, February, 1981, Pages 848-856.

Deri, Tevan, Semlyen and Castanhe, "The Complex Ground Return Plane - A Simplified Model for Homogenous and Multilayer Earth Return," PAS 100, Number 8, August, 1981, Pages 3686-3693.

Marti, J. R., "Accurate Modelling of Frequency-Dependent Transmission Lines in Electromagnetic Transient Simulations," PAS 101, Number 1, January, 1982, Pages 147-157.

Menemenlis and Zhu Tong Chun, "Wave Propagation on Nonuniform Lines," PAS 101, Number 4, April, 1982, Pages 833-839.

Makram, Koerber and Kruempel, "An Accurate Computer Method for Obtaining Boundary Conditions in Faulted Power Systems," PAS 101, Number 9, September, 1982, Pages 3252-3260.

L. Marti, "Low-Order Approximation of Transmission Line Parameters for Frequency-Dependent Models," PAS 102, Number 11, November, 1983, Pages 3582-3589.

Harrington and Afghahi, "Implementation of a Computer Model to Include the Effects of Corona in Transient Overvoltage Calculations," PAS 102, Number 4, April, 1983, Pages 902-910.

Harrington and Afghahi, "Effect of Corona on Surges on Polyphase Transmission Lines," PAS 102, Number 7, July, 1983, Pages 2294-2299.

Lee, "Nonlinear Corona Models in an Electromagnetic Transients Program (EMTP)," PAS 102, Number 9, September, 1983, Pages 2936-2942.

Chisholm, Chow and Srivastava, "Lightning Surge Response of Transmission Towers," PAS 102, Number 9, September, 1983, Pages 3232-3242.

Semlyen and Abdel-Rahman, "State Equation Modelling of Untransposed Three-Phase Lines," PAS 103, Number 11, November, 1984, Pages 3402-3408.

Semlyen and Brierly, "Stability Analysis and Stabilizing Procedure for a Frequency Dependent Transmission Line Model," PAS 103, Number 12, December, 1984, Pages 3579-3586.

Dommel, "Overhead Line Parameters from Handbook Formulas and Computer Programs," PAS 104, Number 2, February, 1985, Pages 366-372.

Inoue, "Propagation Analysis of Overvoltage Surges with Corona Based Upon Charge Versus Voltage Curve," PAS 104, Number 3, March, 1985, Pages 655-662.

Semlyen and Deri, "Time Domain Modelling of Frequency Dependent Three-Phase Transmission Line Impedances," PAS 104, Number 6, June, 1985, Pages 1549-1555; PAS 104, Number 9, September, 1985, Page 2577 (correction).

Saied and Al-Fuhaid, "Electromagnetic Transients in a Line-Transformer Cascade by a Numerical Laplace Transform Technique," PAS 104, Number 10, October, 1985, Pages 2901-2909.

Chisholm, Chow and Srivastava, "Travel Time of Transmission Towers," PAS 104, Number 10, October, 1985, Pages 2922-2928.

Faria and Silva, "Wave Propagation in Polyphase Transmission Lines - A General Solution to Include Cases Where Ordinary Modal Theory Fails," 85 SM 379-1, Presented at the 1985 Summer Power Meeting.

Semlyen and Wei-Gang, "Corona Modelling for the Calculation of Transients on Transmission Lines," 85 SM 380-1, Presented at the 1985 Summer Power Meeting.

IEEE Papers Index - Machines Category

Brandwajn, Meyer and Dommel, "Synchronous Machine Initialization for Unbalanced Network Conditions within an Electromagnetic Transients Program," PICA Conference Record, Volume 11, 1979, Pages 38-41.

Brandwajn and Dommel, "A New Method for Interfacing Generator Models with an Electromagnetic Transients Program," PICA Conference Record, Volume 10, 1977, Pages 260-265, PAS 97, Number 2, Mar/Apr, 1978, Page 319 (abstract).

Gross and Hall, "Synchronous Machine and Torsional Dynamics Simulation in the Computation of Electromagnetic Transients," PAS 97, Number 4, July/Aug, 1978, Pages 1074-1086.

Brandwajn, "Representation of Magnetic Saturation in the Synchronous Machine Model in an Electromagnetic Transients Program," PAS 99, Number 5, Sept/Oct, 1980, Pages 1996-2002.

Van Dommelen, "Optimization of Initial Values of Mechanical Variables of Turbine-Generator Units in an Electromagnetic Transients Program," PAS 100, Number 12, December, 1981, Pages 4990-4994.

Lauw and Meyer, "Universal Machine Modeling for the Representation of Rotating Electric Machinery in an Electromagnetic Transients Program," PAS 101, Number 6, June, 1982, Pages 1342-1351.

Woodford, Gole and Menzies, "Digital Simulation of dc Links and ac Machines," PAS 102, Number 6, June, 1983, Pages 1616-1623.

Gole, Menzies, Turanli, Woodford, "Improved Interfacing of Electrical Machine Models to Electromagnetic Transients Programs," PAS 103, Number 9, September, 1984, Pages 2446-2451.

Gole and Menzies, "Modelling of Capacitive Loads for the Study of Transients in Synchronous Machines," PAS 104, Number 8, August, 1985, Pages 2093-2098.

Lauw, "Interfacing for Universal Multimachine Modeling in an Electromagnetic Transients Program," PAS 104, Number 9, September, 1985, Pages 2367-2373.

IEEE Papers Index - Sources Category

Sabir and Lee, "Dynamic Load Models Derived from Data Acquired During System Transients," PAS 101, Number 9, September, 1982, Pages 3365-3372.

Morched and Brandwajn, "Transmission Network Equivalents for Electromagnetic Transients Studies," PAS 102, Number 9, September, 1983, Pages 2984-2994.

IEEE Papers Index - Studies Category

IEEE SPD & Education Committees, "Surge Protection in Power Systems," (Tutorial Course Text 79 EH0144-6-PWR), Pages 1-118.

IEEE T&D and Education Committees "Power System Harmonics," (Tutorial Course Text 84 EH0221-2-PWR), Pages 1-158.

IEEE Transformers & Education Committees, "Power Transformer Considerations of Current Interest to the Utility Engineer," (Tutorial Course Texts 84 EH0209-7-PWR, 76 CH1159-3-PWR), Pages 1-70,1-79.

IEEE Papers Index - TACS Category

Dube and Dommel, "Simulation of Control Systems in an Electromagnetic Transients Program with TACS," PICA Conference Record, Volume 10, 1977, Pages 266-271; PAS 97, Number 2, Mar/Apr, 1978, Page 319 (abstract).

Lasseter and Lee, "Digital Simulation of Static VAR System Transients," PAS 101, Number 10, October, 1982, Pages 4171-4177.

Woodford, Gole and Menzies, "Digital Simulation of dc Links and ac Machines," PAS 102, Number 6, June, 1983, Pages 1616-1623.

Reeve and Chen, "Versatile Interactive Digital Simulator Based on EMTP for ac/dc Power System Transient Studies," PAS 103, Number 12, December, 1984, Pages 3625-3633.

Woodford, "Validation of Digital Simulation of DC Links," PAS 104, Number 9, September, 1985, Pages 2588-2595.

Ino, Mathur, Iravani and Sasaki, "Validation of Digital Simulation of DC Links - Part II," PAS 104, Number 9, September, 1985, Pages 2596-2603.

IEEE Papers Index - Transformers Category

IEEE Transformers & Education Committees, "Power Transformer Considerations of Current Interest to the Utility Engineer," (Tutorial Course Texts 84 EHD209-7-PWR, 76 CH1159-3-PWR), Pages 1-70, 1-79.

Degeneff, "A Method for Constructing Terminal Models for Single-Phase n-Winding Transformers," PAS 98, Number 1, Jan/Feb, 1979, Page 6 (abstract).

Dick and Watson, "Transformer Models for Transient Studies Based on Field Measurements," PAS 100, Number 1, January, 1981, Pages 409-419.

Avila-Rosales and Alvarado, "Nonlinear Frequency Dependent Transformer Model for Electromagnetic Transient Studies in Power Systems," PAS 101, Number 11, November, 1982, Pages 4281-4288.

Brandwajn, Dommel and Dommel, "Matrix Representation of Three-Phase N-Winding Transformers for Steady-State and Transient Studies," PAS 101, Number 6, June, 1982, Pages 1369-1378.

Degeneff, McNutt, et. al., "Transformer Response to System Switching Voltages," PAS 101, Number 6, June, 1982, Pages 1457-1470.

Frame, Mohan and Liu, "Hysteresis Modeling in an Electromagnetic Transients Program," PAS 101, Number 9, September, 1982, Pages 3403-3412.

Avila-Rosales and Semlyen, "Iron Core Modeling for Electrical Transients," PAS 104, Number 11, November, 1985, Pages 3189-3194.

Ewart, "Digital Computer Simulation Model of a Steel-Core Transformer," 85 SM 377-3, presented at the 1985 Summer Power Meeting.

Dommel, Yan and Wei, "Harmonics from Transformer Saturation," 85 SM 381-9, presented at the 1985 Summer Power Meeting.

1-9. EMTP NEWSLETTER REFERENCES

The EMTP Newsletter and its back issues constitutes a valuable reference for all EMTP users. The articles describe both models and studies in a form specific to the EMTP, whereas the IEEE papers tend to be broader in scope, more theoretical and/or less specific in the details of developing EMTP input data. An index of past EMTP Newsletter articles follows, with groupings in the same eleven categories cited for IEEE papers, plus an additional category for field test comparisons. The EMTP Newsletter has been published at the University of British Columbia, but it will be published at the Catholic University of Leuven in Belgium beginning in 1986.

EMTP Newsletter Articles - General Category

Meyer, "Current Bonneville Power Administration EMTP Research and Development Contracts," Volume 1, Number 1, July, 1979, pages 1-4.

Lauw, "Design Recommendations for Numerical Stability of Power Electronic Converters," Volume 1, Number 4, November, 1980, pages 2-6.

Meyer, "Real-Time EMTP Plotting, and the Beginning of Interactive EMTP Execution," Volume 1, Number 5, February, 1981, pages 2-7.

Lauw, "Discussion of: Design Recommendations for Numerical Stability of Power Electronic Converters," Volume 1, Number 5, February, 1981, pages 25.

Meyer, "Interactive EMTP Execution, Observation and Control Via Shared COMMON," Volume 2, Number 2, September, 1981, pages 26-27.

Dommel and Meyer, "A Note From the Editors - Artificial Oscillations," Volume 2, Number 3, February, 1982, pages 1-2.

Brandwajn, "Damping of Numerical Noise in the EMTP Solution," Volume 2, Number 3, February, 1982, pages 10-19.

Alvarado, "Eliminating Numerical Oscillations in Trapezoidal Integration," Volume 2, Number 3, February, 1982, pages 20-32.

Brandwajn, "Influence of Numerical Noise on the Stability of Type 59 SM Model," Volume 2, Number 3, February, 1982, pages 37-43.

Meyer and Ren-ming, "Generalization of EMTP Switch and Source Logic to Allow Nearly Arbitrary Interconnections of Switches, Ungrounded Voltage and Current Sources, Ideal Transformers, Rigorous Checking of the Isolation of Multiphase Nonlinearities, and Floating Subsystems," Volume 2, Number 4, May, 1982, pages 36-42.

Meyer and Ren-ming, "Successful Generalization of EMTP Switch and Source Logic," Volume 3, Number 1, August, 1982, pages 70-74.

Meyer, "User-Supplied EMTP FORTRAN for the Solution of Coupled Single-Phase Nonlinearities Using a Standard Compensation-Based Interface," Volume 3, Number 3, February, 1983, pages 37-42.

Van Dommelen, "About the Discretization Error and the Frequency Scan Usage with Synchronous Machines," Volume 3, Number 3, February, 1983, pages 49-52.

Meyer, "Third-Generation Interactive EMTP Execution, Observation and Control: Near-Universality Via FORTRAN 77 Addition to the UTPF," Volume 4, Number 1, August, 1983, pages 4-13.

Meyer, "EMTP Data Modularization and Sorting by Class: A Foundation Upon Which EMTP Data Bases Can Be Built," Volume 4, Number 2, November, 1983, pages 28-40.

Brandwajn, "Use of the New RAMP Command for Interactive (SPY) Modification of Series RLC Elements," Volume 4, Number 2, November, 1983, pages 41-44.

Domme1, "Brief Summary of EMTP Related Work at UBC," Volume 4, Number 4, August, 1984, pages 23-27.

Li Guang Qi and Domme1, "Comparison of Fourier Analysis Routine in EMTP with FFT Routines," Volume 5, Number 2, April, 1985, pages 39-40.

Ramanujam, "A Note on Trapezoidal Rule and its Relationship to Backward Euler and Gear's Second Order Methods," Volume 5, Number 3, July, 1985, pages 1-7.

Yan, "Error Analysis of Some Numerical Integration Methods in Frequency Domain," Volume 5, Number 3, July, 1985, pages 8-14.

J. R. Marti, "Numerical Integration Rules and Frequency-Dependence Line Models," Volume 5, Number 3, July, 1985, pages 27-39.

Domme1, "DCG/EPRI EMTP Development," Volume 5, Number 4, October, 1985, page 26.

EMTP Newsletter Articles - Arresters Category

Meyer, "Experimentation with Zinc-Oxide Surge Arrester Modeling in EMTP," Volume 1, Number 2, December, 1979, pages 6-9.

Brandwajn, "Modelling of Surge Arresters in the Analysis of Electromagnetic Transients," Volume 1, Number 3, April, 1980, pages 8-13.

Teixeira and Charles, "Active Gap Arrester Model," Volume 1, Number 5, February, 1981, pages 13-20.

Brandwajn, "Generalization of Zinc-Oxide (ZnO) Surge Arrester Modeling," Volume 4, Number 2, November, 1983, pages 2-6.

Shirmohammadi, "Fitting ZnO Surge Arrester Characteristics for EMTP," Volume 4, Number 3, February, 1984, pages 18-29.

Brandwajn, "Generalization of Parameter Calculation of Zinc-Oxide (ZnO) Surge Arresters," Volume 4, Number 4, August, 1984, pages 19-21.

Durbak, "Zinc-Oxide Arrester Model for Fast Surges," Volume 5, Number 1, January, 1985, pages 1-9.

EMTP Newsletter Articles - Breakers Category

Meyer and Ren-ming, "Generalization of EMTP Switch and Source Logic to Allow Nearly Arbitrary Interconnections of Switches, Ungrounded Voltage and Current Sources, Ideal Transformers, Rigorous Checking of the Isolation of Multiphase Nonlinearities, and Floating Subsystems," Volume 2, Number 4, May, 1982, pages 36-42.

Meyer and Ren-ming, "Successful Generalization of EMTP Switch and Source Logic," Volume 3, Number 1, August, 1982, pages 70-74.

Teixeira, "Dynamic Arc Model in EMTP," Volume 4, Number 2, November, 1983, pages 14-27.

Lima, "Open Breaker Protection Study Using TACS Models," Volume 5, Number 1, January, 1985, pages 10-20.

Kizilcay, "Dynamic Arc Modeling in EMTP," Volume 5, Number 3, July, 1985, pages 15-26.

EMTP Newsletter Articles - Cable Category

Ametani and Liu, "Calculation of Cable Transients by EMTP," Volume 1, Number 1, July, 1979, pages 5-7.

Liu, "Status Report on Transient Cable Calculations Using the EMTP," Volume 1, Number 2, December, 1979, pages 3-6.

Hauer, "Dynamic Models for Frequency Dependence in Lines and Cables," Volume 1, Number 3, April, 1980, pages 3-4.

Ametani, "Cable Constants and Transient Calculations with the EMTP," Volume 1, Number 4, November, 1980, pages 7-9.

Brandwajn, "Use of 'Weighting Functions' in the Modelling of Frequency Dependence of dc Cables," Volume 2, Number 1, June, 1981, pages 14-21.

Brandwajn, "Guidelines for the Use of the Support Routine WEIGHTING for Cables," Volume 2, Number 1, June, 1981, pages 22-31.

Brandwajn, "User's Instructions for the Adjustment of Exponential Tail in the Weighting Functions Model of Frequency Dependence," Volume 2, Number 2, September, 1981, pages 27-29.

Ametani and Nagaoka, "Transients Calculations on a Crossbonded Cable by EMTP and Pi-Circuit Modeling of an Overhead Line and a Cable in 'Cable Constants'," Volume 2, Number 4, May, 1982, pages 20-29.

Brierly, "Modification of SEMLYEN SETUP to fit Cable Characteristics Provided by CABLE CONSTANTS," Volume 3, Number 3, February, 1983, pages 42-48.

Eteiba and Brierly, "Transient Analysis of Short Crossbonded Cable System Using SEMLYEN SETUP," Volume 3, Number 4, May, 1983, pages 8-16.

Brandwajn, "Evaluation of Various EMTP Cable Models," Volume 4, Number 3, February, 1984, pages 1-12.

EMTP Newsletter Articles - Field Tests Category

Brandwajn, "Duplication of TNA Simulation Results," Volume 1, Number 3, April, 1980, pages 4-8.

Vaz and Lima, "Portuguese 400-kV Network Field Tests. Simulation Studies.," Volume 2, Number 2, September, 1981, pages 3-24.

Lima, "Details about the Portuguese 400-kV Field Test Simulation Studies," Volume 2, Number 4, May, 1982, pages 2-10.

Koschik, "EMTP Transmission Line Simulation: Evaluation of Models, Simulation of HVDC Staged Line Fault," Volume 3, Number 1, August, 1982, pages 2-25.

Mork, Rao and Stuehm, "Modeling Ferroresonance with EMTP," Volume 3, Number 4, May, 1983, pages 2-7.

EMTP Newsletter Articles - Initial Conditions Category

Brandwajn, "Calculation of Initial Conditions for Combined Power Network and Control System Simulation," Volume 1, Number 5, February, 1981, pages 8-12.

Brandwajn, "Improvements to the Initialization of Combined ac and dc Networks," Volume 2, Number 1, June, 1981, pages 32-38.

Lauw, "Data Initialization and Other Additional Options of the UM Module," Volume 2, Number 3, February, 1982, pages 44-54.

Toyoda, "Setting Initial Conditions on Lines with Shunt Reactors for Reclosing Studies," Volume 2, Number 4, May, 1982, pages 43-54.

Yan, "Steady-State Solution with Harmonic Distortion," Volume 3, Number 2, November, 1982, pages 14-21.

Ramanujam and Diwakar, "Computation of Harmonics for Initializing Synchronous Machine Variables for Transient Studies," Volume 3, Number 4, May, 1983, pages 27-41.

Ramanujam and Diwakar, "Correction to: Computation of Harmonics for Initializing Synchronous Machine Variables for Transient Studies," Volume 4, Number 2, November, 1983, pages 46-49

Ino, Iravani and Mathur, "An Initialization Method for Simulation of HVDC Systems by EMTP," Volume 5, Number 1, January, 1985, pages 34-42.

EMTP Newsletter Articles - Lines Category

J. R. Marti, "New Approach to the Problem of Frequency Dependence of Transmission Line Parameters," Volume 1, Number 3, April, 1980, pages 17-20.

Hauer, "Dynamic Models for Frequency Dependence in Lines and Cables," Volume 1, Number 3, April, 1980, pages 3-4.

Liu, "A Practical New EMTP Model for Untransposed Transmission Lines - The Constant-Parameter Distributed Option Provided by K. C. Lee of UBC," Volume 2, Number 1, November, 1981, pages 7-13.

Brandwajn, "User's Instructions for the Adjustment of Exponential Tail in the Weighting Functions Model of Frequency Dependence," Volume 2, Number 2, September, 1981, pages 27-29.

J. R. Marti, "Implementation at BPA of a New Frequency Dependence Model," Volume 2, Number 3, February, 1982, pages 33-37.

Dommel, "Double-Circuit Lines with Zero Sequence Coupling Only," Volume 2, Number 3, February, 1982, pages 57-60.

L. Marti, "Low Order Approximation of the Frequency Dependent Line Parameters in J. Marti's Model," Volume 2, Number 4, May, 1982, pages 10-16.

L. Marti, "Voltage and Current Profiles Along Transmission Lines," Volume 2, Number 4, May, 1982, pages 17-19.

Lima, "Details about the Portuguese 400-kV Field Test Simulation Studies," Volume 2, Number 4, May, 1982, pages 2-10.

Ametani and Nagaoka, "Transients Calculations on a Crossbonded Cable by EMTP and Pi-Circuit Modeling of an Overhead Line and a Cable in 'Cable Constants'," Volume 2, Number 4, May, 1982, pages 20-29.

Dommel and Torres, "Simple Overhead Line Models for Lightning Surge Studies," Volume 2, Number 4, May, 1982, pages 30-35.

Brandwajn, "Initial Experience with the New Frequency-Dependent Line Model," Volume 2, Number 4, May, 1982, pages 54-58.

Lee, Sawada and L. Marti, "Comparison of Various EMTP Transmission Line Models - Part I (Line with Three Phases in Triangular Configuration)," Volume 2, Number 4, May, 1982, pages 58-69.

Koschik, "EMTP Transmission Line Simulation: Evaluation of Models, Simulation of HVDC Staged Line Fault," Volume 3, Number 1, August, 1982, pages 2-25.

Lima, "Temporary Overvoltage Studies," Volume 3, Number 1, August, 1982, pages 31-45.

Brandwajn, "Modification of User's Instructions for MARTI SETUP," Volume 3, Number 1, August, 1982, pages 76-80.

Hauer, "Benchmark Checks on Semlyen and Marti Simulation Logic for State-Space Modeling of Transmission Line Dynamics," Volume 3, Number 2, November, 1982, pages 2-13.

Sawada and Lee, "Comparison of Various EMTP Transmission Line Models - Part II (Line with Three Phases in Horizontal Configuration)," Volume 3 Number 3, February, 1983, pages 2-13.

Liu, "Summary of Questions About Complex or Real Transformation Matrices [T] of Untransposed, Distributed Transmission Line Models," Volume 4, Number 1, August, 1983, pages 15-17.

L. Marti, "Limitations of Frequency-Dependent Transmission Line Models in the EMTP," Volume 4, Number 2, November, 1983, pages 50-53.

Lima, "Open Breaker Protection Study Using TACS Models," Volume 5, Number 1, January, 1985, pages 10-20.

Shirmohammadi and Morched, "Improved Evaluation of Carson Correction Terms for Line Impedance Calculations," Volume 5, Number 2, April, 1985, pages 28-38.

EMTP Newsletter Articles - Machines Category

Dommel, "Data Conversion of Synchronous Machine Parameters," Volume 1, Number 3, April, 1980, pages 13-17.

Lauw, "The Importance of Recent EMTP Modeling Extensions, as Illustrated by Transient Studies Involving Unconventional Rotating Electric Machinery," Volume 1, Number 5, February, 1981, pages 23-24.

Van Dommelen, "Elimination of Predisturbance Mechanical Oscillations When Modeling Turbo-Generator Sets with Larger Time Increments," Volume 2, Number 1, June, 1981, pages 39-46.

Brandwajn, "Influence of Numerical Noise on the Stability of Type 59 SM Model," Volume 2, Number 3, February, 1982, pages 37-43.

Lauw, "Data Initialization and Other Additional Options of the UM Module," Volume 2, Number 3, February, 1982, pages 44-54.

Brandwajn, "Modifications to the User's Instructions for the Type 59 SM," Volume 2, Number 3, February, 1982, pages 55-56.

Ogihara, "EMTP Simulation of Load Rejection Shows Possible Self-Excitation of a 1300 MVA Generator Which Remains Connected to a UHV Line," Volume 3, Number 1, August, 1982, pages 26-27.

Ramanujam, "A Method of Interfacing Olive's Model of Synchronous Machine in an Electromagnetic Transients Program," Volume 3, Number 1, August, 1982, pages 46-59.

Lauw, "Extension of EMTP Universal Machine (UM) Modeling so as to Accept Type 50 (SCE) or Type 59 (Brandwajn) EMTP SM Data Cards as Input," Volume 3, Number 1, August, 1982, pages 60-69.

Brandwajn, "Removal of the SCE's Synchronous Machine Model," Volume 3, Number 2, November, 1982, pages 31-34.

Ramanujam, "A Note on Synchronous Machine Data Conversion," Volume 3, Number 2, November, 1982, pages 35-40.

Brandwajn, "Discussion of: A Method of Interfacing Olive's Model of Synchronous Machine in an Electromagnetic Transients Program," Volume 3, Number 2, November, 1982, pages 40-42.

Ramanujam, "Closure to: A Method of Interfacing Olive's Model of Synchronous Machine in an Electromagnetic Transients Program," Volume 3, Number 2, November, 1982, pages 42-45.

Lauw, "Multi-Machine System Simulation with the Universal Machine," Volume 3, Number 3, February, 1983, pages 14-24.

Lian, Ren-ming and Lauw, "Series-Capacitor Compensated Line Results in Unstable UM Self-Excitation Which is Explained Using Hurwitz Stability Theory," Volume 3, Number 4, May, 1983, pages 17-22.

Ramanujam, "A Note on Computation of High-Frequency Currents in Synchronous Machine Rotor Due to Unbalanced Stator Currents," Volume 3, Number 4, May, 1983, pages 23-26.

Ramanujam and Diwakar, "Computation of Harmonics for Initializing Synchronous Machine Variables for Transient Studies," Volume 3, Number 4, May, 1983, pages 27-41.

Brandwajn, "Planned Modifications to the Type 59 EMTF Generator Model," Volume 4, Number 1, August, 1983, pages 2-3.

Ramanujam and Diwakar, "Correction to: Computation of Harmonics for Initializing Synchronous Machine Variables for Transient Studies," Volume 4, Number 2, November, 1983, pages 46-49.

Brandwajn, "Investigation and Improvement of Long-Term Stability for the Type 59 Synchronous Machine (SM) Model," Volume 4, Number 2, November, 1983, pages 54-57.

Lauw, "Recent Developments of the EMTF Universal Machine: Load-Flow, Mechanical Network Sharing and Saturation Evaluation," Volume 4, Number 4, August, 1984, pages 12-18.

Brandwajn, "Discussion of: Recent Developments of the Universal Machine Load-Flow, Mechanical Network Sharing and Saturation," Volume 4, Number 4, August, 1984, pages 18-19.

Shirmohammadi and Lauw, "Limitations of Synchronous Machine Models in EMTF," Volume 4, Number 4, August, 1984, pages 7-11.

Shirmohammadi, "Universal Machine Modelling in Electromagnetic Transient Program (EMTF)," Volume 5, Number 2, April, 1985, pages 5-27.

Mechenbier, "Simulation of Synchronous Machines in Cases with Large Speed Changes," Volume 5, Number 4, October, 1985, pages 3-7.

H. W. Dommel, Bhattacharya, I. I. Dommel, Brandwajn and Ye Zhong-liang, "Canay's Data Conversion of Synchronous Machine Parameters," Volume 5, Number 4, October, 1985, pages 8-25.

EMTP Newsletter Articles - Sources Category

Meyer and Ren-ming, "Generalization of EMTP Switch and Source Logic to Allow Nearly Arbitrary Interconnections of Switches, Ungrounded Voltage and Current Sources, Ideal Transformers, Rigorous Checking of the Isolation of Multiphase Nonlinearities, and Floating Subsystems," Volume 2, Number 4, May, 1982, pages 36-42.

Meyer and Ren-ming, "Successful Generalization of EMTP Switch and Source Logic," Volume 3, Number 1, August, 1982, pages 70-74.

EMTP Newsletter Articles - Studies Category

Brandwajn, "Duplication of TNA Simulation Results," Volume 1, Number 3, April, 1980, pages 4-8.

Teixeira and Charles, "Statistical Reclosing Studies," Volume 1, Number 5, February, 1981, pages 21-23.

Vaz and Lima, "Portuguese 400-kV Network Field Tests. Simulation Studies," Volume 2, Number 2, September, 1981, pages 3-24.

Even, "EMTP Simulation of Resonant Overvoltage in HV Power Transformers," Volume 2, Number 3, February, 1982, pages 3-9.

Lima, "Details about the Portuguese 400-kV Field Test Simulation Studies," Volume 2, Number 4, May, 1982, pages 2-10.

Toyoda, "Setting Initial Conditions on Lines with Shunt Reactors for Reclosing Studies," Volume 2, Number 4, May, 1982, pages 43-54.

Ogihara, "EMTP Simulation of Load Rejection Shows Possible Self-Excitation of a 1300 MVA Generator Which Remains Connected to a URV Line," Volume 3, Number 1, August, 1982, pages 26-27.

Lima, "Temporary Overvoltage Studies," Volume 3, Number 1, August, 1982, pages 31-45.

Lauw, "Multi-Machine System Simulation with the Universal Machine," Volume 3, Number 3, February, 1983, pages 14-24.

Lima, "Open Breaker Protection Study Using TACS Models," Volume 5, Number 1, January, 1985, pages 10-20.

Goldsworthy, "EMTP Simulation of the Pacific HVDC Intertie," Volume 5, Number 2, April, 1985, pages 1-4.

EMTP Newsletter Articles - TACS Category

Dube, "Treatment of Limiters in TACS," Volume 1, Number 3, April, 1980, page 2.

Lauw, "Design Recommendations for Numerical Stability of Power Electronic Converters," Volume 1, Number 4, November, 1980, pages 2-6.

Teixeira and Charles, "Active Gap Arrester Model," Volume 1, Number 5, February, 1981, pages 13-20.

Lauw, "Discussion of: Design Recommendations for Numerical Stability of Power Electronic Converters," Volume 1, Number 5, February, 1981, pages 25.

Brandwajn, "Calculation of Initial Conditions for Combined Power Network and Control System Simulation," Volume 1, Number 5, February, 1981, pages 8-12.

Brandwajn, "Improvements to the Initialization of Combined ac and dc Networks," Volume 2, Number 1, June, 1981, pages 32-38.

Lima, "Temporary Overvoltage Studies," Volume 3, Number 1, August, 1982, pages 31-45.

Teixeira, "Dynamic Arc Model in EMTP," Volume 4, Number 2, November, 1983, pages 14-27.

Ren-ming and Goldsworthy, "Warning About Possibly Erroneous Order of EMTP TACS Variable Calculation for Typical Controller Modeling of HVDC Studies," Volume 4, Number 2, November, 1983, pages 7-9.

Van Dommelen and Maene, "TACS: A Note on an Additional Delay of One Time Step," Volume 4, Number 3, February, 1984, pages 13-17.

Ren-ming, "The Challenge of Better EMTP TACS Variable Ordering," Volume 4, Number 4, August, 1984, pages 1-6.

Shirmohammadi, "Unnecessary TACS Delays (EMTP Version M35 or Earlier)," Volume 4, Number 4, August, 1984, pages 22.

Lima, "Open Breaker Protection Study Using TACS Models," Volume 5, Number 1, January, 1985, pages 10-20.

Lima, "Numerical Instability Due to EMTP - TACS Interrelation," Volume 5, Number 1, January, 1985, pages 21-33.

Ino, Iravani and Mathur, "An Initialization Method for Simulation of HVDC Systems by EMTP," Volume 5, Number 1, January, 1985, pages 34-42.

Goldsworthy, "EMTP Simulation of the Pacific HVDC Intertie," Volume 5, Number 2, April, 1985, pages 1-4.

Kizilcay, "Dynamic Arc Modeling in EMTP," Volume 5, Number 3, July, 1985, pages 15-26.

EMTP Newsletter Articles - Transformer Category

Brandwajn and Brierly, "Model of Three-Leg Core Transformer," Volume 1, Number 2, December, 1979, pages 9-13.

Lembo, "Development and Testing of a 138-kV ± 25 degree Phase Shifter Transformer Model," Volume 2, Number 1, June, 1981, pages 2-6.

Even, "EMTP Simulation of Resonant Overvoltage in HV Power Transformers,"
Volume 2, Number 3, February, 1982, pages 3-9.

Mork, Rao and Stuehm, "Modeling Ferroresonance with EMTP," Volume 3 Number 4,
May, 1983, pages 2-7.

Part 2

COMPONENT GUIDE

Section 2

DVERHEAD LINES

This section discusses overhead transmission line models available in the EMTP and presents typical ranges of transmission line parameters to aid the user in performing studies. This section includes:

1. Abbreviated Reference List.
2. Defining Equations for Transmission Line Models.
3. Summary of Model Types.
4. Example One: Typical 500-kV Line Faulting and Comparison With Field Test Data For:
 - a. Constant parameter transposed model
 - b. Constant parameter nontransposed model (Lee's Model)
 - c. Transposed, frequency-dependent zero sequence coupling model (Dommel-Meyer model)
 - d. Nontransposed, constant transformation matrix, frequency dependent model (Marti's model)
5. Example Two: Flat 500-kV Line.
6. Recommendations for Use of the Line Models.
7. Typical Data for Transmission Lines.
8. Appendix - Input File Listings

2-1. ABBREVIATED REFERENCE LIST

The Introduction contains a detailed list of references on transmission lines. An abbreviated list of those references considered basic to the understanding of EMTP line model theory follows.

- A. W. S. Meyer and H. W. Dommel, "Numerical Modelling of Frequency-Dependent Transmission Line Parameters in an Electromagnetic Transients Program," IEEE Transactions On Power Apparatus and Systems, Vol. PAS-93, 1974, pp. 1401-1409 (Paper No. T74-080-8).
- B. J. R. Marti, "Accurate Modeling of Frequency-Dependent Transmission Lines in Electromagnetic Transients Simulation," IEEE Transactions On Power Apparatus and Systems, Vol. PAS-101, 1982, pp. 147-157.

- C. A. Semlyen and A. Dabuleanu, "Fast and Accurate Switching Transient Calculations on Transmission Lines with Ground Return Using Recursive Convolutions," IEEE Transactions On Power Apparatus and Systems, Vol. PAS.-94, 1975, pp. 561-571.

2-2 DEFINING EQUATIONS FOR TRANSMISSION LINE MODELS

The differential equations for a uniform transmission line are defined by analyzing an infinitesimal section of the line Δz , see Figure 2-1, located at coordinate z on the line. Initially, we do not consider line terminations. By inspection of Figure 2-1, one can write the following equations for a two-conductor line:

$$\Delta v(z,t) = v(z + \Delta z,t) - v(z,t) = - R \Delta z i(z,t) - \frac{L \Delta z}{\Delta t} \frac{\partial i(z,t)}{\partial t} \quad (2-1)$$

$$\Delta i(z,t) = i(z + \Delta z,t) - i(z,t) = - G \Delta z v(z,t) - C \Delta z \frac{\partial v(z,t)}{\partial t} \quad (2-2)$$

where R , L , G , and C are the per unit length resistance, inductance, conductance and capacitance of the line, respectively.

Dividing (2-1) by Δz and letting $\Delta z \rightarrow 0$ leads to the well-known partial differential equations for transmission lines.

$$- \frac{\partial v(z,t)}{\partial z} = R i(z,t) + L \frac{\partial i(z,t)}{\partial t} = Z i \quad (2-3)$$

$$- \frac{\partial i(z,t)}{\partial z} = G v(z,t) + C \frac{\partial v(z,t)}{\partial t} = Y v \quad (2-4)$$

where $Z = R + L \frac{\partial}{\partial t}$ (2-5)

$$Y = G + C \frac{\partial}{\partial t} \quad (2-6)$$

For a multi-conductor line with N conductors or phases, equations similar to (2-3) and (2-4) can be written in matrix form, i.e.:

$$- \frac{\partial V}{\partial z} = [Z] i \quad (2-7)$$

$$-\frac{\partial I}{\partial z} = [Y] V \quad (2-8)$$

$$\text{where } Z_{ij} = R_{ij} + L_{ij} \frac{\partial}{\partial t} \quad (2-9)$$

$$Y_{ij} = G_{ij} + C_{ij} \frac{\partial}{\partial t} \quad (2-10)$$

Hereafter, the analysis will encompass multiconductor lines.

For excitation of the system at any one particular frequency, one can write:

$$-\frac{\partial V}{\partial z} = [Z] I \quad (2-11)$$

$$-\frac{\partial I}{\partial z} = [Y] V \quad (2-12)$$

$$\text{where } Z_{ij} = R_{ij} + j\omega L_{ij} \quad (2-13)$$

$$Y_{ij} = G_{ij} + j\omega C_{ij} \quad (2-14)$$

or, by differentiating, these equations become:

$$\frac{\partial^2 V}{\partial z^2} = [Z][Y] V \quad (2-15)$$

$$\frac{\partial^2 I}{\partial z^2} = [Y][Z] I \quad (2-16)$$

where V and I are "phase" quantities, also denoted by V_{phase} and I_{phase} .

It can be proven that (2-15) and (2-16) can be decoupled by modal transformations using two eigenvector matrices, T_V and T_I , for $[Z][Y]$ and $[Y][Z]$ respectively. That is:

$$[I] = [I_{\text{phase}}] = [T_I][I_{\text{mode}}] \quad (2-17)$$

$$[V] = [V_{\text{phase}}] = [T_V][V_{\text{mode}}] \quad (2-18)$$

$$\text{and } [T_I]^{-1} = [T_V]^t \quad (2-19)$$

By using the modal transformations, the original N phase coupled system can be transformed into N uncoupled single phase (or single conductor) systems, like the one shown in Figure 2-1. In essence, the decoupling of the modes is the diagonalization of the impedance and admittance matrices (only the diagonal elements are nonzero). Therefore:

$$[Z_{\text{mode}}] = [T_V]^{-1} [Z_{\text{phase}}][T_I] \quad (2-20)$$

$$[Y_{\text{mode}}] = [T_I]^{-1} [Y_{\text{phase}}][T_V] \quad (2-21)$$

Where Z_{mode} and Y_{mode} are diagonal matrices.

Hence, for any "single-phase" mode, Equations 2-3 and 2-4 have a solution of the form:

$$V(z) = V_1 e^{-\gamma z} + V_2 e^{+\gamma z} \quad (2-22)$$

$$I(z) = I_1 e^{-\gamma z} - I_2 e^{+\gamma z} \quad (2-23)$$

$$\text{where } \gamma^2 = (R + j\omega L)(G + j\omega C) \quad (2-24)$$

V_1 , V_2 , I_1 and I_2 are incident and reflected voltage and current waves, respectively. All of the quantities R , L , G and C are modal quantities per unit length.

Equation 2-23 can be rewritten as:

$$I(z) = \frac{1}{Z_c} \{ V_1 e^{-\gamma z} - V_2 e^{+\gamma z} \} \quad (2-25)$$

where Z_c is the modal surge impedance of the line, defined by:

$$Z_c = \sqrt{\frac{R + j\omega L}{G + j\omega C}} \quad (2-26)$$

In general, R , L , G , and C vary with frequency.

Equation 2-25 implies that the current at any point on the line is the sum of two current waves, one travelling forward ($e^{-\gamma z}$) and one travelling backward ($e^{+\gamma z}$). It also implies that there is a voltage wave corresponding to each current wave, and the ratio between each is determined by Z_c .

Referring to Figure 2-2, which depicts a single-conductor line with terminals k and m, we can relate the forward travelling wave at one terminal to the backward travelling wave at the other terminal. This will lead to a relationship between voltages and currents at the line terminals, which will define a branch model to be used with branches representing the rest of the system (i.e., transformers, shunt capacitors, etc.).

The time-domain branch equation for node k is:

$$i_k = \frac{e_k}{z_c} - \frac{e_m(t-\tau)}{z_c} - i_m(t-\tau) \quad (2-27)$$

The branches defined by (2-27) are shown in Figure 2-2b. one branch at each node. The branch consists of a resistance equal to the line surge impedance and a "past-history" term corresponding to a wave arriving from the other line terminal.

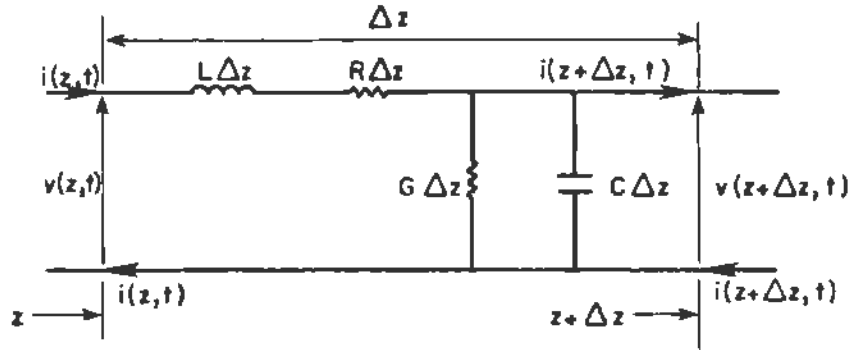
In its simplest form, the model in Figure 2-2 has constant z_c and no losses. The total line resistance is, therefore, lumped at each terminal and at midline in quantities of $R/4$, $R/4$, and $R/2$, respectively. Thus, the line model will have two travelling wave sections. Normally, this lumping of losses will not cause any computational problems. The incorporation of frequency-dependent z_c and losses is discussed later.

At each time step, the EMTP solves the model in Figure 2-2 for each mode, and phase quantities are then calculated by Equations 2-17, 2-18, and 2-19. One thing worthy of note is that T_I , in general, is frequency-dependent and complex, having both real and imaginary parts. T_V is also frequency-dependent and complex. Models for frequency-dependent lines require that the user specify T_I , which can be obtained from the different supporting routines, i.e., LINE CONSTANTS, WEIGHTING, etc.

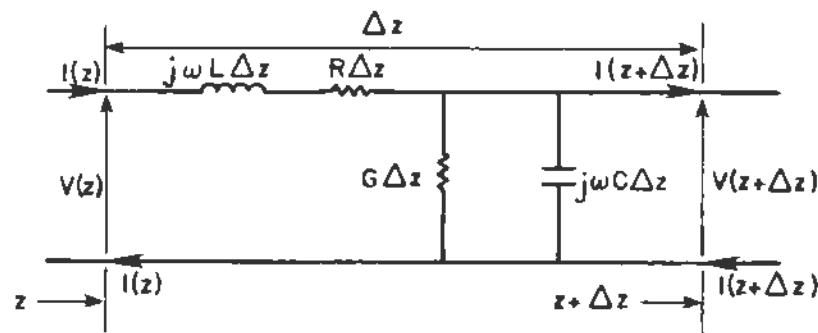
In general, only the real part of T_I should be used. The real T_I supplied by the line model SETUP routines are optimized to minimize the effect of neglecting the imaginary part of T_I . Use of a complex T_I in the time-step loop could produce totally erroneous results. A constant real T_I calculated at 500 Hz will produce good results under the following conditions.

- 1) flat lines, with or without ground wires.
- 2) any line configuration with no ground wires or with segmented ground wires.
- 3) single-circuit lines.

Under other conditions, the results may be less accurate, but are normally still usable.



a) Time Domain



b) Frequency Domain

Figure 2-1. Infinitesimal Section of a Two-Conductor Transmission Line in the a) Time Domain and b) Frequency Domain

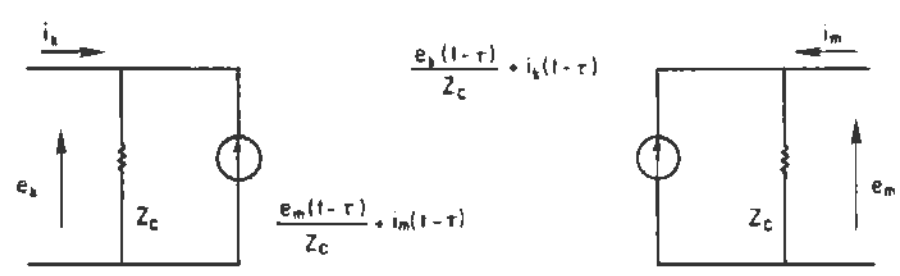
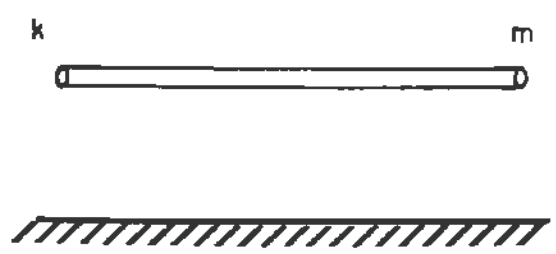


Figure 2-2. EMTP Single-Conductor Line Model

The K. C. Lee model automatically uses the complex T_I for an "exact" phasor solution, and then switches to a real T_I for the time step simulation. This changeover has not caused any observed or noticeable efforts on the results.

2-3. SUMMARY OF TRANSMISSION LINE MODELS IN THE EMTP

The EMTP contains two major categories of transmission line models: 1) constant-parameter models; and, 2) frequency-dependent models. Among the constant-parameter line models the EMTP provides a variety of options, such as:

- a) Positive sequence lumped parameter representation (balanced circuits).
- b) Positive and zero-sequence lumped parameter representation.
- c) Pi-section representation.
- d) Distributed parameter transposed line representation.
- e) Distributed parameter nontransposed line representation (K. C. Lee model).

If frequency dependence of lines is required, the EMTP provides several options, such as:

- a) The Meyer-Dommel setup.
- b) Semlyen setup.
- c) Marti setup.

Table 2-1 shows the recommended usage of the above models.

Transposed line models are often adequate for representing outlying portions of the system or for low-frequency phenomena, such as subsynchronous resonance. Switched lines should generally be represented by nontransposed line models for improved accuracy. Transposed, frequency-independent models are particularly suited for the input of typical positive and zero sequence surge impedances and wave velocities, and may, therefore, be the model of choice for parametric studies of unbuilt lines. Untransposed models require some knowledge or assumptions about the line conductors and tower configuration.

As frequency increases, the positive and zero-sequence line resistances increase while the zero-sequence inductance decreases. The positive-sequence inductance and both sequence capacitances remain relatively constant over frequencies of interest to the power system engineer. Including these frequency-dependent effects in a line model will reduce the peak magnitude and increase the damping of line switching transients. It is often desired to employ one of the EMTP's frequency-dependent line models in switching surge studies to improve the accuracy of the results.

Only distributed parameter lines (both transposed and nontransposed) have been chosen for illustration from among the frequency-independent models. From among the frequency-dependent models, the Meyer-Dommel and the Marti setups were chosen.

Distributed parameter lines are preferred over pi-section representations because of running time and core-storage considerations. Only as a last resort is the user encouraged to use pi-section representation. In this case, sections representing short untransposed lengths of line should be used. Ten to twenty miles per section is a good rule of thumb. By connecting many such sections in series (keeping track of any actual transpositions), a model for a long line can be built. Unfortunately, the use of pi-sections will add many buses or nodes to the system model, and therefore increase the computing time.

2-3-1. Principles of Frequency-Dependent Models in the EMTP

It is outside the scope of this guide to present the exact formulation of the frequency-dependent line models used in the EMTP, two of which are used in this section (the Marti and the Meyer-Dommel models). If the reader wishes to examine the details of the models, he is referred to the papers included in the list of references. It suffices to say here that both models illustrated use the principle of the modal transformation described above, and both methods also use "Weighting Functions" (described below) to find the frequency-dependent solutions of the transmission line equations. They differ in limitations imposed on the subject line and the use of the Weighting Functions. The modal transformation matrices used in both models are assumed to be frequency independent.

Before we describe the weighting functions, it should be noted that the Meyer-Dommel Model has the following limitations, according to Reference A:

1. The transmission line is assumed to be perfectly transposed.
2. No distributed branches are so short that $\tau < \Delta t$, where τ is the travel time and Δt is the time step of the simulation.
3. Frequency dependence is only allowed in the zero sequence mode.
4. Only distortionless lines or lines with with zero shunt conductance ($G=0$) are allowed.

Table 2-1

SUMMARY OF MODELS FOR TRANSMISSION LINES

MODEL	BEST FIT FOR
A) <u>Frequency-Independent Line</u>	In general are best for parametric studies, power frequency or low frequency phenomena, or where exact data is unavailable.
--Positive sequence lumped parameter representation (Branch Type 0)	<ul style="list-style-type: none"> --Unswitched lines --Balanced conditions --Load flow --Initial conditions for balanced systems --Remote source equivalencing
--Positive and zero sequence representation lumped parameter representation (Type 51, 52, 53)	<ul style="list-style-type: none"> --Unswitched lines, if computer resources are limited --Unbalanced conditions --Load flow --Initial conditions for unbalanced systems --Remote source equivalencing
--Pi-section representation (Type 1, 2, 3, ----N)	<ul style="list-style-type: none"> --Can be used for switched lines, although not recommended --Data in similar format to TNA (Transient Network Analyzer) data
--Distributed Parameter - Frequency-independent transposed line model (Type -1, -2, -3)	<ul style="list-style-type: none"> --General purpose studies --Switched lines --Lightning and high-frequency studies where travelling wave analysis is important --Where typical and line-specific data is available.
--Distributed Parameter - Frequency-independent nontransposed line model (Type -1, -2, -3, etc.) (K. C. Lee's model)	<ul style="list-style-type: none"> --Nontransposed lines --High ground resistivity and unbalanced circuits --General purpose studies --Modal analysis --Travelling wave analysis
B) <u>Frequency Dependent Line</u>	When frequency dependence is important, i.e., for switching surge studies, and those studies dealing with transients/system resonances in excess of 1 kHz.
--Meyer-Dommel setup (Type -1, -2, -3)	<ul style="list-style-type: none"> All frequency-dependent lines have the same usage except as noted below. --Switched transposed lines --Only zero sequence frequency-dependence
--Marti	<ul style="list-style-type: none"> --Can be used for transposed or non-transposed lines

These assumptions are not excessively restrictive because the predominant frequency-dependent effects do occur in the zero-sequence mode. If the user must represent frequency-dependent parameters for nontransposed line models, then Marti's model should be used.

2-3-2. Meaning of the Weighting Equations

The weighting functions, referred to as $a_1(t)$ and $a_2(t)$, can be defined per Figure 2-3, according to Meyer and Dommel. R_1 is defined as the limit $z_c(\omega)$, where

$z_c(\omega)$ is the surge impedance of the line.

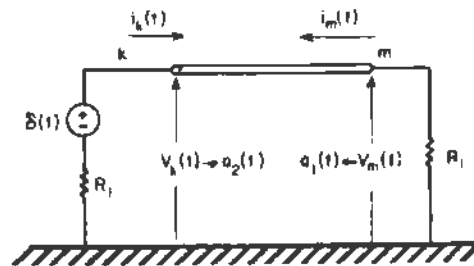


Figure 2-3. Physical Interpretation of Meyer-Dommel Weighting Function^(B)

In Figure 2-3, $a_1(t)$ is the voltage at node m , and $a_2(t)$ is the voltage at node k . The shapes of both $a_1(t)$ and $a_2(t)$ depend on the reflections from both ends of the line, and, therefore, can be complex and difficult to define as seen in Figure 2-4.

The effect of $a_1(t)$ on the model of Figure 2-2 is to incorporate more of the line's "past history." This attenuates and distorts the travelling waves. A frequency-independent model defined by Equation 2-27 would have a single-valued $a_1(t)$ at the point $t = \tau$.

The effect of $a_2(t)$ is to incorporate frequency variations in z_c . A frequency-independent model would have $a_2(t) = 0$ for all $t > 0$.

The weighting functions are approximated by exponentials, which permit the use of a numerically efficient recursive convolution algorithm for the EMTP simulation.

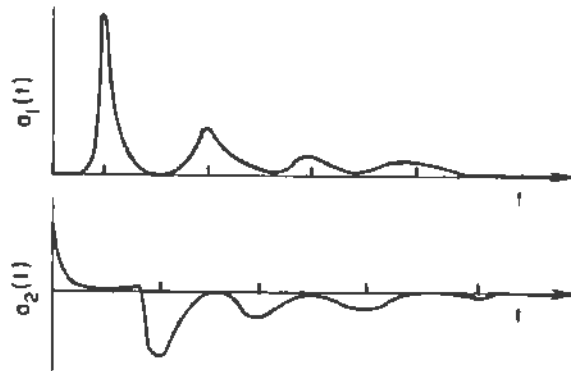


Figure 2-4. Weighting Functions in Meyer and Dommel's Formulation (B)

The increase in computing time is not great, but variations in the weighting functions, especially $a_2(t)$, sometimes lead to instabilities in the Meyer-Dommel model.

Marti suggested that the resistance R_1 be replaced by a network of RC elements which represents the surge impedance of the line for all frequencies. Because no reflections will result from either end of the line, $a_1(t)$ will have only the first "spike," and $a_2(t)$ will become zero for time $t > 0$, as shown in Figure 2-5. The effect of $a_2(t)$ is "taken over" by the frequency-dependent characteristic impedance, $Z_c(\omega)$, in Marti's model. Hence, in practice, the Marti model is only concerned with one rather than two weighting functions.

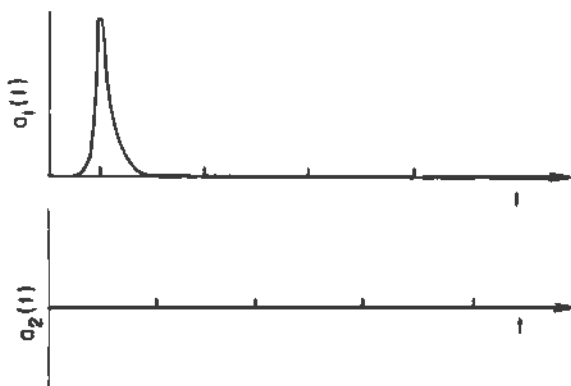


Figure 2-5. Weighting Functions $a_1(t)$ and $a_2(t)$ in the Marti Formulation (B)

The Marti setup routine determines the RC network for each mode, as well as $a_1(t)$ and T_1 . Each mode could have a different number of RC elements. Marti's model has the significant advantages of nontransposed line capability and enhanced stability (because $a_2(t) = 0$ and $a_1(t)$ has been simplified). It still has the limitation that the line travel time must exceed the simulation time step.

Any of the frequency-dependent line models which employ weighting functions must use a T_1 evaluated at one frequency, usually 500 to 5000 Hz. Fortunately, this is an acceptable approximation for frequencies of 60 Hz to 10 kHz, for overhead lines. At present, this limitation on T_1 precludes effective modeling of frequency-dependent cable or double-circuit overhead line parameters in the EMTP.

All of the weighting function models have inaccuracies in their low-frequency response as well. The practical significance of this is that trapped charges on lines can often not be used with the frequency-dependent line models. The Semlyen model in particular exhibits bizarre behavior at dc. When simulating line reclosing with trapped charge, any results obtained with the frequency-dependent models must be carefully checked. It is, in fact, recommended that a constant-parameter model be used instead.

The line parameters for a constant-parameter model used in a switching study can be calculated at the predominant transient frequency. Although this frequency may vary, a good estimate would be based on the positive sequence travel time of the line, where $f = 1/(4\tau)$. In other words,

$$f = \frac{50000}{d} \quad (2-28)$$

where d is the line length in miles.

Trapped charges can be specified for a constant-parameter line with no difficulty, and parameters based on the frequency given by (2-28) should improve the accuracy of the simulated transients. There may be some concern over the initial conditions calculated with higher frequency line parameters. However, because the capacitances and positive sequence inductance do not vary significantly with frequency, the initial conditions should be acceptably accurate.

At 500 Hz, the parameters R_0 and R_1 increase two to three times, the zero-sequence surge impedance decreases 15 to 20 percent, and the zero-sequence wave velocity increases 15 to 20 percent. The positive sequence travelling wave parameters are essentially unchanged.

2-4. EXAMPLE ONE: TYPICAL 500-KV LINE FAULTING

The system for the illustration of the different line models is obtained from Reference A. As shown in Figure 2-6, the system simulated is made up of an open-ended, 138 mile, three-phase, 500-kV line. A single-line-to-ground fault is applied to Phase C through a 2-ohm resistance.

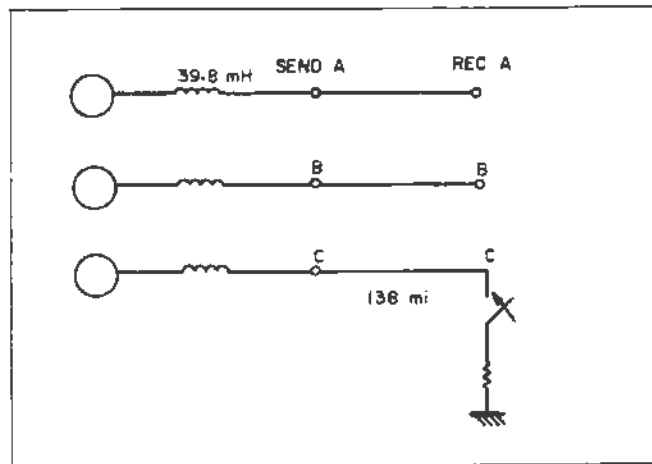


Figure 2-6. System Used for Example 1 for Comparing Results of Different Line Models. A single-line-to-ground fault is applied at Phase C of a 138 mile open-ended line. The fault is not allowed to clear for the duration of the run.

The results of the different simulations are compared to results of a field test, also obtained from Reference A.

2-4-1. Models Used

The following line models were considered:

- Constant-parameter, transposed line model ($f = 60$ Hz)
- Constant-parameter, nontransposed line model ($f = 60$ Hz)

- Constant-parameter, transposed line model ($f = 500$ Hz)
- Constant-parameter, nontransposed line model ($f = 500$ Hz)
- Meyer-Dommel transposed line model with zero-sequence frequency-dependence
- Marti's frequency-dependent transposed line model
- Marti's frequency-dependent nontransposed line model

The objectives of this example are to:

- Provide benchmarks for setup of the different models.
- Compare the computational effort needed for setup of each model.
- Run transient cases with the different models to: a) show setup and b) compare computational effort.
- Compare results obtained by the different models to those from the field test data reported in Reference A.
- Compare results from a frequency-independent line model to the above.
- Caution the user to any "problems" which may arise from using certain models, eg, numerical instability or sensitivity to time step, etc.
- Make recommendations on the use of the different models.

2-4-2. Setups for the Different Models

All setups for the various models are based on the "LINE CONSTANTS" supporting routine of the EMTP. For the frequency-dependent models, LINE CONSTANTS is used in conjunction with other supporting routines: JMARTI SETUP for Marti's model and WEIGHTING for the Meyer-Dommel model. Table 2-2 contains a brief description of the input data structures (files) for the different line models which are included in Tables 2-3 through 2-6 (Appendix). Comment cards have been extensively used in the input data to help the user identify different parameters. The users are cautioned here that some (very few) default input parameters for the LINE CONSTANTS routine vary with different versions of the EMTP. One such variable is ITRNSF. Hence, when using this document as a guide, the users should consult with their Operation Manual to check the default value of the different variables on their in-house EMTP version.

Table 2-2

CROSS REFERENCE BETWEEN MODELS USED AND FILE NAMES

LINE MODEL	EXAMPLE 1		EXAMPLE 2	
	SET UP FILE NAME	TRANSIENT CASE FILE NAME	SET UP FILE NAME	TRANSIENT CASE FILE NAME
1. Distributed parameter and constant-parameter, transposed model. Line parameters obtained for 60 Hz.	LINE	LNTL	LINE500LEE	L500TL
2. Distributed parameter and constant-parameter, transposed model. Line parameters obtained for 500 Hz.	LINE	LNTL5	LINE500LEE	L500TL5
3. Distributed parameter and constant-parameter, nontransposed K. C. Lee line model. Line parameters obtained for 60 Hz.	LINELEE	LNLEE	LINE500LEE	L500LEE
4. Distributed parameter and constant-parameter nontransposed K. C. Lee line model. Line parameters obtained for 500 Hz.	LINELEE	LNLEE5	LINE500LEE	L500LEE5
5. Distributed parameter, transposed, frequency-dependent (zero sequence) Meyer-Dommel line model.	LINEMD	LNMDT	LINE500MD	L500MDT
6. Frequency-dependent transposed Marti model.	LINEMARTI	LNMRM	LINE500MRT	L500MRT
7. Frequency-dependent nontransposed Marti model.	LINEMARTI	LNMRNT	LINE500MRT	L500MRNT

2-4-3. Computational Efforts for the Setup of the Different Line Models

The CPU times on a CRAY 1-S computer for the different line model setups are shown in Table 2-7. It is evident from this table that the Marti frequency-dependent model consumes considerable computational effort when compared to the constant-parameter models or the Meyer-Dommel model.

Table 2-7
RESULTS OF EXAMPLE 1

CASE	CPU TIMES [SEC]		PEAK OVERVOLTAGES [kV]					
	LINE	TRANSIENT	SENDING END			RECEIVING END		
	CONSTANTS	CASE	A	B	C	A	B	C
<u>Constant-Parameter Models</u>								
Transposed, 60-Hz	.110	.665	356.7	375.2	331.1	427.1	643.5	320.7
Transposed, 500-Hz	.110	.665	358.7	392.8	368.9	397.1	576.4	320.5
Nontransposed, 60-Hz	.114	.559	358.9	377.0	353.2	430.6	641.0	319.9
Nontransposed, 500-Hz	.115	.559	371.0	373.5	390.4	447.1	521.1	318.8
<u>Frequency-Dependent Models</u>								
Meyer-Dommel	.944	.863	315.7	335.5	347.1	396.5	485.1	429.8
Marti's Transposed	85.464	.852	312.2	332.4	307.8	430.0	551.7	320.8
Marti's Nontransposed	71.736	.833	312.2	335.7	307.7	425.1	566.2	320.7

2-4-4. Using Keypunched Card Output

The Marti, Meyer-Dommel, Pi-section and Semlyen setups may output the line model input data on punched cards, which are then added to the input data deck of the transient case. Punch card machines are becoming scarce nowadays, and it is becoming customary not to use cards. Hence, the user can avoid generating cards by specifying computer files to receive the card images. The card images are generated on Logical Unit No. 7. Hence, by assigning a permanent file name to that logical unit, one can catalog the card images under a file name which can then be attached to the file containing the input data for the rest of the system. Remember to delete the marking images which are placed at the beginning and end of the file, which have nothing to do with the line model. These images are usually generated for the control of the card punch machine.

2-4-5. Transient Simulation Using the Different Line Models

Transient simulations were made with the different line models discussed above. In all cases, a time step of 50 μ s was used with a run time of 60 ms. The case with the Meyer-Dommel setup was also run with a time step of 10 μ s. The CPU times for running the above cases on a CRAY 1-S computer are shown in Table 2-7.

Tables 2-9 through 2-13 (Appendix) contain the card images for the input for the different simulations.

2-4-6. Comparison of Results from Different Line Models

Figure 2-7 shows the Phase B receiving end voltage to ground of Example 1 as obtained from a field test on the subject line reported in Reference A. Figures 2-8 through 2-13 show the voltages at the same point (REC B) as obtained from the different line models. Peak overvoltage results from the various models are in Table 2-7. One may conclude that:

- Marti's model setup requires about two orders of magnitude more CPU time than the other model setups (see Table 2-7).
- Cases run with the different models require CPU time in the same order of magnitude, although frequency-dependent line models require approximately 60% more CPU time (see Table 2-7).
- Some instabilities appear with the Meyer-Dommel line model. This is clear from the "hash" in the 60-Hz prefault steady-state condition (see Figure 2-11). Using a time step of 10 μ s did not cure this problem. Running other cases with totally different parameters seemed to give similar problems, which leads one to think that the problem may be with the M34+ version of the EMTP used for the examples. Even though the Meyer-Dommel model is potentially unstable, the results reported in Reference A did not have this problem.
- The results of the constant-parameter line models with 60 Hz parameters yield higher peak overvoltages with less damping compared to the field test results. The overall waveshape and response may be satisfactory, albeit conservative.
- The constant-parameter, 500-Hz models produce lower peak overvoltages and better damping of the transients, as compared to the 60-Hz constant-parameter models. However, the steady-state and sending-end overvoltages are increased.

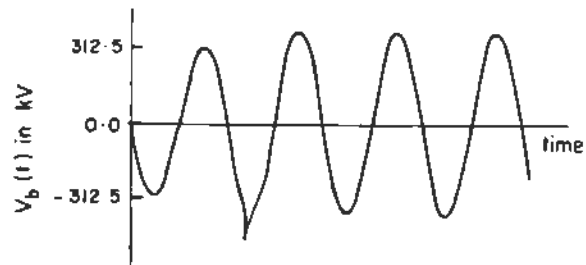


Figure 2-7. Phase B Voltage at the Open Receiving End (REC B) of the 138 Mile Line of Example 1 as Obtained by a Field Test. Reference (A).

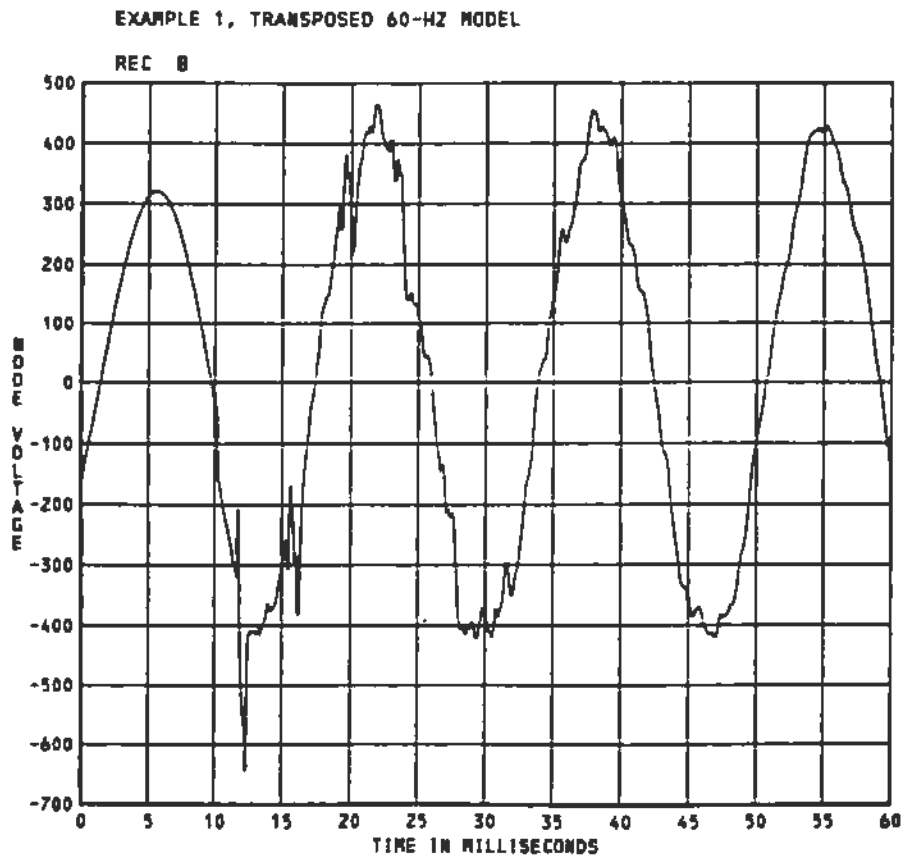


Figure 2-8. REC B Voltage to Ground for Example 1 Using a Distributed and Transposed Constant-Parameter Line Model. Line Parameters Calculated at 60 Hz.

EXAMPLE 1, TRANPOSED 500-HZ MODEL

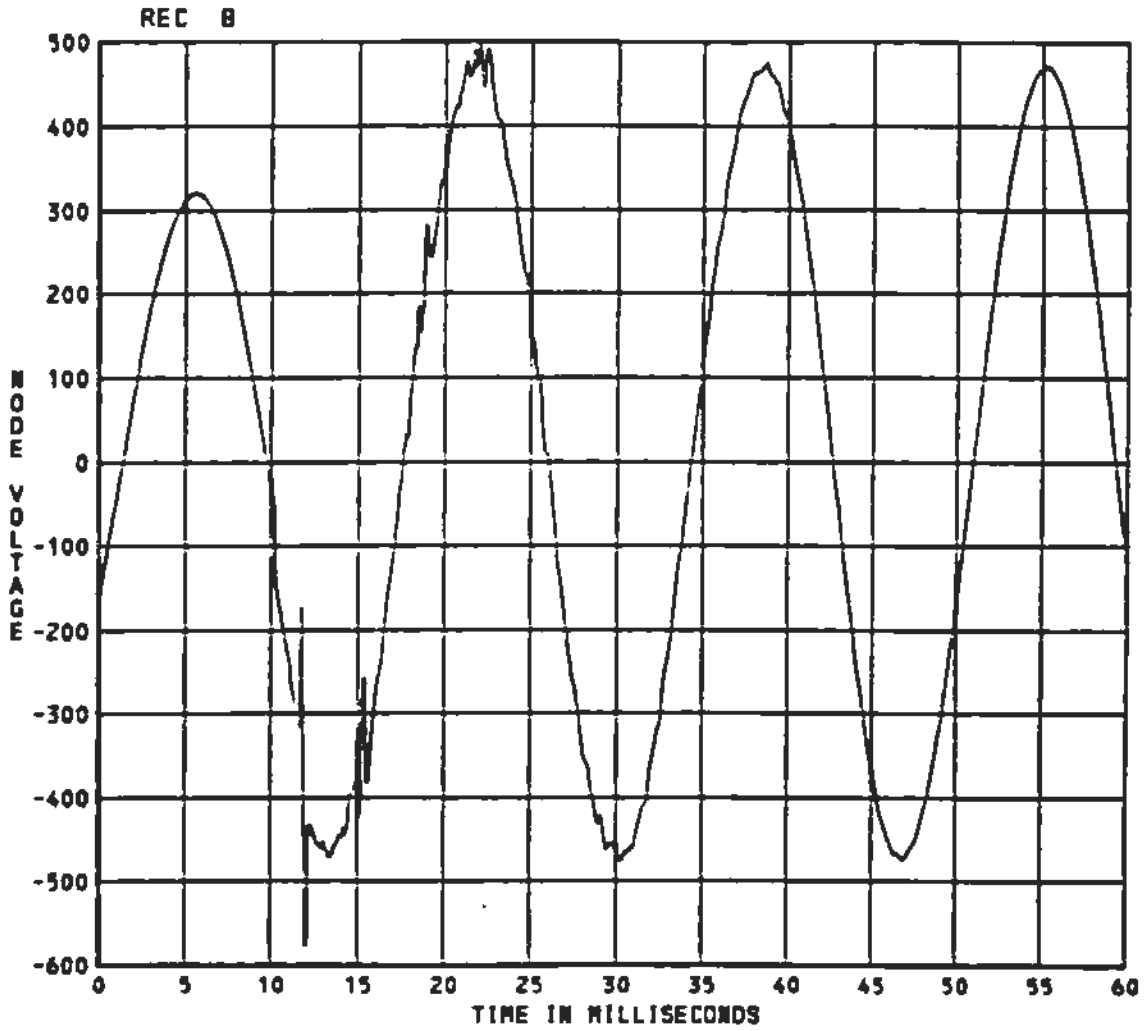


Figure 2-9. REC B Voltage to Ground for Example 1 Using Constant-Parameter Transposed Line Model. Line Parameters Calculated at 500 Hz.

EXAMPLE 1, NONTRANPOSED 60-HZ MODEL

REC B

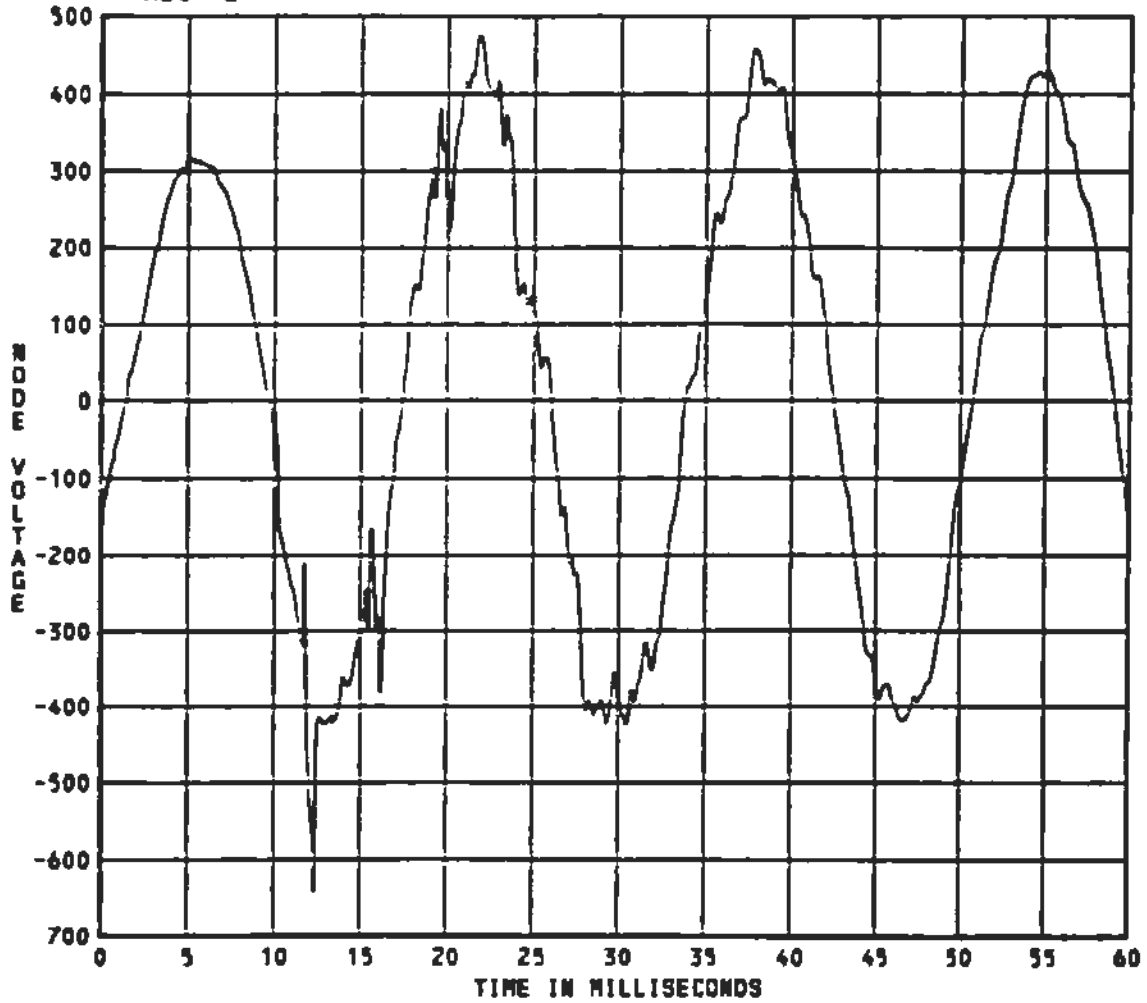


Figure 2-10. REC B Voltage to Ground for Example 1 Using Lee's Nontransposed Line Model, Line Parameters Calculated at 60 Hz.

EXAMPLE 1, MEYER-DOMMEL MODEL

REC B

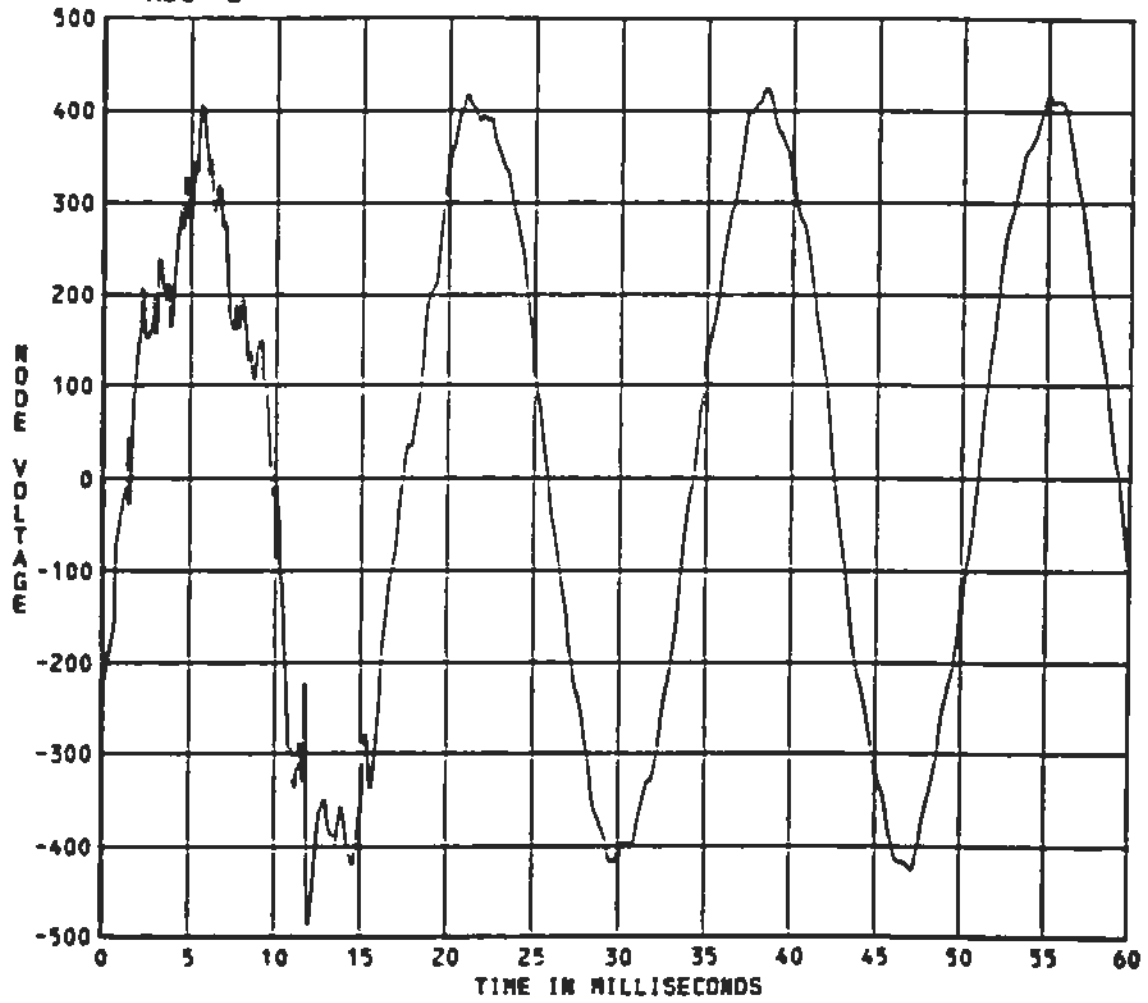


Figure 2-11. REC B Voltage to Ground for Example 1 Using Meyer-Dommel Frequency-Dependent Line Model

EXAMPLE 1, MARTI'S NONTRANPOSED MODEL

REC B

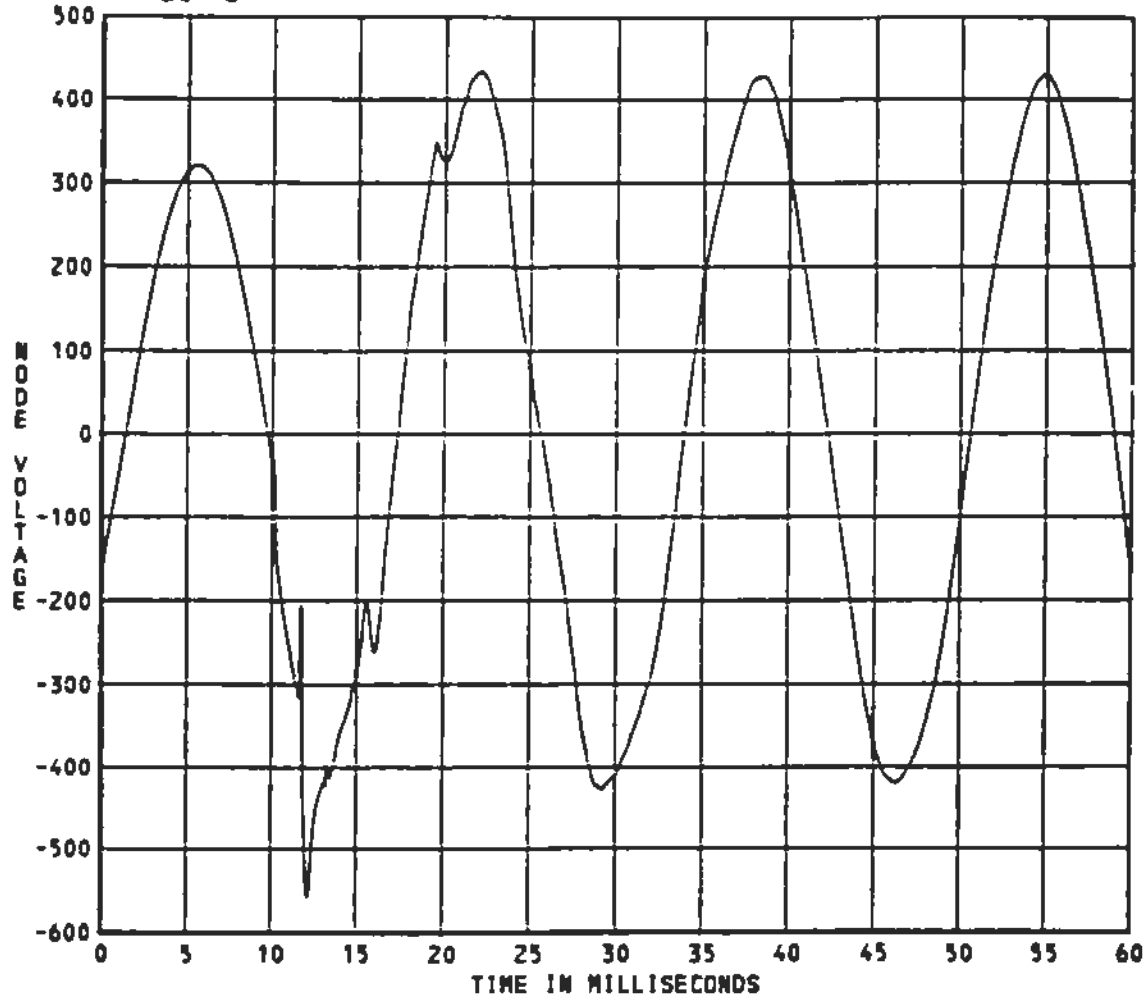


Figure 2-12. REC B Voltage to Ground for Example 1 Using Marti's Frequency-Dependent Nontransposed Line Model

EXAMPLE 1, MARTI'S TRANSPOSED MODEL

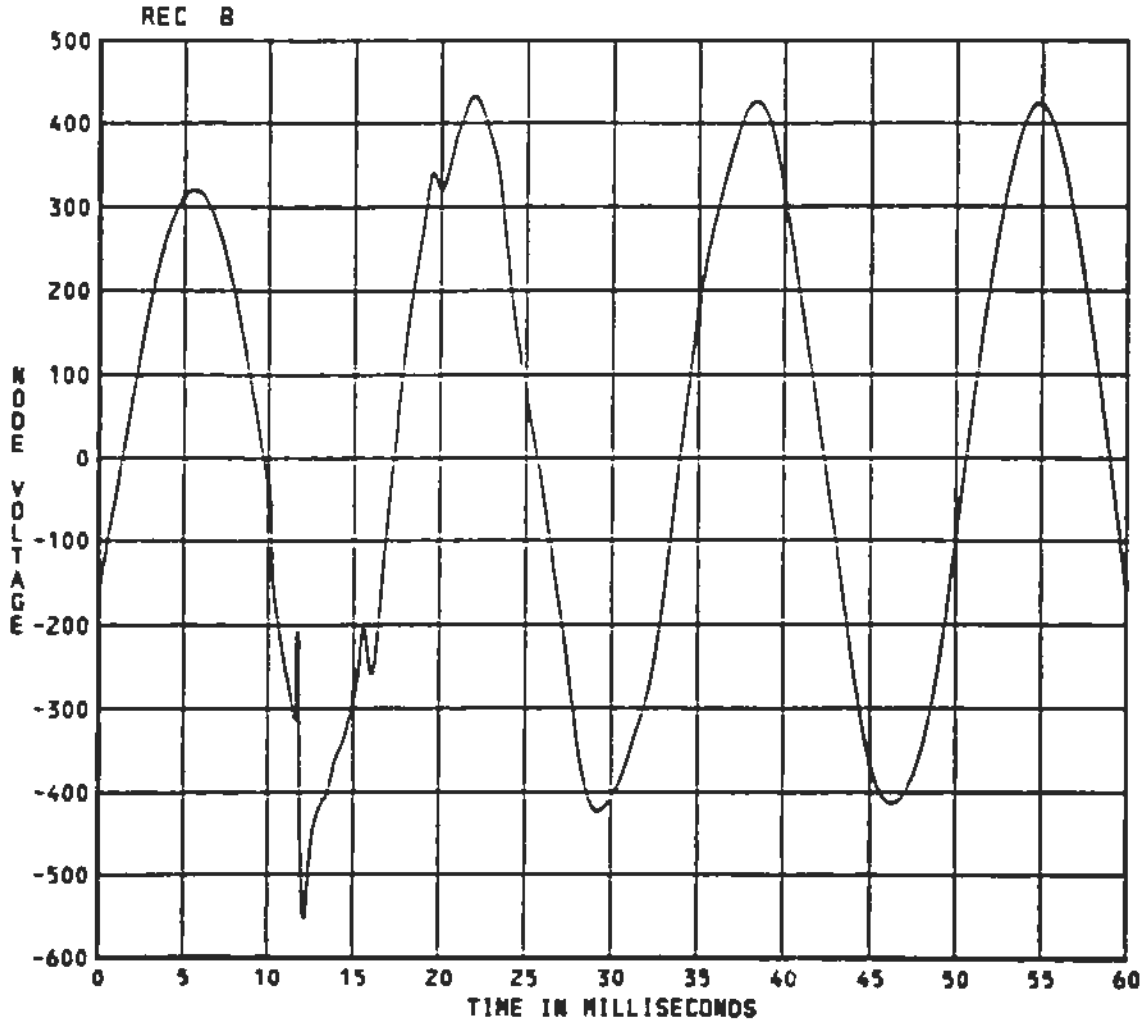


Figure 2-13. REC B Voltage to Ground for Example 1 Using Marti's Frequency-Dependent Transposed Line Model

- The transposed and nontransposed assumptions produce very similar results because the line conductors are in a delta configuration, which is a nearly balanced configuration. The 500-Hz constant-parameter models do differ, probably because of differences in the T_I matrix.

2-5. EXAMPLE 2: FLAT 500-KV LINE FAULTING

A more realistic circuit, shown in Figure 2-14, was used to compare the results of the different line models. Frequency-dependent and constant-parameter models for transposed and nontransposed line assumptions were tested. In this case, a line-to-ground fault on the receiving end Phase B (node REC B) was applied at near maximum voltage, as shown in Figure 2-15. The fault was applied at 33 milliseconds. This induced worst-case transients on the other two phases which are open-circuited. The fault is not allowed to clear in the time span of the case. Table 2-14 (Appendix) shows system input data for the case using Marti's nontransposed line model.

Figures 2-16 through 2-19 show the voltage at the receiving end Phase A using several different line models. Table 2-8 summarizes the results of these cases. Here, as in the previous example, one can note the following:

- The constant-parameter line models with parameters evaluated at 60 Hz yield results with the highest overvoltages and least damping. These conservative results are still acceptable in terms of wave shape and peak magnitude when compared to the Marti line model results.
- The Meyer-Dommel models still produced instabilities which could not be attributed to any system parameter in the pre-fault steady-state conditions. Many efforts to eliminate these instabilities were made with no success. These instabilities may be the same "numerical difficulties" which Marti refers to in his paper, Reference (B), or may be due to a "bug" in the EMTP version (M34+) used for these examples. No efforts were made to check the code for any possible bugs.

- Because the line conductors are in a flat, or unbalanced, configuration, the transposed and nontransposed model results show a noticeable difference.
- The 500-Hz constant-parameter model results are out of line with the other models. The damping of the transients is improved in these models, but the steady-state conditions are distorted, as compared to the 60-Hz constant-parameter models.

Table 2-8
RESULTS OF EXAMPLE 2

CASE	CPU TIMES [SEC]		PEAK OVERTAGES [kV]					
	LINE	TRANSIENT	SENDING END			RECEIVING END		
	CONSTANTS	RUN	A	B	C	A	B	C
<u>Constant-Parameter Models</u>								
Transposed, 60-Hz	.105	2.788	502.7	481.2	475.4	578.2	442.0	579.3
Transposed, 500-Hz	.105	2.787	475.8	452.9	450.1	642.4	441.8	501.1
Nontransposed, 60-Hz	.110	2.800	493.7	462.1	474.2	581.1	443.6	547.3
Nontransposed, 500-Hz	.110	2.802	464.9	441.4	455.0	616.1	443.7	501.6
<u>Frequency-Dependent Models</u>								
Meyer-Dommel	.926	3.328	458.6	483.7	448.7	604.4	527.2	608.4
Marti's Transposed	41.626	3.215	442.8	438.9	438.0	586.6	442.2	539.4
Marti's Nontransposed	108.606	3.332	435.3	431.5	427.3	552.8	443.8	526.6

2-6. RECOMMENDATIONS FOR USE OF THE LINE MODELS

The preceding material should have convinced the user that selection of an EMTP line model involves a balance of many factors. Application rules will not be valid for every conceivable situation, so that the user may have to experiment. The following recommendations are presented in condensed form as a summary of this section so far.

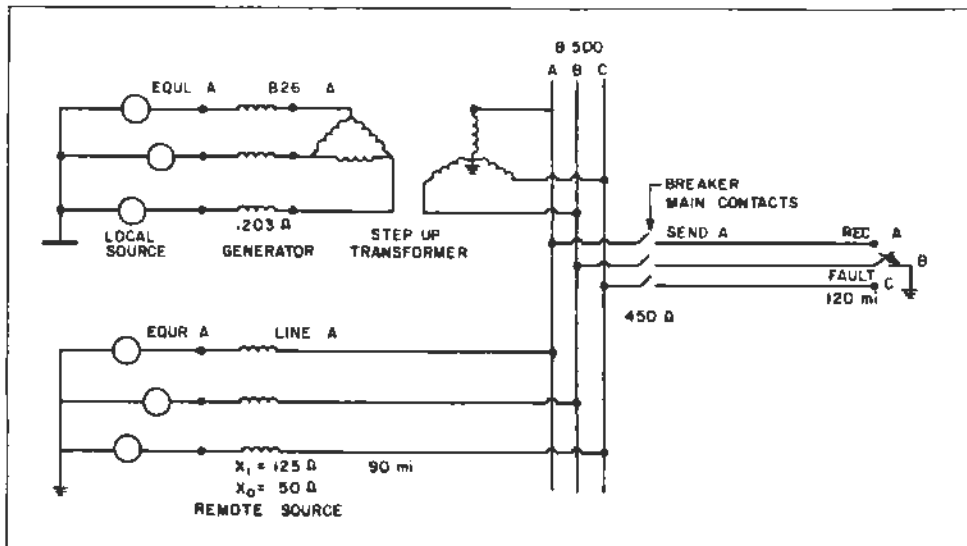


Figure 2-14. Circuit of Example 2. A single-line-to-ground fault is applied to Phase B of an open-ended transmission line, 120 miles long. Fault is not allowed to clear for the duration of the run.

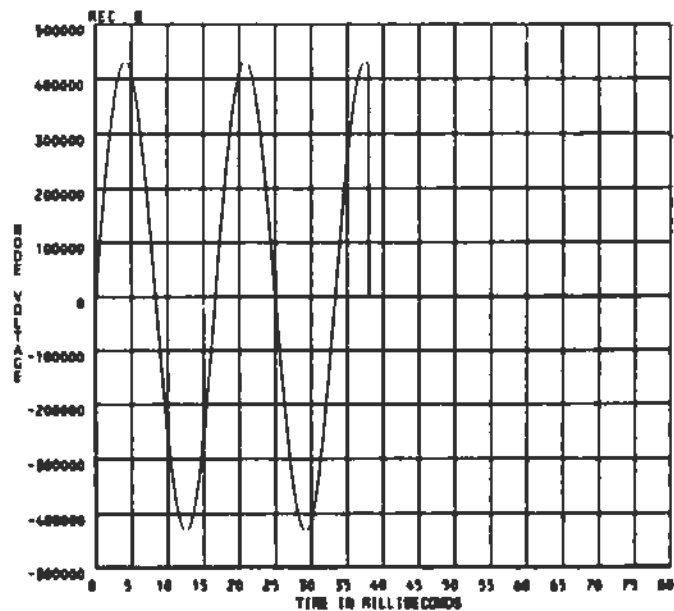
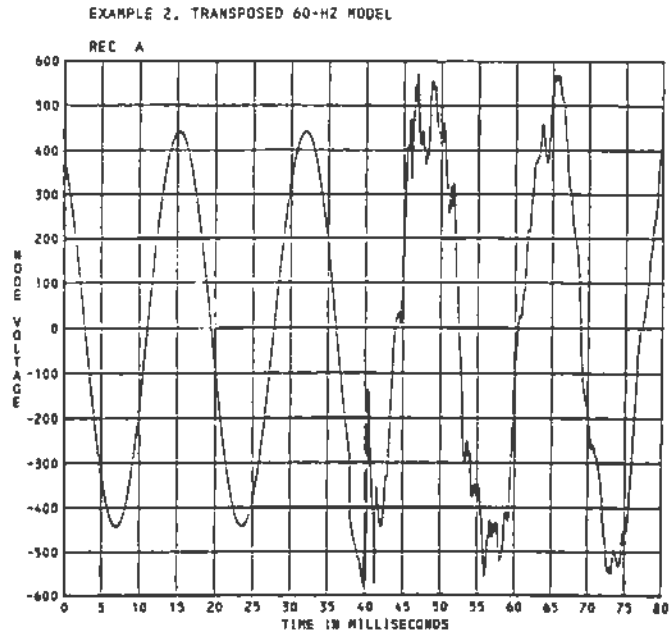
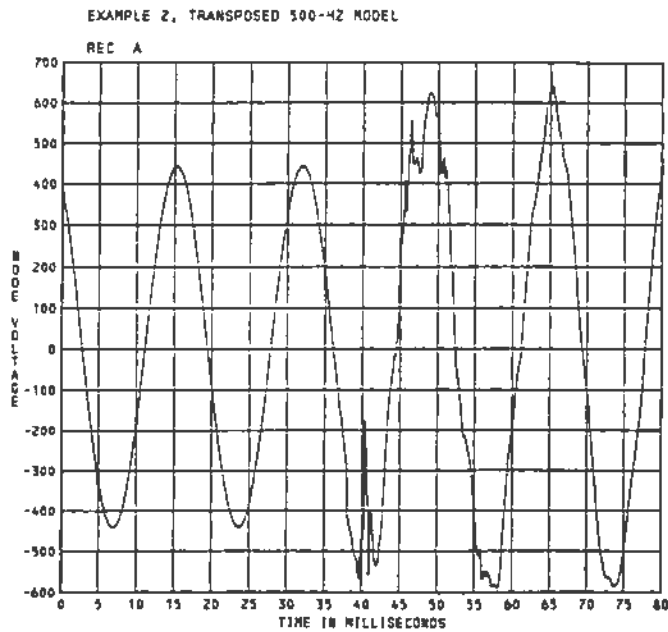


Figure 2-15. Faulting Conditions for Example 2. Node Voltage at Faulted Node REC B.

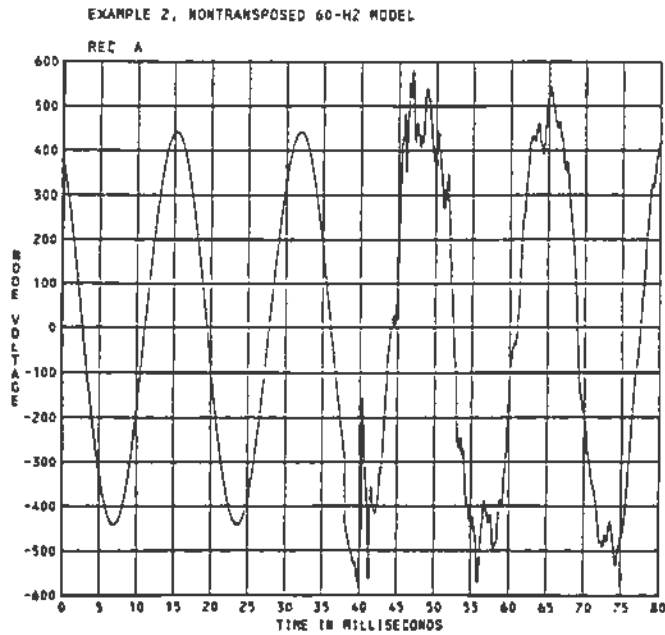


a) 60-Hz Parameters

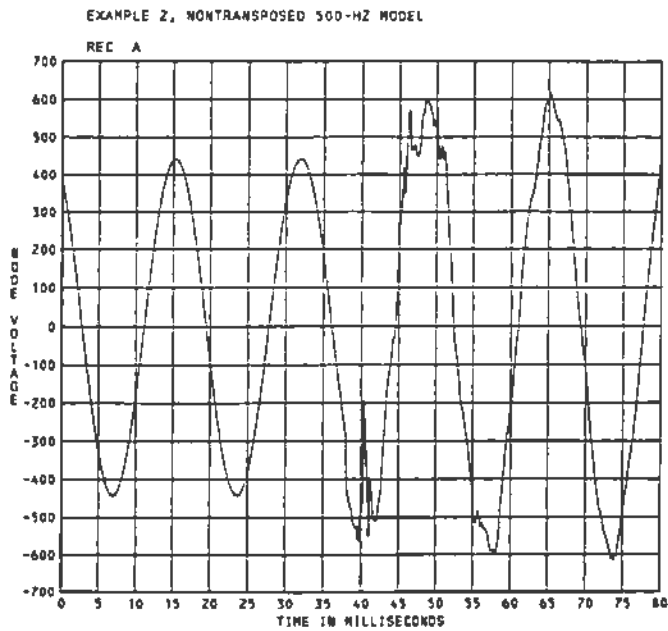


b) 500-Hz Parameters

Figure 2-16. REC A Voltage to Ground For Example 2, Using the Constant-Parameter Transposed Line Model



a) 60-Hz Parameters



b) 500-Hz Parameters

Figure 2-17. REC A Voltage to Ground For Example 2, Using the Constant-Parameter Nontransposed Line Model

EXAMPLE 2, MEYER-DOMMEL MODEL

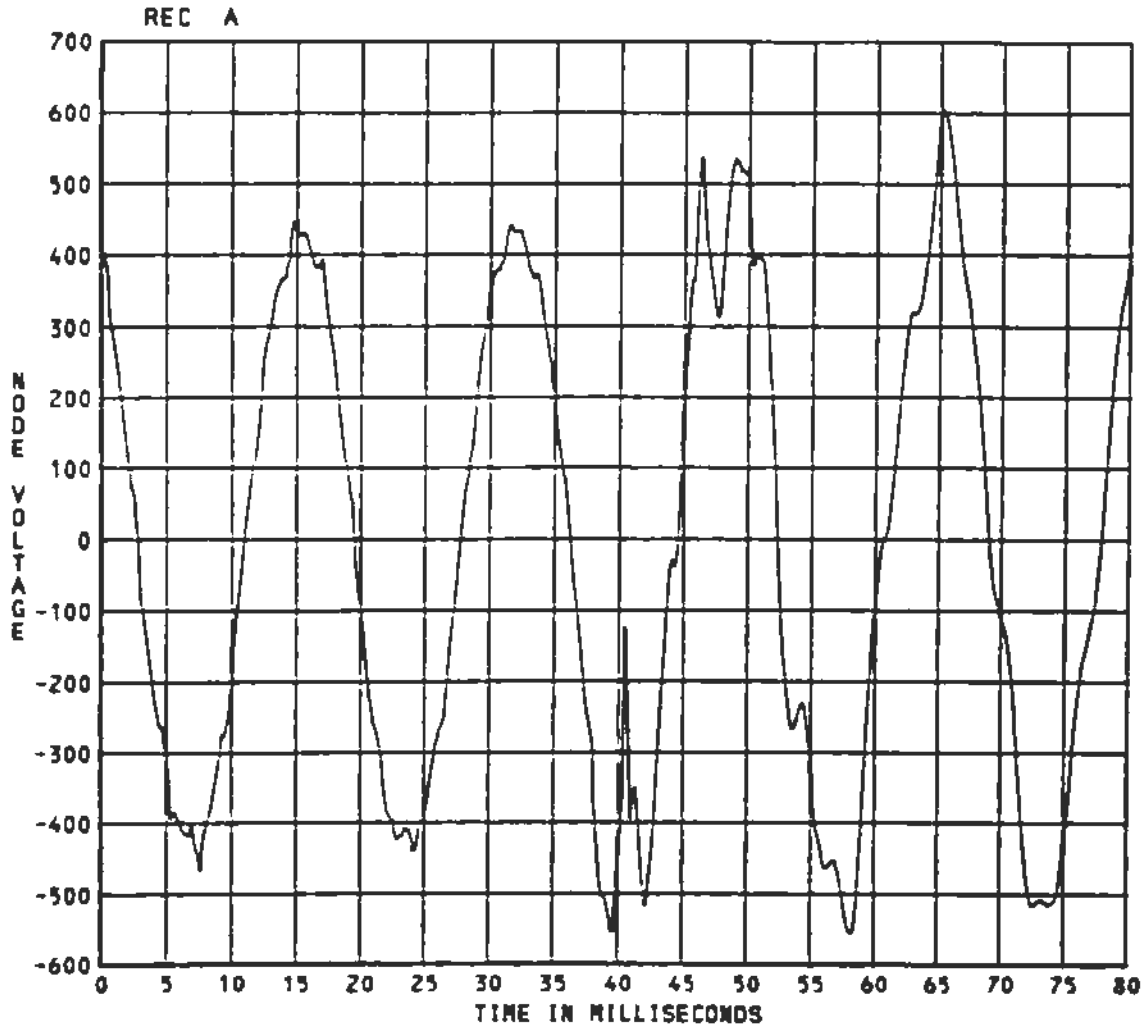
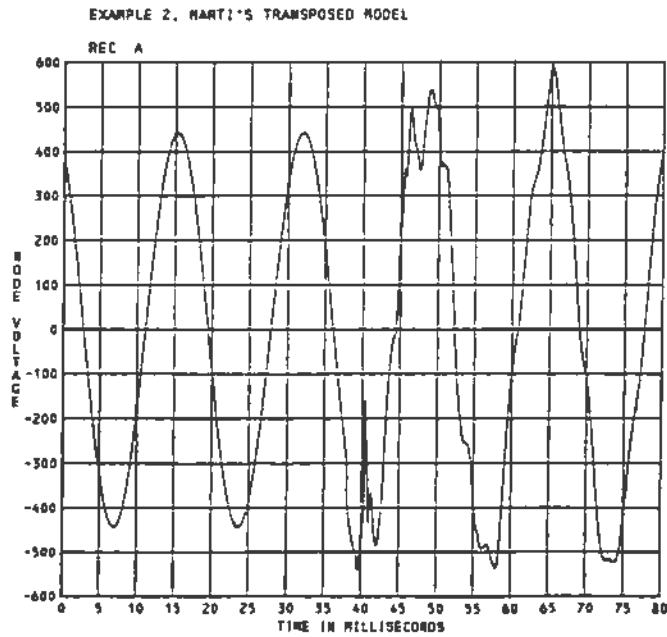
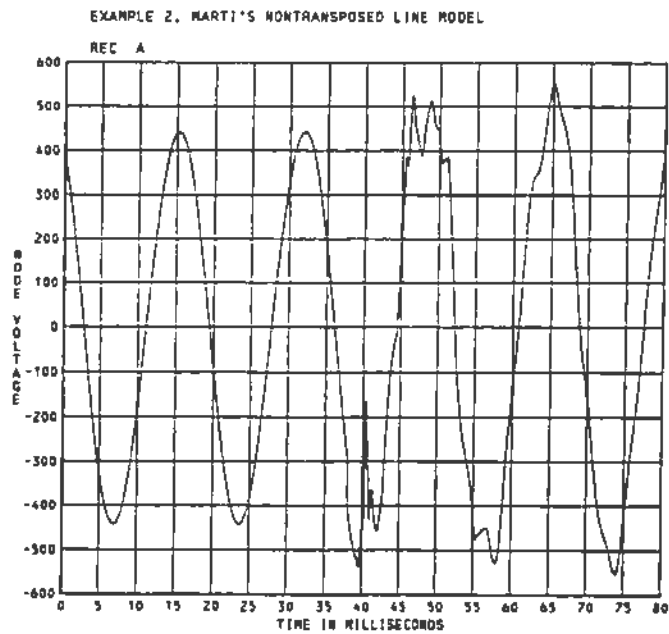


Figure 2-18. REC A Voltage to Ground for Example 2, Using the Meyer-Dommel Transposed Line Model



a) Transposed Line



b) Nontransposed Line

Figure 2-19. REC A Voltage to Ground for Example 2, Using the Marti Frequency-Dependent Model

1. Use lumped RL branch models only for steady-state calculations or to represent remote unswitched lines.
2. Cascaded pi-sections should not be used for overhead lines because the distributed parameter models simulate the same effects much more efficiently.
3. Constant-parameter models, either transposed or nontransposed, should be used in most cases, including statistical switching studies.
4. Constant-parameter line model parameters may be calculated for a predominant transient frequency, rather than 60 Hz.
5. If the user wants to use a frequency-dependent model:
 - a. Use extreme caution in applying trapped charge to the model.
 - b. Attempt to use the Meyer-Dommel model first, because its setup time is much less than the Marti model setup time.
 - c. If the Meyer-Dommel model appears to be unstable, or if the user must represent a nontransposed line, use the Marti model with real T_1 matrix.
6. Double-circuit overhead lines require special care if frequency-dependent models will be used. The constant-parameter, nontransposed model may be preferable. This can be set up to represent two transposed lines with zero-sequence coupling between them, as described by Dommel in the February, 1982, EMTP Newsletter.
7. Although cable modeling has not been addressed in this section, it may be stated that:
 - a. Frequency-dependent models should not be used.
 - b. Cascaded pi-sections may be required to simulate pipe-type cables, sheaths, etc.
8. The Marti model setup routine requires as much CPU time as is required for a 200-shot probability case. However, the transient case CPU times for frequency-dependent line models should not be considered a deterrent to their use.

2-7. TYPICAL DATA FOR TRANSMISSION LINES

This section presents typical data for transmission lines. It is intended that this data provide boundaries for transmission line parameters to use in the EMTP or other system studies. These ranges are plotted in several figures on the

following pages. The dots or crosses inside the boundaries indicate concentration of the data, i.e., many lines having the same parameters. The data presented in the figures is based on over 160 lines.

Unless otherwise stated, all data presented is for 60 Hz. This especially applies to the resistance and inductance of the lines. Capacitance is generally considered independent of frequency. Figures 2-20, 2-21, and 2-22 show the variation with frequency of the zero and positive sequence resistance, inductance, and surge impedance of a typical flat 500-kV line configuration shown in Figure 2-23. The 60-Hz parameters are adequate for most studies such as steady state, temporary overvoltages, subsynchronous resonance and other lower frequency studies. For higher frequency studies such as switching surges and lightning etc., the use of the 60-Hz parameters results in conservative answers.

The data as plotted is in a format suitable for the EMTP distributed parameter (ITYPE = -1, -2, -3), transposed or nontransposed configuration. It can be used with ILINE input options 1 or 0. It is suggested, however, to use Option 1 in all studies because the percentage variation of the positive-sequence surge impedance with frequency, as shown in Figure 2-22, is small when compared to the changes in the inductance or resistance. This is due to the square root relationship with frequency. This will make use of the typical data more convenient. It is also suggested that for the higher frequency studies, specifically switching surge studies, the user should consider either using one of the frequency-dependent lines described in Section 2-3, or calculating the line parameters at a higher frequency.

Many transmission towers were, and still are in some cases, oversized for their voltage level. Therefore, when an upgrading of voltage level was made (e.g., from 69 kV to 115 kV or from 115 kV to 230 kV), many utilities used the same tower configurations for the higher voltage. The upgrade may be accompanied by changes in the number of insulators and phase conductors to achieve more insulation and lower losses, corona, and radio and television interference.

This factor and others, such as NESC or local codes, cause overlaps in the range of parameters for transmission lines of different voltage levels. This is especially demonstrated in the following parameters:

2. The minimum clearances and, hence, the strike distances phase-to-phase. This is shown in Figure 2-27 for lines above 69 kV.

1. The equivalent number of standard insulators (5-3/4" x 10") as shown in Figures 2-24 and 2-25 and the minimum clearance to tower as shown in Figure 2-26. The vertical lines in those two figures reflect the range of the values used for that voltage level. For the lower voltage levels, the horizontal lines reflect the most-used values in the industry. Figure 2-25 shows the same data of Figure 2-24 for voltage levels above 69 kV on a linear scale, rather than the logarithmic scale of Figure 2-24. As mentioned above, the vertical axis of those figures represents the equivalent number of standard insulators for the different voltage levels, although the sampled lines might have had other types of insulators (e.g., 6-3/4" x 11", 7-3/4" x 12-5/8", 6-1/2 x 12-5/8", or long rod, etc.).
3. The phase conductor heights at tower and mid-span, as illustrated in Figure 2-28.

Figures 2-29 through 2-34 show the other parameters of transmission lines.

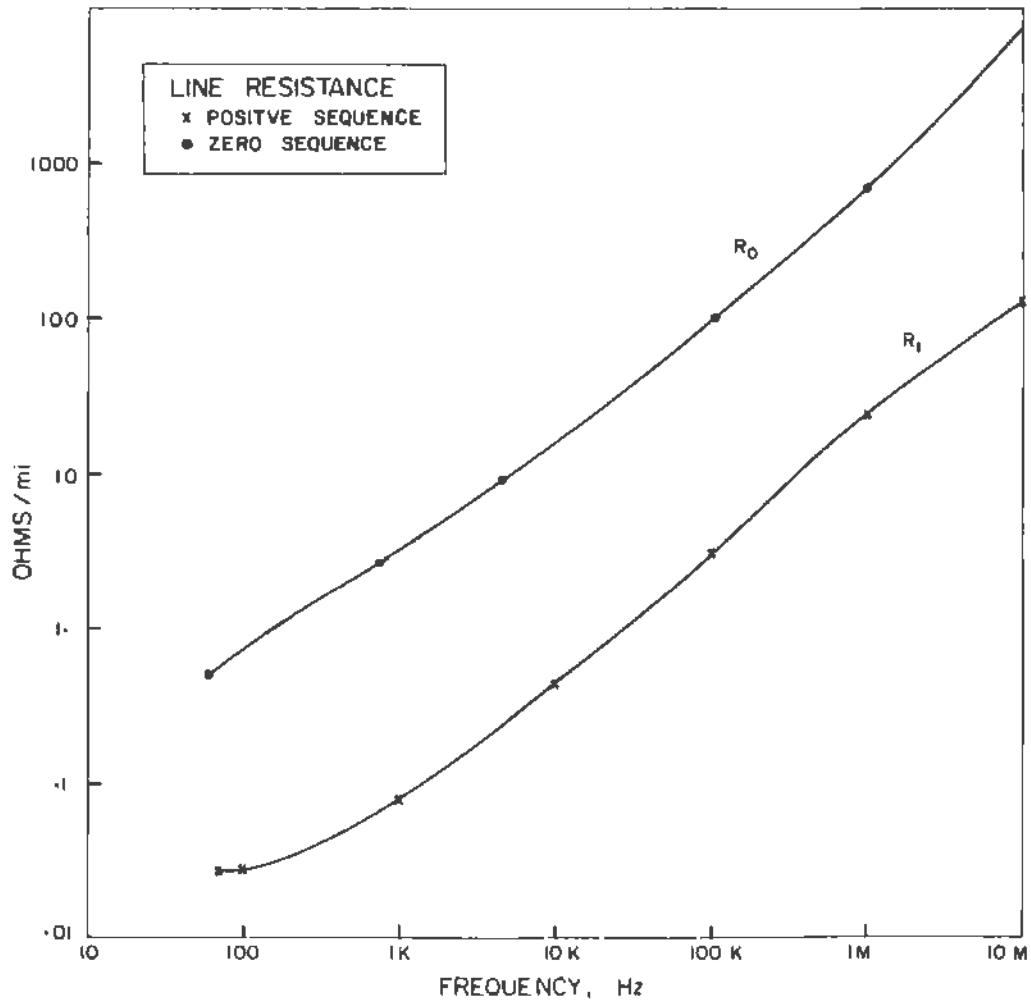


Figure 2-20. Variation of the Sequence Resistances Per Unit Length of a Typical 500-kV Flat Configuration Transmission Line Shown in Figure 2-23

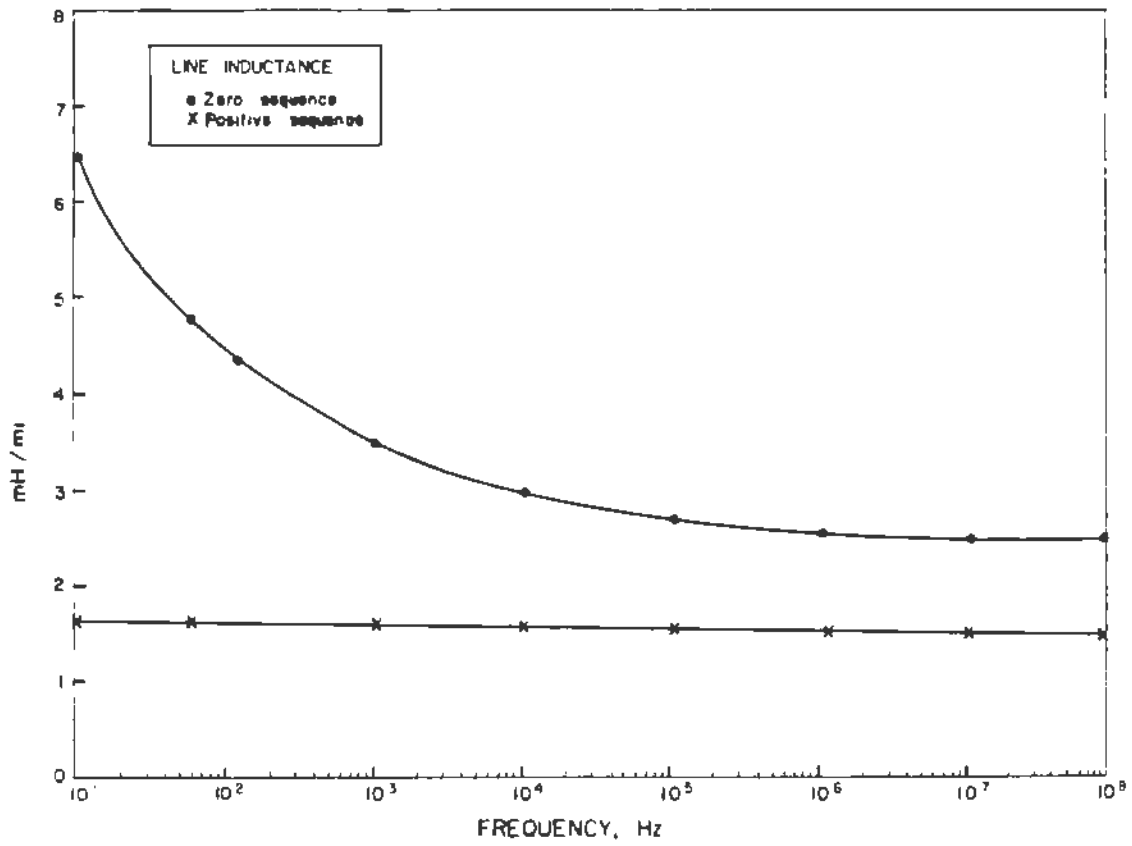


Figure 2-21. Variation of the Sequence Inductances Per Unit Length of a Typical 500-kV Flat Configuration Transmission Line Shown in Figure 2-23

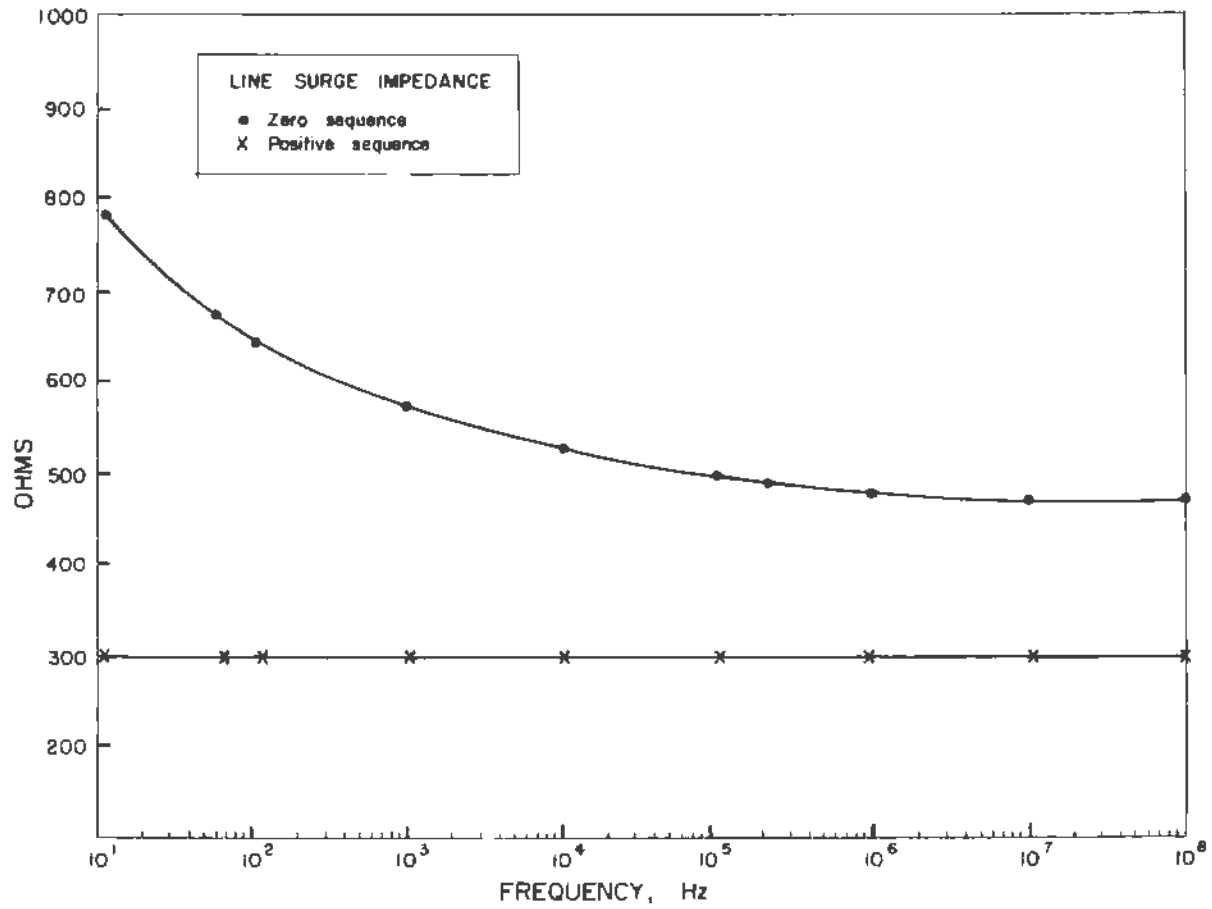


Figure 2-22. Variation of the Sequence Surge Impedances for a Typical 500-kV Flat Configuration Transmission Line Shown in Figure 2-23

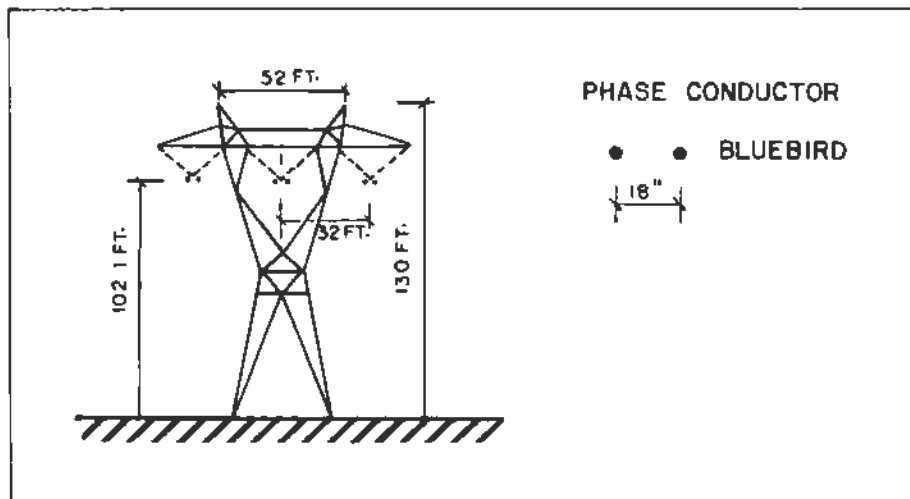


Figure 2-23. Tower Dimensions for the 500-kV Flat Configuration Transmission Line

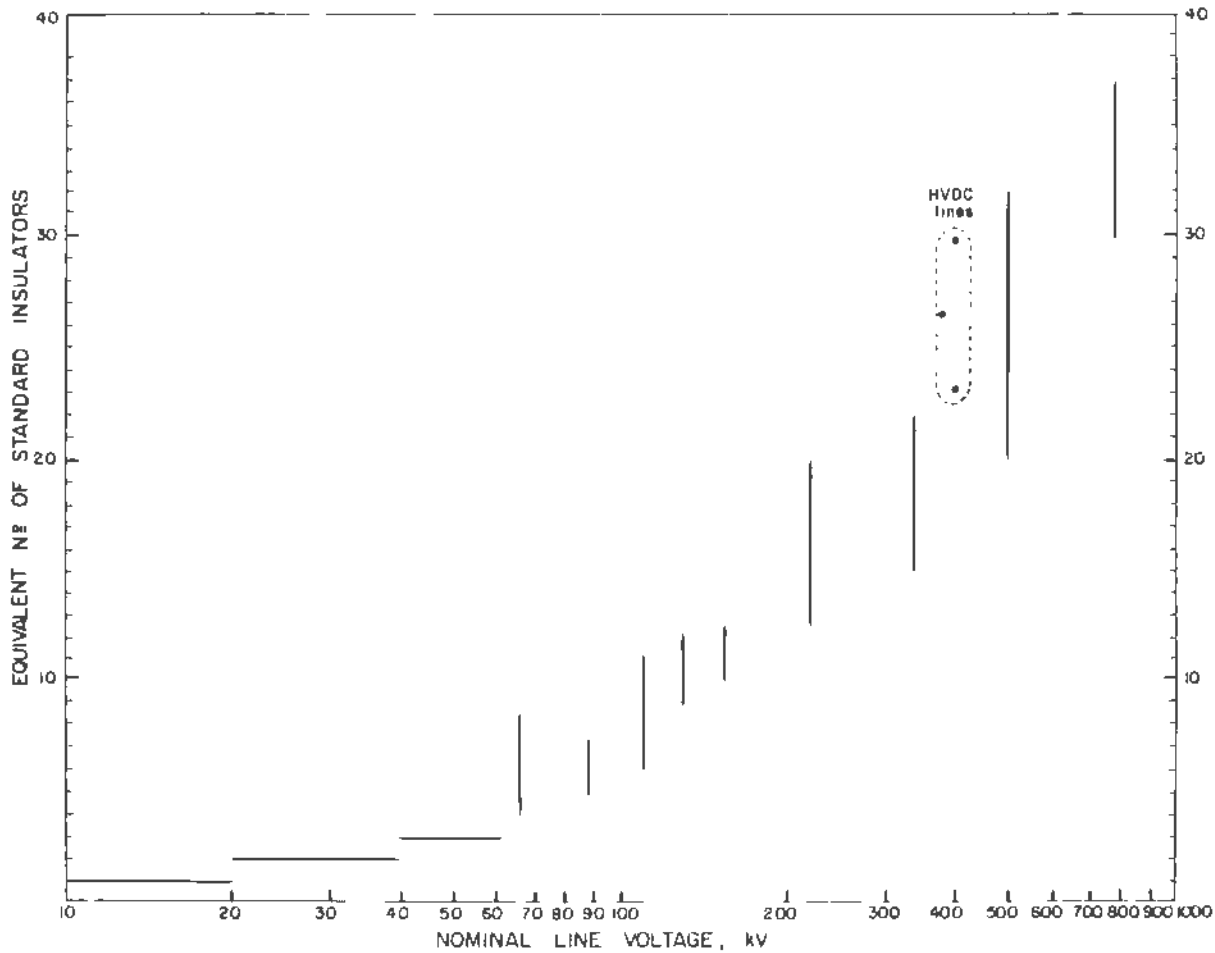


Figure 2-24. Equivalent Number of Standard Suspension Insulators (5-3/4" x 10") Which Are Used on Different Voltage Levels. Values Reflect the Range In Use.

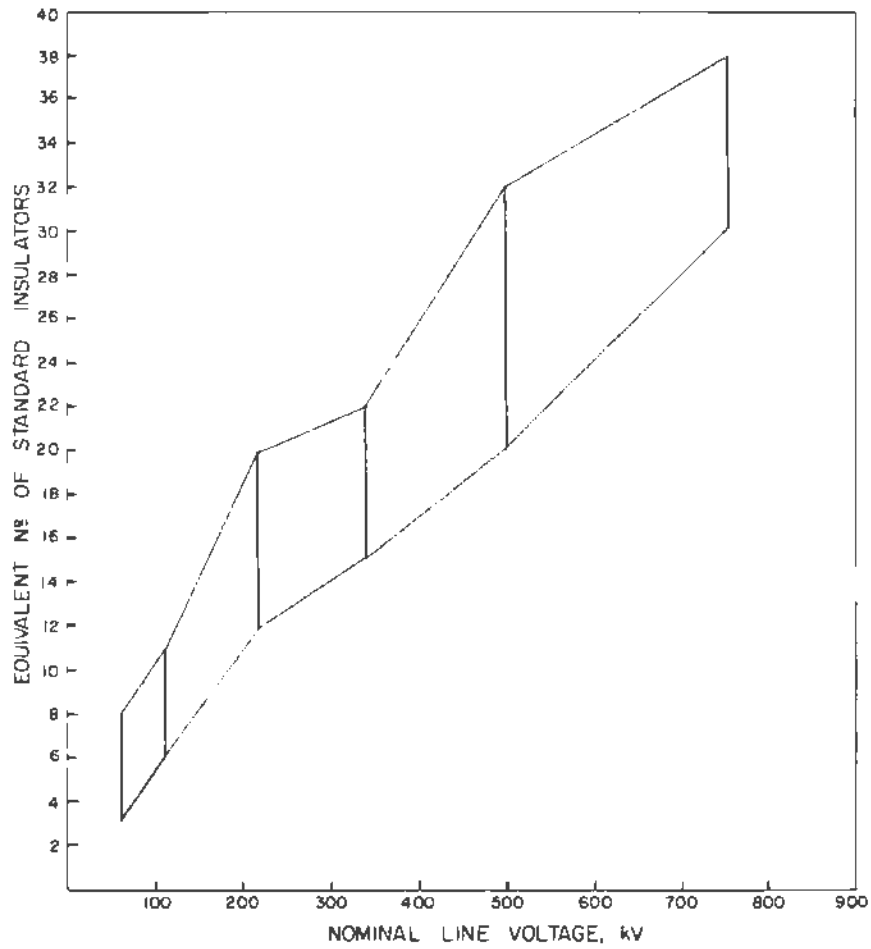


Figure 2-25. Equivalent Number of 5-3/4" x 10" Standard Insulators Used at Voltage Levels Equal To and Greater Than 69 kV

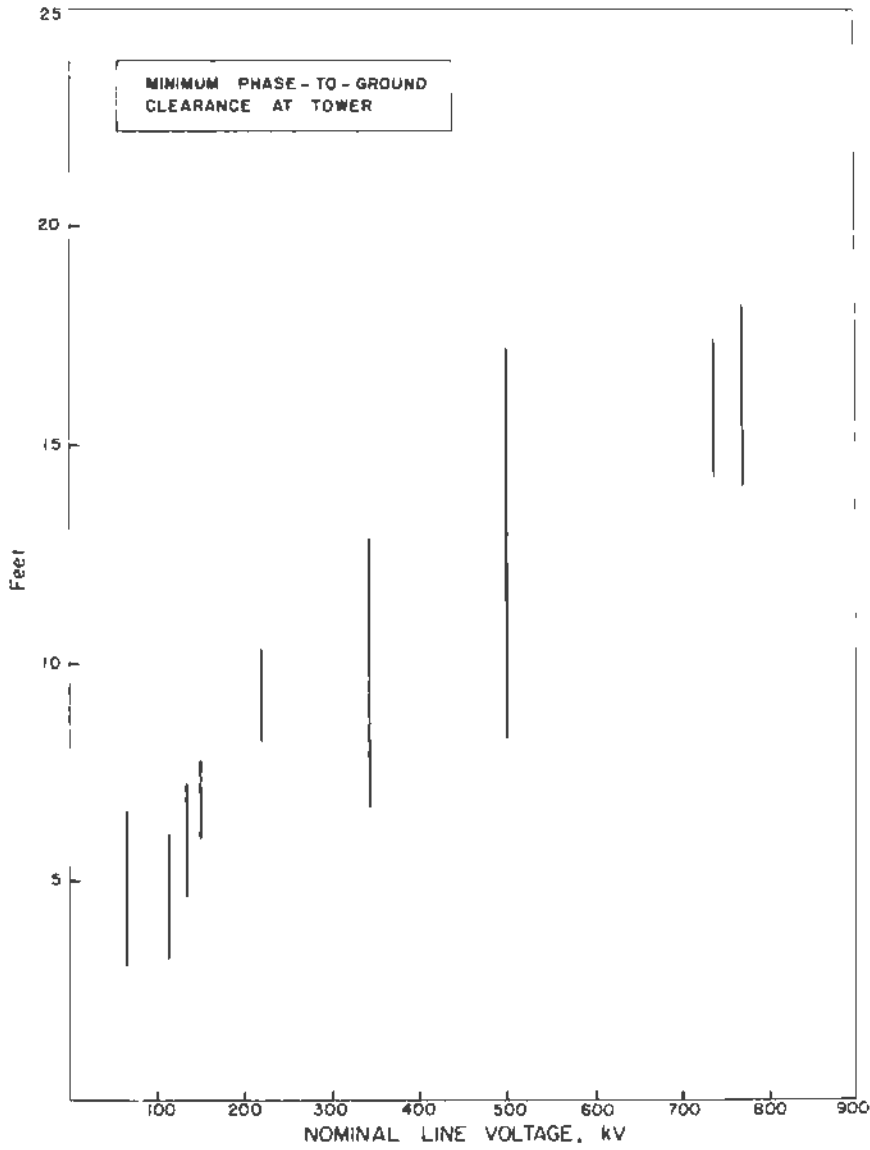


Figure 2-26. Minimum Phase-to-Ground Clearances at Tower for Lines at Nominal Voltage Levels Equal to and Greater Than 69 kV

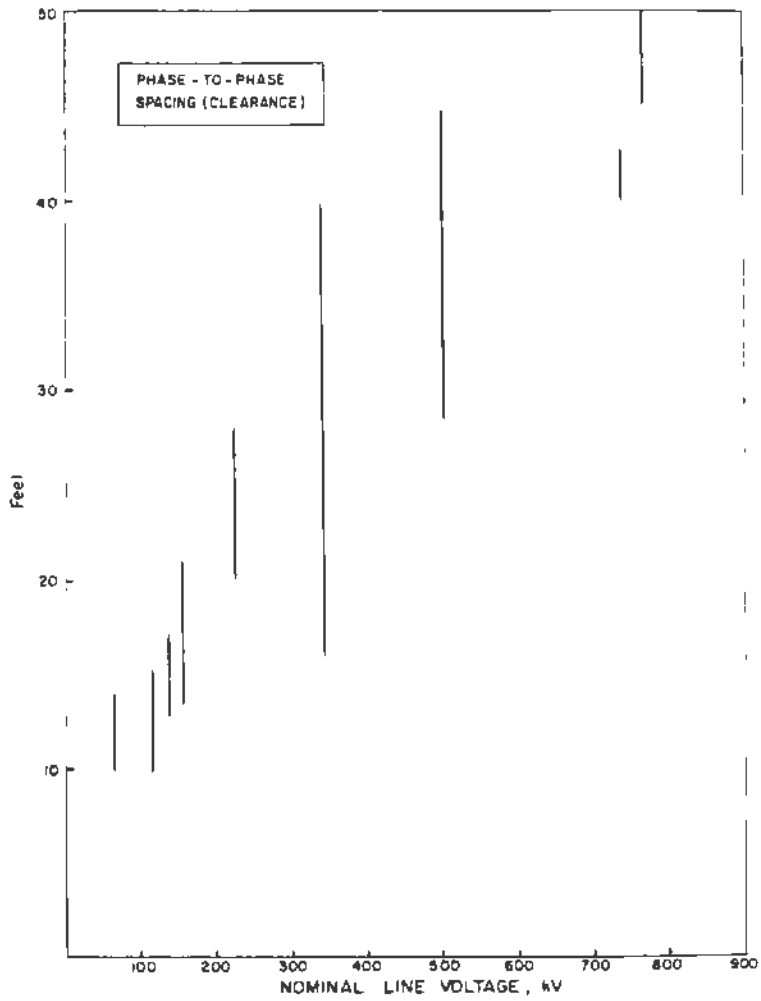


Figure 2-27. Minimum Phase-to-Phase Clearances for Lines at Nominal Voltage Levels Equal To and Greater Than 69 kV

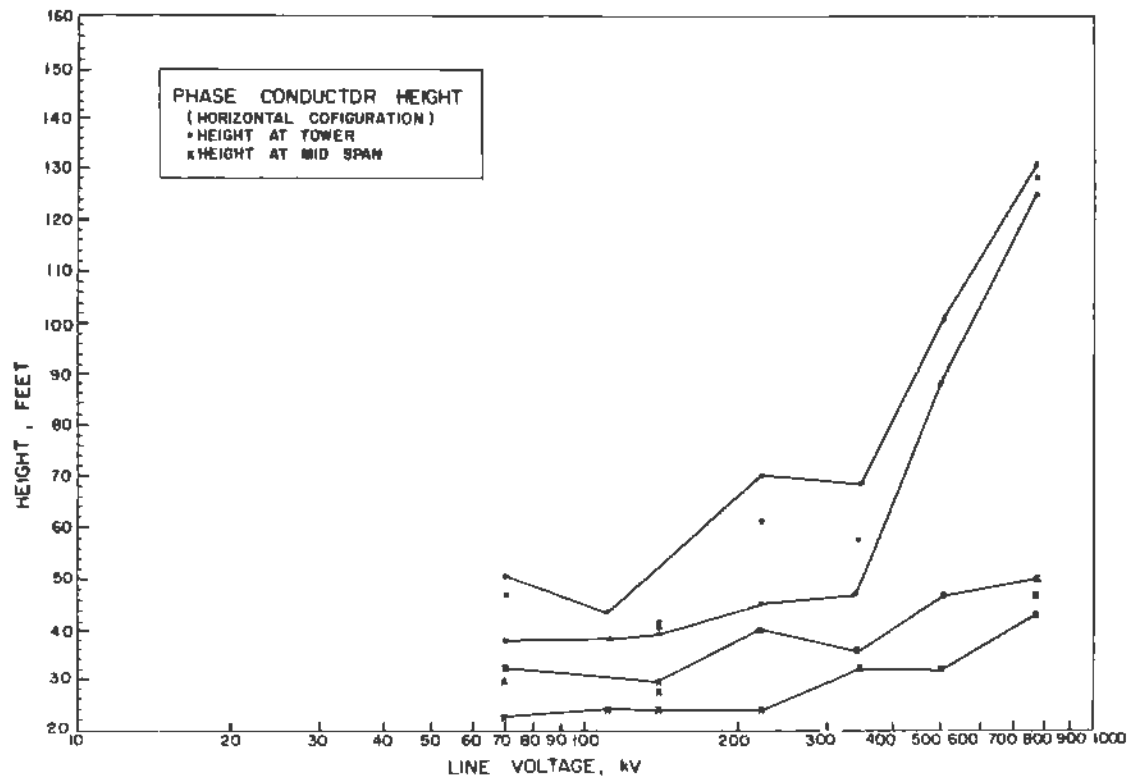


Figure 2-28. Phase Conductor Heights for Transmission Lines at Nominal Voltage Levels Equal To and Greater Than 69 kV

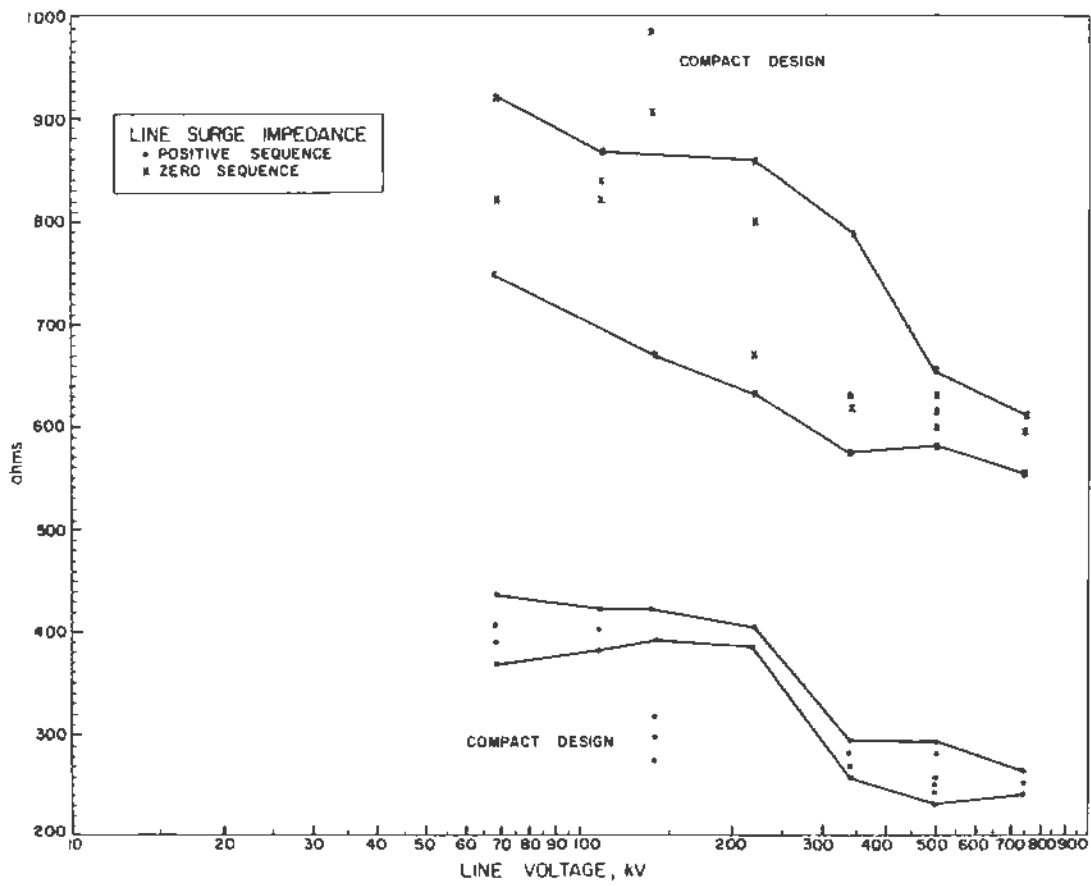


Figure 2-29. Positive and Zero Sequence Surge Impedance for Transmission Lines

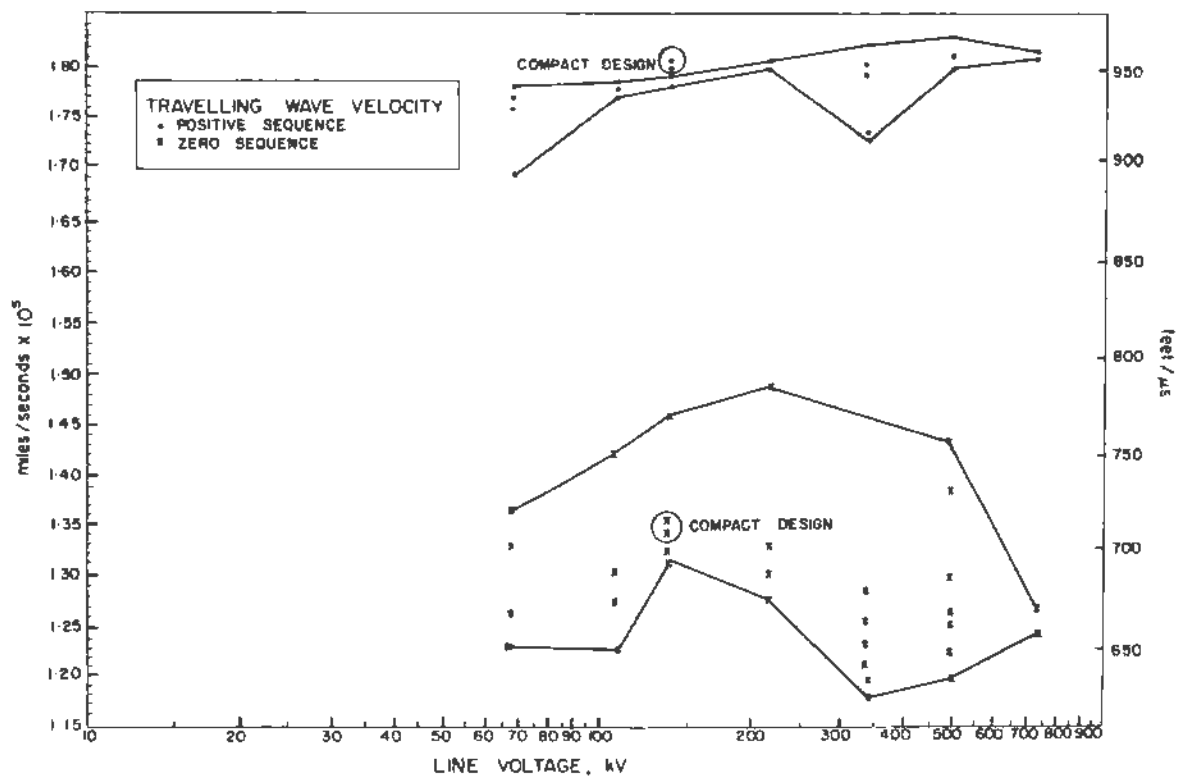


Figure 2-30. Positive and Zero-Sequence Travelling Wave Velocities for Typical Transmission Lines. To be Used in Conjunction with Figure II.A.28 When Using Distributed Parameter Lines (ITYPE = -1, -2, -3).

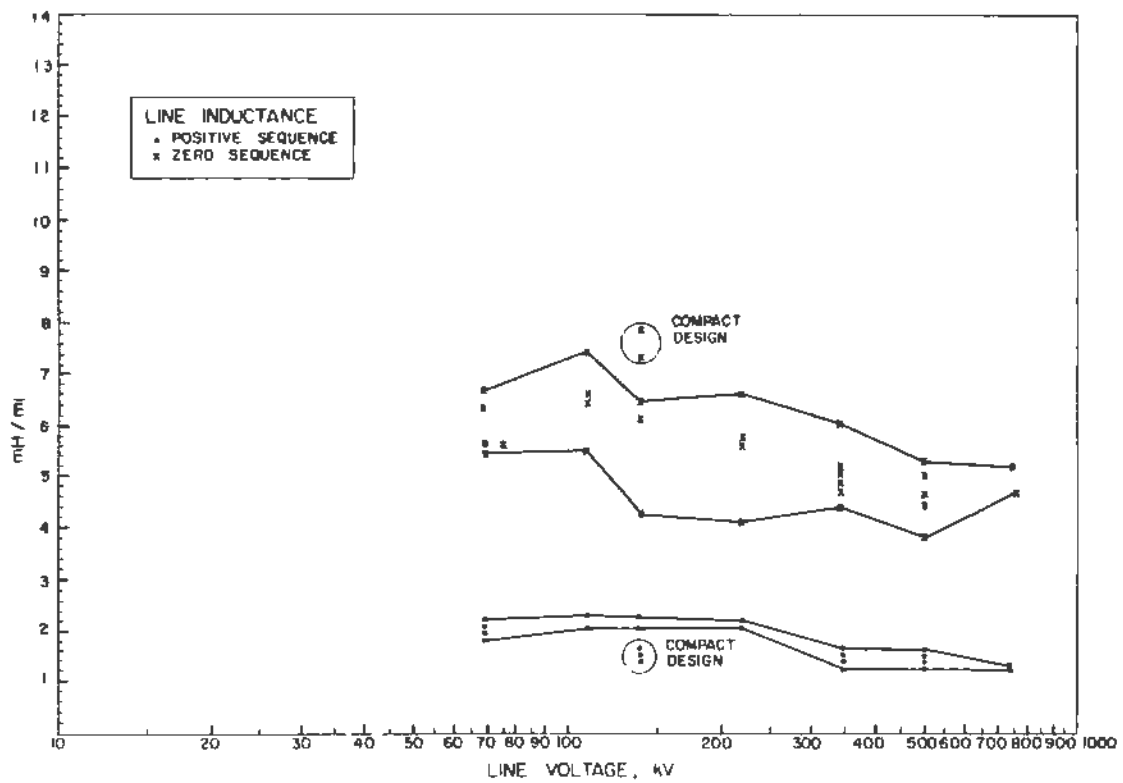


Figure 2-31. Positive and Zero-Sequence Line Inductances for Typical Transmission Lines

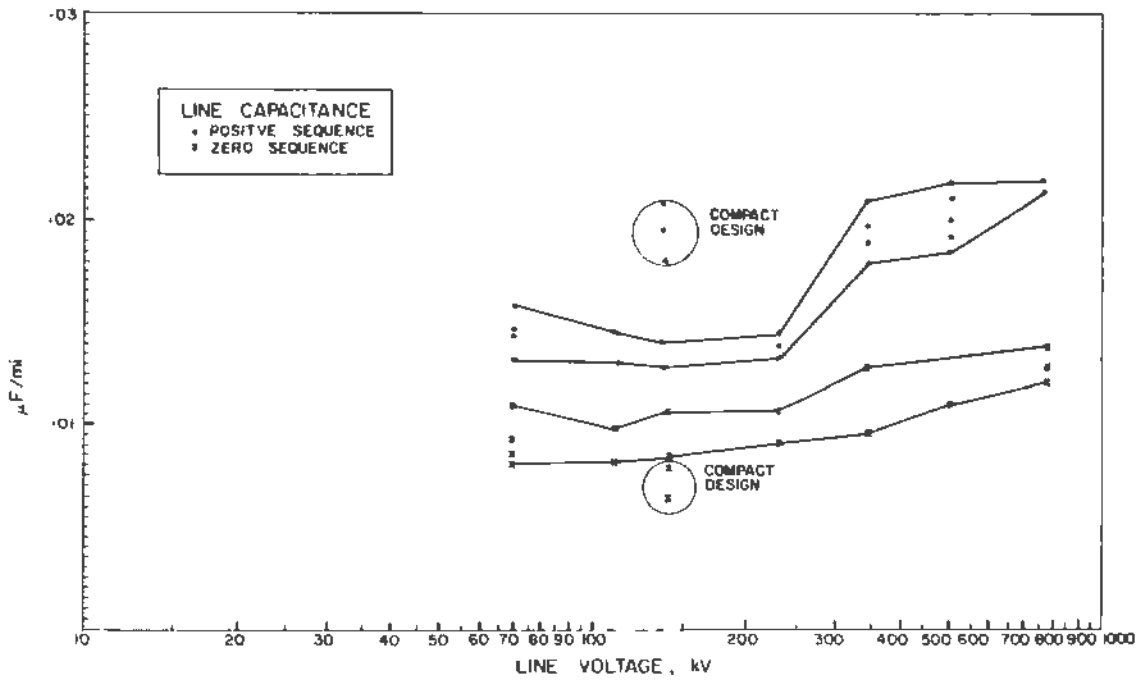


Figure 2-32. Positive and Zero-Sequence Capacitances for Typical Transmission Lines

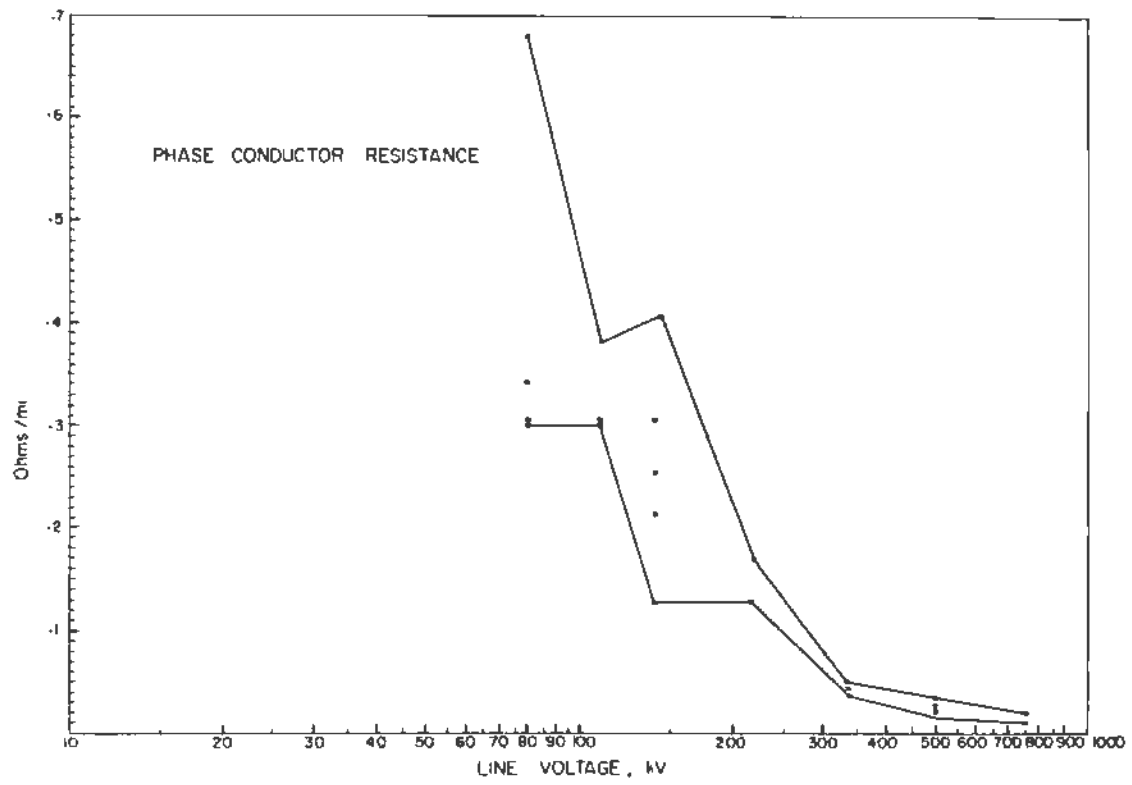


Figure 2-33. DC Resistance of the Phase Conductor (Single or Bundled, as Applicable) for Typical Transmission Lines

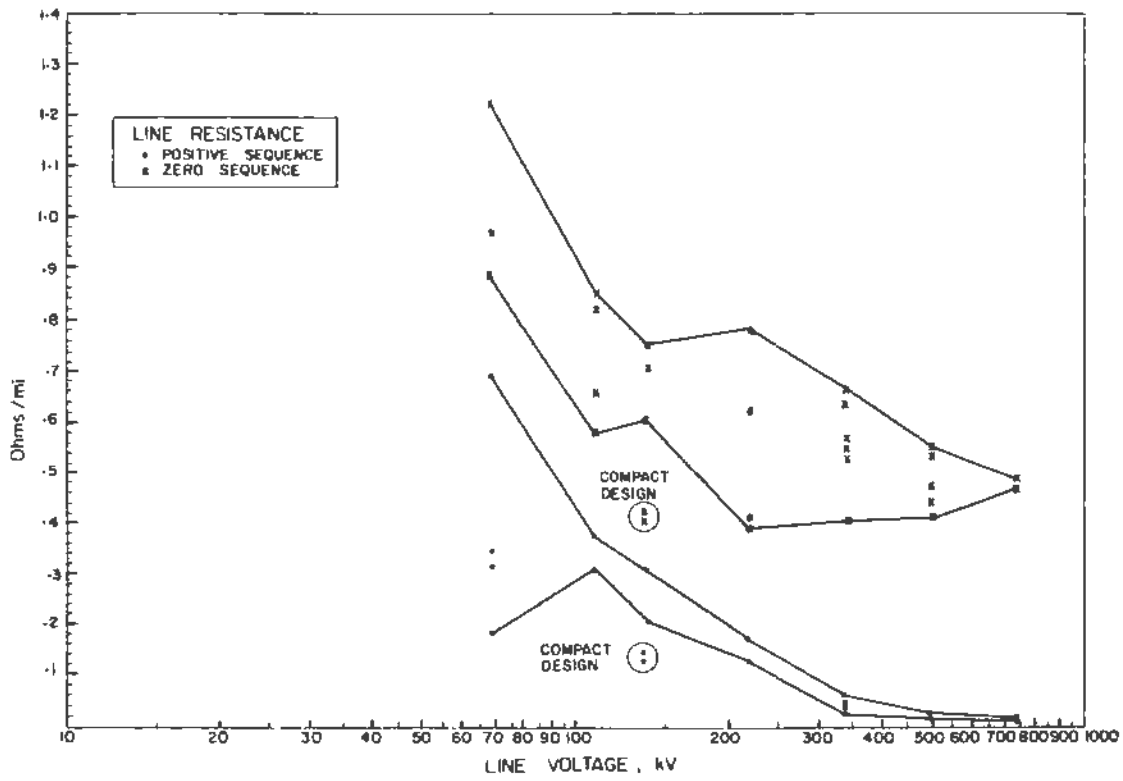


Figure 2-34. Positive and Zero Sequence Resistances for Typical Transmission Lines

2-8. APPENDIX - INPUT FILE LISTINGS

Table 2-3

SETUP FOR A UNIFORMLY DISTRIBUTED TRANSPOSED CONSTANT-PARAMETER
LINE TO BE USED IN EXAMPLE 1

```

C FILE NAME "LINELEE"
C THE LINE CONSTANTS FOR A TYPICAL 500-KV LINE WILL BE CALCULATED
C FOR EXAMPLE 1, TRANSPOSED 500-HZ MODEL
BEGIN NEW DATA CASE
LINE CONSTANTS
C 34567890123456789012345678901234567890123456789012345678901234567890
C COLUMN 1-3: PHASE NUMBER
C COLUMN 17,18: USUALLY A "4"
C COLUMN 80: NUMBER OF CONDUCTORS IN THE BUNDLE
C 4-8 9-16 19-26 27-34 35-42 43-50 51-58 59-66 69-72 73-78
C SKIN RESIS REACT DIAM HORIZ VTOWER VMID SEPAR ALPHA NAME
C
C
1.3636 .05215 4 1.602 -20.75 50. 50.
1.3636 .05215 4 1.602 -19.25 50. 50.
2.3636 .05215 4 1.602 -75 77.5 77.5
2.3636 .05215 4 1.602 .75 77.5 77.5
3.3636 .05125 4 1.602 19.25 50. 50.
3.3636 .05125 4 1.602 20.75 50. 50.
0 5 2.61 4 .386 -12.9 98.5 98.5
0 5 2.61 4 .386 12.9 98.5 98.5
BLANK CARD TERMINATING CONDUCTOR CARDS
C FREQUENCY CARDS
C COLUMN 44: ICAP 0 FOR SHUNT Y OUTPUT, 1 FOR SHUNT C OUTPUT
C COLUMN 58: ISEG 1 FOR SEGMENTED GROUND WIRES, 0 FOR CONTINUOUS WIRES
C COLUMNS 60-62: IDEC NUMBER OF DECADES SPANNED BY FREQUENCY-DEPENDENT
C WEIGHTING AND JMARTI SETUPS
C COLUMNS 63-65: IPNT NUMBER OF POINTS PER DECADE FOR FREQUENCY-DEPENDENT
C WEIGHTING AND JMARTI SETUPS
C COLUMNS 66-68: IPUN 88 FOR "WEIGHTING" SETUP OF ZERO SEQUENCE MODE
C 44 TO PUNCH P1-SECTION CARDS
C COLUMN 70: MODAL 0 FOR TRANSPOSED LINE, NO TI MATRIX OUTPUT
C 1 FOR NONTRANSPOSED LINE, WILL OUTPUT A TI MATRIX
C COLUMNS 71-72: ITPNSF MUST BE -2 FOR MARTI'S MODEL WHEN MODAL=0 TO GET
C REAL TI MATRIX
C 1-8 9-18 19-28 30-35 37-42
C EARTH FREQUENCY CARSON PRINT PRINT
C RESIS HZ ACCURACY (C) (Z)
C 1 2 3 4 5 6 7 8
C 34567890123456789012345678901234567890123456789012345678901234567890
100 500.0 1 111111 111111 1
BLANK CARD TERMINATING FREQUENCY CARDS
BLANK CARD TERMINATING LINE CONSTANTS CASES
BLANK CARD TERMINATING THE CASE

```

Table 2-4

SETUP FOR A UNIFORMLY DISTRIBUTED NONTRANPOSED CONSTANT-PARAMETER
LINE TO BE USED IN EXAMPLE 1

```

C FILE NAME: "LINELEE"
C THE LINE CONSTANTS FOR A TYPICAL 500-KV LINE WILL BE CALCULATED
C FOR EXAMPLE 1, NONTRANPOSED 60-HZ MODEL
BEGIN NEW DATA CASE
LINE CONSTANTS
C 34567890123456789012345678901234567890123456789012345678901234567890
C COLUMN 1-3: PHASE NUMBER
C COLUMN 17,18: USUALLY A "4"
C COLUMN 80: NUMBER OF CONDUCTORS IN THE BUNDLE
C 4-8 9-16 19-26 27-34 35-42 43-50 51-58 59-66 59-72 73-78
C SKIN RESIS REACT DIAM HORIZ VTOWER VMIO SEPAR ALPHA NAME
C
C
1.3636 .05215 4 1.602 -20.75 50 50.
1.3636 .05215 4 1.602 -19.25 50 50.
2.3636 .05215 4 1.602 -.75 77.5 77.5
2.3636 .05215 4 1.602 -.75 77.5 77.5
3.3636 .05125 4 1.602 19.25 50 50.
3.3636 .05125 4 1.602 20.75 50 50.
0.5 2.61 4 .386 -12.9 98.5 98.5
0.5 2.61 4 .386 12.9 98.5 98.5
BLANK CARD TERMINATING CONDUCTOR CARDS
C FREQUENCY CARDS
C COLUMN 44: ICAP 0 FOR SHUNT Y OUTPUT, 1 FOR SHUNT G OUTPUT
C COLUMN 58: ISEG 1 FOR SEGMENTED GROUND WIRES, 0 FOR CONTINUOUS WIRES
C COLUMNS 60-62: IDEC NUMBER OF DECADES SPANNED BY FREQUENCY-DEPENDENT
WEIGHTING AND JMARTI SETUPS
C COLUMNS 63-65: IPNT NUMBER OF POINTS PER DECADE FOR FREQUENCY-DEPENDENT
WEIGHTING AND JMARTI SETUPS
C COLUMNS 66-68: IPUN 88 FOR "WEIGHTING" SETUP OF ZERO SEQUENCE MODE
44 TO PUNCH PI-SECTION CARDS
C COLUMN 70: MODAL 0 FOR TRANPOSED LINE, NO TI MATRIX OUTPUT
1 FOR NONTRANPOSED LINE, WILL OUTPUT A TI MATRIX
C COLUMNS 71-72: ITRANSF MUST BE -2 FOR MARTI'S MODEL WHEN MODAL=0 TO GET
REAL TI MATRIX
C 1-8 9-18 19-28 30-35 37-42
C EARTH FREQUENCY CARSON PRINT PRINT
C RESIS HZ ACCURACY (C) (Z)
C 1 2 3 4 5 6 7 8
C 34567890123456789012345678901234567890123456789012345678901234567890
100. 60.0 1 111111 111111 1
BLANK CARD TERMINATING FREQUENCY CARDS
BLANK CARD TERMINATING LINE CONSTANTS CASES
BLANK CARD TERMINATING THE CASE

```

Table 2-5

MEYER-DDMMEL SETUP FOR A FREQUENCY-DEPENDENT LINE MODEL
TO BE USED IN EXAMPLE 1

```

BEGIN NEW DATA CASE
C FILE NAME: "LINEMD"
C MEYER-DDMMEL SETUP FOR A TYPICAL 500-KV LINE IN EXAMPLE 1
C WITH TRANSPSED ASSUMPTION AND ZERO-SEQUENCE FREQUENCY DEPENDENCE
WEIGHTING
LINE CONSTANTS
C 34567890123456789012345678901234567890123456789012345678901234567890
C COLUMN 1-3: PHASE NUMBER
C COLUMN 17,18: USUALLY A "4"
C COLUMN 80: NUMBER OF CONDUCTORS IN THE BUNDLE
C   4-8   9-16   19-25   27-34   35-42   43-50   51-58   59-66   59-72   73-78
C SKIN   RESIS   REACT   DIAM   HORIZ   VTOWER   VMID   SEPAR ALPHA NAME
C
1 3636 05215 4      1.602  -20.75  50.      50
1.3636 05215 4      1.602  -19.25  50.      50
2.3636 05215 4      1.602  -.75    77.5    77.5
2.3636 05215 4      1.602  -.75    77.5    77.5
3.3636 05125 4      1.602  19.25  50.      50.
3.3636 05125 4      1.602  20.75  50.      50.
0.5    2.61   4      .386   -12.9   98.5    98.5
0.5    2.61   4      .386   12.9    98.5    98.5
BLANK CARD TERMINATING CONDUCTOR CARDS
C FREQUENCY CARDS
C COLUMN 44: ICAP      0 FOR SHUNT Y OUTPUT, 1 FOR SHUNT C OUTPUT
C COLUMN 58: ISEG     1 FOR SEGMENTED GROUND WIRES, 0 FOR CONTINUOUS WIRES
C COLUMNS 60-62: IDEC NUMBER OF DECADES SPANNED BY FREQUENCY-DEPENDENT
C                      WEIGHTING AND JMARTI SETUPS
C COLUMNS 63-65: IPNT NUMBER OF POINTS PER DECADE FOR FREQUENCY-DEPENDENT
C                      WEIGHTING AND JMARTI SETUPS
C COLUMNS 66-68: TPUN 88 FOR "WEIGHTING" SETUP OF ZERO SEQUENCE MODE
C                      44 TO PUNCH PI-SECTION CARDS
C COLUMN 70: MODAL    0 FOR TRANSPSED LINE, NO TI MATRIX OUTPUT
C                      1 FOR NONTRANSPSED LINE, WILL OUTPUT A TI MATRIX
C COLUMNS 71-72: ITPNSF MUST BE -2 FOR MARTI'S MODEL WHEN MODAL=0 TO GET
C                      REAL TI MATRIX
C   1-8   9-18   19-28   30-35   37-42
C EARTH FREQUENCY CARSON PRINT PRINT
C RFSIS   HZ   ACCURACY (C) (Z)
C   1     2     3     4     5     6     7     8
C 34567890123456789012345678901234567890123456789012345678901234567890
C FIRST FREQUENCY CARD IN WEIGHTING SETUP IS NEAR DC
100.    .001    1
C SECOND FREQUENCY CARD IN WEIGHTING SETUP IS AT POWER FREQUENCY
100.    60.0    1
C THIRD FREQUENCY CARD LOOPS OVER 8 DECADES AT 4 POINTS PER DECADE
C STARTING AT 1E-1 HERTZ AND ENDING AT 1E7 HERTZ
100.    1    1
8 4 88
BLANK CARD TERMINATING FREQUENCY CARDS
BLANK CARD TERMINATING LINE CONSTANTS CASE
C LINE LENGTH IN MILES
138.
BLANK INTEGER MISC DATA CARD FOR WEIGHTING (USE DEFAULTS)
BLANK CARD TERMINATING WEIGHTING
BLANK CARD TERMINATING CASE

```

Table 2-6

MARTI SETUP FOR A FREQUENCY-DEPENDENT NONTRANPOSED LINE MODEL TO BE USED IN EXAMPLE 1

```

BEGIN NEW DATA CASE
C FILE NAME, "LINEMARTI"
C MARTI SETUP FOR A TYPICAL 500-KV LINE IN EXAMPLE 1.
C USING NONTRANPOSED ASSUMPTION
JMARTI SETUP
C FOLLOWING CARD INCLUDES NODE NAMES ON THE "PUNCHED-CARD" OUTPUT
C IO LOGICAL UNIT 7
BRANCH SEND AREC ASEND BREC BSEND CREC C
LINE CONSTANTS
C 34567890123456789012345678901234567890123456789012345678901234567890
C COLUMN 1-3: PHASE NUMBER
C COLUMN 17,18, USUALLY A "4"
C COLUMN 80: NUMBER OF CONDUCTORS IN THE BUNDLE
C 4-8 9-16 19-26 27-34 35-42 43-50 51-58 59-66 59-72 73-78
C SKIN RESIS REACT DIAM HORIZ VTOWER VMID SEPAR ALPHA NAME
C
C 1 2 3 4 5 6 7
C 3456789012345678901234567890123456789012345678901234567890123456789
1 3636 .05215 4 1.602 -20.75 50 50
1 3636 .05215 4 1.602 -19.25 50 50
2 3636 .05215 4 1.602 -7.5 77.5 77.5
2 3636 .05215 4 1.602 7.5 77.5 77.5
3 3636 .05125 4 1.602 19.25 50 50
3 3636 .05125 4 1.602 20.75 50 50
0 5 2.61 4 .386 -12.9 98.5 98.5
0 .5 2.61 4 .386 12.9 98.5 98.5
BLANK CARD TERMINATING CONDUCTOR CARDS
C FREQUENCY CARDS
C COLUMN 44: ICAP 0 FOR SHUNT Y OUTPUT, 1 FOR SHUNT C OUTPUT
C COLUMNS 45-52: OIST LINE LENGTH IN MILES, USED ONLY FOR JMARTI SETUP
C COLUMN 58: ISEG 1 FOR SEGMENTED GROUND WIRES, 0 FOR CONTINUOUS WIRES
C COLUMNS 60-62: IOEC NUMBER OF DECADES SPANNED BY FREQUENCY-DEPENDENT
WEIGHTING AND JMARTI SETUPS
C COLUMNS 63-65: IPNT NUMBER OF POINTS PER DECADE FOR FREQUENCY-DEPENDENT
WEIGHTING AND JMARTI SETUPS
C COLUMNS 66-68: IPUN 88 FOR "WEIGHTING" SETUP OF ZERO SEQUENCE MODE
44 TO PUNCH PI-SECTION CARDS
C COLUMN 70: MODAL 0 FOR TRANPOSED LINE, NO TI MATRIX OUTPUT
1 FOR NONTRANPOSED LINE, WILL OUTPUT A TI MATRIX
C COLUMNS 71-72: ITRNSF MUST BE -2 FOR MARTI'S MODEL WHEN MODAL=0 TO GET
REAL TI MATRIX
C 1-8 9-18 19-28 30-35 37-42 45-52
C EARTH FREQUENCY CARSON PRINT PRINT OIST IN
C RESIS HZ ACCURACY (C) (Z) MILES
C 1 2 3 4 5 6 7 8
C 3456789012345678901234567890123456789012345678901234567890123456789
C FIRST FREQUENCY CARD IN NONTRANPOSED JMARTI SETUP IS FOR CALCULATION
OF THE TI MATRIX, AT 5000 HERTZ IN THIS CASE
C THIS CARD IS OMITTED FOR TRANPOSED JMARTI SETUP
100. 5000. 1 138. 1-2
C NEXT FREQUENCY CARD IN JMARTI SETUP IS AT POWER FREQUENCY
100. 60.0 1 138 1
C LAST FREQUENCY CARD IN JMARTI SETUP LDOPS FROM 1E-2 HERTZ
C TO 1E7 HERTZ AT 10 POINTS PER DECADE
100. .01 1 138. 9 10 1
BLANK CARD TERMINATING FREQUENCY CARDS
BLANK CARD TERMINATING LINE CONSTANTS CASE
C THE FOLLOWING CARD INDICATES USE OF THE DEFAULT FITTING PARAMETERS
DEFAULT
BLANK CARD TERMINATING MARTI SETUP
BLANK CARD TERMINATING CASE

```

Table 2-9

TRANSIENT RUN FOR EXAMPLE 1 WITH A UNIFORMLY
DISTRIBUTED TRANSPOSED CONSTANT-PARAMETER LINE MODEL

```

C FILE NAME: LNTL UNIFORMLY DISTRIBUTED, TRANSPOSED, CONSTANT PARAMETER
C LINE MODEL FOR EXAMPLE 1
C RESULTS OF FIELD TEST ARE OBTAINED FROM IEEE PAPER
C NO T74-080-8 BY MEYER AND DOMMEL
C
C A SINGLE LINE TO GROUND FAULT IS APPLIED TO PHASE C OF THE RECEIVING
C END AT 10 15 MS. THIS FAULT IS NOT ALLOWED TO BE CLEARED WITHIN THE TIME
C FRAME OF THIS CASE.
C BEGIN NEW DATA CASE
C FIRST MISCELLANEOUS DATA CARD:
C 34567890123456789012345678901234567890123456789012345678901234567890
C   1-8   9-16  17-24  25-32
C I-STEP  T-MAX  X-OPT  C-OPT
C SECONDS SECONDS  O=MH  O=UF
C           F(HZ)  F(HZ)
50.00E-6   06     0     0
C
C SECOND MISCELLANEOUS DATA CARD
C   1-8   9-16  17-24  25-32  33-40  41-48  49-56  57-64  65-72  73-80
C PRINT  PLOT NETWORK PR. SS  PR. MAX  I PUN  PUNCH  DUMP  MULTI  DIAGNOS
C O=EACH  O=EACH  O= NO  O= NO  O= NO  O= NO  O= NO  INTD  NENERG  PRINT
C K=K-TH  K=K-TH  1=YES  1=YES  1=YES  1=YES  1=YES  DISK  STUDIES  O=NO
C           050     1     1     1     1     1     0     0     1     0
C
C 3456789012345678901234567890123456789012345678901234567890123456789
SEND ASENDXA          .001          3
EQUA ASENDYA          1. E9          3
EQUA ASENDXA          39.8           1
EQUA BSEND B          39.8           4
EQUA CSEND C          39.8           4
C FAULT AT THE RECEIVING END, PHASE C
C   1     2     3     4     5     6     7
C 3456789012345678901234567890123456789012345678901234567890123456789
FAULTCFF          2.0           4
FF              0001           3
C *****
C
C TRANSPOSED LINE MODEL
C
C COLUMN 52: ILINE  0 FOR INPUT OF L AND C PER UNIT LENGTH IN EACH MODE
C                  1 FOR INPUT OF Z AND V FOR EACH MODE
C                  2 FOR INPUT OF Z AND TAU FOR EACH MODE
C COLUMNS 53-54: IPUNCH  0 FOR LUMPED-RESISTANCE LOSSES (CONSTANT PARAMETER)
C                       -1 FOR MEYER-DOMMEL MODEL OF THIS MODE
C                       -2 FOR MARTI MODEL
C COLUMNS 55-56: IPOSE  0 FOR TRANSPOSED LINE
C                       N. NUMBER OF PHASES FOR NONTRANSPOSED LINE
C                       IF N IS NOT ZERO, AN N X N T J MATRIX WILL BE INPUT
C COLUMNS 27-32: SKIP  FOR MARTI MODEL ONLY, 0. FOR FULL INPUT ECHO,
C                       2 FOR SUPPRESSION OF INPUT ECHO (RECOMMENDED)
C
C
C
C
C           FOR ILINE=1.
C           R     Z     V     L
C           1     2     3     4     5     6     7
C 3456789012345678901234567890123456789012345678901234567890123456789
-1SEND AREC  A          564  541  1303E4  138  1
-2SEND BREC  B          .0294  283  5  1823E4  138  1
-3SEND CREC  C
C *****
C
C BLANK CARD TERMINATING BRANCH CARDS
C
C SWITCH CARDS

```

Table 2-9(Cont'd)

TRANSIENT RUN FOR EXAMPLE 1 WITH A UNIFORMLY
DISTRIBUTED TRANSPOSED CONSTANT-PARAMETER LINE MODEL

```

C   3-8  9-14    15-24    25-34    35-44    45-54    55-64    65-74
C                                     (OUTPUT OPTION IN COLUMN 80)
C   NODE NAMES                                IE FLASHOVER  SPECIAL  REFERENCE
C                                     OR  VOLTAGE  REQUEST SWITCH-NAME
C   BUS1  BUS2    CLOSE  OPEN  NSTEP          WORD  BUS5  BUS6
C   REC CFAULTC  01015  .0960
C 3456789012345678901234567890123456789012345678901234567890123456789
BLANK CARD TERMINATING SWITCH CARDS
C SOURCE CARDS
C 34567890123456789012345678901234567890123456789012345678901234567890
C COLUMN 1,2: TYPE OF SOURCE 1 - 17,(E.G. 11-13 ARE RAMP FUNCTIONS, 1A = CDSINE)
C COLUMN 9,10: 0=VOLTAGE SOURCE, -1=CURRENT SOURCE
C   3-8      11-20      21-30      31-40      41-50      51-60      61-70      71-80
C   NODE  AMPLITUDE  FREQUENCY  TD  IN SEC  AMPL-A1  TIME-T1  T-START  T-STOP
C   NAME  IN HZ      IN DEGR  DEGR  SECONDS  SECONDS  SECONDS  SECONDS
14EQUA  A      303000.    60.0      0      0      -1.0
14EQUA  B      303000.    60.0     -120    -1.0
14EQUA  C      303000.    60.0     -240    -1.0
C
BLANK CARD TERMINATING SOURCE CARDS
C NODE VOLTAGE OUTPUT
C 34567890123456789012345678901234567890
SEND ASEND BSEND CREC AREC BREC C
BLANK CARD TERMINATING NODE VOLTAGE OUTPUT
C PLOTTING CARDS
C CALCOMP PLOT 2
C (CASE TITLE UP TO 78 CHARACTERS)
2 EXAMPLE 1, TRANSPOSED 60-HZ MODEL
C THE FOLLOWING IS FORMAT OF THE PLOT REQUEST CARDS
C COLUMN 2, "1"
C COLUMN 3, 4=NODE VOLTAGE
C 8=BRANCH VOLTAGE
C 9=BRANCH CURRENT
C COLUMN 4, UNITS OF HORIZONTAL SCALE 1=DEGREES
C 2=CYCLES
C 3=SEC
C 4=MSEC
C 5=USEC
C COLUMNS 5-7 HORIZONTAL SCALE (UNITS PER INCH)
C COLUMNS 8-11 TIME WHERE PLOT STARTS
C COLUMNS 12-15 TIME WHERE PLOT ENDS
C COLUMNS 16-20 VALUE OF BOTTOM VERTICAL SCALE
C COLUMNS 21-24 VALUE OF TOP VERTICAL SCALE
C COLUMNS 25-48 UP TO FOUR NODE NAMES
C COLUMNS 49-64 GRAPH HEADING LABEL
C COLUMNS 65-80 VERTICAL AXIS LABEL
144 B 80 REC AREC BREC C
144 B, 80. SEND ASEND BSEND C
BLANK CARD TERMINATING PLOT REQUESTS
BLANK CARD TERMINATING THE CASE

```

Table 2-10

TRANSIENT RUN FOR EXAMPLE 1 WITH A UNIFORMLY DISTRIBUTED
NONTRANPOSED CONSTANT-PARAMETER LINE MODEL (LEE'S MODEL)

```

C FILE NAME: LNLEE: UNIFORMLY DISTRIBUTED, NONTRANPOSED, CONSTANT PARAMETER
C LINE MODEL AT 60 HERTZ FOR EXAMPLE 1
C RESULTS OF FIELD TEST ARE OBTAINED FROM IEEE PAPER
C NO 174-080-8 BY MEYER AND DOMMEL
C
C A SINGLE LINE TO GROUND FAULT IS APPLIED TO PHASE C OF THE RECEIVING
C END AT 10 MS. THIS FAULT IS NOT ALLOWED TO BE CLEARED WITHIN THE TIME
C FRAME OF THIS CASE
C BEGIN NEW DATA CASE
C FIRST MISCELLANEDUS DATA CARD:
C 34567890123456789012345678901234567890123456789012345678901234567890
C 1-B 9-16 17-24 25-32
C T-STEP T-MAX X-OPT C-OPT
C SECONDS SECONDS O-MH O-UF
C F(HZ) F(HZ)
C 50.00E-6 .06 0 0
C
C SECOND MISCELLANEDUS DATA CARD
C 1-B 9-16 17-24 25-32 33-40 41-48 49-56 57-64 65-72 73-80
C PRINT PLOT NETWORK PR SS PR MAX I PUN PUNCH DUMP MULT. DIAGNDS
C O=EACH O=EACH O= NO O= NO O= NO O= NO O= NO INTD NENERG PRINT
C K=K-TH K=K-TH 1=YES 1=YES 1=YES 1=YES 1=YES 1=YES DISK STUDIES O=NO
C 20000 1 1 1 1 1 0 0 1 0
C 3456789012345678901234567890123456789012345678901234567890123456789
C EQU L ASEND A 39.8
C EQU L BSEND B 39.8
C EQU L CSEND C 39.8
C FAULT AT THE RECEIVING END, PHASE C
C 1 2 3 4 5 6 7
C 3456789012345678901234567890123456789012345678901234567890123456789
C FAULTC 2 0
C
C *****
C
C NONTRANPOSED LINE MODEL AT 60 HERTZ
C
C COLUMN 52: ILINE 0 FOR INPUT OF L AND C PER UNIT LENGTH IN EACH MODE
C 1 FOR INPUT OF Z AND V FOR EACH MODE
C 2 FOR INPUT OF Z AND TAU FOR EACH MODE
C COLUMNS 53-54: IPUNCH 0 FOR LUMPED-RESISTANCE LOSSES (CONSTANT-PARAMETER)
C -1 FOR MEYER-DOMMEL MODEL OF THIS MODE
C -2 FOR MARTI MODEL
C COLUMNS 55-56: IPOSE 0 FOR TRANPOSED LINE
C N, NUMBER OF PHASES FOR NONTRANPOSED LINE
C IF N IS NOT ZERO, AN N X N TI MATRIX WILL BE INPUT
C COLUMNS 27-32: SKIP 0 FOR MARTI MODEL ONLY, 0. FOR FULL INPUT ECHO,
C 2. FOR SUPPRESSION OF INPUT ECHO (RECOMMENDED)
C
C FOR ILINE=1,
C R Z V L
C 1 2 3 4 5 6 7
C 3456789012345678901234567890123456789012345678901234567890123456789
C -1SEND AREC A .5662 638.7 1304E4 138 1 3
C -2SEND BREC B .028 291 1828E4 138 1 3
C -3SEND CREC C .032 277 1818E4 138 1 3
C
C TI MATRIX
C ALTERNATE ROWS OF REAL AND IMAGINARY ELEMENTS
C 1 2 3 4 5 6 7
C 3456789012345678901234567890123456789012345678901234567890123456789
C .58714 7C314 -.41072
C -.022956 .0050697 -.0046215
C .54864 .0084544 81636
C -.093359 -.0088059 087089

```

Table 2-10 (Cont'd)

TRANSIENT RUN FOR EXAMPLE 1 WITH FOR A UNIFORMLY DISTRIBUTED
NONTRANPOSED CONSTANT-PARAMETER LINE MODEL (LEE'S MODEL)

```

58694      - .71092      - .39613
- 022627   0044579     - .018238
C
C          FND OF LFE S MODEL
C .....
C
BLANK CARD TERMINATING BRANCH CARDS
C
C SWITCH CARDS
C   3-8  9-14      15-24      25-34      35-44      45-54      55-64      65-74
C                                     (OUTPUT OPTION IN COLUMN 80)
C   NODE NAMES      IE FLASHOVER   SPECIAL REFERENCE
C   BUS1  BUS2      TIME TO      TIME TO      OR VOLTAGE   REQUEST SWITCH-NAME
C   REC  CFAULTC  01015      0960      NSTEP      WORD  BUS5  BU56
C 3456789012345678901234567890123456789012345678901234567890123456789
BLANK CARD TERMINATING SWITCH CARDS
C SOURCE CARDS
C 34567890123456789012345678901234567890123456789012345678901234567890
C COLUMN 1,2 TYPE OF SOURCE 1 - 17, I.E. G. 11-13 ARE RAMP FUNCTIONS, 14 = COSINE
C COLUMN 9,10 0=VOLTAGE SOURCE, -1=CURRENT SOURCE
C   3-8      11-20      21-30      31-40      41-50      51-60      61-70      71-80
C   NODE  AMPLITUDE FREQUENCY TO IN SEC  AMPL-A1  TIME-T1  T-START  T-STOP
C   NAME  IN HZ      DEGR      SECONDS  SECONDS  SECONDS  SECONDS
14EQUL A      303000      60.0      0          -1 0
14EQUL B      303000      60.0     -120       -1 0
14EQUL C      303000      60.0    -240       -1 0
C
BLANK CARD TERMINATING SOURCE CARDS
C NODE VOLTAGE OUTPUT
C 34567890123456789012345678901234567890
SEND ASEND BSEND CREC AREC BREC C
BLANK CARD TERMINATING NODE VOLTAGE OUTPUT
C PLOTTING CARDS
C CALCOMP PLDT 2
C (CASE TITLE UP TO 78 CHARACTERS)
2 EXAMPLE 1. NONTRANPOSED 60-HZ MODEL
C THE FOLLOWING IS FORMAT OF THE PLOT REQUEST CARDS
C COLUMN 2. "1"
C COLUMN 3. 4=NODE VOLTAGE
C           8=BRANCH VOLTAGE
C           9=BRANCH CURRENT
C COLUMN 4. UNITS OF HORIZONTAL SCALE 1=DEGREES
C           2=CYCLES
C           3=SEC
C           4=MSEC
C           5=USEC
C COLUMNS 5-7 HORIZONTAL SCALE (UNITS PER INCH)
C COLUMNS 8-11 TIME WHERE PLOT STARTS
C COLUMNS 12-15 TIME WHERE PLOT ENDS
C COLUMNS 16-20 VALUE OF BOTTOM VERTICAL SCALE
C COLUMNS 21-24 VALUE OF TOP VERTICAL SCALE
C COLUMNS 25-48 UP TO FOUR NODE NAMES
C COLUMNS 49-64 GRAPH HEADING LABEL
C COLUMNS 65-80 VERTICAL AXIS LABEL
144 B 80. REC AREC BREC C
144 B 80. SEND ASEND BSEND C
BLANK CARD TERMINATING PLOT REQUESTS
BLANK CARD TERMINATING THE CASE

```

Table 2-11

TRANSIENT RUN FOR EXAMPLE 1 USING MEYER-DDMMEL
FREQUENCY-DEPENDENT LINE MODEL

```

C FILE NAME: " LNMDT " UNIFORMLY DISTRIBUTED, TRANSPOSED, FREQUENCY
C DEPENDENT REPRESENTATION USING MEYER DOMMEL LINE MODEL FOR EXAMPLE 1
C ZERO SEQUENCE FREQUENCY DEPENDENCE ONLY
C RESULTS OF FIELD TEST ARE OBTAINED FROM IEEE PAPER
C NO T74-080-8 BY MEYER AND DOMMEL
C
C A SINGLE LINE TO GROUND FAULT IS APPLIED TO PHASE C OF THE RECEIVING
C END AT 10.15 MS. THIS FAULT IS NOT ALLOWED TO BE CLEARED WITHIN THE TIME
C FRAME OF THIS CASE.
BEGIN NEW DATA CASE
C FIRST MISCELLANEOUS DATA CARD:
C 34567890123456789012345678901234567890123456789012345678901234567890
C 1-B 9-16 17-24 25-32
C T-STEP T-MAX X-DPT C-DPT
C SECONDS SECONDS O=MH O=UF
C F(HZ) F(HZ)
50.00E-6 06 60 0
C
C SECOND MISCELLANEOUS DATA CARD
C 1-B 9-16 17-24 25-32 33-40 41-48 49-56 57-64 65-72 73-80
C PRINT PLDT NETWORK PR.SS PR.MAX I PUN PUNCH DUMP MULT. DIAGNOS
C O=EACH O=EACH O= NO O= NO O= NO O= NO INTO NENERG PRINT
C K=K-TH K=K-TH 1=YES 1=YES 1=YES 1=YES 1=YES 1=YES DISK STUDIES O=NO
C 20000 1 1 1 1 1 0 0 1 0
C 1 2 3 4 5 6 7
C 3456789012345678901234567890123456789012345678901234567890123456789
EQU L ASEND A 15.0
EQU L BSEND B 15.0
EQU L CSEND C 15.0
C FAULT AT THE RECEIVING END, PHASE C
C 1 2 3 4 5 6 7
C 3456789012345678901234567890123456789012345678901234567890123456789
FAULTC 2.0
*****
C
C TRANSPOSED LINE MODEL WITH ZERO-SEQUENCE FREQUENCY DEPENDENCE
C
C COLUMN 52: ILINE 0 FOR INPUT OF L AND C PER UNIT LENGTH IN EACH MODE
C 1 FOR INPUT OF Z AND V FOR EACH MODE
C 2 FOR INPUT OF Z AND YAU FOR EACH MODE
C COLUMNS 53-54: IPUNCH 0 FOR LUMPED-RESISTANCE LOSSES (CONSTANT-PARAMETER)
C -1 FOR MEYER-DDMMEL MODEL OF THIS MODE
C -2 FOR MARTI MODEL
C COLUMNS 55-56: IPOSE 0 FOR TRANSPOSED LINE
C N, NUMBER OF PHASES FOR NONTRANSPOSED LINE
C IF N IS NOT ZERO, AN N X N TI MATRIX WILL BE INPUT
C COLUMNS 27-32: SKIP FOR MARTI MODEL ONLY, 0 FOR FULL INPUT ECHO,
C 2 FOR SUPPRESSION OF INPUT ECHO (RECOMMENDED)
C
C FOR ILINE=1,
C R Z V L
C 1 2 3 4 5 6 7
C 3456789012345678901234567890123456789012345678901234567890123456789
-ISEND AREC A 5641 641 1303E4 108 1-1
C THE FOLLOWING CARDS ARE OBTAINED FROM THE LOGICAL UNIT 7 "PUNCHED-CARD"
C OUTPUT OF A WEIGHTING SETUP
200 309 10 179 445 987 1
694.4590 0.00 709 3643 0.00 724 2695 0.00 739 1748 0.00
754.0800 0.97 768 9853 60.31 783 8905 911.02 798 7957 3332.00
813.7010 6017.61 828 6062 7217.67 843 5115 6952.28 858 4167 5992.08
873.3220 4892.48 888 2272 3917.08 903 1325 3125.47 918 0377 2486.19
932.9430 1980.22 947 8482 1601.51 962 7535 1325.07 977 6587 1110.83
992.5640 934.12 1007 4692 784.94 1022 3745 658.44 1037 2797 557.69
1052.1850 475.21 1067 0902 421.71 1081 9955 383.21 1096 9007 349.40
1111.8060 317.16 1126 7112 285.15 1141 6165 256.41 1156 5217 229.19
1171.4269 206.29 1186 3322 196.28 1201 2374 166.76 1216 1427 148.20
1231.0479 133.42 1245 9532 123.61 1260 8584 118.18 1275 7637 116.07
1290.6689 115.40 1305 5742 113.43 1320 4794 108.98 1335 3847 103.36
1350.2899 98.01 1365 1952 93.10 1380 1004 88.19 1395 0057 83.36
1409.9109 78.40 1424 8162 73.21 1439 7214 68.59 1454 6267 65.53
1469.5319 63.62 1484 4372 61.61 1499 3424 58.80 1514 2477 55.26
1529.1529 51.20 1544 0582 47.32 1558 9534 44.57 1573 8686 43.30
1588.7739 42.84 1603 6791 42.57 1618 5844 42.53 1633 4895 42.90
1648.3949 43.54 1653 3001 44.36 1678 2054 45.16 1693 1106 45.33
1708.0159 44.34 1722 9211 42.47 1737 8264 40.48 1752 7316 38.85
1767.6369 37.65 1782 5421 36.88 1797 4474 36.28 1812 3526 35.45
1827.2579 34.30 1842 1631 33.22 1857 0684 32.43 1871 9736 31.72
1886.8789 30.85 1901 7841 29.81 1916 6894 28.61 1931 5946 27.42
1946.4999 26.63 1961 4051 25.52 1976 3103 26.88 1991 2156 27.23
2006.1208 27.29 2021 0261 27.02 2035 9313 26.42 2050 8366 25.63

```

Table 2-11 (Cont'd)

TRANSIENT RUN FOR EXAMPLE 1 USING MEYER-DOMMEL
FREQUENCY-DEPENDENT LINE MODEL

2065.7418	24.88	2080.6471	24.18	2095.5523	23.32	2110.4576	22.29
2125.3628	21.33	2140.2681	20.72	2155.1733	20.50	2170.0786	20.67
2184.9838	21.08	2199.8891	21.41	2214.7943	21.43	2229.6996	21.26
2244.6048	21.14	2259.5101	21.18	2274.4153	21.34	2289.3206	21.58
2304.2258	21.82	2319.1311	21.97	2334.0363	22.06	2348.9415	22.28
2363.8468	22.61	2378.7520	22.86	2393.6573	22.85	2408.5625	22.60
2423.4678	22.25	2438.3730	22.06	2453.2783	22.34	2468.1835	23.27
2483.0888	24.72	2497.9940	26.41	2512.8993	28.16	2527.8045	29.90
2542.7098	31.52	2557.6150	32.99	2572.5203	34.26	2587.4255	35.20
2602.3308	35.68	2617.2360	35.71	2632.1413	35.50	2647.0465	35.24
2661.9518	35.00	2676.8570	34.80	2691.7623	34.59	2706.6675	34.23
2721.5728	33.67	2736.4780	33.01	2751.3832	32.35	2766.2885	31.72
2781.1937	31.07	2796.0990	30.38	2811.0042	29.66	2825.9095	28.95
2840.8147	28.38	2855.7200	28.07	2870.6252	27.99	2885.5305	28.01
2900.4357	27.97	2915.3410	27.83	2930.2462	27.58	2945.1515	27.25
2960.0567	26.93	2974.9620	26.65	2999.8672	26.34	3004.7725	25.94
3019.6777	25.50	3034.5830	25.10	3049.4882	24.79	3064.3935	24.58
3079.2987	24.43	3094.2040	24.24	3109.1092	23.92	3124.0145	23.47
3138.9197	23.03	3153.8249	22.68	3168.7302	22.43	3183.6354	22.30
3198.5407	22.24	3213.4459	22.20	3228.3512	22.16	3243.2564	22.19
3258.1617	22.30	3273.0669	22.42	3287.9722	22.47	3302.8774	22.39
3317.7827	22.17	3332.6879	21.87	3347.5932	21.59	3362.4984	21.40
3377.4037	21.32	3392.3089	21.26	3407.2142	21.19	3422.1194	21.10
3437.0247	21.01	3451.9299	20.94	3466.8352	20.90	3481.7404	20.88
3496.6457	20.80	3511.5509	20.63	3526.4561	20.44	3541.3614	20.31
3556.2666	20.26	3571.1719	20.29	3586.0771	20.37	3600.9824	20.40
3615.8876	20.33	3630.7929	20.15	3645.6981	19.94	3660.6034	19.70
0.0100	111194.13	0.0102	111125.70	0.0104	111056.02	0.0106	110985.10
0.0108	110912.94	0.0110	110839.54	0.0112	110764.91	0.0114	110689.06
0.0116	110611.98	0.0117	110533.68	0.0119	110454.16	0.0121	110373.75
0.0129	110038.83	0.0137	109684.87	0.0145	109312.16	0.0152	108921.04
0.0160	108511.81	0.0168	108084.81	0.0176	107640.41	0.0183	107178.97
0.0191	106700.87	0.0199	106206.50	0.0207	105696.73	0.0238	103505.63
0.0269	101095.97	0.0300	98498.28	0.0331	95744.80	0.0362	92868.82
0.0393	89904.08	0.0424	86884.16	0.0455	83841.91	0.0486	80808.84
0.0517	77814.66	0.0548	74887.10	0.0672	64285.27	0.0795	56129.23
0.0920	50601.75	0.1044	47172.88	0.1168	44952.77	0.1292	43086.88
0.1416	41044.33	0.1540	38713.30	0.1664	36307.35	0.1788	34159.96
0.1912	32517.46	0.2409	29373.66	0.2905	25094.45	0.3401	22647.20
0.3897	20750.34	0.4394	19685.17	0.4890	17820.95	0.5386	16459.28
0.5882	15311.92	0.6378	14643.13	0.6875	13879.37	0.7371	13186.35
0.9356	10988.89	1.1341	9508.95	1.3326	8649.66	1.5310	7640.49
1.7295	6737.90	1.9280	6140.20	2.1265	5726.65	2.3250	5446.14
2.5235	5149.56	2.7220	4729.98	2.9205	4340.12	3.1144	3529.61
4.5084	3103.41	5.3024	2534.24	6.0963	2205.54	6.8903	2004.05
7.6842	1903.55	8.4782	1701.55	9.2721	1498.11	10.0661	1362.40
10.8601	1271.39	11.6540	1212.00	14.8299	1006.51	18.0057	770.66
21.1815	672.20	24.3574	629.53	27.5332	535.47	30.7090	464.02
33.8849	416.43	37.0607	392.42	40.2366	370.65	43.4124	363.38
46.5882	336.57	59.2916	249.39	71.9949	220.07	84.6983	197.24
97.4016	167.20	110.1050	151.91	122.8083	142.00	135.5117	141.09
148.2150	131.69	160.9184	118.05	173.6217	112.57	186.3251	107.29
237.1385	98.66	287.9519	85.01	338.7653	78.02	389.5786	73.61
440.3920	71.71	451.2054	66.87	542.0188	63.13	592.8022	60.22
643.6456	58.11	694.4590	55.57	709.3643	55.14	724.2695	54.85
733.1748	54.69	754.0800	54.50	768.9853	54.16	783.8905	53.56
798.7957	53.16	813.7010	52.60	828.6062	52.12	843.5115	51.31
858.4167	50.73	873.3220	49.81	888.2272	49.11	903.1325	48.22
918.0377	47.86	932.9430	47.21	947.8482	46.87	962.7535	46.18
977.6587	45.86	992.5640	45.14	1007.4692	44.80	1022.3745	44.20
1037.2797	44.04	1052.1850	43.45	1067.0902	43.22	1081.9955	42.70
1096.9007	42.62	1111.8060	42.21	1126.7112	42.24	1141.6165	41.98
1156.5217	41.98	1171.4269	41.52	1186.3322	41.30	1201.2374	40.74
1216.1427	40.42	1231.0479	39.77	1245.9532	39.43	1260.8584	38.86
1275.7637	38.52	1290.6689	38.01	1305.5742	37.85	1320.4794	37.63
1335.3847	37.67	1350.2899	37.58	1365.1952	37.63	1380.1004	37.38
1395.0057	37.05	1409.9109	36.49	1424.8162	36.02	1439.7214	35.53
1454.6267	35.24	1469.5319	35.01	1484.4372	34.79	1499.3424	34.41
1514.2477	34.00	1529.1529	33.63	1544.0582	33.27	1558.9634	32.81
1573.8686	31.41	1588.7739	25.44	1603.6791	7.84	1618.5844	-26.45
1633.4896	-75.17	1648.3949	-129.32	1663.3001	-179.13	1678.2054	-217.77
1693.1106	-242.38	1708.0159	-255.39	1722.9211	-257.55	1737.9264	-252.01
1752.7316	-241.55	1767.6369	-228.17	1782.5421	-213.73	1797.4474	-198.97
1812.3526	-184.67	1827.2579	-170.87	1842.1631	-158.01	1857.0684	-145.99
1871.9736	-135.16	1886.8789	-125.38	1901.7841	-116.86	1916.6894	-109.19
1931.5946	-102.48	1946.4999	-96.33	1961.4051	-90.89	1976.3103	-85.80
1991.2156	-81.22	2006.1208	-76.91	2021.0261	-73.03	2035.9313	-69.34
2050.8366	-66.07	2065.7418	-63.08	2080.6471	-60.54	2095.5523	-58.23
2110.4576	-56.28	2125.3628	-54.48	2140.2681	-52.90	2155.1733	-51.37
2170.0786	-50.00	2184.9838	-48.65	2199.8891	-47.39	2214.7943	-46.12
2229.6996	-44.93	2244.6048	-43.77	2259.5101	-42.69	2274.4153	-41.64

Table 2-11 (Cont'd)

TRANSIENT RUN FOR EXAMPLE 1 USING MEYER-DDMMEL
 FREQUENCY-DEPENDENT LINE MDEL

2289.3206	-40.69	2304.2258	-39.76	2319.1311	-38.86	2334.0363	-37.98
2348.9415	-37.14	2363.8468	-36.34	2378.7520	-35.58	2393.6573	-34.89
2408.5625	-34.25	2423.4678	-33.70	2438.3730	-33.17	2453.2783	-32.74
2468.1835	-32.35	2483.0888	-32.02	2497.9940	-31.67	2512.8993	-31.37
2527.8045	-31.01	2542.7098	-30.68	2557.6150	-30.30	2572.5203	-29.99
2587.4255	-29.62	2602.3308	-29.31	2617.2360	-28.94	2632.1413	-28.65
2647.0465	-28.30	2661.9518	-28.02	2676.8570	-27.69	2691.7623	-27.43
2706.6675	-27.10	2721.5728	-26.82	2736.4780	-26.49	2751.3832	-26.24
2766.2885	-25.94	2781.1937	-25.73	2796.0990	-25.47	2811.0042	-25.29
2825.9095	-25.03	2840.8147	-24.83	2855.7200	-24.58	2870.6252	-24.38
2885.5305	-24.11	2900.4357	-23.89	2915.3410	-23.61	2930.2462	-23.38
2945.1515	-23.10	2960.0567	-22.89	2974.9620	-22.67	2989.8672	-22.49
3004.7725	-22.29	3019.6777	-22.13	3034.5830	-21.95	3049.4882	-21.80
3064.3935	-21.63	3079.2987	-21.50	3094.2040	-21.37	3109.1092	-21.23
3124.0145	-21.10	3138.9197	-20.98	3153.8249	-20.87	3168.7302	-20.75
3183.6354	-20.64	3198.5407	-20.52	3213.4459	-20.40	3228.3512	-20.24
3243.2564	-20.09	3258.1617	-19.94	3273.0669	-19.81	3287.9722	-19.66
3302.8774	-19.56	3317.7827	-19.45	3332.6879	-19.38	3347.5932	-19.30
3362.4984	-19.27	3377.4037	-19.22	3392.3089	-19.19	3407.2142	-19.13
3422.1194	-19.10	3437.0247	-19.01	3451.9299	-18.95	3466.8352	-18.86
3481.7404	-18.80	3496.6457	-18.70	3511.5509	-18.62	3526.4561	-18.50
3541.3614	-18.41	3556.2666	-18.27	3571.1718	-18.16	3586.0771	-18.02
3600.9824	-17.91	3615.8876	-17.75	3630.7929	-17.63	3645.6981	-17.49
3650.6034	-17.38						

C THE NEXT TWO LINE MODEL CARDS ARE THE SAME AS FOR THE
 C CONSTANT-PARAMETER TRANSDUCED LINE MODEL
 -2SEND BREC B 0294 289 5 1823E4 138 1
 -3SEND CREC C
 C END OF MEYER-DDMMEL SETUP
 BLANK CARD TERMINATING BRANCH CARDS
 C
 C SWITCH CARDS
 C 3-8 9-14 15-24 25-34 35-44 45-54 55-64 65-74
 C (OUTPUT OPTION IN COLUMN 80)
 C NODE NAMES IE FLASHOVER SPECIAL REFERENCE
 C DR VOLTAGE REQUEST SWITCH-NAME
 C BUS1 BUS2 CLOSE OPEN NSTEP WORD BUS5 BUS6
 REC CFAULTC .01015 .0960
 C 34567890123456789012345678901234567890123456789012345678901234567890
 BLANK CARD TERMINATING SWITCH CARDS
 C SOURCE CARDS
 C 34567890123456789012345678901234567890123456789012345678901234567890
 C COLUMN 1,2: TYPE OF SOURCE 1 = 17, (E.G. 11-13 ARE RAMP FUNCTIONS, 14 = COSINE)
 C COLUMN 9,10: 0=VOLTAGE SOURCE, -1=CURRENT SOURCE
 C 3-8 11-20 21-30 31-40 41-50 51-60 61-70 71-80
 C NODE AMPLITUDE FREQUENCY TO IN SEC AMPL-A1 TIME-T1 T-START T-STOP
 C NAME IN HZ DEGR SECONDS SECONDS SECONDS
 14EQU A 303000. 60.0 0. -1.0
 14EQU B 303000. 60.0 -120. -1.0
 14EQU C 303000. 60.0 -240. -1.0
 C
 BLANK CARD TERMINATING SOURCE CARDS
 C NODE VOLTAGE OUTPUT
 C 34567890123456789012345678901234567890
 SEND ASEND BSEND CREC AREC BREC C
 BLANK CARD TERMINATING NODE VOLTAGE OUTPUT
 C PLOTTING CARDS
 C CALCOMP PLOT 2
 C (CASE TITLE UP TO 78 CHARACTERS)
 2 EXAMRLE 1, MEYER-DDMMEL MODEL
 C THE FOLLOWING IS FORMAT OF THE PLOT REQUEST CARDS
 C COLUMN 2, "1"
 C COLUMN 3, 4=NODE VOLTAGE
 C 8=BRANCH VOLTAGE
 C 9=BRANCH CURRENT
 C COLUMN 4, UNITS OF HORIZONTAL SCALE 1=DEGREES
 C 2=CYCLES
 C 3=SEC
 C 4=MSEC
 C 5=USEC
 C COLUMNS 5-7 HORIZONTAL SCALE (UNITS PER INCH)
 C COLUMNS 8-11 TIME WHERE PLOT STARTS
 C COLUMNS 12-15 TIME WHERE PLOT ENDS
 C COLUMNS 16-20 VALUE OF BOTTOM VERTICAL SCALE
 C COLUMNS 21-24 VALUE OF TOP VERTICAL SCALE
 C COLUMNS 25-48 UP TO FOUR NODE NAMES
 C COLUMNS 49-64 GRAPH HEADING LABEL
 C COLUMNS 65-80 VERTICAL AXIS LABEL
 144 B. 80. REC AREC BREC C
 144 B. 80. SEND ASEND BSEND C
 BLANK CARD TERMINATING PLOT REQUESTS
 BLANK CARD TERMINATING THE CASE

Table 2-12

TRANSIENT RUN FOR EXAMPLE 1 USING MARTI
 FREQUENCY-DEPENDENT TRANSPOSED LINE MODEL

```

C FILE NAME: LNMRT: UNIFORMLY DISTRIBUTED, TRANSPOSED, FREQUENCY
C DEPENDENT REPRESENTATION USING MARTI'S LINE MODEL IN EXAMPLE 1
C RESULTS OF FIELD TEST ARE OBTAINED FROM IEEE PAPER
C NO T74-080-8 BY MEYER AND DOMMEL
C
C A SINGLE LINE TO GROUND FAULT IS APPLIED TO PHASE C OF THE RECEIVING
C END AT 10.15 MS THIS FAULT IS NOT ALLOWED TO BE CLEARED WITHIN THE TIME
C FRAME OF THIS CASE
C BEGIN NEW DATA CASE
C FIRST MISCELLANEOUS DATA CARD.
C 34567890123456789012345678901234567890123456789012345678901234567890
C   1-8   9-16  17-24  25-32
C T-STEP T-MAX X-DPT C-DPT
C SECNOS SECONDS O=MH O=UF
C           F(HZ)  F(HZ)
50.00E-6   .06   50.   0
C
C SECOND MISCELLANEOUS DATA CARD
C   1-8   9-16  17-24  25-32  33-40  41-48  49-56  57-64  65-72  73-80
C PRINT PLOT NETWORK PR 55 PR MAX I PUN PUNCH DUMP MULT DIAGNDS
C O=EACH O=EACH O= NO O= NO O= NO O= NO O= NO INTO NENERG PRINT
C K=K-TH K=K-TH 1=YES 1=YES 1=YES 1=YES 1=YES DISK STUDIES O=NO
   20000      1      1      1      1      0      0      1      1      0
C
C   1      2      3      4      5      6      7
C 3456789012345678901234567890123456789012345678901234567890123456789
EQUIL ASEND A      15.0
EQUIL BSEND B      15.0
EQUIL CSEND C      15.0
C FAULT AT THE RECEIVING END, PHASE C
C   1      2      3      4      5      6      7
C 3456789012345678901234567890123456789012345678901234567890123456789
FAULTC      2.0
C
C TRANSPOSED MARTI LINE MODEL
C
C THE LOGICAL UNIT ? "PUNCHED-CARD" OUTPUT OF A JMARTI SETUP INCLUDES THE
C FOLLOWING ECHO OF THE LINE CONSTANTS INPUT DATA
C
C PUNCHED CARD OUTPUT OF "JMARTI SETUP" WHICH BEGAN AT 07:40:00 08/20/86
C 1.3636 .05215 4 1.602 -20.75 50. 50.
C 1.3636 .05215 4 1.602 -19.25 50. 50.
C 2.3636 .05215 4 1.602 .75 77.5 77.5
C 2.3636 .05215 4 1.602 .75 77.5 77.5
C 3.3636 .05125 4 1.602 19.25 50. 50.
C 3.3636 .05125 4 1.602 20.75 50. 50.
C 0.5 2.61 4 .386 -12.9 98.5 98.5
C 0.5 2.61 4 .386 12.9 98.5 98.5
C
C 100. 60.0 1 138. 1 0
C 100. 01 1 138. 1 9 10 0
C
C COLUMNS 53-54: IPUNCH 0 FOR LUMPED-RESISTANCE LOSSES (CONSTANT-PARAMETER)
C -1 FOR MEYER-DOMMEL MODEL OF THIS MODE
C -2 FOR MARTI MODEL
C COLUMNS 55-56: IPOSE 0 FOR TRANSPOSED LINE
C N, NUMBER OF PHASES FOR NONTRANSPOSED LINE
C IF N IS NOT ZERO, AN N X N T1 MATRIX WILL BE INPUT
C COLUMNS 27-32: SKIP FOR MARTI MODEL ONLY, 0. FOR FULL INPUT ECHO,
C 2. FOR SUPPRESSION OF INPUT ECHO (RECOMMENDED)
C
C   1      2      3      4      5      6      7
C 3456789012345678901234567890123456789012345678901234567890123456789
-1SEND AREC A      2. -2
   17 0 47451827929384489834E+03
-0.117280677200854910E+01 -0.327280220926280662E+01 -0.101011460882380674E+02
    
```

Table 2-12 (Cont'd)

TRANSIENT RUN FOR EXAMPLE 1 USING MARTI
FREQUENCY-DEPENDENT TRANSPDSED LINE MDEL

```

-0 244832503757004360E+02 -0 120985031296926990E+03 0 130135442657187377E+04
0 587125218452641274E+04 0 316954878555831965E+05 0 100827179836694151E+06
0 164949745502145588E+07 0 779308815921717882E+07 0 141201591057665944E+08
0 264045258237400054E+08 0 997078440304487943E+07 0 222569184234302043E+08
0 297130796350537538E+08 0 476757389647240638E+08
0 312339952010773913E+00 0 905908981294849979E+00 0 160846467144267535E+01
0 196074489935897844E+01 0 241149368828202170E+01 0 203227805940717871E+02
0 124008524754663540E+03 0 707230498805248226E+03 0 246911548574706830E+04
0 219948313839646289E+05 0 229310271622575819E+06 0 886938567203734070E+06
0 335327854953779280E+07 0 525548301790785789E+07 0 114825443797491192E+08
0 155532854419242739E+08 0 252577090434361696E+08
13 0 8676499707795555160E-03
0 548860304792078146E-01 0 270215295450645598E+00 0 367050860320457417E+00
0 797755155305289065E+00 0 390073991956225540E+01 0 114998077936546110E+02
0 646852894162889242E+02 0 363211358042552092E+03 0 136342935896832204E+04
0 925181415229431877E+03 0 442935452080323011E+04 0 420091991679456550E+05
0 164139493613499999E+08 -0 164631223129197955E+08
0 215698813095414152E+02 0 102855777242496060E+03 0 142075955392425132E+03
0 275106438085345871E+03 0 347238096713441336E+03 0 518752252370566566E+03
0 124856763804709771E+04 0 266934723538784601E+04 0 449603907944451202E+04
0 620257474557743989E+04 0 110439473599084303E+05 0 273488804550659118E+05
0 201209147800548234E+05 0 201410356948336120E+05
-2SEND BREC B 2 -2
13 0 27318408871936480863E+03
0 223251478525677521E+04 -0 115099593419909059E+04 0 558984152406424982E+03
0 130455458196277504E+03 0 805896654965072229E+02 0 135899071341194940E+03
0 634158442765094605E+02 0 674214110490761413E+02 0 103157960715124772E+03
0 229360333306409302E+04 0 335051942848868202E+04 0 610447048386642709E+05
0 258364383836477994E+07 0 371389583212514651E+01 0 740696447731448870E+01
0 339145798939918563E+01 0 135604963835547209E+02 0 237116653593797082E+02
0 104642864508485899E+02 0 730430189218600389E+02 0 109418113924930366E+03
0 383083915332563265E+02 0 327612183402094524E+04 0 591999282200587913E+05
0 218993045825045555E+04
0 251368194157055020E+07
20 0 74599757394747806538E-03
0 181858848956385488E-01 0 331566863826618885E-01 0 319192389464984671E+01
0 570358929665571045E+01 0 764381878023101535E+01 0 117991708479343060E+02
0 179947692057775157E+02 0 514515900363599030E+02 0 361254238938807247E+03
0 207208548732903727E+04 0 257280679718424798E+05 0 285428326613020617E+05
0 132103697982693463E+07 -0 122866159766508638E+07 0 323217251252388581E+06
0 604109472211927175E+06 -0 562959409755119323E+09 -0 553248695570976257E+09
0 346055391419599533E+09 -0 356842613068454742E+09
0 748555664723940594E+01 0 129364870752799470E+01 0 136603575045245815E+04
0 231637065536323643E+04 0 313894493420961953E+04 0 478985602195386309E+04
0 729494792026357026E+04 0 214077248189528472E+05 0 174056935807927511E+05
0 476247360044827219E+05 0 170995294086223468E+06 0 230041899438361637E+06
0 345403344186253845E+06 0 346917639953350648E+06 0 676302136565778404E+06
0 921180737239833921E+06 0 205335711417751759E+07 0 205541047129156440E+07
0 180516879910421134E+07 0 180697396820349991E+07
-35END CREC C 2 -2
13 0 27918408871936480863E+03
0 223251478525677521E+04 -0 115099593419909069E+04 0 558984152406424982E+03
0 130455458196277504E+03 0 805896654965072229E+02 0 135899071341194940E+03
0 634158442765094605E+02 0 674214110490761413E+02 0 103157960715124772E+03
0 229360333306409302E+04 0 335051942848868202E+04 0 610447048386642709E+05
0 258364383836477994E+07 0 371389583212514651E+01 0 740696447731448870E+01
0 339145798939918563E+01 0 135604963835547209E+02 0 237116653593797082E+02
0 104642864508485899E+02 0 730430189218600389E+02 0 109418113924930366E+03
0 383083915332563265E+02 0 327612183402094524E+04 0 591999282200587913E+05
0 218993045825045555E+04
0 251368194157055020E+07
20 0 74599757394747806538E-03
0 181858848956385488E-01 0 331566863826618885E+01 0 319192389464984671E+01
0 570368929665571045E+01 0 764381878023101535E+01 0 117991706479313060E+02
0 179947692057775157E+02 0 514515900363599030E+02 0 361254238938807247E+03
0 207208548732903727E+04 0 257280679718424798E+05 0 285428326613020617E+05
0 132103697982693463E+07 -0 122866159766508638E+07 0 323217251252388581E+06
0 604109472211927175E+06 -0 562959409755119323E+09 -0 553248695570976257E+09
0 346055391419599533E+09 -0 356842613068454742E+09
0 748555664723940594E+01 0 129364870752799470E+01 0 136603575045245815E+04
0 231637065536323643E+04 0 313894493420961953E+04 0 478985602195386309E+04
0 729494792026357026E+04 0 214077248189528472E+05 0 174056935807927511E+05
0 476247360044827219E+05 0 170995294086223468E+06 0 230041899438361637E+06
0 345403344186253845E+06 0 346917639953350648E+06 0 676302136565778404E+06
0 921180737239833921E+06 0 205335711417751759E+07 0 205541047129156440E+07
0 180516879910421134E+07 0 180697396820349991E+07
-35END CREC C 2 -2
13 0 27918408871936480863E+03
0 223251478525677521E+04 -0 115099593419909069E+04 0 558984152406424982E+03
0 130455458196277504E+03 0 805896654965072229E+02 0 135899071341194940E+03
0 634158442765094605E+02 0 674214110490761413E+02 0 103157960715124772E+03
0 229360333306409302E+04 0 335051942848868202E+04 0 610447048386642709E+05
0 258364383836477994E+07 0 371389583212514651E+01 0 740696447731448870E+01
0 339145798939918563E+01 0 135604963835547209E+02 0 237116653593797082E+02
0 104642864508485899E+02 0 730430189218600389E+02 0 109418113924930366E+03
0 383083915332563265E+02 0 327612183402094524E+04 0 591999282200587913E+05
0 218993045825045555E+04
0 251368194157055020E+07
20 0 74599757394747806538E-03
0 181858848956385488E-01 0 331566863826618885E+01 0 319192389464984671E+01
0 570368929665571045E+01 0 764381878023101535E+01 0 117991706479313060E+02
0 179947692057775157E+02 0 514515900363599030E+02 0 361254238938807247E+03
0 207208548732903727E+04 0 257280679718424798E+05 0 285428326613020617E+05

```

Table 2-12 (Cont'd)

TRANSIENT RUN FOR EXAMPLE 1 USING MARTI
FREQUENCY-DEPENDENT TRANPOSED LINE MODEL

```

O. 132103697982693463E+07 -O 122866159766508638E+07 O 923217251252388581E+06
O. 604109472211927176E+06 O 562959409755119323E+09 -O. 553248695570976257E+09
O. 346055391419599533E+09 -O 356842613068454742E+09
O. 748555664723940594E+01 O. 129364870752799470E+04 O. 136603575045245815E+04
O. 231637065536323643E+04 O 313894493420961953E+04 O. 478985602195386309E+04
O. 729494792026357026E+04 O. 214077248189528472E+05 O. 174056935807927511E+05
O. 476247360044827219E+05 O. 170995294086223458E+06 O. 230041899438361637E+06
O. 345403344186253845E+06 O 346917639953350648E+06 O. 676302136565778404E+06
O. 921180737239833921E+06 O. 205335711417751759E+07 O. 205541047129156440E+07
O. 180516879940421134E+07 O. 180697396820349991E+07
C
C END OF MARTI LINE MODEL INPUT
C NO TI MATRIX IS INPUT BECAUSE THE MDEL IS TRANPOSED
C
C *****
C
C BLANK CARD TERMINATING BRANCH CARDS
C
C SWITCH CARDS
C 3-8 9-14 15-24 25-34 35-44 45-54 55-64 65-74
C (OUTPUT OPTION IN COLUMN 80)
C NODE NAMES IE FLASHOVER SPECIAL REFERENCE
C OR VOLTAGE REQUEST SWITCH-NAME
C BUS1 BUS2 CLOSE OPEN NSTEP WORD BUSS BUSG
C REC CFAULTC 01015 0960
C 3456789012345678901234567890123456789012345678901234567890123456789012345678901234567890
C BLANK CARD TERMINATING SWITCH CARDS
C SOURCE CARDS
C 3456789012345678901234567890123456789012345678901234567890123456789012345678901234567890
C COLUMN 1,2: TYPE OF SOURCE 1 - 17, (E.G. 11-13 ARE RAMP FUNCTIONS, 14 = COSINE)
C COLUMN 9,10: 0=VOLTAGE SOURCE, -1=CURRENT SOURCE
C 3-8 11-20 21-30 31-40 41-50 51-60 61-70 71-80
C NODE AMPLITUDE FREQUENCY TO IN SEC AMPL-A1 TIME-T1 T-START T-STOP
C NAME IN HZ DEGR SECONDS SECONDS SECONDS
14EQL A 303000. 60.0 0 -1.0
14EQL B 303000. 60.0 -120. -1.0
14EQL C 303000 60.0 -240 -1.0
C
C BLANK CARD TERMINATING SOURCE CARDS
C NODE VOLTAGE OUTPUT
C 34567890123456789012345678901234567890
C SEND ASEND BSEND CREC AREC BREC C
C BLANK CARD TERMINATING NODE VOLTAGE OUTPUT
C PLOTTING CARDS
C CALCOMP PLOT 2
C (CASE TITLE UP TO 78 CHARACTERS)
2 EXAMPLE 1, MARTI'S TRANPOSED MODEL
C THE FOLLOWING IS FORMAT OF THE PLOT REQUEST CARDS
C COLUMN 2, "1"
C COLUMN 3, 4=NODE VOLTAGE
C 8=BRANCH VOLTAGE
C 9=BRANCH CURRENT
C COLUMN 4, UNITS OF HORIZONTAL SCALE 1=DEGREES
C 2=CYCLES
C 3=SEC
C 4=MSEC
C 5=USEC
C
C COLUMNS 5-7 HORIZONTAL SCALE (UNITS PER INCH)
C COLUMNS 8-11 TIME WHERE PLOT STARTS
C COLUMNS 12-15 TIME WHERE PLOT ENDS
C COLUMNS 16-20 VALUE OF BOTTOM VERTICAL SCALE
C COLUMNS 21-24 VALUE OF TOP VERTICAL SCALE
C COLUMNS 25-48 UP TO FOUR NODE NAMES
C COLUMNS 49-64 GRAPH HEADING LABEL
C COLUMNS 65-80 VERTICAL AXIS LABEL
144 B 80 REC AREC BREC C
144 B 80 SEND ASEND BSEND C
C BLANK CARD TERMINATING PLOT REQUESTS
C BLANK CARD TERMINATING THE CASE

```

Table 2-13

TRANSIENT RUN FOR EXAMPLE 1 USING MARTI
 FREQUENCY-DEPENDENT NONTRANPOSED LINE MODEL

```

C FILE NAME: LNMRT: UNIFORMLY DISTRIBUTED, NONTRANPOSED, FREQUENCY
C DEPENDENT REPRESENTATION USING MARTI'S LINE MODEL FOR EXAMPLE 1
C RESULTS OF FIELD TEST ARE OBTAINED FROM IEEE PAPER
C NO 174-080-8 BY MEYER AND DUMMEL
C
C A SINGLE LINE TO GROUND FAULT IS APPLIED TO PHASE C OF THE RECEIVING
C END AT 10.15 MS. THIS FAULT IS NOT ALLOWED TO BE CLEARED WITHIN THE TIME
C FRAME OF THIS CASE.
C BEGIN NEW DATA CASE
C FIRST MISCELLANEOUS DATA CARD:
C 34567890123456789012345678901234567890123456789012345678901234567890
C 1-8 9-16 17-24 25-32
C T-STEP T-MAX X-DPT C-DPT
C SECONDS SECONDS 0=MH 0=UF
C K=K-TH K=K-TH 1=YES 1=YES 1=YES 1=YES 1=YES 1=YES 1=YES 1=YES
C 20000 1 1 1 1 1 0 0 1 0
C
C SECOND MISCELLANEOUS DATA CARD
C 1-8 9-16 17-24 25-32 33-40 41-48 49-56 57-64 65-72 73-80
C PRINT PLOT NETWORK PR SS PR MAX I PUN PUNCH DUMP MULT DIAGNOS
C 0=EACH 0=EACH 0=NO 0=ND 0=NO 0=NO 0=NO 0=NO INTO NENERG PRINT
C K=K-TH K=K-TH 1=YES 1=YES 1=YES 1=YES 1=YES 1=YES 1=YES 1=YES 1=YES 1=YES
C 20000 1 1 1 1 1 0 0 1 0
C
C 34567890123456789012345678901234567890123456789012345678901234567890
C EQU L ASEND A 15.0
C EQU L BSEND B 15.0
C EQU L CSEND C 15.0
C FAULT AT THE RECEIVING END, PHASE C
C 1 2 3 4 5 6 7
C 34567890123456789012345678901234567890123456789012345678901234567890
C FAULTC 2.0
C
C .....
C
C NONTRANPOSED MARTI LINE MODEL INPUT
C
C THE LOGICAL UNIT 7 "PUNCHED-CARD" OUTPUT OF A JMARTI SETUP INCLUDES
C THE FOLLOWING ECHO OF LINE CONSTANTS INPUT DATA
C
C PUNCHED CARD OUTPUT OF "JMARTI SETUP" WHICH BEGAN AT 07:26:08 08/20/86
C 1.3636 .05215 4 1.602 -20.75 50. 50.
C 1.3636 .05215 4 1.602 -19.25 50. 50.
C 2.3636 .05215 4 1.602 -75 77.5 77.5
C 2.3636 .05215 4 1.602 75 77.5 77.5
C 3.3636 .05125 4 1.602 19.25 50. 50.
C 3.3636 .05125 4 1.602 20.75 50. 50.
C 0.5 2.61 4 .386 -12.9 98.5 98.5
C 0.5 2.61 4 .386 12.9 98.5 98.5
C
C 100 5000 1 138. 1 1-2
C 100 60.0 1 138. 1 1
C 100 0.1 1 138. 1 9 10 1
C
C COLUMNS 53-54 IPUNCH 0 FOR LUMPED-RESISTANCE LOSSES (CONSTANT-PARAMETER)
C -1 FOR MEYER-DUMMEL MODEL OF THIS MODE
C -2 FOR MARTI MODEL
C COLUMNS 55-56 IPOSE 0 FOR TRANPOSED LINE
C N, NUMBER OF PHASES FOR NONTRANPOSED LINE
C IF N IS NOT ZERO, AN N X N PI MATRIX WILL BE INPUT
C COLUMNS 27-32 SKIP FOR MARTI MODEL ONLY, 0 FOR FULL INPUT ECHO,
C 2 FOR SUPPRESSION OF INPUT ECHO (RECOMMENDED)
C
C 1 2 3 4 5 6 7
C 34567890123456789012345678901234567890123456789012345678901234567890
    
```

Table 2-13 (Cont'd)

TRANSIENT RUN FOR EXAMPLE 1 USING MARTI
 FREQUENCY-DEPENDENT NONTRANPOSED LINE MODEL

-1	SEND AREC A	2.	-2	3
	17	0.47487160101434164971E+03		
-0	119503162881184010E+01	-0.326892601062597520E+01	-0	627808926196377115E+01
-0	296091297300037250E+02	-0.120940702598478310E+03	0.	129894631960505648E+04
0.	596887191395767149E+04	0.308722954951382707E+05	0.	102373272753268014E+06
0.	163868433379027379E+07	0.774502284435054659E+07	0.	140388716978837847E+08
0.	262452849599930047E+08	0.105621145496204495E+08	0.	208106200736043453E+08
0.	322252816738244295E+08	0.456690440688078403E+08		
0.	318444474143245059E+00	0.906096217634441813E+00	0.	167177938571877149E+01
0.	174796362283244377E+01	0.250648280540679024E+01	0.	203071838411721046E+02
0.	126086361452913024E+03	0.031053425657395564E+03	0.	250486261316612944E+04
0.	218726637948580319E+05	0.2280449045703150333E+06	0.	882424120872419327E+06
0.	333829584227986633E+07	0.554420757319149374E+07	0.	108020610457895994E+08
0.	167498016560479402E+08	0.242748545638475418E+08		
	14	0.86849776031173650525E-03		
0.	580152500887889388E-01	0.269715412131610321E+00	0.	358631515126138111E+00
0.	775336897427621352E+00	0.512143539928851510E+01	0.	838209310849589428E+01
0.	700175437339662494E+02	0.393050276108977632E+03	0.	138210011332239082E+04
0.	706195382845908170E+03	0.527256019310418893E+04	0.	528343713697134517E+05
0.	178312894597945213E+08	-0.178919627301954030E+08		
0.	228209546828926477E+02	0.102740809713908220E+03	0.	139218430692429137E+03
0.	269604535948668853E+03	0.389215132609942884E+03	0.	427779656728098416E+03
0.	132142832278849527E+04	0.277173164577853458E+04	0.	449345095170973218E+04
0.	596609131708205677E+04	0.114715205510469968E+05	0.	266318187900488264E+05
0.	204029603396488819E+05	0.204233632999883266E+05		
-2	SEND BREC 8	2.	-2	3
	13	0.28580869799709216749E+03		
0.	385515816224028822E+04	-0.274354792610088770E+04	0.	440518055835420454E+03
0.	212138590145010311E+03	0.890863548201764388E+02	0.	132353020343727621E+03
0.	645192966703452839E+02	0.750292241530855790E+02	0.	131858775319442065E+04
0.	254936968728188367E+04	0.189269194926329655E+05	0.	393530510881239548E+06
0.	563432534131550788E+07			
0.	358040160814492480E+01	0.375515841399830208E+01	0.	703336502229472808E+01
0.	109079723441776650E+02	0.139655108920660495E+02	0.	235557497490131027E+02
0.	391131493700968749E+02	0.802992445140744166E+02	0.	127512692695625416E+04
0.	247570514289243146E+04	0.184291678156175184E+05	0.	383273491829002276E+06
0.	551032769475838541E+07			
	13	0.74131424386504260470E-03		
0.	192161620394728061E+02	0.207910737034382009E+01	0.	557816466590047639E+02
0.	305960456859098712E+02	0.621685103276831796E+03	-0	628857275150040281E+04
0.	28091244867577995E+05	0.719621640659067779E+05	0.	497277641526484489E+07
0.	450129768301306152E+11	-0.396352275575622558E+11	0.	371705995049687499E+11
-0.	425504160481909179E+11			
0.	326602047053036221E+04	0.361602043874112496E+03	0.	949599225381627911E+04
0.	518764668271355913E+04	0.245885512760987039E+05	0.	115386381066317204E+06
0.	109532546357007231E+06	0.236641409942938014E+06	0.	621691137498479336E+06
0.	989526558376729488E+06	0.990516084935054183E+06	0.	974420807294171303E+06
0.	975395228101465851E+06			
-3	SEND CREC C	2.	-2	3
	10	0.27248374249323933327E+03		
0.	808834440886188531E+03	0.345736033868844970E+03	0.	508297808607803744E+03
0.	126310666107660836E+03	0.766057568123051169E+02	0.	132480050033297629E+03
0.	647982112475506255E+02	0.125343032112450146E+03	0.	315292547711625229E+04
0.	152879411366682499E+06			
0.	285857956077185804E+01	0.428887408777180212E+01	0.	738274598892382982E+01
0.	104853389347954025E+02	0.135583552569445373E+02	0.	234345539231809425E+02
0.	381678841224575080E+02	0.712899103916602143E+02	0.	15281595642076135RE+04
0.	743505614391937851E+05			
	20	0.74871320732244506498E-03		
0.	250540215342772709E-01	0.508290136582746754E+01	0.	445989262313648282E+01
0.	683271827229521022E+01	0.122652357573056178E+02	0.	100295491201804338E+02
0.	136653923162496416E+02	0.103375148863896811E+03	0.	648487388943168955E+03
0.	221433098950574640E+04	0.164135666585447033E+05	0.	518069280577083118E+05
0.	394136421795912086E+06	-0.101332083318735240E+05	-0	174303419874725863E+06
0.	524342866126023232E+06	0.704492951271683593E+12	-0.	555056496773761718E+12
0.	578211839151425781E+12	-0.727649098931671875E+12		

Table 2-13 (Cont'd)

TRANSIENT RUN FOR EXAMPLE 1 USING MARTI
 FREQUENCY-DEPENDENT NONTRANPOSED LINE MODEL

```

O. 891708457795169806E+01 O. 180867430329040507E+04 O. 154837406059516059E+04
O. 241721129928615118E+04 O. 391603796888153010E+04 O. 400132197801065922E+04
O. 497359886148633086E+04 O. 253968020139539148E+05 O. 272612219294871902E+05
O. 475723224750750232E+05 O. 149898516330461017E+06 O. 334040507539352402E+06
O. 541780942881010472E+06 O. 671199632035642862E+06 O. 569908394622657448E+06
O. 12645006401353329E+07 O. 440567216178667545E+07 O. 441007783394834399E+07
O. 436803542484822869E+07 O. 437240346027284860E+07

C
C THE FOLLOWING IS A 3 X 3 TI MATRIX FOR THE NONTRANPOSED LINE MODEL
C WITH ALTERNATE ROWS OF REAL AND IMAGINARY ELEMENTS
C THE IMAGINARY ELEMENTS ARE ZERO TO ACHIEVE STABLE RESULTS
C
O.57155537 O.70673359 -O.41818745
O.00000000 O.00000000 O.00000000
O.58880356 O.00066892 O.80696214
O.00000000 O.00000000 O.00000000
O.57151975 -O.70747946 -O.41705079
O.00000000 O.00000000 O.00000000

C
C
C END OF MARTI'S SETUP
C
C *****
C BLANK CARD TERMINATING BRANCH CARDS
C
C
C SWITCH CARDS
C 3-8 9-14 15-24 25-34 35-44 45-54 55-64 65-74
C (OUTPUT OPTION IN COLUMN 80)
C NODE NAMES IE FLASHOVER SPECIAL REFERENCE
C OR VOLTAGE REQUEST SWITCH-NAME
C BUS1 BUS2 CLOSE OPEN NSTEP WORD BUS5 BUS6
C REC CFAULTC O1015 O960
C 34567890123456789012345678901234567890123456789012345678901234567890
C BLANK CARD TERMINATING SWITCH CARDS
C SOURCE CARDS
C 34567890123456789012345678901234567890123456789012345678901234567890
C COLUMN 1,2: TYPE OF SOURCE 1 - 17, (E.G. 11-13 ARE RAMP FUNCTIONS, 14 = COSINE)
C COLUMN 9,10: 0=VOLTAGE SOURCE, -1=CURRENT SOURCE
C 3-8 11-20 21-30 31-40 41-50 51-60 61-70 71-80
C NODE AMPLITUDE FREQUENCY TO IN SEC AMPL-A1 TIME-T1 T-START T-STOP
C NAME IN HZ DEGR SECONDS SECONDS SECONDS
14E0UL A 303000. 60.0 O. -1.0
14E0UL B 303000. 60.0 -120. -1.0
14E0UL C 303000. 60.0 -240. -1.0

C
C BLANK CARD TERMINATING SOURCE CARDS
C NODE VOLTAGE OUTPUT
C 34567890123456789012345678901234567890
C SEND ASEND BSEND CREC AREC BREC C
C BLANK CARD TERMINATING NODE VOLTAGE OUTPUT
C PLOTTING CARDS
C CALCOMP PLOT 2
C (CASE TITLE UP TO 78 CHARACTERS)
C EXAMPLE 1, MARTI'S NONTRANPOSED MODEL
C THE FOLLOWING IS FORMAT OF THE PLOT REQUEST CARDS
C COLUMN 2, "1"
C COLUMN 3, 4=NODE VOLTAGE
C 8=BRANCH VOLTAGE
C 9=BRANCH CURRENT
C COLUMN 4, UNITS OF HORIZONTAL SCALE 1=DEGREES
C 2=CYCLES
C 3=SEC
C 4=MSEC
C 5=USEC
C COLUMNS 5-7 HORIZONTAL SCALE (UNITS PER INCH)
C COLUMNS 8-11 TIME WHERE PLOT STARTS
C COLUMNS 12-15 TIME WHERE PLOT ENDS
C COLUMNS 16-20 VALUE OF BOTTOM VERTICAL SCALE
C COLUMNS 21-24 VALUE OF TOP VERTICAL SCALE
C COLUMNS 25-48 UP TO FOUR NODE NAMES
C COLUMNS 49-64 GRAPH HEADING LABEL
C COLUMNS 65-80 VERTICAL AXIS LABEL
144 B. 80. REC AREC BREC C
144 B. 80. SEND ASEND BSEND C
C BLANK CARD TERMINATING PLDT REQUESTS
C BLANK CARD TERMINATING THE CASE
    
```

Table 2-14

TRANSIENT RUN FOR EXAMPLE 2 USING MARTI'S
FREQUENCY-DEPENDENT NONTRANPOSED LINE MODEL

```

C FILE NAME: L500MRNT: UNIFORMLY DISTRIBUTED, NONTRANPOSED, FREQUENCY-
C DEPENDENT REPRESENTATION USING MARTI'S LINE MODEL IN EXAMPLE 2.
C A SINGLE LINE TO GROUND FAULT IS APPLIED TO PHASE B OF THE RECEIVING
C END AT 38 MS. THIS FAULT IS NOT ALLOWED TO BE CLEARED WITHIN THE TIME
C FRAME OF THIS CASE.
BEGIN NEW DATA CASE
C FIRST MISCELLANEOUS DATA CARD:
C 34567890123456789012345678901234567890123456789012345678901234567890
C   1-8   9-16  17-24  25-32
C T-STEP T-MAX  X-OPT  C-OPT
C SECONDS SECONDS  O=MH  O=UF
C                               F(HZ)  F(HZ)
33.30E-6   .08   60.    0
C
C SECOND MISCELLANEOUS DATA CARD
C   1-8   9-16  17-24  25-32  33-40  41-48  49-56  57-64  65-72  73-80
C PRINT PLOT NETWORK PR SS PR MAX I PUN PUNCH DUMP MULT. DIAGNOS
C O=EACH O=EACH O= NO O= NO O= NO O= NO O= NO O= NO O= NO O= NO
C K=K-TH K=K-TH 1=YES 1=YES 1=YES 1=YES 1=YES 1=YES 1=YES 1=YES
C 20000 1 1 1 1 0 0 1 0
C LOCAL SOURCE (GENERATOR)
B26 AEQU A .203
B26 BEQU B .203
B26 CEQU C .203
C
C FAULT AT THE RECEIVING END, PHASE B
FAULTB .01
C
C REMOTE SOURCE (MUTUALLY COUPLED)
C 34567890123456789012345678901234567890123456789012345678901234567890
C                               SEQUENCE VALUES
C                               27-32  33-44
C                               R L (FIRST ZERO, THEN PDS SEQUENCE)
51LINE AEQU A 50
52LINE BEQU B 125
53LINE CEQU C
C
C TRANSMISSION LINES
C *****
C
C COLUMN 52 ILINE 0 FOR INPUT OF L AND C PER UNIT LENGTH IN EACH MODE
C 1 FOR INPUT OF Z AND V FOR EACH MODE
C 2 FOR INPUT OF Z AND TAU FOR EACH MODE
C COLUMNS 53-54: IPUNCH 0 FOR LUMPED-RESISTANCE LOSSES (CONSTANT-PARAMETER)
C -1 FOR MEYER-DOMMEL MODEL OF THIS MODE
C -2 FOR MARTI MODEL
C COLUMNS 55-56: IPOSE 0 FOR TRANPOSED LINE
C N, NUMBER OF PHASES FOR NONTRANPOSED LINE
C IF N IS NOT ZERO, AN N X N TI MATRIX WILL BE INPUT
C COLUMNS 27-32: SKIP FOR MARTI MODEL ONLY, 0 FOR FULL INPUT ECHO,
C 2. FOR SUPPRESSION OF INPUT ECHO (RECOMMENDED)
C
C FOR ILINE=0.
C R L C LE
C 1 2 3 4 5 6 7
C 34567890123456789012345678901234567890123456789012345678901234567890
-1B500 ALINE A 55801.6722 01268 90 0
-2B500 BLINE B .0310 .5816 01340 90 0
-3B500 CLINE C
C *****
C
C NONTRANPOSED MARTI LINE MODEL FOR 120-MILE FLAT LINE
C
C THE LOGICAL UNIT 7 "PUNCHED-CARD" OUTPUT FROM A JMARTI SETUP INCLUDES
C THE FOLLOWING ECHO OF LINE CONSTANTS INPUT DATA

```

Table 2-14 (Cont'd)

TRANSIENT RUN FOR EXAMPLE 2 USING MARTI'S
FREQUENCY-DEPENDENT NONTRANSPOSED LINE MODEL

```

C
C PUNCHED CARD OUTPUT OF "JMARTI SETUP" WHICH BEGAN AT 08:01:12 08/20/86
C 1 .5 .0426 4 1.762 -32. 102.1 32. 18. 0.
C 2 .5 .0426 4 1.762 0. 102.1 32. 18. 0.
C 3 .5 .0426 4 1.762 32. 102.1 32. 18. 0.
C 0 5 2 4 4 .385 -19.8 130. 83.5
C 0 5 2 4 4 .385 19.8 130. 83.5
C
C 100. 5000 1 120. 1-2
C 100. 60 0 1 120. 1
C 100. .1 1 120. 9 10 1
C
C COLUMNS 53-54: IPUNCH 0 FOR LUMPED-RESISTANCE LOSSES (CONSTANT-PARAMETER)
C -1 FOR MEYER-DOMMEL MODEL OF THIS MODE
C -2 FOR MARTI MODEL.
C COLUMNS 55-56: IPOSE 0 FOR TRANSPOSED LINE
C N, NUMBER OF PHASES FOR NONTRANSPOSED LINE
C IF N IS NOT ZERO, AN N X N TI MATRIX WILL BE INPUT
C COLUMNS 27-32: SKIP FOR MARTI MODEL ONLY, 0. FOR FULL INPUT ECHO,
C 2 FOR SUPPRESSION OF INPUT ECHO (RECOMMENDED)
C
C 1 2 3 4 5 6 7
C 345678901234567890123456789012345678901234567890123456789
-1SEND AREC A 2. -2 3
18 0.43908714577912724053E+03
-0.613456154821199106E+02 -0.248909503579607189E+03 0.188431420077086659E+04
0.126728751123631955E+05 0.274602961208898341E+05 0.288714939206590643E+05
0.518169993180953897E+05 0.312250771488523110E+06 0.898558032685820013E+06
0.267490554193986952E+07 0.981705632698440551E+07 0.944515428711032867E+07
0.545678162847658991E+07 0.818220061406037211E+07 0.120511728238770365E+08
0.228509647070652246E+08 0.548098095734786987E+08 0.248506299108313560E+09
0.232311265979521408E+01 0.280036038678284171E+01 0.259337956870298285E+02
0.205236028688341320E+03 0.330271065715402073E+03 0.808502138020223355E+03
0.285157748511199315E+04 0.168533333606205579E+05 0.505956085722462739E+05
0.157212716656896285E+06 0.600097940235644578E+06 0.229748028592777252E+07
0.280351154508358240E+07 0.419503481365057826E+07 0.616022595928063988E+07
0.116538127130455970E+08 0.278747926713114738E+08 0.127330113245054721E+09
16 0.68953070291821738635E-03
0.912735546530067942E-01 0.2032498276866568629E+00 0.242126883701613948E+00
0.493068873661499651E+00 0.589191212476123382E+01 0.498459030003013481E+01
0.156868560961148091E+02 0.542382626669823366E+02 0.290474739478839182E+03
0.852758618441919679E+03 0.209198706509763724E+04 0.434940543544414686E+04
0.668343709602896124E+05 0.142692563715297146E+05 0.647491457877287268E+07
-0.656368466330218315E+07
0.351580504035341618E+02 0.768221609057009118E+02 0.979356863958619214E+02
0.169904440635394166E+03 0.308842822170965519E+03 0.318618750919704325E+03
0.422220681810456881E+03 0.131137177527571475E+04 0.464809327517563360E+04
0.691149894123375997E+04 0.113963911611079238E+05 0.154190092708375304E+05
0.298413238071723608E+05 0.762585138342198915E+05 0.372673669357534963E+05
0.373046343026892282E+05
-2SEND BREC B 2. -2 3
11 0.30597931831209703523E+03
0.108477692709104309E+04 0.107807995884714273E+03 0.120407914742370394E+03
0.107405034960793727E+03 0.613207824723745074E+02 0.699609646259837063E+02
0.110230796489788644E+03 0.306421103210833098E+04 0.298834183373817941E+05
0.870026494605936110E+06 0.142901710593068003E+08
0.364696990765830264E+01 0.575537761737186315E+01 0.857144693375158794E+01
0.126829545754029027E+02 0.219732683990231407E+02 0.426009221113524745E+02
0.660690307226009281E+02 0.166723846081422379E+04 0.163414609271768713E+05
0.477699375563645735E+06 0.790390235502752661E+07
13 0.64575885362810545031E-03
0.206751774714240355E+02 0.309626367995366535E+01 0.419636820855162113E+02
0.394723122049051653E+02 0.934422406462246726E+03 -0.327285042751838045E+04
0.192558330821749987E+05 0.113862228568045888E+06 0.181077421172747761E+07
0.202424176986039876E+08 -0.200864652794187068E+08 -0.161976168613557815E+09
0.159878557141596794E+09

```

Table 2-14 (Cont'd)

TRANSIENT RUN FOR EXAMPLE 2 USING MARTI'S
FREQUENCY-DEPENDENT NONTRANPOSED LINE MODEL

```

O .369429782479224377E+04 O 568767013518488965E+03 O .777601669745121034E+04
O 675351278696910594E+04 O 337928317967629991E+05 O 879998009815993718E+05
O .831876045986590906E+05 O .221279499230219051E+06 O .424281452553659677E+06
O .135176408091928809E+07 O 1353115845000019252E+07 O 542536329516507685E+06
O .543078865845989435E+06
-3SEND CREC C 2. -2 3
14 O .26064673431699702632E+03
-O .229512079686121069E+03 O .121843824813449464E+04 O .284820323286936400E+03
O .152586797149669652E+03 O 903064739529431790E+02 O .114411221243246018E+03
O 277060229590096014E+02 O 660498415211186511E+02 O 852903920779544932E+02
O .408310123273817225E+03 O 101456894600433588E+04 O .147768284714019682E+04
O .547744735815079184E+04 O .238245287216002121E+06
O .387532520047027162E+01 O 325992292970566666E+01 O 626465704275560142E+01
O .964980752225204696E+01 O .130470194024973125E+02 O 219116302194250920E+02
O 365991316282718344E+02 O 766755446329229926E+02 O .992050482717686463E+02
O .444736952244840722E+03 O 109120424323075712E+04 O .161456014446861081E+04
O .595523567953618476E+04 O .259590281317977234E+06
24 O .64838282149290438205E-03
O .405768691270227410E-01 O .308442250449014920E+01 O .325631167368719331E+01
O .532650270521122592E+01 O .110063579443270782E+02 O 190264213653849765E+02
O .252033086183040495E+02 O 389498562014580329E+02 O 882208823832834241E+04
O .135238573661135887E+03 O 210330252772223502E+03 O 427487864216024172E+02
O .194733221029511187E+05 O .601266521653125528E+05 O 440204546355731785E+06
-O .319750435147410025E+05 O .176460012284470722E+06 O 163440999408705532E+07
-O .215104443622888326E+08 O .207535603698037862E+08 O .206004284393372535E+08
-O .203240772640591859E+08 O 378791526875427246E+09 O .380614508104217529E+09
O .156418283016661234E+02 O .124905515629517321E+04 O 118975069399582571E+04
O 205696883086915477E+01 O .428429166453299694E+04 O 718358024414203828E+04
O 968982363382010953E+04 O 140659445789696183E+05 O .199783788092497969E+05
O 269463439069999149E+05 O .186893113310560584E+05 O .951210113855907693E+05
O 219461273728646337E+06 O 560900024122186005E+06 O .112439465183116495E+07
O .121524437057208439E+07 O 167372380056462436E+07 O .307846187230658531E+07
O 577865662774130702E+07 O 578443528436896204E+07 O 285428582118804454E+08
O .285714010700901746E+08 O .881002197423481941E+07 O .881883199620848884E+07

```

```

C THE FOLLOWING CARDS COMPRISE A 3 X 3 TI MATRIX FOR THE NONTRANPOSED LINE
C WITH ALTERNATE ROWS OF REAL AND IMAGINARY ELEMENTS
C THE IMAGINARY ELEMENTS ARE ZERO TO ACHIEVE STABLE RESULTS

```

```

C
O .59691238 -O .70710678 -O .41040583
O .00000000 O .00000000 O .00000000
O .53608882 O .00000000 O .81433047
O .00000000 O .00000000 O .00000000
O .59691238 O .70710678 -O .41040583
O .00000000 O .00000000 O .00000000

```

```

C
C END OF MARTI'S SETUP
C
C *****

```

```

C TRANSFORMER
C 345678901234567890123456789012345678901234567890
C 3-13 15-20 27-32 33-38 39-44 45-50
C REQUESTWORD BUS I FLUX BUS R-MAG
C TRANSFORMER 2 33 1137 X 3 E5

```

```

C
C 1-16 17-32
C CURRENT FLUX
C 2 33 1137.0
C 5 44 1250.0
C 23 33 1364.0
C 1579 00 2274.0
C 9999

```

```

C TRANSFORMER WINDINGS
C COLUMN 1,2: WINDING NUMBER

```

Table 2-14 (Cont'd)

TRANSIENT RUN FOR EXAMPLE 2 USING MARTI'S
FREQUENCY-DEPENDENT NONTRANSPOSED LINE MODEL

```

C 3456789012345678901234567890123456789012345678901234567890
C   3-8  9-14                27-32 33-38 39-44
C   BUS1  BUS2                R-K   L-K  TURNS
1B500 A                27.55 11 66
2B26  AB26  B                2026   1.
   TRANSFORMER           X
1B500 B
2B26  BB26  C                2026   1.
   TRANSFORMER           X                Z
1B500 C
2B26  CB26  A
BLANK CARD TERMINATING BRANCH CARDS
C
C SWITCH CARDS
C 34567890123456789012345678901234567890123456789012345678901234567890
C   3-8  9-14   15-24   25-34   35-44   45-54   55-64   65-74
C                                     (OUTPUT OPTION IN COLUMN 80)
C   NODE NAMES                IE FLASHOVER SPECIAL REFERENCE
C                               OR VOLTAGE REQUEST SWITCH-NAME
C   BUS1  BUS2    CLOSE    OPEN    NSTEP    WORD  BUS5  BUS6
C  B500  ASEND A    -1.      9999
C  B500  BSEND B    -1.      9999
C  B500  CSEND C    -1.      9999
C  REC  BFAULTB    .038    .0960
BLANK CARD TERMINATING SWITCH CARDS
C SOURCE CARDS
C 34567890123456789012345678901234567890123456789012345678901234567890
C COLUMN 1,2: TYPE OF SOURCE 1 - 17, (E G 11-13 ARE RAMP FUNCTIONS, 14 = COSINE)
C COLUMN 9,10: O=VOLTAGE SOURCE, -1=CURRENT SOURCE
C   3-8   11-20   21-30   31-40   41-50   51-60   61-70   71-80
C   NODE  AMPLITUDE  FREQUENCY  TO IN SEC  AMPL-A1  TIME-T1  T-START  T-STOP
C   NAME  IN HZ      DEGR
14E0UL A    18863.    60 0    0.
14E0UL B    18863.    60 0   -120.
14E0UL C    18863.    60.0   -240.
C REMOTE SOURCE
14EQUR A    380281.    60.0    30.
14EQUR B    380281.    60.0   -90.
14EQUR C    380281.    60.0  -210.
BLANK CARD TERMINATING SOURCE CARDS
C NODE VOLTAGE OUTPUT
C 34567890123456789012345678901234567890
C  B500  AB500  BB500  CSEND  ASEND  BSEND  CREC  AREC  BREC  C
BLANK CARD TERMINATING NODE VOLTAGE OUTPUT
C PLOTTING CARDS
C CALCOMP PLOT                2
C (CASE TITLE UP TO 78 CHARACTERS)
2 EXAMPLE 2, MARTI'S NONTRANSPOSED LINE MODEL
C THE FOLLOWING IS FORMAT OF THE PLOT REQUEST CARDS
C COLUMN 2, "1"
C COLUMN 3, 4-NODE VOLTAGE
C           B=BRANCH VOLTAGE
C           9=BRANCH CURRENT
C COLUMN 4, UNITS OF HORIZONTAL SCALE 1=DEGREES
C                                           2=CYCLES
C                                           3=SEC
C                                           4=MSEC
C                                           5=USEC
C COLUMNS 5-7 HORIZONTAL SCALE (UNITS PER INCH)
C COLUMNS 8-11 TIME WHERE PLOT STARTS
C COLUMNS 12-15 TIME WHERE PLOT ENDS
C COLUMNS 16-20 VALUE OF BOTTOM VERTICAL SCALE
C COLUMNS 21-24 VALUE OF TOP VERTICAL SCALE
C COLUMNS 25-48 UP TO FOUR NODE NAMES
C COLUMNS 49-64 GRAPH HEADING LABEL
C COLUMNS 65-80 VERTICAL AXIS LABEL
144 8. 80. REC AREC BREC C
144 8. 80. SEND ASEND BSEND C
BLANK CARD TERMINATING PLOT REQUESTS
BLANK CARD TERMINATING THE CASE

```

Section 3

TRANSFORMERS

3-1. REFERENCE LIST AND DEFINING EQUATIONS

There have been several IEEE and EMTF Newsletter articles written on the subject of EMTF transformer modeling. These are listed in the Introduction of Section 1. For a good, brief introduction, the user is referred to the following three papers.

1. Brandwajn, Dommel and Dommel, "Matrix Representation of Three-Phase N-Winding Transformers for Steady-State and Transient Studies," PAS-101, Number 6, June 1982, pp. 1369-1378.
2. Degeneff, McNutt, Neugebauer, Panek, McCallum and Honey, "Transformer Response to Switching Overvoltages," PAS-101, Number 6, June 1982, pp. 1457-1470.
3. Ewart, "Digital Computer Simulation of a Steel-Core Transformer," PWRD-1, Number 3, July 1986, pp. 174-183.

The following outline of transformer modeling in the EMTF is largely taken from Reference 1. The general case of three-phase core-form transformers is considered. Shell-form or single-phase transformers can be treated with the same equations by setting the zero sequence quantities equal to the positive sequence quantities. For single-phase transformers, the resulting model matrices are smaller and simpler.

All of the equations presented are valid when per-unit impedances and currents are used. The MVA base should be consistent, which may require base conversions on the transformer test data. Once the model matrices are derived, it is best to use physical units for input to the EMTF. To convert R and X from per-unit to ohms:

$$Z_{ik\text{-physical}} = Z_{ik\text{-pu}} (3 * kV_{i\text{-rated}} * kV_{k\text{-rated}}) / \text{MVA}_{\text{base}} \quad (3-1)$$

where $kV_{i\text{-rated}}$ and $kV_{k\text{-rated}}$ are the rms kV ratings of the windings in question. These physical impedances in the matrix will automatically account for the correct winding turns ratios.

The transformer turns ratios and winding impedances can be described by an impedance matrix. For example, an N-winding single-phase transformer would have the following matrix equation.

$$\begin{matrix} V_1 & Z_{11} & \dots & Z_{1n} & I_1 \\ \cdot & \dots & \dots & \dots & \cdot \\ \cdot & \dots & \dots & \dots & \cdot \\ V_n & Z_{n1} & \dots & Z_{nn} & I_n \end{matrix} \quad (3-2)$$

The elements of the Z matrix could be determined from open-circuit excitation tests applied to one winding at a time.

$$Z_{ik} = V_i / I_k \quad (3-3)$$

The commonly measured short circuit impedances would be

$$Z_{ik-sc} = Z_{ii} - (Z_{ik} * Z_{ki}) / Z_{kk} = Z_{ii} (1 - k^2) \quad (3-4)$$

where k is the coupling factor. Because iron-core power transformers are very tightly coupled, k is close to 1.0 and the short circuit impedances are a very small percentage of the Z matrix elements. This is a problem with excitation tests to determine Z_{jk} ; the short circuit impedances are "lost" if the measurements are not made to 6-digit accuracy, which is an impractical task.

If the Z matrix formulation is used, the EMTP will split the matrix into resistive and inductive components so that

$$V = RI + L d/dt I \quad (3-5)$$

The series RL matrix can be directly input to the EMTP. A practical method of determining the Z matrix elements is to first obtain the diagonal elements from excitation tests. It is desired to let Z_{ii} be purely reactive. If excitation losses were included in Z_{ii} , they would be modeled as a series RL rather than the preferred parallel RL. Therefore

$$Z_{ij} = jX_{ij} = 1.0/I_{mij} \quad (3-6)$$

$$I_{mij} = \sqrt{I_e^2 - P_e^2} = I_e \approx 0.01 \text{ p.u.} \quad (3-7)$$

As noted, I_{mij} should be at least 1% to avoid near-singularity problems with the Z matrix. Having obtained the diagonal matrix elements from n excitation tests, the off-diagonal elements are obtained with the aid of short-circuit tests.

$$Z_{ik} = Z_{ki} = \sqrt{(Z_{ii} - Z_{ik-sc}) * Z_{kk}} \quad (3-8)$$

For a three-phase transformer, the same equations may be used if each element is replaced with a 3x3 submatrix which represents the coupling between phases of each winding, and also between different phases of different windings. For example, if positive and zero sequence excitation tests are performed, X_{ij} is a 3x3 matrix.

$$X_{\text{self-}ij} = 1/3(X_{0-ii} + 2X_{1-ii}) \quad (3-9)$$

$$X_{\text{mutual-}ij} = 1/3(X_{0-ii} - X_{1-ii}) \quad (3-10)$$

Positive and zero sequence short-circuit tests are handled in a similar fashion. If short-circuit tests are performed on a three-phase three-winding transformer with delta tertiary, as depicted in Figure 3-1, the zero sequence tests will also have the delta tertiary effectively short-circuited.

The measured impedances in the positive sequence test will be

$$Z_{12} = Z_1 + Z_2 \quad (3-11)$$

$$Z_{13} = Z_1 + Z_3 \quad (3-12)$$

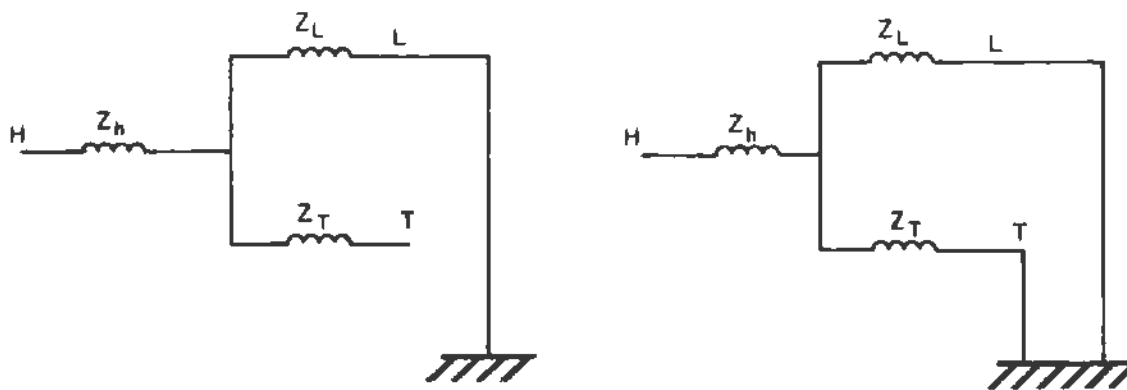
$$Z_{23} = Z_2 + Z_3 \quad (3-13)$$

These are the impedances to use in calculating Z matrix elements. The zero sequence test results will be

$$Z_{12(\text{closed delta})} = Z_1 + (Z_2 * Z_3) / (Z_2 + Z_3) \quad (3-14)$$

$$Z_{13} = Z_1 + Z_3 \quad (3-15)$$

$$Z_{23} = Z_2 + Z_3 \quad (3-16)$$



a) positive sequence

b) zero sequence

Figure 3-1. Equivalent Circuits for Short-Circuit Tests

The impedances required are

$$Z_{12} = Z_1 + Z_2 \tag{3-17}$$

$$Z_{13} = Z_1 + Z_3 \tag{3-18}$$

$$Z_{23} = Z_2 + Z_3 \tag{3-19}$$

where

$$Z_1 = Z_{13} - \frac{\sqrt{Z_{23} * Z_{13}} - Z_{12}(\text{closed delta}) * Z_{23}}{Z_{23}} \tag{3-20}$$

$$Z_2 = Z_{23} - Z_{13} + Z_1 \tag{3-21}$$

$$Z_3 = Z_{13} - Z_1 \tag{3-22}$$

It is also possible to describe the transformer with an admittance matrix. Voltage drops between windings are first defined with respect to a reference winding, n, using a reduced impedance matrix.

$$I = YV \quad (3-23)$$

$$\begin{bmatrix} V_1 - V_n \\ \cdot \\ \cdot \\ V_{n-1} - V_n \end{bmatrix} = \begin{bmatrix} Z_{11\text{red}} & \cdots & Z_{1n-1\text{red}} \\ \cdots & \cdots & \cdots \\ \cdots & \cdots & \cdots \\ Z_{n-11\text{red}} & \cdots & Z_{n-1n-1\text{red}} \end{bmatrix} * \begin{bmatrix} I_1 \\ \cdot \\ \cdot \\ I_{n-1} \end{bmatrix} \quad (3-24)$$

If we ignore exciting current for the time being, $\sum I_k = 0$ for all n windings. The advantage of this formulation is that the elements of Z_{red} are easily determined from the short-circuit impedances for both the positive and zero sequence.

$$Z_{iired} = Z_{in-sc} \quad (3-25)$$

$$Z_{ikred} = 1/2(Z_{in-sc} + Z_{kn-sc} - Z_{ik-sc}) \quad (3-26)$$

We can invert Z_{red} to obtain Y_{red} , but it remains to account for winding n in the new Y matrix. This is done by adding a row and column based on the current constraint.

$$Y_{in} = Y_{ni} = - \sum_{k=1}^{n-1} Y_{ikred} \quad \text{for } i \neq n \quad (3-27)$$

$$Y_{nn} = - \sum_{i=1}^{n-1} Y_{in} \quad (3-28)$$

It is generally preferred to represent load losses separately as series resistances. Therefore, resistive components are left out of the short-circuit impedances when forming the Y matrix.

$$X_{ik-sc} = \sqrt{[Z_{ik-sc}]^2 - (R_i + R_k)^2} \quad (3-29)$$

where R_i and R_k are the winding resistances. We can then define the transformer by

$$L^{-1} = j\omega Y \quad (3-30)$$

$$dI/dt = L^{-1} [V - R * I] \quad (3-31)$$

The three-phase core-form units have zero sequence exciting current in the order of 100%, which should not be ignored. The delta tertiary winding should be open for the zero sequence excitation test. Otherwise, a virtual short-circuit test will result. Excitation branches can be represented as shunt admittance elements

$$Y_{\text{self}} = -j1/3(I_{e0} + 2 I_{e1}) \quad (3-32)$$

$$Y_{\text{mutual}} = -j1/3(I_{e0} - I_{e1}) \quad (3-33)$$

These could be added across the winding closest to the core, or divided up among all the windings.

The transformer magnetizing impedance can be represented separately by a shunt element which is usually connected across the winding closest to the core, which is usually the lowest voltage winding. A two-slope nonlinear inductance is probably adequate to specify L_m , as shown in Figure 3-2. A saturation level of 1.0 to 1.2 may be assumed, with an air-core reactance equal to 2 to 4 times the short-circuit impedance. If the high impedance linear portion of L_m has been included in the Y or Z matrix, then a single-slope or "switched" inductance should be added to the model, also shown in Figure 3-2.

When available, the saturation characteristic is usually given as rms voltage vs. rms current. The EMTP piecewise nonlinear inductance models require the characteristic to be specified as flux vs. current. An auxiliary program CONVERT performs this data conversion. First, the flux points are merely rescaled voltage points according to

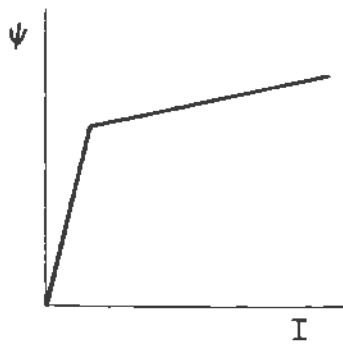
$$\psi = V_{\text{rms}} \sqrt{2} / \omega \quad (3-34)$$

The first current point in Figure 3-3 is given by

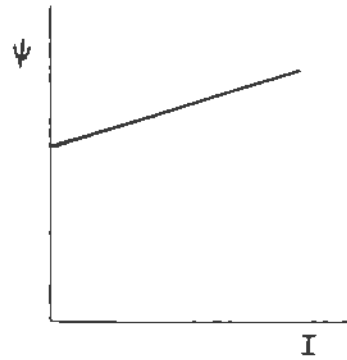
$$I_b = I_{\text{rms-b}} \sqrt{2} \quad (3-35)$$

The remaining current points are found recursively as follows.

1. Assume the current points up to I_{k-1} are known, and we need I_k .

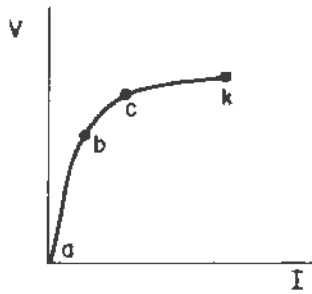


a) Nonlinear L_m

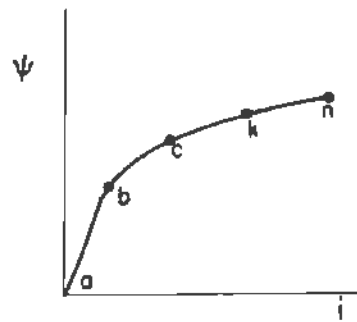


b) External Air-Core Reactance
with Linear Portion in Matrix

Figure 3-2. Nonlinear Magnetizing Impedances



a) V_{rms} vs. I_{rms}



b) ψ vs. I

Figure 3-3. Piecewise Nonlinear Inductance

2. Let $Y = Y_k \sin \omega t$. Since we know the points up to I_{k-1} , the current $I = f(t, I_k)$.
3. Set $F = (I_{\text{rms-k}})^2 = 2/\pi \int I^2 d(\omega t)$. If we use trapezoidal integration, $F = a + bI_k + cI_k^2$, which can be solved for I_k since $I_{\text{rms-k}}$ is already known.

Core losses can be represented with a resistance in parallel with L_m . A better simulation of core hysteresis is obtained with the use of an RL network as shown in Figure 3-4. These models were described by Dommel and Avila-Rosales. Unfortunately, the model parameters may be difficult to obtain.

In Dommel's model, R_m can be a nonlinear resistance with the resistance of each segment given by

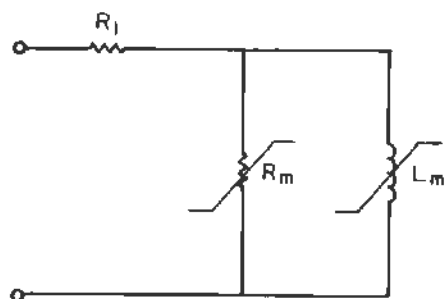
$$R_m = 2V / dI \quad (3-36)$$

where dI is the width of the hysteresis loop at that flux level. R_1 is chosen to achieve the correct total core losses.

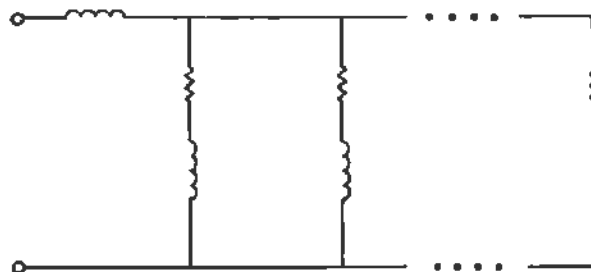
The EMTP also includes a Type 96 branch to represent a hysteretic iron core. This model consists of a variable resistance paralleled by a current source. The user inputs the steady-state characteristic, residual flux, and saturation characteristic as shown in Figure 3-5. This model can be difficult to use because of the abrupt changeover from the steady-state characteristic to the hysteresis loop when the time-step simulation begins, and because of the difficulty in obtaining input data. The EMTP does have the shape of a hysteresis loop for one core material cataloged in the supporting routine HYSDAT. The user specifies the size of the core, and HYSDAT generates Type 96 branch data for input to the EMTP.

3-2. SUMMARY OF MATRIX MODELS

The EMTP employs various matrix formulations to represent transformer turns ratios, leakage impedances, winding resistances, and terminal connections. The magnetizing inductance and core losses are modeled with separate nonlinear flux-current characteristics, which are usually connected across the winding which is



a) Dommel's



b) Avila-Rosaes'

Figure 3-4. Hysteresis Model with RI Components

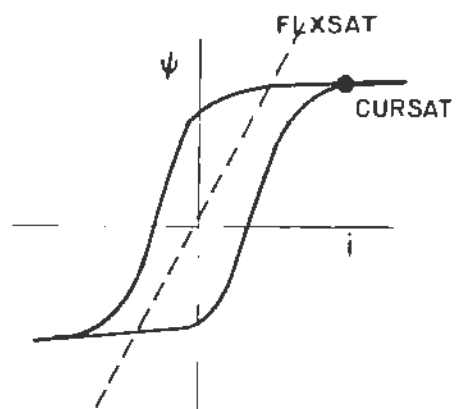
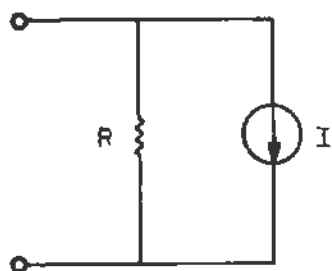


Figure 3-5. Type 96 Hysteretic Iron Core Model

closest to the core. The electrostatic couplings which are important at high frequency must be represented with external capacitance networks connected at the terminals of the matrix model.

The various matrix models available in the EMTP are listed below.

TRANSFORMER branch type

Input - leakage impedances, winding resistances, and turns ratios are input with the EMTP branch data

Advantages - simplest input format

Disadvantages - limited to single-phase, or three-phase bank of single-phase units
- may be numerically unstable for three-winding units

XFORMER matrix setup

Input - manufacturer's data, generates RL matrix branch cards

Advantages - results in stable model for multi-winding transformers

Disadvantages - limited to single-phase banks

TRELEG matrix setup

Input - manufacturer's data (including zero sequence tests), generates RL matrix branch cards or R-1 and L-1 matrix branch cards.

Advantages - properly represents three-phase core-form transformers BCTRAN matrix setup

Input - manufacturer's data (including zero sequence tests), generates RL matrix branch cards

Advantages - properly represents three-phase core-form transformers
- may be more stable than TRELEG matrix model

It is generally recommended that the EMTP's saturable TRANSFORMER branch be used whenever possible because of its simplicity. For three-winding transformers, the XFORMER matrix may be necessary. If the zero sequence behavior of a three-phase core-form transformer must be represented, the user should choose either the TRELEG setup or the BCTRAN setup. When a three-winding core-form transformer has a closed delta tertiary, it is usually not necessary to model the zero sequence effects because the delta terminal connections will predominate.

3-3. SUMMARY OF CORE MODELS

The saturable TRANSFORMER has a built-in exciting impedance which is connected at the star-point of the wye equivalent circuit for the transformer. A piecewise linear flux-current curve is defined point-by-point, with a linear resistance connected in parallel. As an approximation, the manufacturer's rms saturation curve of voltage vs. current may be input, after converting the voltage to peak flux linkages and the current to peak current. For most studies, this will be accurate enough, but there is an auxiliary program called CONVERT which may be used to recursively determine a more accurate flux-current relationship.

The matrix models will require the piecewise linear Type 98 branch to represent the core. This branch should be connected across the terminals of the winding closest to the core, which is usually the low voltage winding. No internal "star" point is available for connection. However, it is probably more accurate to put the exciting impedance across the winding closest to the core than it is to connect it at a fictitious internal node. The core losses can be represented by an externally-added linear resistance, or by a more complicated circuit which accounts for frequency dependent losses. Input data for the Type 98 branch is defined the same way as for the TRANSFORMER branch - including the optional use of auxiliary program CONVERT.

A Type 96 hysteretic inductor model may also be used with the matrix models. This model can be difficult to initialize properly, and the data for various core materials is not readily available.

3-4. TRANSFORMER MATRIX SETUP EXAMPLES

This section contains illustrations of the use of saturable TRANSFORMER, XFORMER, TRELEG and 8CTRAN setups for a three-phase core-form unit with data as given in Table 3-1. There is also a discussion of how to handle the special cases of autotransformers and phase shifters.

The user will generally convert test data for use in the saturable TRANSFORMER branch himself. The number of equivalent branches is usually limited to 3. The exciting branch will be connected to the fictitious star point in the equivalent circuit. The EMTP input for this branch type is shown in Table 3-2.

The XFORMER, TRELEG and BCTRAN models require the use of auxiliary setup routines. The outputs from these programs comprise the required EMTF input data. This data can also be punched on cards or, equivalently, written to Logical Unit 7 for subsequent inclusion in the user's EMTF input file. The sample inputs and outputs for these setup routines are presented in the following tables.

	<u>Input</u>	<u>Output</u>
XFORMER	Table 3-3	Table 3-4
TRELEG	Table 3-5	Table 3-6
BCTRAN	Table 3-7	Table 3-8

Table 3-1

SAMPLE TRANSFORMER TEST DATA

Winding	rms kV	R_{wdg} [ohms]	Windings	Short-Circuit Tests			
				Z_1 [%] / MVA_{base}	Z_0 [%] / MVA_{base}		
Grd-Y	230.0	0.2054666	1-2	8.74	300.0	7.34	300.0
Grd-Y	109.8	0.0742333	1-3	8.68	76.0	26.26	300.0
Delta	50.0	0.0822	2-3	5.31	76.0	18.55	300.0

Excitation Test on Winding 1: $I_{e1} = 0.428\%$ on 300.0 MVA
 $P_{e1} = 135.73$ kW
 $I_{e0}, P_{e0} =$ essentially short-circuit tests due to
delta winding, set $I_{e0} = 100.0\%$ and
 $P_{e0} = 200.0$ kW.

Table 3-2

EMTP SATURABLE TRANSFORMER BRANCH INPUT

$$I_{SS} = \frac{300 \text{ MVA}}{\sqrt{3} \times 230 \text{ kV}} \times 0.00428 \times \sqrt{2} = 0.0045587 \text{ kA} = 4.5582 \text{ A}$$

$$V_{SS} = \frac{132790 \times \sqrt{2}}{377} = 498.13 \text{ V-sec}$$

$$R_m = \frac{(230 \text{ kV})^2}{135.73 \text{ kW}} = 390 \text{ k}\Omega$$

Calculation of X on 300-MVA base:

$$L_{12} = 0.0874 \quad L_1 = 1/7 \times (0.0874 + 0.3426 - 0.2096) = 0.1102$$

$$L_{13} = \frac{0.0868 \times (300)}{76} \quad L_2 = 1/7 \times (0.0874 + 0.2096 - 0.3426) = -0.0279$$

$$= 0.3426$$

$$L_{23} = \frac{0.0531 \times (300)}{76} \quad L_3 = 1/7 \times (0.3426 + 0.2096 - 0.0874) = 0.2322$$

$$= 0.2096$$

$$X_1 = \frac{0.1102 \times (230^2)}{7600} = 19.432 \text{ ohms}$$

$$X_2 = \frac{-0.0279 \times (109.8^2)}{7600} = -0.9203 \text{ ohms}$$

$$X_3 = \frac{0.2322 \times (50^2) \times 3}{7600} = 5.805 \text{ ohms}$$

```

C SATURABLE TRANSFORMER MODEL INPUT
C KEYWORD          I-SS FLUX-SS  NAME R-EXC          I-EXC
C                                     OUTPUT
C
C COLUMNS 3-13    27-32 33-38 39-44 45-50
C TRANSFORMER      4.5582498.13 XFA390.E3          1
C MAGNETIZING INDUCTANCE PIECEWISE LINEAR CHARACTERISTIC
C CURRENT          FLUX
C (AMPS-PK)        (VOLT-SEC)
C      E16.0        E16.0
C      5.0140      547.94
C      9999
C WINDING PARAMETERS
C # NODE NAMES          R          X          N
C                                     (USE WINDING KV RATING IN RMS)
C 12  2A6          12X          E6.0 E6.0 E6.0
C 1HIGH A          2054719.432132 79
C 2LOW A          07423-.9203 63 39
C 3TERT ATERT B          .0822 5.805 50.00
C INPUT SECOND PHASE BY REFERENCE BRANCH PROCEDURE
C EXCITING BRANCH PARAMETERS ARE COPIED BY REFERENCE BRANCH PROCEDURE
C KEYWORD          REF. NAME          NAME
C COLUMNS 3-13  15-20          39-44
C TRANSFORMER    XFA          XFB
C WINDING CONNECTIONS - R, X, AND N COPIED BY REFERENCE BRANCH PROCEDURE
C 1HIGH B
C 2LOW B
C 3TERT BTERT C
C INPUT THIRD PHASE BY REFERENCE BRANCH PROCEDURE
C EXCITING BRANCH PARAMETERS ARE COPIED BY REFERENCE BRANCH PROCEDURE
C KEYWORD          REF. NAME          NAME
C COLUMNS 3-13  15-20          39-44
C TRANSFORMER    XFA          XFC
C WINDING CONNECTIONS - R, X, AND N COPIED BY REFERENCE BRANCH PROCEDURE
C 1HIGH C
C 2LOW C
C 3          TERT A
    
```

Table 3-3

XFORMER INPUT

```

BEGIN NEW DATA CASE
XFORMER
BRANCH HIGH A      LOW A      TERT ATERT B
C NW CMAGN PBCUR      IPUNCH
C IM% 1-PH BASE MVA O=YES, 1=NO
C I1 E9.0 E10.0 I12
3 0.428 100.0 1
C VOLTS PLDSS-IJ Z-SC PBASE-ZSC
C RMS KV KW LOAD LOSS % 1-PH MVA BASE
C E10.0 E10.0 E10.0 E10.0
132.79 0.0 8.74 100.00
63.39 0.0 8.68 25.33
50.00 0.0 5.31 25.33
BLANK CARD ENDING XFORMER SETUPS
END LAST DATA CASE
    
```

Table 3-4

XFORMER OUTPUT

```

SINGLE-PHASE 3-WINDING TRANSFORMER. 'IMAGN' = 0.42800 PER CENT BASED ON 100.000 MVA
VOLTAGE ACROSS WINDING LOSSES IMPEDANCE BASED ON
(KV) (KW) (PER CENT) (MVA)
HIGH 132.79 HIGH TO MEDIUM 0.00 8.7400 100.000
MEDIUM 63.39 HIGH TO LOW 0.00 8.6800 25.330
LOW 50.00 MEDIUM TO LOW 0.00 5.3100 25.330

IMPEDANCE MATRIX AS REQUIRED FOR EMTF STUDIES (WITH X' IN OHMS AT THE POWER FREQUENCY)
R X R X R X
HIGH 0.0000000E+00 0.4121177E+05
MEDIUM 0.0000000E+00 0.1966773E+05 0.0000000E+00 0.9389655E+04
LOW 0.0000000E+00 0.1550763E+05 0.0000000E+00 0.7404286E+04 0.0000000E+00 0.5843946E+04
    
```

80-COLUMN CARD-IMAGE LISTING OF PUNCHED-CARD OUTPUT FOLLOWS (TYPE-51-53 EMTF BRANCH CARDS)

```

-----
1 2 3 4 5 6 7 8
0 0 0 0 0 0 0 0
-----
51. HIGH A, . . . . . 0 0000000000000E+00 , 0.4121177066059E+05 , . . . .
52. LOW A, . . . . . 0 0000000000000E+00 , 0.1966772065495E+05 $
0 0000000000000E+00 , 0.9389655222303E+04 , . . . .
53. TERT A, TERT B, . . . . . 0 0000000000000E+00 , 0.1550762750127E+05 $
0 0000000000000E+00 , 0.7404285723481E+04 $
0 0000000000000E+00 , 0.5843946384859E+04 , . . . .
-----
    
```

```

SHORT-CIRCUIT INPUT IMPEDANCES WHICH ARE OBTAINED FROM THE JUST-PRINTED IMPEDANCE MATRIX, BY REVERSE
COMPUTATION. THIS IS SORT OF A CHECK ON THE COMPUTATION.
HIGH TO MEDIUM 0.00000 15.40935
HIGH TO LOW 0.00000 60.38171
MEDIUM TO LOW 0.00000 8.41805
REPEAT OF PRECEDING CALCULATION, ONLY THIS TIME THE STARTING POINT WILL BE THE IMPEDANCE MATRIX WITH ALL
ELEMENTS ROUNDED TO FIVE DECIMAL DIGITS
HIGH TO MEDIUM 0.00000 15.58807
HIGH TO LOW 0.00000 60.58246
MEDIUM TO LOW 0.00000 8.41779
    
```

Table 3-5
TRELEG INPUT

```

BEGIN NEW DATA CASE
C TRELEG SETUP IS FLAGGED BY 33. IN COLUMNS 38-40
XFORMER          33.
C N NDELTA      FREQ      MVA-BASE
C N=# WINDINGS, <=5
C NDELTA=# DELTA WINDINGS, <=2
C I2 I3        E12.0      E12.0
  3 1          60.0       300.0
C I J          TPR        TPX          TZR          TZX
C WDGs        POSITIVE SEQUENCE      ZERO SEQUENCE
C           R-SC        X-SC          R-SC        X-SC
C I3 I2        E12.0      E12.0      E12.0      E12.0
  1 2          0.0090     0.0873     0.0060     0.0732
  1 3          0.0111     0.3424     0.0200     0.2618
  2 3          0.0117     0.2093     0.0250     0.1838
BLANK CARD ENDING SHORT CIRCUIT TESTS
C KZOUT 0=P.U. OUTPUT, 1=OHMS OUTPUT
C I3
  1
C J INOD      VRATED      RDC OHMS      NAMES
C           0=Y
C           1=D
C I3 I2        E13.0      E12.0      6A6
  1 0          132.79     0.2054666HIGH A      HIGH B      HIGH C
  2 0          63.39      0.0742333LOW A      LOW B      LOW C
  3 1          50.0       0.0822      TERT ATERT BTERT BTERT CTERT CTERT A
BLANK CARD ENDING WINDINGS
C NT 0=EXCITATION TESTS FOR FIRST WINDING DN, Y
C           1=EXCITATION TESTS FOR ALL WINDINGS
C I3
  0
C           XPOS      XZERO
C           E13.0      E12.0
           233.64      1.0
BLANK CARD ENDING MAGNETIZING IMPEDANCES
BLANK CARD ENDING TRELEG SETUPS
END LAST DATA CASE

```

Table 3-6

TRELEG OUTPUT

***** 80-COLUMN CARD-IMAGE LISTING OF UNIT-7 PUNCHED CARDS *****								
1	2	3	4	5	6	7	8	
O	O	O	O	O	O	O	O	O
51, HIGH A.	...		0.205466600000E+00.		0.275242248345E+05		
52, LOW A.	...		-0.366596732259E-01.		0.131344308015E+05	\$		
			0.742333000000E-01.		0.627111675896E+04		
53, TERT A, TERT B...			-0.395878214402E+00.		0.103491974543E+05	\$		
			-0.201357058337E+00.		0.494198218838E+04	\$		
			0.822000000000E-01.		0.389986166667E+04		
54, HIGH B.	...		0.000000000000E+00.		-0.136739464967E+05	\$		
			-0.371904524455E-01.		-0.652500341574E+04	\$		
			-0.175178879147E+00.		-0.514211707485E+04		
			0.205466600000E+00.		0.275242248345E+05		
55, LOW B.	...		-0.371904524455E-01.		-0.652500341574E+04	\$		
			0.000000000000E+00.		-0.311371293448E+04	\$		
			-0.973243121042E-01.		-0.245383687756E+04		
			-0.366596732259E-01.		0.131344308015E+05	\$		
			0.742333000000E-01.		0.627111675896E+04		
56, TERT B, TERT C...			-0.175178879147E+00.		-0.514211707485E+04	\$		
			-0.973243121042E-01.		-0.245383687756E+04	\$		
			0.000000000000E+00.		-0.193372333333E+04		
			-0.395878214402E+00.		0.103491974543E+05	\$		
			-0.201357058337E+00.		0.494198218838E+04	\$		
			0.822000000000E-01.		0.389986166667E+04		
57, HIGH C.	...		0.000000000000E+00.		-0.136739464967E+05	\$		
			-0.371904524455E-01.		-0.652500341574E+04	\$		
			-0.175178879147E+00.		-0.514211707485E+04		
			0.000000000000E+00.		-0.136739464967E+05	\$		
			-0.371904524455E-01.		-0.652500341574E+04	\$		
			-0.175178879147E+00.		-0.514211707485E+04		
			0.205466600000E+00.		0.275242248345E+05		
58, LOW C.	...		-0.371904524455E-01.		-0.652500341574E+04	\$		
			0.000000000000E+00.		-0.311371293448E+04	\$		
			-0.973243121042E-01.		-0.245383687756E+04		
			-0.371904524455E-01.		-0.652500341574E+04	\$		
			0.000000000000E+00.		-0.311371293448E+04	\$		
			-0.973243121042E-01.		-0.245383687756E+04		
			-0.366596732259E-01.		0.131344308015E+05	\$		
			0.742333000000E-01.		0.627111675896E+04		
59, TERT C, TERT A...			-0.175178879147E+00.		-0.514211707485E+04	\$		
			-0.973243121042E-01.		-0.245383687756E+04	\$		
			0.000000000000E+00.		-0.193372333333E+04		
			-0.175178879147E+00.		-0.514211707485E+04	\$		
			-0.973243121042E-01.		-0.245383687756E+04	\$		
			0.000000000000E+00.		-0.193372333333E+04		
			-0.395878214402E+00.		0.103491974543E+05	\$		
			-0.201357058337E+00.		0.494198218838E+04	\$		
			0.822000000000E-01.		0.389986166667E+04		

Table 3-7

BCTRAN INPUT

```

BEGIN NEW DATA CASE
C BCTRAN SETUP, NOTE 44 IN COLUMNS 38-40
XFORMER 44
C COLUMNS 73-74 NPHASE (1=SINGLE-PHASE BANK, 0=THREE-PHASE UNIT)
C COLUMNS 75-76 ITEST (WINDING # USED FOR EXCITATION TEST)
C COLUMNS 77-78 IPUT (WINDING # TO CONNECT EXCITATION BRANCH)
C COLUMNS 79-80 IPRINT (0 FOR R AND L-INV, 1 FOR R AND X, -1 FOR BOTH)
C N F-HZ IE % MVA-BASE PE1-KW IEO % MVA-BASE PEO-KW
C I2 E10.2 E10.2 E10.2 E10.2 E10.2 E10.2 E10.2 412
3 60.0 0.428 300.0 135.73 100.0 300.0 200.0 0 1 3-1
C K KV-RATED RDC NAMES
C I3 E10.2 E10.2 6A6
1 132.79 0.2054666 HIGH A HIGH B HIGH C
2 63.39 0.0742333 LOW A LOW B LOW C
3 50.00 0.0822 TERT ATERT BTERT BTERT CTERT CTERT A
C I K LOAD-LOSS 2-PDS MVA-PDS 2-ZERO % MVA-ZERO
C WOGS KW
C COLUMNS 55-56 IDELTA (0=ALL WOGS OPEN FOR ZERO-SEQUENCE TEST,
#=ADDITIONAL SHORT-CIRCUITED WDG)
C COLUMNS 57-58 ILOSS (0=USE RDC FOR WINDING RESISTANCE,
1=USE LOSS FOR WINDING RESISTANCE, N<4 ONLY)
C 2 I2 E10.2 E10.2 E10.2 E10.2 E10.2 2 I2
1 2 0 0 8.74 300.0 7.34 300.0 3 0
1 3 0.0 8.68 76.0 26.26 300.0
2 3 0.0 5.31 76.0 18.55 300.0
BLANK CARD ENDING SHDRT CIRCUIT DATA
BLANK CARD ENDING BCTRAN SETUPS
END LAST DATA CASE

```

Table 3-8

BCTTRAN OUTPUT

SHUNT RESISTANCES FOR REPRESENTATION OF EXCITATION LOSSES
 ZERO SEQUENCE SHUNT RESISTANCE REDUCED TO BE EQUAL TO POSITIVE SEQUENCE VALUE
 PLACE SHUNT RESISTANCE MATRIX ACROSS WINDING 3 WITH R(SELF/OHM)= 0.550983E+05

AND R(MUTUAL/OHM)= 0.000000E+00

BRANCH DATA - RESISTANCE MATRIX (OHMS) AND INVERSE INDUCTANCE MATRIX (1/HENRIES)

1HIGH A	0.2054666000E+00	0.2651716326E+02
2LOW A	0.0000000000E+00	-0.5959489439E+02
	0.7423330000E-01	0.1809119693E+03
3TERT ATERT B	0.0000000000E+00	0.5130124928E+01
	0.0000000000E+00	-0.7108807411E+02
	0.8220000000E-01	0.8335996693E+02
4HIGH B	0.0000000000E+00	0.1321666189E+01
	0.0000000000E+00	-0.1058091858E+01
	0.0000000000E+00	-0.2168632207E+01
	0.2054666000E+00	0.2651716326E+02
5LOW B	0.0000000000E+00	-0.1058091858E+01
	0.0000000000E+00	0.1400067417E+00
	0.0000000000E+00	0.2632579808E+01
	0.0000000000E+00	-0.5959489439E+02
	0.7423330000E-01	0.1809119693E+03
6TERT BTERT C	0.0000000000E+00	-0.2168632207E+01
	0.0000000000E+00	0.2632579808E+01
	0.0000000000E+00	0.9216689096E+01
	0.0000000000E+00	0.5130124928E+01
	0.0000000000E+00	-0.7108807411E+02
	0.8220000000E-01	0.8335996693E+02
7HIGH C	0.0000000000E+00	0.1321666189E+01
	0.0000000000E+00	-0.1058091858E+01
	0.0000000000E+00	-0.2168632207E+01
	0.0000000000E+00	0.1321666189E+01
	0.0000000000E+00	-0.1058091858E+01
	0.0000000000E+00	-0.2168632207E+01
	0.2054666000E+00	0.2651716326E+02
8LOW C	0.0000000000E+00	-0.1058091858E+01
	0.0000000000E+00	0.1400067417E+00
	0.0000000000E+00	0.2632579808E+01
	0.0000000000E+00	-0.1058091858E+01
	0.0000000000E+00	0.1400067417E+00
	0.0000000000E+00	0.2632579808E+01
	0.0000000000E+00	-0.5959489439E+02
	0.7423330000E-01	0.1809119693E+03
9TERT CTERT A	0.0000000000E+00	-0.2168632207E+01
	0.0000000000E+00	0.2632579808E+01
	0.0000000000E+00	0.9216689096E+01
	0.0000000000E+00	-0.2168632207E+01
	0.0000000000E+00	0.2632579808E+01
	0.0000000000E+00	0.9216689096E+01
	0.0000000000E+00	0.5130124928E+01
	0.0000000000E+00	-0.7108807411E+02
	0.8220000000E-01	0.8335996693E+02

Table 3-8 (Cont'd)

BCTRAN OUTPUT

```

BRANCH DATA - RESISTANCE MATRIX (OHMS) AND REACTANCE MATRIX (OHMS) AT 60.00 HZ
1HIGH A      0.2054666000E+00  0.2767997811E+05
2LOW A       0.0000000000E+00  0.1320530369E+05
              0.7423330000E-01  0.6303181862E+04
3TERT ATERT B 0.0000000000E+00  0.1040148766E+05
              0.0000000000E+00  0.4965361115E+04
              0.8220000000E-01  0.3916517680E+04
4HIGH B     0.0000000000E+00-0  0.1375182324E+05
              0.0000000000E+00-0  0.6563730577E+04
              0.0000000000E+00-0  0.5176262775E+04
              0.2054666000E+00  0.2767997811E+05
5LOW B       0.0000000000E+00-0  0.6563730577E+04
              0.0000000000E+00-0  0.3133049215E+04
              0.0000000000E+00-0  0.2470994031E+04
              0.0000000000E+00  0.1320530369E+05
              0.7423330000E-01  0.6303181862E+04
6TERT BTERT C 0.0000000000E+00-0  0.5176262775E+04
              0.0000000000E+00-0  0.2470994031E+04
              0.0000000000E+00-0  0.1949040882E+04
              0.0000000000E+00  0.1040148766E+05
              0.0000000000E+00  0.4965361115E+04
              0.8220000000E-01  0.3916517680E+04
7HIGH C     0.0000000000E+00-0  0.1375182324E+05
              0.0000000000E+00-0  0.6563730577E+04
              0.0000000000E+00-0  0.5176262775E+04
              0.0000000000E+00-0  0.1375182324E+05
              0.0000000000E+00-0  0.6563730577E+04
              0.0000000000E+00-0  0.5176262775E+04
              0.2054666000E+00  0.2767997811E+05
8LOW C       0.0000000000E+00-0  0.6563730577E+04
              0.0000000000E+00-0  0.3133049215E+04
              0.0000000000E+00-0  0.2470994031E+04
              0.0000000000E+00-0  0.6563730577E+04
              0.0000000000E+00-0  0.3133049215E+04
              0.0000000000E+00-0  0.2470994031E+04
              0.0000000000E+00-0  0.2470994031E+04
              0.0000000000E+00-0  0.1949040882E+04
              0.0000000000E+00  0.1040148766E+05
              0.0000000000E+00  0.4965361115E+04
              0.8220000000E-01  0.3916517680E+04
9TERT CTERT A 0.0000000000E+00-0  0.5176262775E+04
              0.0000000000E+00-0  0.2470994031E+04
              0.0000000000E+00-0  0.1949040882E+04
              0.0000000000E+00-0  0.5176262775E+04
              0.0000000000E+00-0  0.2470994031E+04
              0.0000000000E+00-0  0.1949040882E+04
              0.0000000000E+00  0.1040148766E+05
              0.0000000000E+00  0.4965361115E+04
              0.8220000000E-01  0.3916517680E+04
1BLANK CARD ENDING BCTRAN SETUPS

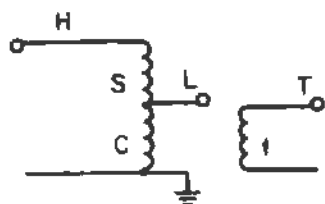
```

Autotransformer short-circuit tests are conducted in a similar fashion to tests on other transformers. The results could be used to generate a model matrix in the normal way, probably with acceptable results. However, the user should more properly represent the autotransformer with its three windings, series, common, and tertiary, as shown in Figure 3-6. If the short-circuit test results are Z_{h1} , Z_{ht} and Z_{1t} , then the short-circuit impedances to use in developing the model matrix would be called Z_{sc} , Z_{st} and Z_{ct} . These new impedances are derived from the measured impedances and the actual winding voltage ratings, V_s , V_c , and V_t . The final autotransformer model is developed with the proper terminal connections of the three-winding banks.

$$Z_{sc} = Z_{h1} * (V_h / (V_h - V_1))^2 \quad (3-37)$$

$$Z_{ct} = Z_{1t} \quad (3-38)$$

$$Z_{st} = Z_{h1} * (V_h * V_1) / (V_h - V_1)^2 + Z_{ht} * V_h / (V_h - V_1) - Z_{1t} * V_1 / (V_h - V_1) \quad (3-39)$$



$$V_s = V_h - V_1 \quad (3-40)$$

$$V_c = V_1 \quad (3-41)$$

$$V_t = V_t \quad (3-42)$$

Figure 3-6. Autotransformer Windings

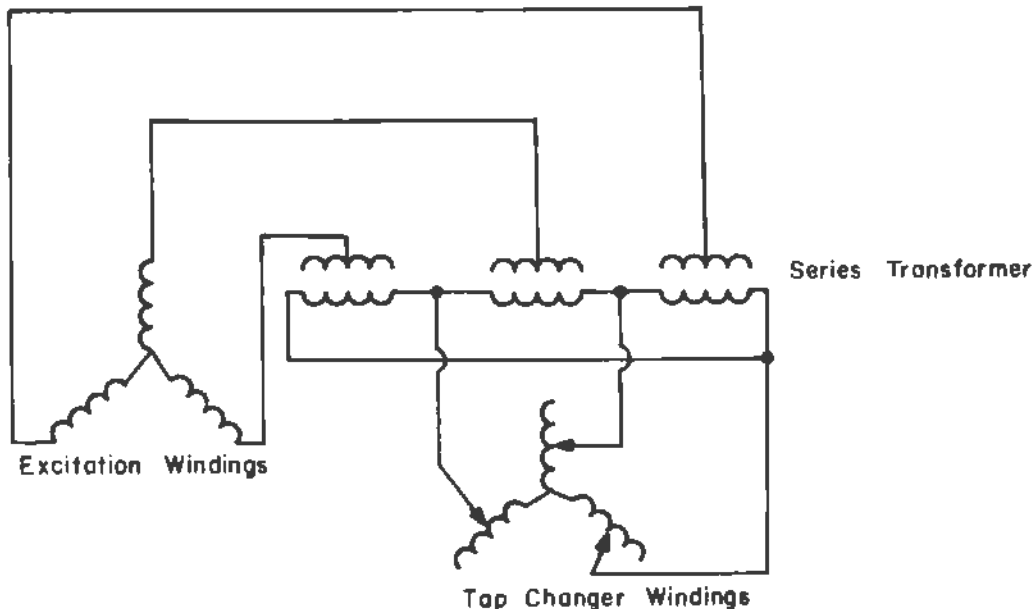


Figure 3-7. Phase Shifting Transformer Winding Connections

A phase shifting transformer can also be represented in the EMTP by deriving a matrix for the physical windings and then making the proper terminal connections, as described by Lembo in the June 1981 issue of the EMTP Newsletter. Figure 3-7 shows the schematic connections of the windings for a device which performs phase shifting by injecting a series line voltage. The necessary impedance data for deriving the matrix must be obtained from the transformer manufacturer. The desired phase shift angle, and corresponding series voltage, will determine the polarity and tap setting of the transformer. This will require a new matrix for each phase shift angle to be simulated. It is assumed that the tap setting will not change during any simulated switching transients.

3-5. TRANSFORMER CORE SETUP EXAMPLES

This section contains examples of the nonlinear magnetizing impedance setup for the transformer in Table 3-1. Two of the EMTP auxiliary setup routines are illustrated. The first example uses CONVERT to generate the data for a piecewise linear inductance, while the second example uses HYSDAT to generate Type 96 hysteretic inductance branch data. Both branches are to be connected across the 50-kV delta tertiary windings, because those windings are closest to the core.

The typical data is taken from Section 3-8. For the 300-MVA transformer, excitation currents of 0.25% at 100% voltage and 1.0% at 110% voltage are assumed. These points define the inputs to CONVERT. The current at 110% voltage could be used to define the saturation point for input to HYSOAT; the flux at saturation would be $(50000.0 \cdot \sqrt{2}) / 377$ and the current at saturation would be $(100 \text{ MVA} / 50 \text{ kV}) \cdot 0.0025 \cdot \sqrt{2} = 7.071$ amperes peak. However, for reasons described in Section 3-6, it may be necessary to specify a higher saturation flux and current to permit successful initialization of the Type 96 model for an EMTP transient run. The output from CONVERT was used to define the saturation point for input to HYSOAT; flux = 206.32 volt-seconds and current = 50.0 amperes. The subroutine HYSOAT has the shape for one core material stored within it. The input and output for CONVERT are shown in Table 3-9, while the input and output for HYSOAT are shown in Table 3-10.

Table 3-9
 CONVERT INPUT AND OUTPUT

```

BEGIN NEW DATA CASE
SATURATION
C USING THE PROGRAM CONVERT
C FREQ-HZ   KV-BASE   MVA-BASE   IPUNCH   KTHRD
C          60.0     50.00     100.0     1=NO     1=1ST AND 3RD QUADRANT POINTS
C          EB.0     EB.0     EB.0     IB       IB
C          I-RMS P.U.   V-RMS P.U.
C          E16.0     E16.0
C          0.0025     1.0
C          0.0100     1.1
C          9999
BLANK CARD ENDING SATURATION CASES
END LAST DATA CASE

DERIVED SATURATION CURVE GIVING PEAK CURRENT VS. FLUX
ROW      CURRENT (AMP)      FLUX (VOLT-SEC)
1        0.000000000      0.000000000
2        7.0710678119     187.5658991994
3        49.5702631919    206.3224891193
          9999

CHECK OF DERIVED CURVE BY INDEPENDENT REVERSE COMPUTATION.
ASSUMING SINUSOIDAL VOLTAGE (FLUX) AT LEVEL OF EACH POINT,
RMS CURRENT IS FOUND NUMERICALLY.
THIS CURVE SHOULD BE EQUAL TO THE ORIGINAL I-V POINTS INPUTTED.

ROW      CURRENT IN P.U.      VOLTAGE IN P.U.
2        0.00250000         1.00000000
3        0.01000000         1.10000000

BLANK CARD TERMINATING ALL SATURATION CASES      1BLANK CARD ENDING SATURATION CASES
  
```

Table 3-10

HYSDAT INPUT AND OUTPUT

```

BEGIN NEW DATA CASE
SATURATION
C USE OF THE SUBPROGRAM, HYSDAT, IS FLAGGED BY FREQ=88
C FREQ
C   EB.O
C   88.
C ITYPE      LEVEL      IPUNCH
C MUST=1     1=4-5 PTS   0=YES
C ARMCD M4   2=10 PTS    1=NO
C ORIENTED   3=15 PTS
C SILICON    4=20-25 PTS
C STEEL
C   18       18       18
C   1        3        1
C CUPSAT     FLUXSAT
C (AMPS)     (VOLT-SEC)
C   EB.O     EB.O
C   50.000   206.32
BLANK CARD ENDING HYSDAT CASES
BLANK CARD ENDING SATURATION CASES
END LAST DATA CASE

```

DERIVED TYPE-96 CHARACTERISTIC FOLLOWS%

CURRENT	FLUX
-0.1875000E+02	-0.2014654E+03
-0.9375000E+01	-0.1990381E+03
-0.3125000E+01	-0.1929699E+03
-0.6250000E+00	-0.1869016E+03
0.1093750E+01	-0.1723379E+03
0.2062500E+01	-0.1456376E+03
0.3750000E+01	0.1043736E+03
0.5937500E+01	0.1492786E+03
0.8437500E+01	0.1674833E+03
0.1250000E+02	0.1820471E+03
0.1843750E+02	0.1917562E+03
0.2875000E+02	0.1990381E+03
0.5000000E+02	0.2063200E+03
0.6875000E+02	0.2075336E+03
0.9990000E+04	

BLANK CARD ENDING HYSTERESIS-CURVE REQUESTS
 BLANK CARD TERMINATING ALL SATURATION CASES

1BLANK CARD ENDING HYSDAT CASES
 1BLANK CARD ENDING SATURATION CASES

3-6. TRANSFORMER TEST CASES

This section includes four cases of initiating a single-line-to-ground fault on the transformer low-voltage winding terminals shown in Figure 3-8. The case is run with the saturable TRANSFORMER and BCTRAN models taken from the setup examples, both with and without the delta tertiary closed.

Two test cases of initiating the fault are then performed with saturation represented. One contains a Type 98 piecewise linear inductance branch generated by CONVERT, and the other contains a Type 96 hysteresis branch generated by HYSDAT.

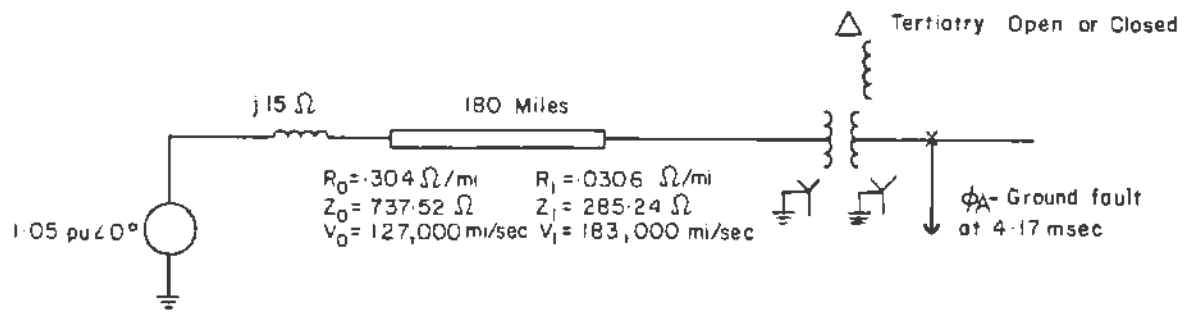


Figure 3-8. Transformer Test Case System

The EMTP input for the system in Figure 3-8, minus the transformer model, is shown in Table 3-11. Transformer and saturation models from Sections 3-4 and 3-5 are plugged into this input file. The case results are shown in Table 3-12. The fault currents and the phase B primary voltages for each case are presented in Figures 3-9 through 3-14.

Results from the saturable TRANSFORMER branches and the BCTRAN matrix are equivalent when the delta tertiary winding is closed. When the delta tertiary is opened, the transformer voltages increase and the fault current decreases in the saturable TRANSFORMER model. This occurs because the zero-sequence impedance changes drastically when the delta tertiary is opened. The BCTRAN matrix includes 100% zero-sequence excitation current, so that the results are not affected as much when the delta tertiary is opened. Therefore, if a three-phase three-winding transformer includes a closed delta tertiary, it is probably not necessary to use the matrix setup routines.

The cases with saturation represented are not directly comparable to the first four cases because the branches from Section 3-5 were directly added to the tertiary terminals, thereby increasing the total excitation current. The delta winding was open-circuited. Saturation slightly increased the overvoltages,

although the Type 98 results differed from the Type 96 results. The shapes of the exciting branch currents also differed, as the user may observe by running the cases and plotting the currents.

The Type 96 branches were automatically initialized by the EMTP, this feature being requested with a "8888." in columns 27-32. The initial flux and current point is obtained by constructing a trajectory from the origin to the saturation point which was inputted to HYS DAT, and then determining the current from this curve at 70% of the saturation flux. The user can input his own value of initial flux and current, but this point must lie within the major hysteresis loop. In the first case attempted, two of the branches were initialized outside the major hysteresis loop, which generated a warning message and an adjustment by the EMTP. Numerical instabilities were noted in the tertiary terminal voltages.

The saturation flux and current were increased, as described in Section 3-5, to allow initialization of the Type 96 model within its major hysteresis loop. This was accomplished, but the tertiary terminal voltages were still unstable, and ferroresonance also appeared at the other terminals. It is difficult to match the characteristic generated by HYS DAT with that generated by CONVERT. The first Type 96 model had much less magnetizing current, while the second Type 96 model had larger magnetizing current which produced ferroresonance.

An attempt to model saturation at the star point of the saturable TRANSFORMER branch yielded grossly distorted waveshapes. It is therefore recommended that separate external branches be used to simulate saturation at the terminals of the lowest voltage windings.

If transformer saturation must be represented, the Type 98 branch connected across the lowest voltage winding terminals appears to be the most reliable model. Core losses should be represented by separate parallel resistances. The Type 96 branch without the extra resistances is theoretically attractive, but great care must be taken in using it, especially with regard to initialization. The Type 96 branch must not be initialized outside of its major hysteresis loop. The choice of only one core material in the subroutine HYS DAT may restrict the user from accurately modelling the desired shape of the saturation curve. Finally, the outputs from an EMTP case using the Type 96 branch should be inspected carefully.

Computation times for all of these cases fell within the same order of magnitude. As might be expected, the Type 96 CPU time was slightly higher than the other cases.

Table 3-11

EMTP INPUT FOR SINGLE-LINE-TO-GROUND FAULTS

```

BEGIN NEW DATA CASE
49.18E-6 60.E-3 60.0 60.0
20000 1 1 1 1
SRCE ASWT A 15.0
SRCE BSWT BSRCE ASWT A
SRCE CSWT CSRCE ASWT A
-1LINE AHIGH A 0.304737 521.27E5 180.0 1
-2LINE BHIGH B 0.0360285 241.83E5 180.0 1
-3LINE CHIGH C
LOW AFAULTA 0.1
C
C TRANSFORMER MODEL BRANCH CARDS ARE INSERTED HERE
C
BLANK CARD ENDING BRANCHES
SWT ALINE A -0.005 1.0
SWT BLINE B -0.005 1.0
SWT CLINE C +0.005 1.0
FAULTA 0.004167 1.0
BLANK CARD ENDING SWITCHES
14SRCE A 197184.0 60.0 0.0 -1.0
14SRCE B 197184.0 60.0 240.0 -1.0
14SRCE C 197184.0 60.0 120.0 -1.0
BLANK CARD ENDING SOURCES
1
BLANK CARD ENDING CALCOMP PLOTS
BLANK CARD ENDING THE CASE

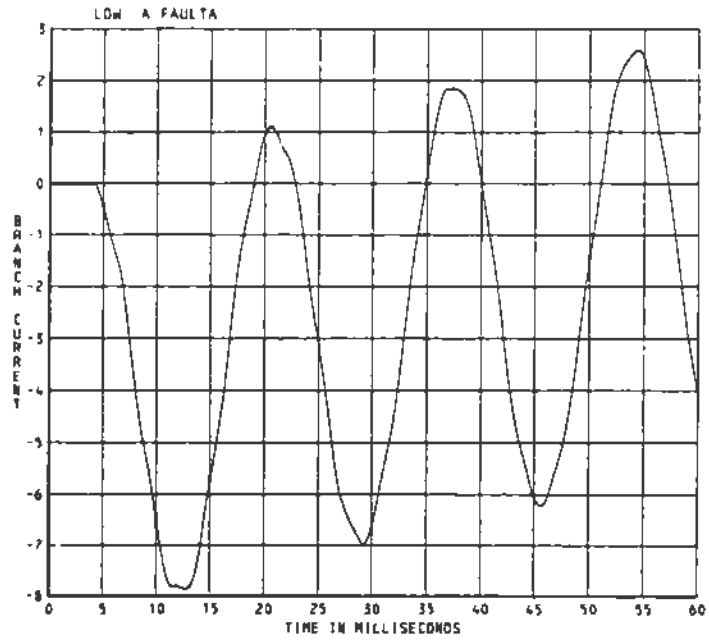
```

Table 3-12

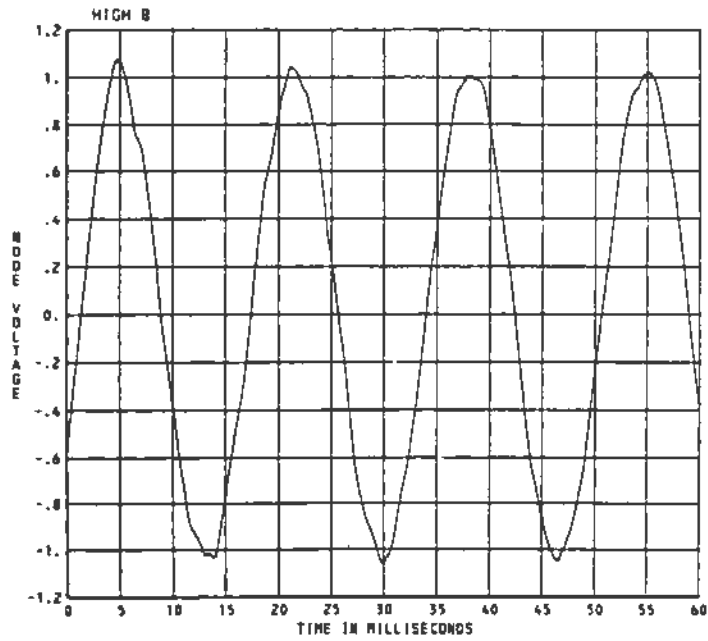
SINGLE-LINE-TO-GROUND FAULT CASE RESULTS PEAK TRANSIENT MAGNITUDES

Case	Primary Voltages			Secondary Voltages			Tertiary Voltages			Fault [kA]
	[kV]			[kV]			[kV]			
	A	B	C	A	B	C	A	B	C	
Sat. XF, D closed	215.3	201.8	215.3	102.7	93.8	102.7	81.0	70.5	-	7.87
Sat. XF, D open	215.3	281.8	290.4	102.7	134.5	138.6	3.3	109.6	165.0	3.27
BCTTRAN, 0 closed	215.3	200.5	215.3	102.7	93.6	102.7	81.0	70.6	-	7.95
BCTTRAN, D open	201.2	220.2	221.3	102.7	103.6	104.0	59.6	81.0	81.0	6.23
BCTTRAN, Type 98	213.9	230.5	232.4	102.5	108.5	108.8	60.2	81.8	81.9	6.20
BCTTRAN, Type 96	271.7	298.8	290.1	102.6	141.1	135.7	75.2	81.5	105.6	6.18

	Saturation Branch Currents			Cray 1-S CPU Time
	[Amperes]			
	B-A	C-B	Grnd-C	
Sat. XF, D closed	-	-	-	1.469
Sat. XF, D open	-	-	-	1.474
BCTTRAN, D closed	-	-	-	1.305
BCTTRAN, D open	-	-	-	1.331
BCTTRAN, Type 98	61.8	133.7	135.8	1.416
BCTTRAN, Type 96	112.4	558.1	565.7	1.636

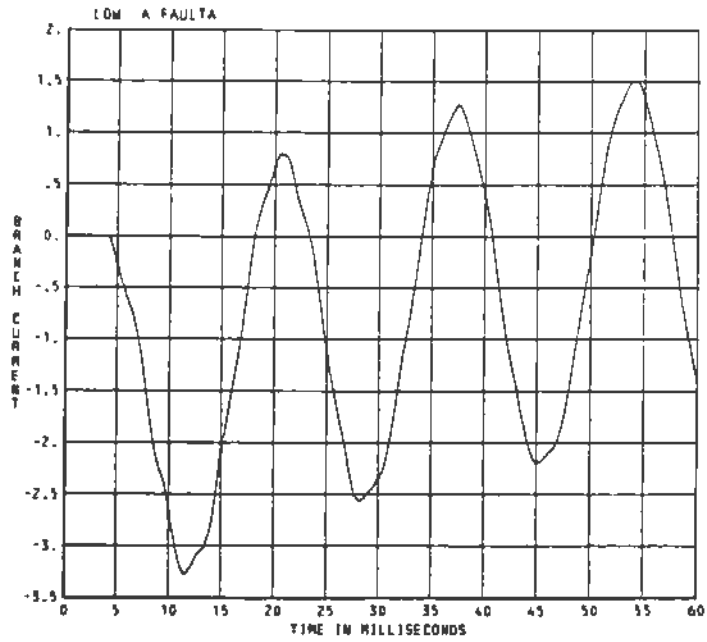


a) Phase A Fault Current

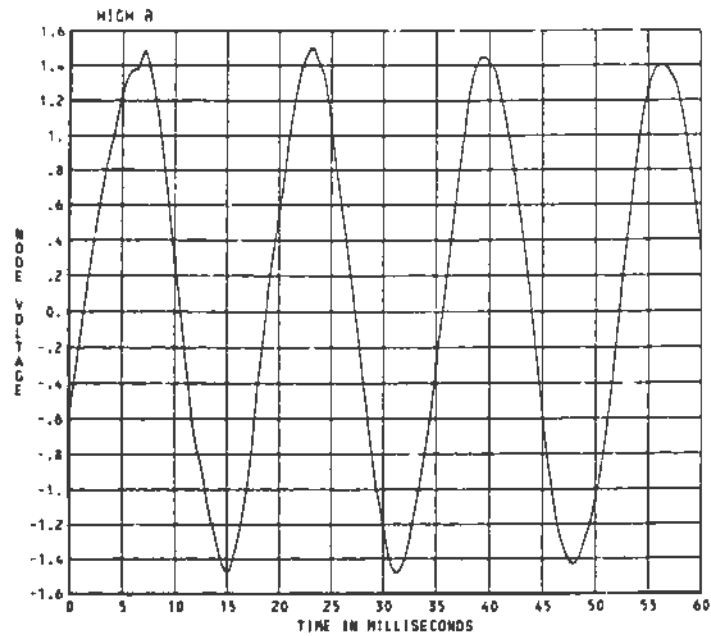


b) Phase B Primary Voltage

Figure 3-9. Single-Line-to-Ground Low Side Fault Saturable TRANSFORMER, Closed Delta Tertiary

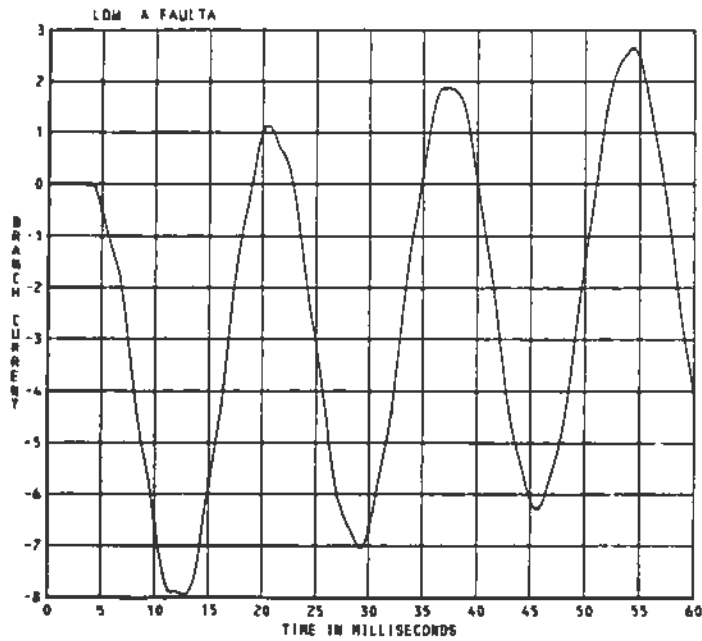


a) Phase A Fault Current

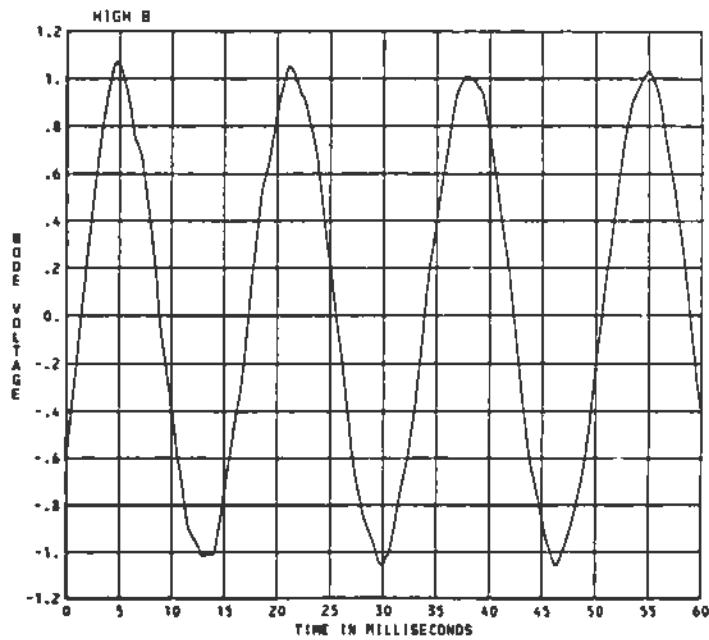


b) Phase B Primary Voltage

Figure 3-10. Single-Line-to-Ground Low Side Fault Saturable TRANSFORMER, Open Delta Tertiary

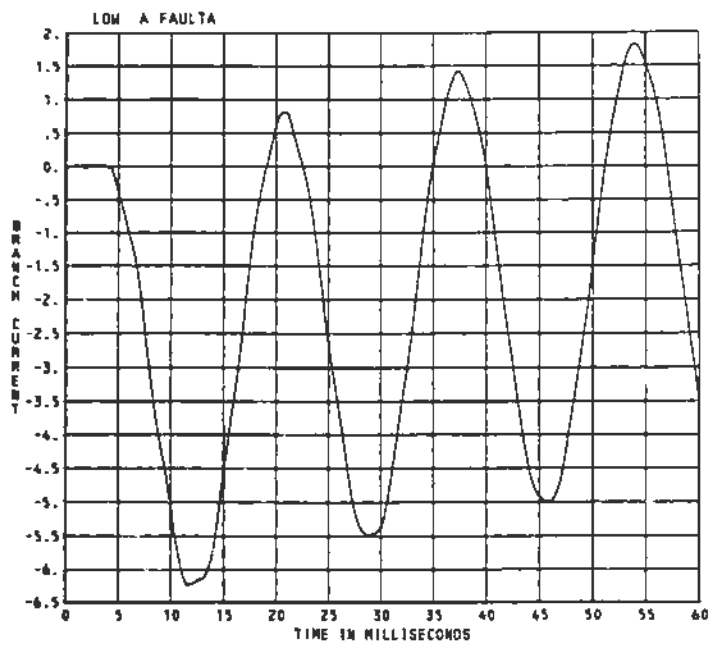


a) Phase A Fault Current

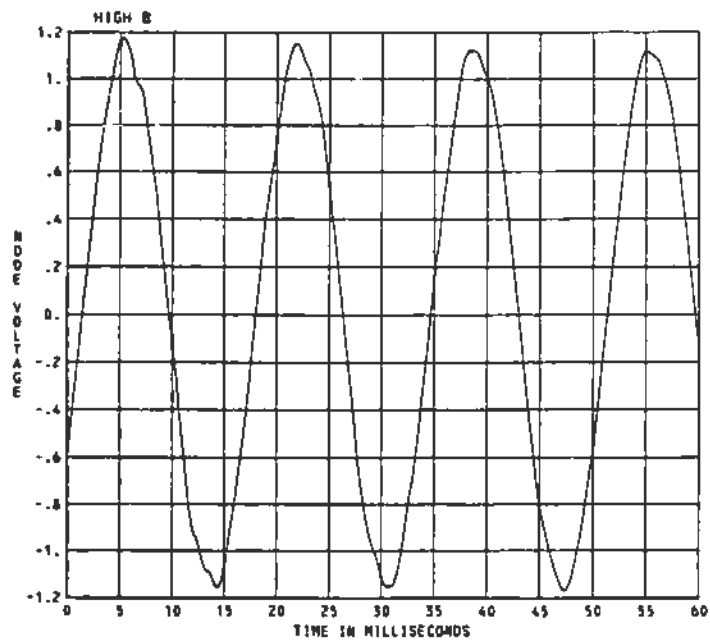


b) Phase B Primary Voltage

Figure 3-11. Single-Line-to-Ground Low Side Fault
BCTAN, Closed Delta Tertiary

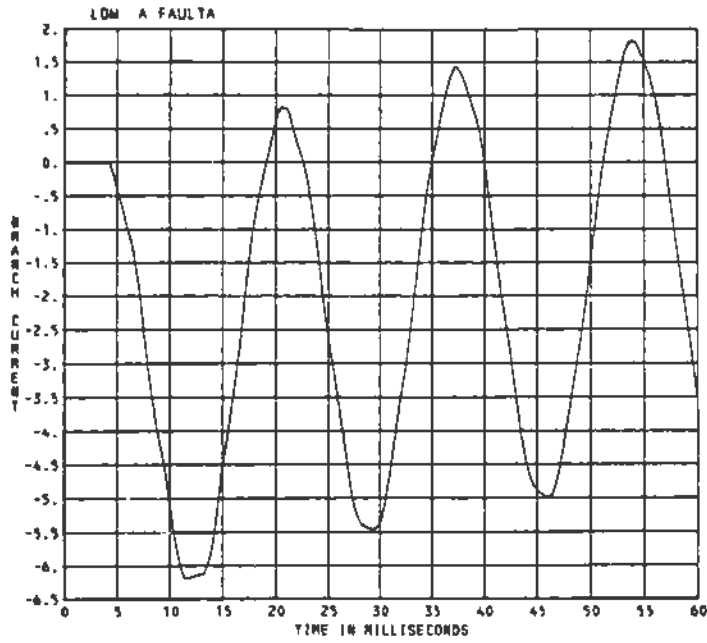


a) Phase A Fault Current

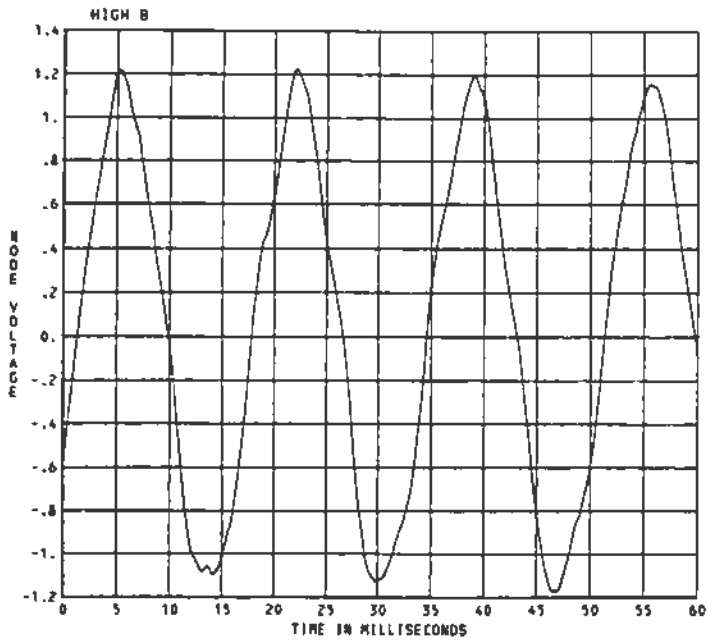


b) Phase B Primary Voltage

Figure 3-12. Single-Line-to-Ground Low Side Fault
BCTAN, Open Delta Tertiary

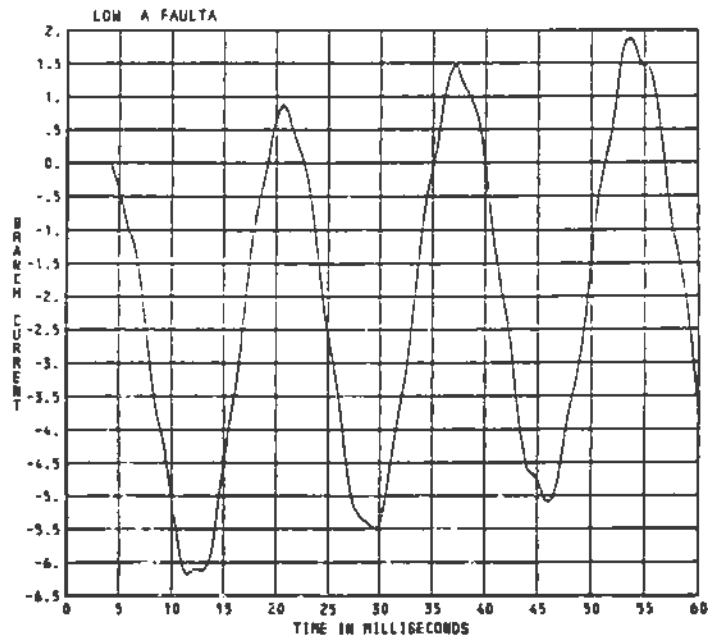


a) Phase A Fault Current

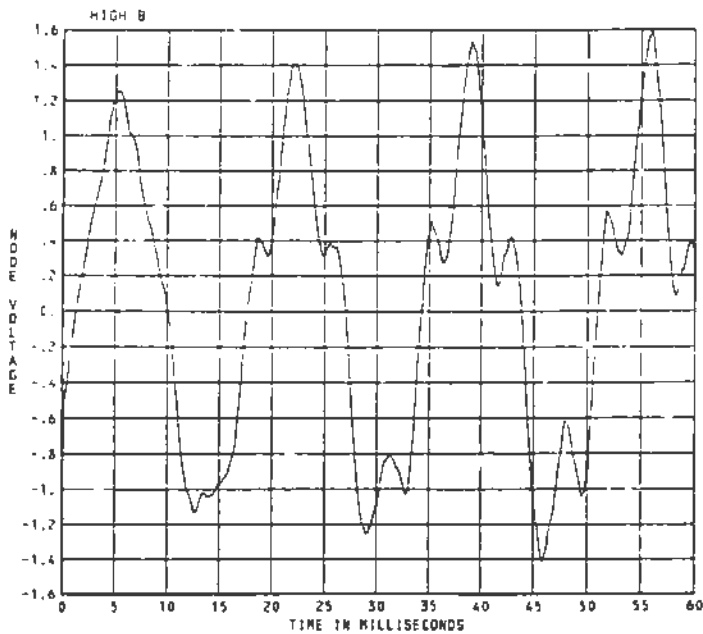


b) Phase B Primary Voltage

Figure 3-13. Single-Line-to-Ground Low Side Fault BCTAN, Open Delta Tertiary, Type 98 Saturation



a) Phase A Fault Current



b) Phase B Primary Voltage

Figure 3-14. Single-Line-to-Ground Low Side Fault BCTAN, Open Delta Tertiary, Type 96 Hysteresis

3-7. HIGH-FREQUENCY MODEL SETUP EXAMPLE

This section contains an illustration of applying typical transformer capacitances to the BCTRAN model taken from the setup examples. Two cases of response to a single-phase 2x100 microsecond surge are simulated, one with and one without the capacitances. The capacitance data is taken from Section 3-9. Typical values of 10 nF for C_{lg} and C_{hl} were read from the Figures, and C_{hg} was then assumed to be half of C_{lg} :

$$\begin{aligned}C_{hg} &= 5 \text{ nF} \\C_{lg} &= 10 \text{ nF} \\C_{hl} &= 10 \text{ nF}\end{aligned}$$

These are 60-Hz capacitances. For impulses, the values were divided by 2. The effect of the capacitances was tested with a single-phase, 1200-kV, 2 x 100 microsecond surge input to the phase B primary, as illustrated in Figure 3-15. The EMTP input for the capacitances is shown in Table 3-13. The capacitances are simply added as extra branches connected to the transformer terminals.

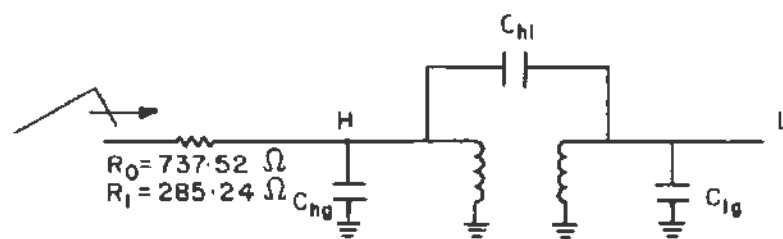


Figure 3-15. Single-Phase Surge Applied to Transformer

Table 3-13

TRANSFORMER CAPACITANCE BRANCH INPUT

C	TRANSFORMER CAPACITANCES	
C	HIGH-TO-GROUND	COLUMNS 39-44
	HIGH A	0.0025
	HIGH B	0.0025
	HIGH C	0.0025
C	LOW-TO-GROUND	COLUMNS 39-44
	LOW A	0.0050
	LOW B	0.0050
	LOW C	0.0050
C	HIGH-TO-LOW	COLUMNS 39-44
	HIGH ALOW A	0.0050
	HIGH BLOW B	0.0050
	HIGH CLOW C	0.0050
	BLANK CARD ENDING BRANCHES	

The results are given in Table 3-14. The phase B primary and secondary voltages, with and without transformer capacitances, are plotted in Figures 3-16 and 3-17. It may be seen that the capacitances lengthen the wavefront and slightly reduce the peak magnitudes. A natural frequency of 18.2 kHz is evident in the secondary terminal voltage with the capacitances. This frequency can be estimated from the parameters in Figure 3-15, as viewed from the low-voltage terminal.

$$C_{eq} = 0.005 + (0.005 * 0.0025) / (0.005 + 0.0025) \quad (3-43)$$

$$= 0.0067 \mu\text{F}$$

$$L_{eq} = 0.0874 * (109.8 * 109.8) / (300 * 377) \quad (3-44)$$

$$= 9.32 \text{ mH}$$

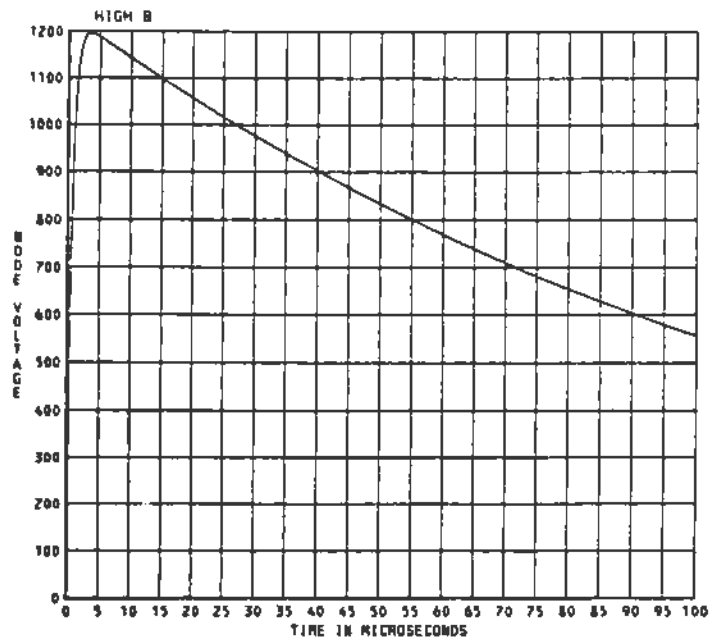
$$f = 1 / (2\pi \sqrt{LC}) = 20.2 \text{ kHz} \quad (3-45)$$

The surge front and tail times were varied in an attempt to produce higher over-voltages by exciting one of the transformer resonant frequencies, but none of the cases with a single surge input produced exceptionally higher overvoltages. There has been concern that repetitive excitation, such as from a prestriking or restriking circuit breaker, might excite a transformer resonant frequency and

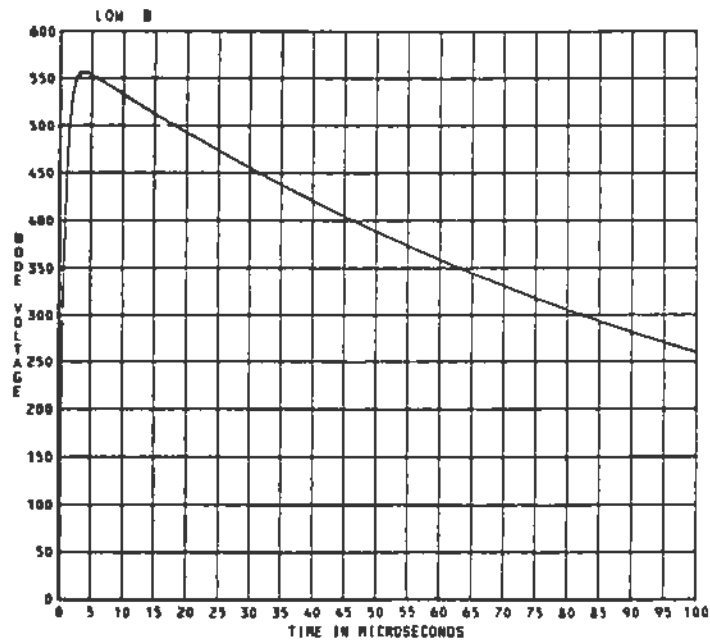
generate damaging overvoltages inside the windings. Lumped capacitances at the transformer terminals can be used in an attempt to represent only the terminal behavior, in a coarse way. Any investigation of internal transformer winding resonances must be undertaken with the close collaboration of the transformer's manufacturer.

Table 3-14
SURGE TRANSFER CASE RESULTS

Case	Primary [kV]		Secondary [kV]		Tertiary [kV]			Wavefronts [μsec]	
	<u>B</u>	<u>A/C</u>	<u>B</u>	<u>A/C</u>	<u>A</u>	<u>B</u>	<u>C</u>	<u>High-B</u>	<u>Low-B</u>
	Without Caps	1197	- 41.9	556.5	-25.7	331.2	370.7	-40.0	3.5
With Caps	1130	-129.4	549.8	-64.5	324.6	365.2	-66.8	10.4	8.8

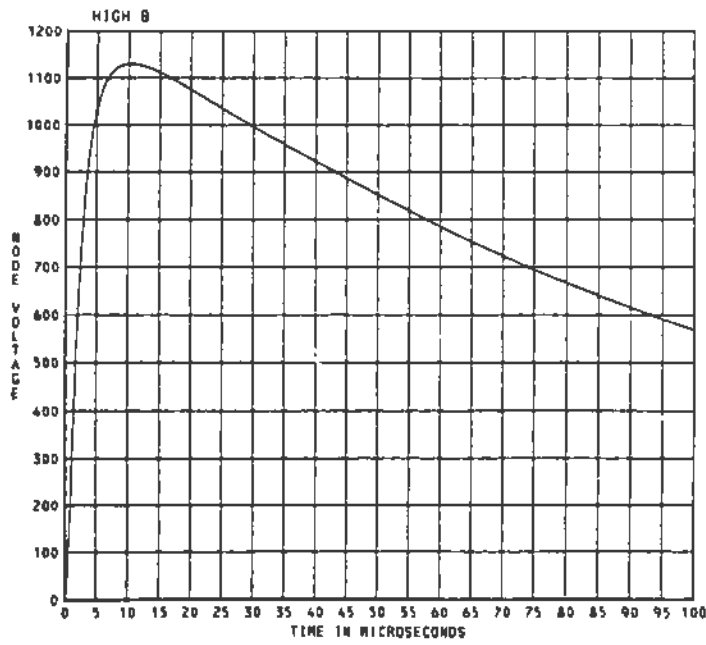


a) Phase B Primary Voltage

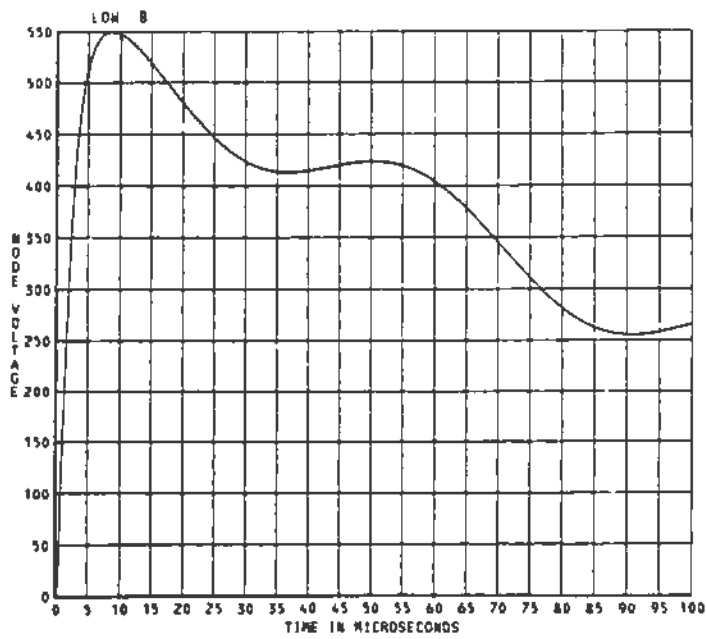


b) Phase B Secondary Voltage

Figure 3-16. Surge Transfer Without Transformer Capacitances



a) Phase B Primary Voltage



b) Phase B Secondary Voltage

Figure 3-17. Surge Transfer With Transformer Capacitances

3-8. TRANSFORMER MODEL CHARACTERISTICS AND TYPICAL DATA

Power system transformers have several different characteristics which may be important in transient studies. The relative importance of these parameters varies with the type of study and the frequency range of interest, as summarized in Table 3-15, based on Ardito and Santagostino, "A Review of Digital and Analog Methods of Calculation of Overvoltages in Electric Systems," Cigre SC 33, Overvoltages and Insulation Coordination Colloquium in Budapest, 23-25 September 1985.

Table 3-15
TRANSFORMER MODEL CHARACTERISTICS

Characteristic	Frequency Band			
	0-5kHz	3-30kHz	5kHz-3MHz	50kHz-30MHz
Leakage Inductance	X	X		
Phase-to-Phase Coupling	X	X		
Saturation	X	X		
Asymmetry of Phases	X			
Frequency-Dependent Losses	X	X		
Hysteresis & Core Losses	X*	X*		
Capacitive Coupling		X**	X	X

* usually important only for ferroresonance or no-load switching

** in this frequency range, usually important only for surge transfer or no-load switching

Figures on the following pages illustrate the ranges of typical data for auto-transformers, core-form transformers and shell-form transformers. The data is plotted against either the transformer MVA rating or the nominal system voltage. The parameters considered include:

- Figure 3-18. Transformer Lowest Insulation Strength (vs. kV)
- Figure 3-19. Positive Sequence Impedance of Non-Autotransformers (vs. BIL)
- Figure 3-20. Positive Sequence Impedance of Autotransformers (vs. BIL)
- Figure 3-21. Core Loss (vs. MVA)
- Figure 3-22. Load Loss (vs. MVA)
- Figure 3-23. Exciting Current at 100% Voltage (vs. MVA)
- Figure 3-24. Exciting Current at 110% Voltage (vs. MVA)
- Figure 3-25. Leakage Reactance (vs. MVA)

Typical data drawn from these plots may be used to develop EMTF transformer models as illustrated in the previous examples.

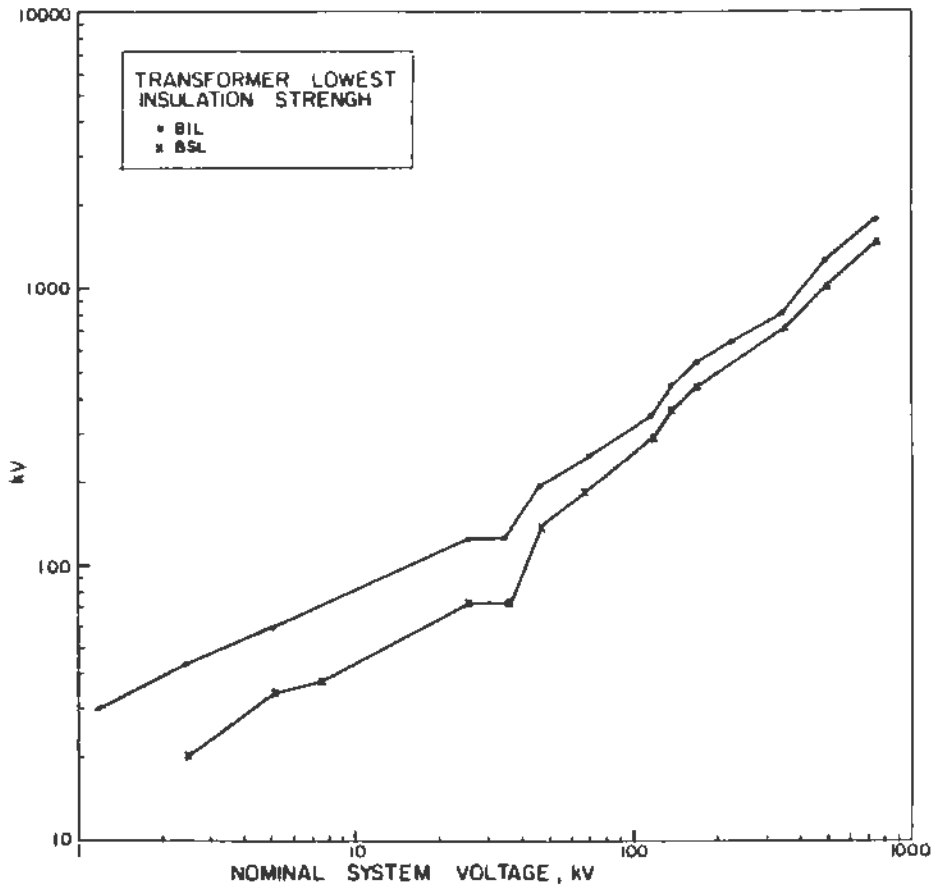


Figure 3-18. Transformer Lowest Insulation Strength (vs. kV)

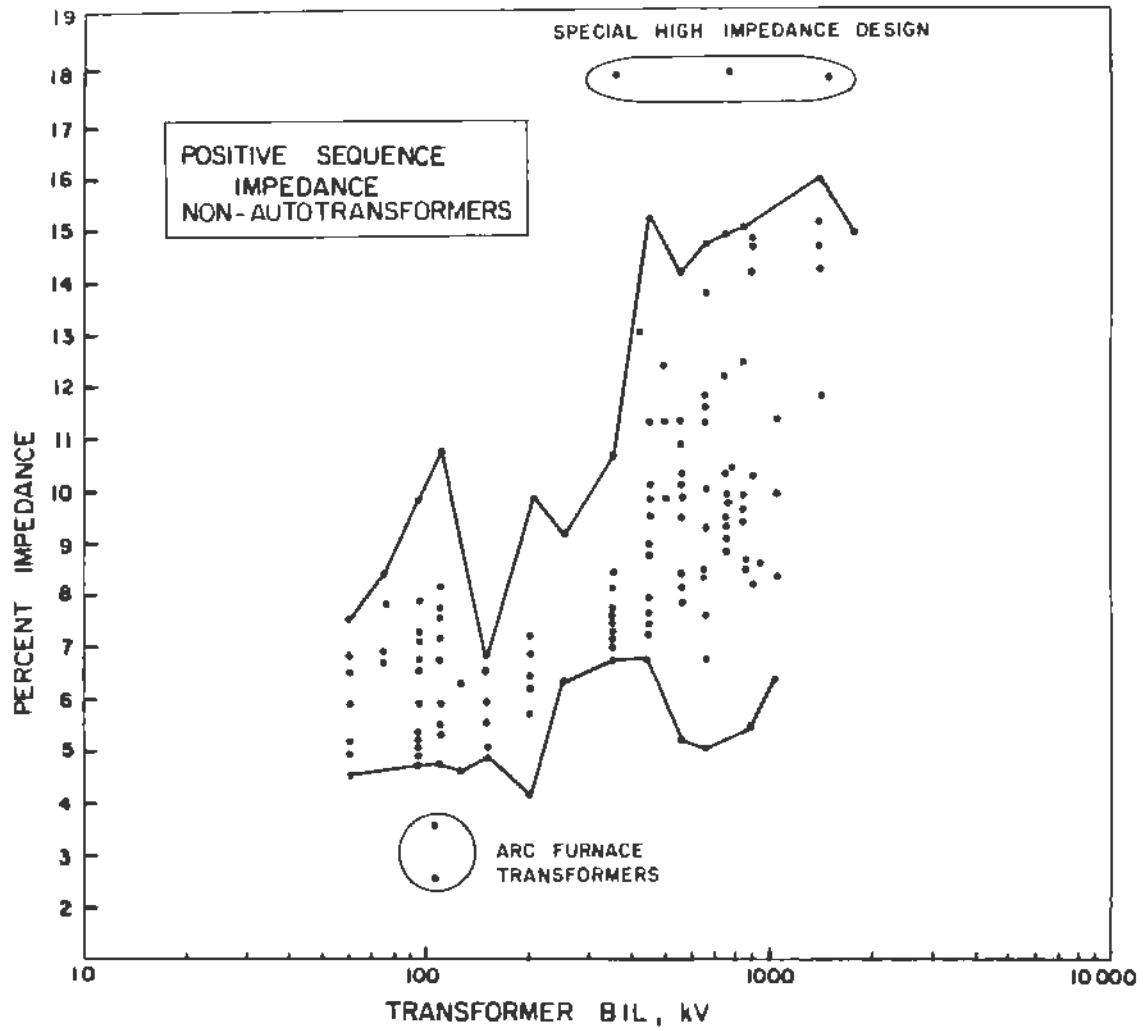


Figure 3-19. Positive Sequence Impedance of Non-Autotransformers (vs. BIL)

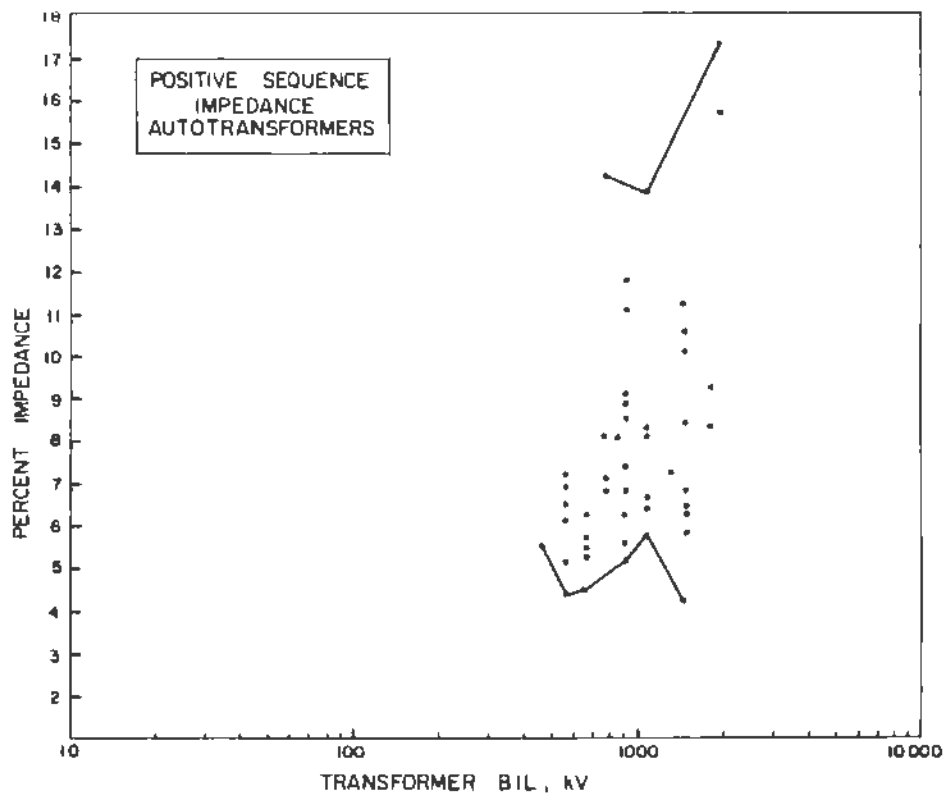


Figure 3-20. Positive Sequence Impedance of Autotransformers (vs. BIL)

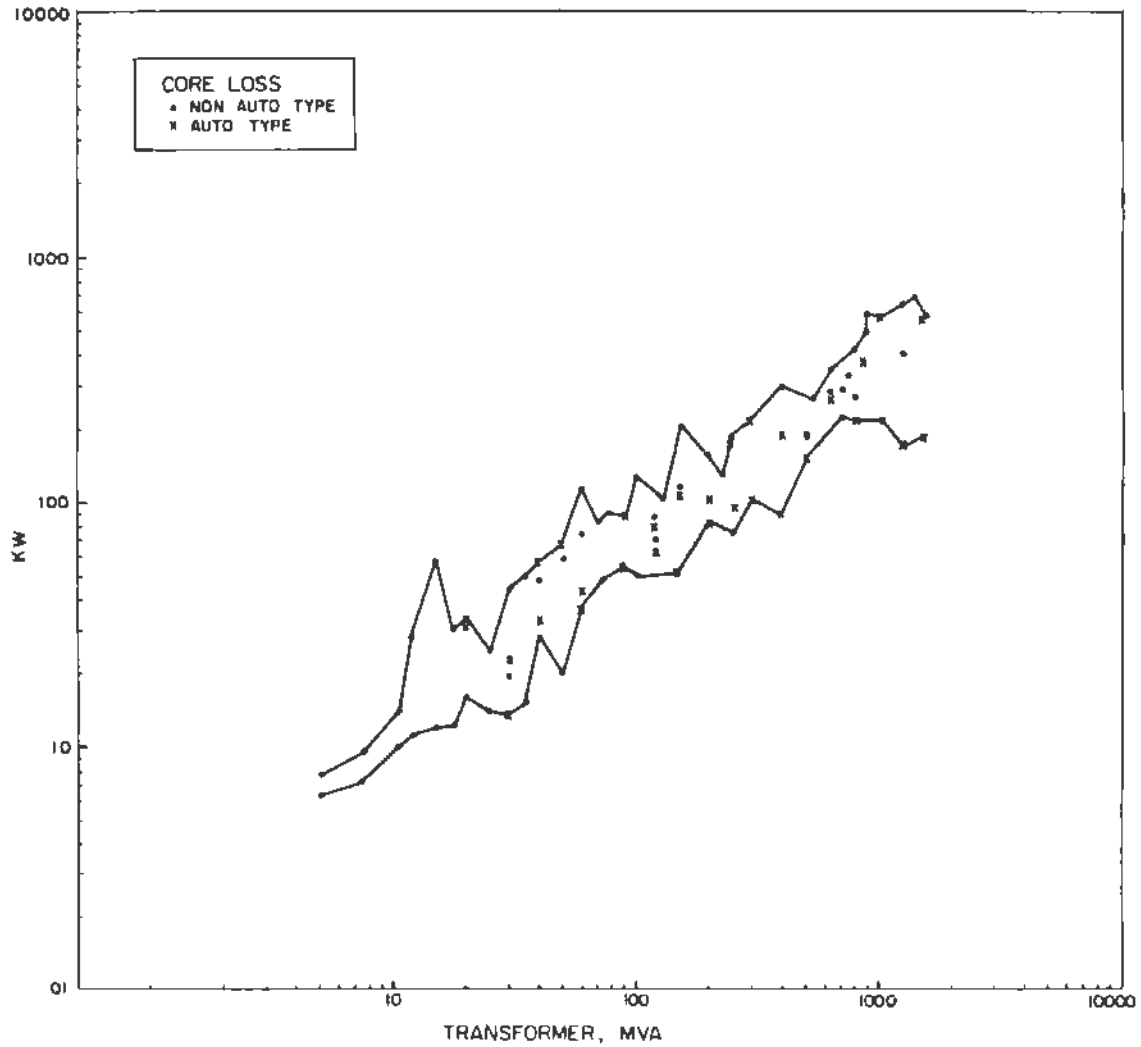


Figure 3-21. Core Loss (vs. MVA)

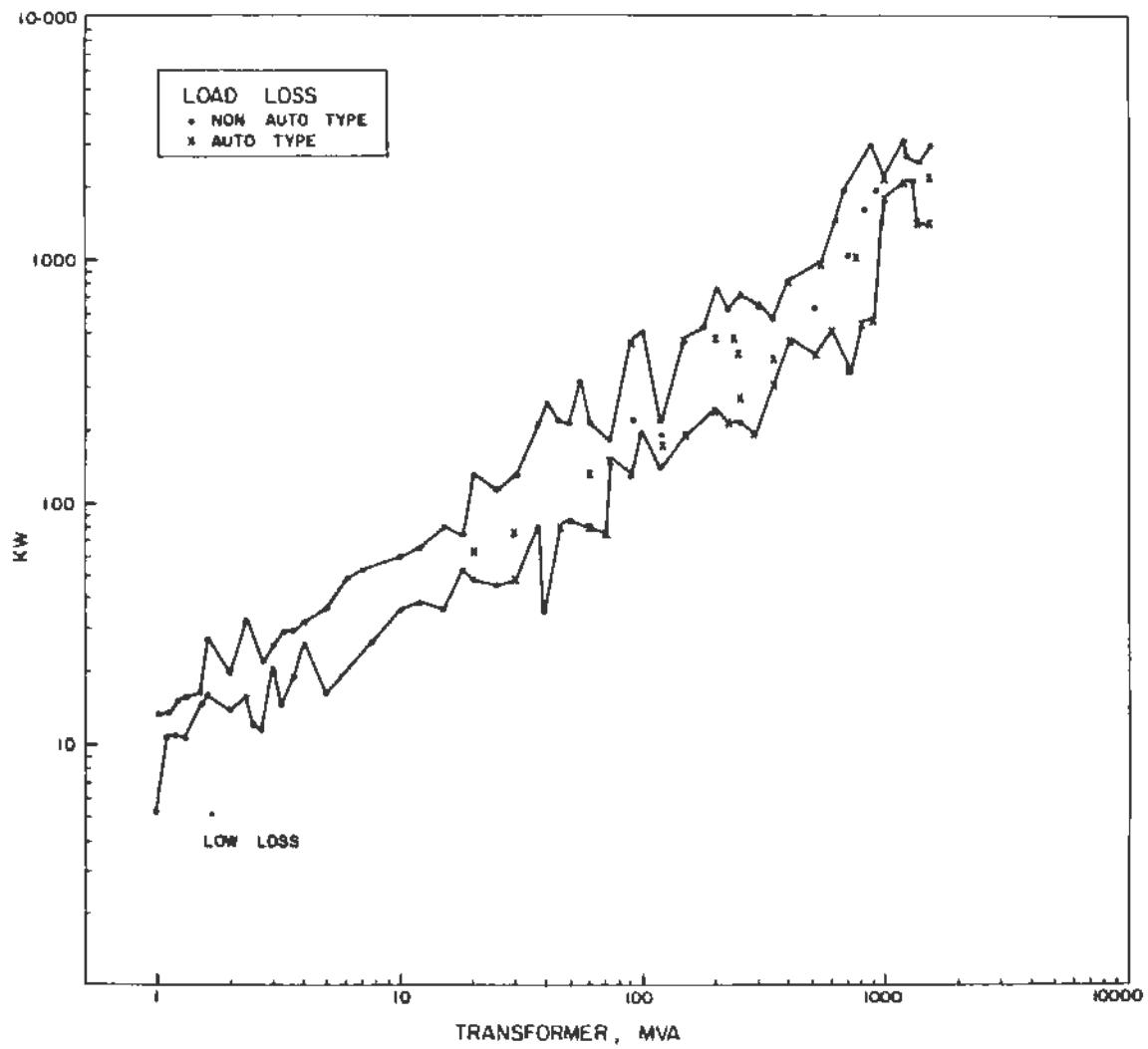


Figure 3-22. Load Loss (vs. MVA)

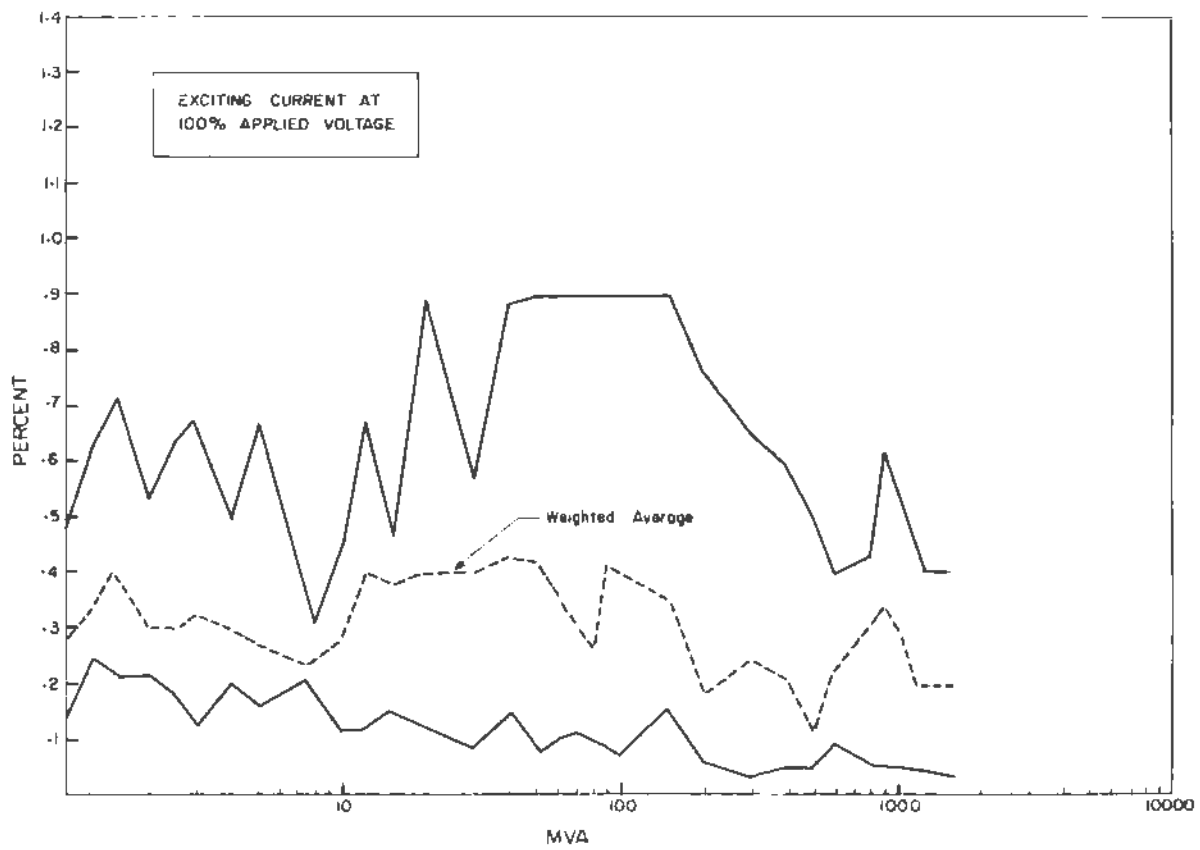


Figure 3-23. Exciting Current at 100% Voltage (vs. MVA)

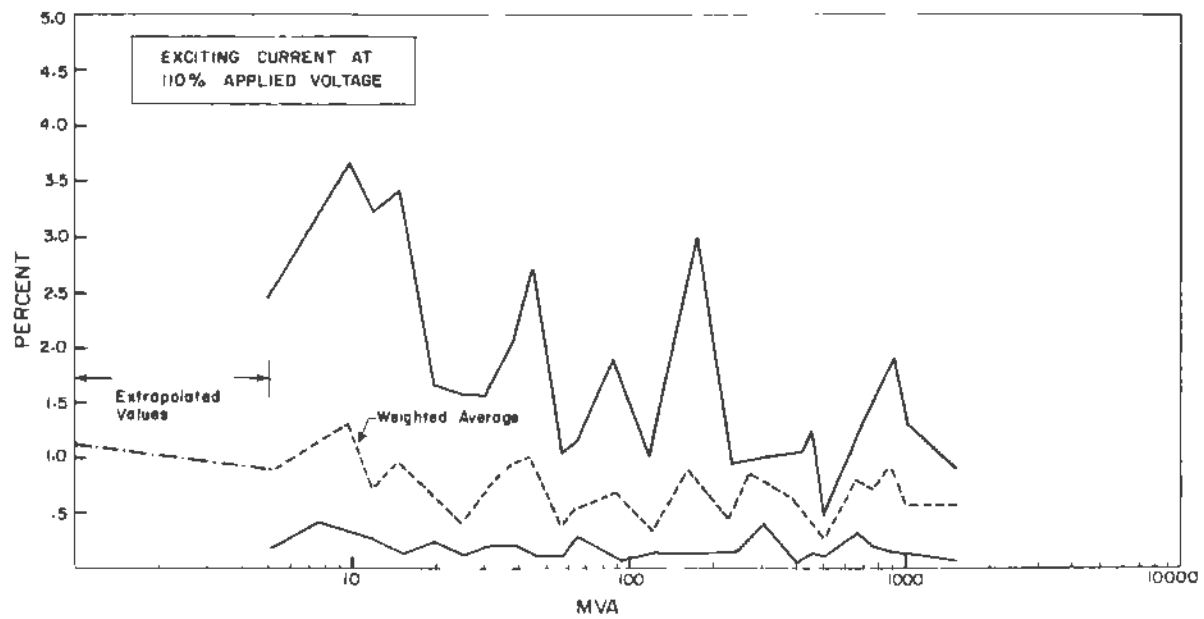


Figure 3-24. Exciting Current at 110% Voltage (vs. MVA)

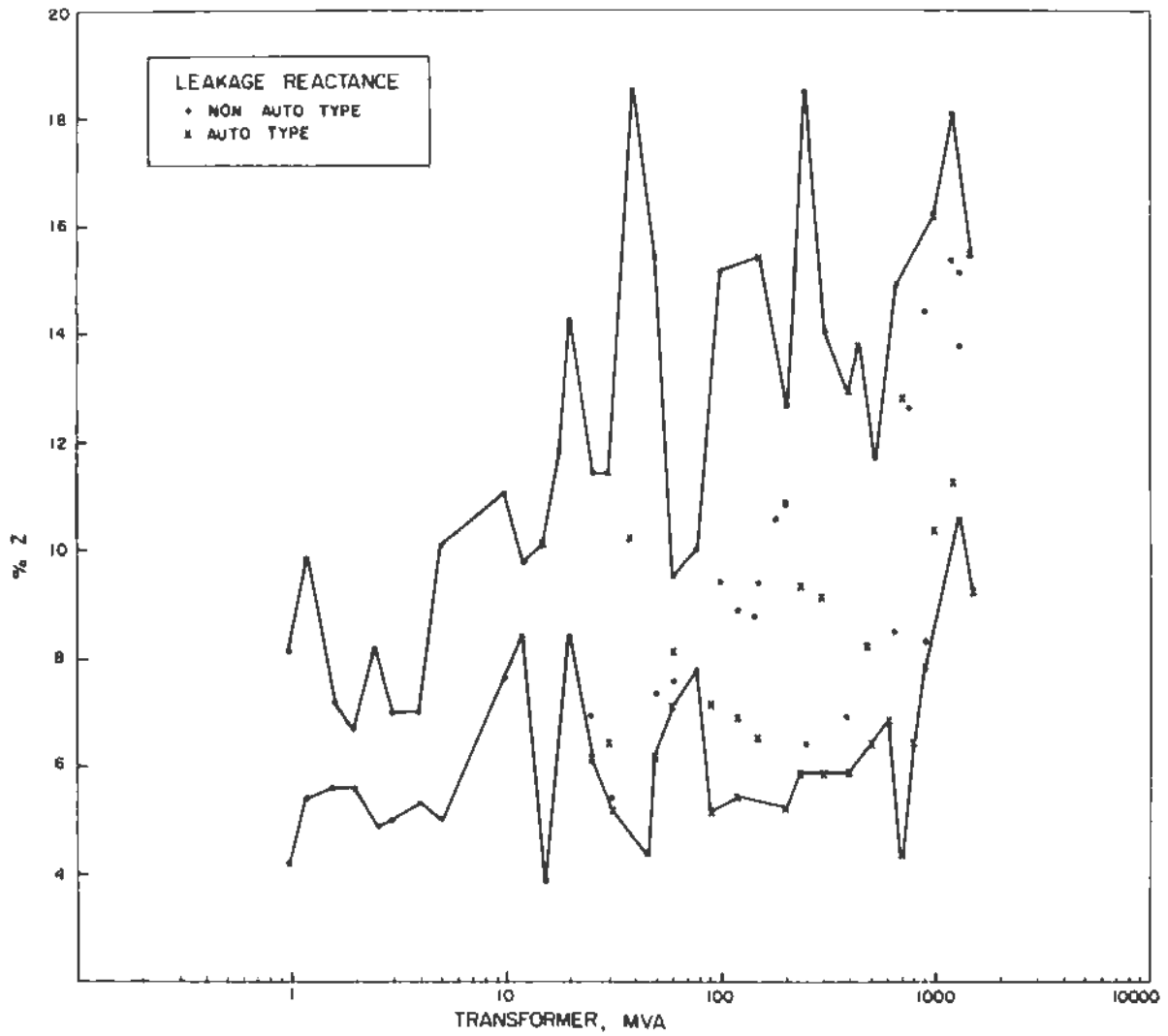


Figure 3-25. Leakage Reactance (vs. MVA)

3-9. TRANSFORMER TERMINAL CAPACITANCES

Considerable scatter occurs in the capacitance values of transformers with similar MVA and kV ratings. This is due mainly to the physical arrangement of the transformer windings. In order to estimate where a particular transformer might fall within the range of capacitance for a given MVA and kV rating, the physical arrangement of the transformer windings should be determined and compared with the "normal" arrangement.

For core-type transformers, the winding capacitances can usually be approximated by parallel plate capacitance formulas in which the capacitance is proportional to the area of the plates and inversely proportional to the separation between the plates. The size of the plates can be approximated as being proportional to the square root of the MVA, while their separation can be approximated as being proportional to the BIL level for higher of the two windings involved. For a two-winding transformer, one would expect the capacitance of the HV winding to ground to be less than the capacitance of the LV winding to ground because of the increased clearance needed for the HV winding.

Based on the analogy of the parallel plates model, it is also reasonable to assume that the capacitances of the dry-type transformers would be less than those of oil transformers, or those with any other insulating fluid medium of higher permittivity.

The capacitances are also very dependent on the physical arrangement of the windings. For example, the HV to LV capacitance is approximately doubled if a tap winding which is electrically connected to the LV winding is physically located outside of the HV winding. This winding arrangement will, however, reduce the HV to ground capacitance by approximately 50% and increase the LV to ground capacitance by approximately 10%. If a tertiary winding is located inside the LV winding, the LV to ground capacitance is reduced by approximately 80%. Electrostatic grading has a very noticeable impact on the values of the transformer capacitances, increasing both the HV and LV to ground capacitances while reducing the HV to LV capacitance.

For shell-type transformers, the parallel plate model for transformer winding to ground capacitance calculations is not as accurate or as applicable. However, it

can still be used as a rough approximation. For HV to LV capacitance, the parallel plate representation is quite reasonable and accurate. The HV to LV capacitance is proportional to the number of HV to LV gaps. The presence of a tertiary winding can affect the capacitances considerably.

The following pages contain plots of typical transformer capacitances. These values were measured at 60 Hertz. Actual impulse capacitances may be smaller. For example, the full-winding distributed capacitance is often halved and lumped at each end of the winding. The applicable impulse capacitance may be 1/3 to 1/2 of this value, depending on the impulse wavefront. If the surge fully penetrates the winding, the effective capacitance is larger. Some lower-voltage transformers which have been designed with "line shields" will have impulse capacitances essentially equal to the 60-Hz values.

Ranges of typical equivalent circuit capacitances are plotted in the following figures:

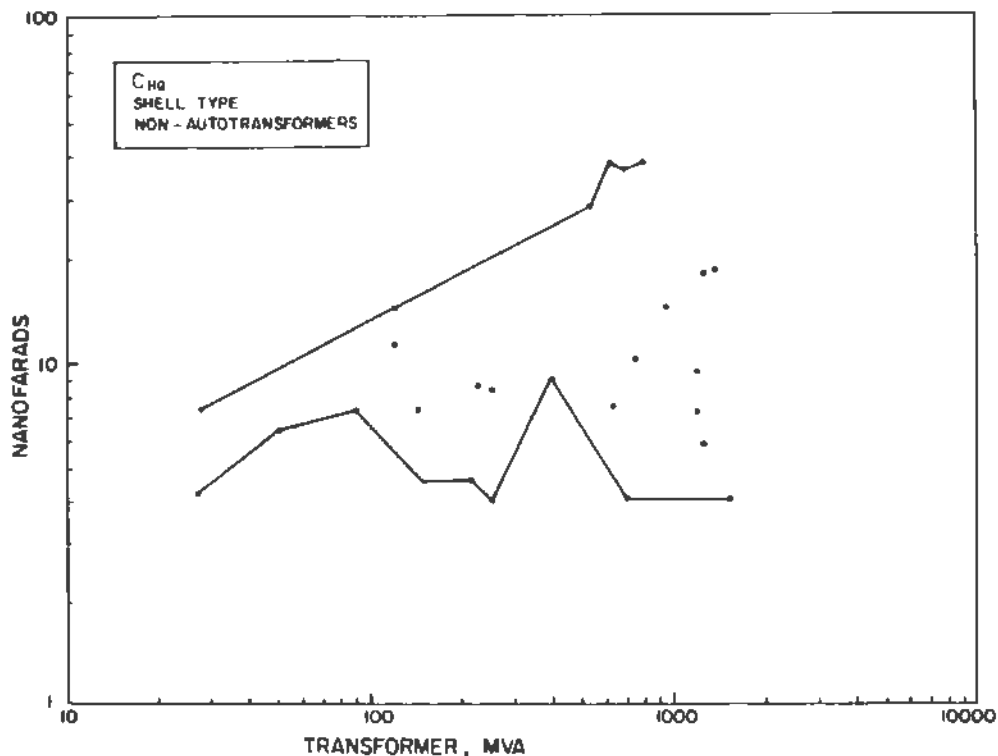


Figure 3-26. Shell-Form C_{Hg} (vs. MVA)

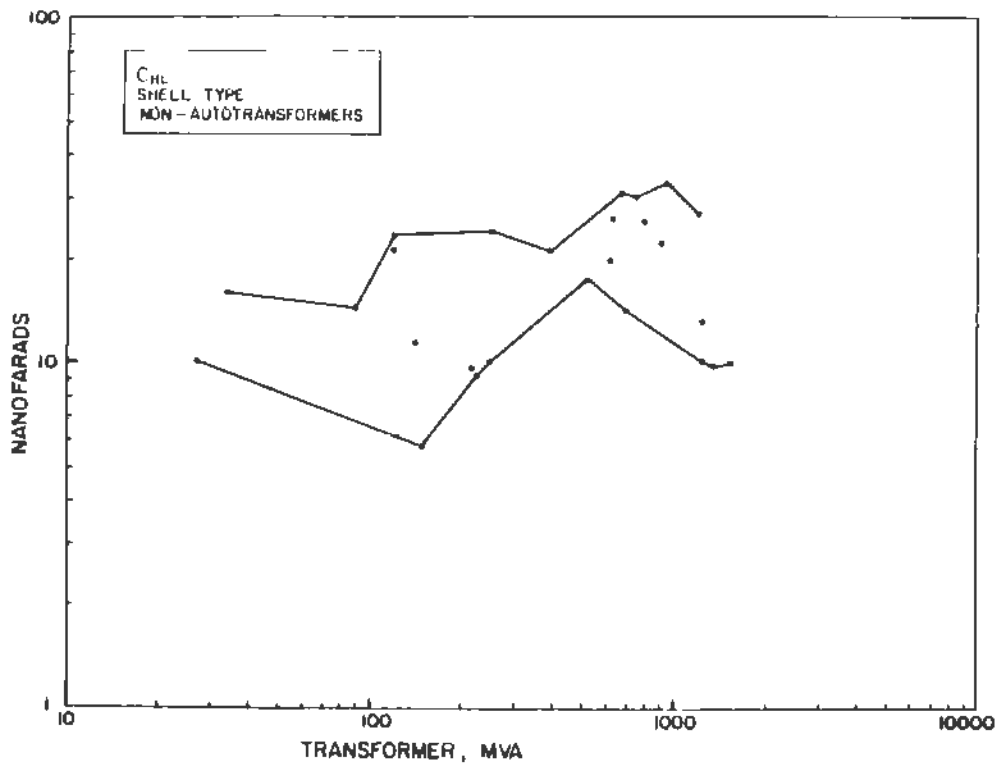


Figure 3-27. Shell-Form C_{h1} (vs. MVA)

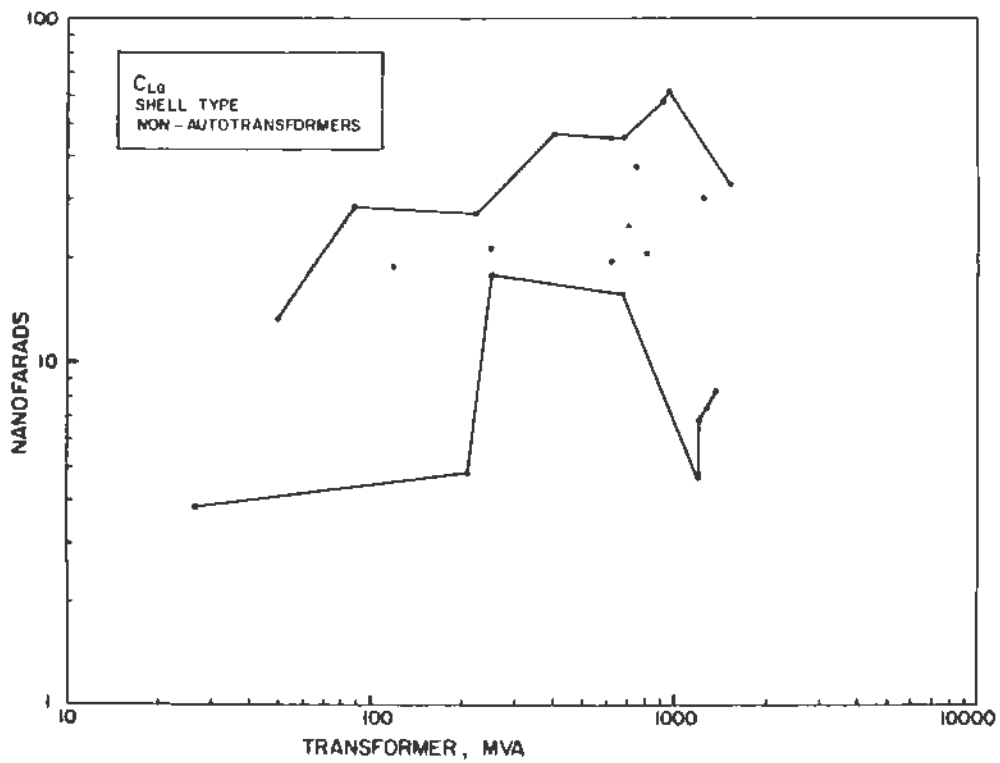


Figure 3-28. Shell-Form C_{1g} (vs. MVA)

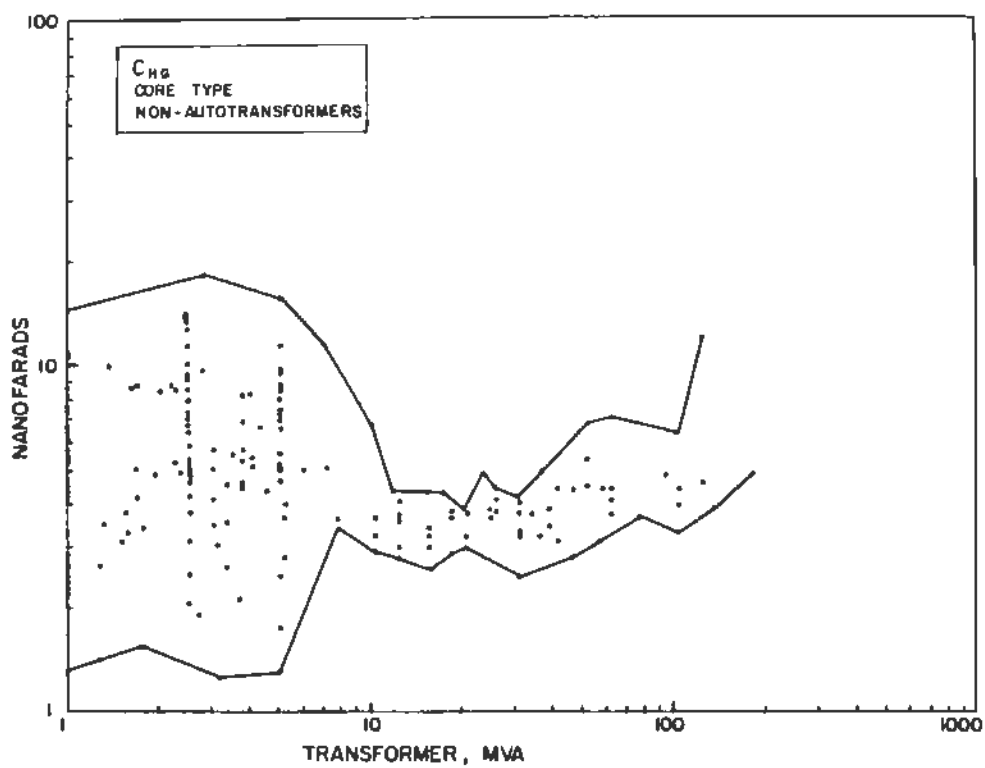


Figure 3-29. Core-Form C_{hg} (vs. MVA)

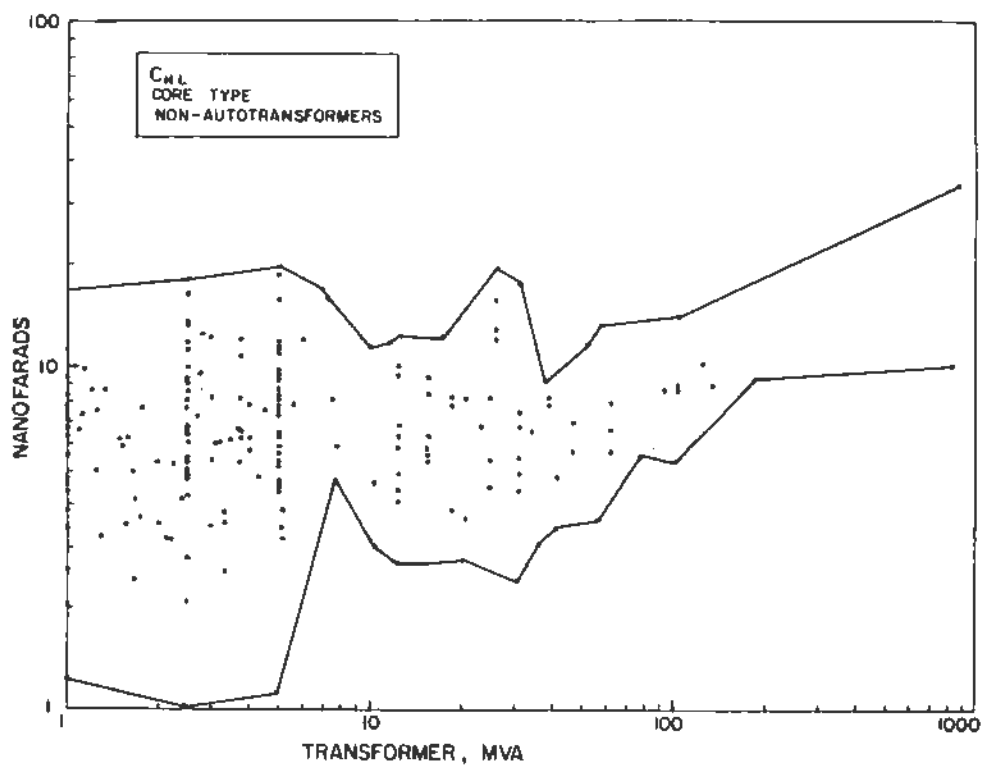


Figure 3-30. Core-Form C_{hl} (vs. MVA)

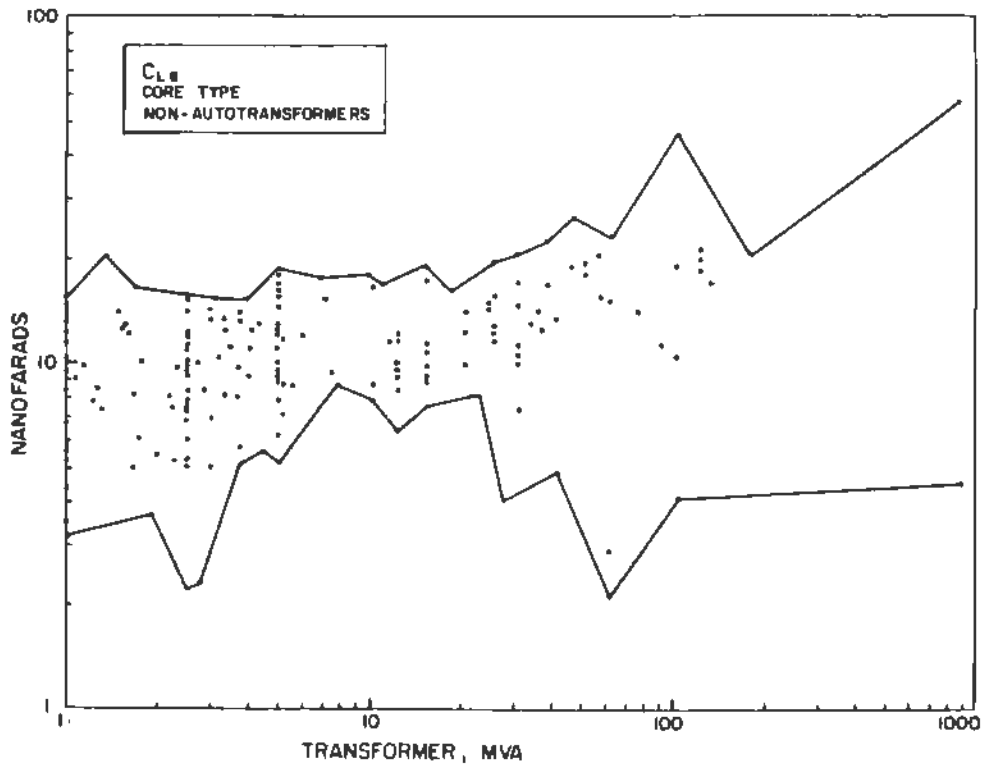


Figure 3-31. Core-Form C_{1g} (vs. MVA)

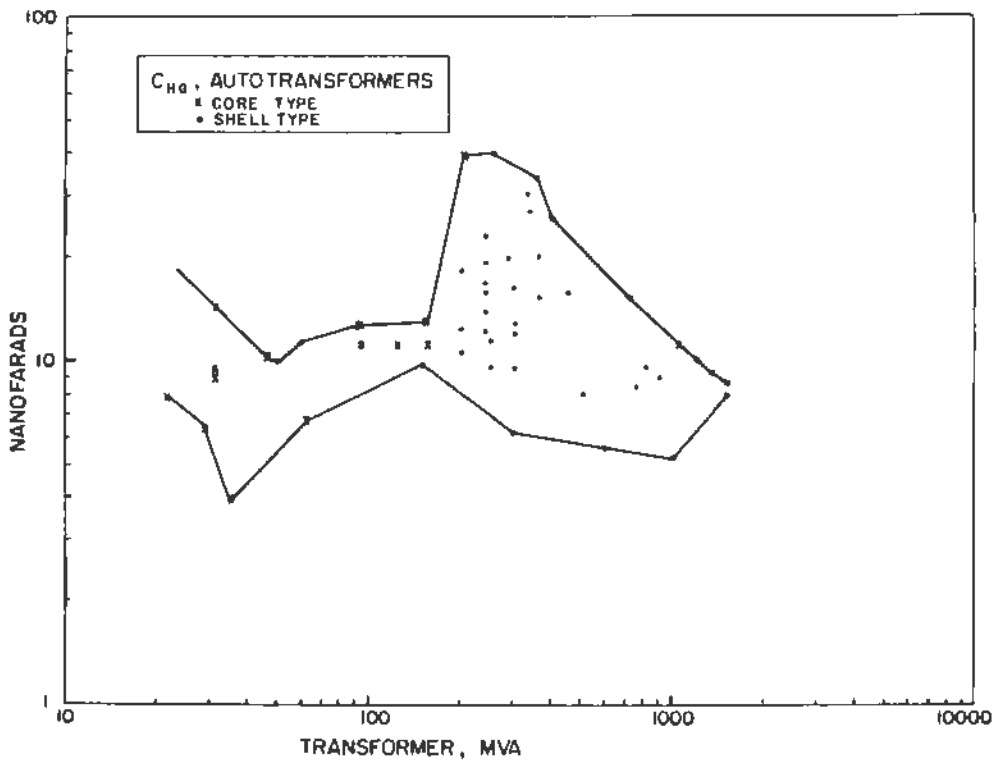


Figure 3-32. Autotransformer C_{1g} (vs. MVA)

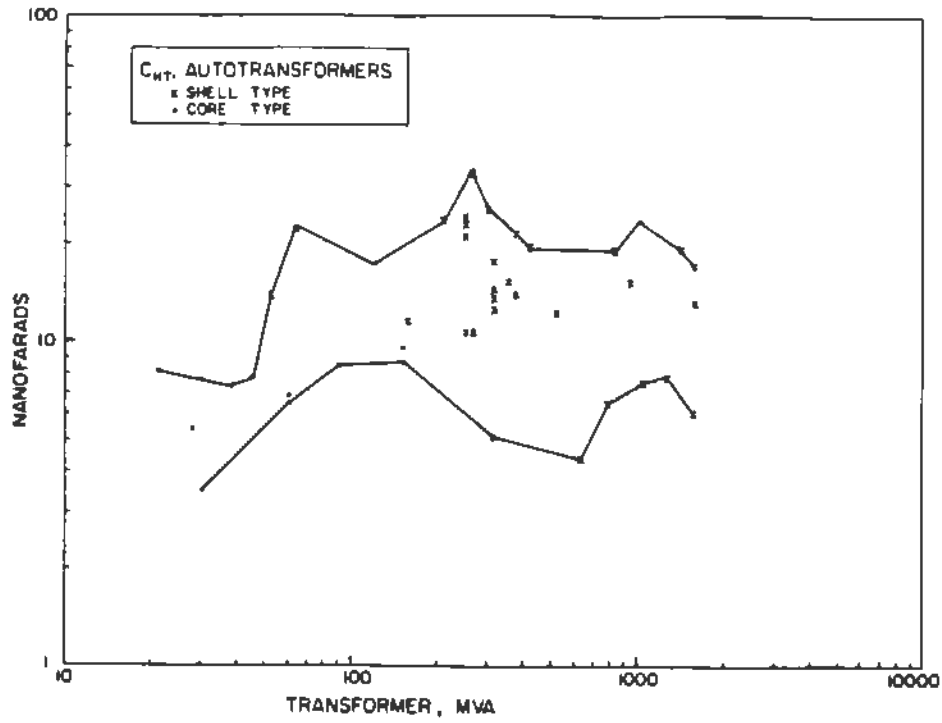


Figure 3-33. Autotransformer C_{ht} (vs. MVA)

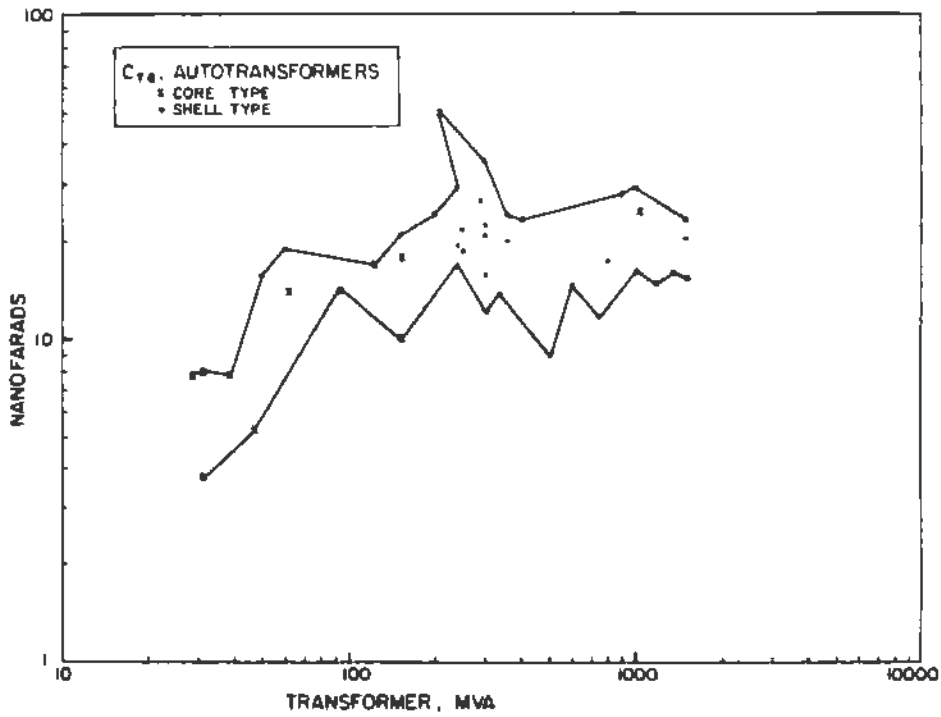


Figure 3-34. Autotransformer C_{tg} (vs. MVA)

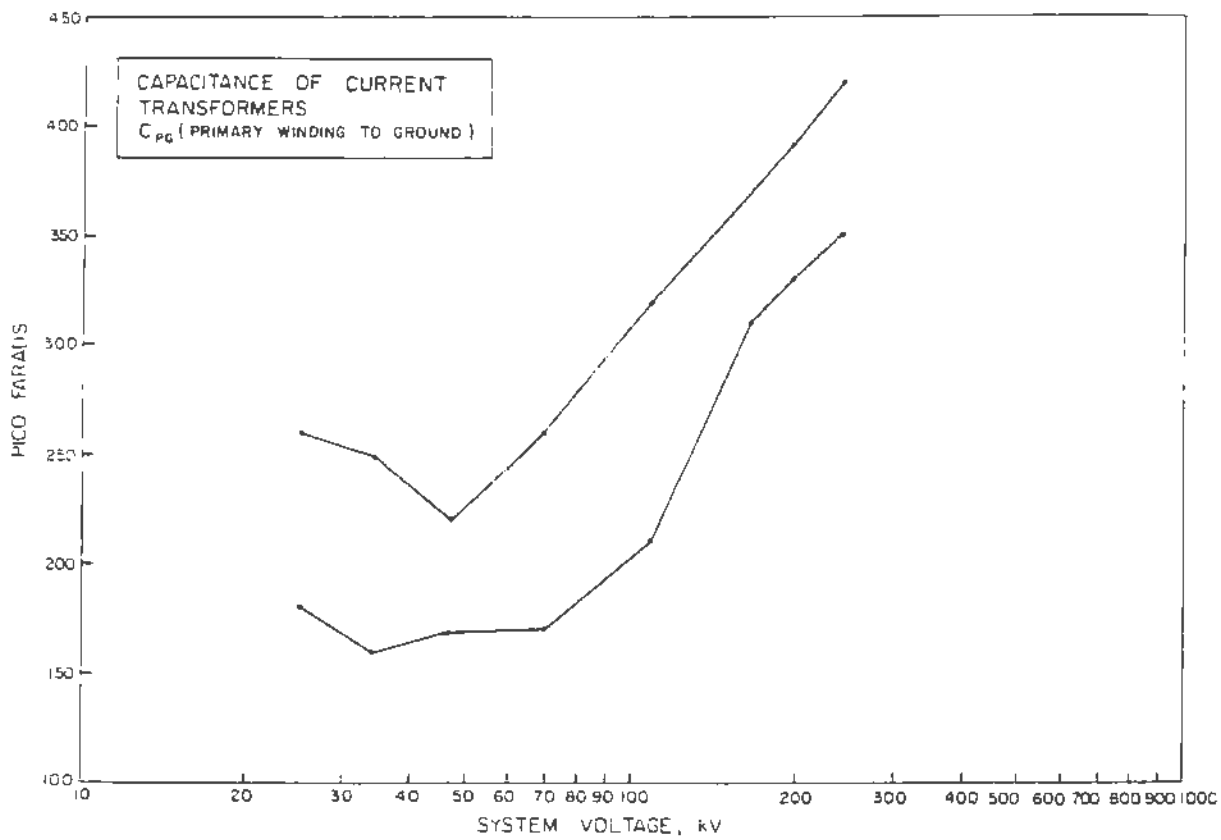


Figure 3-35. Capacitance of Current Transformers (vs. kV)

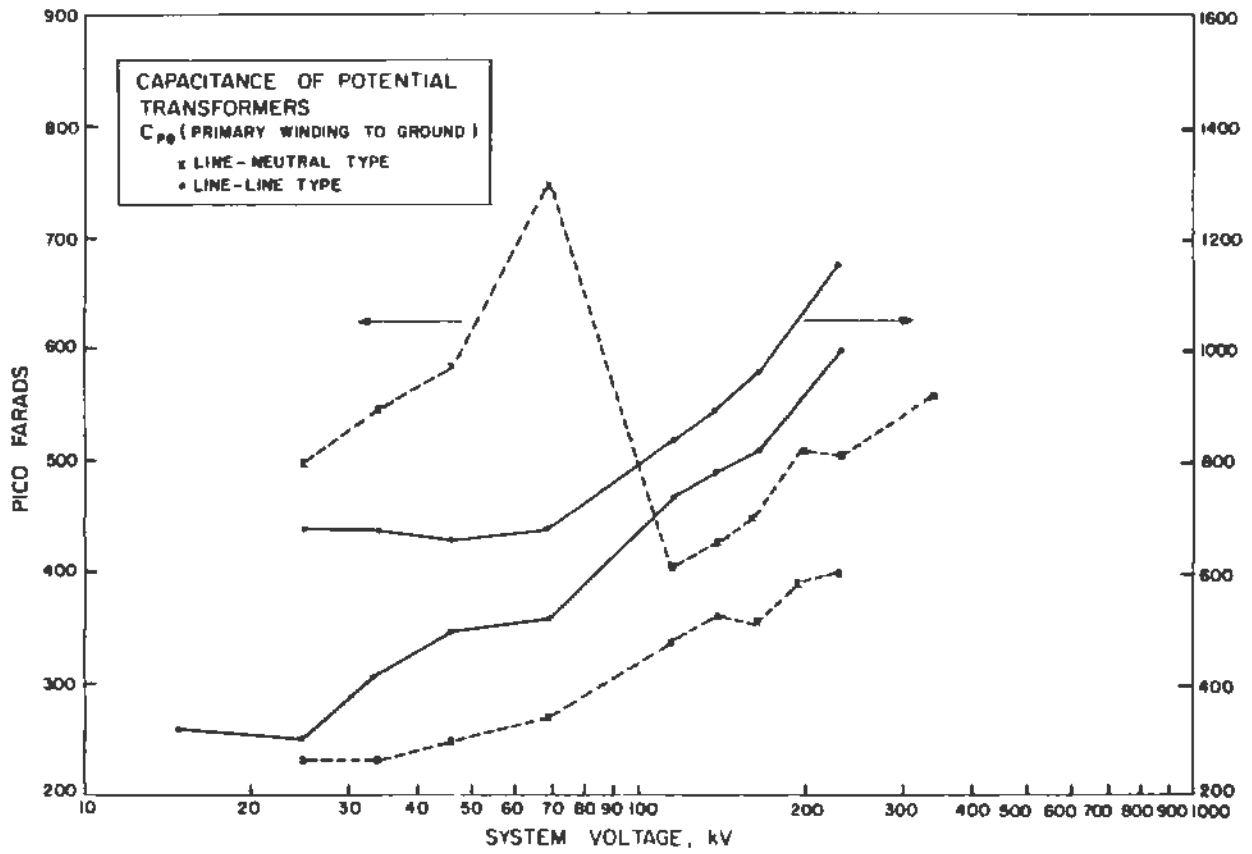


Figure 3-36. Capacitance of Potential Transformers (vs. kV)

3-10. SHUNT REACTORS

At system voltages of 34.5 kV and below, air-core reactors are used. These are tertiary reactors, harmonic filter reactors, and reactors used in static VAR compensators. Most tertiary reactors in service have a rated voltage of 13.8 kV, and the capacity can range from 5 MVAR to 150 MVAR. Often, two or more sets of reactors rated approximately 30 to 50 MVAR and switched individually are connected in parallel. The Q of these air core reactors is approximately 200 to 250. The majority of the tertiary reactors are connected in ungrounded wye. Because the available fault currents on the tertiary sides of transformers are generally 20 to 80 kA, tertiary reactors are switched with a three-pole breaker in the neutral circuit.

At system voltages of 230 kV and above, shunt reactors are used to control voltages during light load or open line conditions. The majority of these shunt reactors are connected to the transmission lines. These reactors are connected in solidly grounded wye. The MVA rating can be as high as 350 MVAR. All of these shunt reactors are oil filled, and the majority of them use a gapped iron core. Saturation levels of the core can vary from approximately 1.15 to 1.50 per-unit voltage at 60 Hz. The Q ranges from 500 to 700. The terminal-to-ground capacitance can vary from approximately 1500 pF to 7000 pF.

Section 4
CIRCUIT BREAKERS

4-1. GENERAL INPUT CONSIDERATIONS

Circuit breakers are simulated with a switch which is either open or closed. An example of circuit breaker input data is shown in Table 4-1. The output options are input in column 80. At time zero the switch is open if TCLOSE is positive, and it closes at $t > TCLOSE$. If TCLOSE is zero or negative, the switch is closed in the initial steady-state solution and at time zero. The switch opens at the first current zero after $t > TOPEN$. The current zero can be detected in two different ways, as shown in Figure 4-1.

Table 4-1
INPUT DATA FOR A TIME-CONTROLLED SWITCH

1		2		3		4		5		6		7		8	
1234567890	1234567890	1234567890	1234567890	1234567890	1234567890	1234567890	1234567890	1234567890	1234567890	1234567890	1234567890	1234567890	1234567890	1234567890	1234567890
NODE NAMES		TIME CRITERIA				CURRENT MARGIN		OUTPUT REQUESTS							
BUS1	BUS2	T-CLOSE	T-OPEN												
A6	A6	E 10.0	E 10.0	E 10.0				1 1							
		SECONDS	SECONDS	AMPERES											
BUS-1			001					1							
BUS-1	BUS2-A	.001	01					2							
BUS-1	BUS2-B	.001	01					2							
BUS-1	BUS2-C	.001	01					2							
B500	AB5001A	-1.0	.12	.1				3							
B500	BB5001B	-1.0	.12	.1				3							
B500	CB5001C	-1.0	.12	.1				3							
B501	B5001	.160	1 0												
B500	B501	.152	1 0												

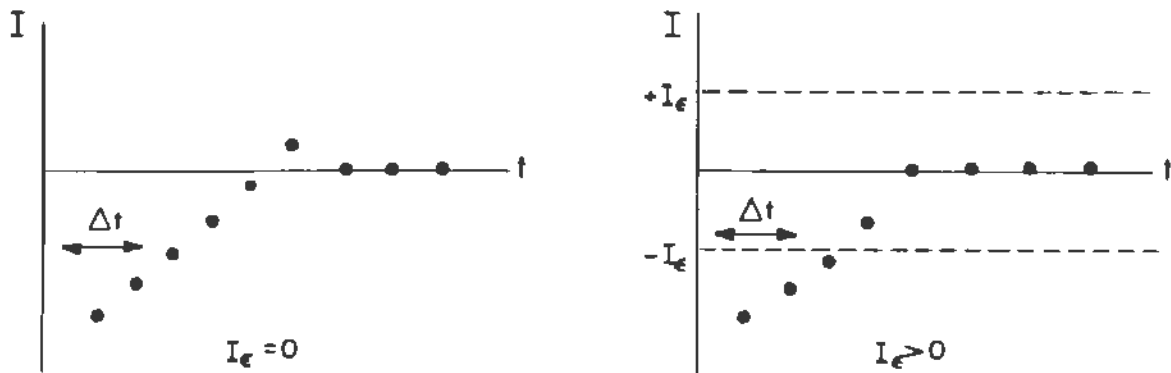


Figure 4-1. Determination of Switch Opening Time

Network topology considerations for circuit breakers are discussed in the Introduction. In essence, the user should not permit switches to interrupt purely inductive current unless there will be another discharge path available for that current.

Input data for simple time controlled circuit breakers is shown in Table 4-1. The examples presented are:

1. Breaker Pole "BUS-1" to GROUND closes at $t = 0$ and opens at the first current zero after $t > 0.001$ seconds. The switch current output is requested with a 1 in column 80.
2. Phases A, B and C of the circuit breaker are connected from nodes "BUS-1" to "BUS-2". The breaker closes at $t > 0.001$ seconds and opens at the first current zero after $t > 0.01$ seconds. The switch voltage, across the contacts, is requested with a 2 in column 80.
3. Phases A, B and C of the circuit breaker are connected between nodes "B500" and "B5001". The breaker closes at $t = -1.0$ seconds, and therefore the switch is considered closed when the phasor steady-state solution is performed by the EMTP. The breaker opens as soon as the absolute value of the switch current is less than 0.1 Amperes after 0.12 seconds. The switch current and voltage outputs are requested with a 3 in column 80.
4. One pole of a circuit breaker with a preinsertion resistor as shown in Figure 4-10. The auxiliary contact A closes at 0.152 seconds. The resistor R is inserted for 8 milliseconds, and then the main contact M shorts it out by closing at 0.160 seconds. Both contacts remain closed for the remainder of the simulation. Therefore, an opening time of 1.0 seconds, which is greater than TMAX, was specified.

4-2. PRESTRIKE

When a circuit breaker closes, the voltage across the contacts stresses the insulation of the contact gap and may lead to a prestrike at the time the stress exceeds the strength, as shown in Figure 4-2. The contact closing time should be adjusted (advanced) to account for prestrike. For lower frequency switching surges, prestrike may alter the probability distribution of contact closing as shown in Figure 4-3.

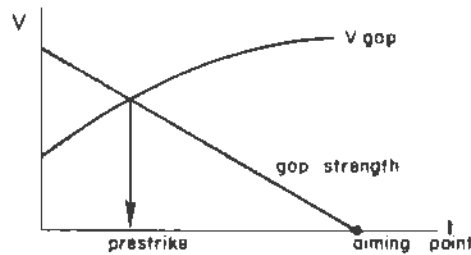


Figure 4-2. Prestriking Circuit Breaker

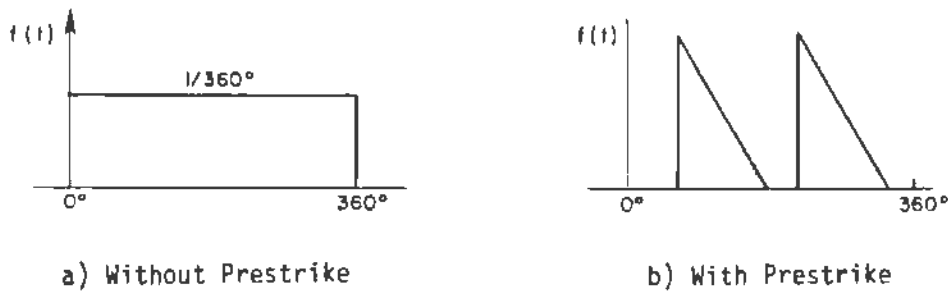


Figure 4-3. Distribution of Contact Closing Times

During higher frequency transients, the current after a prestrike may be interrupted. As the recovery voltage builds up across the switch contacts, another breakdown will occur because the gap dielectric strength decreases as the contacts approach each other. A succession of high-frequency transients may result. The block diagram of a TACS model for prestrike is shown in Figure 4-4,

and is applied to the circuit in Figure 4-5 with the results shown in Figures 4-6 and 4-7. This example makes use of a TACS-controlled thyristor, which is switch Type 11. The switch is instructed to close only when the TACS variable SPARK exceeds zero, and it interrupts when the current falls below a small threshold.

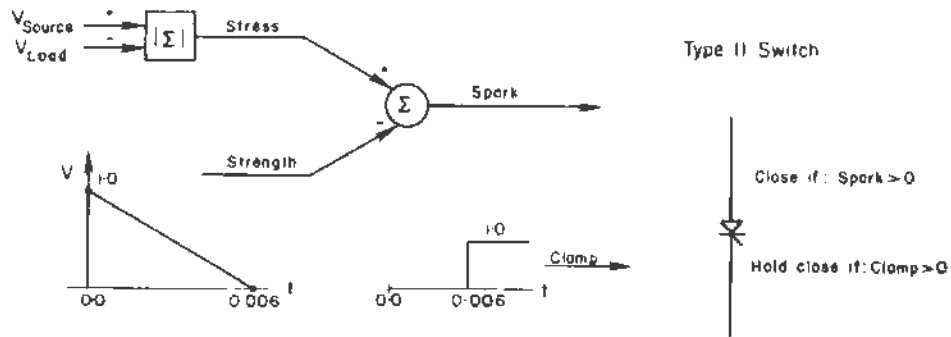
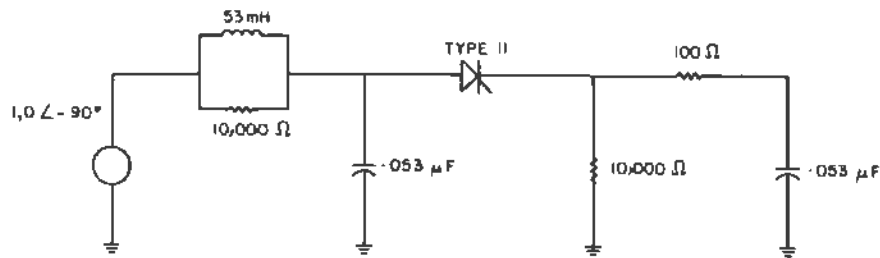


Figure 4-4. TACS Prestrike Logic



Type II closes if spark > 0

Type II held closed if clamp > 0

Figure 4-5. Prestrike Circuit Example

PRESTRIKING SWITCH, LOAD R = 10000

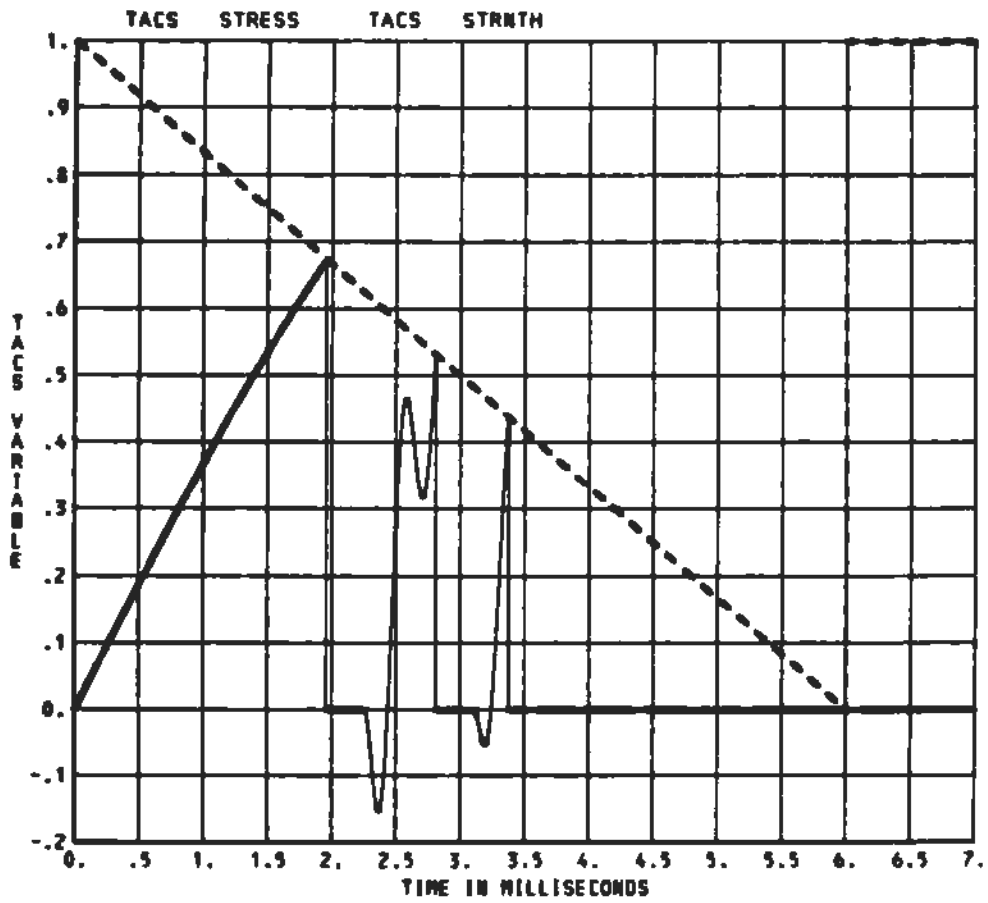


Figure 4-6. TACS Control Signals

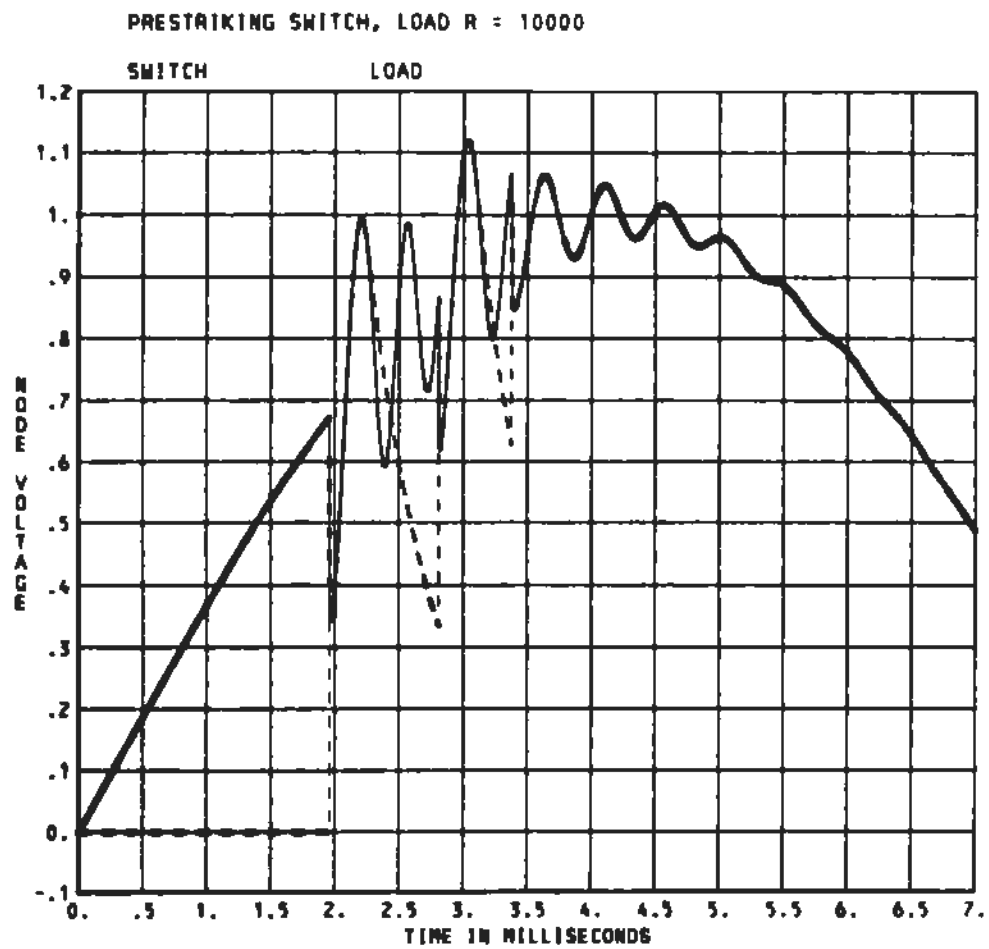


Figure 4-7. Load Voltage During Prestrike

4-3 RESTRIKE

Restrikes are similar to prestrikes, except that they occur during switch opening. The gap dielectric strength increases when the contacts move apart so that restrikes are not as common as prestrikes. However, the consequences may be more severe because the gap voltage at breakdown is generally higher, which leads to higher transient voltage magnitudes.

A TACS Logic model may be used to simulate restrikes as discussed above. However, for single restrikes a simpler model will suffice. A flashover switch, or voltage-controlled switch, is used to simulate the restriking of a circuit breaker. The flashover switch is connected in parallel with the circuit breaker as shown in Figure 4-8. The parameter VFLASH is equal to the desired voltage across the switch contacts at the instant of restrike.

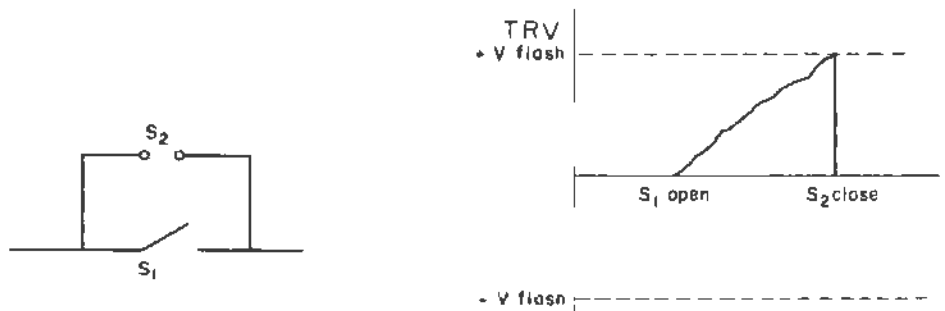


Figure 4-8. Simulation of a Restrike

Input data for the flashover switch in Figure 4-8 is given in Table 4-2. After circuit breaker S1 opens, the recovery voltage across the switch will build up. If the voltage across the breaker contacts exceeds the dielectric strength of the opening contacts (950 kV), a restrike will occur. Current will then flow for at least 96 milliseconds before interruption occurs. The simulation should be done in two steps. First, the magnitude and shape of the recovery voltage after the switch opens should be determined. Second, the recovery voltage is compared with the interrupter's insulation strength to determine if a restrike

Table 4-2

INPUT DATA FOR FLASHOVER SWITCH

1		2		3		4		5		6		7		8	
1234567890	1234567890	1234567890	1234567890	1234567890	1234567890	1234567890	1234567890	1234567890	1234567890	1234567890	1234567890	1234567890	1234567890	1234567890	1234567890
NODE NAMES		TIME CRITERIA		CURRENT		FLASHOVER						OUTPUT			
BUS1 BUS2		T-NO FD T-DELAY		MARGIN		LEVEL						REQUESTS			
A6 A6		E10.0 E10.0		E10.0 E10.0		E10.0 E10.0						11			
		SECONOS SECONDS		AMPERES		VOLTS									
B5003 B5004		0 .096				950 0E3						2			

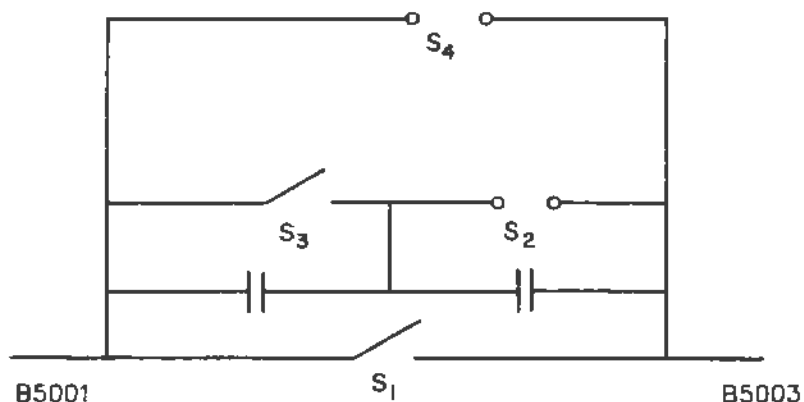


Figure 4-9. Circuit Connection for the Simulation of Multiple Restrikes

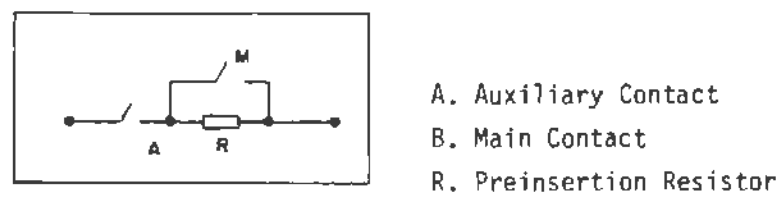
will occur, and if so, the recovery voltage magnitude at the time of restrike. The EMTP case can then be rerun with an appropriate flashover level for the voltage-controlled switch.

The switch connections for a multiple restrike simulation are shown in Figure 4-9. The flashover switch is connected between nodes "B5001" and "B5003". The time before which the switch is prevented from flashing over is 0.0 seconds. The switch flashes over or closes when the voltage across the

contacts of S2 reaches 950 kV. The elapsed time, TDELAY, before which switch opening will not be allowed is 0.096 seconds. Therefore, S2 opens at the first natural current zero 0.096 seconds or more after S2 closed. These values must be coordinated with the opening time of S1. After S2 opens, the recovery voltage again builds up and another restrike is possible when the recovery voltage reaches 950 kV. A second flashover of the circuit breaker at higher recovery voltage could be represented by putting another switch S3 in series with S2. S3 is set to open after S2 opens. To simulate the second restrike, S4 with the proper flashover voltage is connected in parallel with S1. To represent more restrikes, additional switches with increasing levels of flashover voltage must be added to Figure 4-9.

4-4. PREINSERTION RESISTORS

Preinsertion resistors are added to EHV circuit breakers to reduce the switching overvoltages. The circuit breaker has two contacts per pole, an auxiliary contact A and a main contact M. The schematic of one pole of an EHV circuit breaker with a preinsertion resistor is shown in Figure 4-10.



- A. Auxiliary Contact
- B. Main Contact
- R. Preinsertion Resistor

Figure 4-10. One Pole of an EHV Circuit Breaker With Preinsertion Resistor

The effect of preinsertion resistors is illustrated by the single-phase system depicted in Figure 4-11. The receiving end voltage with and without a resistor is shown in Figure 4-12. With a single switch closing at 0.001 seconds (Figure 4-12a), the peak receiving end voltage exceeds 2.0 per-unit. With two smaller transients at 0.001 and 0.0933 seconds (Figure 4-12b), the peak voltage

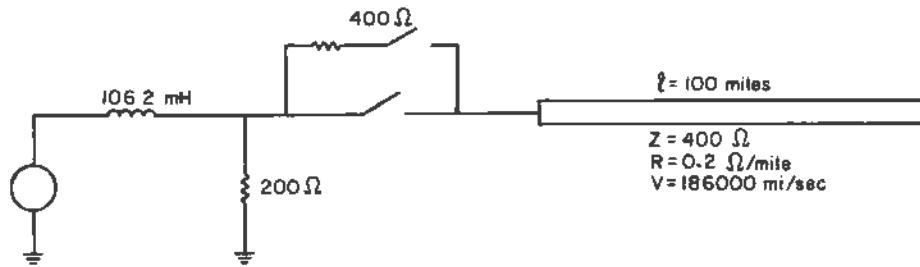


Figure 4-11. Single-phase Line Energization

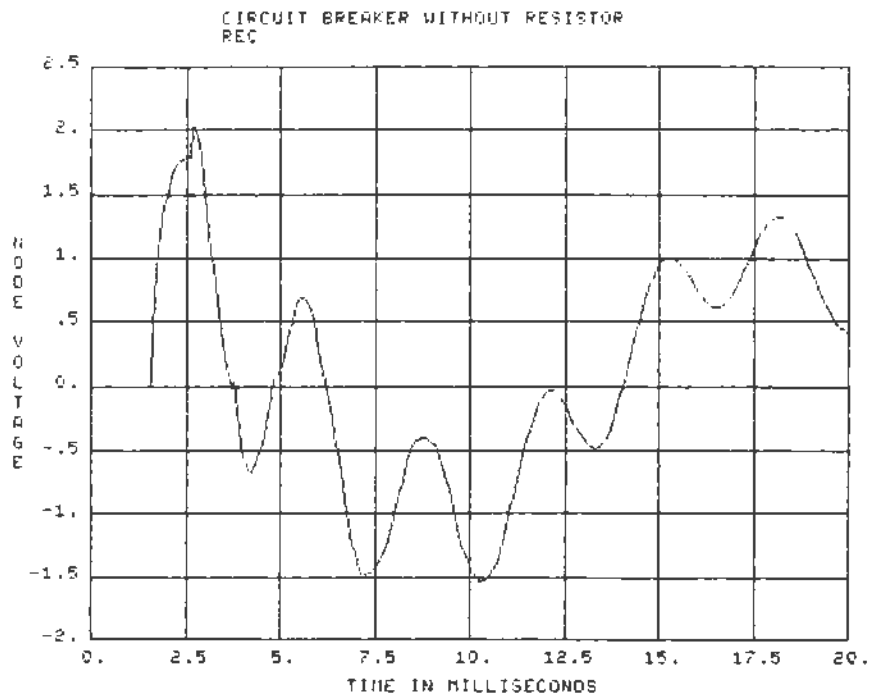


Figure 4-12a. Receiving End Voltage with No Resistor

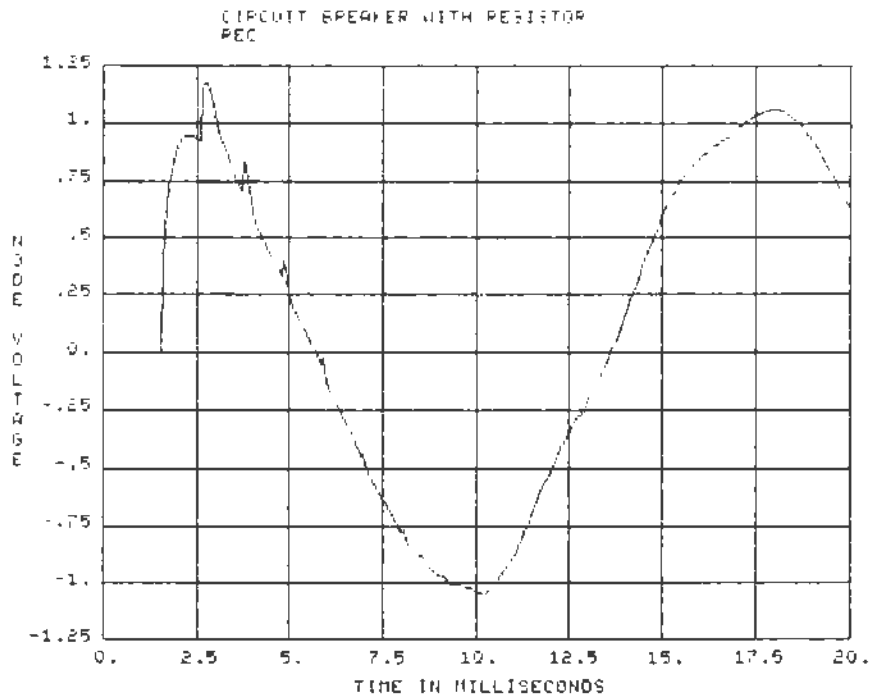


Figure 4-12b. Receiving End Voltage with Resistor

is less than 1.2 per-unit and the lower frequency oscillations are rapidly damped out by the preinsertion resistor.

4-5. STATISTICAL PARAMETERS

When a circuit breaker closes, the three poles aim for the same closing time. Because of the possible delays in the closing mechanism's mechanical linkages, and possible electrical prestrikes, the actual closing time differs from the aiming point. The time between the first and last pole to close is called the pole span. The closing times of a pole can be represented by a Normal distribution as shown in Figure 4-13. The mean value of the distribution is the aiming point. If the distribution is terminated at $+3\sigma$ and -3σ , the circuit breaker pole span will be equal to six times the distribution's standard deviation. Typical values for circuit breaker closing times and pole spans range from 16 to 20 milliseconds and 8 to 10 milliseconds, respectively.

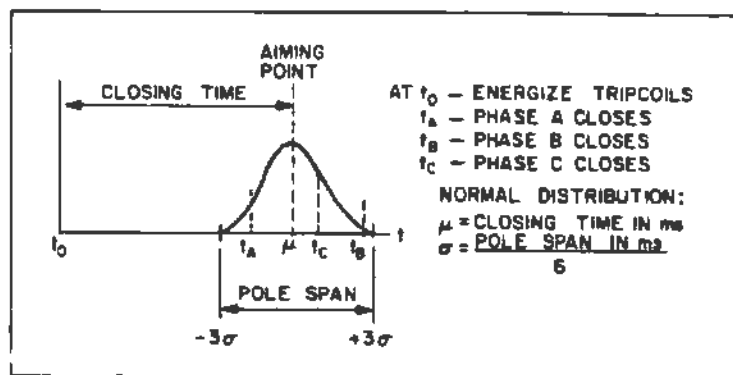


Figure 4-13. Closing Time of the Circuit Breaker Main Contact

The relationship of the contact closing times to t_0 , which is the aiming point relative to the power frequency voltage, is also a random variable. The magnitude of switching overvoltages depends on the power frequency voltage at time of contact closure. An added delay, which is referred to as the "reference angle," is applied equally to all STATISTICS switches. The random delay always follows a uniform distribution with specified parameters. Figure 4-14 shows a uniform distribution for reference angles from 0 to 360 degrees.

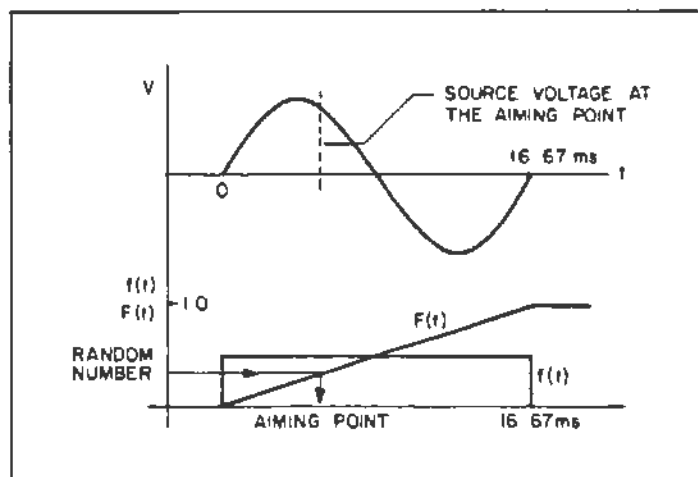


Figure 4-14. Uniform Distribution for Selecting the Aiming Point Reference Angle Boundaries at 0 and 360 Degrees

Reference angles from 0 to 360 degrees take into account all possible power frequency voltages at the instant of contact closure. This data is included on the third miscellaneous data card rather than the switch cards, because it applies to all STATISTICS switches in the simulation.

In order to represent the statistical nature of contact closing, the EMTP uses STATISTICS type switches. The closing time of each STATISTICS switch is randomly varied according to a Normal distribution. The input data is shown in Table 4-3. Inputs in four sections are required:

1. On the second miscellaneous data card a non-zero entry in columns 65-72 specifies the number of line breaker operations for energizing or reclosing. Typically, 200 operations are simulated. This also indicates the presence of a third miscellaneous data card.
2. The third miscellaneous data card specifies the statistical parameters of the breakers and the format for output of the case results.
 - a. ISW should be equal to 1 if the user wants the actual switching times for each shot. This will permit rerunning the single maximum case to obtain waveform plots of the highest overvoltage.
 - b. ITEST is normally equal to 0, which randomly varies the aiming point over a 360 degree cycle.
 - c. IOIST is normally equal to 0, because switch closing times follow a Normal distribution.
 - d. AINCR is usually 0.05 or 0.10. The user should select AINCR to obtain 10 to 20 histogram classes in the statistical output of per-unit overvoltages.
 - e. XMAXMX should be rather high, eg. 5.0. If the resulting overvoltages appear unreasonably high, the user should look for inaccuracies in the model rather than decrease XMAXMX.
 - f. DEGMIN should be 0.0 degrees.
 - g. DEGMAX should be 360.0 degrees for cases of reclosing into a trapped charge. For line energization cases with no trapped charge, DEGMAX could be set equal to 180.0 degrees because each power frequency half cycle will be symmetrical.
 - h. STATFR is usually 60.0 Hertz.

Table 4-3

INPUT DATA FOR STATISTICAL SWITCHING

INPUT ON THE SECOND MISCELLANEOUS DATA CARD

1	2	3	4	5	6	7	8
1234567890	1234567890	1234567890	1234567890	1234567890	1234567890	1234567890	1234567890
							NENERG
200							

INPUT ON THE THIRD MISCELLANEDUS DATA CARD

COLUMNS 1-8: ISW (I8) 1=OUTPUT ALL VARIABLE SWITCH CLOSING AND OPENING TIMES FOR EVERY ENERGIZATION.
 0=NO PRINTED OUTPUT FOR INDIVIDUAL ENERGIZATIONS

COLUMNS 9-16: ITEST (I8) 0=ADD AN EXTRA RANDOM OFFSET DETERMINED BY THE PARAMETERS "DEGMIN", "DEGMAX", AND "STATFR".
 1=TIMING POINT IS ALWAYS 0 DEGREES. NO EXTRA RANDOM OFFSET IS ADDED.
 2=ADD THE RANDOM OFFSET TO SWITCH CLOSING TIMES ONLY.
 3=ADD THE RANDOM OFFSET TO SWITCH OPENING TIMES ONLY.

COLUMNS 17-24: IDIST (I8) 0=USE GAUSSIAN DISTRIBUTION FOR ALL CLOSING TIMES
 1=USE UNIFORM DISTRIBUTION FOR ALL CLOSING TIMES

COLUMNS 25-32: AINCR (FB.O) PER-UNIT VOLTAGE INCREMENT FOR THE OVERVOLTAGE HISTOGRAMS. DEFAULT VALUE IS 0.05 PER-UNIT.

COLUMNS 33-40: XMAXMX (FB.O) CUT-OFF VOLTAGE FOR THE OVERVOLTAGE HISTOGRAMS. DEFAULT VALUE IS 2.0 PER-UNIT.

THE FOLLOWING THREE PARAMETERS DEFINE THE WINDOW OF ADDITIONAL RANDDM OFFSETS TO THE RANDOM SWITCH CLOSING TIMES. SEE FIGURE 4-14

COLUMNS 41-48: DEGMIN (FB.O) MINIMUM RANDOM OFFSET. DEFAULT VALUE IS 0 DEGREES.
 COLUMNS 49-56: DEGMAX (FB.O) MAXIMUM RANDOM OFFSET. DEFAULT VALUE IS 360 DEGREES
 COLUMNS 57-64: STATFR (FB.O) POWER FREQUENCY FOR THE PURPOSE OF DEFINING THE WINDOW OF RANDDM OFFSETS. DEFAULT VALUE IS 60 HZ.

COLUMNS 65-72: SIGMAX (FB.O) TRUNCATION POINT OF BREAKER POLE SPAN, IN NUMBER OF STANDARD DEVIATIONS. DEFAULT VALUE IS 4 SIGMA.

COLUMNS 73-80: NSEED (I8) 0=RANDOM NUMBERS DEPEND ON THE TIME OF DAY
 1=RANDOM NUMBERS USE A CONSTANT "SEED", AND WILL BE IDENTICAL FOR SUBSEQUENT EMTP RUNS.

1	2	3	4	5	6	7	8		
1234567890	1234567890	1234567890	1234567890	1234567890	1234567890	1234567890	1234567890		
ISW	ITEST	IDIST	AINCR	XMAXMX	DEGMIN	DEGMAX	STATFR	SIGMAX	NSEED
I8	I8	I8	FB.O	FB.O	FB.O	FB.O	FB.O	FB.O	I8
1	0	0	0.1	4.0	0.0	360.0	60.0	3.0	0

Table 4-3 (Cont'd)

INPUT DATA FOR BREAKER WITH PREINSERTION RESISTOR

INPUT IN THE "SWITCH CARDS" SECTION

1		2		3		4		5		6		7		8	
1234567890	1234567890	1234567890	1234567890	1234567890	1234567890	1234567890	1234567890	1234567890	1234567890	1234567890	1234567890	1234567890	1234567890	1234567890	1234567890
NODE NAMES										SPECIAL REQUEST WORD		REFERENCE SWITCH			
BUS1	BUS2	MEAN CLOSING TIME		STANDARD DEVIATION								BUS5	BUS6		
A6	A6	E10.0	E10.0							A10	A6	A6			
		SECONDS		SECONDS		STATISTICS									
B501	AB5001A	.0165	.0014	STATISTICS											
		DELAY TIME IN SECONDS													
B500	B502	-.01	.0007	STATISTICS						B501	AB5001A				

STATISTICAL OUTPUT CARDS: THESE CARDS CAN BE MIXED IN ANY ORDER IN THE STATISTICAL OUTPUT REQUEST SECTION

HISTOGRAM REQUEST CARD

COLUMNS 1-2: IBROPT (I8) 0=NODE VOLTAGE HISTOGRAM
 -1=BRANCH OR DIFFERENTIAL VOLTAGE HISTOGRAM
 -2=BRANCH CURRENT HISTOGRAM
 -3=BRANCH POWER HISTOGRAM
 -4=BRANCH ENERGY HISTOGRAM
 COLUMNS 3-14: BASE (E12.0) PER-UNIT BASE IN VOLTS, AMPS, WATTS, OR JOULES FOR THIS HISTOGRAM
 COLUMNS 15-80: BUS (11A6) SINGLE BUS NAMES FOR NODE VOLTAGE HISTOGRAM, OR UP TO 5 PAIRS OF BUS NAMES FOR BRANCH HISTOGRAMS

HISTOGRAM CLASS CARD: THIS CARD CHANGES THE EFFECTIVE AINCR AND XMAXMX, UNTIL ANOTHER OF THESE CARDS IS INPUT.

COLUMNS 1-24: (24X) LEAVE BLANK.
 COLUMNS 25-32: AINCR (F8.0) IF >0, THIS IS A NEW VALUE OF AINCR TO BE USED FOR ALL SUBSEQUENT HISTOGRAMS.
 IF <0 AND AN INTEGER, ALL SUBSEQUENT HISTOGRAMS WILL HAVE -AINCR CLASSES.
 COLUMNS 33-40: XMAXMX (F8.0) THIS IS A NEW VALUE OF XMAXMX TO BE USED FOR ALL SUBSEQUENT HISTOGRAMS.
 COLUMNS 41-61: (A21) INPUT THE STRING "MISC STATISTICS DATA"

BLANK CARD TERMINATING NODE VOLTAGE OUTPUT

BLANK CARD TERMINATING PLOT REQUESTS

C OUTPUT FOR THE "STATISTICS" CASE

C COLUMN 2: 0 = NODE VOLTAGES

C -1 = BRANCH VOLTAGES

C 34567890123456789012345678901234567890

C 3-14 15-20 21-26 27-32 33-38

C BASE VOLT BUS1 BUS2 BUS3 BUS4

C REQUEST FOR LINE-TO-GROUND HISTOGRAMS

0 408269.SEND ASEND BSEND C

0 408270.REC AREC BREC C

C REQUEST FOR LINE-TO-LINE HISTOGRAMS

-1 408271.SEND ASEND BSEND CSEND CSEND A

-1 408272.REC AREC BREC CREC CREC A

BLANK CARD TERMINATING STATISTICS OUTPUT

BLANK CARD TERMINATING THE CASE

3. Inputs in the Switch cards section. In the example of Table 4-4, the STATISTICS switch for the main contacts connects nodes "B501 A" and "B5001A". The mean closing time is 16.5 milliseconds. The standard deviation is 1.4 milliseconds, resulting in a pole span of $6 \times 1.4 = 8.4$ milliseconds.
4. Inputs in the node voltage output section. Here the user specifies a per-unit base for each of the node voltages to be included in the statistical output. As discussed in the Introduction, the user should group all three phases of one bus on a single output card, each card having a slightly different voltage base. The program will then tabulate case peaks as well as phase peaks for each bus. The user may also include differential voltages (e.g., transformer phase-to-phase voltages) on these output cards.

If a circuit breaker has preinsertion resistors, the closing of the auxiliary contact can also be modeled with a Normal distribution. The actual closing time of the auxiliary contacts is determined relative to the closing of the main contacts as seen in Figure 4-15.

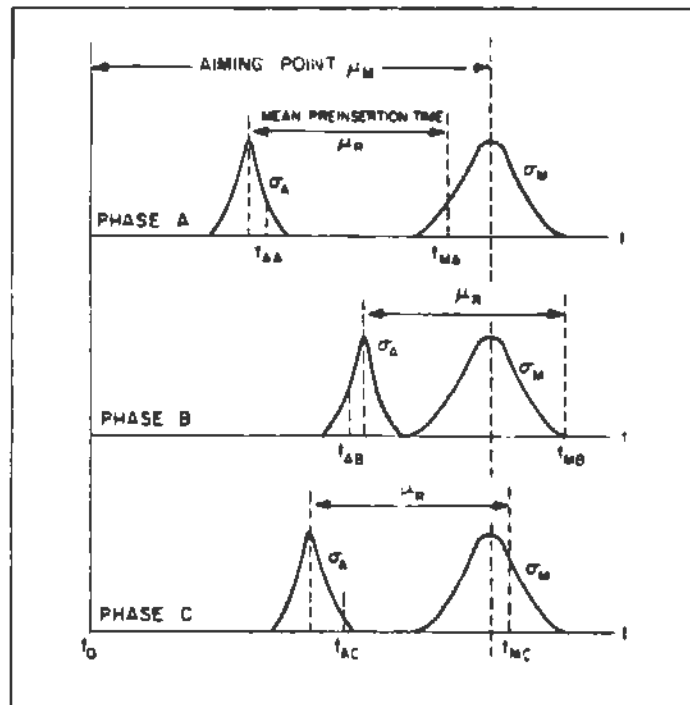


Figure 4-15. Closing Times of the Auxiliary and Main Contacts

The input data for the auxiliary contact is shown at the bottom of Table 4-3. The DELAY TIME is -10 milliseconds because the auxiliary contact closes before the main contact. Therefore, the mean preinsertion time of the resistor is 10 milliseconds. The standard deviation of the auxiliary contacts is .7 milliseconds. Typical values for the mean preinsertion time are 8 to 12 milliseconds, with a standard deviation typically one-half that of the main contacts.

The STATISTICS switches are always open for the steady-state solution. They close once at the appropriate randomly determined time and then remain closed for the remainder of the simulation.

4-6. CURRENT CHOPPING

Oil and SF6 circuit breakers interrupt arcs at natural current zeros, which results in no high-frequency transient voltages associated with current interruption. Vacuum circuit breakers have a tendency to chop current. The amount of chopped current depends on the contact material and the contact geometry. In general, older breaker designs chop higher levels of current than newer designs.

The amount of current chopped varies significantly with the design and the manufacturer. If the effect of current chopping in a given device is investigated the manufacturer should be consulted for the current chopping characteristics. Typical values of mean chopped current range from 2 to 5 amperes, while the maximum chopped current typically ranges from 6 to 10 amperes.

Current chopping is easily simulated by inputting the level of chopped current as " I_e " on the switch cards.

4-7. BREAKER CAPACITANCES

Some circuit breakers have built-in capacitors to modify the TRV waveshape. These capacitors modify the line-side voltage component of the TRV to be within the capabilities of the interrupter. The capacitance reduces the rate-of-rise, which may be important during short-line faults. The value of capacitance depends on the number of interrupters per breaker pole.

Circuit breakers with several interrupters in series have grading capacitors and/or resistors across the interrupters to obtain the proper voltage division between the breaks. These capacitors vary significantly with the type and manufacturer. Typical values are 800-2000 pF per break.

4-8. ARC RESISTANCE

For most simulations the arc resistance can be neglected. If the user wishes to include arc resistance, it can be modeled as a time-varying resistance branch Type 91. An alternative would be to model arc dynamics in TACS. Teixeira describes a dynamic arc model in the November 1983 issue of the EMTP Newsletter, and Kizilcay describes another arc model in the July, 1985, issue of the EMTP Newsletter.

The EMTP dynamic arc models which have been documented represent the arc with an exponentially decaying conductance which approaches zero as the arc extinguishes. Thermal reignitions can also be simulated. Two representative differential equations for the arc conductance are:

$$\frac{dg}{dt} = \frac{1}{T} (G - g)$$

or
$$\frac{dg}{dt} = \frac{g}{T} \left(\frac{vi}{P_0} - 1 \right)$$

where g = dynamic conductance,
 G = steady-state conductance as a function of current,
 T = arc time constant,
 P_0 = steady-state arc power loss
 v = arc voltage
 i = arc current

It is possible to implement these equations in TACS and represent the arc with injected current sources at the breaker terminals. However, this technique requires a very small time step, and it is often unstable. The dynamic arc model cannot be initialized properly at time zero, so it must be activated at some predetermined time in the simulation. Kizilcay describes a modified EMTP

which allows TACS to control an electrical resistance, which avoids the stability problem. However, obtaining data for the equation's parameters presents another problem.

The characteristics of the arc resistance depend mainly on the number of breaks, fault current magnitude, type of interrupter and interrupting media (air, oil, vacuum or SF6). The arc characteristics for a given circuit breaker must generally be obtained from the manufacturer.

4-9. TYPICAL DATA

Circuit breaker characteristics which are important to a particular EMTP study will vary with the frequency range of interest, as shown in Table 4-4 based on Ardito and Santagostino, "A Review of Digital and Analog Methods of Calculation of Overvoltages in Electric Systems," Cigre SC 33 Overvoltages and Insulation Coordination Colloquium in Budapest, September 23-25, 1985.

Table 4-4
CIRCUIT BREAKER CHARACTERISTICS

Characteristic	Frequency Band			
	.01-5kHz	3-30kHz	5kHz-3MHz	50kHz-30MHz
Pole Span	X	X		
Prestrike				X
Current Chopping		X*		X
Restrikes		X*	X	X
High Frequency Interruption		X*	X	X
Stray Capacitance		X*	X	X
Arc Voltage	X	X**		X

- * important for interruption of small inductive currents
- ** important when determining actual time and di/dt at interruption

The most commonly used interrupting media are vacuum, oil and SF6. The interrupting media determines many of the characteristics of the circuit breaker. Most 345-kV and all 500-kV and 800-kV breakers have several interrupters in series to achieve the necessary recovery voltage capability.

In systems 345-kV and up the switching surge level is a major factor in determining the insulation design, and one way to limit switching surges is to use preinsertion resistors. The range of available preinsertion resistors varies from 250 to 800 ohms, with 400 ohms being a commonly used value.

Some circuit breakers use opening resistors to control the transient recovery voltage. The simulation of the opening resistor is the same as for the preinsertion resistor, except that STATISTICS switches are not normally required. An auxiliary contact and a main contact are used.

Some circuit breakers have built-in capacitors to slope off the transient recovery voltage. The values of these capacitors are supplied by the circuit breaker manufacturers. Depending on the breaker design, these capacitors are added as branches either across the contacts or from one terminal to ground.

The pole span is defined as the time between the first pole and last pole closings. Tests have shown that the breaker closings can be described by a Normal distribution where the pole span is defined as ± 3 standard deviations ($\pm 3\sigma$) of the distribution. Typical pole spans range from 1/4 to 1/2 cycle.

Preinsertion time is the time the preinsertion resistors are inserted before the main contacts close and short them out. Typical values are 1/3 to 2 cycles. The pole span of the auxiliary contacts, including prestrike, is approximately one half of the main contact pole span, or 1/8 to 1/4 cycle.

As the contacts of a circuit breaker close a prestrike can occur. The prestrike time depends very much on the breaker design, because the speed of the closing contacts has a major effect. In general the prestrike time is less than 6 milliseconds.

All circuit breakers meet the transient recovery voltage (TRV) capabilities as defined in the ANSI standards. The preferred ratings are given in C37.06-1979, or its latest revision. The TRV capability at rated current of breakers 72.5 kV and below is defined by a $(1 - \cos)$ envelope. Breakers rated 121 kV and above use the $(\exp - \cos)$ envelope. Some circuit breakers have a capability above the standard requirements. This information must be obtained from the manufacturer.

Section 5
SURGE ARRESTERS

5-1. INTRODUCTION

Surge arresters are devices which are used to protect equipment with non self-restoring insulation, such as power transformers, large shunt reactors, cables, etc. The arrester is designed to sparkover at a given level and to carry the impulse current to ground. The magnitude and duration of the power follow current must be limited, and the arrester must be able to reseal when the applied voltage decreases to normal values.

In the past, the active-gap silicon carbide arrester was applied. Presently, the use of metal oxide arresters is increasing. Silicon carbide arresters are made up of air gaps in series with a nonlinear resistor. The gaps are necessary to limit the high leakage currents that would occur at normal voltage. The active gap design forces the arc to elongate, producing a back voltage which limits the current. The flashover level of the gap depends on the steepness of the applied surge voltage.

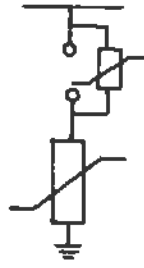
Many metal oxide arresters are simply made up of a series of nonlinear resistor blocks. At rated voltage, only a few milliamperes flow. The volt-current characteristic of the metal oxide (MOx) arrester is much flatter than the characteristic of the silicon carbide (SiC) block. The three basic types shown in Figure 5-1 are:

- 1) The completely gapless arrester;
- 2) A gap shunted by MOx;
- 3) A gap shunted by a linear circuit.

The simplest model of a surge arrester can be made up of a resistor with a nonlinear V-I characteristic with a flashover voltage. After the flashover voltage, V_{fo} , is reached, a jump to a specified segment occurs as shown in Figure 5-2. In this example, the characteristic after flashover jumps to segment 2.



a) Gapless



b) Shunt Gap



c) Series Gap

Figure 5-1. Types of Metal Oxide Arresters

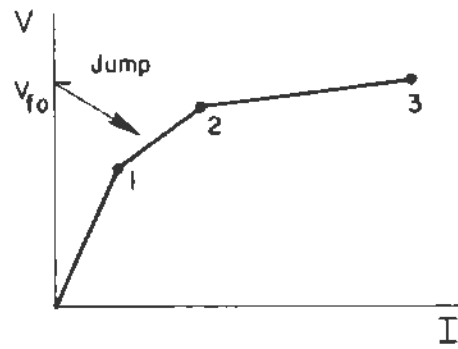


Figure 5-2. Nonlinear V-I Characteristic with Flashover

This principle can be extended to include several linear segments which approximate the nonlinear V-I characteristic. The linear segments may be thought of as switched resistors in parallel.

The piecewise linear characteristic with switched resistors suffers from a time-step delay in changing segments as the voltage changes. When the arrester voltage exceeds the voltage limit for segment 1 in Figure 5-2, the arrester should begin operating on segment 2. However, the EMTP does not sense the voltage change until the time-step computations are completed, so that the change is not made until the next time step.

The EMTP also has a true nonlinear model for the arrester which is solved by compensation techniques. As illustrated in Figure 5-3, the system external to the arrester is reduced to a Thevenin equivalent, which defines a load line. A subroutine in the EMTP iteratively determines the intersection of the load line with the arrester's nonlinear characteristic and then updates the network node voltages. Thus the arrester simulation is truly simultaneous with the network solution.

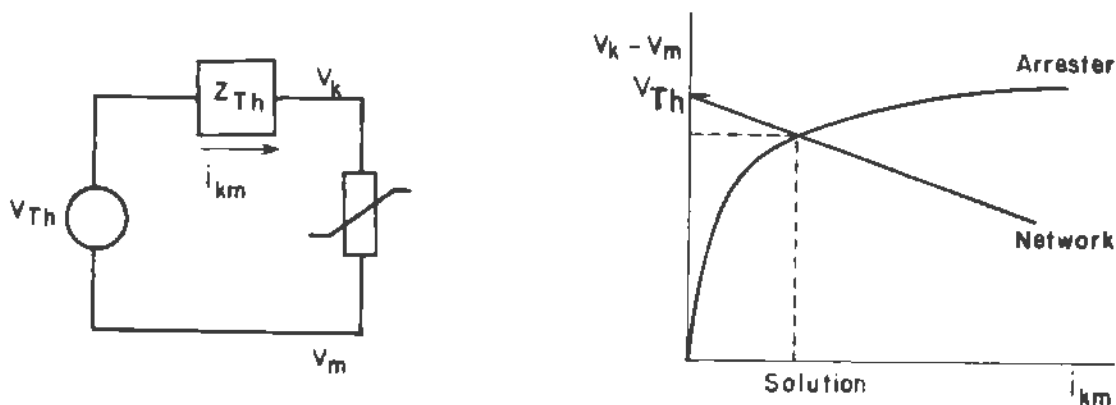


Figure 5-3. Nonlinear Arrester Solution by Compensation

The iterative solution uses the Newton-Raphson method, which should converge at each time step if the time step is small enough and if the initial phasor solution is in the arrester model's linear region. Because of the Thevenin network reduction, only one bus in each system is allowed to have an arrester model. However, portions of the system which are completely isolated from the rest of the system by traveling wave line models may each have an arrester model. Referring to the discussion of overhead lines in Section 2, it may be recalled that the terminals of traveling wave models are not directly connected. The original implementation of the model in Figure 5-3 was single-phase, which was a serious limitation. However, each arrester can now be multiphase.

The data cards associated with MOx arresters are split. A Type 92 element (with a special MOx flag) has to be in the branch data section, and the V-I characteristic of the MOx arrester is defined immediately before the request for node voltage outputs. For each arrester, a V-I characteristic has to be input. Ordering of the characteristics must correspond exactly to the input ordering of the associated Type 92 branch cards.

The following characteristics may be specified:

- * Single exponential without gap.
- * Multi-exponential with gap.

The approach demonstrated in this section uses the single exponential models for both metal oxide and silicon carbide arresters. Gaps are represented with voltage-controlled switches, which are placed in the switch cards section of the EMTP input file.

The nonlinear characteristic in Figure 5-3 is defined by one or more exponential segments as shown in Figure 5-4. For lower voltages with currents in the milliamperes range, the arrester characteristic is defined by a high linear resistance which is also used in the phasor solution. Shunt gaps may be represented by additional exponential segments, also shown in Figure 5-4.

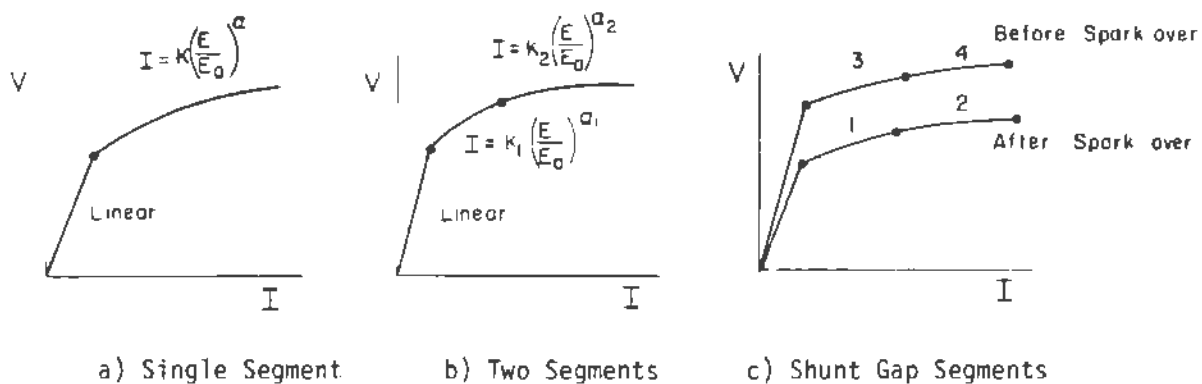


Figure 5-4. Exponential Segments Defining Arrester Characteristic

5-2. SUMMARY OF MODELS AND BEST USAGE

Several arrester models are available in the EMTP.

1. Type-99 pseudo-nonlinear resistance, which is equivalent to a set of paralleled switched resistors. Can be multiphase.
2. Type-92 "MOx" model with exponential segments. Can be multiphase.
3. Type-92 piecewise linear resistance solved by compensation techniques. Single-phase only.
4. Type-94 Active Gap SiC model. Single-phase only.

The Type-92 MOx model is preferred for all arresters, including the SiC type. The Type-94 model is very difficult to obtain input data for, and in addition, is limited to one phase. One of the setup examples illustrates the use of TACS to simulate the active gap in a SiC arrester. There may be rare applications for the Type-99 model or the Type-92 piecewise linear resistance model.

5-3. SETUP EXAMPLES

Eight single-phase test cases are presented covering lightning impulse and switching surge. All of the test cases employ the exponential form of arrester model. Arresters with series gaps also include a simple flashover switch. The following test cases were run.

Lightning Impulse (Figure 5-5)

- SAM001: No arrester
- SAM002: SiC arrester
- SAM003: MOx arrester

Switching Surge (Figure 5-6)

- SAM004: No arrester
- SAM005: MOx arrester
- SAM006: MOx arrester with Shunt Gap
- SAM007: SiC arrester with Active Gap
- SAM008: SiC arrester with Passive Gap

The lightning test system simulates a surge entering a 500-kV station on one of the incoming lines. The voltages impressed on a transformer and circuit breaker are of interest. Due to the fast wavefront of the surge, the separation between the arrester and the protected equipment becomes important. The arrester lead length and the travel time of the pedestal are also represented. The magnitude of the incoming surge is 1330 kV, which was derived from a typical backflash two spans out from the 500-kV station. A typical 500-kV line CFO is 1900 kV, and the magnitude of the incoming surge was taken as 70% of this value. A voltage steepness of 1667 kV/ μ sec is typical of the incoming surge from a backflash two spans out, and the wave tail would be relatively short. Therefore, a 0.8×10 microsecond waveshape was assumed. A Thevenin equivalent impedance of 20 ohms is used to represent the flashed-over tower's footing resistance. The Thevenin equivalent surge magnitude would be 1406 kV, as shown in Figure 5-5.

The switching surge test system consists of a simple 350-ohm surge impedance with a 1890-kV, 200×2000 microsecond surge input. This 4.63 per-unit surge results in approximately 3 kA discharge current, which is the manufacturer's switching surge coordination current for the published protective level data. The SiC

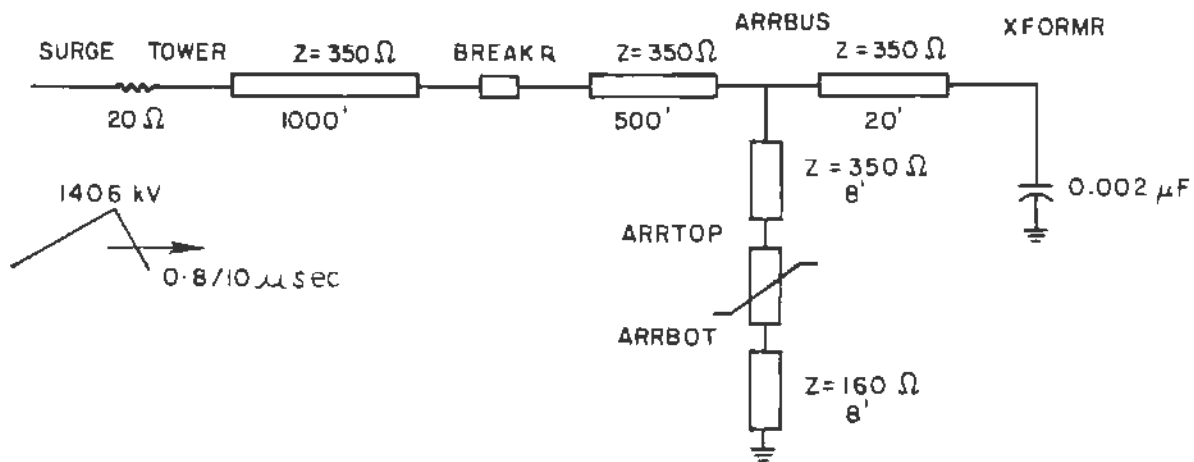


Figure 5-5. System for Lightning Impulse Test Cases

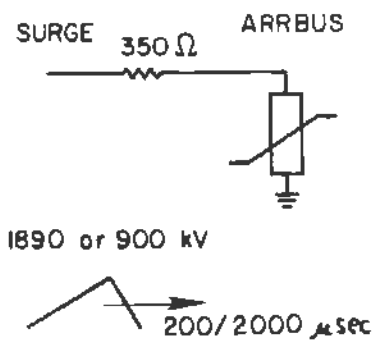


Figure 5-6. System for Switching Surge Test Cases

discharge current is lower, but the discharge voltage is higher, in comparison to the MOx arrester. The total energy dissipated would be approximately the same in either case. For the MOx arrester with a shunt gap, and the active-gap SiC arrester, a more reasonable 900-kV (2.2 per-unit) surge magnitude was simulated.

All of the arresters are 396-kV arresters with parameters based on the data of Section 5-4. The crest voltage rating of this arrester is $396 * \sqrt{2} = 560$ kV, and the Maximum Continuous Operating Voltage (MCOV) rating for the MOx type is $396 * 0.81 = 321$ kV rms. This arrester rating could be applied on effectively-grounded 500-kV systems.

For the SiC arrester, the sparkover levels will depend on the wavefront:

$$\begin{aligned} \text{Front-of-Wave Sparkover} &= 2.05 * 560 = 1148 \text{ kV} \\ 1.2 \times 50 \text{ } \mu\text{sec Sparkover} &= 1.70 * 560 = 952 \text{ kV} \\ \text{Switching Surge Sparkover} &= 1.55 * 560 = 868 \text{ kV} \\ \text{Power Frequency Sparkover} &= 1.35 * 560 = 756 \text{ kV} \end{aligned}$$

These sparkover levels can be simulated in the EMTP with a flashover type switch in series with the nonlinear Type 92 resistance. The flashover voltage depends on the transients to be studied.

An active gap for the silicon carbide arrester can be simulated with a back-emf generated by TACS, as shown in Figure 5-7. Typical parameters of the back-emf are:

$$\begin{aligned} \text{Amplitude} &= 50\text{-}70\% \text{ of the Arrester Rating in Volts Peak} \\ \text{Dead Time} &= 70 \text{ microseconds} \\ \text{Rise Time} &= 400 \text{ microseconds} \end{aligned}$$

It is evident that the active gap is only important during longer-duration switching surges, and is safely ignored in lightning studies.

The nonlinear Type 92 branch input to the EMTP requires a reference voltage, an exponent, and a multiplying coefficient for the equation:

$$I = k * (E/E_a)^\alpha \tag{5-1}$$

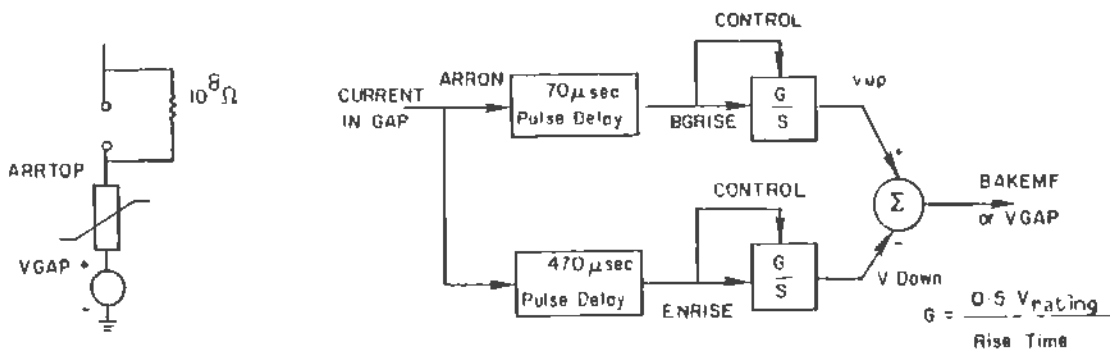


Figure 5-7. 396-kV SiC Arrester Active Gap in TACS

The arrester rating, E_a , will be 560000.0 volts for all test cases as discussed above. The parameters k and α depend on the arrester type, discharge current level, and discharge current steepness as detailed in Section 5-5. Although the EMTP allows several exponential segments, the approach taken here is to use the single-exponential segment with appropriately chosen k and α .

For the silicon carbide arrester, $\alpha=14$ for both switching and lightning discharge. To find k for switching, we set $E = 868$ kV (the sparkover level), at $I = 3000$ amperes for arrester ratings ≥ 48 kV, and use (5-1) to solve for $k = 6.5$. To find k for lightning, we assume a current steepness and calculate k from (5-17) in Section 5-5-1. The current steepness is estimated from the steepness of the incoming surge and the line surge impedance (350 ohms). This yields

$$S_i = 2 S_v / Z = (2 * 1330 \text{ kV}) / (0.8 \text{ } \mu\text{sec} * 350 \text{ ohms}) \quad (5-2)$$

$$= 9.5 \text{ kA}/\mu\text{sec}$$

Equation 5-17 then produces $k = 1.0858$ for the lightning impulse.

For the metal oxide arrester, an average value of $\alpha=26$ is often quoted. However, it is more appropriate to adjust α based on the simulated current magnitudes and steepnesses. For high switching surge currents up to 3 kA, we can use $\alpha=21$ and $k=(1/1.306)^{21}=0.0037$. For I in amperes as required by the EMTP, $k = 3.675$. For lightning impulses, a current steepness of 9.5 kA/ μ sec is assumed. Equation 5-18 in Section 5-5-2 provides two alternatives for k and α , depending on the peak discharge current. For peak currents less than 10 kA, $k = 8.02E-10$ and $\alpha = 52.0$. For peak currents greater than 10 kA, $k = 0.6954$ and $\alpha = 16.9$. Both cases were run.

Section 5-5-2 contains the data needed for setting up a MOx arrester with shunt gaps. This can be modelled with the multi-exponential segment option as described in the Operation Manual. The "flashover" voltage, at which point the arrester changes from the low-current to the high-current characteristic, occurs at 100 amperes, or 1.314 per-unit of 560 kV.

$$0.1 \text{ kA} = (1.314/1.38)^{47} \tag{5-3}$$

Although the EMTP allows the low and high current characteristics to be represented with two separate exponential segments, only one characteristic for each would be used here. This is accomplished by specifying identical k and α for the segments. The high-current characteristic has the same k and α calculated above, while the low-current characteristic has $\alpha=47$ and $k=0.0002665$ for I in amperes. The multi-exponential model in the version of the EMTP used for the example cases did not work properly, in that the shunt gap never sparked over, for any set of input parameters. An alternate means of representing the shunt gap was used in case SAMOD6, which may be employed if the multi-exponential model does not work.

The input for case SAMOD6 includes two nonlinear arrester characteristics in series, each with $k = 3.675$ and $\alpha = 21$. The main characteristic has a voltage rating of 560 kV, while the shunted characteristic has a voltage rating of 0.12 times E_a , or 67.2 kV. This represents 12 percent more MOx blocks in series with the main set of blocks. The series characteristic is shunted with a gap having a flashover voltage of 0.1404 times E_a , or 78.624 kV. This gap will spark over when the total arrester voltage is 733.824 kV, or 1.31 per-unit of the arrester rating. The gap has a series resistance of one ohm, which is necessary to avoid numerical problems which would be caused by shorting the gapped nonlinear resistance. A

large (1E7-ohm) resistance from the main nonlinear resistance terminal to ground is also necessary to meet connectivity requirements before the shunt gap sparks over. Because the main and the shunted nonlinear resistances are connected directly in series, it is necessary to model them as two "phases" of the same arrester.

The input data for case SAMOD3 is presented in Table 5-1. It illustrates the lightning test system and the input for a simple gapless, single-exponential MOx arrester. The data for a passive-gap SiC arrester is given in Table 5-2 for case SAMOD8, the data for a shunt-gap MOx arrester is given in Table 5-3 for case SAMOD6, and the data for an active-gap SiC arrester is given in Table 5-4 for case SAMOD7 (see also Figure 5-7).

The results of the cases are presented in Tables 5-5 and 5-6. Sample plotted results of cases SAMOD1 through SAMOD8 are presented in Figures 5-8 through 5-15. Energy dissipation results in Table 5-6 were obtained by rerunning the cases with a "4" punched in column 80 of the arrester branch card, to obtain branch power and energy outputs in lieu of branch voltage and current. The TACS logic presented in Section 8-5-6-1 is an alternate means of calculating the surge arrester energy dissipation.

For the lightning impulse cases, it may be seen that the MOx arrester has a lower discharge voltage and higher discharge current than the SiC arrester. The arrester lead length and pedestal allow a voltage which is higher than the discharge voltage to appear on the arrester bus. At other points in the substation, such as the transformer terminal and the breaker terminal, the voltage is even higher. The predominant transient frequency can be verified using the lumped parameter equivalents of the lines.

$$L = d (Z/L) = 1520 \text{ ft.} * (350 \text{ ohms} / 1E9 \text{ ft./sec}) = 0.532 \text{ mH} \quad (5-4)$$

$$C = C_{xfmr} + d / (V*Z) \quad (5-5)$$

$$= 0.002 \text{ } \mu\text{F} + 1520 \text{ ft.} / (1E9 * 350 \text{ ohms}) = 0.0063 \text{ } \mu\text{F}$$

$$f = 1.0 / (2\pi \sqrt{LC}) = 87 \text{ kHz} \quad (5-6)$$

$$T = 1/f = 11.5 \text{ } \mu\text{sec} \quad (5-7)$$

Table 5-1

INPUT DATA FOR CASE SAMOD3, LIGHTNING TEST
SYSTEM WITH GAPLESS METAL OXIDE ARRESTER

```

BEGIN NEW DATA CASE
  002E-6 30 0E-6
  20000      3      1      1      1      0      0      1      0
-1TOWER BREAKR      350.0 1.0E9 1000. 1
  TOWER SURGE      20.0
-1BREAKRARRBUS      350.0 1.0E9 500. 1
-1ARRBUSXFORMR      350.0 1.0E9 20. 1
  XFORMR      .002
C ARRESTER LEAD AND PEDESTAL
-1ARRBUSARRTOP      350.0 1.0E9 8. 1
-1ARRBOT      160.0 1.0E9 8. 1
C ARRESTER TERMINAL CONNECTIONS. FLAGGED BY 5555.
92ARRTOPARRBOT      5555
  -1.      -1
  1.      1
  9999.
BLANK CARD ENDING BRANCHES
BLANK CARD ENDING SWITCHES
15SURGE 1592000.0 +82876. -3178600.
BLANK CARD ENDING SOURCES
C ARRESTER CHARACTERISTIC
C      K      A      EA
  -1      8.02E-10      52.0      0.5      0.0 560000.
C MAXIMUM # ITERATIONS PER TIME STEP = 20
  20
  TOWER BREAKRARRBUSXFORMRSURGE ARRBOT
BLANK CARD ENDING NODE VOLTAGE REQUESTS
BLANK CARD ENDING CALCOMP PLOT REQUESTS
BLANK CARD ENDING THE EMTF CASE
  
```

Table 5-2

INPUT DATA FOR CASE SAMOD8, SWITCHING SURGE TEST
SYSTEM WITH PASSIVE-GAP SILICON CARBIDE ARRESTER

```

BEGIN NEW DATA CASE
1.0E-61000.E-6
20000 1 1 1 1 0 0 1 0
SURGE ARRBUS 350.0
C ARRESTER TERMINAL CONNECTIONS. CHARACTERISTIC IS INPUT AFTER SOURCES.
C AS FLAGGED BY 5555 IN COLUMNS 28-32
92ARRTOP 5555.
C DUMMY CHARACTERISTIC
C E16.0 E16.0
-1 -1
1 1.
9999.
BLANK CARD ENDING BRANCHES
C ARRESTER GAP FLASHOVER LEVEL
ARRTOPARRBUS 10.E-6 10.E-6 868000.0
BLANK CARD ENDING SWITCHES
1SSURGE 2219691 6 -434.422 -12068 80
BLANK CARD ENDING SOURCES
C ARRESTER CHARACTERISTIC
C IPHASE K A V-MIN V-O EA
C (<0) P.U., USE LINEAR P.U.
RESISTANCE BELOW INITIAL
V-MIN VOLTAGE
E16.0 E16.0 E8.0
0.5 0.0 560000.
C MAXZND
C MAXIMUM # ITERATIONS AT EACH TIME STEP
C 18
20
ARRBUSSURGE
BLANK CARD ENDING NODE VOLTAGE REQUESTS
BLANK CARD ENDING CALCOMP PLOT REQUESTS
BLANK CARD ENDING THE EMTP CASE
    
```

Table 5-3

INPUT DATA FOR CASE SAMOD6, SWITCHING SURGE
TEST SYSTEM WITH SHUNT-GAP METAL OXIDE ARRESTER

```

BEGIN NEW DATA CASE
1.0E-61000.E-5
20000 1 1 1 1 0 0 1 0
SURGE ARREUS 350.0
ARRGAPARRDUM 1.0
ARRGAP 1.0E7
C ARRESTER TERMINAL CONNECTIONS CHARACTERISTIC IS INPUT AFTER SOURCES.
C AS FLAGGED BY 5555 IN COLUMNS 28-32
92ARRGAP 5555 3
C DUMMY CHARACTERISTIC
C E16.0 E16.0
-1. -1.
1. 1.
9999.
92ARRBUSARRGAPARRGAP 5555. 3
BLANK CARD ENDING BRANCHES
C ARRESTER SHUNT GAP FLASHOVER LEVEL
ARRDUMARRBUS 10.E-6 10.E-6 78624.0
BLANK CARD ENDING SWITCHES
15SURGE 1056996.0 -434.422 -12068.80
BLANK CARD ENDING SOURCES
C ARRESTER CHARACTERISTIC
C IPHASE K A V-MIN V-O EA
C (-0) P.U., USE LINEAR P.U.
C RESISTANCE BELOW INITIAL
C V-MIN VOLTAGE
C 18 E16.0 E16.0 E16.0 E8.0
-1 3.675 21.0 0.5 0.0 560000
C SHUNTED CHARACTERISTIC
-2 3.675 21.0 0.5 0.0 67200.
C MAXZNO
C MAXIMUM # ITERATIONS AT EACH TIME STEP
C 18
20
ARRBUSSURGE
BLANK CARD ENDING NODE VOLTAGE REQUESTS
BLANK CARD ENDING CALCOMP PLOT REQUESTS
BLANK CARD ENDING THE EMTF CASE

```

Table 5-4

INPUT DATA FOR CASE SAMOD7, SWITCHING SURGE
TEST SYSTEM WITH ACTIVE-GAP SILICON CARBIDE ARRESTER

```

BEGIN NEW DATA CASE
1.0E-64000.E-6
20000 1 1 1 1 0 0 1 0
TACS HYBRID
DOWNTM +DEADTM +RISETM
BLANK CARD ENDING TACS FUNCTIONS
91ARRTOP
C ARRESTER PARAMETERS: PEAK RATING = 560 KV
C RISE TIME = 400 USEC
C DEAD TIME = 70 USEC
1VRATED 560000.
1DEADTM 70.E-6
1RISETM 400.E-6
BLANK CARD ENDING TACS SOURCES
C TACS BLOCK DIAGRAM LOGIC TO GENERATE ACTIVE GAP EMF
C
C CHECK THAT GAP HAS FLASHED OVER
C
98BPOLAR = SIGN (ARRTOP)
98ARRON = ABS (ARRTOP) .GT 1 0
C WAIT FOR DEAD TIME DELAY
C
98BGRISE54+ARRON DEADTM
C RAMP UP THE EMF UNTIL THE RISE TIME HAS PASSED
C
98ENRISE54+ARRON DOWNTM
98VUP 58+BGRISE 1 0 BGRISE
98VDOWN 58+ENRISE 1 0 ENRISE
C GENERATE THE BACK EMF
C
98BAKEMF = 0.5 * (VRATED / RISETM) * (VUP - VODWN) * POLAR * ARRON
BLANK CARD ENDING TACS DEVICES
ARRTOPDOWNTMPOLAR ARRON BGRISEENRISEVUP VODWN BAKEMF
BLANK CARD ENDING TACS OUTPUTS
BLANK CARD ENDING TACS INITIAL CONDITIONS
SURGE ARRBUS 350.
ARRTOP 1.00E5
VGAP 1.00E5
ARRTOPARRBUS 1.00E8
ARRBOTVGAP 1.0
C ARRESTER TERMINAL CONNECTIONS. THE CHARACTERISTIC IS INPUT AFTER THE SOURCES,
C AS FLAGGED BY 5555. IN COLUMNS 28-32.
92ARRTOPARRBOT 5555. 3
C DUMMY CHARACTERISTIC
C E16.0 E16.0
-1. -1.
1. 1.
9999
BLANK CARD ENDING BRANCHES
C ARRESTER GAP
C T-CLOSE T-DELAY I-MARGIN V-FLASH
C COLUMNS 15-24 25-34 35-44 45-54
ARRBUSARRTOP 0.000100 0.000200 2 0 86000. 3
BLANK CARD ENDING SWITCHES
15SURGE 1056996 0 -434.422 -12068 80
C TACS-GENERATED BACK EMF TO SIMULATE ACTIVE GAP
17BAKEMF
11VGAP 1 0
BLANK CARD ENDING SOURCES
C ARRESTER CHARACTERISTIC
C IPHASE K A V-MIN V-0 EA
C (<0) P.U., USE LINEAR P.U.
C RESISTANCE BELOW INITIAL
C V-MIN VOLTAGE
C E16.0 E16.0 E8.0
C -1 E16.0 14.0 E16.0 E16.0 560000.
C 6.5 0.5 0.0
C MAXZND
C MAXIMUM # ITERATIONS AT EACH TIME STEP
C 18
C 20
ARRBUSARRTOPVGAP SURGE
BLANK CARD ENDING NODE VOLTAGE REQUESTS
BLANK CARD ENDING CALCOMP PLOT REQUESTS
BLANK CARD ENDING THE EMTF CASE

```

The higher frequencies result from the conductor travel times. The 20-ohm resistance at TOWER and the 2nF capacitance at XFORMR may each be considered short circuits for the travelling waves, to a first-order approximation. The travel times are 1 microsecond from TOWER to BREAKR, 1/2 microsecond from BREAKR to ARRBUS, 20 nanoseconds from ARRBUS to XFORMR, and 8 nanoseconds each for the arrester lead length and pedestal.

The preferred BIL's for 500-kV transformers and circuit breakers range from 1300 to 1675 kV, with a desired protective margin of 15%, or 195 kV to 250 kV. Table 5-5 shows that it might be desirable to use line entrance arresters to protect the circuit breakers. It also shows that the transformer BIL should be at least 1450 kV for this severe condition.

The switching surge cases also indicate that the MOx arrester will tend to have a lower discharge voltage and higher discharge current than the SiC arrester, for the same switching surge. The active gap in some SiC arresters will actually increase the discharge voltage, but not to a level which exceeds the arrester sparkover level. The main effect of the active gap is to limit the discharge current, and hence the dissipated energy, during long-tailed surges. The shunt gap in some MOx arresters will usually spark over quickly, and reduce the discharge voltage by 10 to 12 percent of what it would have been with the same number of blocks and no shunt gap. Table 5-7 compares the MOx arrester performance to the SiC arrester performance during switching surges.

The nonlinear Type 92 resistance approximately doubles the running time of each case. The simulation of an active gap in TACS multiplies the CPU time by five.

Table 5-5

LIGHTNING IMPULSE TEST SYSTEM RESULTS

Case	V_{tower} [kV]	V_{brkr} [kV]	V_{xfmr} [kV]	V_{arbus} [kV]	Arrester Discharge		CPU
					E [kV]	I [kA]	Time [seconds]
SAMOD1-no arrester	1330	2784	2727	2675	-	-	3.588
SAMOD2-SiC arrester	1330	1344	1230	1102	1049	7.09	8.084
SAMOD3-MOx arrester $\alpha=16.9$	1330	1324	1165	1030	970	7.46	7.751
SAMOD3-MOx arrester $\alpha=52.0$	1330	1324	1255	1088	996	8.19	7.706

Table 5-6

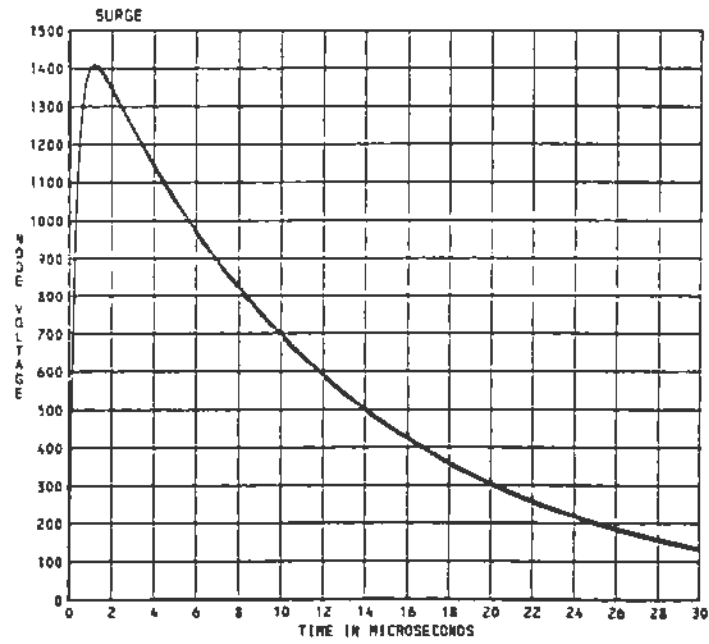
SWITCHING SURGE TEST SYSTEM RESULTS

Case	Discharge Voltage [kV]	Current [Amperes]	Energy [MJoules]	CPU Time [seconds]
SAMOD4-no arrester, 900-kV surge	900	-	-	0.212
SAMOD4-no arrester, 1890-kV surge	1890	-	-	0.212
SAMOD5-MOx gapless, 1890-kV surge	773	3192	2.97	0.414
SAMOD5-MOx gapless, 900-kV surge	710	542	0.22	0.419
SAMOD6-MOx shunt gap, 900-kV surge	733	541	-	0.710
SAMOD7-SiC active gap, 900-kV surge	869	416	-	2.741
SAMOD8-SiC passive gap, 1890-kV surge	866	2925	2.88	0.440
SAMOD8-SiC passive gap, 900-kV surge	754	417	0.16	0.440

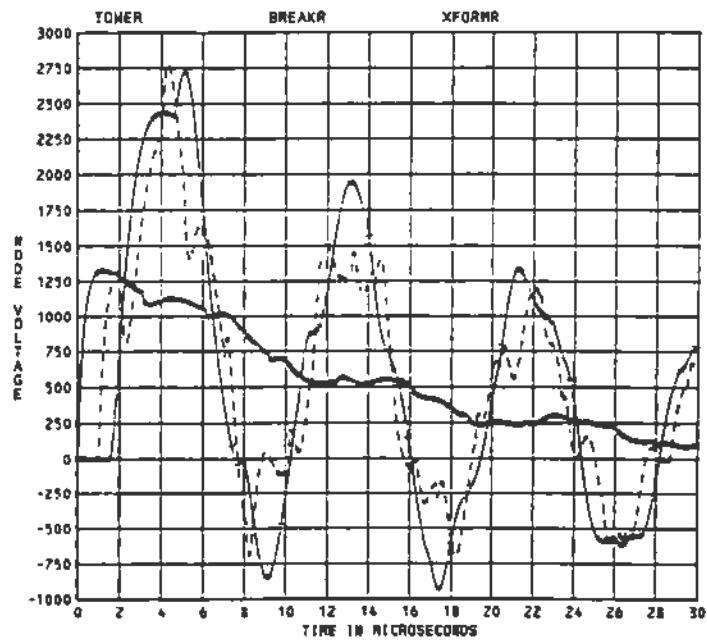
Table 5-7

SWITCHING SURGE RESULTS - COMPARISON OF METAL OXIDE TO
SILICON CARBIDE ARRESTERS

Surge Input [kV/p.u.]	Metal Oxide		Silicon Carbide	
	Voltage [kV/p.u.]	Energy [MJoules]	Voltage [kV/p.u.]	Energy [MJoules]
1890/4.63	773/1.89	2.97	866/2.12	2.88
900/2.12	710/1.74	0.22	754/1.85	0.16

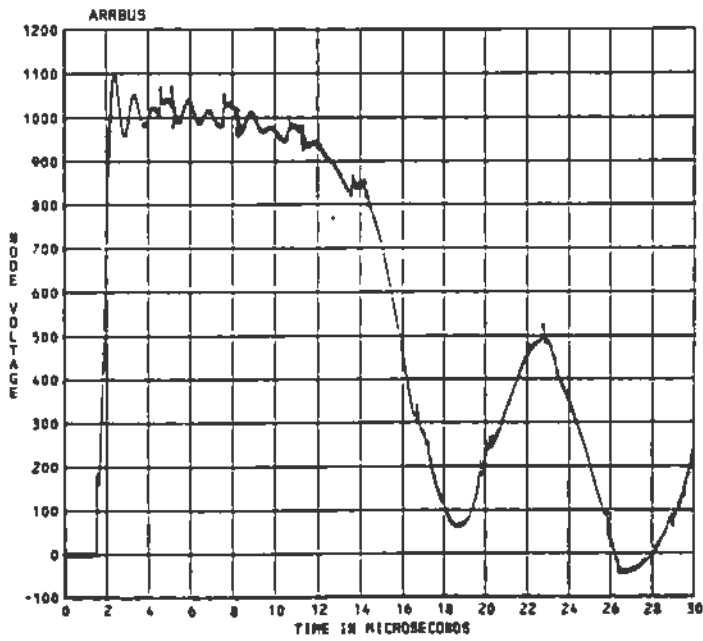


a) Incoming Surge

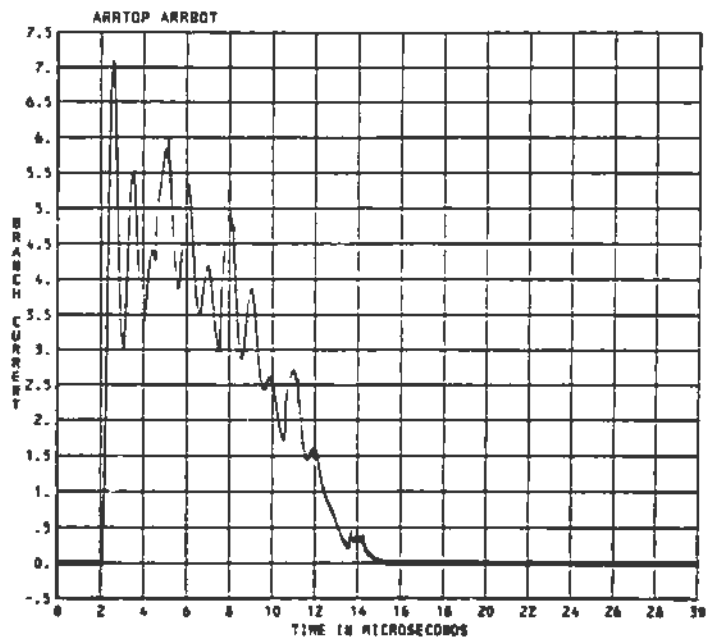


b) Equipment Stresses

Figure 5-8. Case SAMOD1, Lightning Impulse, No Arrester

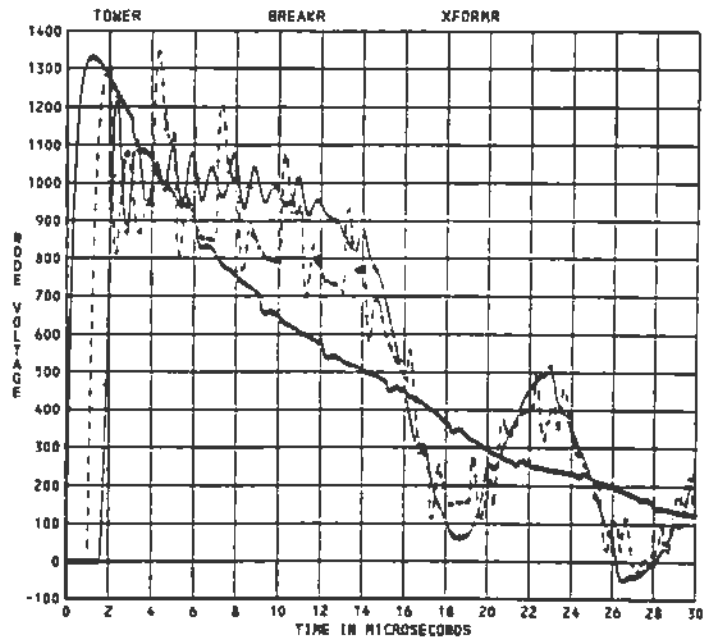


a) Arrester Bus Voltage



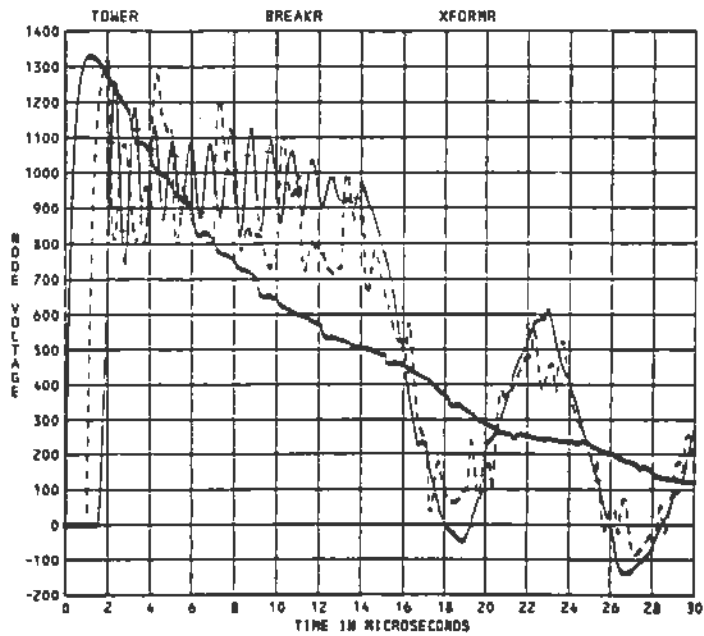
b) Arrester Discharge Current

Figure 5-9. Case SAM0D2, Lightning Impulse, SiC Arrester



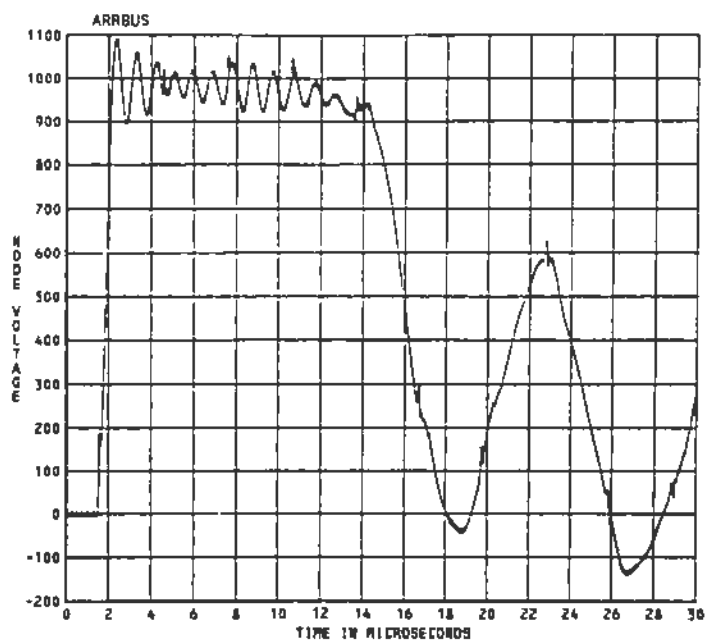
c) Equipment Stresses

Figure 5-9 (cont.). Case SAMOD2, Lightning Impulse, SiC Arrester

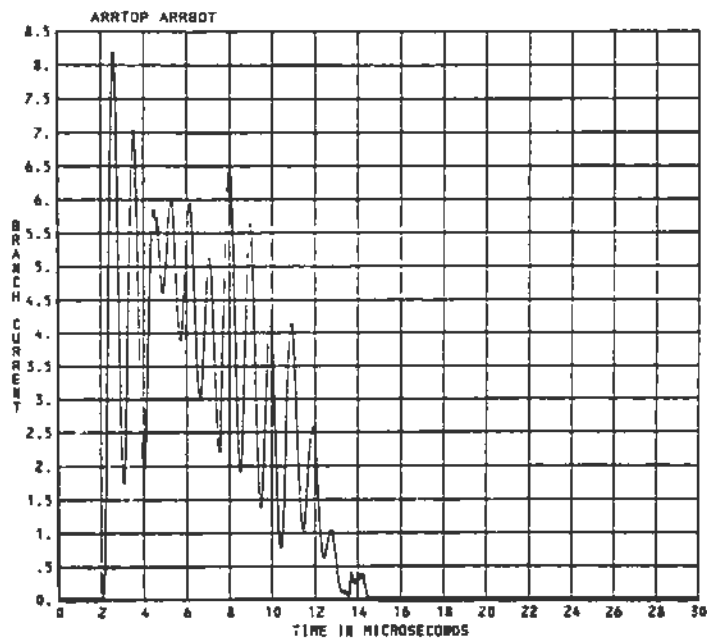


a) Equipment Stresses

Figure 5-10. Case SAMOD3, Lightning Impulse, MOx Arrester

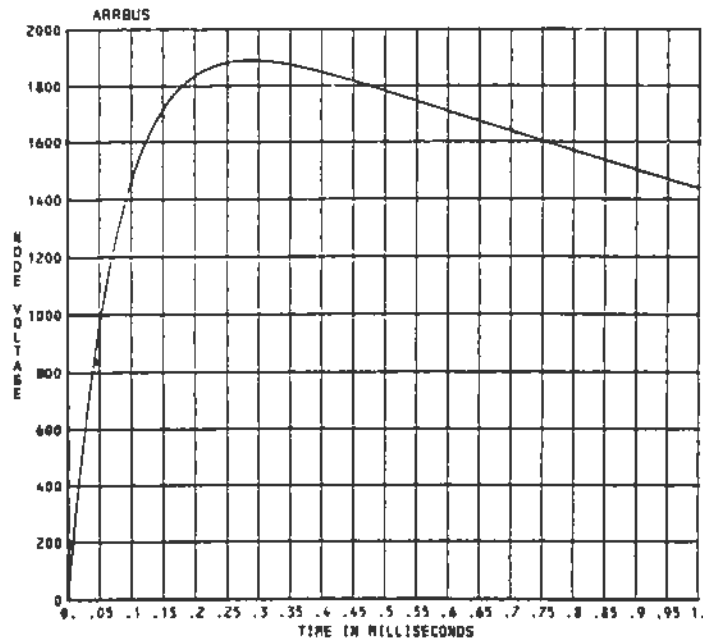


b) Arrester Bus Voltage

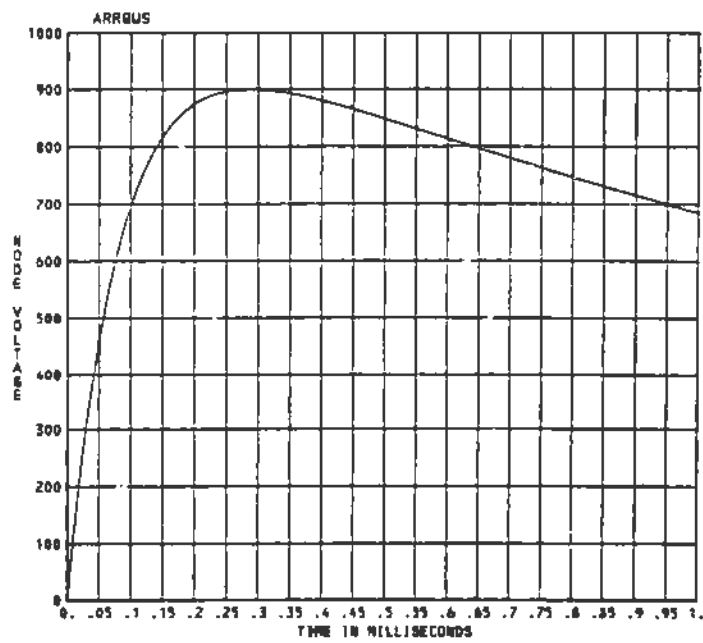


c) Arrester Discharge Current

Figure 5-10 (cont.) Case SAMOD3, Lightning Impulse, MOx Arrester

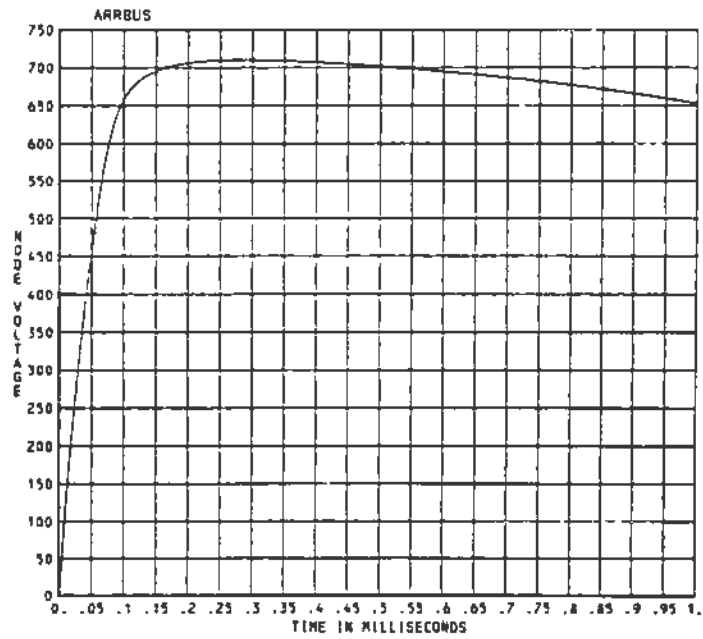


a) Switching Surge Waveshape - 1890 kV peak

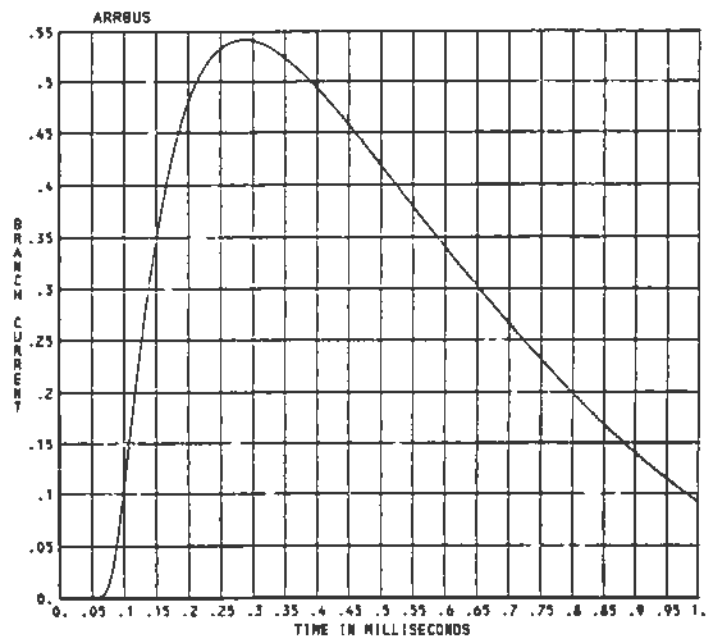


b) Switching Surge Waveshape - 900 kV peak

Figure 5-11. Case SAMOD4, Switching Surge, No Arrester

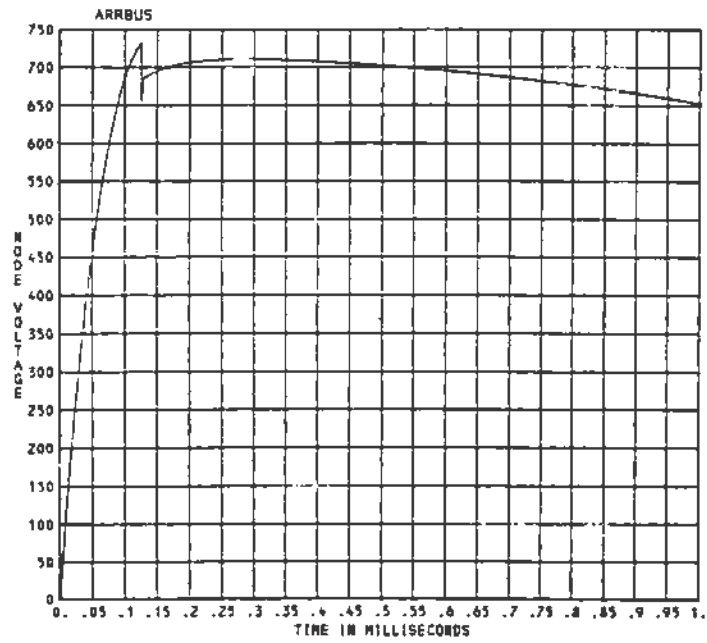


a) Arrester Discharge Voltage

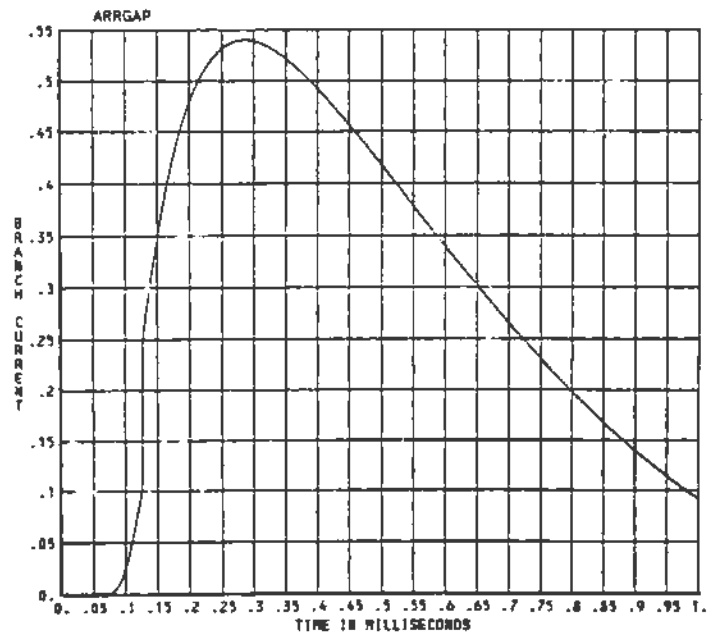


b) Arrester Discharge Current

Figure 5-12. Case SAMOD5, Switching Surge, MOx Gapless, 9DD-kV Surge

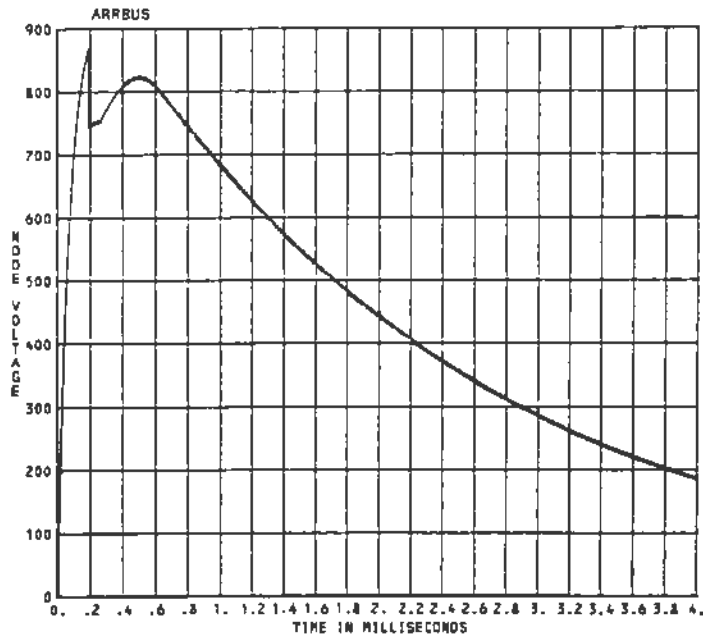


a) Arrester Discharge Voltage

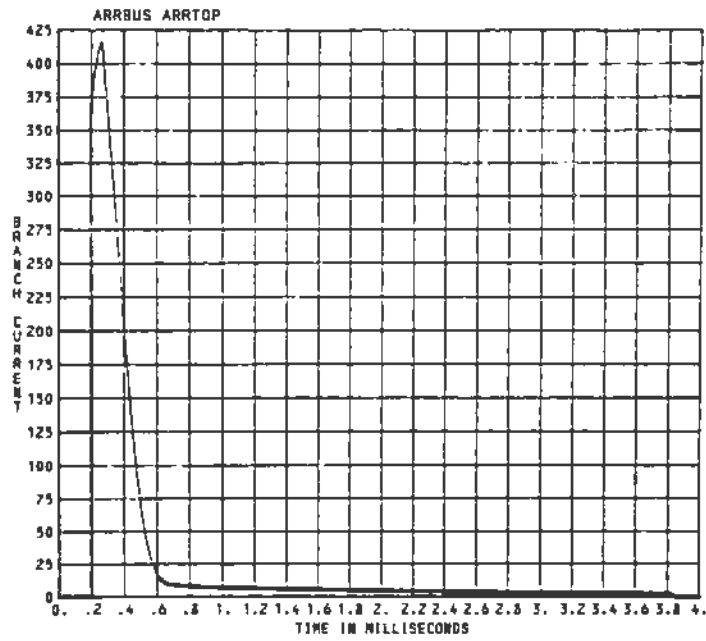


b) Arrester Discharge Current

Figure 5-13. Case SAMOD6, Switching Surge, MOx Shunt Gap, 900-kV Surge

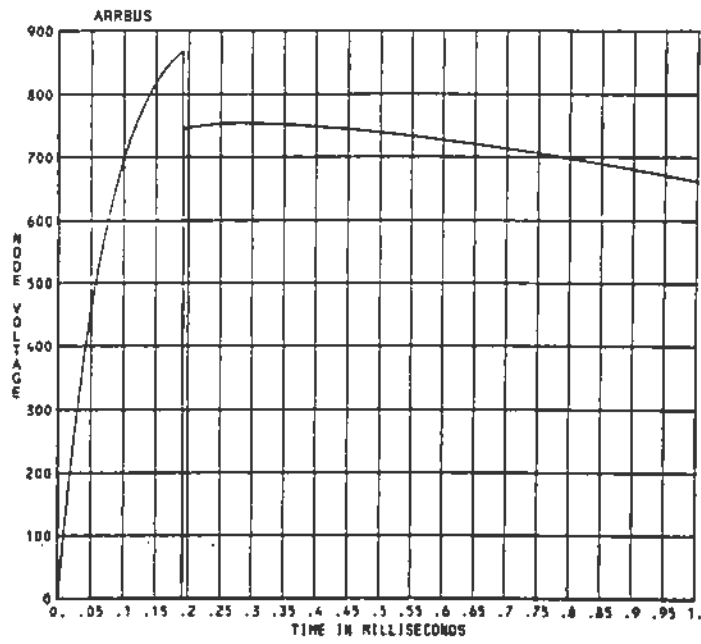


a) Arrester Discharge Voltage

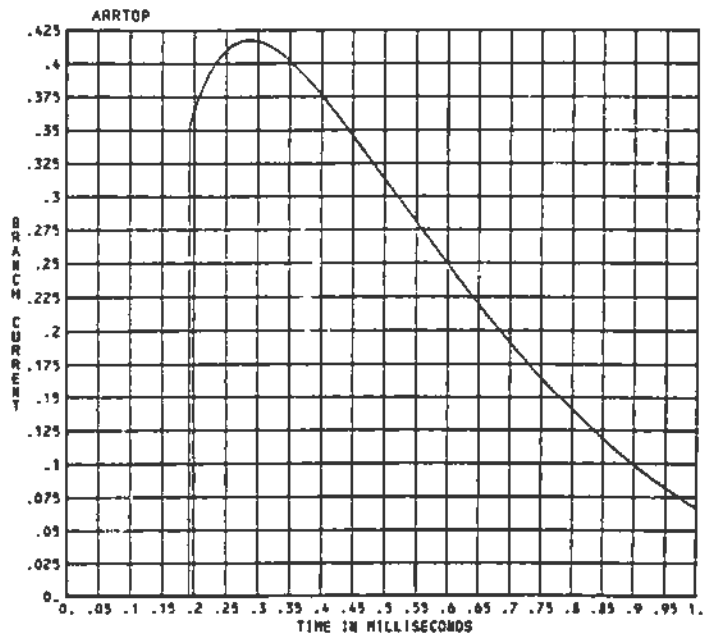


b) Arrester Discharge Current

Figure 5-14. Case SAMOD7, Switching Surge, SiC Active Gap, 900-kV Surge



a) Arrester Discharge Voltage



b) Arrester Discharge Current

Figure 5-15. Case SAM0D8, Switching Surge, SiC Passive Gap, 900-kV Surge

5-4. APPROXIMATE SOLUTIONS FOR ARRESTER DISCHARGE VOLTAGE AND CURRENT

The discharge voltage for either type of arrester during switching surges can be estimated by solving the following two equations.

$$I = (E_s - E_d)/Z \quad (5-8)$$

$$I = k * (E_d/E_a)^\alpha \quad (5-9)$$

The parameter E_s is the peak switching surge voltage magnitude, and the parameter E_d is the arrester discharge voltage. These can be combined into one equation, which is solved for the discharge current by iteration.

$$I = k * [(E_s - Z * I)/E_a]^\alpha \quad (5-10)$$

In the examples of Section 5-3, Z is 350 ohms and E_s is either 1890 kV or 900 kV. It will be seen that the discharge currents in Table 5-6 satisfy (5-10).

The energy during a switching surge discharge may be estimated pessimistically by assuming that the entire line is charged to the same voltage, and that the arrester discharges all of the energy. Under these conditions,

$$E = I * E_d * (2\tau) \quad (5-11)$$

where τ is the line's travel time. In more convenient terms,

$$E = 0.0000111 * I * E_d * d \quad (5-12)$$

where d is the line length in miles. For I in kA and E_d in kV, the energy will be in MegaJoules. Equation 5-12 can be used to estimate the energy dissipated given a line length, or to estimate the maximum permissible line length given a switching surge to be discharged. Table 5-8 compares the MOx and SiC energy dissipation capabilities to the results from Table 5-7. The estimated maximum permissible line lengths are also included in Table 5-8. In general, the energy dissipation during transmission line switching surges will not be critical, but the energy dissipation during shunt capacitor switching overvoltages may be of concern.

Table 5-8

ARRESTER ENERGY DISSIPATION APPROXIMATIONS

	Metal Oxide			Silicon Carbide		
	Capability	Actual	Line Length	Capability	Actual	Line Length
1890-kV Surge	5.2 MJ	2.97 MJ	189 miles	2.8 MJ	2.88 MJ	100 miles
900-kV Surge	5.2 MJ	0.22 MJ	1216 miles	2.8 MJ	0.16 MJ	801 miles

The lightning surge discharge current and voltage can be estimated by iteratively solving two equations.

$$I = (2E_s - E_d)/Z \quad (5-13)$$

$$I = k * (E_d/E_a)^\alpha \quad (5-14)$$

In this case, the term $2E_s$ represents a Thevenin equivalent voltage for the lightning impulse. As described in Section 5, k will depend on the current steepness for lightning impulses. The current steepness can be estimated from the voltage surge steepness.

$$S_i = 2S_v/Z = E_s/(\tau_f * Z) \quad (5-15)$$

where τ_f is the voltage surge front time. For the examples in Section 5-3, it was determined that $S_i = 9.5$ kA/ μ sec. Many iterations are required to solve the equations because the value of I is very sensitive to E_d . The results are shown in Table 5-9, with a comparison to the actual results from Table 5-5. It should be noted that the approximations exclude the effects of the arrester pedestal, arrester lead length, and transformer capacitance.

Table 5-9

APPROXIMATIONS TO LIGHTNING IMPULSE DISCHARGE VOLTAGE AND CURRENT

Arrester Type	k	a	Estimated		Actual	
			I	Ed	I	Ed
Metal Oxide	8.02E-13	52	4.8 kA	985 kV	8.2 kA	996 kV
Silicon Carbide	0.00109	14	4.7 kA	1019 kV	7.1 kA	1049 kV

5-5 TYPICAL ARRESTER DATA

The characteristics of surge arresters which are important depend on the frequency range of interest, as shown in Table 5-10 based on Ardito and Santagostino, "A Review of Digital and Analog Methods of Calculation of Overvoltages in Electric Systems," Cigre SC 33, Overvoltages and Insulation Coordination Colloquium in Budapest, 23-25 September 1985.

Table 5-10
SURGE ARRESTER MODEL CHARACTERISTICS

Characteristic	Frequency Band			
	.01-5kHz	3-30 kHz	5kHz-3MHz	50kHz-30MHz
V-I Characteristic	X	X	X	X
Gap Flashover Voltage	X	X	X	X
Parasitic Inductance			X	X
Lead Lengths			X	X
Surge Steepness Effects			X	X
Thermal Characteristics	X	X		

The typical data in this section cover switching and lightning impulse discharge voltages, gap sparkover voltages, charge and energy capabilities, and temporary overvoltage capabilities for station class MOx and silicon carbide arresters. The data was developed from information published by several manufacturers. For critical applications, the particular arrester manufacturer should be consulted for more information.

Parasitic inductance in the arrester has the effect of delaying the discharge current peak, so that it does not coincide with the discharge voltage peak. It affects the discharge current waveshape only for surges which have front times on the order of one microsecond or less. Even in these cases, the practical effect of parasitic inductance on the peak current and voltage is not significant. Surge arrester inductance is not treated in this section. If the user needs to simulate the inductance's effect on the discharge current waveshape, Durbak's article in the January, 1985 EMTP Newsletter contains further information.

The surge arrester has three major regions of operation. The first region, for low voltages, includes resistive and capacitive current conduction in the milliAmpere range. This region is modelled with a linear resistance in the EMTP, usually for voltages up to one half of the peak arrester rating. The capacitive current effects are of little practical importance.

The second region is the range of voltage limiting for currents up to 3 kiloAmperes peak for switching surges, or up to 40 kiloAmperes peak for lightning surges. This region is treated in sections 5-5-1 and 5-5-2 below.

The third region is thermal runaway, which occurs if excessive energy is dissipated during a switching surge, or if a lightning surge discharge current is excessively high. The energy dissipation capabilities are covered in sections 5-5-1 and 5-5-2. Surge arresters are designed to safely discharge currents of at least 100 kiloAmperes peak. If thermal runaway occurs, the arrester characteristic curves upward and becomes almost linear. It is not necessary to model the third region in detail for EMTP simulations, because the arrester will eventually fail and become a short circuit.

5-5-1. Silicon Carbide - Station Class

This section covers sparkover levels and discharge characteristics for the silicon carbide surge arrester. The discharge characteristics assume a single- exponential formulation of the model. This formula has been used in the past because it fits the silicon carbide nonlinear resistance very well. The EMTP also allows piecewise linear arrester models. The single-exponential equations presented here could be used to generate the I-V points for these models.

For the SiC Arrester's switching impulse discharge characteristic, use the single exponential characteristic in (5-16).

$$I = k * (E/E_a)^{14} \tag{5-16}$$

where E_a is the arrester rating in kV crest

E is the arrester discharge voltage in kV

I is the arrester discharge current in kA

To find k, set E = switching impulse sparkover level in kV, and
 I = 500 Amps (arrester rating \leq 48 kV)
 I = 3000 Amps (arrester rating \geq 48 kV)

For the SiC arrester's lightning impulse discharge characteristic, use the single exponential characteristic in (5-17).

$$I = [0.7692/(S^{0.1})]^{14} * [E/E_a]^{14} = k * (E/E_a)^{14} \quad (5-17)$$

where S is an assumed steepness in kA/ μ sec
 E_a is the arrester rating in kV crest
 E is the arrester discharge voltage in kV
 I is the arrester discharge current in kA

Table 5-II
 SPARKOVER LEVELS

<u>Sparkover Test</u>	<u>Duty Cycle Rating</u>	<u>Crest Voltage [p.u.]</u>
FOW	60-144 (100 kV/us-12 kV)	2.00
	168-240 (100 kV/us)	2.10
	258-312 (2000 kV/us)	2.00
	396-468 (2000 kV/us)	2.05
1.2x50 microsecond Switching Impulse	60-468	1.70
	60-168	1.60
	180-312	1.57
60-Hz	396-468	1.55
	3-60	1.50
	60-468	1.35

Table 5-12

SiC ARRESTER ENERGY DISCHARGE CAPABILITY [kJ/kV]

Duty Cycle Rating [kV]	Current Range [kV]		
	<3400	3400-5000	>5000
60-312	4	3	4 Coulombs/operation
396-468	7	6	4 Coulombs/operation

5-5-2. Metal Oxide - Station Class

Unfortunately, the single-exponential formula which works so well for silicon carbide arresters does not fit the metal oxide discharge characteristic very well. The implementation of multi-exponential characteristics in the EMTP reflects this fact. Figure 5-16 illustrates that the exponential parameter, α , is a variable for metal oxide arresters. A piecewise linear resistance solved by compensation techniques would be a better and more efficient model for metal oxide arresters than the multi-exponential, but it has not been implemented in the EMTP. It is suggested that, for the time being, users select a single-exponential model for metal oxide arresters, with a chosen appropriate to the frequency range being simulated.

Metal oxide arrester ratings are now given on a duty cycle basis according to standards. The actual duty cycle test is not applicable to metal oxide arresters, so in the past manufacturers have specified Maximum Continuous Operating Voltages (MCOV) for their metal oxide arresters. The MCOV rating is the maximum system operating voltage that the arrester should be subjected to. Thus, the MCOV rating is a very useful number, but the duty cycle ratings have the advantage of compatibility with the traditional arrester ratings. Generally, a metal oxide arrester's MCOV rating can be calculated as 0.81 times the duty cycle rating.

For the metal oxide arrester's lightning impulse discharge characteristic, use the single exponential characteristic in (5-18).

$$I = [1.0/(c * S^{1/\beta})]^\alpha * [E/E_a]^\alpha = k * (E/E_a)^\alpha \quad (5-18)$$

where S is an assumed steepness in kA/usec

E_a is the arrester rating in kV crest

E is the arrester discharge voltage in kV

I is the arrester discharge current in kA

α , β and c are parameters selected from Table 5-13

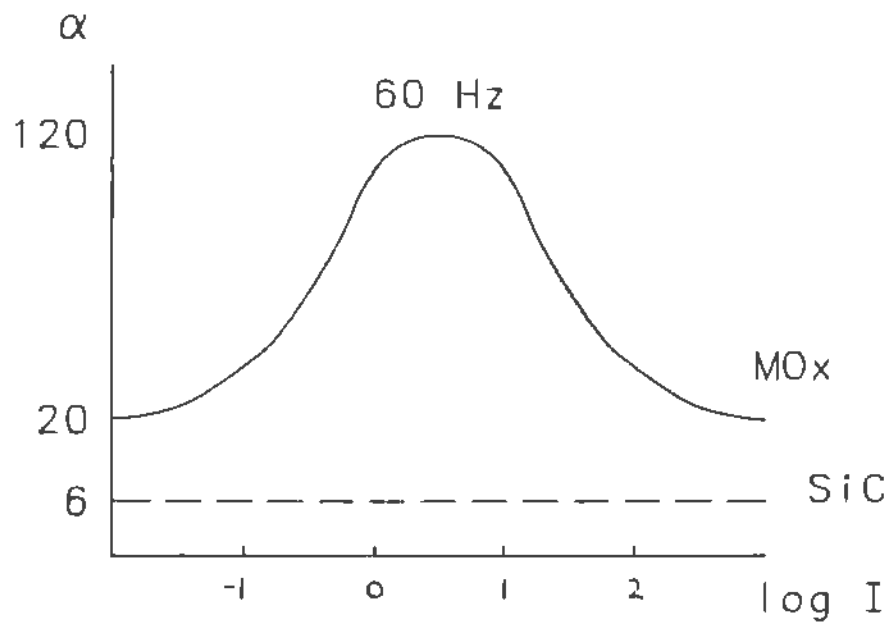


Figure 5-16. Variation of α vs. I for a Metal Oxide Arrester

Table 5-13

METAL OXIDE LIGHTNING DISCHARGE PARAMETERS

Duty Cycle	Current Range	c	α	β	%error
60-360	3-10	1.454	31.1	17.7	1.0
	10-40	1.182	8.2	17.7	1.0
396-588	3-10	1.500	52.0	17.3	1.2
	10-40	1.350	16.9	17.3	1.2

For the metal oxide arrester's switching impulse discharge characteristic, use the single exponential characteristic in (5-19).

$$I = (1.0/c)^\alpha * (E/E_a)^\alpha = k * (E/E_a)^\alpha \quad (5-19)$$

- where E_a is the arrester rating in kV crest
- E is the arrester discharge voltage in kV
- I is the arrester discharge current in kA
- α and c are parameters selected from Table 5-14

Table 5-14 presents the parameters for modelling a MOx surge arrester during switching surges, including the parameter k for use in (5-1). The parameters of the shunt gap are also included in Table 5-14, for use as described in the example of Section 5-3.

Table 5-14

METAL OXIDE ARRESTER SWITCHING DISCHARGE PARAMETERS
 METAL OXIDE ARRESTER WITH SHUNT GAP - 45/90 IMPULSE TEST

		<u>Duty Cycle Rating</u>	
		<u>54-360</u>	<u>396-444</u>
Before Sparkover	k (5-1)	.0221	.0002665
	c	1.398	1.380
	α	32	47
	I_{range}	1-500 A	1-100 A
After Sparkover	k (5-1)	12.20	3.675
	c	1.292	1.306
	α	17.2	21
	I_{range}	250-3k A	50-3k A
Shunt Gap	V_{rat}	0.10 E_a	0.12 E_a
	V_{spark}	0.1241 E_a	0.1404 E_a

Table 5-15

METAL OXIDE ARRESTER ENERGY DISCHARGE CAPABILITY

<u>Duty Cycle Rating</u> [kV]	<u>Energy</u> [kJ/kV]	<u>Maximum Current</u> [kA/kV]
2.7-48	4.0	1.0
54-360	7.2	1.5
396-588	13.1	2.7

Section 6

INITIAL CONDITIONS

The EMTP time-step simulations must start from an initial state. In most cases, the EMTP's a.c. steady-state phasor solution is adequate to initialize the system voltages and currents prior to beginning the time-step simulations. The phasor solution is also a valuable study tool in itself to study steady-state coupling and resonance problems. However, the phasor solutions are presently limited to one frequency - normally, the power frequency. Other frequencies such as d.c. and harmonics must be ignored in the phasor solution.

The single frequency limitation of the phasor solution will sometimes cause problems when significant harmonic or d.c. components exist in the pretransient state. Some examples of these states include:

1. Switching capacitor banks or transmission lines with trapped charge.
2. Saturated nonlinear inductances which generate harmonics.
3. HVDC and SVC systems.

One approach is to approximately initialize the system considering only the power frequency phasor solution. During the ensuing time step solution, the EMTP model will normally reach a steady-state condition with all frequencies present, provided the user waits long enough. This method can be expensive in terms of computing resources. More efficient methods are available for special cases, as discussed below.

6-1. SETTING UP LOAD FLOWS

Load flows often provide the initial conditions for EMTP transient simulations. The load flow output contains a set of bus voltages and line currents which are to be duplicated in the EMTP. In general, the EMTP voltage sources are not at the load flow buses, but are connected behind source impedances. Therefore, a precise matching of the load flow condition is not straightforward and may require a manual iterative approach.

In general, the user should attempt to match bus voltages and phase angles rather than line currents. The first iteration could begin with the EMTP voltage source magnitudes and phase angles equal to the load flow voltage at the nearest bus. If the source impedance represents lines and/or transformers for which the load flow currents are available, then the user may add the voltage drop across the source impedance to the initial guess for the phasor source voltage. Several steady-state solutions with adjusted source voltages may be required before the user is satisfied with the results.

After the bus voltage magnitudes and phase angles are matched, the line and transformer currents may still not match the load flow values. This occurs because the EMTP model includes more detail and slightly different parameters than the load flow model. This is usually not a cause for concern. In most cases the initial bus voltages will have a greater impact on transient overvoltages. One exception would be in series-capacitor compensated systems, where the stored energy in the capacitor depends significantly on the initial line currents.

6-2. CAPACITOR BANK SWITCHING

Shunt capacitor banks are normally energized only after a sufficient waiting time from the most recent deenergization. Typically, 5 minutes are sufficient to allow the trapped charge to decay. However, a restrike simulation involves trapped charges on the capacitor bank. Since restrikes in capacitor bank switching occur one-quarter to one-half cycle after the first pole opens, and the ensuing transients contain high-frequency components, the simulation of recovery voltage buildup across the switch contacts will waste considerable computing resources. It is more efficient to study a switch closing operation with trapped charges on the bank, which simulates a restrike.

For grounded three-phase banks, the specification of trapped charge is straightforward. In the initial condition cards which come immediately before node voltage output requests, each capacitor bank terminal voltage is specified to have a d.c. voltage corresponding to the trapped charge. The branch initial condition cards should specify zero branch current and the d.c. branch voltage - which is also the d.c. node voltage to ground. All of the d.c. voltages on capacitors which have opened will be approximately ± 1.0 per-unit, because capacitive current interruption occurs at a voltage peak.

For ungrounded three-phase banks, one pole interrupts the capacitive current and then the other two poles normally interrupt simultaneously one-quarter cycle later. In the meantime, the capacitor bank neutral voltage has shifted. The peak recovery voltage across the first pole to open reaches approximately 2.5 per-unit.

The remaining two poles could fail to interrupt one-quarter cycle after the first pole, in which case they will not interrupt until at least three-quarters of a cycle after the first pole. In the meantime, the capacitor bank neutral shift causes a peak 3.0 per-unit recovery voltage across the first pole to open.

Typically, restrikes of an ungrounded capacitor bank will occur with one or two phases of the bank still connected to the system. There will be a combination of d.c. and power frequency voltages on each capacitance. To properly initialize the bank with trapped charge, several rules must be followed:

1. Interrupted phases will have zero branch current and either 1.0 per-unit or 0.87 per-unit d.c. branch voltage.
2. Uninterrupted phases will have power frequency branch currents and voltages.
3. The stray neutral capacitance will have 0.5 per-unit d.c. voltage plus 0.5 per-unit power frequency voltage.

To determine the initial branch voltages and currents, the user must perform two phasor solutions.

1. One with the capacitor bank energized to determine the voltage trapped on the interrupted phase.
2. One with the capacitor bank unbalanced, i.e., one or more poles of the switch open. This determines the capacitor branch currents and phase angles.

The capacitor node voltages are derived by summing the appropriate branch voltages, while the branch currents are obtained from the unbalanced phasor solution. This ensures that inductive currents will not undergo sudden changes during the first time step of the transient.

When simulating the restrike with a small time step, the EMTP will calculate the proper capacitor currents and will initialize the remaining system. The user then overrides these initial conditions by specifying d.c. voltages on the

node voltage initial condition cards and on the branch cards for the capacitances. The user must also respecify the same capacitor branch currents, because the use of initial condition cards destroys any values previously calculated in the phasor solution.

An example of this technique is shown in Figure 6-1. It is desired to simulate a restrike 5 milliseconds after the first pole interrupts, where the second and third poles have failed to interrupt. The first balanced phasor solution produces 11175 volts to ground at the capacitor terminals. If phase C is the pole which interrupts, we have the following initial conditions.

$$\begin{aligned}
 V_n &= 11175 \\
 I_{cn} &= 0 \\
 V_{cn} &= 11175 [0.5 + 0.5 \sin (\omega t - 90^\circ)] \\
 &\quad \text{with } t = 0.005, V_n = 7314
 \end{aligned}$$

The unbalanced phasor solution should be performed with source voltage angles corresponding to the instant of restrike - i.e., 5 milliseconds or 108° after a peak voltage on phase C. The instantaneous voltages and currents at time zero from this phasor solution produce:

$$\begin{aligned}
 V_n &= 3251.6 & I_{an} &= -497.35 \\
 V_{bn}^{an} &= -14172.1 & I_{bn}^{an} &= 497.57 \\
 & & I_{cn}^{an} &= .22 \\
 V_a &= V_n + V_{an} = 10565.6 \\
 V_b &= V_n + V_{bn}^{an} = -6858.1 \\
 V_c &= V_n + V_{cn}^{an} = 18489.0
 \end{aligned}$$

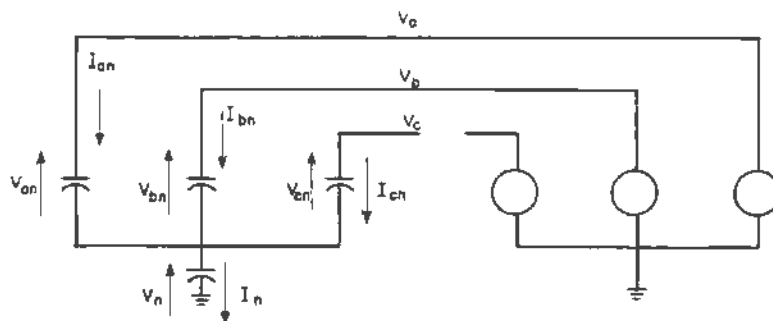


Figure 6-1. Ungrounded Capacitor Bank with Trapped Charge

As an alternative to specifying the initial conditions, the user could simulate the entire switch opening and restrike operation. However, this must all be performed at the same small time step to accurately simulate the restriking transients. If the user's computer installation includes the MEMSAV and START AGAIN options mentioned in the Operation Manual, then the buildup of recovery voltage need only be simulated once for each set of initial conditions, thereby saving considerable CPU time.

6-3. OVERHEAD LINE SWITCHING

Reclosing into lines which have experienced a single-phase or two-phase fault is similar to a capacitor bank restrike in that the unfaulted phases will have trapped charges which significantly affect the ensuing transients. For the simulation of distributed parameter lines without shunt reactors, these trapped charges may be represented as d.c. voltages. The user should simulate a fault clearing case to determine the trapped line voltages, and then input these d.c. voltages as initial conditions for the line terminals when simulating the reclose. The line conductor currents and differential voltages should be specified as zero in all three phases. An example of this technique is given in Case 7 of the Primer.

When shunt reactors are installed on the line, slowly decaying 45-55 Hz oscillations will be superimposed on the d.c. line voltages after opening the breakers. These initial conditions are difficult to specify on the initial condition cards, but a technique for doing so is described by Teixeira and Charles in the February 1981 EMTP Newsletter. Another initialization technique which uses internal sources is described by Toyoda in the May 1982 issue of the EMTP Newsletter.

As an alternative to specifying the initial conditions, the user could simulate the entire fault initiation, fault clearing and reclosing operation. However, this must all be performed at the same small time step to accurately simulate the reclosing transients. Since the dead time between fault clearing and reclosing usually ranges from 0.5 to several seconds, significant computing time will be wasted. Numerical stability problems may also surface due to the excessively large number of time steps to be simulated. If the user's computer installation includes the MEMSAV and START AGAIN options mentioned in the Operation Manual, then the dead time need only be simulated once for each set of initial conditions, thereby saving considerable CPU time in statistical studies.

6-4. NONLINEAR ELEMENTS

The EMTP phasor solution assumes linear impedances as well as a single steady state frequency. Nonlinear elements are approximated with a linear impedance, which is usually the first segment of a piecewise linear resistance or inductance characteristic. The EMTP will print a warning if the phasor solution lies outside the range of this first linear segment, but the system will be initialized at that linear impedance. An error will be introduced at the first time step, as illustrated in Figure 6-2.

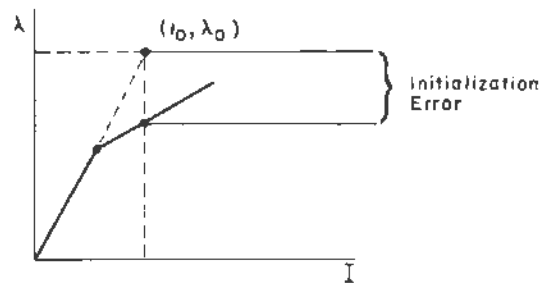


Figure 6-2. Initialization of Nonlinear Inductance

A significant flux linkage error in the initialization of a nonlinear inductance will generally lead to sustained oscillations as soon as the time step simulation begins. These will eventually decay. Even if the initial condition lies within the linear range of the inductance characteristic, any harmonic distortion components which exist in the steady state will have been ignored by the EMTP. Therefore, a waiting time will be required before the time step simulation reaches a quasi steady state with all of the harmonics. This waiting time is usually less than that associated with initialization outside the linear range, but could still amount to several cycles of power frequency voltage.

At the present time, there is no method of accounting for nonlinearities in the EMTP initialization process. The user can minimize the amount by which nonlinear inductances are initialized outside their linear range by letting one of the phase voltage angles be approximately zero degrees. The flux is in phase with the current, which lags the voltage by 90 degrees. Therefore, one of the phase flux linkages will be zero and the other two will be ± 0.87 times their peak values, as shown in Figure 6-3.

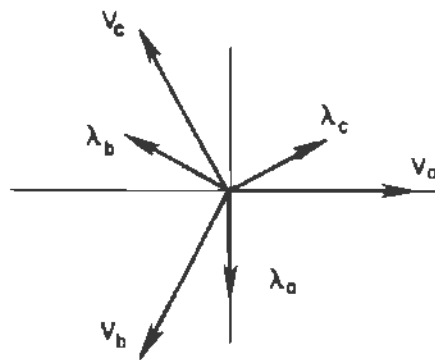


Figure 6-3. Phasor Diagram of Three-Phase Inductance Initialization

Nonlinear resistances do not cause the same degree of difficulty in initialization. Because resistors do not store energy, errors in the initial conditions will usually dissipate soon after the time step simulation begins. The EMTP's surge arrester model is defined as a linear resistance for normal operating voltages during the time step simulation, which further reduces initial condition errors. The initial currents in surge arresters and other nonlinear resistors will usually be very small.

6-5. SYNCHRONOUS MACHINE EXCITATION SYSTEMS

TACS initialization is difficult because the EMTP will not perform the process automatically. The electrical network is initialized first, so that TACS sources which depend on electrical voltages, currents or switches are available in the steady state. However, TACS control signals are not available to the electrical network in the steady state. Furthermore, the user must provide the initial states and past histories of integrators, s-blocks and delay blocks manually. TACS initialization for HVDC and Static VAR Compensators is addressed in some of the EMTP Newsletter articles. These entries may be found under the TACS category of the reference list.

One special case which will be treated in this module is that of synchronous machine excitation systems and governors. The EMTP Type 59 machine model calculates its initial field voltage and mechanical torque input to satisfy its initial conditions based on the electrical network phasor solution. The TACS excitation system and governor outputs then serve as scaling factors for the initial values of field voltage and torque.

If the user sets up the initial output of the TACS exciter and governor equal to 1.0, then those outputs during the time domain simulation will be in per-unit of the machine's initial condition. This system is convenient to use if the following procedure is followed:

1. For each new set of load flows, run a phasor solution to determine the Type 59 model's initial field voltage and mechanical torque.
2. Set initial outputs of the TACS control systems equal to 1.0.
3. Adjust gains, limits and reference values in the TACS data to reflect the actual Type 59 initial condition.
4. Perform the actual time step simulation. As an example, consider the exciter and hydrogovernor block diagrams shown in Figure 6-4. Initial conditions of the machine are:

$$\begin{aligned}P_o &= .95 \text{ per-unit of rating} \\I_D &= 300 \text{ amperes} \\I_f &= 300 \text{ amperes} \\V_t &= 1.05 \text{ per-unit}\end{aligned}$$

The field current for one per-unit voltage on the air gap line, input as parameter AGLINE with the Type 59 data, is 270 amperes. The machine's rated speed is 257 rpm, or 26.913 rad/sec. The block diagrams are adjusted as shown in Figure 6-5 for input to TACS.

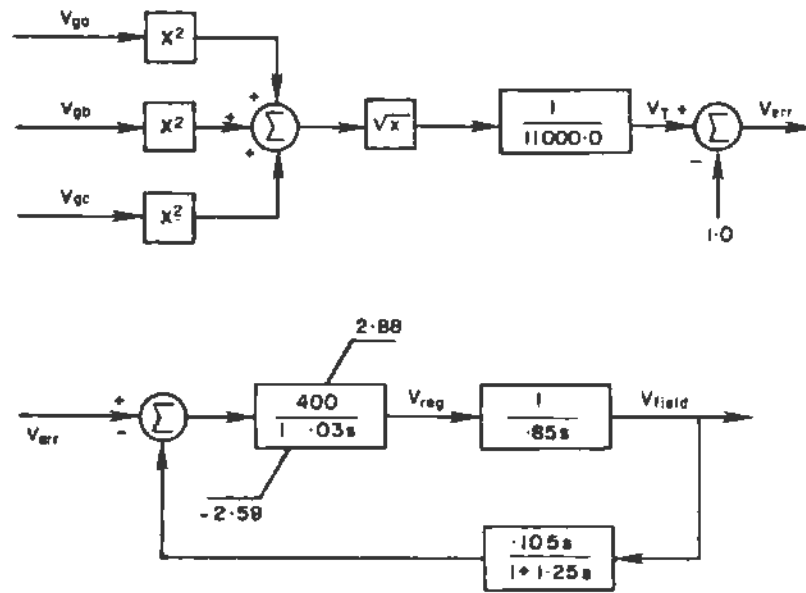


Figure 6-4a. Excitation System Block Diagram

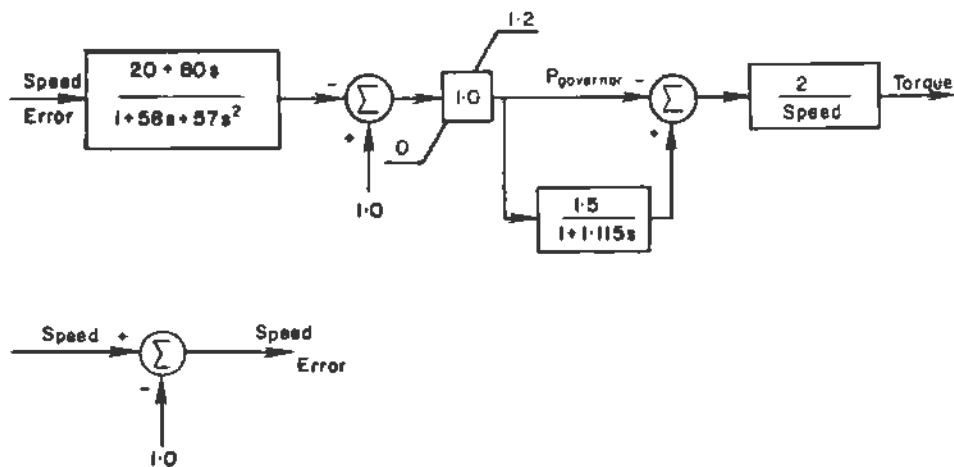


Figure 6-4b. Hydrogovernor Block Diagram

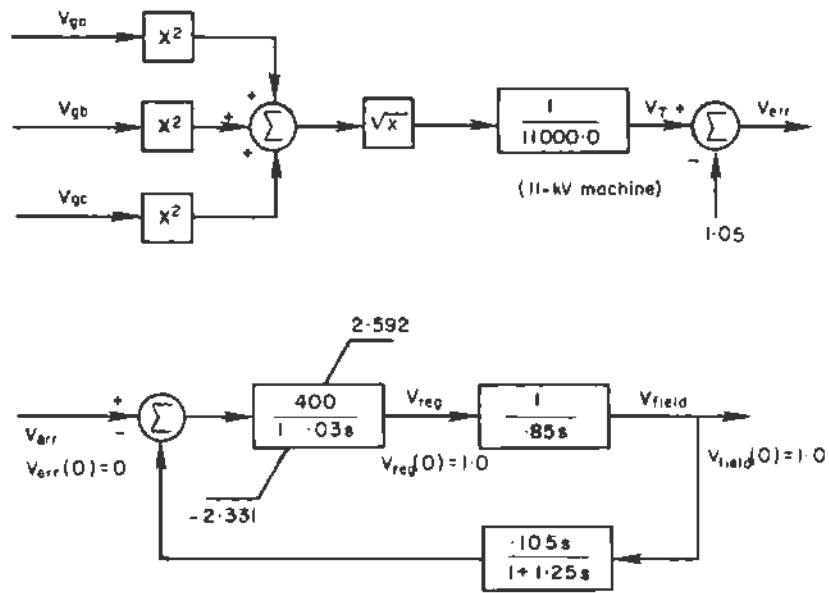


Figure 6-5a. TACS Excitation System Block Diagram

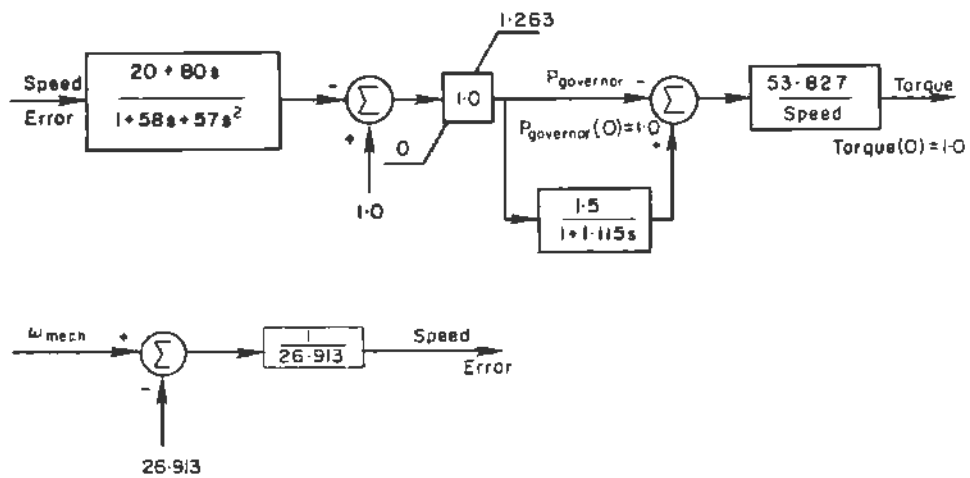


Figure 6-5b. TACS Hydrogovernor Block Diagram

Section 7

SOURCES

EMTP sources include both rotating machines and voltage sources behind equivalent source impedances. This module will cover the specification of source impedances, modeling of loads and surge impedances for transient studies, and synchronous generator parameters. The initial source voltages are often determined by load flow study results or other considerations. More information on source voltage magnitudes may be found in the Initial Conditions section.

7-1. SETTING UP MATRIX IMPEDANCES

The source data can be given in several different forms:

1. Three-phase fault or line-to-ground fault data in either MVA or kA.
2. Positive and zero sequence impedances in either ohms or per-unit on a given base (usually 100 MVA).

If the data is not given in ohms, it usually must be converted to ohms for input to the EMTP. The following example shows the conversion of short circuit data given in kA to either Type 1-2-3 or Type 51-52-53 impedances.

Example: 230-kV system

3-phase fault current = 10.5 kA $\angle -86^\circ$

Line-to-ground fault current = 7.5 kA $\angle -84^\circ$

Ignoring the angle differences between the three-phase and line-to-ground fault currents, we get

$$\begin{aligned} Z_1 &= E_{1n} / I_{3p} = 230 / (\sqrt{3} \times 10.5) = 12.64 \text{ ohms} \\ Z_0 &= (3 \times E_{1n} / I_{1p}) - (2 \times Z_1) \\ &= [(3 \times 230) / \sqrt{3} \times 7.5] - (2 \times 12.64) = 27.84 \text{ ohms} \end{aligned}$$

More accurately, with the phase angles included, we get

$$Z_1 = R_1 + jX_1 = .882 + j12.61 \text{ ohms}$$

$$Z_0 = R_0 + jX_0 = 2.91 + j27.69 \text{ ohms}$$

The sequence impedances can be input directly for the Type 51-52-53 branch type.

51BUS1 ABUS2 A	R_0	L_0
52BUS1 BBUS2 B	R_1	L_1
53BUS1 CBUS2 C		

The sequence impedances can also be converted to self and mutual impedances for the Type 1-2-3 branch type. If the zero sequence impedance is less than the positive sequence impedance, then the mutual impedances will be negative.

$$Z_{11} = Z_{22} = Z_{33} = Z_s = 1/3 \times (Z_0 + 2 \times Z_1)$$

$$Z_{12} = Z_{13} = Z_{23} = Z_m = 1/3 \times (Z_0 - Z_1)$$

$$R_s = 1/3 \times (2.91 + 2 \times .882) = 1.558 \text{ ohms}$$

$$X_s = 1/3 \times (27.69 + 2 \times 12.61) = 17.64 \text{ ohms}$$

$$R_m = 1/3 \times (2.91 - .882) = .676 \text{ ohms}$$

$$X_m = 1/3 \times (27.69 - 12.61) = 5.02 \text{ ohms}$$

1BUS1 ABUS2 A	R_s	L_s	C_s						
2BUS1 BBUS2 B	R_m	L_m	C_m	R_s	L_s	C_s			
3BUS1 CBUS2 C	R_m	L_m	C_m	R_m	L_m	C_m	R_s	L_s	C_s

The Type 51-52-53 branches are usually more convenient to use, but the Type 1-2-3 branches offer more flexibility. Shunt source capacitances can be included and nontransposed source impedances can be input. The Type 1-2-3 branches are often useful for simulating unbalanced loads connected to ground.

7-2. SURGE IMPEDANCE TERMINATIONS

Travelling wave studies often truncate the system model at a bus which has lines connected to it. The proper source equivalent for these lines is a surge impedance termination connected to ground. Capacitances and inductances can be used to represent buswork, transformers, shunt reactors and shunt capacitors on the bus as described in other modules of this guide. However, when surge impedance

terminations are used, the user should avoid initializing with 60-Hz phasor solutions. The initial load flows will be too high and the initial bus voltages too low due to the shunt resistances. It is better to inject the surge into a network with zero initial conditions. The power frequency voltage, which can usually be assumed constant during the transient, can be superimposed on the transient during the analysis of the results.

A single-phase line surge impedance termination is simply a resistor connected to ground, as depicted in the example of Figure 7-1. The reflection coefficient at this termination is zero, which means that traveling waves entering the bus "disappear" into the outgoing line. The surge impedance termination by itself has no effect on the bus voltage - the bus voltage is equal to the incoming waveshape. However, if there are other lumped elements connected to the bus (shunt capacitor, for instance) then the net reflection coefficient is not zero and there will be an effect on the bus voltage.

If several lines terminate at the bus, the surge impedance terminations should be paralleled as shown in Figure 7-2. In this situation, the net reflection coefficient is -0.5, which will tend to reduce the bus voltage.



Figure 7-1. Single-phase Surge Impedance Termination

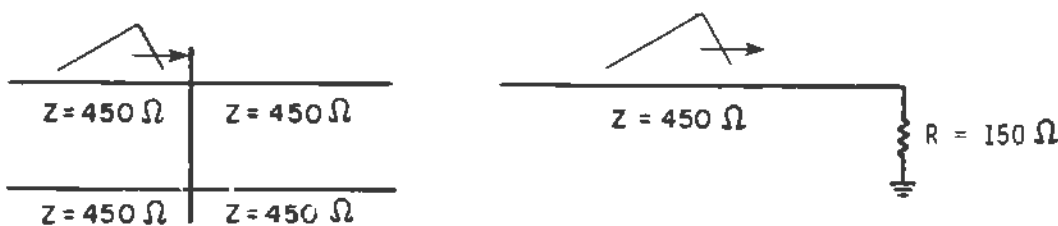


Figure 7-2. Paralleled Surge Impedance Terminations

Multi-phase lines will require a matrix of resistances for the proper surge impedance termination. If the line is transposed, then the self and mutual resistances for this matrix are given by:

$$R_s = Z_1 + 1/3(Z_0 - Z_1)$$

$$R_m = 1/3(Z_0 - Z_1)$$

where Z_0 and Z_1 are the zero sequence and positive sequence surge impedances. These resistances can be input as a Type 1-3 or as a Type 51-53 branch as discussed above. The Type 51-53 branch is more convenient because $R_0 = Z_0$ and $R_1 = Z_1$. Figure 7-3 illustrates a surge impedance termination for the 90-mile 500-kV line from Case 7 of the Primer.

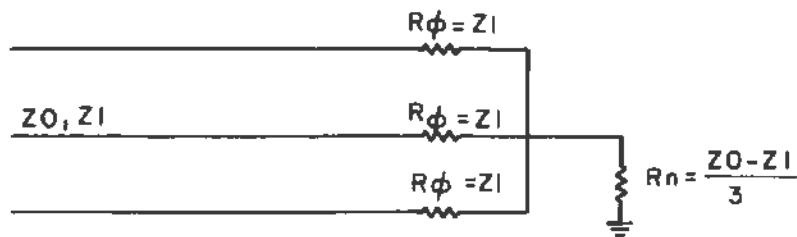


Figure 7-3. Multi-phase Surge Impedance Termination

If the line is not transposed, then the resistance matrix will have unequal self and mutual terms. The Type 1-3 branch must be used to accommodate this. The user should run the LINE CONSTANTS program to obtain the surge impedance termination matrix, which is labelled "ZSURGE IN PHASE DOMAIN" in the printout. These values are to be inserted directly into the resistance matrix. An example for a two-phase line is given in Case 3 of the Primer, where $R_{11} = 478.54$ ohms, $R_{12} = 93.77$ ohms and $R_{22} = 316.23$ ohms. This termination is used in Case 4 of the Primer.

If one of the frequency-dependent line models is used, the surge impedance varies with frequency. It is probably best to use a surge impedance termination evaluated at the predominant frequency of the transient.

7-3. LOADS AND DAMPING

The effect of loads on harmonics and electromagnetic transients is often ignored during studies. However, field test results indicate that the loads can have an important impact on these phenomena, particularly in reducing peak values, increasing damping and determining harmonic magnitudes at resonance. Very little is presently known about how to properly model loads at high frequencies. The simple load models used for load flow and stability studies will generally yield incorrect results.

The load model should satisfy two requirements which are of equal importance. The power frequency watt and VAR load must be accurate in order to evaluate the initial conditions. The high-frequency characteristics of the model should also match the physical load to properly represent its effect on harmonics and transients.

Series RL and parallel RL circuits can produce the correct initial conditions, but are very inaccurate at higher frequencies. An added step in complexity is to represent the load as a combination of series and parallel RL circuits, usually with 10% of the load dissipated in the series RL element and 90% in the parallel RL element, or vice versa. Four load circuit configurations are shown in Figure 7-4. The total load impedance in each circuit is 1.0 at an angle of 25 degrees, which can be rescaled to provide 1 p.u. MVA at .9 lagging power factor. A physical justification for the Series-Parallel configuration in Figure 7-4c is often given - namely, that the small series RL depicts distribution transformers and overhead conductors, while the parallel RL depicts the customer load. Customer-owned power factor correction capacitors could be added across the parallel load.

The resistance and reactance of these load circuits are plotted as functions of frequency in Figure 7-5. All of the loads will provide the correct power frequency initial conditions. However, the Series RL model provides little damping at high frequencies due to the increasing series reactance. The Parallel RL model becomes a constant damping resistance at high frequencies, which usually overdamps electromagnetic transients. The two dynamic load models provide better high frequency damping characteristics. The Series-Parallel circuit resistance approaches a constant value, but the increasing series

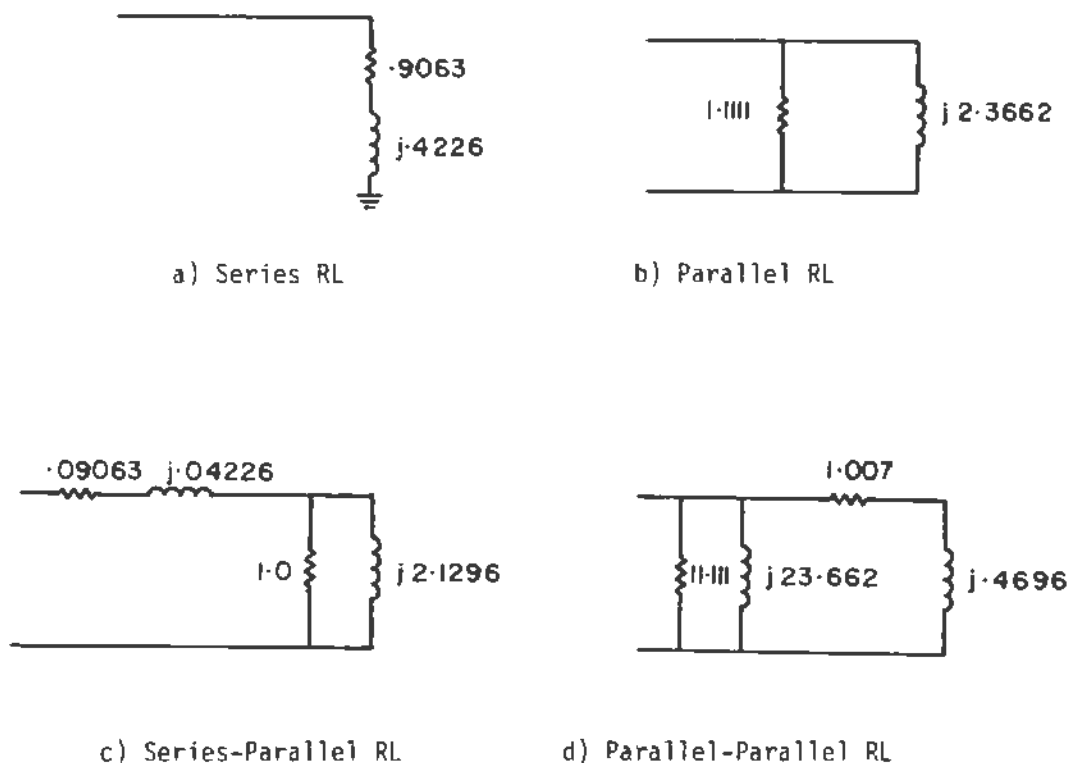
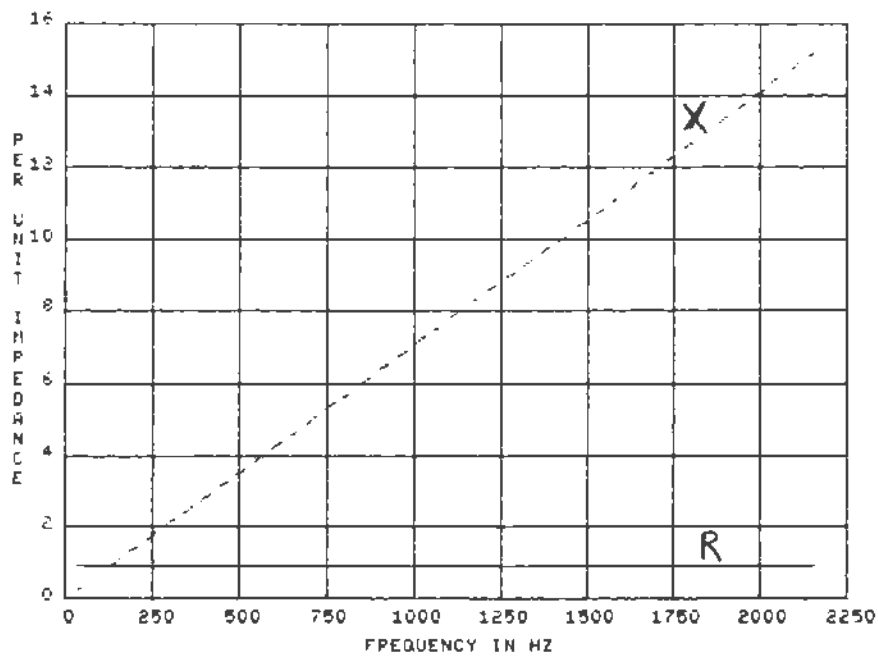


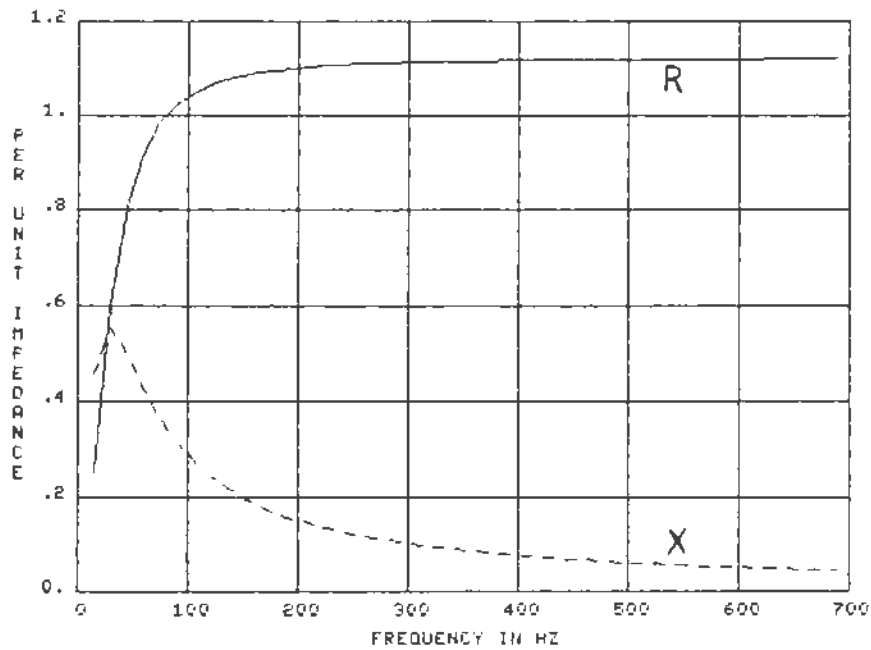
Figure 7-4. Load Equivalent Circuits

reactance will limit its damping effect. The Parallel-Parallel RL resistance asymptotically approaches a higher value as frequency increases, but this value is effective in damping high-frequency transients because there is no high reactance in series with it. Of the four simple load models considered, the Parallel-Parallel RL Circuit is recommended for EMTP studies.

None of the load models considered in Figure 7-4 contain the series and parallel resonance phenomena which have been observed during field tests. If shunt capacitors are part of the load, they could be lumped in parallel across the load circuit terminals, thereby producing one of the lower frequency parallel resonances in the load. Overhead lines and cables also have shunt capacitance. Even if there are no capacitor banks in the load, both transmission and distribution system load equivalents will generally have a parallel resonance in the 500-1000 Hz range, so the user could incorporate this with a paralleled capacitance.

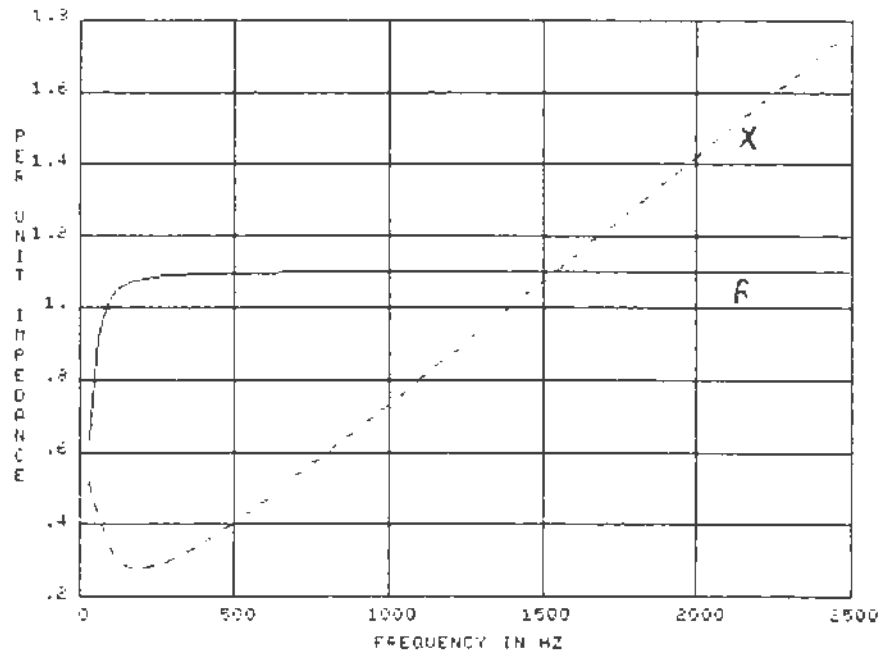


a) Series RL Circuit

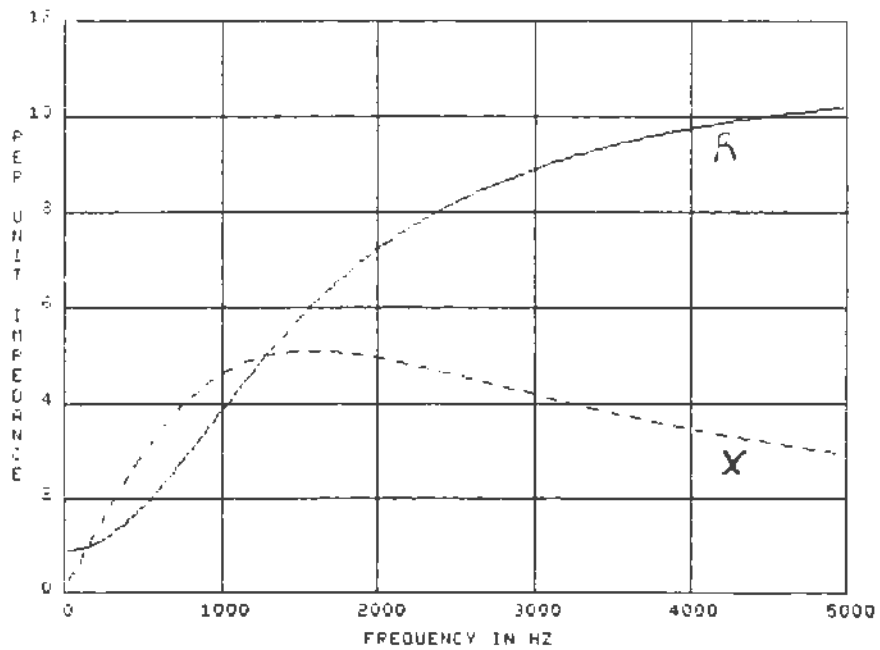


b) Parallel RL Circuit

Figure 7-5. Frequency Characteristics of Load Models



c) Series-Parallel RL Circuit



d) Parallel-Parallel RL Circuit

Figure 7-5 (cont.). Frequency Characteristics of Load Models

More detailed and accurate load models do exist, but the data required to define them is usually unavailable. The user could employ field test results to derive more detailed load models. At present, the state of knowledge is not sufficient to derive more detailed load models based solely on knowledge of the load composition.

7-4. DDUBLE-EXPONENTIAL WAVESHAVE

Impulse voltages and currents are usually defined in terms of their peak value, front time and tail time. The front time for voltage surges, for both full waveshapes and chopped-on-tail waves, is defined as 1.67 times the length of time required to increase from 30% to 90% of the peak voltage. For voltage waves chopped-on-front, the front time is defined as 2.5 times the length of time between 50% and 90% of the chopped voltage value. The front time for current surges is defined as 1.25 times the length of time required to increase from 10% to 90% of the peak current. The time to half value is defined as the time between virtual zero and the 50% magnitude point on the wave tail. The virtual zero is defined as the intersection of the line which determines front time (30-90 or 10-90) with the horizontal axis. Figure 7-6 shows a waveform with these parameters defined.

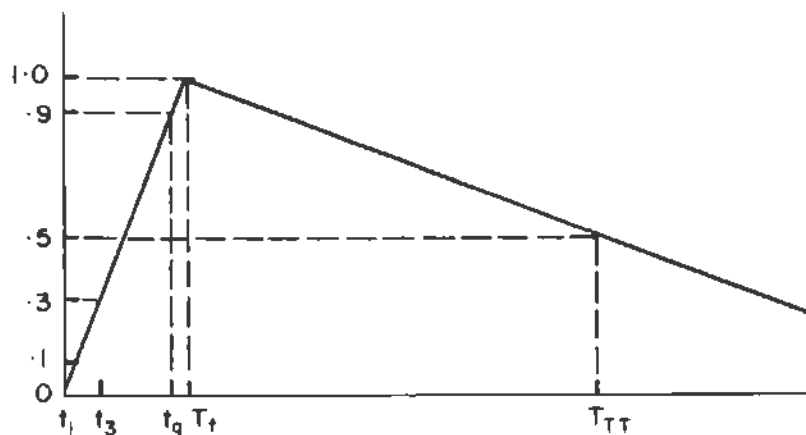


Figure 7-6. Impulse Waveshape

The wavefront and wavetail can be simulated with straight lines in the EMTP by using source Type 13. However, the discontinuous changes in slope at the peak and zero values may lead to spurious oscillations in the simulation. The double exponential source Type 15 will not cause these problems. The equation for this source is:

$$v = E (e^{-at} - e^{-bt})$$

The parameters E, a and b must be derived from the standard parameters of T_f and T_t for a one per-unit peak surge. An example of the equations for Newton-Raphson iteration for a 30-90 voltage surge follows. These nonlinear equations define a 7x7 matrix to be solved for E, a, b, B, T_t , T_3 and T_9 .

Nonlinear System:

$$T_f = 1.67 (T_9 - T_3)$$

$$0.9 = E (e^{-aT_9} - e^{-bT_9})$$

$$0.3 = E (e^{-aT_3} - e^{-bT_3})$$

$$0.5 = E (e^{-aT_t} - e^{-bT_t})$$

$$1.0 = E (e^{-B} - e^{-B(b/a)})$$

$$\ln(b/a) = B [(b/a) - 1]$$

$$T_{tt} = T_t + 0.9T_f - T_9$$

Initial Guess:

$$e^{-aT_{tt}} = 0.5$$

$$e^{-bT_f} = 0.1$$

$$E = 1.05$$

$$T_9 = 0.8T_f$$

$$T_3 = 0.2T_f$$

$$B = \ln(b/a) / [(b/a) - 1]$$

$$T_t = T_{tt}$$

The standard 1.2 x 50 microsecond lightning impulse voltage is a waveshape defined for testing purposes. For EMTP studies, the front time should have median values of 4 microseconds for the first stroke and 0.6 microseconds for subsequent strokes. The tail time should have median values of 78 microseconds

for the first stroke and 30 microseconds for subsequent strokes. A useful "average" waveshape might be 2×100 microseconds. The Type 15 parameters for this shape are

$$\begin{aligned} E &= 1.03128 \\ a &= 7266.34 \\ b &= 1499840 \end{aligned}$$

where the peak magnitude is normalized to 1.0. This waveshape is shown in Figure 7-7.

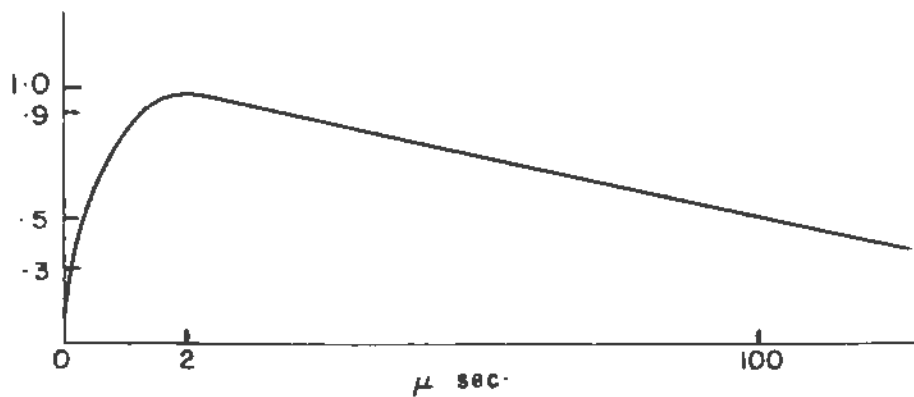


Figure 7-7. Double Exponential Representation of 2×100 Wave

Lightning stroke parameters can be assumed to follow a Log-Normal distribution. The Normal probability tables are used with this distribution, except that the reduced variate is

$$Z = \ln(x/M)/B$$

The distribution parameters are shown in Table 7-1.

Table 7-1

LIGHTNING STROKE PARAMETERS

	First Stroke		Subsequent Strokes	
	Median	Spread	Median	Spread
	M	β	M	β
30-90				
Front time [usec]	3.83	.56	.583	1.004
Tail time [usec]	77.5	.577	30.2	.933
Crest [kA] for $3 < I < 20$	61.00	1.33	12.3	.52
Crest [kA] for $I \geq 20$	33.3	.605	12.3	.52

7-5. TYPICAL SOURCE DATA

Typical source data is not as easy to define as typical data for components such as generators and transformers, which is largely determined by hardware and/or manufacturing constraints. The past growth of utility systems was governed by many different factors such as the availability of generation sites, distance from generating plants to load centers, etc. Therefore, it is difficult to define a typical source.

Several general statements can be made. At stations with local generation the zero sequence impedance is lower than the positive sequence impedance because of the delta-wye connected generator stepup transformers. At stations which are remote from generating plants the zero sequence impedance is larger than the positive sequence impedance because overhead line impedances predominate, and the X_0/X_1 ratio of a transmission line usually lies between 2 and 3.

Ranges for the phase angles of positive and zero sequence impedances at stations with and without local generation are given in Table 7-2.

Table 7-2

TYPICAL PHASE ANGLES OF SEQUENCE IMPEDANCES

<u>Positive Sequence</u>	<u>Zero Sequence</u>	
	<u>With Local Generation</u>	<u>Without Local Generation</u>
84-89°	84-89°	80-87°

The higher phase angles are associated with the stronger sources.

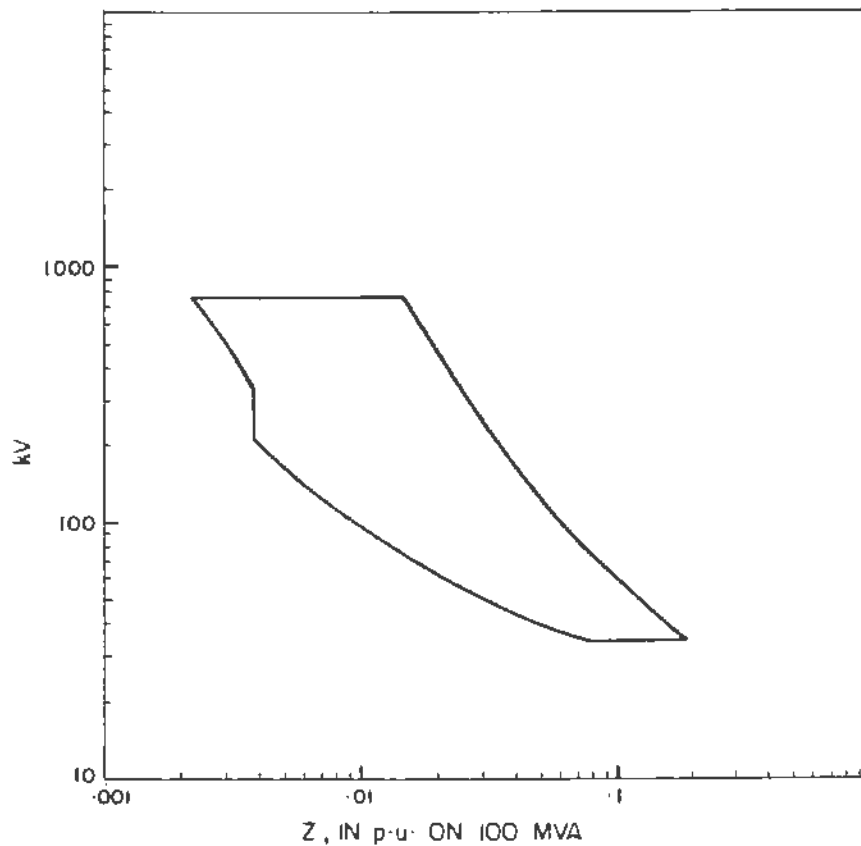


Figure 7-8. Typical Source Impedances

Figure 7-8 gives a typical range of positive sequence impedances for systems from 34.5 kV to 765 kV. The lower impedance boundary is given by the maximum interrupting ratings of circuit breakers because the short circuit capacity at a station will be less than the rated interrupting current of the circuit breakers. The upper impedance boundary was determined by assuming a typical low fault current. Substations on weak systems or very remote from generation can have larger source impedances than those given in Figure 7-8.

The source impedance at a given point changes with the amount of generation connected and therefore the source impedance for the system has to be determined or estimated for both minimum and maximum generation conditions. The ratio of Z_0/Z_1 is determined by how close the equivalent source bus is to generation.

The number of incoming lines at a station can vary significantly. In general, substations rated 345-kV or higher have fewer lines connected than stations rated 230-kV or below. At the highest voltage level in a utility the number of incoming lines per substation typically ranges between 1 and 4. At lower voltage levels the number can range from 4 to 10, or more in high load density areas. The actual number of incoming lines can be obtained from station or system one-line diagrams, which are usually readily available.

7-6. TYPICAL MACHINE IMPEDANCES

The transient characteristics of generators which are important to a study vary with the frequency range of interest, as illustrated in Table 7-3, which is based on Ardito and Santagostino's "A Review of Digital and Analog Methods of Calculation of Overvoltages in Electric Systems," Cigre SC 33 Overvoltages and Insulation Coordination Colloquium in Budapest, September 23-25, 1985.

Table 7-3
IMPORTANT GENERATOR CHARACTERISTICS

Characteristic	Frequency Band			
	.01-5kHz	3-30kHz	5kHz-3MHz	50kHz-30MHz
Constant EMF, X_d''	X	X		
d and q axis dynamics	X*			
Governor System (less than 1 Hz)	X			
Excitation System (less than 10 Hz)	X			
High-Frequency Losses	X	X		
Capacitive Coupling			X	X

* only if the generator is electrically close to the disturbance

ANSI Standard C37.011-1979 provides typical generator terminal capacitances to ground as listed Table 7-4. The numbers should be divided by three to obtain capacitance per phase. These values may be used in TRV, machine surge protection and surge transfer studies. The capacitances do not vary in proportion to generator MVA within the ranges given.

The data was obtained from a generator manufacturer and from the book, Power System Control and Stability, by Anderson and Fouad, pp. 424-450.

Table 7-5 presents typical machine parameters for steam and hydro generators. The parameters in Table 7-5 can be used directly in the Type 59 machine model.

Table 7-4
GENERATOR TERMINAL CAPACITANCE TO GROUND

Generator MVA	Total Three-Phase Winding Capacitance [Microfarads]
Steam Turbines	
Conventional Cooled	
2-pole machines	
15-30	0.17 - 0.36
30-50	0.22 - 0.44
50-70	0.27 - 0.52
70-225	0.34 - 0.87
225-275	1.49
4-pole machines	
125-225	0.94 - 1.41
Conductor-cooled (Gas)	
2-pole machines	
100-300	0.33 - 0.47
Conductor-cooled (Liquid)	
2-pole machines	
190-300	0.27 - 0.67
300-850	0.49 - 0.68
4-pole machines	
250-300	0.37 - 0.38
300-850	0.71 - 0.94
>850	1.47
Hydro Generators	
360-720 rpm, 10-30 MVA	0.26 - 0.53
85-225 rpm, 25-100 MVA	0.90 - 1.64

Table 7-5
TYPICAL GENERATOR IMPEDANCES

	Turbine Generators			
	2-POLE		4-POLE	
	Conventional Cooled	Conductor Cooled	Conventional Cooled	Conductor Cooled
X_d	1.76 1.7-1.82	1.95 1.72-2.17	1.38 1.21-1.55	1.87 1.6-2.13
X_d'	.21 .18-.23	.33 .264-.387	.26 .25-.27	.41 .35-.467
X_d''	.13 .11-.14	.28 .23-.323	.19 .184-.197	.29 .269-.32
X_q	1.66 1.63-1.69	1.93 1.71-2.14	1.35 1.17-1.52	1.82 1.56-2.07
X_q'	.245-1.12	.245-1.12	.47-1.27	.47-1.27
X_q''	.116-.332	.116-.332	.12-.308	.12-.308
T_{do}'	8.3 7.1-9.6	5.08 4.8-5.36	6.9 5.4-8.43	6.2 4.81-7.713
T_{do}''	.032-.059	.032-.059	.032-.055	.032-.055
T_{qo}'	.3-1.5	.3-1.5	.38-1.5	.38-1.5
T_{qo}''	.042-.218	.042-.218	.055-.152	.055-.152
X_o	-----0.1 to 0.7 of X_d'' -----			
X_1	.16 .118-.21	.35 .27-.42	.19 .16-.27	.35 .29-.41
R_a	.00081-.00119	.00145-.00229	.00146-.00147	.00167-.00235
H	2.5-3.5	2.5-3.5	3-4	3-4

Reactances and resistances are in per-unit.

Time constants are in seconds.

Values given are typical values, ranges of values, or both.

Older machines will generally tend to be close to the minimum values.

Notes:

- X_o varies so critically with armature winding pitch that an average value can hardly be given. Variation is from .1 to .7 of X_d'' .
- $H = (.231 WR^2 \text{ RPM}^2 \times 10^{-6}) / (\text{kVA})$, where WR^2 is in lbm-ft².

Table 7-5 (Cont'd)
TYPICAL GENERATOR IMPEDANCES

	Salient-Pole Generators		Combustion Turbines	Synchronous Condensers
	With Dampers	Without Dampers		
X_d	1 .6-1.5	1 .6-1.5	1.64-1.85	1.08-2.48
X_d'	.32 .25-.5	.32 .25-.5	.159-.225	.244-.385
X_d''	.2 .13-.32	.3 .2-.5	.102-.155	.141-.257
X_q	.6 .4-.8	.6 .4-.8	1.58-1.74	.72-1.18
X_q'	= X_q	= X_q	.306	.58-1.18
X_q''	.135-.402	.135-.402	.1	.17-.261
T_{do}'	9 4-10	9 8-10	4.61-7.5	6-16
T_{do}''	.029-.051	.029-.051	.054	.039-.058
T_{qo}'	-----	-----	1.5	.15
T_{qo}''	.033-.08	.033-.08	.107	.188-.235
X_o	-----0.1 to 0.7 of X_d'' -----			
X_1	.2 .17-.4	.2 .17-.4	.113	.0987-.146
R_a	.003-.015	.003-.015	.034	.0017-.006
H	3-7	3-7	9-12	1-2

Reactances and resistances are in per-unit.
Time constants are in seconds.
Values given are typical values, ranges of values, or both.
Older machines will generally tend to be close to the minimum values.

Notes:

1. X_o varies so critically with armature winding pitch that an average value can hardly be given. Variation is from .1 to .7 of X_d'' .
2. $H = (.231 WR^2 RPM^2 \times 10^{-6}) / (kVA)$, where WR^2 is in $lbm-ft^2$.

The bottom row in Table 7-5 contains typical H constants (rotational inertia). These values can be converted to million lbm-ft² as required by the EMTP.

$$\omega R^2 \text{ [million lbm-ft}^2\text{]} = \frac{(\text{MVA}) H}{0.000231 N^2}$$

Where MVA is the machine rating and N is the machine rated speed in rpm. The speed is 3600 for two-pole machines (fossil fuel plants) and 1800 for four-pole machines (nuclear plants). Assuming H = 3 for the 600 MVA machine used in Case 10 of the Primer, a total inertia of .6 million lbm-ft² is estimated, compared to .54 million lbm-ft² in Table 10.2 of the Primer.

The total inertia can be used in a single-mass model of the mechanical system. If shaft torques are of interest, the user must obtain a lumped mass-spring-damping model from the machine manufacturer.

For synchronous machines, the EMTP user has the choice of inputting either matrix inductances and resistances in per-unit, or the manufacturer-supplied reactances and time constants. If the manufacturer's data is used, the EMTP makes assumptions about the stator leakage inductance to derive the complete machine parameters. This assumption sometimes breaks down during iterative "parameter optimization." The EMTP user may control the data conversion process by inputting parameters in matrix form. Two methods will be described:

1. Assume the stator leakage inductance is in the d-axis power coil. This is the normal EMTP assumption whenever a 1.0 is specified on the PARAMETER FITTING card.
2. Use Olive's model. This is obtained by specifying R and L matrix parameters in the Type 59 input, or by using manufacturer's data with a 2.0 on the PARAMETER FITTING card.

Only the d-axis equations are presented below; the q-axis equations are completely analogous with the following parameter substitutions:

$$\begin{array}{l}
 X_d \leftrightarrow X_q \quad X_d' \leftrightarrow X_q' \quad X_d'' \leftrightarrow X_q'' \quad T_{do}' \leftrightarrow T_{qo}' \quad T_{do}'' \leftrightarrow T_{qo}'' \\
 X_l \text{ and } R_a \text{ are the same for both d and q axes.} \\
 L_f \leftrightarrow L_g \quad L_{kd} \leftrightarrow L_{kq} \quad L_{af} \leftrightarrow L_{ag} \quad L_{akd} \leftrightarrow L_{akq} \quad L_{fkd} \leftrightarrow L_{gkq} \\
 R_f \leftrightarrow R_g \quad R_{kd} \leftrightarrow R_{kq}
 \end{array}$$

Method 1: First test that

$$\frac{X_d X_d' + X_d' X_d'' - X_d X_d'' - X_d'^2}{X_d X_d' + X_d' X_d'' - X_d X_d'' - X_1(2X_d' - X_1)} \leq \frac{(T_{do}' - T_{do}'')^2}{(T_{do}' + T_{do}'')^2}$$

If not, then use Method 2

$$R_a = R_a \quad L_d = X_d \quad L_{af} = X_d - X_1 \quad L_f = \frac{(X_d - X_1)^2}{X_d - X_d'}$$

$$L_{akd} = L_{fkd} = L_{af}$$

$$L_{kd} = \frac{2L_{af} - L_f - (X_d - X_d'')}{1 - \frac{L_f}{L_{af}^2} (X_d - X_d'')}$$

$$TD = \frac{T_{do}' + T_{do}''}{2} - \sqrt{\frac{(T_{do}' + T_{do}'')^2}{2} - \frac{T_{do}' T_{do}''}{1 - \frac{L_{af}^2}{L_f L_{kd}}}}$$

$$R_{kd} = L_{kd} / 377TD$$

$$R_f = \frac{L_f}{377(T_{do}' + T_{do}'' - TD)}$$

Method 2:

$$R_a = R_a \quad R_f = \frac{(X_d - X_1)^2}{377(X_d - X_d')T_{do}' } \quad R_{kd} = \frac{(X_d' - X_1)^2}{377(X_d' - X_d'')T_{do}'' }$$

$$L_d = X_d$$

$$L_{af} = L_{akd} = L_{fkd} = X_d - X_1$$

$$L_f = \frac{(X_d - X_1)^2}{X_d - X_d'}$$

$$L_{kd} = X_d - \frac{X_d'(2X_1 - X_d'') - X_1^2}{X_d' - X_d''}$$

Olive's model does not assume equal mutual inductances and is simplest to input. Method 1 employs a questionable leakage inductance assumption which is not based on physical reality. The equivalent star point of the d or q axis circuit has no physical meaning, and it is erroneous to associate the leakage inductance purely with one coil. The situation is similar to that for transformer wye equivalent circuits, where the magnetizing impedance should not necessarily be connected at the star point.

The conversion of Method 1 fails if a negative argument appears under the square root. Dommel describes a modification which ensures a positive argument in the April 1980 issue of the EMTP Newsletter, but the rotor resistances and inductances are significantly affected. Ramanujam describes an improved method in the November 1982 issue of the EMTP Newsletter. In the October 1985 EMTP Newsletter, Dommel et. al. present a method of using Canay's parameter conversion in the EMTP. Canay's method is more physically correct, but has the same potential problem with a negative square root argument as Method 1 above. Canay's method can be used with either the stator leakage inductance or, in its place, a "characteristic inductance" which produces derived model time constants more in agreement with test results. In general, the choice of machine parameter calculation method will affect transient rotor quantities such as field current, but will not affect calculated initial conditions, stator currents, air gap torques or mechanical torques.

The equations may be used for machines which do not have three coils on each axis, or for which the user does not have a complete set of data. To remove one coil from either the d or q axis, set $X' = X$ and $T_0' = 0$. To remove two coils from the q axis, set $X_q'' = X_q' = X_q$ and ignore T_{q0}' and T_{q0}'' . The user may calculate the impedance matrix values or use the modified manufacturer's data with the PARAMETER FITTING option.

Manufacturer's and matrix model parameters for the IEEE Second Benchmark Model for Subsynchronous Resonance Studies are presented in Table 7-6. This 600-MVA machine is the same one used in Case 10 of the Primer. The Method 1 conversion broke down in the calculation of R_g and R_{kq} . Canay's parameter conversion as described by Dommel et. al. also broke down. Therefore, Olive's model was used (PARAMETER FITTING = 2.0).

It should be noted that Olive's method yields parameters very close to the results from both Canay's method and Method 1 and that it is amenable to hand calculations. Therefore, Olive's method is recommended. A comparison between the derived model time constants from Olive's method and Canay's method is shown in Table 7-7. Method 1 has recently been removed from the EMTP, and replaced with Canay's method.

Table 7-6

MACHINE PARAMETER CONVERSION RESULTS

Parameter	Method 1	Domme1's	Olive's	Canay's
$R_a = .0045$				
$X_l = .14$				
$T_{do}' = 4.5$				
$T_{do}'' = .04$				
$T_{qo}' = .55$				
$T_{qo}'' = .09$				
$X_d = 1.65$				
$X_d' = .25$				
$X_d'' = .20$				
$X_q = 1.59$				
$X_q' = .46$				
$X_q'' = .20$				
Parameter	Method 1	Domme1's	Olive's	Canay's
R_a	.0045	.0045	.0045	.0045
R_f	.00102	.00176	.00096	.001021
R_{kd}	.01517	.0017	.01605	.015047
R_g	fails	.02008	.00897	fails
R_{kq}	fails	.01813	.01161	fails
L_d	1.65	1.65	1.65	1.65
L_f	1.6286	1.50249	1.6286	1.6371
L_{kd}	1.6421	1.45067	1.642	1.6329
L_{af}	1.51	1.45034	1.51	1.51
L_{akd}	1.51	1.45034	1.51	1.51
L_{fkd}	1.51	1.45034	1.51	1.51
L_q	1.59	1.59	1.59	1.59
L_g	1.86062	2.42194	1.8606	fails
L_{kq}	1.52385	2.18738	1.5238	fails
L_{ag}	1.45	1.65433	1.45	fails
L_{akq}	1.45	1.65433	1.45	fails
L_{gkq}	1.45	1.65433	1.45	fails
L_o	0.14	0.14	0.14	0.14

Table 7-7

DERIVED MODEL TIME CONSTANTS

Time Constant	Olive's	Canay's
T_f	4.5	4.2521
T_D	.2714	.2879
T_g	.55	fails
T_{kq}	.3482	fails
T_d'	.6993	.6749
T_d''	.0315	.0323
T_q'	.1681	fails
T_q''	.037	fails

Part 3
STUDY GUIDE

Section 8

LINE SWITCHING

This section of the Application Guide addresses some typical power system studies which can be performed with the EMTP for transmission line design. The main emphasis of this section will be studies of switching surges generated by circuit breakers opening or closing. However, other sources of overvoltages, such as temporary overvoltages and lightning, will also be addressed. Finally, the requirements necessary for line design are combined and analyzed.

The approach in this section is twofold. First, this section presents a background to the problem and explains the situations which can occur in a power system, usually giving a simplified technique for analysis. Second, this section presents the necessary techniques to analyze the phenomena and perform the associated study using the EMTP. This section shows the input files for selected cases, but detailed explanations are not provided because the user is assumed to have acquired such expertise.

This section also includes general trends and rules of thumb which are to be expected from certain simulations. These are useful for plausibility checks of the EMTP's results.

The outline of this section is as follows:

- 8-1 Abbreviated List of References
- 8-2 Sources of Overvoltages in Power Systems
- 8-3 Quantifying the Overvoltages
- 8-4 Checklists of Data Required for Performing Overvoltage Studies
- 8-5 Switching Surge Studies
- 8-6 Line Deenergization
- 8-7 Line Energizing and Reclosing
- 8-8 Load Rejection
- 8-9 The Ferranti Effect
- 8-10 Switching Surge Impulse Design
- 8-11 NESC Design Requirements

- 8-12 Power Frequency Contamination Requirements
- 8-13 Lightning Impulse Design
- 8-14 Use of the Different Requirements for Line Design

8-1. ABBREVIATED LIST OF REFERENCES

All references used in this module are listed below.

1. CIGRE Working Group 05 (Analog and Digital Studies of Transient Electrical Phenomena) of Study Committee No. 13, "The Calculation of Switching Surges - Part I," Electra No. 19, pp. 67-122, 1971.
2. IEEE Working Group On Lightning Performance of Transmission Lines, "A Simplified Method for Estimating Lightning Performance of Transmission Lines," IEEE Transactions On Power Apparatus and Systems, Vol. PAS 104, No. 4, pp 919-932, April, 1985.
3. IEEE Working Group on Insulator Contamination, Lightning and Insulator, "Application Guide for Insulators In a Contaminated Environment," IEEE Transactions On Power Apparatus and Systems, pp. 1676-1695.
4. Hileman, A. R., "Transmission Line Insulation Coordination," The Transactions of the South African Institute of Electrical Engineers, Vol. 71, Part 6, June, 1980.
5. The General Electric Company, Transmission Line Reference Book - 345 kV and Above, Published by the Electric Power Research Institute, 1982.
6. Pignini, A, G. Sartorio, M. Moreno, M. Ramirez, R. Cortina, E. Garbagnert, A. C. Britten, and K. J. Sadurski, "Influence of Air Density on the Impulse Strength of External Insulation," IEEE Transactions On Power Apparatus and Systems, pp. 2888-2900, October, 1985.
7. Brown, G. W., "Designing EHV Lines to a Given Outage Rate Using Simplified Techniques," IEEE Transactions On Power Apparatus and Systems, pp. 379-383, March/April, 1978.
8. Taniguchi, Y, N. Arai, and Y. Imano, "Natural Contamination Test of Insulators at Nato Testing Station Near Japan Sea," IEEE Transactions On Power Apparatus and Systems, pp. 239-245, January/February, 1979.
9. Hileman, A. R., P. R. Leblanc, and G. W. Brown, "Estimating the Switching Surge Performance of Transmission Lines," IEEE Transactions On Power Apparatus and Systems, Vol. PAS-89, No. 7, pp. 1455-1469, September/October, 1970.
10. Dillard, J. K., and A. R. Hileman, "UHV Transmission Tower Insulation Tests," IEEE Transactions On Power Apparatus and Systems, pp. 1772-1784, November/December, 1970.
11. The Institute of Electrical and Electronics Engineers, National Electrical Safety Code, ANSI C2, 1984 Edition.

8-2. SOURCES OF OVERVOLTAGES IN POWER SYSTEMS

The overvoltages appearing on transmission lines can be divided into three main categories:

- a) Switching Overvoltages
- b) Lightning Overvoltages
- c) Temporary Overvoltages

8-2-1. Switching Overvoltages

Switching overvoltages, commonly referred to as SOV's, are a result of a breaker operation or a fault. Table 8-1 lists some of the common origins of SOV's.

Table 8-1
COMMON ORIGINS OF SOV'S

<u>Breaker Operation</u>	<u>Fault</u>
Line Energization and Reclosing	Fault Initiation
Line Dropping/Deenergization	Fault Clearing
Switching Capacitive Circuits (Shunt Capacitor Switching)	
Switching Inductive Circuits (Reactor and Transformer Terminated Lines)	
Low-Side Switching (Switching of Lines from the Low Side of a Transformer)	

SOV's are of concern for both phase-to-ground and phase-to-phase overvoltages. The magnitude and waveshape of the SOV's vary considerably with the system parameters and network configuration. Even for the same system parameters and network configuration, the SOV's vary considerably depending on the characteristics of the breaker and the point-on-wave where the switching operation takes place. Thus, the analysis of SOV's is best performed with a probabilistic approach. Hence, although not shown for most example cases in this section, all EMTP switching surge studies should be performed with STATISTICS runs. Input files for "single shots" for different cases are shown in this section. The input for the "probability runs" should be an easy task for the user, following the examples in Section 7 of the EMTP Primer and Section 4 of this Application Guide.

8-2-2. Lightning Overvoltages

Lightning overvoltages are caused by a lightning discharge. These overvoltages, on transmission lines, are caused by one of two phenomena:

- a) Shielding failure
- b) Backflashover of tower insulation

Shielding failures are caused by strokes to the phase conductors due to inadequate shielding of the shield wires. Backflashovers are caused by strokes to the shield wires and towers causing flashovers of line insulation. Induced lightning surges are generally of concern only for distribution lines, and will not be considered in this section.

8-2-3. Temporary Overvoltages

Temporary overvoltages, also known as sustained or dynamic overvoltages, are usually oscillatory in nature and are caused by certain system conditions. These are of relatively much longer duration than both SOV's and lightning overvoltages. Table 8-2 describes some of the causes or system conditions which cause temporary overvoltages.

Table 8-2

SOME CAUSES OF TEMPORARY OVERVOLTAGES

- Ferranti Effect
- Ferroresonance
- Sudden large changes in load
- Induced resonance on double coupled circuits
- Faults
- Operation of circuit breakers, eg., opening of shunt compensated lines

Temporary overvoltages are often sustained on transmission systems because these systems are designed to have low losses, which leads to weak damping.

8-3. QUANTIFYING THE OVERVOLTAGES

Overvoltages are usually quantified in per-unit of the maximum crest (peak) phase-to-ground voltage. This applies for both phase-to-ground and phase-to-phase overvoltages. The maximum phase-to-ground voltage is defined as follows:

$$V_{\text{base}} = \frac{\sqrt{2}}{\sqrt{3}} \times V_n \times 1.05 \quad (8-1)$$

where V_n is the nominal system voltage, e.g., 500 kV. The 1.05 factor accounts for a possible higher-than-nominal operating voltage at the instant of switching.

Some typical values of overvoltages are given in Table 8-3. These values are only listed for reference; actual values may vary considerably with different system conditions.

Table 8-3
TYPICAL MAGNITUDES OF OVERVOLTAGES

<u>Sources</u>	<u>Typical Range in PU*</u>
<u>Temporary Overvoltages:</u>	
SLG Fault - Well-Grounded System	1.3 - 1.4
SLG Fault - Ungrounded System	>1.7
Line Ringing (Shunt Compensated Line)	1.5 - 1.9
Load Rejection	1.2 - 1.6
Ferranti Effect, 100-Mile Line	1.02
200-Mile Line	1.10
300-Mile Line	1.21
500-Mile Line	1.9
Closing of a Transformer-Terminated Line	1.2 - 1.8
<u>Switching Surges</u>	
Reclosing Without Preinsertion Resistors	3 - 3.4
Reclosing With 1 Preinsertion Resistor	2 - 2.2
Reclosing With 2 Preinsertion Resistors	1.4 - 1.6
Fault Initiation - Unfaulted Phase	2.1
Fault Initiation - Coupled Circuit	1.5
Fault Clearing	1.7 - 1.9
<u>Lightning</u>	
Unshielded Line	Median 4800-6400 kV ³
Shielded Lines - 500-kV Lines	Maximum - 1500 kV ^{3,4}
- 138-kV Lines	Maximum - 1000 kV ^{3,4}
Backflashovers	I_C 50-200 kA ⁵

- Notes: * - 1 p.u. as defined in Equation 1.
 3 - Travelling voltage at struck point. Voltages at other towers will be a function of tower insulation, grounding, span lengths, corona, etc.
 4 - Based on a critical current of 10 kA for 500-kV lines and 5 kA for 138-kV lines.
 5 - Peak Lightning discharge current range which will cause backflashover of tower insulation.

8-4. CHECKLISTS OF DATA REQUIRED FOR PERFORMING OVERVOLTAGE STUDIES

In order to facilitate collection of data for switching surge studies, the following tables of data used for Transient Network Analyzer (TNA) studies are included here. The data is divided into the following parts:

- a) Data for Switched Transmission Lines..... Table 8-4
- b) Data for Transmission Lines Not to Be Switched..... Table 8-5
- c) Equivalent Sources..... Table 8-6
- d) Surge Arresters..... Table 8-7
- e) Transformers..... Table 8-8
- f) Circuit Breakers..... Table 8-9
- g) Series and Shunt Compensation..... Table 8-10

The data in Tables 8-4 through 8-10 is generally available from equipment manufacturers or utility drawings. Other sections of this Application Guide describe how to convert the data into EMTP models.

Table 8-4

DATA FOR SWITCHED TRANSMISSION LINES

1. LINE MODEL DATA --

Distance (Miles)	_____
How Many 3-Phase Circuits Per Tower	_____
Conductor: How many per phase	_____
Bundle spacing (inches)	_____
Diameter (inches)	_____
AC resistance (ohm/mile)	_____
X & Y coordinates at Tower (feet):	
Phase A	_____
Phase B	_____
Phase C	_____
Midspan sag (feet)	_____
Overhead Ground Wire: How Many	_____
Diameter (inches)	_____
AC resistance (ohm/mile)	_____

Table 8-4 (Cont'd)

DATA FOR SWITCHED TRANSMISSION LINES

X & Y coordinates at Tower (feet):	
OHGW #1	_____
OHGW #2	_____
Midspan sag (feet)	_____
Average Earth Resistivity (ohm-m)	_____
Insulators: Size	_____
How Many	_____
"V" or "I" Strings	_____
Strike Distance to Ground Under Wind Loading Conditions (feet)	_____
Average Altitude of the Line (feet or km)	_____
Total Number of Towers for the Line	_____

2. Supplemental Data for Line Design (Integration of Contamination and Lightning Performances) --

Contamination Performance/History for Subject Line, or Lines in the Neighborhood of a New Line	_____
Isokeraunic Level	_____
Tower Footing Resistance	_____
Outage Rate Statistics of the Other Lines in the Neighborhood	_____

Table 8-5
DATA FOR TRANSMISSION LINES NOT TO BE SWITCHED

Rated kV		
Length		
Positive Sequence:	R_1 (ohm/mile)	
	X_1 (ohm/mile)	
	C_1 (M Ω /mile)	
Zero Sequence:	R_0 (ohm/mile)	
	X_0 (ohm/mile)	
	C_0 (M Ω /mile)	

Table 8-6
EQUIVALENT SOURCES

<u>Substation</u>	<u>Voltage (kV)</u>	<u>Positive Sequence $Z_1 = R_1 + j X_1$</u>	<u>Zero Sequence $Z_0 = R_0 + j X_0$</u>	<u>Comments (Impedance In Ohms or % On What MVA Base)</u>

Table 8-7
SURGE ARRESTERS

<u>Substation</u>	<u>Manufacturer</u>	<u>Type ZnO or SiC</u>	<u>Rating kV</u>

Table 8-8
TRANSFORMERS

Substation: _____

Manufacturer: _____

	<u>Primary</u>	<u>Secondary</u>	<u>Tertiary</u>
Rated Voltage (kV)	_____	_____	_____
OA-Rating (MVA)	_____	_____	_____
Winding Connection	_____	_____	_____
Impedance (in % on _____ MVA base) H-L:	_____	_____	_____
H-T:	_____	_____	_____
L-T:	_____	_____	_____

Saturation Curve: I_e at 100% V _____
 I_e at 110% V _____
 I_e at 120% V _____
 I_e at 130% V _____

Air Core Impedance _____

Table 8-9
CIRCUIT BREAKERS

<u>Subst.</u>	<u>Manufacturer</u>	<u>Interrupting Medium</u>	<u>Rated Voltage (kV)</u>	<u>Rated Current (kA)</u>	<u>Preinsertion</u>		<u>Maximum Allowable Pole Span (ms)</u>
					<u>Resistor (ohm)</u>	<u>Time (ms)</u>	
_____	_____	_____	_____	_____	_____	_____	_____

Table 8-10
SERIES AND SHUNT COMPENSATION

A. SHUNT REACTORS & TERTIARY REACTORS

<u>Substation (Location)</u>	<u>Rated Voltage (kV)</u>	<u>Rated MVA</u>	<u>Linear or Nonlinear (Saturation Voltage)</u>
_____	_____	_____	_____

B. SERIES CAPACITORS

<u>Substation</u>	<u>Ohmic Value</u>	<u>Spark Gap Protection</u>	<u>Metal Oxide Protection</u>
_____	_____	_____	_____

8-5. SWITCHING SURGE STUDIES

8-5-1. Purpose of Switching Surge Studies

In the design of transmission lines, one usually thinks about switching surge design resulting in the specification of the tower strike distance (the distance from the phase conductor to the tower) and the insulator string length. Lightning overvoltages affect not only the tower insulation requirements but also the need for and placement of overhead ground wires and the need for supplemental grounding. Contamination determines the insulator string creepage distance, which may increase the insulator string length as specified by the switching surge and lightning designs. Codes like the NESC or any applicable local codes define the clearances which may further dictate the tower dimensions. Hence, at least four different factors may act to influence the design of transmission lines, and the integration of these insulation requirements is a must for reliable and conforming designs. This very important task is often referred to as transmission line insulation coordination.

Here we will identify the SOV's which appear on transmission lines, leaving the task of integrating the requirements of lightning, contamination, and NESC for later consideration.

8-5-2. Origin of Switching Surges

Switching surges differ in magnitude and shape depending on the initiating event. Typically, one speaks of three kinds of switching surges; a) those due to fault initiation; b) those due to fault clearing; and c) those due to line energization. For the same initiating event, the waveshape and magnitude of the overvoltage depend on the system parameters, the switching device characteristics, and the point on the voltage wave where switching occurs. In the past, circuit breaker design was oriented towards reducing the overvoltages caused by the arc interruption. This being successful, the overvoltages caused by energizing rather than opening became more critical. Therefore, preinsertion resistors were introduced and implemented on EHV line circuit breakers.

The events of greatest concern for switching surges on EHV and UHV systems are associated with the following:

- Line energization, with the line open-circuited at the far end, or terminated with an unloaded transformer or shunt reactor.
- Line re-energization, with trapped charge.
- Load rejection.
- Transformer switching at no load, or with inductive load.

As mentioned before, the overvoltage waveshape and magnitude depend on the time of switching, the power system parameters, and the characteristics of the switching device. The highest peak magnitudes occur only when specific conditions are met among those three variables, and are relatively rare. To design transmission lines for such overvoltages can produce a very low flashover rate at the expense of economy. It is becoming more customary in the design of EHV and UHV lines to estimate the frequency of occurrence of these overvoltages for a given system condition by using probability analysis techniques. In TNA or EMTP studies, it is more important to quantify the tail of the distribution of overvoltages, because this is directly compared to the insulation strength to determine if flashovers will occur. From this comparison, the switching surge outage rate or flashover rate is calculated.

8-5-3. Objectives of Switching Surge Studies

The objectives for a switching surge study can be summarized as follows:

- To develop switching overvoltage data necessary to determine insulation requirements (clearances and equipment BSL) for lines and stations.
- To ensure that arrester operations during switching surges do not exceed the arrester's energy dissipation capability.
- To identify an acceptable or preferred range of circuit breaker preinsertion resistor values.
- To determine preferred modes of system operation, or conversely determine any "taboo" system configuration which should be avoided.

8-5-4. Background for the Probabilistic Method of Designing Transmission Lines

Switching surge design can be based on either a deterministic approach or a probabilistic one. The deterministic approach is based on:

$$V_3 = E_m \quad (8-2)$$

where the V_3 is defined to be 3σ below the critical flashover voltage (CFO) and E_m is the maximum SOV. The CFO is defined as the voltage level at which a 50% probability of flashover exists. For SOVs, σ is approximately 5% of the CFO.

In the probabilistic approach, one calculates the switching surge flashover rate (SSFOR) by comparing the distribution of the stress (SOV) to that of the strength.

In the past, the deterministic method has been employed for virtually all of the 500-kV and 800-kV lines in the United States. An exception to this is the new generation of lines at BPA. These 500-kV BPA lines have strike distances of 2.24 m plus 0.3 m hand clearance for a total clearance of 2.54 m, compared to clearances of 3.35 to 4.0 m on other 500-kV lines which were designed using the deterministic method. The shortening of the clearances result in substantial savings in the cost of the line. Typically speaking, savings between \$45,000 to \$60,000 per one meter reduction in the strike distance per km are to be expected.

The primary reason for use of the deterministic method was twofold. First, methods to obtain the SOV distribution were not available. Second, given that the distribution could be obtained, methods to combine it with the insulation strength distribution were not available. These deterrents to a probabilistic method were rapidly overcome. SOV distributions were obtained from TNA studies. Techniques used by generation planning engineers to calculate the loss-of-load probability, or by mechanical engineers to calculate the probability of structural failure, were adapted to transmission line design. Following the mechanical engineer's jargon, the word STRESS is used to refer to the SOV distribution and the word STRENGTH is used for insulation strength.

After development of the probabilistic method, it was gradually accepted by the utility industry during the period 1970-1975. This was accomplished by presenting simplified techniques of calculation and, to a large extent, by external pressure placed on utilities to upgrade lower voltage lines, (eg., from 230 kV to 345 kV). Today, within the United States, most new high voltage lines are designed on a probabilistic basis. See Section 8-10 for a simplified method applying the probabilistic design techniques.

8-5-5. Effect of Different System Parameters On the Switching Surge Overvoltages

There are many parameters which affect the magnitude and waveshape of the SOV's obtained during any switching operation. The general effect of these parameters is best presented in Table 8-11, from Reference 1. This table gives the user an idea of what is important when gathering the data for a switching surge study, so that efforts can be directed to the areas where the influence of complete and correct data is the greatest (column 1 of Table 8-11).

8-5-5-1. Source Strength

Generally, the weaker sources result in higher overvoltages when everything else is equal. However, this does not always hold, as shown in Figure 8-1, where the statistical SOV (E_2) is plotted against the source impedance. E_2 is defined as the SOV level which has a 2% probability of being exceeded.

Table 8-11

EFFECT OF DIFFERENT PARAMETERS ON THE RESULTS
OF SWITCHING SURGE STUDIES

Parameters inherent to the network and the circuit breaker influencing the switching overvoltages.	Influence on total overvoltage factors		
	Strong	Medium	Minor
1. Line side parameters			
● Positive and zero sequence inductance, capacitance, and resistance of the line		X	X
● Frequency dependence of the above line parameters		X	X
● Line length	X		
● Degree of parallel compensation	X		
● Degree of series compensation		X	X
● Line termination (open or transformer terminated)	X	X	
● Presence and degree of trapped charge on the line without preinsertion resistors	X		
● Presence and degree of trapped charge on the line with preinsertion resistors		X	X
● Corona effects			X
● Saturation of shunt line reactors		X	
● Damping of shunt line reactors			X
2. Circuit Breaker Parameters			
● Maximum pole span of contacts		X	
● Dielectric characteristics during closing			X
● Presence of preinsertion resistors	X		
● Value (s) of preinsertion resistor (s)	X	X	
● Insertion time of preinsertion resistors		X	X
● Phase angles at instants of switching	X		

Table 8-11 (Cont'd)

EFFECT OF DIFFERENT PARAMETERS ON THE RESULTS OF SWITCHING SURGE STUDIES

Parameters inherent to the network and the circuit breaker influencing the switching overvoltages.	Influence on total overvoltage factors		
	Strong	Medium	Minor
3. Supply side parameters			
● Service voltage			X
● Service frequency			X
● Total short-circuit MVA	X	X	
● Frequency dependent damping factors of transformers and generators			X
● Inductive or "complex" network		X	X
● Lines parallel to switched line			X
● Ratio of positive to zero sequence impedance			X

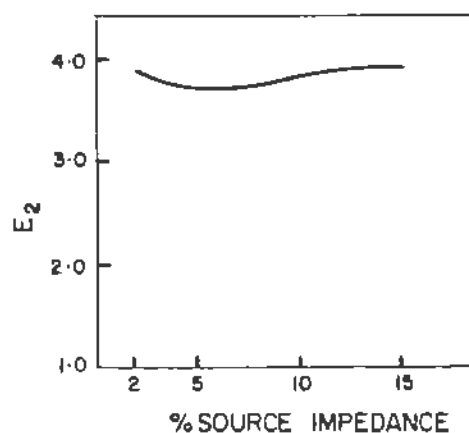


Figure 8-1. Variation of the Statistical Overvoltage, E_2 , With Source Impedance for a Given System. ($X_1 = X_0$ is assumed.)

8-5-5-2. Shunt Reactors

Reactors for shunt compensation normally tend to reduce the SOV magnitude. The amount of surge reduction is small compared to the reduction due to preinsertion resistors and surge arresters. The larger the reactor size at the receiving end, the larger the reduction in SOVs.

8-5-5-3. Transformer Characteristics

In general, the saturation characteristics of transformers have a relatively minor effect on the magnitude of SOVs. However, the effect should be modeled for transformers in the switching substations. Potential dynamic overvoltages may be discovered during the simulated switching operations. The effect of transformer saturation is more pronounced for temporary overvoltages, and an accurate model is necessary for these studies. For lightning studies, transformer saturation models are not necessary at all.

Tertiary windings tend to reduce the SOVs, primarily by supplying a path for the zero sequence currents.

8-5-5-4. Surge Arresters

Surge arresters can be effective in reducing the maximum overvoltages along the switched lines. In reality, surge arresters alter the tail of the SOV distribution, which is the most important part of the distribution because it is the portion compared to the insulation strength in the probabilistic design approach. The limitation of arresters is their "reach." If line-end arresters are used, their effectiveness in reducing the overvoltages in the middle of the line is limited. The maximum overvoltage on a switched line with line-end arresters usually appears somewhere between the middle of the line and the 3/4 point. This effect is shown in Figure 8-2 for a typical 500-kV line.

8-5-5-5. Circuit Breaker Pole Span

The pole span of the circuit breaker is defined as the elapsed time between the first and last poles to close. In general, broader pole spans result in higher overvoltage magnitudes, as shown in Figure 8-3. One possible explanation would be that the wider the pole span, the more independently the poles behave and the

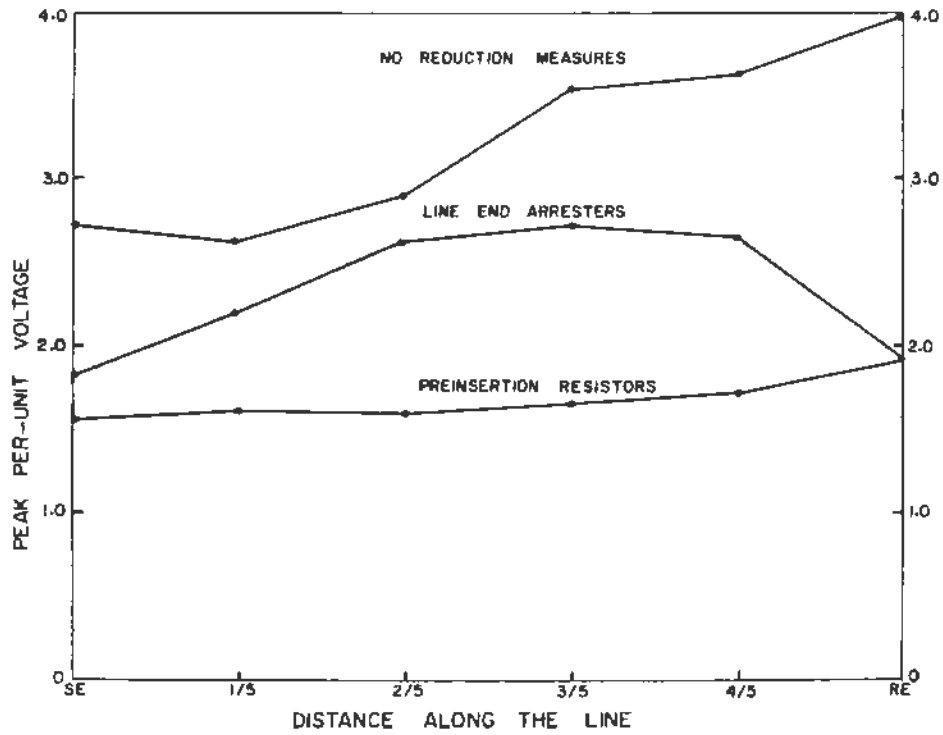


Figure 8-2. Effect of Line End Arresters On Reducing the Maximum SOV's Along a 500-kV Line

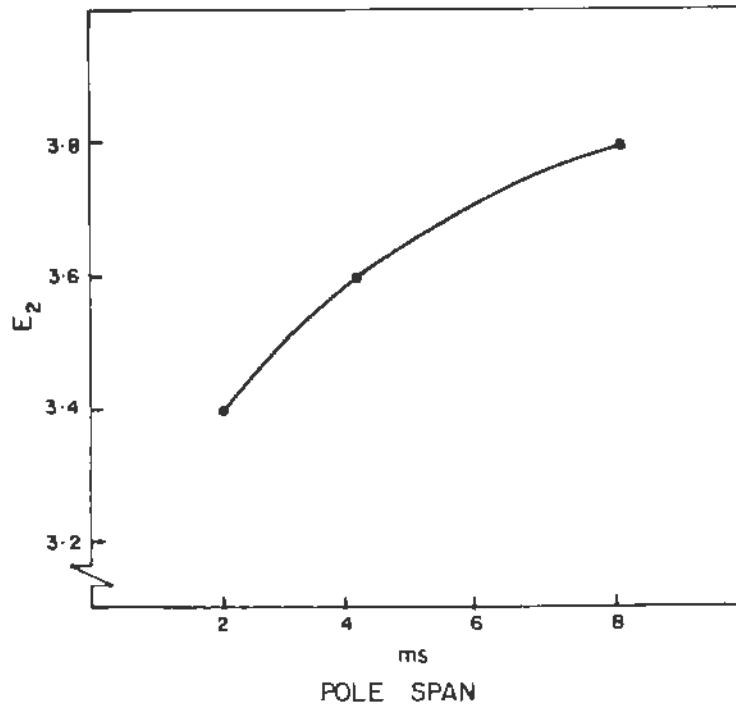


Figure 8-3. Variation of E_2 with Pole Span

more likely that one pole will close at or near the peak source voltage. Figure 8-3 shows the variation of E_2 with three different pole spans, everything else remaining constant.

8-5-5-6. Time of Insertion of the Preinsertion Resistor

It can be shown that shorting the preinsertion resistor before the initial reclosing surge has returned from the receiving end of the line results in the same peak overvoltage as if there were no resistor. For this reason, the insertion time is chosen to be between 7-10 ms. Seven ms is equivalent to the round trip travel time on a 1000-km (600-mile) line, or two round trips on a 500-km (300-mile) line.

8-5-6. Outputs of Interest In Conducting a Switching Surge Study

The outputs shown in Table 8-12 are considered of major importance when conducting switching surge studies. Hence, the user should request them when setting up the input data for the EMTP cases to be studied.

Table 8-12

REQUIRED OUTPUTS FOR CONDUCTING A SWITCHING SURGE STUDY

- Line-to-ground and line-to-line voltages (Phases A, B, and C) on the switched line for:
 - Sending end
 - Receiving end
 - Middle point
 - At least two other points along the line
- Surge arrester voltages, currents, and energy. Most new versions of the EMTP can calculate the energy absorbed in branches by a request of "4" in column 80. This can be applied to surge arresters. There are, however, problems which have been encountered with the energy as calculated by the EMTP this way (negative energy has been witnessed in some cases, and problems with plotting). Hence, an alternative way to calculate energy through TACS is presented later.
- Line currents for the switched line.

As mentioned before, SOV studies usually involve probability runs. Histograms for phase-to-ground and phase-to-phase voltages at different points along the switched line should be requested.

8-5-6-1. TACS Data for Energy Calculation Block

Table 8-13 shows the TACS cards needed for logic to calculate the energy for any branch element connected between nodes "8A" and "9A," as shown in Figure 8-4. Note that for each element, a measuring switch is needed to measure the current into the branch. The branch current, along with the branch voltage, will define the power and the energy consumed by the branch. Either node can be grounded to represent a grounded branch.

8-5-6-2. Special Application of the TACS Energy Calculator Block

The block for calculating the energy described above can be used in some series capacitor studies, where a bypass gap is fired to short the metal oxide voltage limiter and the capacitor bank (see Figure 8-5), if the energy dissipated by the metal oxide exceeds a certain limit. In this case, the energy from the TACS Block 58 is fed into a level-triggered TACS switch, Device Code 52. The output of Device 52 is then used to trigger a TACS-controlled switch (Type 11) in the electrical network.

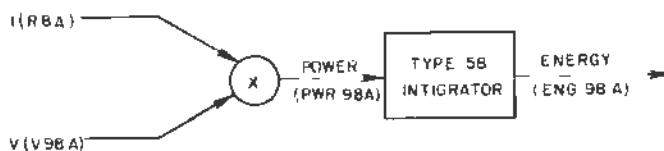


Figure 8-4. TACS Logic for Calculating Energy Dissipated In the Branch Element Between 8A and 9A

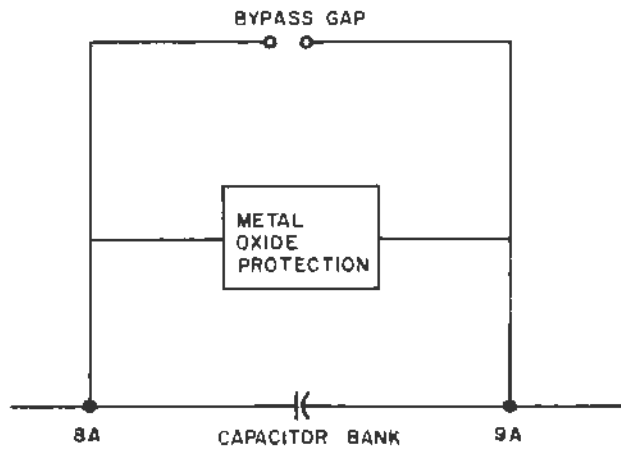


Figure 8-5A. Series Capacitor Bank and Its Protection Scheme

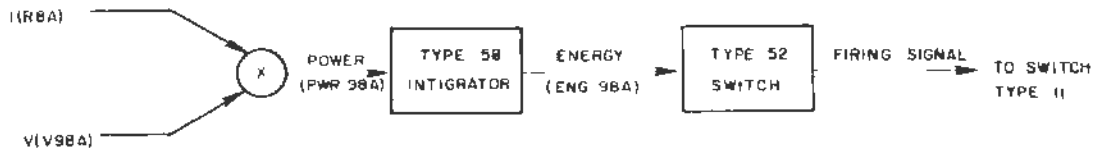


Figure 8-5B. Logic for Firing the Protective Gap Across the Series Capacitor Bank and Its Metal Oxide Protection

Table 8-13

TACS INPUT DATA FOR CALCULATING ENERGY

```

C FILE NAME: "L500ARR-E": SIMULATE RECLOSING OF THE 120 MILE LINE.
C
C TRAPPED CHARGE IS ASSUMED ON THE LINE ARRESTER ENERGIES ARE MONITORED
C THROUGH TACS
C
BEGIN NEW DATA CASE
ABSOLUTE TACS DIMENSIONS
      30      30      50      40      100      100      100      40      50      10
      40      60      200     1000     20
C FIRST MISCELLANEOUS DATA CARD.
C 34567890123456789012345678901234567890123456789012345678901234567890
C   1-8   9-16  17-24  25-32
C T-STEP T-MAX X-OPT C-OPT
C SECONDS SECONDS O=MH O=UF
C F(HZ) F(HZ)
33.30E-7 07 60. 0
C
C SECOND MISCELLANEOUS DATA CARD
C   1-8   9-16  17-24  25-32  33-40  41-48  49-56  57-64  65-72  73-80
C PRINT PLOT NETWORK PR. SS PR. MAX I PUN PUNCH DUMP MULT. DIAGNDS
C O=EACH O=EACH O= NO O= NO O= NO O= NO O= NO INTO NENERG PRINT
C K=K-TH K=K-TH 1=YES 1=YES 1=YES 1=YES 1=YES DISK STUDIES O=NO
      25000      9      1      1      1      1      1      1      000
C
C TACS HYBRID
C ***** TACS SIMULTANEOUS FUNCTION BLOCKS *****
C
C NAME INPUT SIGNAL NAMES GAIN LIMITS
C (3-8) (12-17,20-25,28-33,36-41,44-49) (51-56) (57-62,63-68,69-74,75-80)
C 1 2 3 4 5 6 7
C 3456789012345678901234567890123456789012345678901234567890123456789
C THESE SIX CARDS ARE USED TO DERIVE ARRESTER BRANCH VOLTAGES BY FINDING THE
C DIFFERENCE OF THE TWO TERMINAL VOLTAGES. IN THIS CASE, ONE TERMINAL VOLTAGE
C FOR EACH ARRESTER IS ZERO.
99VRECA -RECA
99VRECB -RECB
99VRECC -RECC
99VSNDA -SENDA
99VSNDB -SENDB
99VSNDC -SENDC
BLANK CARD ENDING TACS FUNCTIONS
C
C ***** TACS SOURCES *****
C
C TYPE NAME AMPLITUDE FREQ. OR T ANGLE OR WIDTH T-START T-STOP
C (3-8) (11-20) (21-30) (31-40) (61-70) (71-80)
C 1 2 3 4 5 6 7
C 3456789012345678901234567890123456789012345678901234567890123456789
C 90= VOLTAGE SOURCE
C 91= CURRENT SOURCE
C VOLTAGE SOURCE CAN BE ANY NODE VOLTAGE OF THE ELECTRICAL SYSTEM
C CURRENT SOURCE IS THE CURRENT FROM NODE X TO NODE Y OF A MEASURING
C SWITCH BETWEEN NODES X AND Y, IN THAT DRDR
C
C THESE SOURCES REPRESENT THE ARRESTER VOLTAGES AND CURRENTS
90RECA
90RECB
90RECC
90SENDA
90SENDB
90SENDC
91SENDMA
91SENDMB

```

Table 8-13 (Cont'd)

TACS INPUT DATA FOR CALCULATING ENERGY

```

91SENDMC
91RECMA
91RECMB
91RECMC
BLANK CARD ENDING TACS SOURCES
C ***** TACS SEQUENTIAL FUNCTIONS AND DEVICES *****
C TYPES: 98=OUTPUT GROUP
C        99=INPUT GROUP
C        88=INSIDE GROUP
C
C ONLY TYPE 98 WILL BE USED HERE
C
C TYPE NAME CODE INPUT SIGNAL NAMES
C (1-2) (3-8) (9-10) (11-17,20-25,28-33,26-41,44-49)
C NUMERICAL PARAMETERS
C (51-56,57-62,63-68,69-74,75-80)
C
C OR, A FREE-FORMAT FORTRAN MATHEMATICAL EXPRESSION, IF COL 11 HAS '='
C TYPE NAME = EXPRESSION
C (1-2) (3-8) (11) (12-80)
C 1 2 3 4 5 6 7
C 3456789012345678901234567890123456789012345678901234567890123456789
C CALCULATION OF POWER CONSUMED, POWER=VOLTAGE*CURRENT
98PWRECA =VPECA*RECMA
98PWRECB =VRECB*RECMB
98PWRECC =VRECC*RECMC
98PWSNA =VSNA*SENDMA
98PWSNB =VSNB*SENDMB
98PWSNC =VSNDC*SENDMC
C
C CALCULATION OF ENERGY CONSUMED = INTEGRAL OF THE POWER
C
C USE DEVICE 58 WITH THE TIME OF SIMULATION, TIMEX, AS THE CONTROL VARIABLE
C 1 2 3 4 5 6 7
C 3456789012345678901234567890123456789012345678901234567890123456789
98ENGRCA58+PWRECA 1 TIMEX
98ENGRCB58+PWRECB 1 TIMEX
98ENGRCC58+PWRECC 1 TIMEX
98ENGSNA58+PWSNA 1 TIMEX
98ENGSNB58+PWSNB 1 TIMEX
98ENGSNC58+PWSNC 1 TIMEX
BLANK CARD ENDING TACS DEVICES
C TACS OUTPUT VARIABLE REQUESTS
C NAMES
C (3-8,9-14, . . .,75-80)
C
C 3456789012345678901234567890123456789012345678901234567890123456789
ENGRCAENGRCBENGRCC
ENGSNAENGSNBENGSNC
PWRECA
PWRECB
PWRECC
PWSNA
PWSNB
PWSNC
BLANK CARD ENDING TACS OUTPUT REQUESTS
C INITIAL CONDITIONS FOR TACS VARIABLES
C NAME INITIAL VALUE
C 3-8 11-20
C NO NEED TO DEFINE ANY INITIAL CONDITIONS FOR THIS CASE
C SINCE ENERGY SHOULD BUILD UP FROM ZERO
BLANK CARD ENDING TACS INITIAL CONDITIONS
C THIS ALSO TERMINATES TACS INPUT
C *****
C ***** ELECTRICAL SYSTEM INPUT DATA *****
C BRANCHES

```

Table 8-13 (Cont'd)

TACS INPUT DATA FOR CALCULATING ENERGY

```

C LINE-END ARRESTERS 396-KV MCOV
C NODE CONNECTIONS INPUTTED WITH DUMMY CHARACTERISTICS HERE
C 5555. CODE REFERS TO ACTUAL CHARACTERISTICS LOCATED
C BEFORE NODE VOLTAGE OUTPUT REQUESTS
C
C *****
92RECMA          5555
   -1.          -1.
   1.           1
   9999.
92RECMB          RECMA          5555.
92RECMC          RECMA          5555.
92SENDMA         RECMA          5555.
92SENDMB         RECMA          5555.
92SENDMC         RECMA          5555.
C *****

```

BLANK CARD TERMINATING BRANCH CARDS

```

C SWITCH CARDS
C      1      2      3      4      5      6      7
C 345678901234567890123456789012345678901234567890123456789
C MEASURING SWITCHES NEEDED TO TRANSFER CURRENTS TO TACS
C FOR THE ENERGY CALCULATION
C RECEIVING END ARRESTER CURRENTS
  RECMA RECA          MEASURING          1
  RECMB RECB          MEASURING          1
  RECMC RECC          MEASURING          1
C SENDING END ARRESTER CURRENTS
  SENDMA SENDA        MEASURING          1
  SENDMB SENDB        MEASURING          1
  SENDMC SENDC        MEASURING          1
C BREAKERS
  B500 ASEDA          .0322316          1.0
  B500 BSENB          .0312096          1.0
  B500 CSENC          .0331682          1.0
BLANK CARD TERMINATING SWITCH CARDS

```

BLANK CARD TERMINATING NODE VOLTAGE OUTPUT

```

C CALCOMP PLOT      2
C (CASE TITLE UP TO 78 CHARACTERS)
2 RECLOSING WITH LINE-END ARRESTERS
C THE FOLLOWING IS FORMAT OF THE PLOT REQUEST CARDS
C COLUMN 2,        "1"
C COLUMN 3,        4=NODE VOLTAGE
C                      8=BRANCH VOLTAGE
C                      9=BRANCH CURRENT
C COLUMN 4,        UNITS OF HORIZONTAL SCALE  1=DEGREES
C                      2=CYCLES
C                      3=SEC
C                      4=MSEC
C                      5=USEC
C COLUMNS 5-7     HORIZONTAL SCALE (UNITS PER INCH)
C COLUMNS 11-15   TIME WHERE PLOT ENDS
C COLUMNS 16-20   VALUE OF BOTTOM VERTICAL SCALE
C COLUMNS 21-24   VALUE OF TOP VERTICAL SCALE
C COLUMNS 25-48   UP TO FOUR NODE NAMES
C COLUMNS 49-64   GRAPH HEADING LABEL
C COLUMNS 65-80   VERTICAL AXIS LABEL
1445.0  70.0      RECA RECB RECC
1445.0  70.0      SENDA SENDB SENOC
1945.0  70.0      TACS ENGRCA
1945.0  70.0      TACS ENGRCB
1945.0  70.0      TACS ENGRCC
1945.0  70.0      TACS ENGSNA
1945.0  70.0      TACS ENGSNB
1945.0  70.0      TACS ENGSNC
BLANK CARD TERMINATING PLOTTED OUTPUT
BLANK CARD TERMINATING THE CASE

```

8.5.7. General Assumptions for Switching Surge Studies

The following assumptions are usually made when performing switching surge studies:

- The pre-switching voltage at the switched bus is set to the maximum system operating voltage (1.05 per-unit of the nominal system voltage).
- For energization cases, it is assumed that no trapped charge exists on the line.
- For reclosing cases, the amount of trapped charge on each phase is determined by the sequence of opening of the circuit breakers, and whether a fault was present on the line prior to opening.
- The reactances of the turbine generators (T-G) are assumed constant during the simulation and equal to X_d'' , the subtransient reactance.
- The switched line is to be represented with a model reflecting the best available data. Lines at the same voltage level and emanating from the same stations as that of the switched lines should also be represented in as much detail as possible, computer storage requirements permitting. Other lines in the system can be lumped together and represented by their positive and zero sequence equivalents.

8-6. LINE DEENERGIZATION

In the past, circuit breakers were designed to reduce the switching overvoltages caused by the interruption process. With the introduction of higher voltages and longer lines, the limiting of the SOV's due to energization and reclosing became more critical. While these newer concerns will be addressed later, the initial concern of line deenergization will be considered now, since it does present some interesting practical problems for shunt compensated lines.

8-6-1. Deenergization of Uncompensated Lines

When the last circuit breaker on an uncompensated line opens, it is switching a capacitive load. Since circuit breakers clear at or very close to current zero, the voltage would be at a maximum, trapping 1.0 per-unit charge on the line.

Figure 8-6 shows the trapped DC voltage on the line following the opening of the circuit breakers at the sending end. No inductive path to ground through a transformer or shunt reactor was assumed to exist. This DC voltage will eventually decay as the trapped charge bleeds off the line across the line insulators.

8-6-2. Deenergization of Shunt Compensated Lines

If an inductive path to ground is available, the charge trapped on the line will attempt to discharge through this path, setting up an oscillation between the line capacitance and the discharge path inductance. The natural frequency of this oscillation, for a transposed line, is determined by $1/2\pi\sqrt{LC}$, where L is the inductance of the transformer or shunt reactor plus the line inductance, and C is the capacitance of the line.

This phenomena is usually referred to as "ring down" or "ringing" of the line. The ringing of untransposed lines is more complicated than described above, because the phase imbalances, together with the presence of multi-modal propagation, produce a multi-frequency waveform.

Figure 8-7 shows the ring down on a transposed line and an untransposed line. Table 8-14 shows the setup for the transposed line case. Table 8-15 shows the setup for the untransposed case. The circuit used for these two cases is shown in Figure 8-8.

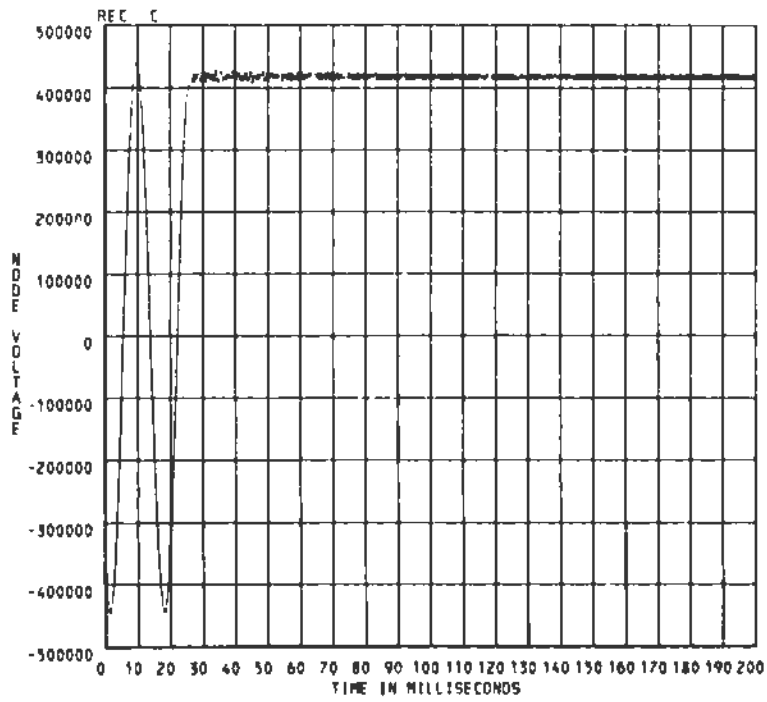


Figure 8-6. Deenergization of An Uncompensated 500-kV Line

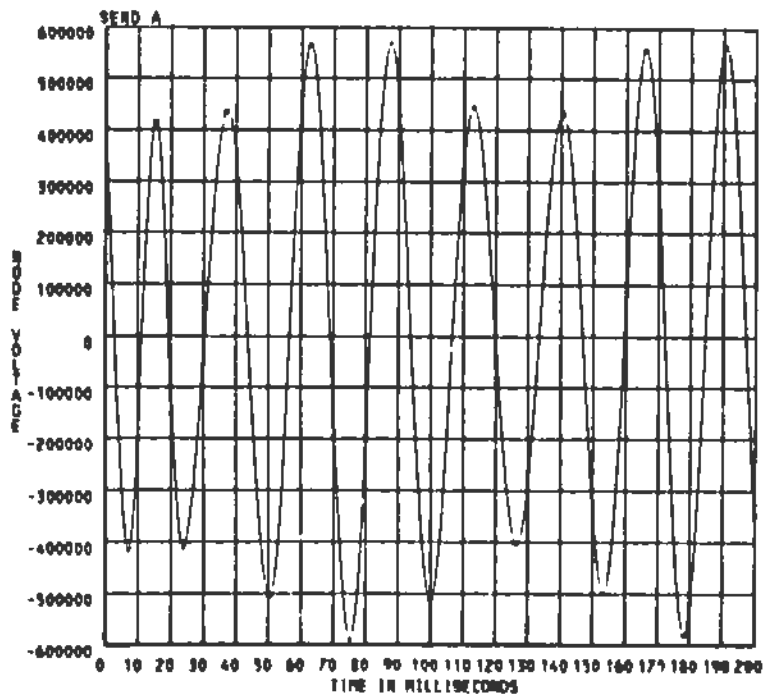


Figure 8-7a. Ringing On Transposed Line - Phase A Sending End Voltage

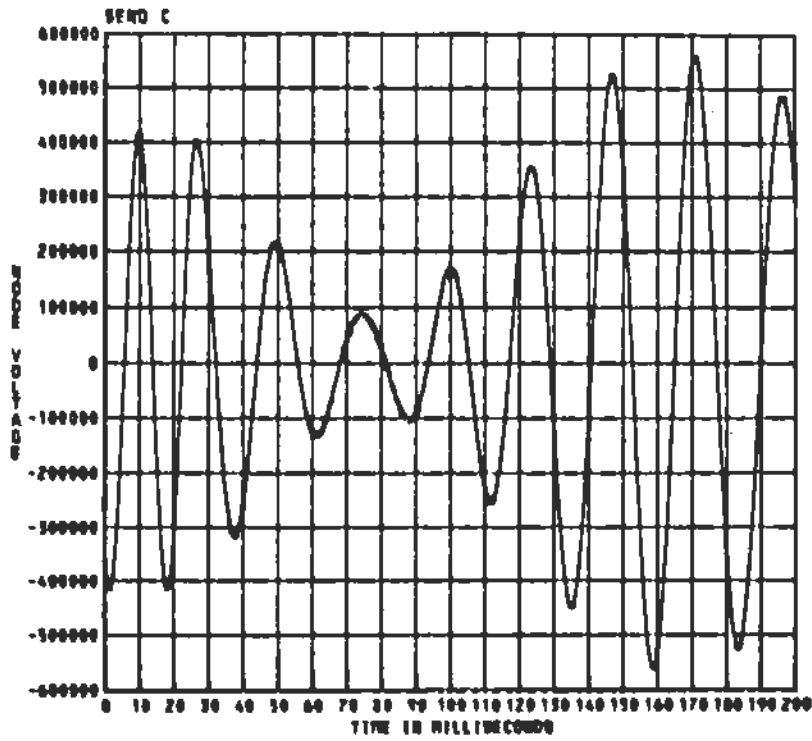
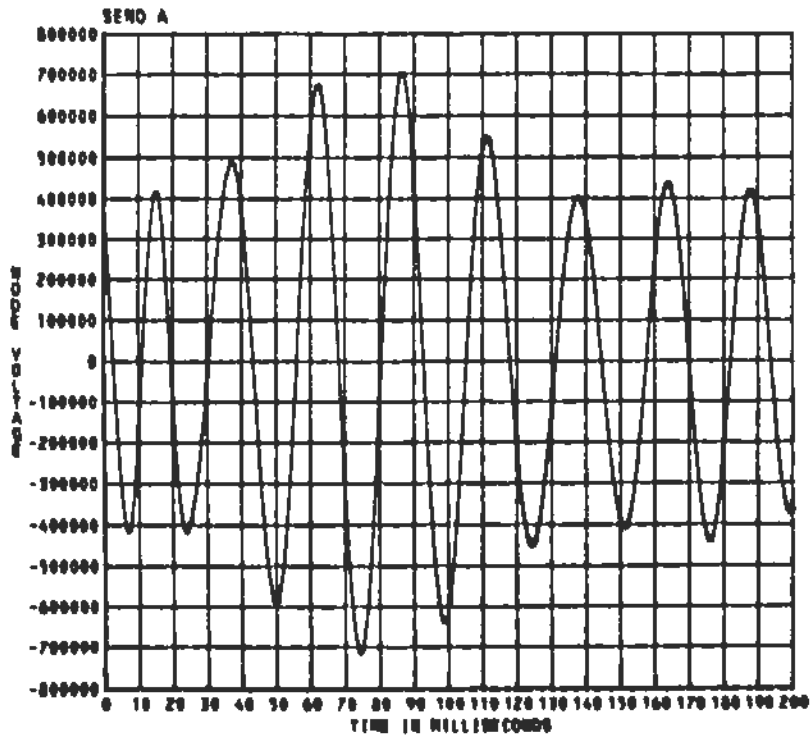


Figure 8-7b. Ringing On an Untransposed Line - Phase A and C Sending End Voltages

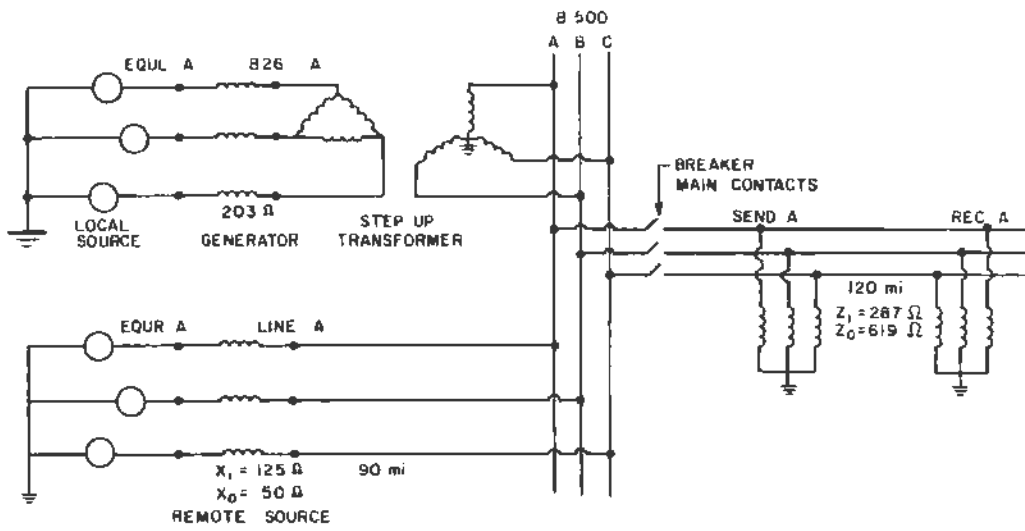


Figure 8-8. Circuit used for Ring Down Cases

Table 8-14

INPUT FOR THE DEENERGIZATION OF A TRANSDPOSED LINE

```

C FILE NAME: "LEOORING-T" DEENERGIZING A TRANSMISSION LINE WITH SHUNT REACTORS
C THE BREAKER OPENS AFTER .02 SEC. THE AUXILIARY SWITCH IS TAKEN OUT. THIS
C RUN WILL SHOW RINGING ON A 120 MILE LINE AFTER BREAKERS AT THE SENDING
C END OPEN. A TRANSDPOSED LINE MODEL IS USED.
BEGIN NEW DATA CASE
C FIRST MISCELLANEOUS DATA CARD
C 34567890123456789012345678901234567890123456789012345678901234567890
C   1-8   9-16  17-24  25-32
C T-STEP T-MAX  A-DPT  C-DPT
C SECNDS SECONDS  O=MH  O=UF
C                               F(HZ)  F(HZ)
33.30E-6      .20      60      0
C
C SECOND MISCELLANEOUS DATA CARD
C   1-8   9-16  17-24  25-32  33-40  41-48  49-56  57-64  65-72  73-80
C PRINT  PLOT NETWORK  PR SS  PR.MAK  I PUN  PUNCH  DUMP  MULT.  DIAGNOS
C O=EACH O=EACH  O= NO  O= NO  O= YES  O= NO  O= NO  INTO  NENERG  PRINT
C K=K-TH K=K-TH  1=YES  1=YES  1=YES  1=YES  1=YES  DISK  STUDIES  O=NO
C 20000      1      1      1      1      1      0      0      1      0
C BRANCHES
C                               27-32  33-38  39-44
C                               R      L      C
C
C SHUNT REACTORS- 50 MVAR AT EACH END OF THE LINE
C   1      2      3      4      5      6      7
C 3456789012345678901234567890123456789012345678901234567890123456789
SEND A                               5512.
SEND B                               5512.
SEND C                               5512.
REC A                               5512.
REC B                               5512.
REC C                               5512.
C LOCAL SOURCE (GENERATOR)
B26 AEQUL A                          203
B26 BEQUL B                          203
B26 CEDUL C                          203
C
C
C REMOTE SOURCE (MUTUALLY COUPLED)
C 3456789012345678901234567890123456789012345
C                               SEQUENCE VALUES
C                               27-32  33-44
C                               R      L (FIRST ZERO, THEN POS. SEQUENCE)
51LINE AEQUR A                          50.
52LINE BEQUR B                          125
53LINE CEQUR C
C
C TRANSMISSION LINES
C 3456789012345678901234567890123456789012345678901234567890
C                               27-32  33-38  39-44  45-50  CODE IN COLUMN "52"
C                               R      L      C      LE  (LE=LENGTH)
C                               (ZERO, POSITIVE SEQUENCE)
-1B500 ALINE A                          .55801 6722 01268 90 0
-2B500 BLINE B                          0310 .5816 01940 90 0
-3B500 CLINE C
C 120 MILE LINE, FLAT CONFIGURATION
C 3456789012345678901234567890123456789012345678901234567890
-1SEND AREC A                          .5294 1.7659 01224 120 0
-2SEND BREC B                          .02499 .59614 01914 120. 0
-3SEND CREC C
C
C TRANSFORMER
C 345678901234567890123456789012345678901234567890
C   3-13  15-20  27-32  33-38  39-44  45-50
C REQUESTWORD  BUS      I  FLUX  BUS R-MAG
C TRANSFORMER      2.33  1137      X  3.E5
C
C   1-16      17-32
C CURRENT      FLUX
C   2 33      1137.0
C   5 44      1250 0
C  23 33      1364 0
C 1579 00      2274 0
C 9999

```

Table 8-14 (Cont'd)

INPUT FOR THE DEENERGIZATION OF A TRANSPOSED LINE

```

C TRANSFORMER WINDINGS
C COLUMN 1,2: WINDING NUMBER
C 345678901234567890123456789012345678901234567890
C   3-8 9-14          27-32 33-38 39-44
C  BUS1  BUS2          R-K   L-K  TURNS
18500 A          27 55 11 66
2826  AB26  B          2026   1
  TRANSFORMER      X          Y
18500 B
2826  BB26  C          2
  TRANSFORMER      /          2
18500 C
2826  CB26  A
BLANK CARD TERMINATING BRANCH CARDS
C
C SWITCH CARDS
C 3456789012345678901234567890123456789012345678901234567890
C   3-8 9-14 15-24 25-34 35-44 45-54 55-64 65-74
C                                     (OUTPUT OPTION IN COLUMN 80)
C   NODE NAMES          IE FLASHOVER   SPECIAL REFERENCE
C                   OR VOLTAGE   REQUEST SWITCH-NAME
C  BUS1  BUS2          CLOSE  OPEN  NSTEP          WORD  BUS5  BUS6
  B500 ASEND A          -1      .020
  B500 BSEND B          -1      .020
  B500 CSEND C          -1      .020
BLANK CARD TERMINATING SWITCH CARDS
C SOURCE CARDS
C 3456789012345678901234567890123456789012345678901234567890
C COLUMN 1,2: TYPE OF SOURCE 1 - 17. (E.G. 11-13 ARE RAMP FUNCTIONS, 14 = COSINE)
C COLUMN 9,10: 0=VOLTAGE SOURCE, -1=CURRENT SOURCE
C   3-8 11-20 21-30 31-40 41-50 51-60 61-70 71-80
C   NODE  AMPLITUDE FREQUENCY TO IN SEC  AMPL-A1  TIME-T1  T-START  T-STOP
C   NAME          IN HZ          DEGR          SECONDS  SECONDS  SECONDS
14EQUL A          18863.  60.0  0          -1.0
14EQUL B          18863.  60.0 -120.         -1.0
14EQUL C          18863.  60.0 -240.         -1.0
C REMOTE SOURCE
14EQUR A          380281  60.0  30          -1.0
14EQUR B          380281  60.0 -90          -1.0
14EQUR C          380281  60.0 -210         -1.0
C
BLANK CARD TERMINATING SOURCE CARDS
C NODE VOLTAGE OUTPUT
C 34567890123456789012345678901234567890
  B500 AB500 BB500 CSEND ASEND BSEND CREC AREC BREC C
BLANK CARD TERMINATING NODE VOLTAGE OUTPUT
C PLOTTING CARDS
CALCOMP PLOT          2
C (CASE TITLE UP TO 78 CHARACTERS)
2 SINGLE-PHASE FAULT CLEARING
C THE FOLLOWING IS FORMAT OF THE PLOT REQUEST CARDS
C COLUMN 2,  "1"
C COLUMN 3,  4=NODE VOLTAGE
C                   8=BRANCH VOLTAGE
C                   9=BRANCH CURRENT
C COLUMN 4,  UNITS OF HORIZONTAL SCALE  1=DEGREES
C                                           2=CYCLES
C                                           3=SEC
C                                           4=MSEC
C                                           5=USEC
C COLUMNS 5-7  HORIZONTAL SCALE (UNITS PER INCH)
C COLUMNS 8-11 TIME WHERE PLOT STARTS
C COLUMNS 12-15 TIME WHERE PLOT ENDS
C COLUMNS 16-20 VALUE OF BOTTOM VERTICAL SCALE
C COLUMNS 21-24 VALUE OF TOP VERTICAL SCALE
C COLUMNS 25-48 UP TO FOUR NODE NAMES
C COLUMNS 49-64 GRAPH HEADING LABEL
C COLUMNS 65-80 VERTICAL AXIS LABEL
14J B  80.          REC AREC BREC C
14A B  80.          SEND ASEND BSEND C
BLANK CARD TERMINATING PLOT REQUESTS
BLANK CARD TERMINATING THE CASE

```

Table 8-15

INPUT FOR THE DEENERGIZATION OF AN UNTRANSPOSED LINE

```

C FILE NAME: "L500RING-N" DEENERGIZING A TRANSMISSION LINE WITH SHUNT REACTORS
C BREAKER OPENS AFTER .02 SEC. THE AUXILIARY SWITCH IS TAKEN OUT. THIS
C RUN WILL SHOW RINGING ON 120 MILE LINE AFTER BREAKERS AT THE
C SENDING END OPEN. A NONTRANSPOSED LINE MODEL IS USED.
BEGIN NEW DATA CASE
C FIRST MISCELLANEOUS DATA CARD:
C 34567890123456789012345678901234567890123456789012345678901234567890
C   1-8   9-16  17-24  25-32
C T-STEP  T-MAX  X-OPT  C-OPT
C SECNDS  SECONDS  O=MH  O=UF
C          F(HZ)   F(HZ)
C 33 30E-6      .20    60.    0
C
C SECOND MISCELLANEOUS DATA CARD
C   1-8   9-16  17-24  25-32  33-40  41-48  49-56  57-64  65-72  73-80
C PRINT  PLOT  NETWORK  PR.SS  PR.MAX  I.PUN  PUNCH  DUMP  MULT.  DIAGNOS
C O=EACH  O=EACH  O=NO  O=NO  O=NO  O=NO  O=NO  INTO  NENERG  PRINT
C K=K-TH  K=K-TH  1=YES  1=YES  1=YES  1=YES  1=YES  DISK  STUDIES  O=NO
C 20000      1      1      1      1      1      0      0      1      0
C BRANCHES
C          27-32  33-38  39-44
C          R      L      C
C
C SHUNT REACTORS- 50 MVAR AT EACH END OF THE LINE BETWEEN SEND-REC
C   1      2      3      4      5      6      7
C 3456789012345678901234567890123456789012345678901234567890123456789
SEND A          5512.
SEND B          5512.
SEND C          5512.
REC A           5512.
REC B           5512.
REC C           5512.
C LOCAL SOURCE (GENERATOR)
B26 AEQUL A          203
B26 BEQUL B          203
B26 CEQUL C          203
C
C REMOTE SOURCE (MUTUALLY COUPLED)
C 3456789012345678901234567890123456789012345
C          SEQUENCE VALUES
C          27-32  33-44
C          R      L (FIRST ZERO, THEN PDS. SEQUENCE)
51LINE AEQUR A          50
52LINE BEQUR B          125.
53LINE CEQUR C
C
C TRANSMISSION LINES
C 345678901234567890123456789012345678901234567890
C          27-32  33-38  39-44  45-50  CODE IN COLUMN "52"
C          R      L      C      LE (LE=LENGTH)
C          (ZERO, POSITIVE SEQUENCE)
-16500 ALINE A          55801 6722 01268 90. 0
-28500 BLINE B          0310 5816 01940 90. 0
-38500 CLINE C
C 120 MILE LINE, FLAT CONFIGURATION
C *****+*****
C
C          DISTRIBUTED PARAMETER UNTRANSPOSED LINE MODEL
C          ( K C LEE MODEL )
C
C 3456789012345678901234567890123456789012345678901234567890
C
C          27-32  33-38  39-44  45-50

```

Table 8-15 (Cont'd)

INPUT FOR THE DEENERGIZATION OF AN UNTRANSPOSED LINE

```

C
C MODAL MODAL MODAL LENGTH
C RES. SURGE VEL
C IMP
-1SEND AREC A .5254 620.871307E4 120. 1 3
-2SEND BREC B .0254 313.991815E4 120. 1 3
-3SEND CREC C .0245 262.731837E4 120. 1 3
C
C TI MATRIX FOR NONTRANSPOSED LINES
C
C 1 2 3 4 5 6 7
C 3456789012345678901234567890123456789012345678901234567890123456789
C
C TI K,1 TI K,2 TI K,3 TI K,4 TI K,5 TI K,6
C ALTERNATE ROWS FOR REAL AND IMAGINARY ELEMENTS
.59603 -.70711 -.41119
-.72864 E-3 -.85711 E-13-.43098 E-3
.53803 .11268 E-12 81353
-.32930 E-2 .16625 E-12 .31168 E-2
.59603 .70711 -.41119
-.7286 E-3 -.77099 E-13-.43098 E-3
C
C TRANSFORMER
C 345678901234567890123456789012345678901234567890
C 3-13 15-20 27-32 33-38 39-44 45-50
C REQUESTWORD BUS I FLUX BUS R-MAG
C TRANSFORMER 2.33 1137. X 3.E5
C
C 1-16 17-32
C CURRENT FLUX
C 2.33 1137.0
C 5.44 1250.0
C 23.33 1364.0
C 1579.00 2274.0
C 9999
C TRANSFORMER WINDINGS
C COLUMN 1,2: WINDING NUMBER
C 345678901234567890123456789012345678901234567890
C 3-8 9-14 27-32 33-38 39-44
C BUS1 BUS2 R-K L-K TURNS
1B500 A 27.55 11 66
2B26 AB26 B .2026 1
TRANSFORMER X Y
1B500 B
2B26 BB26 C
TRANSFORMER Y Z
1B500 C
2B26 CB26 A
C
C BLANK CARD TERMINATING BRANCH CARDS
C
C SWITCH CARDS
C 34567890123456789012345678901234567890123456789012345678901234567890
C 3-8 9-14 15-24 25-34 35-44 45-54 55-64 65-74
C (OUTPUT OPTION IN COLUMN 80)
C NODE NAMES IE FLASHOVER SPECIAL REFERENCE
C OR VOLTAGE REQUEST SWITCH-NAME
C BUS1 BUS2 TIME TO TIME TO NSTEP WORD BUS5 BUS6
C CLOSE OPEN
B500 ASEND A -1 .020
B500 BSEND B -1 .020
B500 CSEND C -1 .020
C
C BLANK CARD TERMINATING SWITCH CARDS
C
C SOURCE CARDS
C 34567890123456789012345678901234567890123456789012345678901234567890
C COLUMN 1,2: TYPE OF SOURCE 1 - 17, (E G 11-13 ARE RAMP FUNCTIONS, 14 = COSINE)
C COLUMN 3,10 0-VOLTAGE SOURCE, -1-CURRENT SOURCE
C 3-8 11-20 21-30 31-40 41-50 51-60 61-70 71-80

```

Table 8-15 (Cont'd)

INPUT FOR THE DEENERGIZATION OF AN UNTRANSPOSED LINE

C	NODE	AMPLITUDE	FREQUENCY	TO IN SEC	AMPL-A1	TIME-T1	T-START	T-STOP
C	NAME		IN HZ	DEGR		SECONDS	SECONDS	SECONDS
14EQUL	A	18863.	60.0	0.			-1.0	
14EQUL	B	18863.	60.0	-120.			-1.0	
14EQUL	C	18863.	60.0	-240.			-1.0	
C REMOTE SOURCE								
14EQUR	A	380281.	60.0	30.			-1.0	
14EQUR	B	380281.	60.0	-90.			-1.0	
14EQUR	C	380281.	60.0	-210.			-1.0	
C								
BLANK CARD TERMINATING SOURCE CARDS								
C NODE VOLTAGE OUTPUT								
C 34567890123456789012345678901234567890								
B500 AB500 BB500 CSEND ASEND BSEND CREC AREC BREC C								
BLANK CARD TERMINATING NODE VOLTAGE OUTPUT								
C PLOTTING CARDS								
CALCOMP PLOT 2								
C (CASE TITLE UP TO 78 CHARACTERS)								
2 SINGLE-PHASE FAULT CLEARING								
C THE FOLLOWING IS FORMAT OF THE PLOT REQUEST CARDS								
C COLUMN 2, "1"								
C COLUMN 3, 4=NODE VOLTAGE								
C 8=BRANCH VOLTAGE								
C 9=BRANCH CURRENT								
C COLUMN 4, UNITS OF HORIZONTAL SCALE 1=DEGREES								
C 2=CYCLES								
C 3=SEC								
C 4=MSEC								
C 5=USEC								
C COLUMNS 5-7 HORIZONTAL SCALE (UNITS PER INCH)								
C COLUMNS 8-11 TIME WHERE PLOT STARTS								
C COLUMNS 12-15 TIME WHERE PLOT ENDS								
C COLUMNS 16-20 VALUE OF BOTTOM VERTICAL SCALE								
C COLUMNS 21-24 VALUE OF TOP VERTICAL SCALE								
C COLUMNS 25-48 UP TO FOUR NODE NAMES								
C COLUMNS 49-64 GRAPH HEADING LABEL								
C COLUMNS 65-80 VERTICAL AXIS LABEL								
144 B 80 REC AREC BREC C								
144 B 80 SEND ASEND BSEND C								
BLANK CARD TERMINATING PLOT REQUESTS								
BLANK CARD TERMINATING THE CASE								

8-6-3. Deenergization of Transformer-Terminated Lines

8-6-3-1 Deenergization From the High-Voltage Side

In the case of a transformer-terminated line, the inductance of the circuit to ground is essentially the very large magnetizing impedance. Thus, the natural frequency of this line is very low compared to the shunt reactor compensated lines. This results in saturation of the transformer, which then discharges the line in a few square-wave shaped oscillations.

Figure 8-9 shows the sending end and receiving end voltages of a transformer-terminated transposed 500-kV line. A saturable transformer model has been used for this case. The input data for this run is shown in Table 8-16. The schematic for the studied system is shown in Figure 8-10.

Figure 8-12 shows the receiving end voltage when deenergizing the 230-kV transmission line depicted in Figure 8-11. Here, however, a Type 98 nonlinear inductor was used to represent the transformer. Table 8-17 shows the input data for this case.

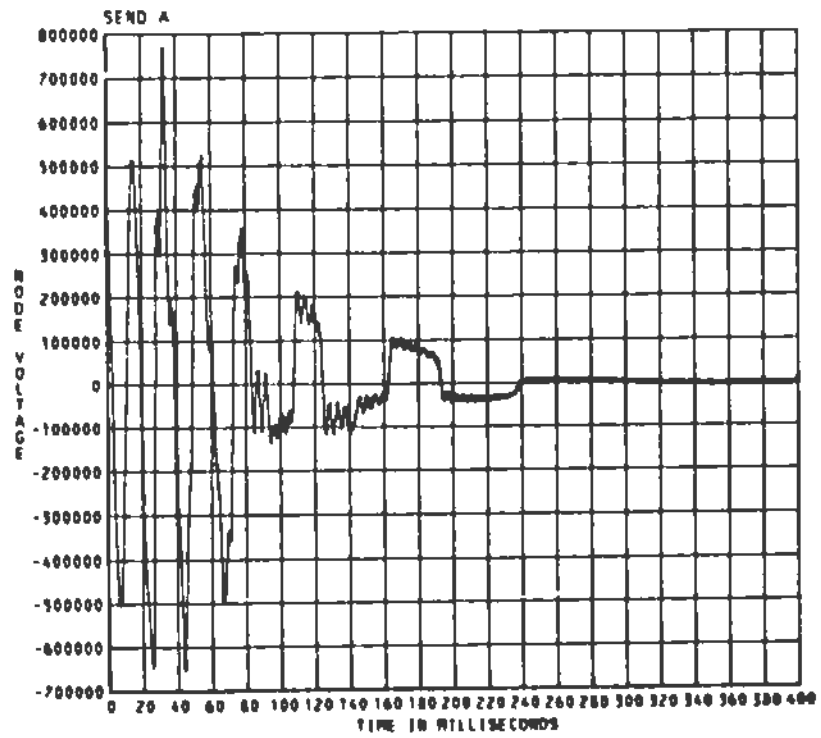
Studying Figures 8-9 and 8-12, one concludes that if a transformer-terminated line is deenergized, the trapped charge decays very rapidly. Hence, for all reclosing cases of transformer-terminated lines, the trapped charge is assumed to be zero.

8-6-3-2 Note On Low-Side Switching

Low-side switching involves switching the line from the low side of a stepup transformer. This is sometimes done in the initial stages of system development when lines of a higher voltage level are added to the system. This would save or defer the cost of a circuit breaker at the higher voltage level.

On deenergization, the transformer remains in the circuit, which means that the line will discharge through the transformer before reclosing, as demonstrated above, unless shunt reactors are used. Because the trapped charge on the line in this case is essentially zero at reclosing, the SOV's are generally lower than for high-side switching.

Sending End
Voltage



Receiving End
Voltage

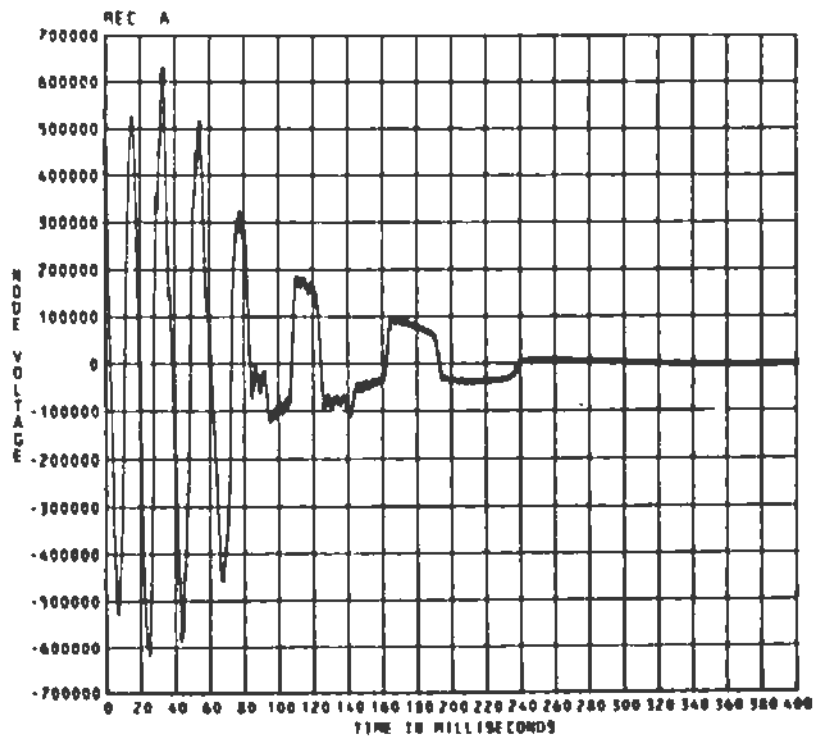


Figure 8-9. Sending End and Receiving End Voltages for a Transformer-Terminated Transposed Line

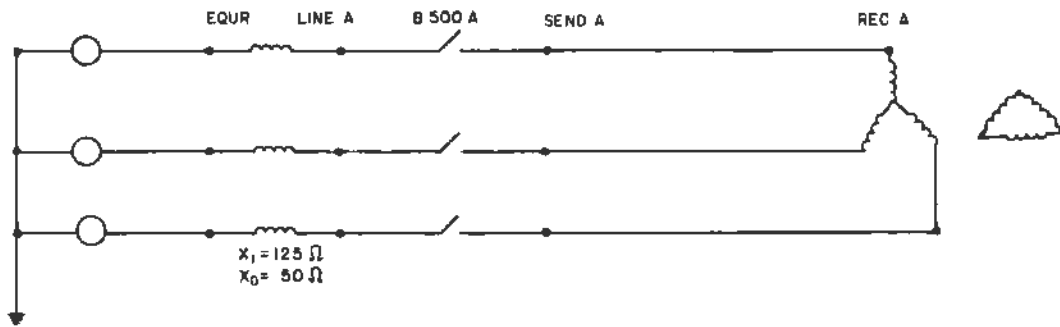


Figure 8-10. Schematic of System Used for the Case of Deenergization of a Transformer-Terminated Line

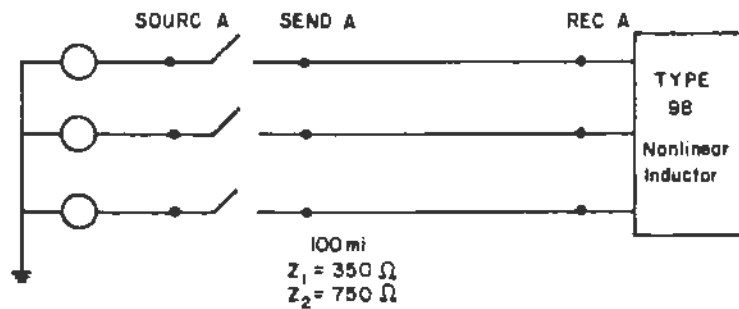


Figure 8-11. Schematic of System Used for Deenergizing a 230-kV Transformer-Terminated Line

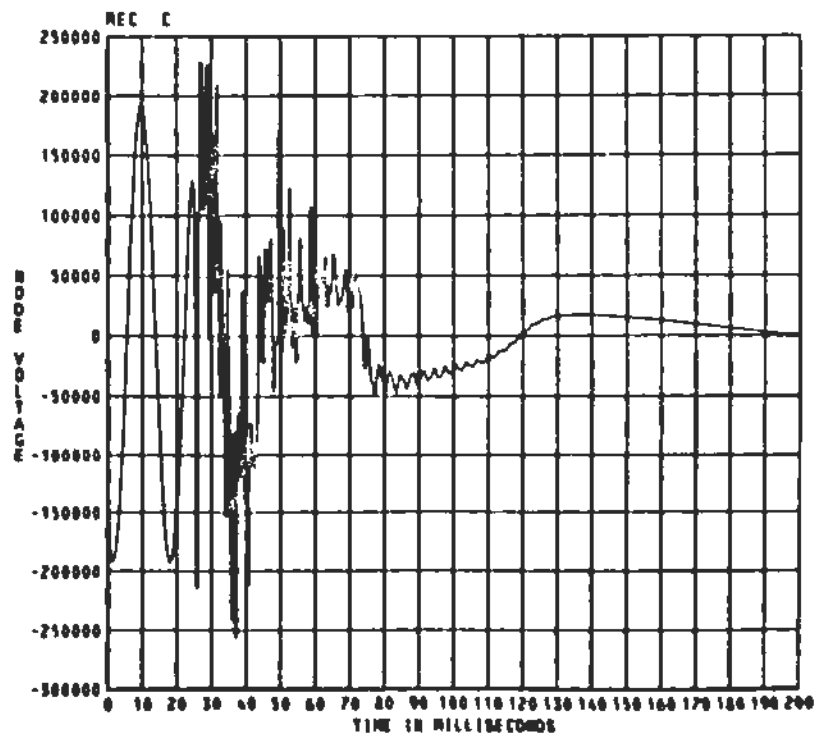


Figure 8-12. Receiving End Voltage When Deenergizing the 100-Mile 230-kV Line.

Table 8-16

INPUT FOR DEENERGIZATION OF A TRANSFORMER-TERMINATED LINE

```

C FILE NAME: "L500XFR-0", DEENERGIZING A 500-KV TRANSFORMER-TERMINATED LINE
C BREAKER OPENS AFTER .02 SEC. THE AUXILIARY SWITCH IS TAKEN OUT.
C
C
C A TRANPOSED LINE IS ASSUMED
BEGIN NEW DATA CASE
C FIRST MISCELLANEOUS DATA CARD:
C 34567890123456789012345678901234567890123456789012345678901234567890
C   1-8   9-16  17-24  25-32
C T-STEP T-MAX X-OPT C-OPT
C SECNDS SECONDS O=MH O=UF
C           F(HZ)  F(HZ)
66.60E-6   .40   60.   0
C
C SECOND MISCELLANEOUS DATA CARD
C   1-8   9-16  17-24  25-32  33-40  41-48  49-56  57-64  65-72  73-80
C PRINT  PLOT NETWORK PR SS PR MAX I PUN PUNCH DUMP MULT DIAGNOS
C O=EACH O=EACH O=ND O=NO O=NO O=NO O=NO INTO NENERG PRINT
C K=K-TH K=K-TH 1=YES 1=YES 1=YES 1=YES 1=YES DISK STUDIES O=NO
C 2000 1 1 1 1 1 0 1 0
C REMOTE SOURCE (MUTUALLY COUPLED)
C 3456789012345678901234567890123456789012345
C           SEQUENCE VALUES
C           27-32 33-44
C           R L (FIRST ZERO, THEN POS. SEQUENCE)
51LINE A FOUR A 50.
52LINE BEOUR B 125.
53LINE CEOUR C
C
C TRANSMISSION LINES
C 345678901234567890123456789012345678901234567890
C           27-32 33-38 39-44 45-50 CODE IN COLUMN "52"
C           R L C LE (LE=LENGTH)
C           (ZERO, POSITIVE SEQUENCE)
-18500 ALINE A 55801.6722 0.1268 90. 0
-28500 BLINE B .0310 .5816 0.1940 90. 0
-38500 CLINE C
C
C
C
C 120 MILE LINE, FLAT CONFIGURATION
C 34567890123456789012345678901234567890123456789012345678901234567890
-1SEND APEC A .5294 1.7659 0.1224 120. 0
-2SEND BREC B .02499 .59614 .01914 120. 0
-3SEND CREC C
C
C TRANSFORMER
C 345678901234567890123456789012345678901234567890
C   3-13 15-20 27-32 33-38 39-44 45-50
C REQUESTWORD BUS I FLUX BUS R-MAG
C TRANSFORMER 2 33 1137 X 3 E4
C   1-16 17-32
C CURRENT FLUX
C   2 33 1137.0
C   5.44 1250.0
C   23.33 1364.0
C   1579.00 2274.0
C 9999
C TRANSFORMER WINDINGS
C COLUMN 1,2: WINDING NUMBER
C 345678901234567890123456789012345678901234567890
C   3-8 9-14 27-32 33-38 39-44
C BUS1 BUS2 P-K L-K TURNS
1REC A 5 27 55 11.66

```

Table 8-16 (Cont'd)

INPUT FOR DEENERGIZATION OF A TRANSFORMER-TERMINATED LINE

```

2B26 AB26 B          004 .2026 1.
TRANSFORMER        y          Y
1REC B
2B26 BB26 C
TRANSFORMER        x          Z
1REC C
2B26 CB26 A
C      1          2          3          4          5          6          7
C 3456789012345678901234567890123456789012345678901234567890123456789
C ADDED CAPACITANCE TO AVOID FLOATING DELTA WINDING
  B26 A          003
  B26 B          003
  B26 C          003
BLANK CARD TERMINATING BRANCH CARDS
C
C SWITCH CARDS
C 34567890123456789012345678901234567890123456789012345678901234567890
C   3-8  9-14    15-24    25-34    35-44    45-54    55-64    65-74
C                                     (OUTPUT OPTION IN COLUMN 80)
C   NODE NAMES                          IE FLASHOVER SPECIAL REFERENCE
C   TIME TO CLOSE      TIME TO OPEN      OR VOLTAGE REQUEST SWITCH-NAME
C   BUS1  BUS2          NSTEP              WORD  BUSS  BUSS
  B500 ASEND A          -1.      .020
  B500 BSEND B          -1.      .020
  B500 CSEND C          -1.      .020
BLANK CARD TERMINATING SWITCH CARDS
C SOURCE CARDS
C 34567890123456789012345678901234567890123456789012345678901234567890
C COLUMN 1,2: TYPE OF SOURCE 1 - 17.(E.G. 11-13 ARE RAMP FUNCTIONS, 14 = COSINE)
C COLUMN 9,10: 0=VOLTAGE SOURCE, -1=CURRENT SOURCE
C   3-8    11-20    21-30    31-40    41-50    51-60    61-70    71-80
C   NAME    AMPLITUDE FREQUENCY TD IN SEC  AMPL-A1  TIME-T1  T-START  T-STOP
C   NAME          TN HZ      DEGR          SECONDS  SECONDS  SECONDS
  14EQUR A      380281.    60.0      30.      -1.0
  14EQUR B      380281.    60.0     -90.      -1.0
  14EQUR C      380281.    60.0    -210.      -1.0
C
BLANK CARD TERMINATING SOURCE CARDS
C NODE VOLTAGE OUTPUT
C 34567890123456789012345678901234567890
  B500 AB500 BB500 CSEND ASEND BSEND CREC AREC BREC C
BLANK CARD TERMINATING NODE VOLTAGE OUTPUT
C PLOTTING CARDS
  CALCOMP PLOT          2
C (CASE TITLE UP TO 78 CHARACTERS)
  2 DEENERGIZING A 500-KV TRANSFORMER-TERMINATED LINE
C THE FOLLOWING IS FORMAT OF THE PLOT REQUEST CARDS
C COLUMN 2,          "1"
C COLUMN 3,          4=NODE VOLTAGE
C                      8=BRANCH VOLTAGE
C                      9=BRANCH CURRENT
C COLUMN 4,          UNITS OF HORIZONTAL SCALE  1=DEGREES
C                      2=CYCLES
C                      3=SEC
C                      4=MSEC
C                      5=USEC
C COLUMNS 5-7      HORIZONTAL SCALE (UNITS PER INCH)
C COLUMNS 8-11     TIME WHERE PLOT STARTS
C COLUMNS 12-15    TIME WHERE PLOT ENDS
C COLUMNS 16-20    VALUE OF BOTTOM VERTICAL SCALE
C COLUMNS 21-24    VALUE OF TOP VERTICAL SCALE
C COLUMNS 25-48    UP TO FOUR NODE NAMES
C COLUMNS 49-64    GRAPH HEADING LABEL
C COLUMNS 65-80    VERTICAL AXIS LABEL
  144 B.  80          REC AREC BREC C
  144 B.  80          SEND ASEND BSEND C
BLANK CARD TERMINATING PLOT REQUESTS
BLANK CARD TERMINATING THE CASE

```

Table 8-17

INPUT DATA DEENERGIZING THE 230-kV
TRANSFORMER-TERMINATED LINE

```

C FILE NAME: "L230*FR" DEENERGIZING A 230-KV TRANSFORMER-TERMINATED LINE
C BREAKER OPENS AFTER .02 SEC
C
C
C A TRANSPOSED LINE IS ASSUMED
BEGIN NEW DATA CASE
C FIRST MISCELLANEOUS DATA CARD
C 34567890123456789012345678901234567890123456789012345678901234567890
C   1-8   9-16  17-24  25-32
C T-STEP T-MAX X-OPT C-OPT
C SECONDS SECONDS O=MH O=UF
C           F(HZ)   F(HZ)
66.60E-6   20     60.     0
C
C SECOND MISCELLANEOUS DATA CARD
C   1-8   9-16  17-24  25-32  33-40  41-48  49-56  57-64  65-72  73-80
C PRINT  PLOT NETWORK PR. SS PR MAX I PUN PUNCH DUMP MULT DIAGNOS
C O=EACH O=EACH O= NO O= NO O= NO O= NO O= NO INTO NENERG PRINT
C K=K-TH K=K-TH 1=YES 1=YES 1=YES 1=YES 1=YES DISK STUDIES O=NO
20000    9      1      1      1      1      0      0      1      0
C
C
C 100 MILE TRANSPOSED LINE
C 3456789012345678901234567890123456789012345678901234567890
C   1      2      3      4      5      6      7
C 3456789012345678901234567890123456789012345678901234567890
-1SEND AREC A           5   750.  1.35E5 100.  1
-2SEND BREC B           03  350.  1.76E5 100.  1
-3SEND CREC C
C
C TRANSFORMER
C TYPE 98 PSEUDO-NONLINEAR INDUCTANCE IS USED FOR THIS ILLUSTRATION
C   1      2      3      4      5      6      7
C 3456789012345678901234567890123456789012345678901234567890
C           I-SS FLUX-SS
98REC A           56  300.
C           1-16  17-32
C           CURRENT FLUX
56           300.
93           400.
1 3           450.
1 8           500.
3           550.
4 9           580.
8.5           600.
13           610.
28 8           620.
55.6           624.
750           628
          9999
C   1      2      3      4      5      6      7
C 3456789012345678901234567890123456789012345678901234567890
98REC B REC A           56  300.
98REC C REC A           56  300
C CORE RESISTANCES
C
REC A           3. E4
REC B           3. E4
REC C           3 E4
BLANK CARD TERMINATING BRANCH CARDS
C
C SWITCH CARDS
C 3456789012345678901234567890123456789012345678901234567890
C   3-8   9-14  15-24  25-34  35-44  45-54  55-64  65-74
C                                     (OUTPUT OPTION IN COLUMN 80)
C NODE NAMES                                     IF FLASHOVER SPECIAL REFERENCE

```

Table 8-17 (Cont'd)

INPUT DATA FOR DEENERGIZING THE 230-kV
TRANSFORMER-TERMINATED LINE

```

C          TIME TO   TIME TO   OR   VOLTAGE   REQUEST SWITCH-NAME
C  BUS1  BUS2   CLOSE   OPEN   NSTEP          WORD  BUS5  BUS6
C  SOURCE SEND A   -1.    .020
C  SOURCE SEND B   -1.    .020
C  SOURCE SEND C   -1.    .020
BLANK CARD TERMINATING SWITCH CARDS
C SOURCE CARDS
C 34567890123456789012345678901234567890123456789012345678901234567890
C COLUMN 1,2: TYPE OF SOURCE 1 - 17, (E.G. 11-13 ARE RAMP FUNCTIONS, 14 = COSINE)
C COLUMN 9,10: 0=VOLTAGE SOURCE, -1=CURRENT SOURCE
C   3-8   11-20   21-30   31-40   41-50   51-60   61-70   71-80
C  NODE  AMPLITUDE FREQUENCY TO IN SEC  AMPL-A1  TIME-T1  T-START  T-STOP
C  NAME  IN HZ      DEGR
C 14SDURCA 188000.  60.0  30.
C 14SOURCB 188000.  60.0  -90.
C 14SOURCC 188000.  60.0  -210.
C
BLANK CARD TERMINATING SOURCE CARDS
C NODE VOLTAGE OUTPUT
C 34567890123456789012345678901234567890
C SOURCE SEND A SEND B SEND C  AREC  BREC  C
BLANK CARD TERMINATING NODE VOLTAGE OUTPUT
C PLOTTING CARDS
C CALCOMP PLDT 2
C (CASE TITLE UP TO 78 CHARACTERS)
2 DEENERGIZING A 230-KV TRANSFORMER-TERMINATED LINE
C THE FOLLOWING IS FORMAT OF THE PLDT REQUEST CARDS
C COLUMN 2, "1"
C COLUMN 3, 4=NODE VOLTAGE
C 8=BRANCH VOLTAGE
C 9=BRANCH CURRENT
C COLUMN 4, UNITS OF HORIZONTAL SCALE 1=DEGREES
C 2=CYCLES
C 3=SEC
C 4=MSEC
C 5=USEC
C COLUMNS 5-7 HORIZONTAL SCALE (UNITS PER INCH)
C COLUMNS 8-11 TIME WHERE PLDT STARTS
C COLUMNS 12-15 TIME WHERE PLDT ENDS
C COLUMNS 16-20 VALUE OF BOTTOM VERTICAL SCALE
C COLUMNS 21-24 VALUE OF TOP VERTICAL SCALE
C COLUMNS 25-48 UP TO FOUR NODE NAMES
C COLUMNS 49-64 GRAPH HEADING LABEL
C COLUMNS 65-80 VERTICAL AXIS LABEL
144 B. 80. REC AREC BREC C
144 B. 80. SEND ASEND BSEND C
BLANK CARD TERMINATING PLOT REQUESTS
BLANK CARD TERMINATING THE CASE

```

8-7. LINE ENERGIZING AND RECLOSING

8-7-1. General Trends In Line Energizing and Reclosing

The only difference between line energizing and line reclosing is in the trapped charge, or the initial conditions, which will exist across the circuit breaker at the time of closure. When energization is simulated, no trapped charge exists on the line. In reclosing, the amount of trapped charge varies with the "speed" of the reclosing. High-speed reclosing is of the most concern, while prolonged or delayed reclosing approaches the energization case.

In high-speed reclosing, the breakers reclose anywhere between 300 and 600 milliseconds after opening, depending on the voltage level and system practices. As a result, some charge will still be trapped on the line when the breakers reclose to reinsert the line. This charge can result in a residual voltage close to 1 per-unit, or even higher on the unfaulted phases, depending on the system on the line side of the breaker. When the contacts of the breaker close, the travelling voltage surge on the line will be equal to the voltage difference between the two sides of the breaker just prior to closing. This surge, which can have a magnitude of 2 per-unit or greater, will double if it reaches the receiving end of an open-ended line.

If preinsertion resistors are used, the peak switching overvoltages on the line are reduced, and their statistical distribution is changed. In this case, the SOV is made up of two components: the Insertion Transient (when the auxiliary contact of the breaker closes, completing the circuit between the source and the line through the preinsertion resistor), and the Shorting Transient (when the main contact of the breaker closes, shorting out the resistor). Ideally, the lowest SOV's are obtained when the two components are made equal. The complicated effect of the system parameters (source characteristics, coupling between phases, multi-modal attenuation, etc.) and the commercial availability of certain preselected resistor values make it necessary to evaluate the system's performance over a range of preinsertion resistor values.

Figure 8-13 shows the result of an investigation in which the value of the preinsertion resistor was varied over a wide range. The maximum overvoltage is shown plotted as a function of resistor value. Note that the energize and reclose curves tend to approach each other on the right-hand side of the curve. This is because the line is "precharged" to almost the same values in these cases, and the

shorting transient then determines the surge magnitude. Also, the curves slope sharply upward from the optimum for lower resistor values, and more gradually upward for higher resistor values. Thus, values at or somewhat above the optimum will be less sensitive to shifts in the curve brought about by changes in source impedance or other system parameters.

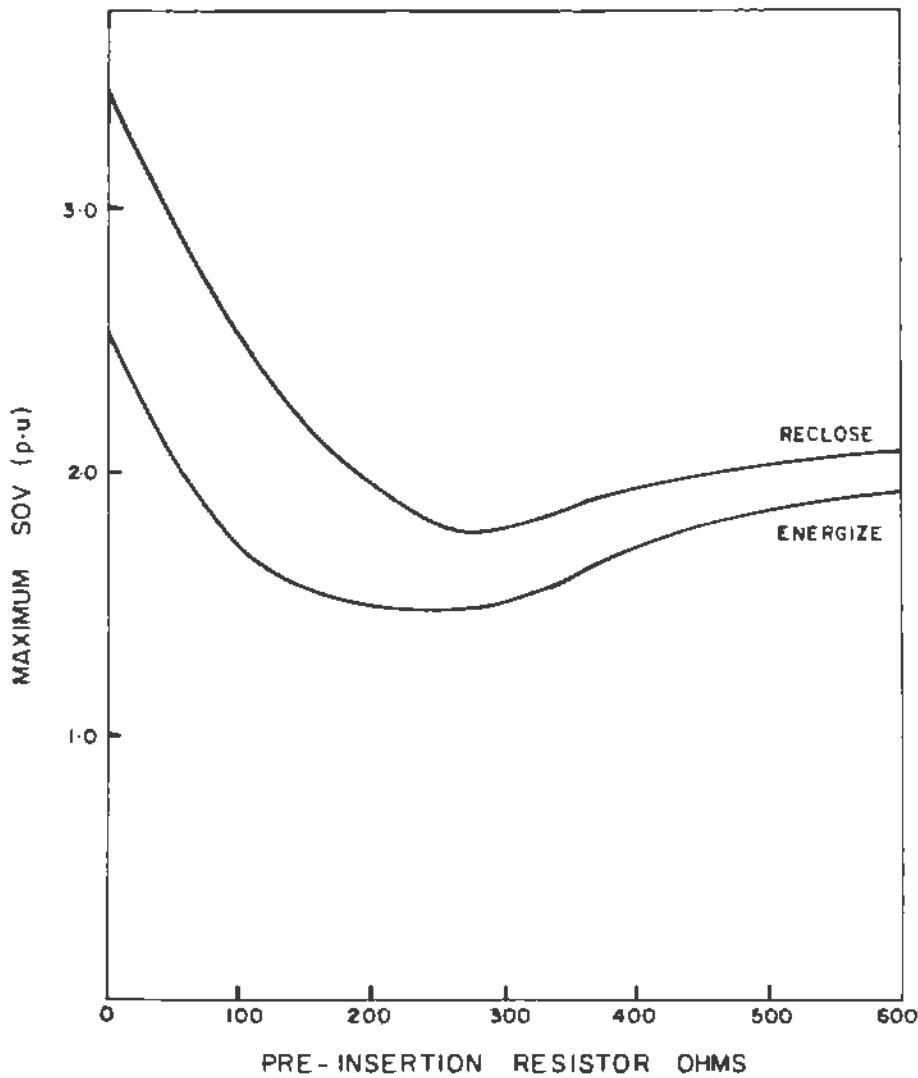


Figure 8-13. Effects of Preinsertion Resistor Size On Maximum Switching Overvoltage

For the extreme values of resistance, zero and infinity, the results are identical to those for a breaker without preinsertion resistors. A resistance of zero ohms causes the full transient to occur during the auxiliary contact closing, while infinite resistance produces the full surge during the shorting transient.

The calculation of the SOV's is an involved task because of the many parameters involved, and the EMTP or a transient network analyzer can be used to do this. It is of academic benefit, however, to simplify this problem and attempt to find approximate answers by hand. For this, a single-phase circuit is considered.

8-7-2. Approximations for the Calculation of SOV's During Energizing and Reclosing

8-7-2-1. Energizing a Line With No Trapped Charge

Consider the circuit in Figure 8-14 for a deenergized, open-ended line with no trapped charge or residual voltage. For this case only, assume that contact 2 of the breaker remains closed so that the preinsertion resistor is not used (i.e., voltages at points B and C are the same). The surge which will travel on the line to the receiving end, RE, depends on the voltage across the switch just before closure of contact 1, i.e., $V_A - V_B$. For the case of a deenergized line, $V_B = 0$, and the surge depends only on V_A , which depends on the point on the voltage waveform where closure occurs. If the closure occurs at maximum voltage, as shown in Figure 8-15, the surge travelling on the line will be E, the peak value of the voltage waveform. When this surge appears at the receiving end, this will double, resulting in $V_{RE} = 2E$, as shown in Figure 8-16.

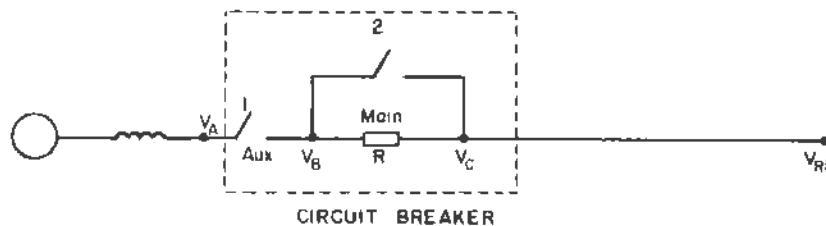


Figure 8-14. Circuit Used in the Approximate Approach for Calculating Energizing and Reclosing SOV's

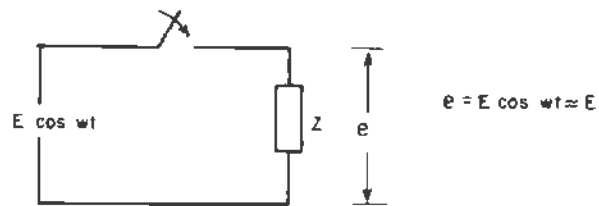


Figure 8-15. Equivalent Circuit for Energizing the Line of Figure 8-14 With No Trapped Charge, as Seen From the Sending End

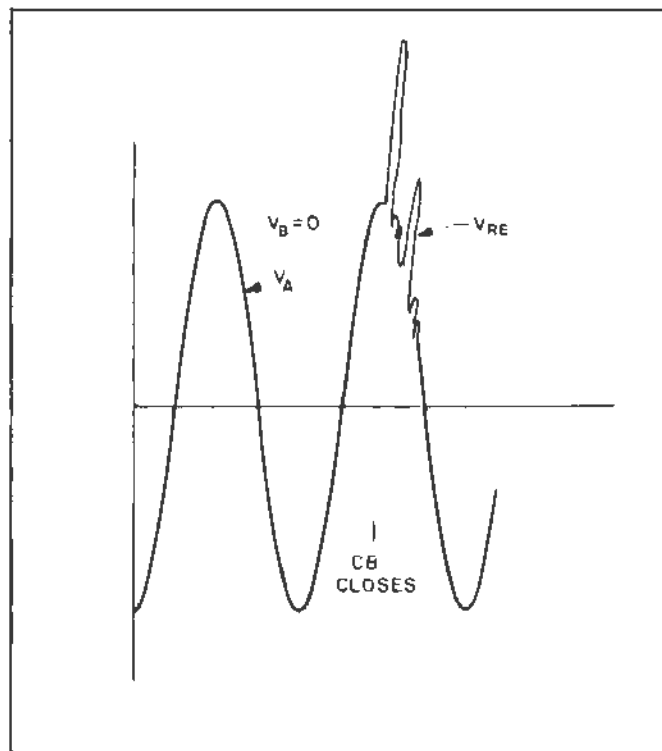


Figure 8-16. Energizing a Line With No Trapped Charge. Circuit Breaker Closing at Maximum Line-to-Ground Voltage.

8-7-2-2. High-Speed Reclosing On a Line With No Preinsertion Resistor

Consider the case of high-speed reclosing on the open-ended line of Figure 8-14 within 20-40 cycles from the time of opening the breaker. No preinsertion resistors are used. If no path to ground exists through a shunt reactor or transformer, the charge will be trapped on the line, resulting in a residual voltage close to 1 per-unit at the time of closure, as shown in Figure 8-17. When the breaker closes, a surge equal to the voltage across the breaker just prior to closing will travel down the line. This magnitude of surge can be close to 2 per-unit, as illustrated in Figure 8-17, resulting in a receiving end surge voltage, V_{RE} , of approximately 4 per-unit. The total voltage at RE in this case is 3 per-unit; 4 per-unit surge magnitude minus 1 per-unit steady-state or initial condition voltage, as shown in Figure 8-18.

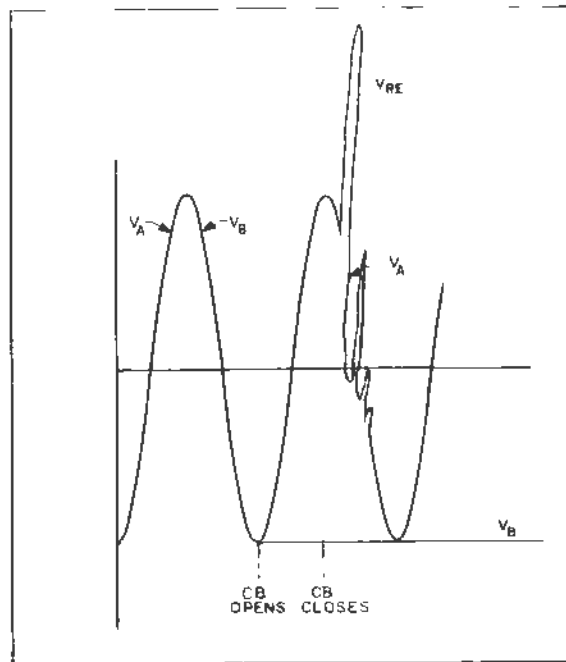


Figure 8-17. Reclosing the Breakers Into Trapped Charge. The reclosing time delay is not shown.

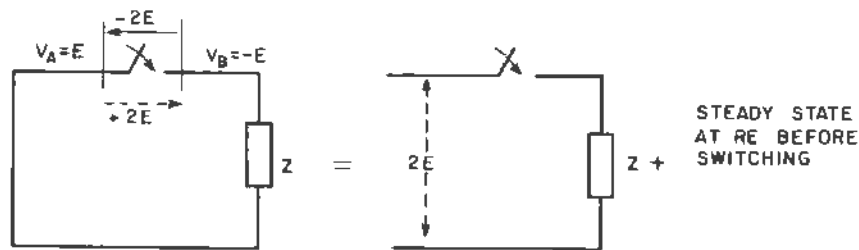


Figure 8-18. Equivalent Circuit for Calculating the Resulting Overvoltage When Reclosing Into 1 Per-Unit Trapped Charge, as Seen from the Sending End

8-7-2-3. High Speed Reclosing On a Line With Preinsertion Resistors

When a preinsertion resistor is used, as shown in Figure 8-14, the SOV is more complicated than in the previous two cases. There exist two components of the SOV, the insertion transient and the shorting transient. As the name indicates, the insertion transient occurs when the auxiliary contacts of the breaker close, thereby reclosing the line through the preinsertion resistor. The shorting transient is the result of the main contact closing, shorting out the resistor. To minimize the overall SOV, these two components should be equal.

The initial conditions for the insertion transient are the following:

$$V_A = +E \quad (8-3)$$

$$V_B = V_C = -E \quad (8-4)$$

$$\text{Voltage across the switch} = V_A - V_B = 2E. \quad (8-5)$$

$$\text{Therefore, cancellation voltage} = V_B - V_A = -2E. \quad (8-6)$$

Figure 8-19 is the equivalent circuit for the travelling wave analysis of the insertion transient. From this circuit, the surge voltage which travels down the line is equal to:

$$e = \frac{Z}{Z + R} 2E \quad (8-7)$$

When this surge gets to the open receiving end, it doubles. The total voltage at the receiving end is the reflected surge voltage minus 1 per-unit steady state voltage, i.e.,

$$V_{RE} = \frac{Z}{Z+R} 4E - E \quad (8-8)$$

The variation of V_{RE} with different values of preinsertion resistance is shown in Figure 8-21.

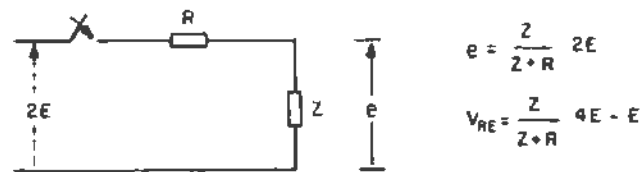


Figure 8-19. Equivalent Circuit for the Making of the Auxiliary Contacts, as Seen from the Sending End

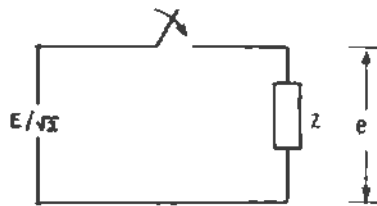


Figure 8-20. Equivalent Circuit for the Making of the Main Contacts, as Seen from the Sending End

When the auxiliary contact is closed and the main contact is open, the steady-state voltage appearing across the preinsertion resistor, R , can be calculated with the help of Figure 8-19. In this circuit,

$$V_B = E \sin \omega t \quad (8-9)$$

If the line is represented by its charging capacitance, C , it can be shown that:

$$V_C = \frac{E}{\omega C} \frac{1}{\sqrt{R^2 + \left(\frac{1}{\omega C}\right)^2}} \sin \omega(t-\tau) \quad (8-10)$$

Where $\omega\tau = \text{arc tan}(\omega RC)$

The variation of the shorting transient with different values of the preinsertion resistance is also shown in Figure 8-21.

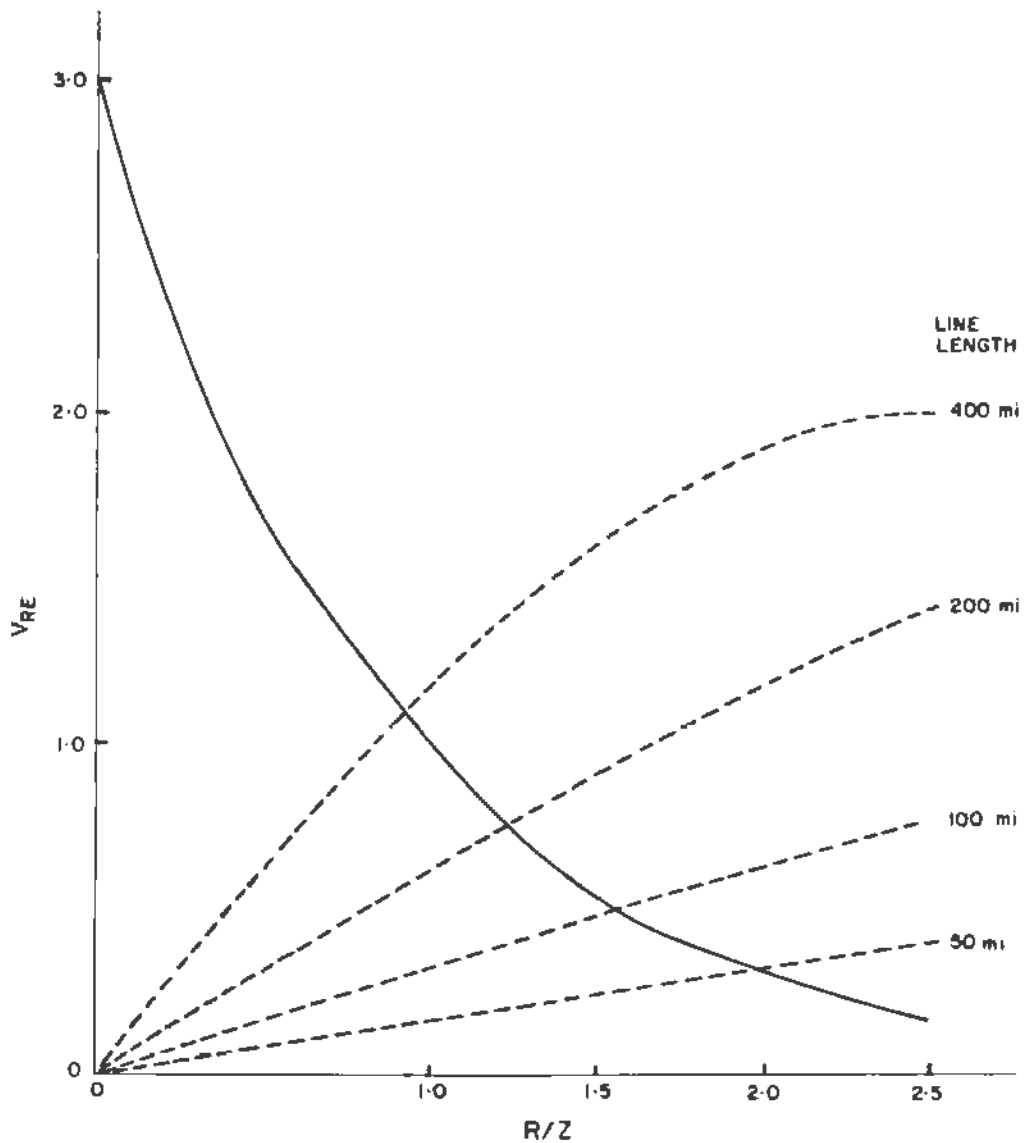


Figure 8-21. Insertion (Solid) and Shorting (Dashed) Transients When Reclosing Into a Line With Trapped Charge Using Preinsertion Resistors

8-7-3. Characteristics of High-Speed Three-Pole Reclosing

High-speed three-pole reclosing is recognized to have the following features:

1. It increases the maximum power which can be transmitted over long high-voltage transmission lines without loss of synchronism following a fault. Reducing the reclosing or dead time can greatly enhance the transient stability of a system.
2. It reduces system disturbances by reclosing before large swings occur between two parts of a system.
3. It reduces line outage times and improves service to customers.

In establishing the dead time, before which the breakers are not allowed to reclose to ensure deionization of the fault arc current, the following factors have to be considered:

1. Magnitude of the short-circuit current. In general, the higher the fault current, the larger the amount of ionized gas generated. This may be offset by greater turbulence in the air and magnetic blowout action, both of which increase with higher current.
2. Duration of the short circuit current. The longer the fault current flows, the greater the amount of ionized gases. This is offset also by greater turbulence, longer magnetic blowout action, and thermal convection currents in the area.
3. Magnitude and duration of capacitive and magnetic coupling currents which may flow due to induced voltages from adjacent energized conductors. This assumes particular importance for single-pole reclosing, or for three-pole reclosing on one circuit of a double-circuit line.
4. Magnitude and duration of resistance-follow current, which flows through shunting resistors on some types of circuit breakers.
5. Magnitude of reenergization voltage applied.
6. Point-on-wave at which the circuit is reenergized. This determines the magnitude of the surge and will account for much of the randomness in the results obtained.
7. Magnetic forces on the arc due to circuit configuration.
8. Length of the insulator string, which determines the minimum length of the flashover path.
9. Weather conditions - particularly the wind effect.
10. Shape of grading rings and other hardware, which determines the dielectric stress on reapplication of the system voltage.

Table 8-18 summarizes the necessary minimum times for deionization of the fault arc at different voltage levels to achieve successful three-pole high-speed reclosing. This table is based on laboratory and field tests plus operating experience. As can be seen from Table 8-18, there is an allowance of about five cycles between the laboratory/field tests and the operating experience.

Table 8-18

ESTIMATED MINIMUM DEIONIZATION OR DEAD TIME (IN CYCLES OF 60 HZ)
REQUIRED FOR AUTOMATIC THREE-POLE RECLOSING

<u>Rated Voltage [kV]</u>	<u>Based on Laboratory and Field Tests</u>	<u>Based On Operating Experience</u>
23	6.5	11
46	7	12
69	7.5	12.5
115	9	14
132	9.5	14.5
230	12.5	17
345	15.5	20.5
400	17	22
500 ⁽¹⁾	20	25

Note (1): At 500 kV and above, closing resistors are generally used. These resistors will significantly alter the shape of the switching surge statistical distribution by both lowering the maximum level and narrowing the band of variations between maximum and minimum. In general, this should produce a significant advantage in the percentage of successful reclosures at a given dead time. Hence, the reclosing times shown are somewhat conservative, and shorter dead times are possible. Laboratory tests confirm that deionization is well advanced for a dead time of 20 to 30 cycles, so there would appear to be no reason to increase deionization times above one-half second at any voltage level. The effect of preinsertion resistors in reducing the magnitude of the reclosing voltage transient can reduce the minimum dead time significantly. Tests indicate an increase in dead time of 5 cycles for 100 percent trapped voltage on reclosing.

8-7-4. Example of High-Speed Three-Pole Reclosing Using Preinsertion Resistors

The system shown in Figure 8-22 was used to simulate high-speed three-pole reclosing into a trapped charge. This system was also studied in Section 7 of the EMTP Primer. Six different values for the preinsertion resistor were used, 0, 100, 200, 300, 450, and 550 ohms. The maximum switching overvoltages at the receiving end are shown in Table 8-19 for the different resistor values. Table 8-20 shows the input data for the case of $R = 300$ ohms.

Table 8-19

VARIATION OF MAXIMUM RECEIVING END VOLTAGE WITH DIFFERENT PREINSERTION RESISTOR VALUES

Resistor Value (ohms)	Maximum V_{REC} (1-g) (per-unit)
0	4.02
100	3.0
200	2.6
300	2.35
450	1.9
550	1.95

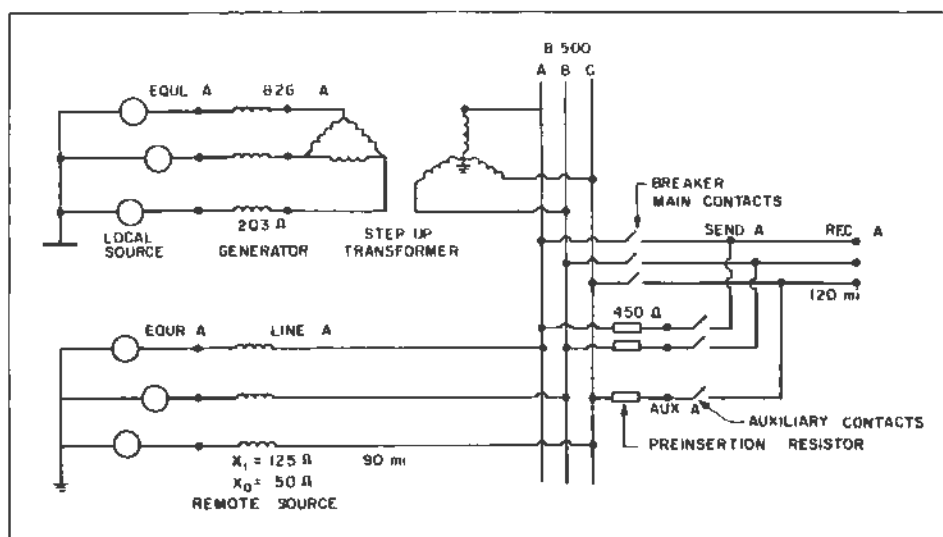


Figure 8-22. System Used for High-Speed Reclosing Into Trapped Charge

Table 8-20

INPUT DATA FOR RECLOSING WITH A 300-OHM PREINSERTION RESISTOR

```

C FILE NAME: "L500STAT-300": SIMULATE RECLOSING OF THE 120 MILE LTNF.
C A 300-OHM PREINSERTION RESISTOR IS USED.
C STATISTICS SWITCHES "MAIN" AND "AUX" CONTROL THE CLOSING. TRAPPED
C CHARGE IS ON THE LINE. 200 CLOSING OPERATIONS WILL BE SIMULATED
C
C BEGIN NEW DATA CASE
C FIRST MISCELLANEOUS DATA CARD:
C 34567890123456789012345678901234567890123456789012345678901234567890
C   1-8   9-16  17-24  25-32
C T-STEP T-MAX  X-OPT  C-DPT
C SECONDS SECONDS O=MH  O=UF
C           F(HZ)   F(HZ)
C 33.30E-6   .07    60.    0
C
C SECOND MISCELLANEOUS DATA CARD
C   1-8   9-16  17-24  25-32  33-40  41-48  49-56  57-64  65-72  73-80
C PRINT  PLOT NETWORK PR SS PR MAX I PUN PUNCH DUMP MULT. DIAGNOS
C O=EACH O=EACH O=NO  O=NO  O=NO  O=NO  O=NO  O=NO  INTO NENERG PRINT
C K=K-TH K=K-TH 1=YES 1=YES 1=YES 1=YES 1=YES 1=YES  DISK STUDIES O=NO
C   5000      1      1      1      1      1      1      1      200
C
C IF ON MISC. CARD#2 "NENERG" COL 65-72 IS NONZERO A THIRD MISC.CARD MUST FOLLOW
C
C THIRD MISCELLANEOUS CARD (FOR STATISTICS DATA FOR THE SWITCHES)
C
C 34567890123456789012345678901234567890123456789012345678901234567890
C   1-8   9-16  17-24  25-32  33-40  41-48  49-56  57-64  65-72  73-80
C ISW  ITST IOIST AINCR XMAXMX DEGMIN DEGMAX STATFR SIGMAX NSEED
C     1      0      0      .05    5.    0.    360.    60.    3      0
C
C BRANCHES
C 34567890123456789012345678901234567890123456789012345678901234567890
C   3-8   9-14  15-20  21-26  27-32  33-38  39-44
C NODE NAMES REFERENCE RES. IND CAP. (OUTPUT IN COLUMN 80)
C           BRANCH MH UF
C BUS1 BUS2 BUS3 BUS4 OHM OHM UMHO
C
C
C   3456789012345678901234567890123456789012345678901234567890
C HIGH RESISTANCE FOR PHASE-TO-PHASE STATISTICS DATA
C REC AREC B 10. E9 2
C REC BREC C 10. E9 2
C REC CREC A 10. E9 2
C SEND ASEND B 10. E9 2
C SEND BSEND C 10. E9 2
C SEND CSEND A 10. E9 2
C PREINSERTION RESISTOR
C B500 AAUX A 300.
C B500 BAUX B 300.
C B500 CAUX C 300.
C LOCAL SOURCE (GENERATOR)
C B26 AEQUL A .203
C B26 BEQUL B .203
C B26 CEQUL C .203
C
C REMOTE SOURCE (MUTUALLY COUPLED)
C 34567890123456789012345678901234567890123456789012345678901234567890
C SEQUENCE VALUES
C 27-32 33-44
C R L (FIRST ZERO, THEN POS. SEQUENCE)
51LINE AEQUR A 50.
52LINE BEQUR B 125
53LINE CEQUR C
C
C TRANSMISSION LINES

```

Table 8-20 (Cont'd)

INPUT DATA FOR RECLOSING WITH A 300-OHM PREINSERTION RESISTOR

```

C 3456789012345678901234567890123456789012345678901234567890
C                               27-32 33-38 39-44 45-50  CODF IN COLUMN "52"
C                               R     L     C     LE   (LE=LENGTH)
C                               (ZERO, POSITIVE SEQUENCE)
-18500 ALINE A                .5580 1.6722 01268   90. 0
-28500 BLINE B                .0310 .5816 01940   90. 0
-38500 CLINE C
C 120 MILE LINE
C 3456789012345678901234567890123456789012345678901234567890
-1SEND AREC A                .5294 1.7659 01224 120 0
-2SEND BREC B                .02499 .59614 01914 120 0
-3SEND CREC C
C
C TRANSFORMER
C 345678901234567890123456789012345678901234567890
C   3-13 15-20                27-32 33-38 39-44 45-50
C REQUESTWORD   BUS          I   FLUX   BUS R-MAG
C TRANSFORMER   2 33 1137      X
C
C   1-16                17-32
C   CURRENT          FLUX
C   2.33                1137 0
C   5 44                1250 0
C   23.33              1364 0
C   1579.00            2274.0
C   9999
C TRANSFORMER WINDINGS
C COLUMN 1,2. WINDING NUMBER
C 345678901234567890123456789012345678901234567890
C   3-8 9-14                27-32 33-38 39-44
C   BUS1 BUS2                R-K   L-K  TURNS
18500 A                27.55 11 66
2826 AB26 B                .2026 1
C TRANSFORMER   Y
18500 B
2826 BB26 C                X
C TRANSFORMER   Z
18500 C
2826 CB26 A
BLANK CARD TERMINATING BRANCH CARDS
C STATISTIC SWITCHES
C 3456789012345678901234567890123456789012345678901234567890
C   3-8 9-14                15-24 25-34                55-64
C   BUS1 BUS2                MEAN STANDARD
C                               CLOSING DEVIATION
C                               TIME MAIN CDNT
8500 ASEND A                .0165 .0014                STATISTICS
8500 BSEND B                0165 .0014                STATISTICS
8500 CSEND C                0165 .0014                STATISTICS
C
C AUXILIARY SWITCHES
C 3456789012345678901234567890123456789012345678901234567890
C   15-24 25-34                REFERENCE
C   RANDDM STANDARD                SWITCH
C   DELAY DEVIATION                65-70 71-76
C   TIME AUXILIARY
AUX ASEND A                - 010 .0007                STATISTICSB500 ASEND A
AUX BSEND B                - 010 .0007                STATISTICSB500 BSEND B
AUX CSEND C                - 010 .0007                STATISTICSB500 CSEND C
BLANK CARD TERMINATING SWITCH CARDS
C SOURCE CARDS
C 3456789012345678901234567890123456789012345678901234567890
C COLUMN 1,2. TYPE OF SOURCE 1 - 17, (E.G. 11-13 ARE RAMP FUNCTIONS, 14 = COSINE)
C COLUMN 9,10. 0=VOLTAGE SOURCE, -1=CURRENT SOURCE
C   3-8 11-20 21-30 31-40 41-50 51-60 61-70 71-80
C   NODE AMPLITUDE FREQUENCY TO IN SEC AMPL-A1 TIME-T1 T-START T-STOP

```

Table 8-20 (Cont'd)

INPUT DATA FOR RECLOSING WITH A 300-OHM PREINSERTION RESISTOR

C	NAME	IN HZ	DEGR	SECONDS	SECONDS	SECONDS
C	LOCAL SOURCE					
	14EQUL A	18863.	60.0	0.	-1.0	
	14EQUL B	18863.	60.0	-120.	-1.0	
	14EQUL C	18863.	60.0	-240.	-1.0	
C	REMOTE SOURCE					
	14EQUR A	380281.	60.0	30.	-1.0	
	14EQUR B	380281.	60.0	-90.	-1.0	
	14EQUR C	380281.	60.0	-210.	-1.0	
C	BLANK CARD TERMINATING SOURCE CARDS					
C	INITIAL CONDITIONS ON THE SWITCHED LINE					
C	345678901234567890123456789012345678901234567890					
C	COLUMN 2: 2 = CARD FOR NODE VOLTAGES					
C	3-8 9-23 (FORMAT E15.8)					
C	BUS1 INST.VOLT.T=0					
	2SEND A	0.				
	2SEND B	525000.				
	2SEND C	415000.				
	2REC A	0.				
	2REC B	525000.				
	2REC C	415000.				
C	COLUMN 2: 3 = CARD FOR LINEAR BRANCH CURRENTS					
C	3456789012345678901234567890					
C	3-8 9-14 15-29					
C	BUS1 BUS2 CURRENT T=0					
	3SEND AREC	A				
	3SEND BREC	B				
	3SEND CREC	C				
C	NODE OUTPUTS					
C	3-8 9-14 15-20 21-26 27-32 33-38 39-44 45-50 51-56 57-62 63-68 69-74 75-80					
C	BUS1 BUS2 BUS3 BUS4 BUS5 BUS6 BUS7 BUS8 BUS9 BUS10 BUS11 BUS12 BUS13					
	B500 AB500 BB500	CSEND ASEND BSEND CREC AREC BREC C				
C	BLANK CARD TERMINATING NODE VOLTAGE OUTPUT					
C	BLANK CARD TERMINATING PLOT REQUESTS					
C	OUTPUT FOR THE "STATISTICS" CASE					
C	COLUMN 2: 0 = NODE VOLTAGES					
C	-1 = BRANCH VOLTAGES					
C	34567890123456789012345678901234567890					
C	3-14 15-20 21-26 27-32 33-38 39-44 45-50					
C	BASE VOLT BUS1 BUS2 BUS3 BUS4 BUS5 BUS6					
C	REQUEST FOR LINE-TO-GROUND HISTOGRAMS					
	0	408269 SEND ASEND BSEND C				
	0	408270 REC AREC BREC C				
C	REQUEST FOR PHASE-TO-PHASE HISTOGRAMS					
	-1	408271 SEND ASEND BSEND CSEND CSEND A				
	-1	408272 REC AREC BREC BREC CREC CREC A				
C	BLANK CARD TERMINATING STATISTICS OUTPUT					
C	BLANK CARD TERMINATING THE CASE					

8-7-5. Characteristics of Single-Pole Switching

Single-pole tripping consists of a protection system which determines that a single-line-to-ground fault has occurred within the trip zone on a particular phase, and then opens only that phase to clear the fault. In contrast to conventional relaying, the two unfaulted phases are left energized, and continue to carry power. Since turbine-generators step out of synchronism more quickly during a fault if the unfaulted phases do not carry power, single-pole tripping improves system stability.

During a multiphase fault, such a relaying system would trip all three phases under the present convention. On EHV lines, nearly all lightning-caused faults involve only one phase and ground, and are temporary. For this reason, single-pole tripping is applicable to the great majority of faults at EHV levels. Single-pole tripping works from a theoretical standpoint because switching out one phase does not introduce as much additional impedance into the transmission system as does tripping all three phases. It is this insertion of reduced impedance that allows greater power transfer and improved system stability.

Single-pole tripping offers the greatest benefits to system stability when only one tie line exists. Single-pole tripping is also useful when two ties exist, since one could be out of service when a fault occurs on the second. But, since the need for such switching falls rapidly as the number of tie lines between two points increases, single-pole tripping appears suited primarily to relatively undeveloped portions of transmission networks.

The reclosing dead time needed for single-pole switching exceeds that for three-pole switching (shown in Table 8-18) on lines where no compensating measures are taken. Such compensating measures include transposition of the phases and the use of shunt reactors. This occurs because coupling between the faulted phase and the others tends to maintain the arc. Conversely, single-pole tripping makes it possible to maintain stability even with the longer dead time, because at least some synchronizing power is transmitted beyond the fault.

Transposition of the phase conductors is often performed when single-pole tripping is used. The transposition acts to equalize the interphase capacitances. When neutral shunt reactors are used, in addition to the line-to-ground reactors,

they act to compensate the line-to-ground capacitance and the net effect is to limit and help extinguish the secondary arc current in the faulted phase. Typically, the secondary arc current which circulates into the fault on the opened phase due to the coupling from other "healthy" phases is limited to 20 amps, and the arc recovery voltage is limited to 50 kV.

8-7-6. Example Of Single-Pole Reclosing

Figure 8-23 shows the circuit used for studying single-pole reclosing. Breakers in Phase A only are assumed to operate when clearing a fault at the receiving end. Table 8-21 contains the input data for this run. Figure 8-24 shows the sending end Phase C voltage, and receiving end Phase A and B voltages.

Table 8-22 shows the input for probability runs for single-pole reclosing. The initialization of the circuit is done in the steady state by assuming Phase A of the line between SENDA and REMA is open, while the other two phases are closed. This can be done in the case of single-pole reclosing while it cannot be done in the case of three-pole reclosing. The trapped charge on the opened Phase A is essentially due to a.c. coupling from the two energized phases.

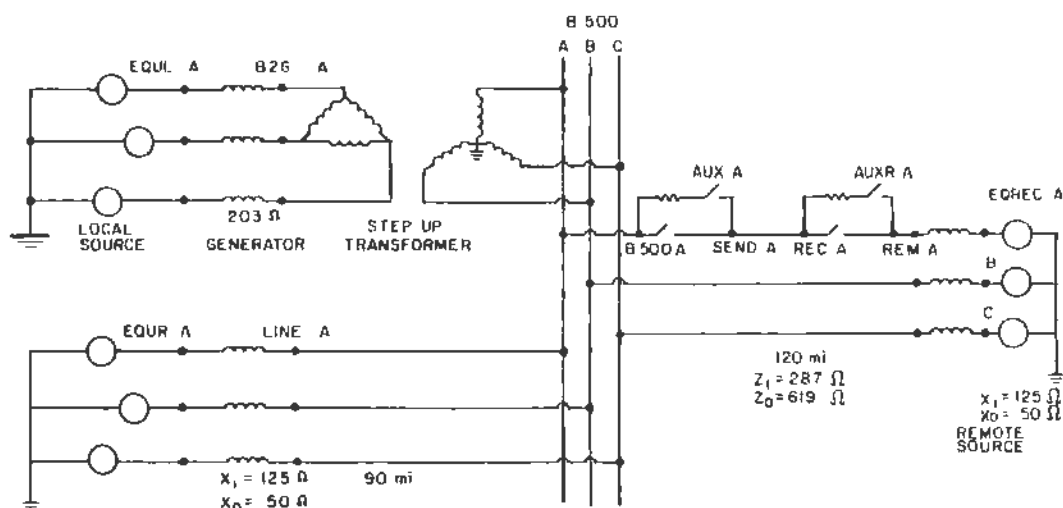


Figure 8-23. System Used for Single-Pole Reclosing Cases

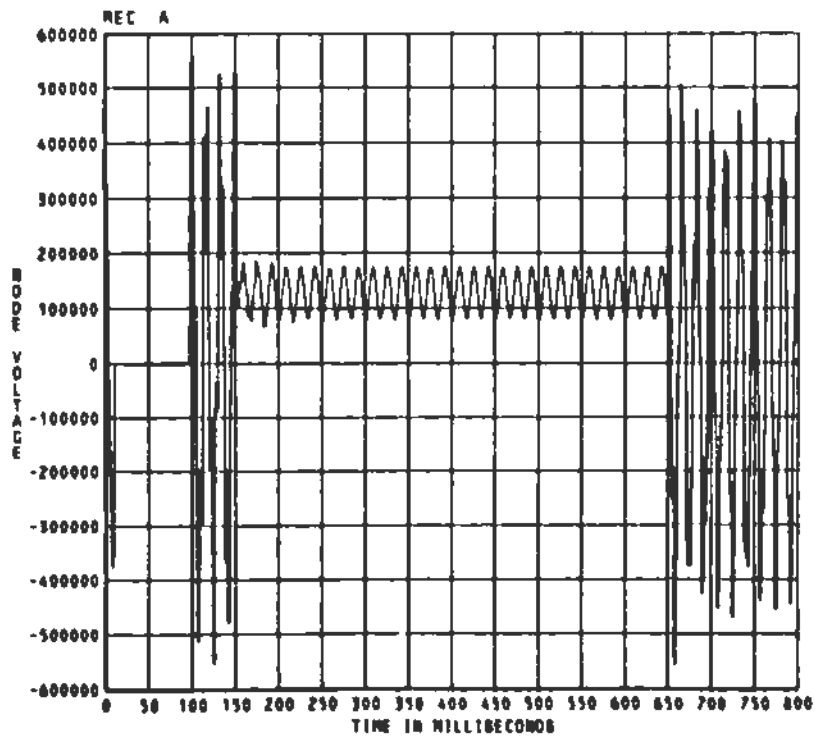


Figure 8-24a. Receiving End Phase A Voltage for Single-Pole Switching Case

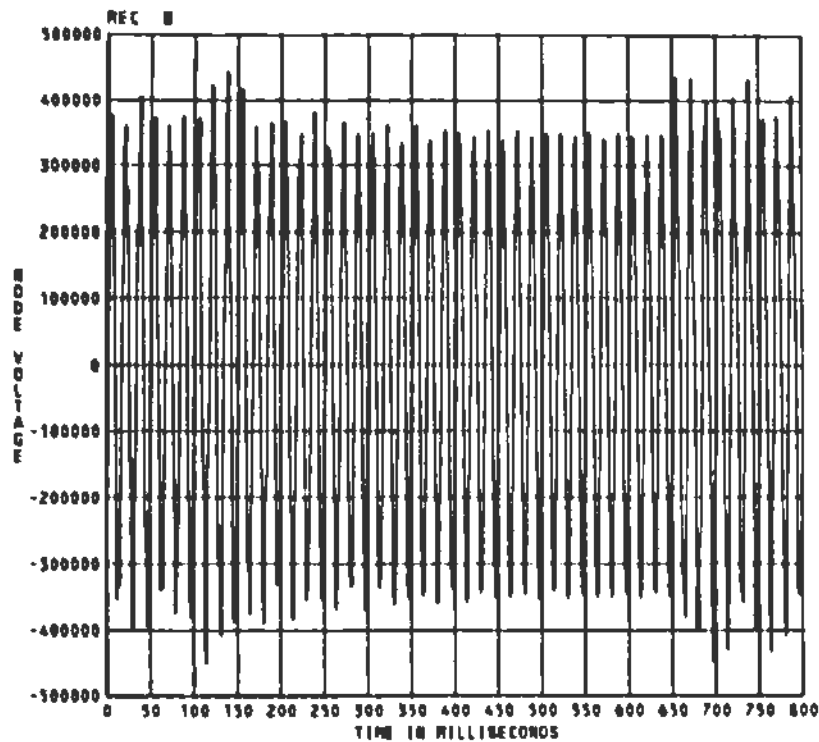


Figure 8-24b. Receiving End Phase B Voltage for Single-Pole Switching Case

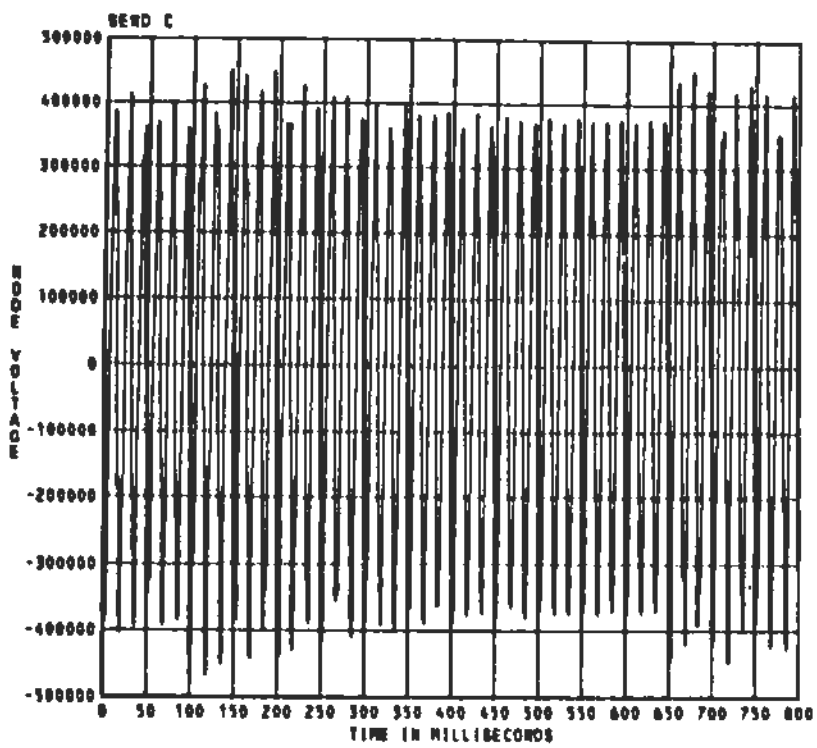


Figure 8-24c. Sending End Phase C Voltage for Single-Pole Switching Case

Table 8-21

INPUT DATA FOR SINGLE-POLE SWITCHING CASE

```

C FILE NAME: "L500SPS". SINGLE-POLE SWITCHING..
C A FAULT IS APPLIED AT NODE "REC A"
C THE PHASE A BREAKER OPENS AFTER 3 CYCLES, AND RECLOSES 30 CYCLES LATER.
C THE FAULT ARC IS EXTINGUISHED AFTER 96 MILLISECONDS
BEGIN NEW DATA CASE
C FIRST MISCELLANEOUS DATA CARD:
C 34567890123456789012345678901234567890123456789012345678901234567890
C   1-8   9-16   17-24   25-32
C T-STEP T-MAX X-OPT C-OPT
C SECNDS SECONDS O=MH O=UF
C                               F(HZ) F(HZ)
66.00E-6      .80      60.      0
C
C SECOND MISCELLANEOUS DATA CARD
C   1-8   9-16   17-24   25-32   33-40   41-48   49-56   57-64   65-72   73-80
C PRINT PLOT NETWORK PR.55 PR.MAX I PUN PUNCH DUMP MULT. DIAGNOS
C O=EACH O=EACH O= NO O= NO O= NO O= NO O= NO INTO NENERG PRINT
C K=K-TH K=K-TH I=YES I=YES I=YES I=YES I=YES DISK STUDIES O=NO
C 20000 13 1 1 1 0 0 1 0
C LOCAL SOURCE (GENERATOR)
B26 AEQUL A .203
B26 BEQUL B .203
B26 CEQUL C .203
C MUTUALLY COUPLED SOURCE EQUIVALENTS
C 3456789012345678901234567890123456789012345
C                               SEQUENCE VALUES
C                               27-32 33-44
C                               R L (FIRST ZERO, THEN POS. SEQUENCE)
51LINE AEQUR A 50.
52LINE BEOUR B 125.
53LINE CEQUR C
C REMOTE SOURCE EQUIVELANTS
51REM AEGRECA 50.
52REC BEORECB 125.
53REC CEGRECC
C
C FAULT AT THE RECEIVING END, PHASE A
FAULTA .01
C
C TRANSMISSION LINES
C 3456789012345678901234567890123456789012345678901234567890
C                               27-32 33-38 39-44 45-50 CODE IN COLUMN "52"
C                               R L C LE (LE=LENGTH)
C                               (ZERO, POSITIVE SEQUENCE)
-18500 ALINE A .55801.6722.01268 90. 0
-28500 BLINE B .0310 5816.01940 90. 0
-38500 CLINE C
C 120 MILE LINE, FLAT CONFIGURATION
C 34567890123456789012345678901234567890123456789012345678901234567890
-1SEND AREC A .5294 1.7659.01224 120. 0
-2SEND BREC B .02499.59614.01914 120. 0
-3SEND CREC C
C
C TRANSFORMER
C 345678901234567890123456789012345678901234567890
C   3-13 15-20 27-32 33-38 39-44 45-50
C REQUESTWORD BUS I FLUX BUS R-MAG
TRANSFORMER 2.33 1137. X 3.E5
C
C   1-16 17-32
C CURRENT FLUX
C 2.33 1137.0
C 5 44 1250 0
C 23 33 1364.0
C 1579.00 2274.0
C 9999
C TRANSFORMER WINDINGS
C COLUMN 1,2: WINDING NUMBER
C 345678901234567890123456789012345678901234567890
C   3-8 9-14 27-32 33-38 39-44
C BUS1 BUS2 R-K L-K TURNS
18500 A 27.55 11.66
2826 AB26 B .2026 1.
TRANSFORMER X Y
18500 B
2826 8826 C

```

Table 8-21 (Cont'd)

INPUT DATA FOR SINGLE-POLE SWITCHING CASE

```

TRANSFORMER      X      Z
18500 C
2B26 CB26 A
(: REINSERTION OR RECLOSING RESISTORS-NONE HAVE BEEN USED FOR THIS CASE(R=.001)
B500 AAUX A      .001
REC AAUXR A      .001
BLANK CARD TERMINATING BRANCH CARDS
C
C SWITCH CARDS
C 34567890123456789012345678901234567890123456789012345678901234567890
C   J-B  9-14    15-24    25-31    35-44    45-54    55-64    65-74
C                                     (OUTPUT OPTION IN COLUMN 80)
C   NODE NAMES      TIME TO      TIME TO      IE FLASHOVER      SPECIAL REFERENCE
C   BUS1  BUS2      CLOSE      OPEN      NSTEP      OR VOLTAGE      REQUEST SWITCH NAME
C   B500 ASEND A      -1.      150
C   AUX  ASEND A      65      999
C   AUXR AREM A      - 010    150
C   REC  AREM A      65      999
C   REC AFAULTA      01      0960
C BREAKERS ON PHASES B AND C NOT ALLOWED TO OPERATE
B500 BSEND B      -1      99
B500 CSEND C      -1      99
BLANK CARD TERMINATING SWITCH CARDS
C SOURCE CARDS
C 34567890123456789012345678901234567890123456789012345678901234567890
C COLUMN 1,2: 1/PE OF SOURCE 1 - 17. (E G 11-13 ARE RAMP FUNCTIONS, 14 - COSINE)
C COLUMN 9,10: 0=VOLTAGE SOURCE, -1=CURRENT SOURCE
C   3-B  11-20    21-30    31-40    41-50    51-60    61-70    71-80
C   NODE  AMPLITUDE  FREQUENCY  TO IN SEC  AMPL-A1  TIME-T1  T-START  T-STOP
C   NAME      IN HZ      DEGR
C 14EQUA A      18863      60 0      0      -1 0
C 14EQUA B      18863      60 0     -120    -1 0
C 14EQUA C      18863      60 0     -240    -1 0
C 14EQUA A      380281     60 0      30     -1 0
C 14EQUA B      380281     60 0     -90     -1 0
C 14EQUA C      380281     60 0    -210     -1 0
C REMOTE SOURCE
C   1      2      3      4      5      6      7
C 3456789012345678901234567890123456789012345678901234567890123456789
14EQUA 380000      60 0     -12 4      -1 0
14EQUA 380000      60 0    -132 4      -1 0
14EQUA 380000      60 0     252 4      -1 0
C
BLANK CARD TERMINATING SOURCE CARDS
C NODE VOLTAGE OUTPUT
C 34567890123456789012345678901234567890
SEND ASEND BSEND CREC AREC BREC C
FAULTAB26 AB26 BB26 C
BLANK CARD TERMINATING NODE VOLTAGE OUTPUT
C PLOTTING CARDS
CALCOMP PLOT      2
C (CASE TITLE UP TO 78 CHARACTERS)
2 SINGLE-POLE SWITCHING OF A TRANSDPOSED 500-KV LINE
C THE FOLLOWING IS FORMAT OF THE PLDT REQUEST CARDS
C COLUMN 2,      "1"
C COLUMN 3,      4-NODE VOLTAGE
C                   8-BRANCH VOLTAGE
C                   3-BRANCH CURRENT
C COLUMN 4,      UNITS OF HORIZONTAL SCALE  1=DEGREES
C                                           2=CYCLES
C                                           3=SEC
C                                           4=MSEC
C                                           5=USEC
C
C COLUMNS 5-7  HORIZONTAL SCALE (UNITS PER INCH)
C COLUMNS 8-11 TIME WHERE PLOT STARTS
C COLUMNS 12-15 TIME WHERE PLOT ENDS
C COLUMNS 16-20 VALUE OF BOTTOM VERTICAL SCALE
C COLUMNS 21-24 VALUE OF TOP VERTICAL SCALE
C COLUMNS 25-48 UP TO FOUR NODE NAMES
C COLUMNS 49-64 GRAPH HEADING LABEL
C COLUMNS 65-80 VERTICAL AXIS LABEL
144 B 80      REC AREC BREC C
144 B 80      SEND ASEND BSEND I
BLANK CARD TERMINATING PLOT REQUESTS
BLANK CARD TERMINATING THE CASE

```

Table 8-22

INPUT DATA FOR SINGLE-POLE SWITCHING PROBABILITY RUNS

```

C FILE NAME: "L500STAT-5PS" SINGLE-POLE RECLOSING PROBABILITY RUN
C ONLY THE PHASE A BREAKER OPERATES.
C THE FAULT ARC IS ASSUMED TO BE EXTINGUISHED.
C
BEGIN NEW DATA CASE
C FIRST MISCELLANEOUS DATA CARD:
C 34567890123456789012345678901234567890123456789012345678901234567890
C   1-8   9-16  17-24  25-32
C T-STEP T-MAX  K-OPT  C-OPT
C SECNDS SECONDS O=MH   O=UF
C                               F(HZ)  F(HZ)
33.30E-6   .07   60.   0
C
C SECOND MISCELLANEOUS DATA CARD
C   1-8   9-16  17-24  25-32  33-40  41-48  49-56  57-64  65-72  73-80
C PRINT  PLOT  NETWORK  PR 55  PR MAX  I PUN  PUNCH  DUMP  MULT  DIAGNOS
C O=EACH O=EACH O=NO   O=NO   O=NO   O=NO   O=NO   INTO  NENERG  PRINT
C K=K-TH K=K-TH 1=YES 1=YES 1=YES 1=YES 1=YES 1=YES 1=NO 0=NO
C   5000   1     1     1     1     1     1     1     1     200
C
C IF ON MISC. CARD#2 "NENERG" COL. 65-72 IS NONZERO A THIRD MISC CARD MUST FOLLOW
C
C THIRD MISCELLANEOUS CARD (FOR STATISTICS DATA FOR THE SWITCHES)
C
C 34567890123456789012345678901234567890123456789012345678901234567890
C   1-8   9-16  17-24  25-32  33-40  41-48  49-56  57-64  65-72  73-80
C ISW  ITST  IDIST  AINCR  XM4XXM  DEGMIN  DEGMAX  STATFR  SIGMAX  NSEED
C   1     0     0     .05     5     0.     360.     60     3.     0
C
C LOCAL SOURCE (GENERATOR)
B26 AEQUL A .203
B26 BEQUL B .203
B26 CEQUL C .203
C MUTUALLY COUPLED SOURCE EQUIVALENTS
C 34567890123456789012345678901234567890123456789012345678901234567890
C                               SEQUENCE VALUES
C                               27-32  33-44
C                               R     L (FIRST ZERO, THEN POS SEQUENCE)
51LINE AEQUR A .50
52LINE BEQUR B 125.
53LINE CEQUR C
C REMOTE SOURCE EQUIVALENTS
51REM AEQRECA .50
52REC BEQRECB 125.
53REC CEQRECC
C
C FAULT AT THE RECEIVING END, PHASE A
FAULTA .01
C
C TRANSMISSION LINES
C 34567890123456789012345678901234567890123456789012345678901234567890
C                               27-32  33-38  39-44  45-50  CODE IN COLUMN "52"
C                               R     L     C     LE (LE=LENGTH)
C                               (ZERO, POSITIVE SEQUENCE)
-1B500 ALINE A .55801 .6722 .01268 90. 0
-2B500 BLINE B .0310 .5816 .01940 90. 0
-3B500 CLINE C
C 120 MILE LINE, FLAT CONFIGURATION
C 34567890123456789012345678901234567890123456789012345678901234567890
-1SEND AREC A .5294 1.7659 .01224 120. 0
-2SEND BREC B .02499 .59614 .01914 120. 0
-3SEND CREC C
C
14EQUR A 380281 . 60.0 30 -1.0
14EQUR B 380281 . 60.0 -90 -1.0
14EQUR C 380281 . 60.0 -210 -1.0
C REMOTE SOURCE
C   1     2     3     4     5     6     7
C 34567890123456789012345678901234567890123456789012345678901234567890
14EQRECA 380000 . 60.0 -12.4 -1.0
14EQRECB 380000 . 60.0 -132.4 -1.0
14EQRECC 380000 . 60.0 -252.4 -1.0
C
BLANK CARD TERMINATING SOURCE CAPS
C MODE VOLTAGE OUTPUT
C 34567890123456789012345678901234567890123456789012345678901234567890
SEND ASEND BSEND CREC AREC BREC C
FAULTAB26 AB26 BB26 C

```

Table 8-22 (Cont'd)

INPUT DATA FOR SINGLE-POLE SWITCHING PROBABILITY RUNS

```

BLANK CARD TERMINATING NODE VOLTAGE OUTPUT
BLANK CARD TERMINATING PLOT REQUESTS
C OUTPUT FOR THE "STATISTICS" CASE
C TRANSFORMER
C 345678901234567890123456789012345678901234567890
C   3-13 15-20 27-32 33-38 39-44 45-50
C REQUESTWORD BUS 1 FLUX BUS R-MAG
C TRANSFORMER 2 33 1137 X 3 E5
C
C   1-16 17-32
C CURRENT FLUX
C   2 33 1137.0
C   5.44 1250.0
C   23.33 1364.0
C   1579.00 2274.0
C   9999
C TRANSFORMER WINDINGS
C COLUMN 1,2: WINDING NUMBER
C 345678901234567890123456789012345678901234567890
C   3-8 9-14 15-24 27-32 33-38 39-44
C BUS1 BUS2 R-K L-K TURNS
C 1B500 A 27.55 11.66
C 2B26 AB26 E 2026 1
C TRANSFORMER X Y
C 1B500 B
C 2B26 BB26 C
C TRANSFORMER X Z
C 1B500 C
C 2B26 CB26 A
C PREINSERTION OF RECLOSING RESISTORS-NONE HAVE BEEN USED FOR THIS CASE(R= 001)
C B500 AAUX A .001
C REC AAUXR A .001
BLANK CARD TERMINATING BRANCH CARDS
C STATISTIC SWITCHES REPRESENTED AT PHASE A ONLY
C
C 34567890123456789012345678901234567890123456789012345678901234567890
C   3-8 9-14 15-24 25-34 55-64
C BUS1 BUS2 MFAN STANDARD
C CLOSING DEVIATION
C TIME MAIN.CONT
C B500 ASEND A .0165 .0014 STATISTICS
C *****
C ORDINARY SWITCH CARDS
C 34567890123456789012345678901234567890123456789012345678901234567890
C   3-8 9-14 15-24 25-34 35-44 45-54 55-64 65-74
C (OUTPUT OPTION IN COLUMN 80)
C NODE NAMES IE FLASHOVER SPECIAL REFERENCE
C OR VOLTAGE REQUEST SWITCH NAME
C BUS1 BUS2 CLOSE OPEN NSTEP WORD BUS5 BUS6
C SWITCHES NOT ALLOWED TO OPERATE
C AUX ASEND A .99 999.
C AUXR AREM A .99 999.
C REC AFAULTA .99 999.
C REC AREM A .99 999.
C BREAKERS ON PHASES B AND C NOT ALLOWED TO OPERATE (ASSUMED TO BE CLOSED )
C B500 BSEND B -1. 99.
C B500 CSEND C -1. 99.
C *****
BLANK CARD TERMINATING SWITCH CARDS
C SOURCE CARDS
C 34567890123456789012345678901234567890123456789012345678901234567890
C COLUMN 1,2: TYPE OF SOURCE 1 = 17.(E.G 11-13 ARE RAMP FUNCTIONS, 14 = COSINE)
C COLUMN 9,10: 0=VOLTAGE SOURCE, -1=CURRENT SOURCE
C   3-8 11-20 21-30 31-40 41-50 51-60 61-70 71-80
C NODE AMPLITUDE FREQUENCY TO IN SEC AMPL-A1 TIME-T1 T-START T-STOP
C NAME IN HZ DEGR SECONDS SECONDS SECONDS
C 14EQUA A 18863. 60 0 0. -1.0
C 14EQUA B 18863. 60 0 -120. -1.0
C 14EQUA C 18863. 60.0 -240. -1.0
C COLUMN 2 0 = NODE VOLTAGES
C -1 = BRANCH VOLTAGES
C 345678901234567890123456789012345678901234567890
C   3-14 15-20 21-26 27-32 33-38 39-44 45-50
C BASE VOLT BUS1 BUS2 BUS3 BUS4 BUS5 BUS6
C REQUEST FOR LINE-TO-GROUND HISTOGRAMS
C 1 PU NODE
C L-G NAMES
C 408270.SEND ASEND BSEND C
C 408271.REC AREC BREC C
C REQUEST FOR PHASE-TO-PHASE HISTOGRAMS
C 1 PU NODE

```

Table 8-22 (Cont'd)

INPUT DATA FOR SINGLE-POLE SWITCHING PROBABILITY RUNS

```

C      L-G   NAMES
-1     408268.SEND ASEND BSEND BSEND CSEND CSEND A
-1     408269.PEC  AREC  BREC  BREC  CREC  CREC  A
BLANK CARD TERMINATING STATISTICS OUTPUT
BLANK CARD TERMINATING THE CASE

```

8-8. LOAD REJECTION

8-8-1. Assumptions In Load Rejection Cases

When long, heavily-loaded transmission lines suddenly experience a loss of load at one end, a sustained power frequency voltage rise will result. The most severe condition is the one in which the line is the only radial feed from a generator to the system, and the breakers at the receiving (load) end of the line trip to initiate the load rejection. Because the line is assumed to be heavily loaded before the load rejection, shunt reactive compensation will be at its minimum value. The overvoltage in this case is brought about by two effects: a) the normal line voltage rise (Ferranti Effect) described in Section 8-9, compounded by b) the generator overspeed. The speed governors and the automatic voltage regulators on the generator will intervene, making the problem a complicated one to analyze. An exact solution requires, in addition to a model of the electrical system, models of the turbine-generator, governor, exciter, regulator, etc. Hence, the simulation of such a case on the EMTP requires an extensive use of TACS and the synchronous machine models as well as the electrical system. No examples will be presented due to the massive amount of data needed for the turbine-generator and its controls (exciter, voltage regulator, governor, etc.) in addition to the power system data. Instead, an approximate method is presented.

In the approximate method, it is assumed that the voltage, E_d'' , behind the subtransient reactance, X_d'' , remains constant at the pre-disturbance value. After a few cycles, the transient voltage, E_d' , becomes the voltage behind the transient reactance, X_d' . Neglecting the subtransient period, the action of the automatic controls, and losses, a reasonable starting value of E_d' is about 1.05 per-unit. This voltage then increases linearly with frequency. The sending end and receiving end voltages, V_{SEND} and V_{REC} , are a function of the line length, the line parameters (at an increased frequency due to the overspeed), and line compensation (series capacitance or shunt reactance).

The determination of the speed and electrical frequency of the generator is a difficult task. For steam turbine-generators, a rule of thumb for the maximum speed after full-load rejection is approximately 10%, attained in less than one second. Hence, a rate of frequency increase of 6 Hz/second is recommended as a conservative estimate. The 10% frequency increase is a reasonable upper limit because the generator breakers must be tripped at such a level to avoid mechanical damage to the turbines. In reality, the governor may limit the generator speed below this level. Nevertheless, a 10% overspeed is reasonable, and sustaining it for a prolonged time will determine the worst possible condition on nearby surge arresters. During the first second, it can also be conservatively assumed that the flux will not change.

For water-wheel generators, the maximum speed increase after full load rejection can be as high as 60%, but it takes up to 10 seconds to reach this level. A fast-acting voltage regulating system will reduce the excitation well before 10 seconds, and the maximum overspeed will be reached around 1 second. A reasonable increase of frequency for a water-wheel generator is about 15%.

Figure 8-25 shows the equivalent circuit for calculating the overvoltages due to load rejection. Figure 8-25a represents a simplified representation of the case where the line is represented by a π equivalent, with no series or shunt compensation. Figure 8-25b represents the same simplified system with shunt compensation at the two ends of the line and series compensation in the middle of the line.

From Figure 8-25, we find that when the frequency of the generator reaches a value, $f > 60$ Hz, assuming the initial value of $E_d' = 1.05$ per-unit, the sending end voltage, V_{SEND} , is given by

$$V_{SEND} = 1.05 \frac{f}{f_0} \frac{A}{A+B} \quad (8-11)$$

where:

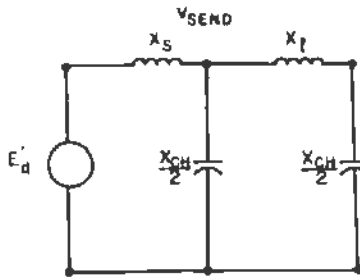
$$A = [X_{series} + X_{shunt}] \parallel X_{shunt} \quad (8-12)$$

$$X_{series} = X_L \frac{f}{f_0} - X_C \frac{f_0}{f} \quad (8-12a)$$

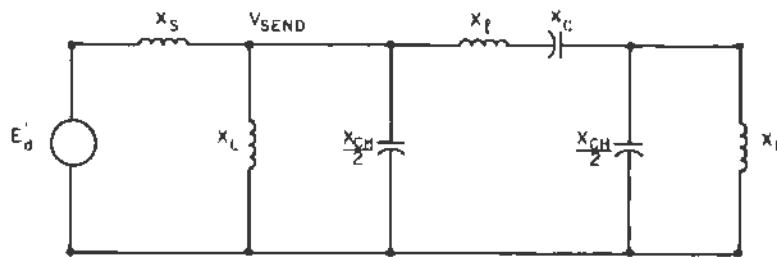
$$X_{shunt} = \frac{X_L X_{CH} \frac{f f_0}{f_0^2}}{X_{CH} \frac{f_0^2}{f^2} - 2 X_L \frac{f^2}{f_0^2}} \quad (8-12b)$$

$$B = (X_d' + X_{XFR}) \frac{f}{f_0} \quad (8-13)$$

and X_{XFR} refers to the generator stepup transformer reactance, so that X_S in Figure 8-25 is given by



a. Line with no shunt compensation.



b. Line with shunt compensation at both ends, and series capacitor compensation in the middle.

Figure 8-25. Simplified Equivalent Circuits for Calculating the Overvoltages Due to Load Rejection

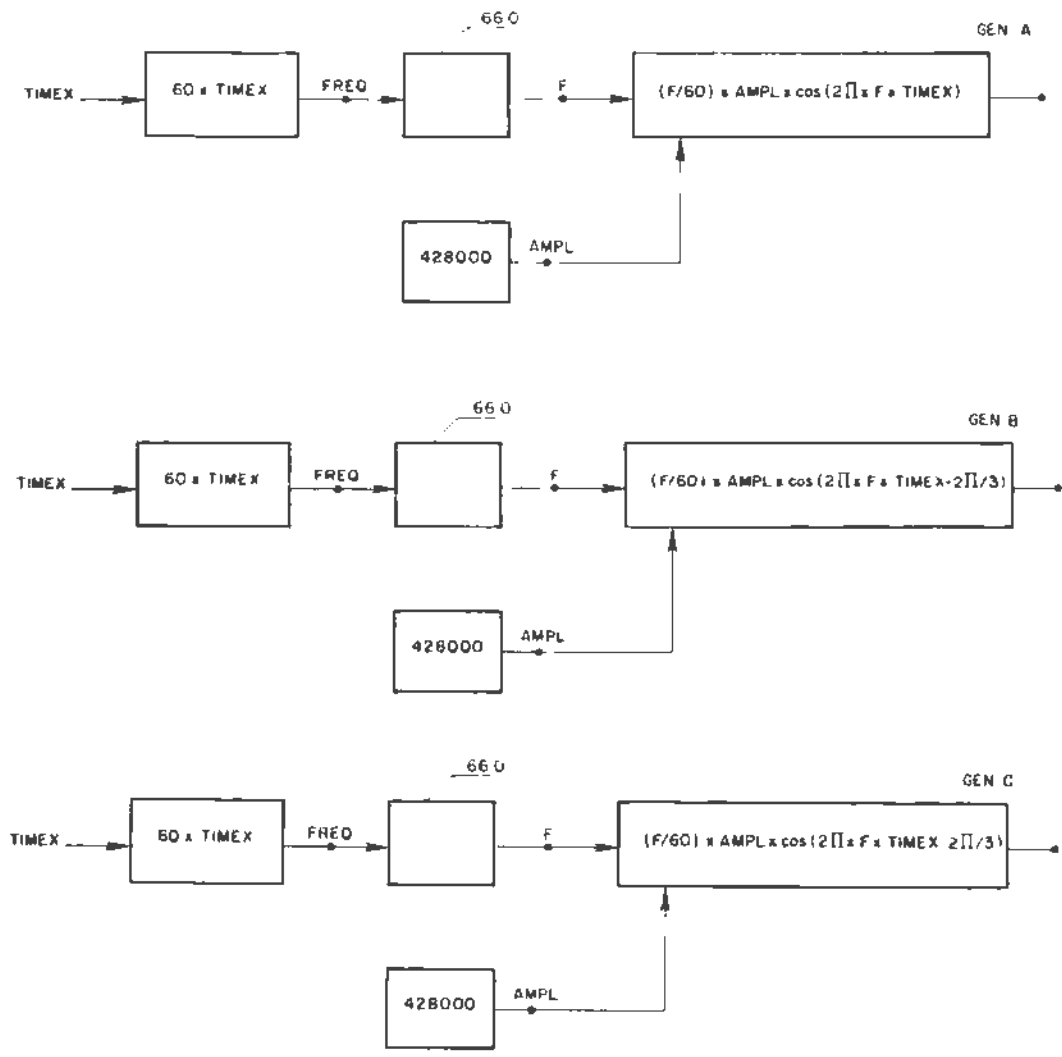


Figure 8-27. TACS Logic for Overspeeding Generator Due to Load Rejection

$$X_S = X_d' + X_{XFR} \quad (8-14)$$

The reactances in Equations 8-12 and 8-13 are at the power frequency, f_0 . The ratio f/f_0 may be assumed to be 1.1 for turbine-generators or 1.15 for water-wheel generators.

The rise in receiving end voltage is considered in Section 8-9 (Ferranti Effect).

8-8-2. Load Rejection Example

Figure 8-26 shows the schematic of the circuit used for the load rejection sample case. Per Section 8-8-1, the frequency is assumed to rise linearly to 66 Hz following load rejection at the receiving end. Voltage is also assumed to be proportional to the frequency in this range because the machine flux is constant. The case is simulated through the use of TACS, as depicted in Figure 8-27. The input data for this case is shown in Table 8-23. Figures 8-28 through 8-30 show the output parameters of interest for the case.

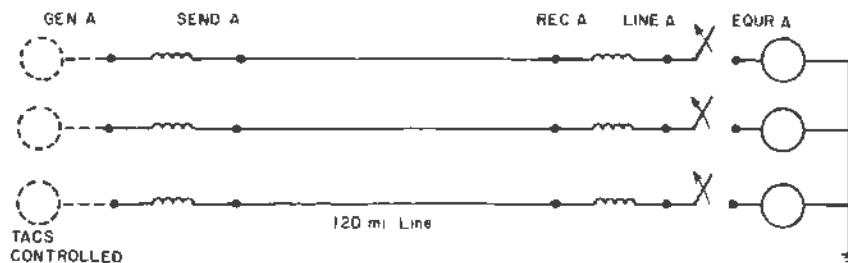


Figure 8-26. Circuit Used for Load Rejection Case

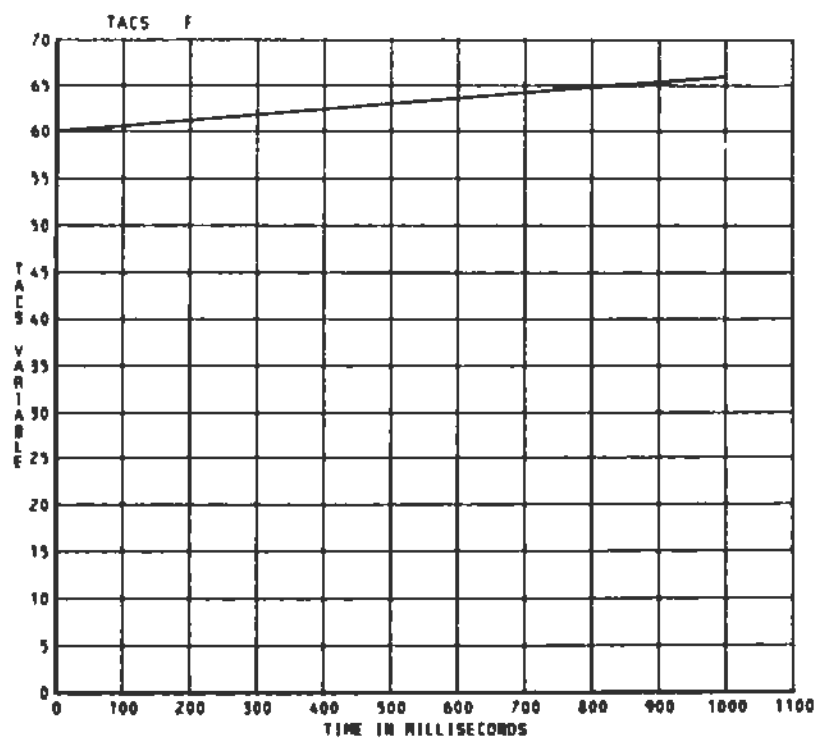


Figure 8-28. Frequency of Overspeeding Generator Due to Load Rejection

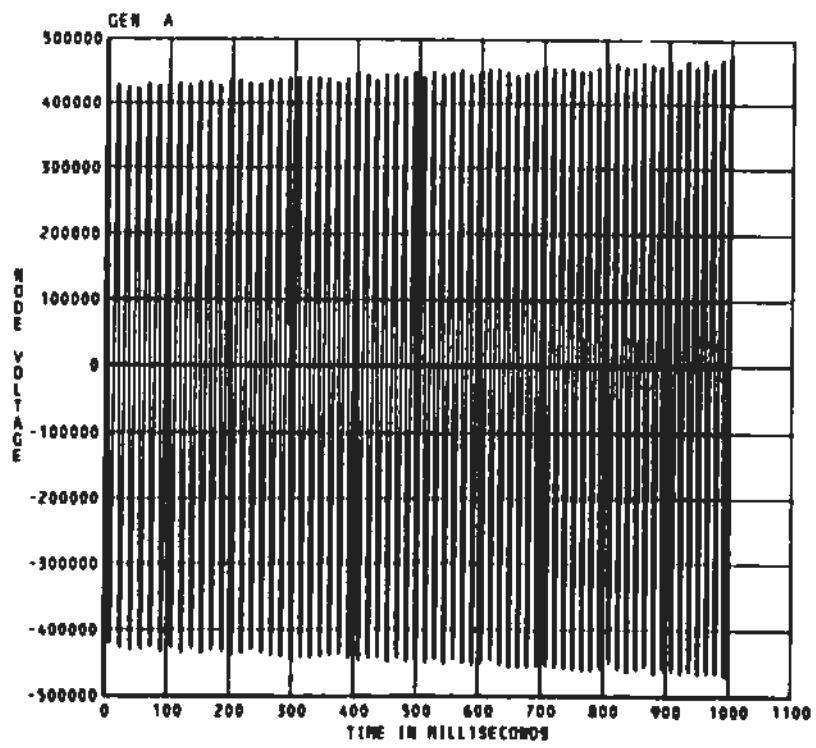


Figure 8-29a. Overspeeding Generator Terminal Voltage to Ground

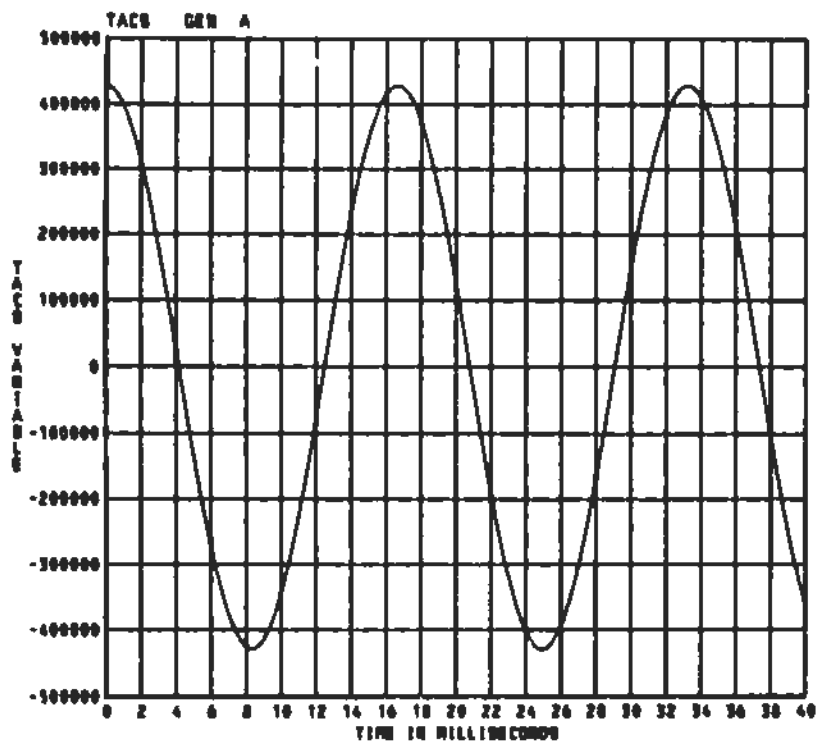


Figure 8-29b. Overspeeding Generator Terminal Voltage - Plotted Only to 40 Milliseconds to Show Details of the Waveform

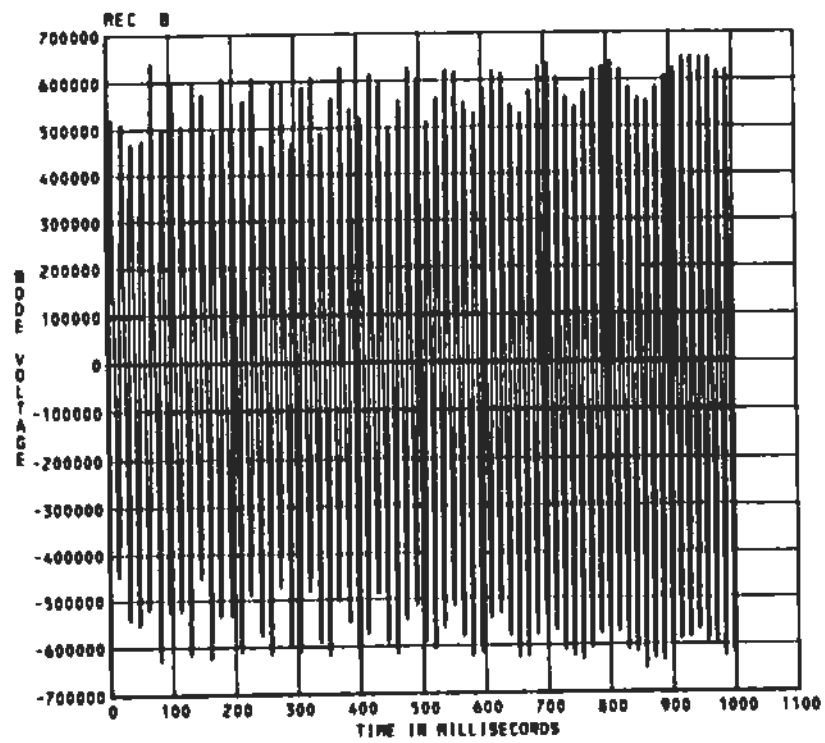


Figure 8-30. Receiving End Terminal Voltage After Load Rejection

Table 8-23

INPUT FOR THE LOAD REJECTION CASE

```

C FILE NAME: LOADREJ-1
C THIS FILE DESCRIBES SETTING UP AN APPROXIMATE MODEL FOR LOAD REJECTION CASES
C USING THE EMTP'S TACS FEATURE.
BEGIN NEW DATA CASE
C FIRST MISCELLANEOUS DATA CARD:
C 34567890123456789012345678901234567890123456789012345678901234567890
C   1-8   9-16  17-24  25-32
C T-STEP  T-MAX  X-OPT  C-OPT
C SECONDS SECONDS  O=MH  O=UF
C           F(HZ)  F(HZ)
C 66.E-6  1.0      60
C
C SECOND MISCELLANEOUS DATA CARD
C   1-8   9-16  17-24  25-32  33-40  41-48  49-56  57-64  65-72  73-80
C PRINT  PLD1 NETWORK  PR 55  PR MAX  I PUN  PUNCH  DUMP  MULTI. DIAGNOS
C O=EACH  O=EACH  O= NO  O= NO  O= NO  O= NO  O= NO  INTO  ENERG.  PRINT
C K=K-TH  K=K-TH  1=YES  1=YES  1=YES  1=YES  1=YES  DISK  STUDIES  O=NO
C 10000   17      1      1      1
C
C THE NEXT CARD SIGNALS THE INPUT OF TACS DATA
TACS HYBRID
C TACS SIMULTANEOUS FUNCTION BLOCKS
C N NAME          INPUT SIGNAL NAMES          GAIN          LIMITS
C (3-8) (12-17,20-25,28-33,36-41,44-49) (51-56) (57-62,63-68,69-74,75-80)
C   1      2      3      4      5      6      7
C 3456789012345678901234567890123456789012345678901234567890123456789
C THIS FUNCTION BLOCK CLAMPS THE OVERSPEED TO 66 HERTZ
99F      +FREQ      66
BLANK CARD ENDING TACS FUNCTIONS
BLANK CARD ENDING TACS SOURCES
C TACS SEQUENTIAL FUNCTIONS AND DEVICES
C TYPES: 98=OUTPUT GROUP
C        89=INPUT GROUP
C        88=INSIDE GROUP
C
C
C TYPE NAME CODE  INPUT SIGNAL NAMES          NUMERICAL PARAMETERS
C (1-2) (3-8) (9-10) (20-25,28-33,36-41,44-49) (51-56,57-62,63-68,69-74,75-80)
C
C OR, A FREE-FORMAT FORTRAN MATHEMATICAL EXPRESSION
C TYPE NAME          EXPRESSION
C (1-2) (3-8) (12-80)
C 3456789012345678901234567890123456789012345678901234567890123456789
C CALCULATION OF FREQUENCY DUE TO OVERSPEED
C AN INCREASE OF 6 HZ PER SEC AND A MAXIMUM LIMIT OF 10 PERCENT OVERSPEED
C ARE ASSUMED
C THE BUILT-IN TIMING SOURCE, TIMEY, IS USED
C   1      2      3      4      5      6      7
C 3456789012345678901234567890123456789012345678901234567890123456789
99FREQ  =60 +TIMEY*6.
C   1      2      3      4      5      6      7
C 3456789012345678901234567890123456789012345678901234567890123456789
98AMPL  = 428000
C CALCULATION OF VOLTAGE SOURCES
C GENA... PHASE A VOLTAGE GEN VOLTAGE
98GEN A  = (F/60.)*AMPL*COS(2.*PI*F*TIMEY)
C GENB... PHASE B VOLTAGE GEN VOLTAGE
98GEN B  = (F/60.)*AMPL*COS(2.*PI*F*TIMEY-2.*PI/3 )
C GENC... PHASE C VOLTAGE GEN VOLTAGE
98GEN C  = (F/60.)*AMPL*COS(2.*PI*F*TIMEY+2.*PI/3 )
BLANK CARD ENDING TACS DEVICES
C TACS OUTPUT VARIABLE REQUESTS
C NAMES
C (3-8,9-14, ...75-80)
C
C   1      2      3      4      5      6      7
C 3456789012345678901234567890123456789012345678901234567890123456789
FREQ F  GEN AGEN  BGENC
BLANK CARD ENDING TACS OUTPUTS
C INITIAL CONDITIONS FOR TACS VARIABLES
C NAME  INITIAL VALUE
C 3-8   11-20
C   1      2      3      4      5      6      7
C 3456789012345678901234567890123456789012345678901234567890123456789
FREQ  60.
F  60.
C INITIAL VOLTAGE ASSUMED TO BE AT 1.05 PU, ANGLE OF 0 DEGREES
GEN A  428000.
GEN B  214000.
GEN C  214000.
AMPL  428000.
BLANK CARD ENDING TACS INITIAL CONDITIONS. THIS ALSO TERMINATES TACS INPUT

```

Table 8-23 (Cont'd)

INPUT FOR THE LOAD REJECTION CASE

```

C
C BRANCHES
C 34567890123456789012345678901234567890123456789012345678901234567890
C   3-8  9-14 15-20 21-26 27-32 33-38 39-44
C   NODE NAMES  REFERENCE RES.  IND.  CAP.  (OUTPUT IN COLUMN 80)
C           BRANCH  MH  UF  I= 1
C   BUS1  BUS2  BUS3  BUS4  OHM  OHM  UMHO  V= 2
C                                           I,V 3
C                                           P,E 4
C ASSUME .30 PU FOR XD' AND XFORMER, DN 525-KV AND 500-MVA BASE
C   GEN  ASEND A           165
C   GEN  BSEND B           165
C   GEN  CSEND C           165.
C 120 MILE LINE, FLAT CDFIGURATION
C .....
C -1SEND AREC A           5294 1.7659 01224 120 0
C -2SEND BREC B           02499.59614.01914 120. 0
C -3SEND CREC C
C .....
C REMOTE SOURCE (MUTUALLY COUPLED)
C 34567890123456789012345678901234567890123456789012345678901234567890
C           SEQUENCE VALUES
C           27-32 33-44
C           R L (FIRST ZERO, THEN POS. SEQUENCE)
C 51LINE AEQR A           50.
C 52LINE BEQR B           125.
C 53LINE CEQR C
C BLANK CARD ENDING BRANCHES
C SWITCH CARDS
C 34567890123456789012345678901234567890123456789012345678901234567890
C   3-8  9-14 15-24 25-34 35-44 45-54 55-64 65-74
C           (OUTPUT OPTION IN COLUMN 80)
C   NODE NAMES  IE FLASHOVER  SPECIAL REFERENCE
C           OR VOLTAGE  REQUEST SWITCH-NAME
C   BUS1  BUS2  TIME TO  TIME TO  NSTEP
C           CLOSE  OPEN  WORD  BUS5  BUS6
C   REC  ALINE A  -1.  .020
C   REC  BLINE B  -1.  .020
C   REC  CLINE C  -1.  .020
C BLANK CARD ENDING SWITCHES
C SOURCE CARDS
C 34567890123456789012345678901234567890123456789012345678901234567890
C COLUMN 1,2: TYPE OF SOURCE 1 - 17,(E.G. 11-13 ARE RAMP FUNCTIONS, 14 = COSINE)
C COLUMN 9,10: 0=VOLTAGE SOURCE, -1=CURRENT SOURCE
C   3-8  9-14 11-20 21-30 31-40 41-50 51-60 61-70 71-80
C   NODE  AMPLITUDE FREQUENCY TO IN SEC  AMPL-A1  TIME-T1  T-START  T-STOP
C   NAME  IN HZ  DEGR  SECONDS  SECONOS  SECONOS
C THE TYPE 60 SOURCES ARE TACS-CONTROLLED.
C0GEN A
C0GEN B
C0GEN C
C THE TYPE 14 SINUSOIDAL SOURCES ARE FOR THE REMOTE "REJECTED" SYSTEM
C14EQR A  428000.  60 0  -30.  -1.0
C14EQR B  428000.  60 0  -150  -1.0
C14EQR C  428000.  60 0  -270  -1.0
C BLANK CARD ENDING SOURCES
C NODE VOLTAGE OUTPUT
C 34567890123456789012345678901234567890123456789012345678901234567890
C   3-8  9-14 15-20 21-26 27-32 33-38 39-44 45-50 51-56 57-62 63-68 69-74 75-80
C   BUS1  BUS2  BUS3  BUS4  BUS5  BUS6  BUS7  BUS8  BUS9  BUS10  BUS11  BUS12  BUS13
C 34567890123456789012345678901234567890
C   SEND ASEND BSEND CREC AREC BREC C
C   LINE ALINE BLINE C
C   GEN AGEN BGEN C
C BLANK CARD TERMINATING NODE VOLTAGE OUTPUT
C
C PLOTTING CARDS
C CALCOMP PLOT 2
C (CASE TITLE UP TO 78 CHARACTERS)
C 2 LOAD REJECTION WITH 10 PERCENT OVERSPEED
C 144 B. 80. REC AREC BREC C
C 144 B. 80. SEND ASEND BSEND C
C BLANK CARD TERMINATING PLDT REQUESTS
C BLANK CARD TERMINATING THE CASE

```

8-9. THE FERRANTI EFFECT

For steady-state conditions, the voltage at the receiving end of a long open-ended uncompensated transmission line will be higher than at the sending end. This is due to what is generally known as the Ferranti Effect. The receiving-end voltage, V_{REC} , can be approximately calculated by the following formula:

$$V_{REC} = V_{SEND} / \cos \beta \ell \quad (8-15)$$

where ℓ is the length of line and β is the phase factor, which is equal to approximately $7.2^\circ/100$ km or $11.59^\circ/100$ Mile.

As a reminder, the phase factor of Equation 8-15 is the imaginary part of the propagation constant, which is defined as:

$$\gamma = \sqrt{(R + j \omega L)(G + j \omega C)} = \alpha + j \beta \quad (8-16)$$

This constant is used to find the voltage at any point on the line at a distance z from a point where the travelling voltage and current are known, i.e.:

$$\begin{aligned} V(z) &= V_1 e^{-\gamma z} + V_2 e^{+\gamma z} \\ I(z) &= I_1 e^{-\gamma z} + I_2 e^{+\gamma z} \end{aligned} \quad (8-17)$$

where V_1 , V_2 , I_1 , and I_2 are the forward and backward (incident and reflected) voltages and current waves at a known point.

From Equation 8-16, it is evident that β is a function of the line parameters R , L , G , and C . Hence, any assumption that β is constant for all lines is invalid. In other words, an assumption that travelling currents and voltages on transmission lines have the same velocity (equal to the speed of light) regardless of the line parameters, is not strictly correct. As was seen in Figure 2-30, the velocity of the travelling waves varies for different lines. This means that one has to calculate the phase factor, β , for every line to determine Ferranti Effect.

As mentioned earlier, Equation 8-15 is a good first approximation. The speed of the travelling voltages and currents will be taken as the speed of light (300 m/μs or 984 ft/μs). One can then calculate β from simple relations:

$$\beta = 2\pi/\lambda \quad (8-18)$$

$$\lambda = c/f \quad (8-19)$$

where λ is the wave length, c is the speed of light, and f = 60 Hz. Equations (8-18) and (8-19) yield:

$$\lambda = 300 \text{ m}/\mu\text{s} \times \frac{1}{60 \text{ Hz}} = 5 \times 10^6 \text{ m} \quad (8-20)$$

and

$$\beta = \frac{2\pi}{5 \times 10^6 \text{ m}} \times \frac{360^\circ}{2\pi \text{ rad}} \times \frac{1000 \text{ m}}{\text{km}} = .072^\circ/\text{km} (.1159^\circ/\text{mile}) \quad (8-21)$$

or, in more convenient terms, 7.2°/100 km or 11.59°/100 mile.

Shunt reactors are commonly installed on transmission lines to compensate for the Ferranti Effect, particularly during periods of light load. The EMTP can replace traditional methods, such as A, B, C, D line constants, which are used for sizing shunt reactors. Only the steady-state solution is needed for this task, so the computational effort is inexpensive when compared to transient solutions. The best model to be used with such a phasor calculation consists of the cascaded pi-sections for untransposed lines. The easiest and most efficient way to make the calculation is to apply one volt to the sending end and monitor the voltage at the receiving end. Note that in some versions of the EMTP (eg., the UBCEMTP), the voltages in the steady-state phasor solution are RMS values. If this is the case, one should compare the voltages in the phasor solution to each other, rather than to the value of the voltage on the source input cards, which are in peak line-to-ground volts.

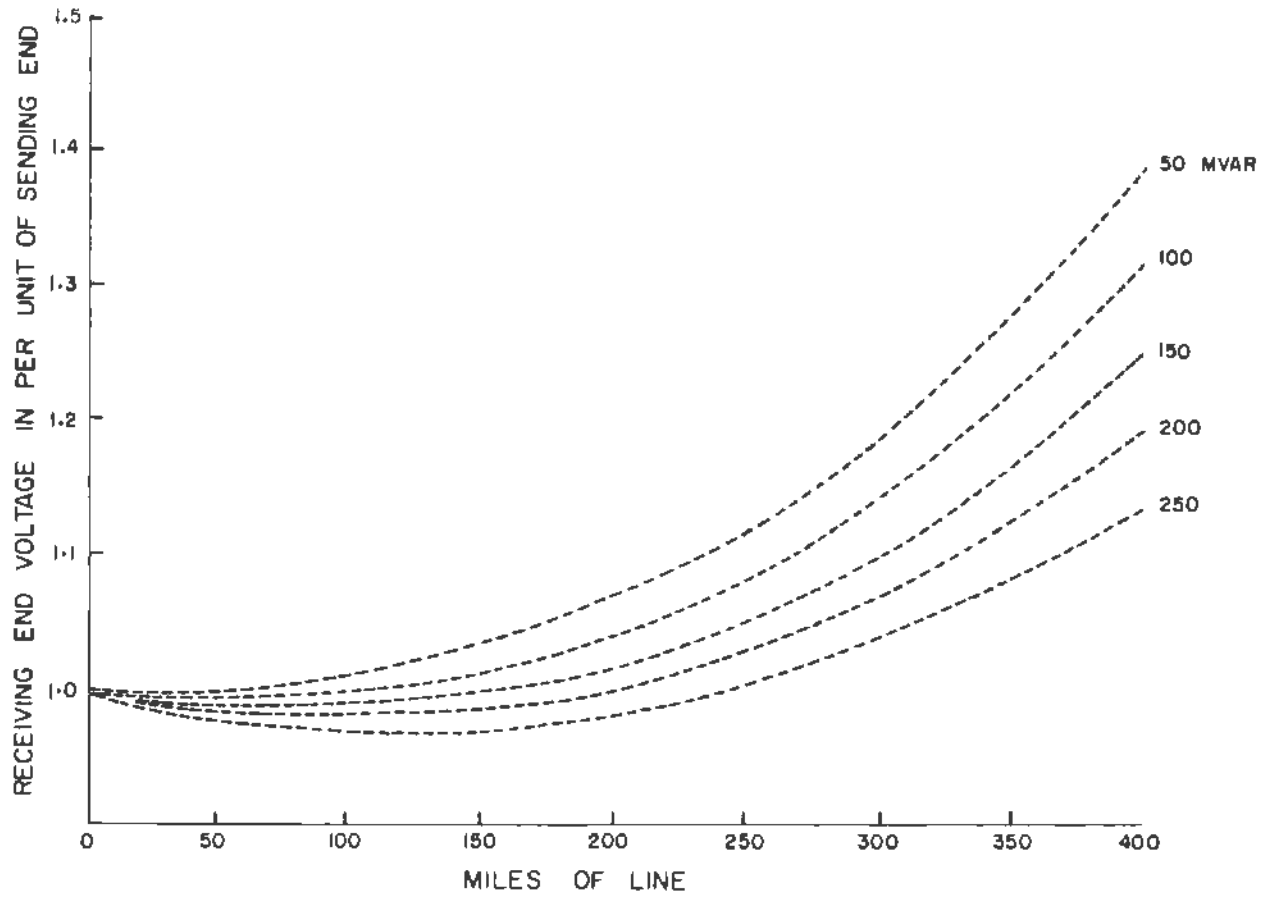


Figure 8-33. 60 Hz Rise in Receiving-End Voltage For An Unloaded 500-kV Line for Various Shunt Reactor Sizes and Different Line Lengths

The example in Figure 8-31 shows a circuit for illustrating the Ferranti Effect. In this example, the surge impedance of the line is assumed to be 280 ohms, and the resistance is assumed to be .05 ohms/mile. The source reactance is assumed to be 40 mH. From the equation,

$$C = \frac{1}{ZV} \quad (8-22)$$

where Z is the surge impedance of the line, and V is the velocity of propagation, the charging capacitance of the line can be calculated as .0189 $\mu\text{f}/\text{mile}$.

Table 8-24 shows the charging MVAR's for different line lengths. Figure 8-32 shows the charging MVAR's (solid line) for the different line lengths. This is also the 100% compensation line if shunt reactors are to be employed to counteract the line charging. Also shown in Figure 8-32 is the amount of shunt reactance for different levels of compensation. There are two uses for Figure 8-32. The first use is to determine the amount of compensation for typical 500-kV lines. One locates the line length and draws a vertical line to intersect the desired compensation level curve. The value of the compensation in MVAR's is then read from the vertical axis. The second use is to determine the areas of overcompensation and undercompensation given a certain size of shunt reactance. Here, one starts at the vertical axis and draws a horizontal line to intersect the compensation level. A vertical line is then drawn perpendicular to the horizontal axis, and the line length is determined. The area to the left of this vertical line represents overcompensation, while that to the right represents undercompensation.

Figure 8-33 shows the results of an investigation to determine the ratio $V_{\text{REC}}/V_{\text{SEND}}$ for different shunt reactance compensation levels. This was obtained with a very simple single-phase representation.

For the uncompensated line case, Table 8-25 shows a comparison between the results obtained from the EMTP and from Equation (8-15). The agreement of the results between the two methods is very good. Although not stated before, the ratio $V_{\text{REC}}/V_{\text{SEND}}$ is independent of the voltage level to a good first-order approximation. In the compensated cases, the $V_{\text{REC}}/V_{\text{SEND}}$ ratios for other voltage levels will be different.

Table 8-24

CHARGING CHARACTERISTICS FOR DIFFERENT LINE LENGTHS
(For a 500-kV Line)

	<u>C(μF)</u>	<u>X_c(ohms)</u>	<u>MVAR</u>
50	.945	2.8×10^3	89
100	1.89	1.4×10^2	178
150	2.835	9.35×10^2	267
200	3.78	7.02×10^2	356
300	5.67	4.68×10^2	534
400	7.56	3.51×10^2	712

Table 8-25

COMPARISON BETWEEN EMTP RESULTS AND THOSE OBTAINED
USING EQUATION 8-15

$$Z = 280, R = .05, X_C = 40 \text{ mH}$$

	<u>By EMTP Calculations</u>				<u>By Formula</u>
	<u>Source</u>	<u>Send</u>	<u>Rec.</u>	<u>V_{REC}/V_{SEND}</u>	<u>V_{REC}/V_{SEND}</u>
100	1.0	1.011	1.032	1.02	1.02
200	1.0	1.023	1.113	1.09	1.09
400	1.0	1.06	1.536	1.45	1.45
500	1.0	1.09	2.061	1.88	1.88
600	1.0	1.16	3.32	2.86	2.86

Note: All of the above voltages are in per-unit.

8-10. SWITCHING IMPULSE DESIGN

The following sections deal with the total design of the transmission line insulation. We will start with switching surge design in this section, and follow it by discussing the National Electric Safety Code (NESC), contamination and lightning designs. Section 8-14 will bring all of these requirements together.

Switching impulse design for transmission lines considers both phase-to-ground and phase-to-phase overvoltages. The basic design approach is similar for both. However, the design parameters are different. In essence, the design is based on

assuming an acceptable switching surge flashover rate (SSFOR) and then specifying the strike distance given the distribution of the SOV's. In this section, a simplified method developed by G. W. Brown in Reference 7 for switching impulses is described. This method, although approximate, is accurate enough for preliminary design. The final design should, of course, be made with more exact methods.

Before we introduce Brown's Method, let us review some of the basic probability distributions and definitions necessary for the SOV design.

The SOV's, as collected from probability runs on the EMTP, are considered as being all of positive polarity. In actual systems, it is expected that the positive and negative polarity SOV's have equal probabilities of occurrence. Laboratory tests in Reference 10 have shown that the tower strength for negative polarity switching impulses is significantly greater than that for positive polarity. Therefore, the SSFOR can be set equal to half of the probability of flashover of the line as determined from all the SOV's collected by the EMTP, i.e.

$$SSFOR = \frac{1}{2} \int P [FO,E] \quad (8-23)$$

$P [FO,E]$ is probability of a flashover on the line given that the SOV = E.

The statistical variations of the SOV's can be represented by any of the distributions shown in Table 8-26.

Table 8-26
TYPICAL DISTRIBUTIONS OF SWITCHING OVERVOLTAGES

<u>Distribution</u>	<u>Parameters</u>
Gaussian	μ_0, σ_0
Extreme Value - Positive Skew	u, β
Extreme Value - Negative Skew	u, β

The distributions are valid from $E = 1$ p.u. to $E = E_m$, where E_m is the maximum obtainable SOV. E_m is often assumed to be $E_2 + 2\sigma_0$ or $E_2 + 2\beta$, depending on the distribution used. E_m could also be taken as the maximum SOV obtained in an EMTP probability run. E_2 is defined as the statistical switching overvoltage, i.e., the probability of exceeding it is 2%, or $P[E \geq E_2] = .02$. Table 8-27 shows the values of E_2 for the distributions of Table 8-26.

Table 8-27

STATISTICAL OVERVOLTAGES FOR DISTRIBUTIONS OF TABLE 8-26

<u>Distribution</u>	<u>E_2</u>
Gaussian	$E_2 = \mu_0 + 2.053 \sigma_0$
Extreme Value (Positive Skew)	$E_2 = u + 3.902 \beta$
Extreme Value (Negative Skew)	$E_2 = u + 1.364 \beta$

The magnitude of the SOV varies with the distance from the sending end, and whether or not surge arresters, preinsertion resistors, shunt reactors, etc., are used. For an uncompensated line where no arresters are used, the SOV at the receiving end, E_R , is the highest, and it is customary to define the voltage at other points on the line as a per-unit of that voltage. Figure 8-34 shows the SOV profile on an uncompensated line. In this figure, E_S is the sending end voltage and E_R is the receiving end voltage.

The strength of tower insulation for switching impulses is defined in terms of the critical flashover voltage (CFO), at which the probability of flashover given $E = \text{CFO}$ is 50%. For wet conditions, the actual switching impulse CFO, CFO_{SI} , is given by:

$$\text{CFO}_{SI} = k (\delta)^n \frac{3450}{1 + 8/s} \text{ [kV]} \quad (8-24)$$

where S is the strike distance in meters and CFO_{SI} is in kV.

For fair weather, the CFO_{SI} is given by

$$\text{CFO}_{SI} = k (\delta/H_c)^n \frac{3450}{1 + 8/s} \text{ [kV]} \quad (8-25)$$

where $\delta = .997 - .106(A)$ (8-26)

and $\delta/H_c = 1.015 - .132(A)$ (8-27)

with A being the line altitude in km.

For center phase V-string insulators, the gap factor k is given by:

$$k = 1.25 + .005 \left(\frac{h}{s} - 6 \right) + .25 \left(e^{-8w/s} - .2 \right)$$
 (8-28)

Where w is the width of tower in m.

s is the strike distance in m.

h is the tower height in m.

For center-phase I-strings, $k = 1.3$.

For the outside phases, multiply the appropriate center-phase k by 1.08.

The SI strength is linear when plotted on cumulative normal probability paper; hence, the strength characteristic is considered normally-distributed, with $\sigma_f/CF0 = .05$. A statistical withstand voltage, V_3 , is defined as being $3\sigma_f$ away from the CF0, i.e.,

$$V_3 = CF0 \left[1 - 3 \frac{\sigma_f}{CF0} \right], \text{ or } V_3 = CF0 (.85)$$
 (8-29)

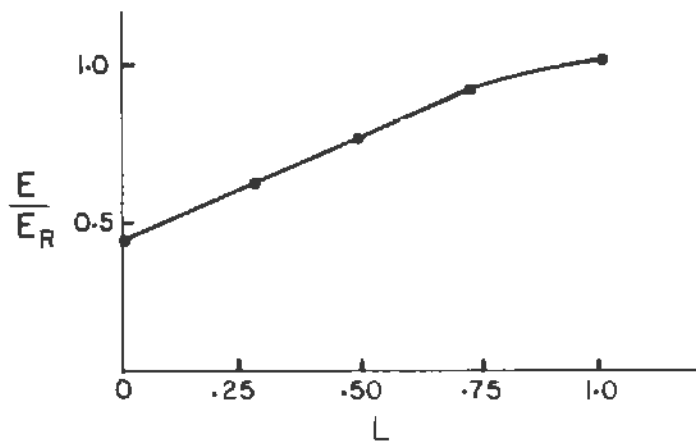


Figure 8-34. Typical Voltage Profile On An Uncompensated Line With No Surge Arresters

For switching as well as lightning impulses, per Reference 10, we have:

$$G_0 = \frac{CFO}{500 (s)} \quad (8-30)$$

Where CFO is for standard conditions ($T = 20^\circ\text{C}$, $P = 760$ mm of Mercury, and $h = 11g$ of water vapor per 1 m^3 of air).

G_0 is a constant such that for:

$$.3 < G_0 < 1, \text{ (the usual case), } n = \frac{G_0 (G_0 - .2)}{.8} \quad (8-31)$$

$$\text{and for } 1 < G_0 < 2 \quad n = \frac{3 - G_0}{2 G_0} \quad (8-32)$$

n is the coefficient to be used in Equations 8-24 and 8-25.

The essentials for using G. W. Brown's method are presented next. The user should refer to Brown's paper, Reference 7, for more details on this method.

Figure 8-35 shows the distribution of SOV's, $f_s(E)$, the strength distribution for 1 tower ($n = 1$), and the strength distribution for a line with n towers. Brown suggests that the strength distribution of n towers can be replaced with a single-valued function at the equivalent CFO for n towers, CFO_n . For this single-valued function, $\delta_{fn} = 0$ as seen in Figure 8-36. The shaded area is, therefore, the probability of flashover.

$$P (FO) = \frac{1}{2} \int_{CFO_n}^{E_m} f_s (E) dE \quad (8-33)$$

Equation (8-33) applies for any SOV distribution.

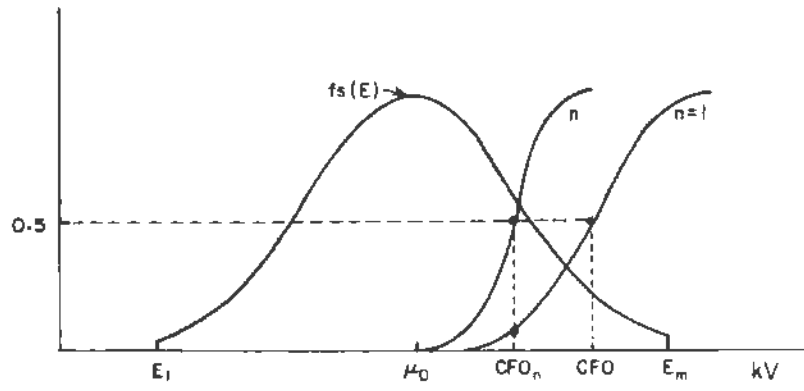


Figure 8-35. Distribution of SOV's Versus Tower Strength for One Tower and for n Towers

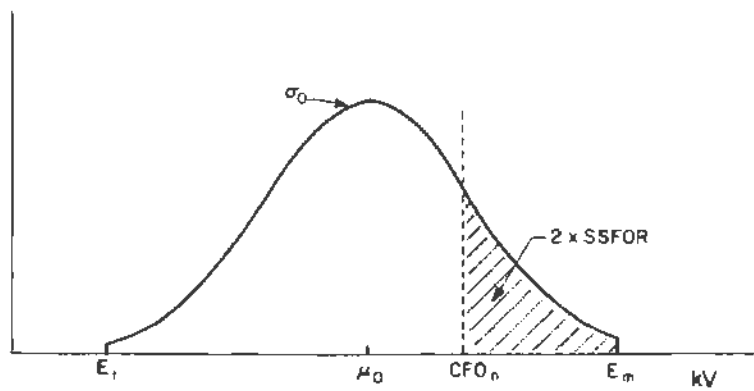


Figure 8-36. Brown's Assumption

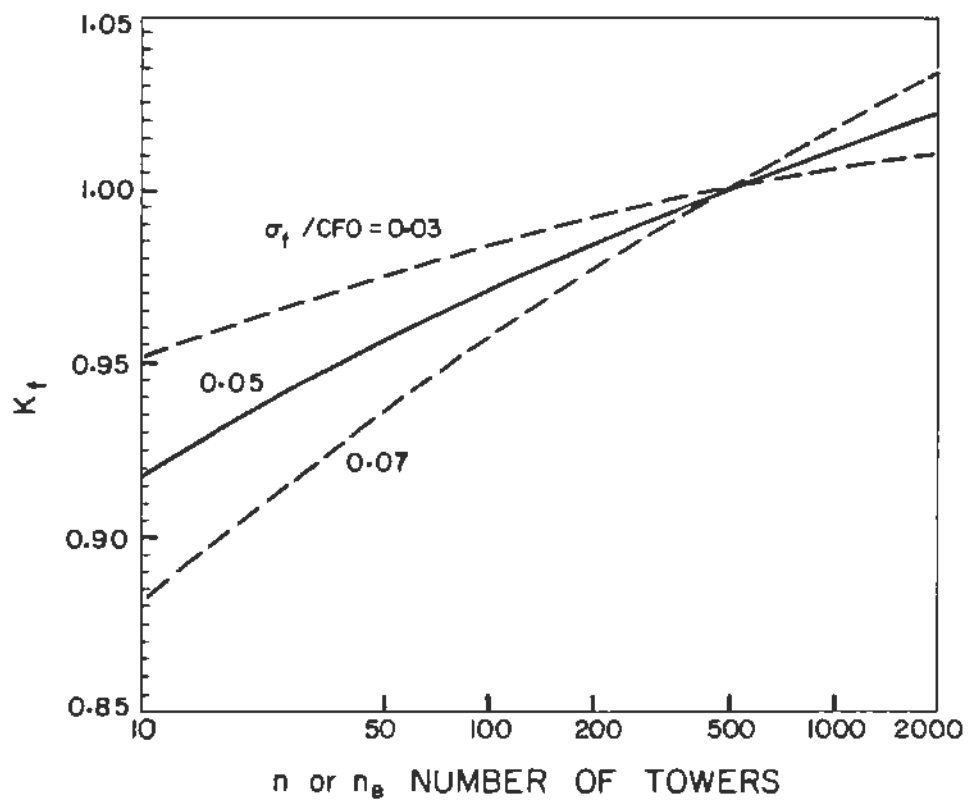


Figure 8-37. Constants for Use in Brown's Method

Brown assumes a linear SOV profile. If n towers have a linear SOV profile characterized by $\rho = E_S/E_R$, they are equivalent to n_e towers having a flat SOV profile characterized by $E_S = E_R$. The value n_e can be approximated by:

$$n_e = \frac{.4}{1-\rho} \frac{\sigma_f}{CFD} n \quad (8-34)$$

The design criterion, $\frac{V_3}{E_2}$, is defined as:

$$\frac{V_3}{E_2} = K_f K_G \quad \text{for a Gaussian SOV distribution.} \quad (8-35)$$

$$\frac{V_3}{E_2} = K_f K_E \quad \text{for an Extreme Value SOV distribution.} \quad (8-36)$$

K_f is shown in Figure 8-37 for three alternate values of $\frac{\sigma_f}{CFD}$.

Values of K_G and K_E are tabulated in Tables 8-28 and 8-29.

Table 8-28
THE CONSTANT K_G AS A FUNCTION OF THE SSFOR

SSFOR Per 100 Operations	K_G			
	$\sigma_f/E_2 = 0.05$	0.07	0.09	0.11
10	0.9394	0.9151	0.8909	0.8666
5	0.9614	0.9460	0.9305	0.9151
1	1.0000	1.0000	1.0000	1.0000
0.5	1.0137	1.0191	1.0246	1.0300
0.1	1.0412	1.0577	1.0742	1.0907

Table 8-29

THE CONSTANT K_E AS A FUNCTION OF THE SSFOR

SSFOR Per 100 Operations	K_E		
	$B/E_2 = 0.05$	0.07	0.09
10	0.8799	0.8319	0.7838
5	0.9174	0.8844	0.8514
1	1.0000	1.0000	1.0000
0.5	1.0349	1.0489	1.0628
0.1	1.1156	1.1618	1.2081

To apply this method in finding the design strike distance for switching impulses, start with the derived values of SSFOR and E_2 , and find V_3 . From V_3 , find the required CFO and the strike distance. For non-standard conditions, one has to iteratively determine the strike distance and the CFO under standard conditions, CFO_S , by Equations (8-24) through (8-32).

The following example illustrates the use of Brown's method.

Example: Determine the strike distances and insulator string length for a 500-kV tower for a design level of SSFOR = 1.0/100 operations. V-strings will be needed on all phases. The line altitude is 1.5 km. Other parameters are:

SOV: Gaussian, $E_2 = 1.8$ p.u., $\sigma_0/E_2 = 0.07$, $E_S/E_R = 0.80$
 Strength: $\sigma_f/CFO = 0.05$ $n = 250$ towers
 $h =$ height of conductor = 18 m $w = 1.6$ m

- $\delta = 0.997 - 0.106 (1.5) = 0.838$
 $n_e = (0.4/0.2)(0.05)(250) = 25$ and $K_f = 0.940$
 $K_G = 1.00$ $V_3/E_2 = 0.940$ $V_3 = 0.940(1.8)(408) = 690$ kV
 $CFO = 812$ kV (non-standard conditions)

- Center Phase:

$$k = 1.25 + 0.005 \left(\frac{18}{5} - 6 \right) + 0.25 \left(e^{-12.8/S} - 0.2 \right)$$

$$n = \frac{G_0 (G_0 - 0.2)}{0.8} \quad 0.3 \leq G_0 \leq 1 \quad G_0 = \frac{CF0_s}{500(s)}$$

$$CF0_s = 0.96 K \frac{3450}{1 + 8/s} \quad CF0 = (\delta)^n CF0_s$$

$$s = \frac{B}{\frac{0.96 k (\delta)^n 3450}{CF0 = 812} - 1}$$

Initial Guess: let $n = 0.5$, $k = 1.2$, and $s = 2.3$ m

Iterating:

\underline{s}	\underline{k}	$\underline{CF0_s}$	$\underline{G_0}$	\underline{n}	\underline{s}
2.3	1.21	895	.778	.562	2.31
2.31	1.21	898	.777	.561	2.31

For Center Phase, $s = 2.31$ m or 7.6 ft.

Insulator Length = $1.05 (2.31 \text{ m}) = 2.43 \text{ m} \rightarrow 17$ insulators

3. Outside Phase

$$CF0_s = 0.96 (1.08) K \frac{3450}{1 + 8/s} \quad CF0 = (\delta)^n CF0_s$$

$$s = \frac{B}{\frac{0.96 (1.08) k 3450 (\delta)^n}{812} - 1}$$

Initial Guess: let $n = 0.5$, $k = 1.2$, and $s = 2.08$ m

\underline{s}	\underline{k}	$\underline{CF0_s}$	$\underline{G_0}$	\underline{n}	\underline{s}
2.08	1.214	896	0.862	.713	2.15
2.15	1.213	919	0.855	.700	2.15

$s = 2.15$ m or 7.05 ft., Insulator Length = 2.26 m \rightarrow 16 Insulators

8-11. NESC DESIGN REQUIREMENTS

The transmission line clearances and strike distances obtained from lightning, switching, and contamination requirements have to be equal to or greater than those specified by the National Electric Safety Code (NESC) or any prevailing local code. In this section we will highlight the NESC's requirements as they apply to the electrical design of transmission lines.

The primary clearances specified by the NESC for transmission lines are the following:

1. Midspan Clearance

Clearance or strike distance between conductor and ground.

2. Tower Strike Distance

Clearance or strike distance from the conductor to the tower body, arm, truss, etc.

The specification of midspan clearance is clearly a safety-related distance, since the general public may walk or ride under a line. Although not explained in the NESC, the limitation on tower strike distance appears to be a safeguard for maintenance personnel.

8-11-1. Midspan Clearance

Midspan clearances are derived by first assuming some type of object, such as a person or truck, is beneath the conductor at the point of lowest clearance, i.e., the midspan. The height of this object is then added to the electrical clearance to obtain the total midspan clearance or strike distance to ground. Such reference heights are described in Table 8-30, which is based on Table 2, No. 232 of the 1984 NESC (Reference 11):

8-11-1-1. Midspan Clearances For Transmission Lines With Maximum Phase-to-Ground Voltages Between 15 and 50 kV

Categories 3 and 4 of Table 8-30 are usually used for the design. For distribution lines with phase-to-ground voltages of 15 to 50 kV, midspan clearances of 17 feet and 22 feet for categories 3 and 4, respectively, should be used based on the loading conditions shown in Table 8-31. For span lengths

exceeding these values, the clearance must be increased by 0.1 feet for each 10 feet of excess span. For example, with heavy loading and a span of 400 feet, the clearance must be increased by 2.3 feet.

Table 8-30
REFERENCE HEIGHTS

<u>Category</u>	<u>Reference Height, Ft.</u>
1. Railroad tracks	22
2. Streets, roads, parking lots	14
3. Spaces accessible only to pedestrians	9
4. Other land traversed by vehicles -- land such as farms, forests, orchards, etc.	14
5. Water - no sailing allowed	14
6. Water - suitable for sail boats	
(1) less than 20 acres	18
(2) 20 to 200 acres	26
(3) 200 to 2000 acres	32
(4) over 2000 acres	38
7. Launching or rigging sail boats	Add 5 ft. to the reference heights of Category 6 above

Table 8-31
SPAN LENGTHS

<u>Loading District</u>	<u>Span Length, Ft.</u>
Heavy	175
Medium	250
Light	350

8-11-1-2. Basic Clearances for Transmission Lines With Phase-to-Ground Voltages Between 50 and 470 kV

For transmission lines having maximum phase-to-ground voltages between 50 and 470 kV (up to 814-kV systems), the clearances listed in Table 8-30 must be increased by 0.4 inches per kV in excess of 50 kV. The increase in strike distance or clearance, Δs , is:

$$\Delta s = \frac{0.4}{12} (V_{LG} - 50) \text{ [ft.]} \quad (8-37)$$

This increase applies to line altitudes of up to 3300 feet. For each 1000 feet in excess of 3300 feet, Δs must be increased by 3%.

8-11-1-3. Basic Clearances for Transmission Lines With Phase-to-Ground Voltages above 470 kV

For voltages greater than 98 kV phase-to-ground (169.7-kV system), the NESC allows the use of an alternate method to the one described above. For voltages greater than 470 kV to ground (814-kV system), this alternate method must be used.

The alternate method of calculating or selecting the electrical component of clearance is by use of the equation:

$$s = 3.28 \frac{a(E_{2\theta})}{500 K}^{1.667} \cdot b \cdot c \quad (8-38)$$

where,

- s = strike distance to reference object in feet
- $E_{2\theta}$ = statistical SOV per breaker operation
- a = 1.15, an allowance for $3\sigma_f$ /CFO
- b = 1.03, an allowance for non-standard atmospheric conditions
- c = 1.2, a safety margin
- K = 1.15, the gap factor

Note that $E_{2\theta}$ is the statistical overvoltage (i.e., 2% of the SOV's exceed it) obtained per single-phase breaker operation. The more familiar and meaningful term E_2 , described before, is defined as the statistical overvoltage per three-phase breaker operation. Hence, we can conclude that the value of $E_{2\theta}$ is a value E_6 obtained from our typical distribution of SOV's per three-phase breaker operation, where E_6 is the voltage at which there exists a 6% probability of being exceeded.

$$E_{2\theta} = E_6 \quad (8-39)$$

Consider first that the SOV distribution is normal, then

$$E_2 = \mu + 2.054\sigma \quad (8-40)$$

$$E_6 = \mu + 1.555\sigma \quad (8-41)$$

Therefore:

$$E_{2\theta} = \frac{1 + 1.555 \frac{\sigma/\mu}{\sigma/\mu}}{1 + 2.054 \frac{\sigma/\mu}{\sigma/\mu}} E_2 \quad (8-42)$$

If, instead, the SOV distribution is an extreme value (positive skew)

$$E_2 = \mu + 3.902\beta \quad (8-43)$$

$$E_6 = \mu + 2.783\beta \quad (8-44)$$

Therefore:

$$E_{2\theta} = \frac{1 + 2.783 \frac{\beta/\mu}{\beta/\mu}}{1 + 3.902 \frac{\beta/\mu}{\beta/\mu}} E_2 \quad (8-45)$$

In either case, $E_{2\theta} < E_2$.

8-11-2. Tower Strike Distance

8-11-2-1. Basic Clearance

The basic clearance or strike distance specified by the NESC from the conductor to the tower side, arm, or truss is 11 inches plus 0.2 inches per kV of maximum system voltage exceeding 50 kV.

$$s = \frac{11}{12} + \frac{0.2}{12} (E_M - 50) \text{ [ft.]} \quad (8-46)$$

For preferred values of E_M , Table 8-32 applies. The clearances in Table 8-32 must be increased by 3% for each 1000 feet of altitude above 3300.

Table 8-32
CLEARANCES

E_M , kV Maximum System Voltage	s, Ft. Strike Distance
169	2.90
242	4.12
362	6.12
550	9.25
800	13.42
1200	20.08

The above clearances apply to insulators restrained from movement, such as V-strings or line posts. Where suspension insulators are used and are not restrained from movement, the above strike distances apply at the design swing angle. This angle should be based on a 6 lbf./ft.² wind, but may be reduced to 4 lbf./ft.² for "sheltered" locations.

8-11-2-2. Alternate Method

As in the case of the midspan clearances, an alternate method for determining the strike distance for lines with phase-to-ground voltages exceeding 98 kV (169.7 kV system) may be used. The alternate method of calculating the required strike distance is by the equation:

$$s = 3.28 \frac{a(E_{2\theta})^{1.667}}{500 K} \cdot b \quad (8-47)$$

where,

$E_{2\theta}$ = statistical SOV per breaker operation

K = 1.2, the gap factor for the center phase

b = 1.03, allowance for non-standard atmospheric conditions

a = 1.15, an allowance for $3\sigma_f$ /CFO for fixed insulator (e.g. V-string)

or,

a = 1.05, an allowance for $1\sigma_f$ /CFO for free-swinging insulator

The values of s calculated by Equations (8-46) and (8-47) must be increased 3% for each 1000 feet of altitude in excess of 1500 feet above mean sea level.

The alternate clearance from Equation (8-47) must not be less than that given in Table 8-32 for the 169-kV system, but, in any case, need not be greater than that given in Table 8-32 for the specific system voltage considered.

Equation (8-47) may be derived in a similar manner as was done for Equation (8-38) for midspan clearance. Note, however, that for fixed insulator strings such as the V-string, the basic design equation used is $V_3 = E_{2\theta}$ or $CF0 - 3\sigma_f = E_{2\theta}$. For the free-swinging insulator, the basic design equation changes to $CF0 - \sigma_f = E_{2\theta}$. In the case of the free-swinging insulator, the strike distance is applied after assuming that the insulator string has been deflected by the wind to a swing angle α . Table 8-33 shows the clearance as calculated by Equation (8-47). Note that clearances which are larger than those shown in Table 8-32 are replaced by the values of that table.

The swing angle, α , is calculated assuming a 6 lbf./ft.² wind pressure (which may be reduced to 4 lbf./ft.² in areas sheltered by buildings, terrain, and other obstacles). This rule applies not only to strike distances calculated using Equation (8-47), but also to the values of Table 8-32.

For a wind pressure, P , and a conductor weight per unit length, W , the force on the conductor caused by the wind pressure, F_{WD} , is:

$$F_{WD} = PDH \quad (8-48)$$

where D is the conductor diameter, and H is the horizontal or wind span length.

The force on the conductor caused by its weight is:

$$F_{WT} = WV \quad (8-49)$$

where V is the vertical or weight span length.

Therefore, the swing angle, α , is

$$\alpha = \tan^{-1} P \frac{D/W}{V/H} \quad (8-50)$$

For:

- P = wind pressure = 6 lbs./ft.²
- D = conductor diameter in inches
- W = conductor weight in lbs./ft.
- H and V in the same units of length

Then:

$$\alpha = \tan^{-1} 0.5 \frac{D/W}{V/H} \quad (8-51)$$

For more details about this section, refer to the 1984 NESC or any later edition.

Table 8-33

MINIMUM TOWER STRIKE DISTANCES
AS CALCULATED BY EQUATION (8-47)

Max. System Voltage, kV	$E_2/$ p.u.	E_2 , p.u. $\sigma/\mu = 9\%$	Min. Clearance or Strike, Ft.			
			Fixed Insulator		Free-Swinging	
362	2.0	2.08	4.16		3.57	
	2.2	2.29	4.88		4.19	
	2.4	2.49	5.64		4.84	
	2.6	2.70	*	6.12	*	
	2.8	2.91	*	6.12	*	6.12
	3.0	3.12	*	6.12	*	6.12
550	1.4	1.46	4.61		3.96	
	1.6	1.66	5.76		4.95	
	1.8	1.87	7.01		6.02	
	2.0	2.08	8.35		7.18	
	2.2	2.29	*	9.25	8.42	
800	1.4	1.46	8.61		7.40	
	1.6	1.66	10.76		9.24	
	1.8	1.87	13.09		11.25	
	2.0	2.08	*	13.42	13.41	
1200	1.4	1.46	16.93		14.54	
	1.5	1.56	18.99		16.31	
	1.6	1.66	*	20.08	18.17	
	1.7	1.77	*	20.08	*	20.08
	1.8	1.87	*	20.08	*	20.08

* Use values given in Table 8-32.

8-12. SUGGESTED DESIGN PROCEDURE FOR CONTAMINATION ON INSULATORS OF TRANSMISSION LINES

Contamination flashovers occur on transmission lines when line insulators become coated with a wet conducting film containing dissolved salts of many kinds, the most common of which is sodium chloride. The conditions primarily responsible for flashovers are fog, dew, and drizzle--heavy rain is beneficial when it washes away surface deposits. Rain water is not usually conductive enough by itself to cause flashover, nor are any dry salt deposits by themselves. Flashover will occur when the salt deposits which build up slowly create a conductive film in the presence of fog, dew, or any other atmospheric moisture. An excellent review of the contamination flashover mechanism is found in Reference 3. The balance of this section deals with the contamination design requirements.

8-12-1. Power Frequency Contamination Requirements

The power frequency requirements for the design of transmission lines are specified by the creepage distance per kV of line-to-ground voltage (based on the maximum system voltage) needed for contamination. The best known and most reliable method to meet the contamination requirements is to analyze data from existing lines. The thought process here is that if an existing line has a satisfactory 60-Hz contamination performance, its design, in terms of creepage/kV, can be copied in the new line. Because this is a 60-Hz phenomena, it is nearly a linear one, and it follows that the required creepage/kV is constant regardless of the voltage level of the line.

It is not always possible to use this method in determining the 60-Hz requirements if documented data is lacking or there are no existing lines in the area where the new lines are to be built. In such conditions, the design engineer should resort to some guidelines established through the testing and experience of others. The first task is to determine if the area traversed by the line falls into any of the following categories:

- 1) None to very light contamination.
- 2) Light contamination.
- 3) Light to moderate contamination.
- 4) Moderate contamination.
- 5) Heavy contamination.

To define the above categories, a quantity referred to as the Equivalent Salt Deposit Density (ESDD) has been defined. The ESDD is measured in mg/cm^2 . For more information about the ESDD and other measures of contamination, refer to References 3, 6, and 8. Table 8-34 describes the range of the ESDD parameter as a function of the contamination category.

Table 8-34
RANGES OF THE EQUIVALENT SALT DEPOSIT DENSITY, ESDD

<u>Area Description</u>	<u>ESDD Range mg/cm^2</u>
None to Very Light Contamination	0 - .03
Light Contamination	.03 - .06
Moderate Contamination	.06 - .1
Heavy Contamination	Over .1

Having quantified the contamination category in terms of the ESDD, it is now necessary to give some guidelines for the required creepage to obtain satisfactory performance.

Reference 3 summarizes some test results from different lines for different contamination levels. Figure 8-38 shows the 50% flashover voltage, V_{50} , in per-unit of the insulator or connection length. In order to interpret the curves of Figure 8-38, the kV/m for a given ESDD is simply multiplied by the length of the insulator. For example, at $\text{ESDD} = .05 \text{ mg}/\text{cm}^2$, the V_{50} for the standard insulator in an I-string configuration would be $(104 \text{ kV}/\text{m}) \times (.146 \text{ m}/\text{ins.}) = 15.2 \text{ kV}/\text{insulator}$.

The IEEE suggests a preliminary design guide for the power frequency strength of contaminated insulators in terms of the withstand voltage in kV/m of the insulator string vs. the ESDD. This is depicted in Figure 8-39, which is obtained from Figure 8-38 by defining the withstand voltage as the level 30% below V_{50} (approximately $V_{50} - 3\sigma$).

Table 8-35 shows the recommended creepage based on the ESDD values from Reference 3 and a CIGRE Working Group 04 Study Committee Report. Table 8-36 from Reference 3 shows the recommended number of standard insulators for 230-kV and 500-kV lines. These values correspond to values used in the field.

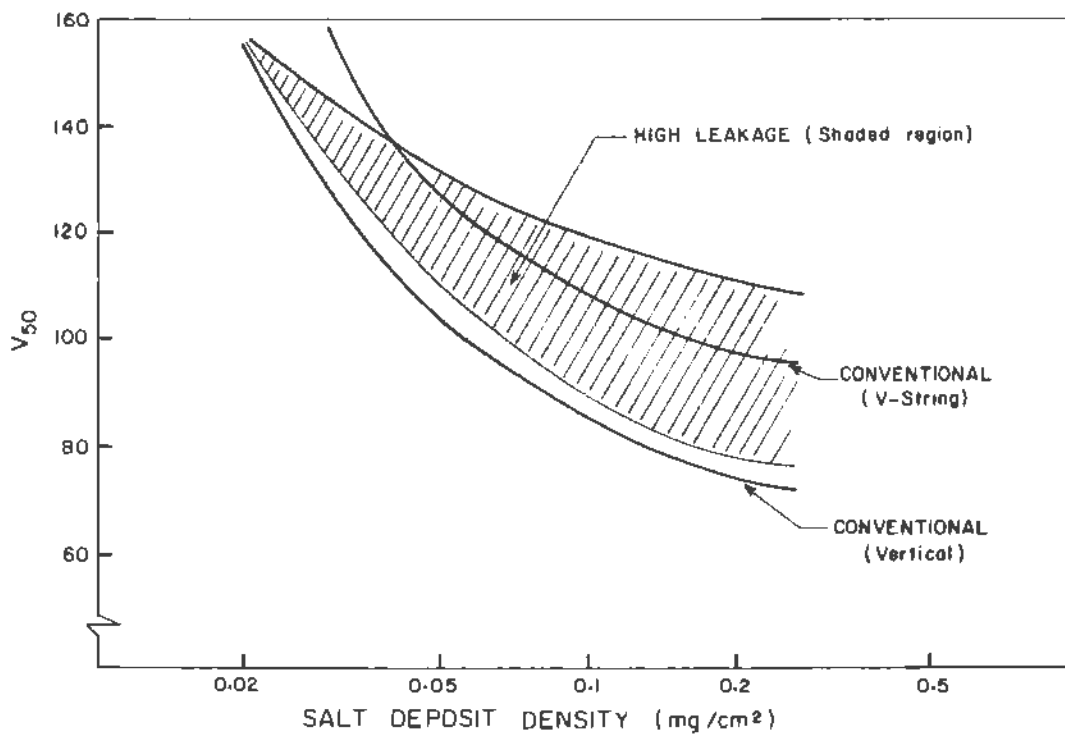


Figure 8-38. 50% Flashover Voltage, V_{50} , in Per-Unit of the Insulation Length As a Function of ESDD⁽³⁾

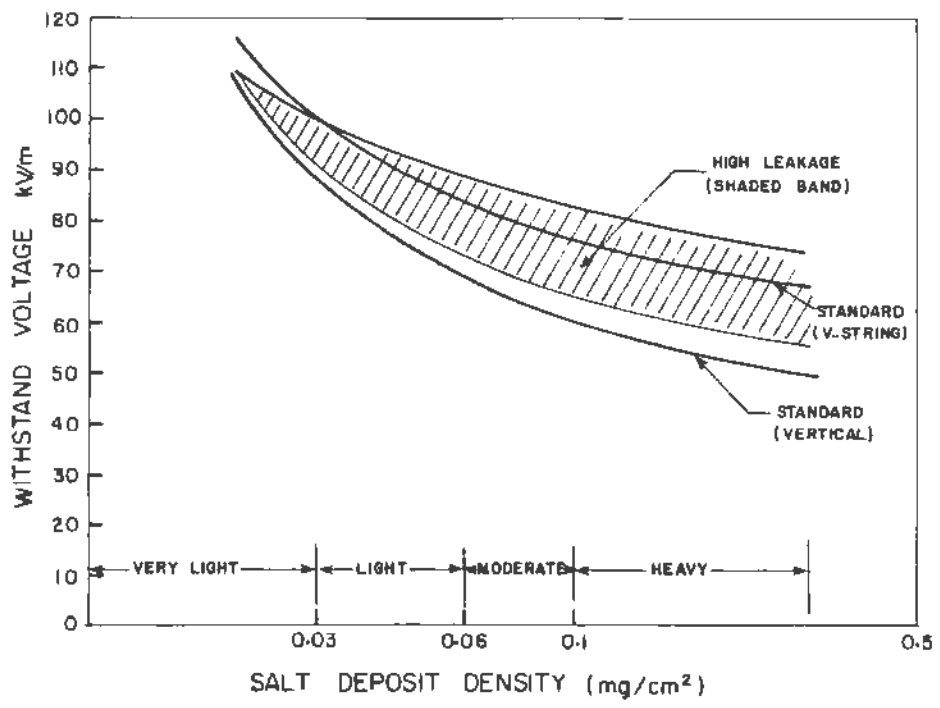


Figure 8-39. Withstand Voltage for Different Insulators Under Different Contamination Conditions (3)

Table 8-35

REQUIRED SPECIFIC CREEP - Inches/kV_{LG}
(cm/kV_{LG})

	Severity (mg/cm ²)	Insulators		V-String	Salt-FOG
		IEEE	CIGRE	IEEE	CIGRE
Very Light	0.02	.75 (1.90)	.75 (1.90)	.71 (1.80)	1.17 (2.97)
	0.03	.95 (2.40)	.87 (2.22)	.83 (2.10)	1.22 (3.10)
Light	0.06	1.22 (3.10)	1.13 (2.88)	1.00 (2.60)	1.48 (3.76)
Moderate	0.10	1.39 (3.50)	1.37 (3.50)	1.09 (2.80)	1.65 (4.19)
Heavy	0.30	1.67 (4.20)	2.08 (5.27)	1.25 (3.20)	2.10 (5.33)

- Notes: (1) For IEEE - For use only with 5-3/4" x 10" units.
 (2) CIGRE - Applies for all insulators.
 (3) CIGRE Salt Fog - Pollution severity is measured in kg/m³ of salinity.
 (4) CIGRE

$$\text{Creep} = 3.26 (\text{ESDD})^{.3756}$$

[in/kV_{LG}] [mg/cm²]

$$\text{Creep} = 0.937 (\text{salinity})^{.2158}$$

[in/kV_{LG}] [kg/m³]

Table 8-36

RECOMMENDED NUMBER OF STANDARD INSULATORS FOR 230-kV and 500-kV
LINES BASED ON POWER FREQUENCY CONTAMINATION CONSIDERATIONS

Voltage kV	Contamination ₂ Severity (mg/cm ²)	Standard Vertical		Standard V-String		Range of Lengths for High Leakage Vertical	
		String Length m (ft)	No. of Insulators	String Length m (ft)	No. of Insulators	String Lengths from m (ft) to m (ft)	
230 ϵ - ϵ 146 _{max} ϵ -g	Very light < 0.03	1.68 (5.51)	12	1.48 (4.85)	10	1.48 (4.85)	1.60 (5.25)
	Light 0.03-0.06	2.16 (7.08)	15	1.78 (5.83)	12	1.66 (5.43)	1.97 (6.47)
	Moderate 0.06-0.01	2.46 (8.06)	17	1.95 (6.39)	13	1.78 (5.83)	2.28 (7.48)
	Heavy > 0.01	2.96 (9.70)	20	2.21 (7.25)	15	2.00 (6.56)	2.60 (8.53)
500 ϵ - ϵ 3.18 _{max} ϵ -g	Very light < 0.03	3.66 (12.00)	25	3.23 (10.58)	22	3.23 (10.58)	3.49 (11.44)
	Light 0.03-0.06	4.71 (15.45)	32	3.88 (12.79)	27	3.62 (11.87)	4.29 (14.09)
	Moderate	5.36 (17.59)	37	4.25 (13.94)	29	3.88 (12.73)	4.97 (16.30)
	Heavy	6.45 (21.15)	44	4.82 (15.80)	33	4.36 (14.30)	5.67 (18.59)

* The 230-kV insulation levels are based on the current practice of 146-kV ϵ -g maximum voltage. If the new standards of 140-kV ϵ -g maximum were used, insulation levels in the table could be reduced by 4% for this voltage class.

8-12-2. Switching Surge Impulse Strength of Contaminated Insulators

The strength of contaminated insulators under switching surge conditions is less well known than the power frequency strength. Limited field and laboratory data, however, seem to indicate that the ratio of the switching surge to power frequency strength in terms of crest line-to-ground values varies from about 2 for heavy contamination to about 3 for light contamination. Hence, one can conclude that if the line insulation is based on the power frequency strength in contaminated conditions, the switching surge requirement will be met in most conditions.

8-12-3. Lightning Impulse Strength of Contaminated Insulators

It is believed that lightning strength of insulators is unaffected by contamination. Hence, contamination requirements are not considered in lightning impulse design.

8-12-4. Leakage Distances For Different Insulators

Table 8-37 shows the leakage distance in mm for the different insulator shapes and types shown in Figure 8-40. Both the table and the figure are from Reference 8.

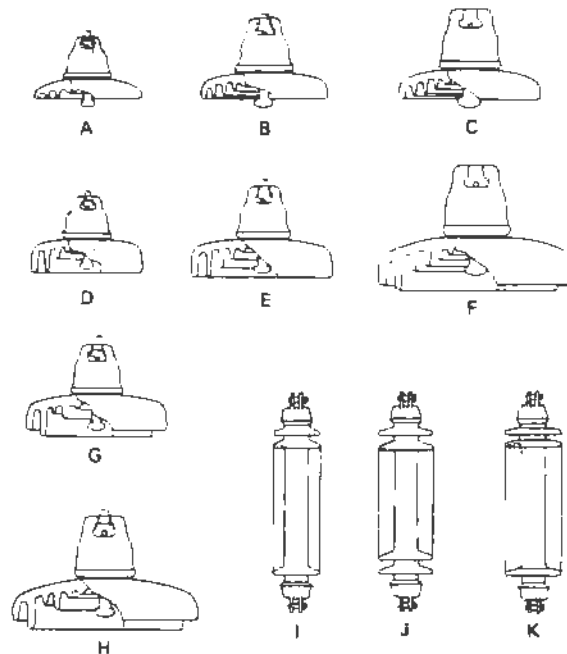


Figure 8-40. Outline of Shapes of Tested Insulators in Table 8-37

Table 8-37
LEAKAGE DISTANCES FOR DIFFERENT INSULATORS⁽⁸⁾
TESTED INSULATORS

Type	Shape	Unit Spacing (mm)	Shed Diameter (mm)	Leakage Distance (mm)
A	250 mm Standard Disc	146	254	280
B	280 mm Standard Disc	170	280	370
C	320 mm Standard Disc	195	320	425
D	250 mm Fog Disc	146	254	430
E	320 mm Fog Disc	170	320	550
F	400 mm Fog Disc	195	400	690
G	320 mm DC Fog Disc	165	320	510
H	420 mm DC Fog Disc	195	420	640
I	Standard Longrod	1,025	160	2,140
J	Longrod	1,025	180	2,530
J'	Longrod	875	180	2,085
K	Longrod Fog	1,025	200	3,215
K'	Longrod Fog	875	200	2,670

8-13. LIGHTNING IMPULSES

Lightning-induced flashovers on transmission lines are divided into two groups:

- a) Those attributed to direct strokes to the phase conductors, better known as Shielding Failures.

- b) Those attributed to strokes to the tower or shield wires, which charge the potential of the tower structure enough to cause flashover to the phase conductor.

This latter phenomena is usually referred to as backflashover, and is the main concern in specifying line insulation, since most new transmission lines are now designed for "perfect shielding."

In order to use the EMTP for lightning impulse design, one has to know the parameters of the first and subsequent lightning strokes. A recommended set of parameters are given in Table 8-38 below. It is believed that the stroke current distribution and steepness are best represented by Log-Normal distributions whose parameters are presented in Table 8-38. For reference, the Log-Normal distribution is of the form:

$$f(I) = \frac{1}{\sqrt{2\pi} \beta} e^{-\frac{1}{2} \left[\frac{\ln(I-I_0) - \ln M}{\beta} \right]^2} \quad (8-52)$$

for the crest current parameter. I_0 represents the minimum current of a stroke and is usually taken as 3 kA. For the other parameters, the equivalent quantity is zero. The correlation coefficient, ρ , in Table 8-38 is that between the crest current magnitude and the steepness. There is no correlation between the magnitudes of the first and subsequent strokes.

Table 8-38

SUGGESTED DISTRIBUTIONS OF LIGHTNING FLASHES FOR ENGINEERING USE

	Crest Current kA		Time to Crest usec		Steepness kA/usec		Correlation Coefficient ρ	Given Current Current	
	M	β	M	ρ	M	β		M	β
	I	f	t	t	s	s		S/1	S/1
<u>First Stroke</u>									
3 < I < 20 kA	61	1.33	2.51	1.23	24.3	0.60	0.38	12.01 ^{0.17}	.555
I > 20 kA	33.3	0.605	1.37	0.671	24.3	0.60	0.38	6.48 ^{0.38}	.555
<u>Subsequent Strokes</u>									
	12.3	0.52	0.308	0.706	39.9	0.85	0.55	4.191 ^{0.90}	.704

With the lightning flash distribution known, the user can set up cases as illustrated in Section 4 of the EMTP Primer to find the voltages across the different phase insulators, and determine if flashover would occur. The probability of flashover given the stroke current is calculated and multiplied by the number of strokes to the line per year to obtain the lightning flashover rate (LFOR).

The method outlined above was followed in Section 4 of the Primer, and will not be repeated here. In addition to this detailed procedure for determining the LFOR, the IEEE offers a simplified method which does not use the EMTP, but uses a program obtainable from the IEEE as documented in Reference 2. This procedure is approximate, but yields results which are accurate enough for performance analysis and parameter evaluations, as seen from Table 8-39. It is recommended that the user obtain this IEEE program and use it in conjunction with the more detailed method outlined here and in the Primer.

Table 8-39

CALCULATED VS. ACTUAL LIGHTNING TRIPOUT RATES PER 100 KM PER YEAR

<u>Line Name</u>	<u>Actual Tripout Rate</u>	<u>Predicted Tripout Rate (1)</u>
Johnsonville-Cordova 500-kV	0.30	0.40
Browns Ferry-West Point 500-kV	0.94	1.50
South Jackson-Cordova 161-kV	0.55	0.48
Sequayah-Charleston 161-kV	3.83	3.90
CIGRE Line #30 - 230 kV	0.24	0.14 (2)
CIGRE Line #31 - 345 kV	3.44	2.48 (2)

- NOTE: 1. Calculated by dividing the line into 4 or 5 component parts by tower type or footing resistance distribution.
2. Data not available for detailed modeling.

In closing this section, Figures 8-41 and 8-42, taken from Reference 2, are provided as initial estimates for LFOR analysis.

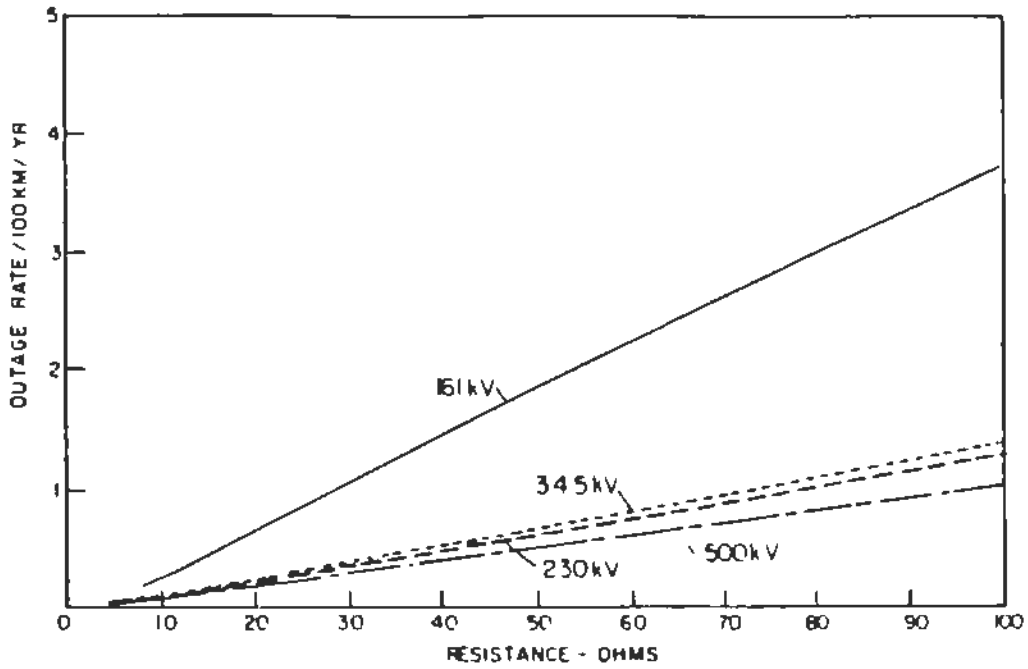


Figure 8-41. Lightning Outage Rates for Single-Circuit Horizontal Lines Versus Tower Footing Impedance ⁽²⁾

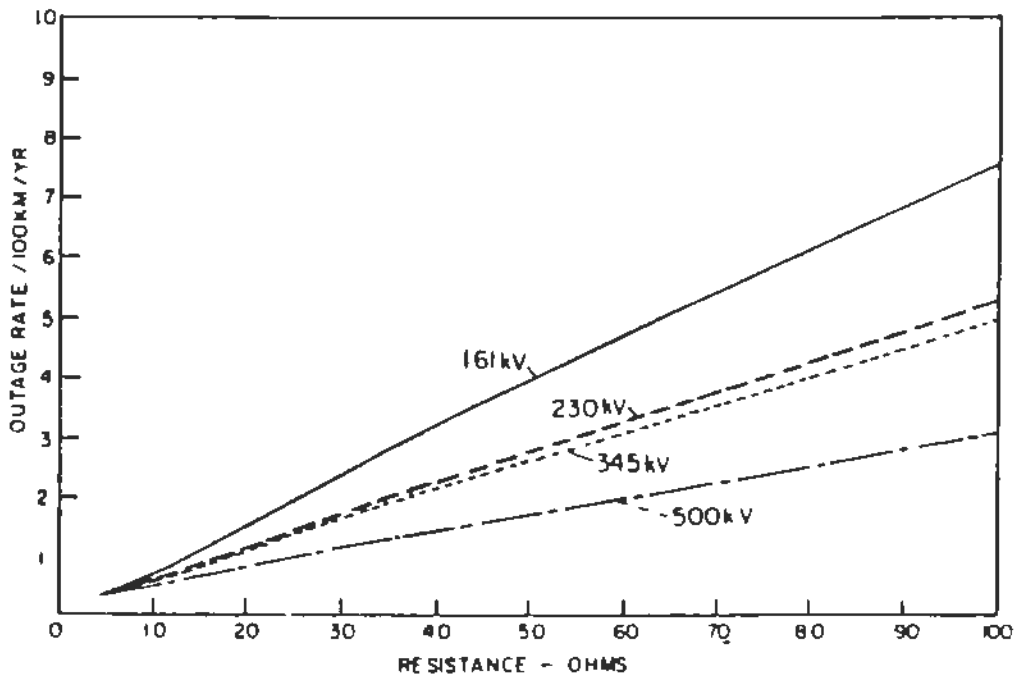


Figure 8-42. Lightning Outage Rates for Double-Circuit Vertical Lines Versus Tower Footing Impedance ⁽²⁾

8-14. COMBINING THE DIFFERENT REQUIREMENTS FOR LINE DESIGN

The strike distances and the clearances obtained from switching impulse, lightning impulse, contamination, and NESC designs are compared, and the most stringent requirements are adopted as dictating the line design. Figure 8-43, from Reference 4, illustrates where the different requirements prevail. In this figure, the required strike distance in meters is plotted against the maximum system voltage for lightning, switching, and power frequency contamination designs. The use of V-string insulator strings is assumed.

The lightning band in Figure 8-43 is for tower footing resistances below 20 ohms. The lower limit of the lightning band is for an isokeramic level (IKL) of 30, which represents an average United States area. The upper limit is for an IKL = 80, which represents a high lightning activity area.

The switching overvoltage curves in Figure 8-43 are drawn assuming a Gaussian SOV distribution for E_2 values of 2.6, 1.8, and 1.4 per-unit. A 4-percent strength decrease for wet conditions and a α_f /CFO of 5 percent are assumed. A statistical overvoltage of 2.6 per-unit represents a typical value for high-speed reclosing of breakers without preinsertion resistors, 1.8 per-unit represents breakers with one preinsertion resistor, and 1.4 per-unit represents an anticipated value for a breaker with one or two preinsertion resistors and controlled closing. A linear voltage profile of $E_R/E_S = 1.4$ is assumed. The line is assumed to have 500 towers.

The power frequency requirements are specified by creepage distance per kV of line-to-ground voltage, based on the maximum system voltage. Using V-string insulators with 146 x 254 mm units, it is assumed that the string length is 1.25 times the strike distance. Three contamination levels are assumed; low (required creepage of 2.2 cm/kV), medium (2.5 cm/kV), and heavy (5.6 cm/kV).

The following general observations on Figure 8-43 can be made.

- The lightning curve is relatively flat, as it should be. If a personality can be ascribed to lightning, it doesn't care whether it hits a 362-kV line or a 550-kV line. Therefore, the lightning requirement should be relatively constant with system voltage. However,

tower heights do increase with system voltage and coupling factors between the ground wires and phase conductors decrease. These effects, together with the increase in power frequency voltage, combine to produce a gentle increase in the required strike distance with increasing system voltage.

- Each of the switching surge curves turns sharply upward, portraying the saturation effect of the CFO with increasing strike distance.
- The contamination performance is assumed to be linear with the system voltage.

8-14-1. Comparison of Design Criteria

Considering Figure 8-43 from an overall viewpoint and comparing the requirements at alternate voltage levels, it is obvious that for severe contamination areas, the contamination criterion dictates design. Neglecting these severe contamination areas, consider only the two lower contamination criteria.

- 362 kV. The lightning curve, the 2.6 per-unit switching surge curve, and the median contamination curve are approximately coincident, illustrating that none of the three criteria dominates the design and an "optimum" point is achieved. A preinsertion resistor in the breaker is not required.
- 550 kV. If the switching surge design is based on a statistical overvoltage of 2.6 per-unit, switching overvoltages dominate the design. Therefore, at 550 kV, a preinsertion resistor in the breaker is used, decreasing the statistical overvoltage to 1.8 per-unit. At this level, lightning tends to dictate design. Note that the median contamination line is in the middle of the lightning band.
- 800 kV. The switching surge curve at 1.8 per-unit meets the upper portion of the lightning band. The lower contamination curve is centered in the lightning band. For improved design, statistical switching surges could be lowered to about 1.7 per-unit, at which point lightning once again dictates design for areas of low to median contamination.

- 1200 kV. If the design were based on a statistical switching overvoltage of 1.8 per-unit, large strike distances would be required, thus economically penalizing the development of this new voltage level. Fortunately, breakers have been built, and newer designs are contemplated, to decrease the switching overvoltage to a statistical level of about 1.4 per-unit. Solving this problem now places the burden on contamination. Here again, however, new insulator designs using semiconducting glazes or non-ceramic insulators have been developed, so that once again the burden of setting the strike distance is on switching surges. Note that switching surges require only 10 percent more insulation than lightning in areas having 80 storm days per year.

To summarize:

1. For practical designs, except for system voltage levels at about 1200 kV, switching surges do not dictate the line design.
2. Below 1200 kV, lightning tends to dominate the design in lightning areas having 30 to 80 storm days per year, except for high contamination areas.
3. At 1200 kV, switching surges control the design.
4. For areas of low lightning activity, having 10 or fewer storm days per year, contamination tends to dominate.

Thus, the conclusion to this point appears obvious. In most regions of the world, where lightning activity is between 30 and 80 storm days per year and contamination is low to medium, lightning dominates and dictates design except at 1200 kV and above. From a philosophical viewpoint, this appears reasonable. Switching surges are "man-made," so they can be "man-controlled," while lightning is a phenomenon of nature and must be accepted. Indeed, even at 1200 kV, lightning may be the dominating design factor.

8-14-2. Integrating NESC Requirements

The NESC requirements are integrated into Figure 8-43, as shown in Figure 8-44. This figure assumes that E_2 can be limited to the values in Table 8-40.

Table 8-40

ASSUMED E_2 FOR THE DIFFERENT VOLTAGE LEVELS

Maximum Voltage Level, kV	E_2 , p.u.
362	2.6
550	1.8
800	1.7
1200	1.4

With these values of E_2 , the NESC requirements for the strike distance can be obtained from Table 8-33 of Section 8-11.

Figure 8-44 shows that two curves can be drawn, depending on the IKL of the area. It can be seen from this figure that if the line is in an area of low contamination, or where measures to successfully combat contamination are available, the NESC requirements are met by reducing the SOV's.

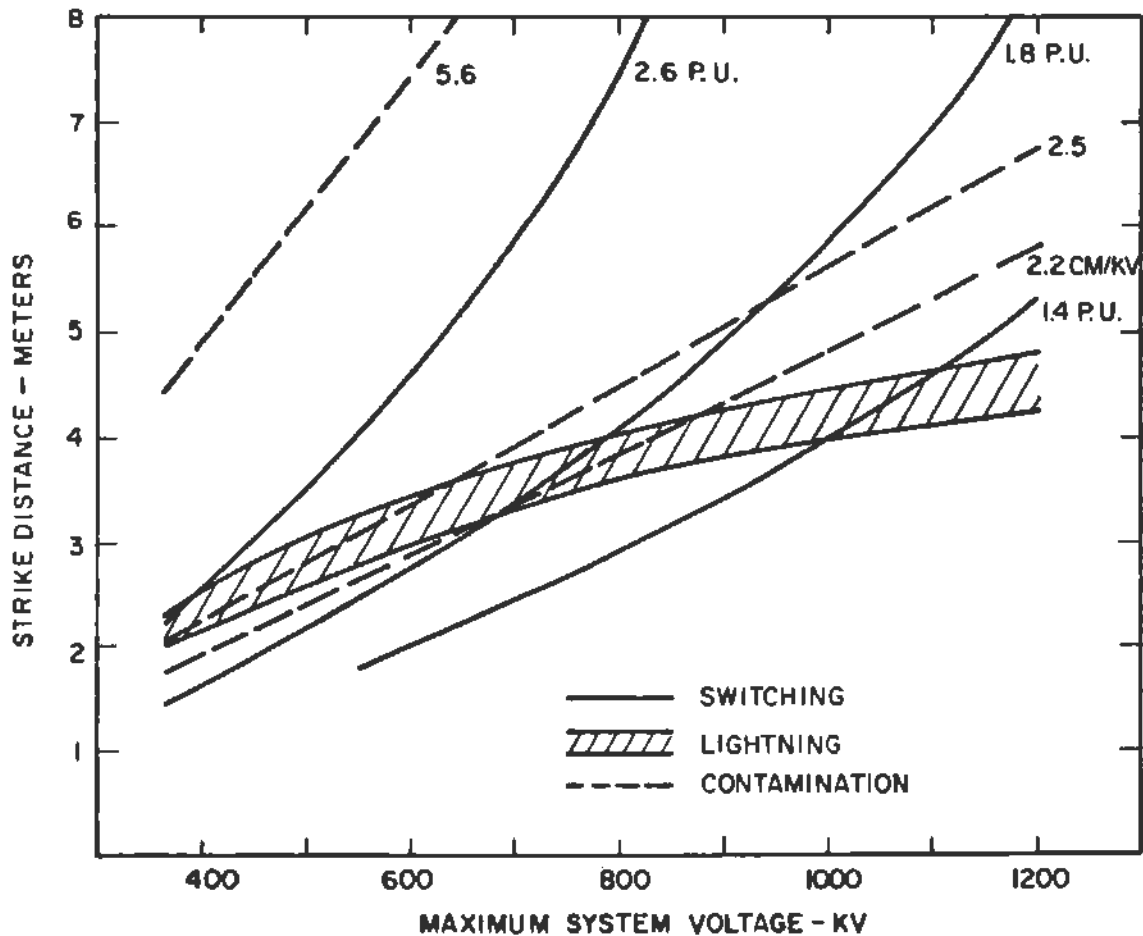


Figure 8-43. Estimates of Line Insulation Requirements⁽⁴⁾

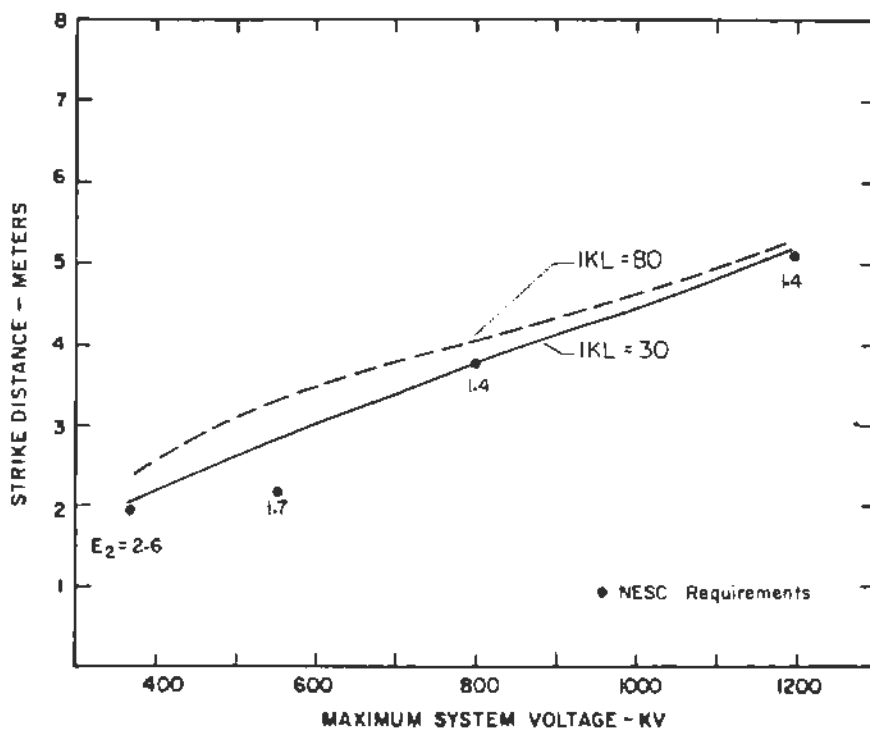


Figure 8-44. Integrating the NESC Requirements Into Figure 8-43

Off-Site Records Management, LLC



F0001883409

Container #: 1037172

ACCT: EP2465
POD

EPRI EL-4650 Vol.2

EMTP

Members of the EMTP Development Coordination Group

Bonneville Power Administration

Canadian Electrical Association-Utility Members

Hydro Quebec

Ontario Hydro

Western Area Power Administration

United States Bureau of Reclamation

Associate Members of the EMTP Development Coordination Group

ASEA

Central Research Institute
of the Electric Power Industry in Japan
